Developing non-isocyanate polyurethane chemistry for more sustainable structural composites in a circular economy

Guillem Seychal

A thesis presented for the degree of
Doctor of Philosophy in Chemical Sciences

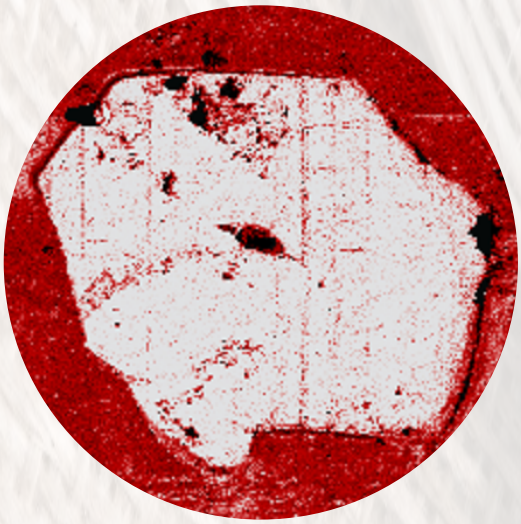

European Joint Doctorate
University of Mons (Belgium)
&
University of the Basque Country (Spain)
Academic year 2024-2025

Jury members

Pr. Jean-Marie Raquez (Promotor)
Pr. Nora Aranburu (Co-promotor)
Pr. Roberto Lazzaroni (President)
Pr. Haritz Sardon (Secretary)
Pr. Veronique Michaud
Pr. Christophe Baley
Pr. Filip Du Prez

"L'utopie a changé de camp : est aujourd'hui utopiste celui qui croit que tout peut continuer comme avant."
Pablo Servigne, Comment tout peut s'effondrer

"Il n'y a pas de produit ou de service plus écologique, économe en ressources, recyclable, que celui que l'on utilise pas. [...] Recycler est très important, mais ne suffit pas et ne peut nous dédouaner de notre consommation matérielle."
Philippe Bihouix, L'âge des low-tech

"Il faut imaginer Sisyphe heureux."
A. Camus, Le Mythe de Sisyphe

Acknowledgments

The following document closes the last three and a half (intense) years. I have sometimes been asked if being a doctoral student was a good situation. If I had to summarize a doctorate today with you, I would say it is above all meetings. It is quite curious to think that chance and encounters forge a destiny. Sometimes, we do not find the interlocutor opposite, I would say the mirror that helps you move forward. So this is not my case, as I said there, since, on the contrary, I was lucky enough to meet these people who help you move forward and whom I now wish to thank.

I would like to thank the European Union, which funded this work through the NIPU-EJD 955700 MSCA project. This project made me move six times, work in four different laboratories across three countries, encounter amazing people, and learn Spanish, a bit of Italian, and three words of Basque (which is not much, but it is a really difficult language). I would also like to thank the various French, Italian, and Belgian administrations for adding amazing side quests throughout these years, such as finding where to pay (or not) taxes, among so many other fun ones. Also, as it will be observed through the abstracts, the joint doctorate allowed this thesis to potentially serve as a Rosetta stone. I must acknowledge Dacia for inventing the Sandero, able to fit an entire apartment and two bikes in it; extremely convenient when you move almost every six months.

As said, the people I encountered have made this thesis, at least from a personal perspective, a success, and a satisfying, enjoyable experience.

My first acknowledgments must obviously go to my supervisors, Nora and Jean-Marie, for giving the opportunity to the least possible chemist to pursue a PhD in chemistry, which was quite a gamble. Thank you, Jean-Marie, for your precious pieces of advice, kindness, and patience, for your guidance, and for sharing your knowledge throughout these years. Nora, no creo que pueda agradecerte lo suficiente por tu apoyo. Un año en San Sebastián fue una experiencia demasiado corta. Tu apoyo, tu disponibilidad, tu amabilidad, tus valiosos consejos han sido para mí mucho más valiosos de lo que imaginas. Eskerrik asko guztiagatik, onena zara. Haritz, fue un placer tenerte como supervisor no oficial. Le agradezco la calidad de sus consejos, tanto sobre ciencia como sobre otros temas, especialmente los escritos de “ciencia ficción”.

I’d also like to thank Dr. Fanny Bonnet, Pr. Christophe Detrembleur, Dr. Bruno Grignard, Pr. Philippe Leclère, Pr. Roberto Lazzaroni, Dr. Vincent Lemaur, and Dr. Leila Bonnaud (and all people of “MaNo”) for their help, support, and advice and for allowing me to use their equipment and waste some of their own, colleagues’ and students’ time, Pierre Nickmielder and Bernard Miranda Campos particularly. I would also like to thank Carpenter Co., and especially Dr. Lucie Imbernon and Bart Haelterman, for welcoming me to their R&D center in Wetteren. I must also kindly thank Pr. Eduard Marenic and Pr. Jean-Charles Passieux for giving me an interesting first view of the research world, 5 years ago, and even more to Dr. Vincent Placet, for making me discover the amazing realm of natural fibers and wanting to continue into PhD studies.

This PhD was the opportunity to meet amazing people and companions on the road and in trouble. My first thoughts must go to the people from Mons, where I arrived on a cold and gray day in October 2021. It was a long time ago, in Covid’s age, covered by the mask, and I had to wait several months before seeing their faces; I had more hairs. Yet, your warm welcome was appreciated and it was always amazing to work in a place where people are not the last for a good laugh or beer, sometimes both together. Thank you so much Nohé, “Mounch” (je l’écris comme je veux), Gab, Chiara, Louis, Anne, Katherine, Sylvie, Caro, Meriam, Samira, Rosica, Jeremy! I must also acknowledge Louis for not letting me sleep in the street for the last 6 months. I do not extend as much as what you deserve as I know I will have the opportunity to thank each one of you, which is a bit better than on a piece of paper no one will ever read.

The NIPU project involved 12 ESR, “early stage researchers”, which amazingly struggled on almost the same things across Europe for 3 years, including (especially?) administration. The terminology MRC “misfortune companion researcher”, might be more suited in the future. Yet, I have been lucky to count on these eleven amazing partners to discuss, debate, laugh, and share some times within the project. It has always been a pleasure to go to NIPU meetings, and I wish we had more. Thank you (by ESR number but not by importance): Francesca, Dr. Federico, Nichollas, Luca, Dr. Florent, Maliheh, Katherine (again), Pavithra, Hsin-Chen “Christy”, Marco, and Pauline! Thank you, Florent, for showing me the darkest secrets of NIPU, Marco for explaining/teaching me chemistry (and more), Katherine for your always good mood, smile, kindness, and wise advice, and Federico for explaining to me the correct spelling of “arancina” and the meaning of some Italian words and sodas that I don’t want to share here and Luca for not being the last doing some supplementary hours after conference and meeting diners.

I expected the year in San Sebastian to be good, but I would not have expected it to be that good. The quality of the people there only made it difficult to leave. I hope not to forget anyone, as so many deserve a warm thank you, which I hope to say in person. Thank you, Marta X, for your fun and kindness, and for keeping my hood closed and turned off (and also amazing graphics, see Chapter 4). Thank you, Xabi, for sharing with me the worst possible day to bike and putting me on the right track to cross the Pyrenees. Thank you, Fernando, for the good times, advice, and ideas. In complete disorder, Aritz, Ainhoa, Paula, Marco (again), Jon, Ion, Giuls, Fermin, Gabby, Flore, Daniele, Alice, Lucas, Bige, Claire, Marta M, Teo, Sergio (also for the Rammstein sessions in the lab), Miryam, Bea, Oihane, eskerik asko a todos! I must thank the rowing club of San Sebastian, Ur Kirolak, for their warm welcome and for letting me row and compete with them; it was good to go back to the past loves. I cannot leave the San Seb section without giving special thanks to Gabriel. Sometimes, unexpectedly, amazing friendships are formed, and I must say this is one of them. I would not have believed in making such a good friend in such a short time, although finding a native Brazilian who speaks English with a French accent might have been a hint. Yet here we are. I have enjoyed discussing life and science and sharing una txuleta or two. We both know it is only a start, but I believe we can say, "What a start." See you soon for more adventures!

Il est désormais temps de passer à quelques remerciements dans la langue de Molière, déjà, parce que je ne peux pas faire confiance dans la qualité de l’anglais des personnes concernées mais également parce que c’est quand même plus sympa.

Dans la catégorie des gens qui ne liront probablement jamais ni cette thèse, ni ces remerciements et ils ont bien raison, je souhaite remercier le triathlon club de Mons : Pierre, Pierre, Pierre, Pierre, Simon, Louis, Anaïs, Aurélien, Manu, Aymeric, Loïc, Marie, Valentin et tant d’autres, sans oublier Pierre, pour leur accueil et pour la motivation à rouler par -8000°C le samedi, à 9 h.

Je souhaiterais également remercier les copaings, JC, Mathieu, Morvan, Antoine Jordan, Jean, Polo, qui, sans le savoir, ont bien facilité ces travaux. Il est parfois difficile de se changer les idées, se vider la tête et les désormais presque traditionnelles vacances d’été et autres nouvel ans ont été capitaux. J’y ai laissé un genou dans cette histoire mais je crois que cela en valait la peine. Dans le registre des amis sur qui on peut toujours compter, merci à toi Rodolphe, avec qui j’ai, après tout, partagé notre premier « projet scientifique », il y a désormais 10 ans, et à vous deux Florian, Maxime!

Je ne souhaite pas remercier mes parents, après tout, s’ils m’avaient aimé à la hauteur de ce que je mérite, jamais ils ne m’auraient laissé partir en Belgique pour faire un doctorat. Aussi, je ne me rappelle pas qu’ils m’aient demandé mon avis avant de me mettre au monde. Il est également arrivé, une fois, que le plateau à fromages soit vide en rentrant. Le temps finira

par guérir cette blessure mais c'est encore trop tôt. Il serait de bon ton tout de même de remercier ma sœur, après tout, elle a quasiment subi les mêmes préjudices que moi, en moins pire. Néanmoins, votre soutien indéfectible et votre amour (réciproque) de tous les 3, ne s'est pas limité à ses trois dernières années mais à bien plus, a minima 26 si mes calculs sont bons, et je sais la chance que j'ai de pouvoir compter sur une famille comme celle-là. Demain, 8h, tests pour savoir si vous avez bien tout suivi à ce que j'ai raconté dans le présent document.

E infine, ma non meno importante, vorrei ringraziare te, Serena. Il tuo sostegno, il tuo sorriso, il tuo amore mi hanno aiutato molto più di quanto a volte lascio sembrare. Mi hai supportato anche se fastidioso quanto sono capace di essere. Abbiamo vissuto tante cose belle e averti al mio fianco negli ultimi anni è stata una benedizione. Sei il miglior partner che chiunque possa chiedere. Ti amo.

Abstract

Natural fiber-reinforced polymer composites (NFC) are key materials for building a more sustainable future, as natural fibers offer a promising low-carbon option. However, they involve the use of fossil-based matrices, hindering their environmental benefits, together with poor adhesion to cellulosic fibers and their non-recyclability. In this respect, this work aims to explore more sustainable matrices in the vision of a circular economy. Polyhydroxyurethanes (PHUs), as obtained from CO_2-based cyclic carbonates and polyamines, are considered to be greener/safer alternatives to conventional polyurethanes but have not been explored as a candidate for composite matrices. The hydroxyurethane moieties present along the PHU's backbone offer unexplored opportunities that could be a breakthrough in many structural applications, particularly a special affinity between PHUs and cellulosic fibers, along with the ability of hydroxyurethane moieties to participate in reversible exchange reactions for further recycling.

As PHUs have never been explored for composite applications, and are relatively new, there is a significant lack of understanding about their advantages and limitations. The relationship between the macromolecular structure, the processability, and the final properties of PHUs was herein evaluated to establish, to a sufficient extent, a comprehensive overview of these emerging thermosets. This allowed us to create an optimized PHU matrix for flax-fiber composites with excellent mechanical performances, 20-30% better than epoxy-based benchmark composites. These exceptional properties are ascribed to the existence of strong hydrogen bonds between PHU and fiber as shown through atomic force microscopy and rationalized by atomistic simulation. These PHU composites also demonstrated self-welding capabilities due to the reversible nature of hydroxyurethane moieties.

To implement these PHUs for large-scale composite and industrial processes, we developed an approach relying on a synergetic copolymerization, which significantly increased dynamic performance and enabled the production of high-performance, re-shapable fiber composites derived from natural fibers as well as carbon fibers. This approach also allowed for efficient fiber recovery. Interestingly, natural fiber mechanical properties after the recycling were demonstrated to be similar, and the chemical composition was similar.

Further investigating this copolymerization strategy, the processability was investigated deeply to provide a better understanding of the systems and efficiently apply it to resin transfer molding with controlled conditions and fast curing. While PHUs were not easily processable, these hybrids can now be infused and cured in an efficient protocol.

Starting from an unexplored pathway, PHU chemistry was explored, developed, and enhanced to enter a new field, composites. Through the implementation of PHUs in composites, particularly NF ones, substantial advantages might be expected in terms of sustainability, possibilities, properties, and economic benefits. Finally, to objectively state the sustainability of our developed materials, an LCA study was conducted to establish the playground of a sustainable discussion and draw future perspectives for implementing PHU chemistry in the realm of composites for structural applications. The LCA results demonstrate that this strategy is environmentally beneficial and could help reduce the footprint of composite materials. Future developments and additional efforts are, however, still required to reach the requirements of sustainability goals wanted by the European Union.

Resumen

Los compuestos poliméricos reforzados con fibras naturales son materiales clave para construir un futuro más sostenible, ya que las fibras naturales ofrecen una opción prometedora con bajas emisiones de carbono en comparación a las fibras empleadas típicamente (vidrio y carbono). Sin embargo, estos compuestos habitualmente implican el uso de matrices de origen fósil, no reciclables, lo que limita sus beneficios ambientales, así como sus prestaciones finales ya que presentan una mala adhesión con las fibras celulósicas. Este trabajo tiene como objetivo explorar los polihidroxiuretanos (PHU) como matrices para compuestos de fibras naturales, de manera que les aporten una mayor sostenibilidad con miras a una economía circular. A pesar de que los PHU se consideran alternativas más ecológicas y seguras que los poliuretanos convencionales ya que se fabrican a partir de carbonatos cíclicos basados en CO_2 y poliaminas, aún no se han explorado como matrices de materiales compuestos. En este sentido, los grupos funcionales hidroxiuretano presentes a lo largo de la estructura principal de los PHU ofrecen oportunidades inexploradas que podrían suponer un gran avance en muchas aplicaciones estructurales, ya que presentan una afinidad especial con las fibras celulósicas, así como la capacidad de participar en reacciones de intercambio reversibles, lo que podría dar lugar a la posibilidad de reciclarlos.

Dada la ausencia de conocimiento acerca de las ventajas y limitaciones que ofrecen los PHU en el campo de los compuestos poliméricos, en esta tesis doctoral se evaluó la relación entre la estructura macromolecular, la procesabilidad y las propiedades finales de los PHU para establecer, en una medida suficiente, una descripción general completa de estos termoestables emergentes. Esto nos permitió desarrollar una matriz de PHU optimizada para compuestos de fibra de lino, que mostraron un excelente rendimiento mecánico, un 20-30% mejor que los compuestos de referencia a base de epoxi. Estas propiedades excepcionales se atribuyen a la existencia de fuertes enlaces de hidrógeno entre el PHU y la fibra, como se demuestró a través de microscopía de fuerza atómica y se racionalizó mediante simulación atomística. Estos compuestos de PHU también demostraron capacidades de auto-reparación debido a la naturaleza reversible de las fracciones de hidroxiuretano. Para implementar estos PHU en procesos industriales y de compuestos a gran escala, se desarrolló un enfoque basado en una copolimerización sinérgica, lo que resultó en un aumento significativo del rendimiento dinámico y permitió la producción de compuestos reforzados tanto con fibras naturales como con fibras de carbono remodelables y con altas prestaciones mecánicas.

Asimismo, se investigó en profundidad el efecto de la estrategia de copolimerización sobre la procesabilidad, con el fin de proporcionar una mejor comprensión de los sistemas y poder aplicarlos de manera satisfactoria al moldeo por transferencia de resina, empleando unas condiciones controladas y un curado rápido. Esto permitió desarrollar híbridos procesables mediante técnicas convencionales, superando la limitación mostrada por los PHU. Por otro lado, la mejorada dinamicidad de los sistemas híbridos permitió la remodelación y soldadura de materiales post-curados y la recuperación de las fibras, incluso utilizando fibras naturales.

Por tanto, en esta tesis doctoral se exploró, desarrolló y mejoró la química de los PHU para aplicarlos a un nuevo campo aún inexplorado, el de los materiales compuestos. A través de la implementación de los PHU en compuestos, particularmente los basados en fibras naturales, se podrían esperar ventajas sustanciales en términos de sostenibilidad, propiedades y beneficios económicos. Con el fin de evaluar objetivamente dicha mejora de la sostenibilidad, se realizó un estudio de ACV, lo que permitió establecer las bases de un debate y trazar perspectivas futuras para la implementación de la química PHU en el ámbito de los compuestos para aplicaciones estructurales.

Résumé

Les composites polymères renforcés de fibres naturelles (NFC) sont des matériaux clés pour construire un avenir plus durable. Les fibres naturelles offrent une option prometteuse à faible empreinte environnementale. Cependant, ils impliquent l'utilisation de matrices à base de ressources fossiles, réduisant leurs avantages environnementaux. Par ailleurs, ces matrices ne fournissent pas systématiquement une interface fibre/matrice de qualité, et ne sont pas recyclables pour la plupart. À cet égard, ce travail vise à explorer des matrices potentiellement plus durables dans une vision de future économie circulaire. Les polyhydroxyuréthanes (PHU), obtenus à partir de carbonates cycliques, dérivables du CO_2, et de polyamines, sont considérés comme des alternatives plus écologiques/plus sûres aux polyuréthanes conventionnels, mais n'ont pas été explorés comme candidats pour les matrices composites. Les fonctions hydroxyuréthanes présents le long de la chaîne principale du PHU offrent des opportunités inexplorées qui pourraient constituer un atout dans de nombreuses applications structurelles. De plus, les fonctions hydroxyuréthanes sont capables de participer à des réactions d'échange réversibles pour un recyclage ultérieur et une meilleur qualité de l'interface fibre matrice est attendue.

Les PHUs n'ayant jamais été explorés pour des applications composites et étant relativement nouveaux, leurs avantages et leurs limites sont mal compris. Afin de remédier à ce problème, la relation entre la structure macromoléculaire, leur aptitude pour les procédés de fabrication et les propriétés finales des PHU a pas été évaluée pour établir un aperçu complet de ces polymères. Cela nous a permis de créer une matrice PHU optimisée pour les composites à base de fibres de lin. D'excellentes performances mécaniques, de 20 à 30 % supérieures à celles des composites de référence à base d'époxy ont été obtenues. Ces propriétés exceptionnelles sont attribuées à l'existence de fortes liaisons hydrogène entre le PHU et la fibre, comme le montre la microscopie à force atomique et rationalisée par simulation atomistique. Ces composites PHU ont également démontré des capacités d'auto-soudage en raison de la nature réversible des groupements hydroxyuréthane.

Pour mettre en œuvre ces PHU pour des procédés composites et industriels à grande échelle, nous avons développé une approche reposant sur une copolymérisation synergique, qui a considérablement augmenté les performances dynamiques et a permis la production de composites remodelables de haute performance dérivés de fibres naturelles ainsi que de fibres de carbone. Cette approche a également permis une récupération efficace des fibres. Les fibres de lin recyclés ont été étudiées chimiquement et mécaniquement et n'ont pas montré de signes de dégradation due au recyclage. Un nouveau composite exploitant les fibres recyclées a été produit et montré des propriétés prometteuses pour des applications intermédiaires.

En approfondissant cette stratégie de copolymérisation, les cinétiques de réticulation ont été étudiées en profondeur pour fournir une meilleure compréhension des systèmes et l'appliquer efficacement au moulage par transfert de résine dans des conditions contrôlées et pour un durcissement rapide. Alors que les PHU n'étaient pas facilement transformables, ces hybrides peuvent désormais être infusés et durcis efficacement.

D'une voie inexplorée, la chimie des PHU a été développée et améliorée pour entrer dans un nouveau domaine, les composites. Grâce à la mise en œuvre des PHU dans les composites, en particulier les composites NF, des avantages substantiels pourraient être attendus en termes de durabilité, de possibilités, de propriétés et d'avantages économiques.

Enfin, une étude ACV a été menée pour évaluer la durabilité des matériaux développés et dessiner des perspectives futures pour la mise en œuvre de la chimie des PHU dans le domaine des composites pour des applications structurelles. Les résultats démontrent que la stratégie est environnementalement prometteuse et peut permettre la réduction de l'empreinte des composites. D'autres efforts sont toutefois nécessaires pour atteindre les ambitions de développement durable annoncée en Europe.

Laburpena

Zuntz naturalekin indartutako material konposatuak funtsezko materialak dira etorkizun iraunkorrago bat eraikitzeko, zuntz naturalek karbono-aztarna baxuko aukera itxaropentsua eskaintzen baitute. Hala ere, konposatu horien matrize bezala lehengai berriztaezinetatik eratorritako polimeroak erabili ohi dira, haien ingurumen-onurak mugatuz. Horrez gain, polimero horiek itsaspen eskasa izan ohi dute zelulosazko zuntzekin eta, gainera, birzikla ezinak dira gehienetan. Honen harira, lan honek matrize iraunkorragoak aztertzea du helburu, zehazki, polihidroxiuretanoak (PHU), zuntz naturalen konposatuen zirkulartasuna handiagotzeko. Nahiz eta CO_2tik eratorritako karbonato zikliko eta poliaminetan oinarritutako PHUak alternatiba berdeago eta seguruago gisa hartu izan diren poliuretano konbentzionalekin alderatuta, ez dira konposatuen matrize gisa aztertu. PHUen kate nagusian dauden hidroxiuretano taldeek aukera berriak eskaintzen dituzte, egitura aplikazio askotan iraultza bat ekar dezaketenak, izan ere PHUen eta zelulosazko zuntzen arteko afinitatea hobe baitezakete. Are eta gehiago,hidroxiuretano taldeek, erreakzio itzulgarrien bitartez, material konposatu hauen birziklapena ahalbidetu dezakete.

PHUek konposatu polimerikoen arloan eskaintzen dituzten abantailei eta mugei buruzko ezagutzarik ez zegoenez, doktoretza-tesi honetan PHUen egitura makromolekularraren, prozesagarritasunaren eta azken propietateen arteko erlazioa ebaluatu zen, neurri handi batean, sortzen ari diren termoegonkor horiei buruzko ikuspegi orokorra ezartzeko. Horri esker, liho-zuntz konposatuetarako PHU matrize optimizatua garatu ahal izan zen, errendimendu mekaniko bikainak erakutsiz, epoxi erretxinan oinarritutako erreferentziazko konposatuak baino %20-30 hobeak. Propietate aparta hauek PHU eta zuntzen arteko hidrogeno-lotura sendoei esleitzen zaizkie, indar atomikoko mikroskopiaren bidez erakutsi eta simulazio atomistikoek arrazoitu bezala. Gainera, PHU konposatuek auto-soldadura gaitasunak erakutsi zituzten hidroxiuretano talde itzulgarriei esker.

PHU horiek eskala handiko konposatuetan eta prozesu industrialetan inplementatzeko, kopolimerizazio sinergikoan oinarritutako hurbilketa bat garatu zen. Horren ondorioz, errendimendu dinamikoa nabarmen handitu zen, eta prestazio mekaniko handidun eta birmoldagarriak ziren konposatuak ekoiztu ahal izan ziren, bai zuntz naturalekin eta baita karbono-zuntzekin ere. Ikuspegi horrek zuntzak eraginkortasunez berreskuratzea ere ahalbidetu zuen.

Era berean, kopolimerizazio-estrategiak prozesagarritasunean duen eragina sakon ikertu zen, sistemak hobeto ulertzeko eta erretxina-transferentziazko moldekatzean (RTM) modu eraginkor batean aplikatu ahal izateko, baldintza kontrolatuak eta ontze azkarra erabiliz. Horri esker eta PHUek erakutsitako muga gainditzuz, hibrido prozesagarriak garatu ahal izan ziren ohiko tekniken bidez. Bestalde, sistema hibridoen dinamikotasun hobeari esker, ondutako materialak birmoldatu eta soldatu ahal izan ziren. Azkenik, zuntzak berreskuratu ahal izan ziren, baita zuntz naturaletan oinarritutako konposatuen kasuan ere.

Beraz, doktorego-tesi honetan PHUen kimika aztertu, garatu eta hobetu zen, oraindik esploratu gabeko eremu berri batean aplikatzeko, material konposatuetan. PHUak konposatuetan inplementatzearen bidez, bereziki zuntz naturaletan oinarritutakoak, abantaila nabarmenak espero litezke iraunkortasunari, propietateei eta onura ekonomikoei dagokienez. Iraunkortasunaren hobekuntza hori objektiboki ebaluatzeko, bizitza-zikloaren azterketa (LCA) bat egin zen, eta, horri esker, jasangarritasunaren inguruko eztabaida baten oinarriak ezarri ahal izan ziren eta PHU kimika egitura-aplikazioetarako konposatuen eremuan ezartzeko etorkizuneko perspektibak zehaztu ahal izan ziren.

Dissemination & Communication

List of Publications - Thesis related

- G. Seychal, C. Ocando, L. Bonnaud, J. De Winter, B. Grignard, C. Detrembleur, H. Sardon, N. Aramburu, J.-M. Raquez, Emerging Polyhydroxyurethanes as Sustainable Thermosets: A Structure–Property Relationship, ACS Appl. Polym. Mater. 5 (2023) 5567–5581. https://doi.org/10.1021/acsapm.3c00879.

- G. Seychal, P. Nickmilder, V. Lemaur, C. Ocando, B. Grignard, P. Leclère, C. Detrembleur, R. Lazzaroni, H. Sardon, N. Aranburu, J.-M. Raquez, A novel approach to design structural natural fiber composites from sustainable CO 2 -derived polyhydroxyurethane thermosets with outstanding properties and circular features, Composites Part A: Applied Science and Manufacturing 185 (2024) 108311. https://doi.org/10.1016/j.compositesa.2024.108311.

- G. Seychal, M. Ximenis, V. Lemaur, B. Grignard, R. Lazzaroni, C. Detrembleur, H. Sardon, N. Aranburu, J. Raquez, Synergetic Hybridization Strategy to Enhance the Dynamicity of Poorly Dynamic CO 2 -derived Vitrimers achieved by a Simple Copolymerization Approach, Adv Funct Materials (2024) 2412268. https://doi.org/10.1002/adfm.202412268.

- G. Seychal, B. Miranda Campos, G. Perli, V. Placet, B. Grignard, G. Bonnet, C. Detrembleur, H. Sardon, N. Aranburu, and J.M. Raquez, Implementing recyclable bio- and CO_2-sourced synergetic dynamic matrices via precise control of curing and properties for natural fiber composites within industrially relevant resin transfer molding, *Accepted in Chemical Engineering Journal*

- G. Seychal, A. Goldberg, G. Perli, H. Sardon, N. Aranburu, and J.M. Raquez, En route to the rational design of circular and sustainable structural fiber-reinforced polymers, ***Manuscript in preparation***

- G. Seychal, P. Bron, O. Talon, N. Aranburu, and J.M. Raquez, Can polyhydroxyurethane Covalent Adaptable Networks, increase the sustainability of composite, a life cycle assessment, ***Submitted***

List of Publications - Collaborations and other works

- G. Seychal, E. Ramasso, P. Le Moal, G. Bourbon, X. Gabrion, V. Placet, Towards in-situ acoustic emission-based health monitoring in bio-based composites structures: Does embedment of sensors affect the mechanical behaviour of flax/epoxy laminates?, Composites Part B: Engineering 236 (2022) 109787. https://doi.org/10.1016/j.compositesb.2022.109787.

- E. Marenić, G. Seychal, J.-C. Passieux, Data driven approach in multiphysics framework: Application to coupled electro-mechanical problems, Computer Methods in Applied Mechanics and Engineering 395 (2022) 114959. https://doi.org/10.1016/j.cma.2022.114959.

- G. Seychal, L. Van Renterghem, C. Ocando, L. Bonnaud, J.-M. Raquez, Towards sustainable reprocessable structural composites: Benzoxazines as biobased matrices for natural fibers, Composites Part B: Engineering 272 (2024) 111201. https://doi.org/10.1016/j.compositesb.2024.111201.

- T. Habets, G. Seychal, M. Caliari, J.-M. Raquez, H. Sardon, B. Grignard, C. Detrembleur, Covalent adaptable networks through dynamic N,S-acetal chemistry: toward recyclable CO_2-based thermosets, JACS 145 (2023) 25450–25462. https://doi.org/10.1021/jacs.3c10080.
- A. Lamas, L. Polo Fonseca, C. Moussard, D.D.M. Zanata, G. Perli, M. Ximenis, X. Lopez De Pariza, G. Seychal, M. Caliari, M. Itxaso, R. Aguirresarobe, I. Calvo, H. Sardon, Exploiting the Base-Triggered Thiol/Vinyl Ether Addition to Prepare Well-Defined Microphase Separated Thermo-Switchable Adhesives, Adv Funct Materials (2024) 2412584. https://doi.org/10.1002/adfm.202412584.
- D. Finazzi, G. Seychal, J.-M. Raquez, G. Robert, K. De Clerck, L. Daelemans, W. Van Paepegem, Study of the temperature-humidity equivalence and the time-temperature superposition principle in the finite-strain response of polyamide-6 and short glass fibre-reinforced polyamide-6, Polymer Testing 141 (2024) 108653. https://doi.org/10.1016/j.polymertesting.2024.108653.
- M. Caliari, F. Vidal, D. Mantione, G. Seychal, M. Campoy-Quiles, L. Irusta, M. Fernandez, X.L. De Pariza, T. Habets, N. Aramburu, J. Raquez, B. Grignard, A.J. Müller, C. Detrembleur, H. Sardon, Advanced Materials (2025) 2417355 https://doi.org/10.1002/adma.202417355.

Patent applications

- Covalent adaptative network, European Patent Application EP24186922, priority 2024
- Foam material, precursor composition and kit thereof, European Patent Application EP24383258, priority 2024

Participation to congress - Poster presentations

- Seychal G., Ocando C., Grignard B., Detrembleur C., Sardon H., Bonnaud L., Aranburu N., Raquez J-M., "Non-Isocyanate Polyurethanes based composites: a new route to more sustainable structural composites", poster presentation, 16th meeting of polymer group the Spanish royal society of chemistry (GEP-SLAP), Donostia-San Sebastian, Spain, 8-12.05.2022
- Seychal G., Ocando C., Grignard B.,Detrembleur C., Sardon H., Bonnaud L., Aranburu N., Raquez J-M., "Non-Isocyanate Polyurethanes based composites: a new route to sustainable fully biobased structural composites" poster presentation, European Conference on Composite Materials, Lausanne, Switzerland, 26-30.06.2022. ***Best poster award***
- Seychal G., Ocando C., Grignard B.,Detrembleur C., Sardon H., Bonnaud L., Aranburu N., Raquez J-M., "Non-Isocyanate Polyurethanes based composites: a new route to sustainable fully biobased structural composites" poster presentation, Mardi des Chercheurs, Mons, Belgium, 06.09.2022
- Seychal G., Ocando C., Grignard B.,Detrembleur C., Sardon H., Bonnaud L., Aranburu N., Raquez J-M., "Non-Isocyanate Polyurethanes based composites: a new route to more sustainable structural composites" poster presentation, BPG annual meeting, Blankenberge, Belgium, 14-15.11.2022

Participation to congress - Oral presentations

- Seychal G., Ocando C., Aranburu N., Raquez J-M., "From epoxides to sustainable PHUs: Can CO_2 enhance natural fiber composite properties?", oral presentation, 6th International Conference on Natural Fibers, Madeira, Portugal, 19-21.06.2023
- Seychal G., Ocando C., Aranburu N., Raquez J-M., "Towards greener composites: are PHUs suitable for natural fiber reinforced composites?", oral presentation, 23rd International Conference on Composite Materials, Belfast, United Kingdom, 31.07-04.08.2023
- Seychal G., Aranburu N., Raquez J-M., "Design of high-performance polyhydroxyurethanes and their derivatives for more sustainable structural natural fiber composites", oral presentation, 50th World Polymer Congress IUPAC MACRO24, Warwick, United Kingdom, 01-04.07.2024

The software Grammarly was used for the publications and throughout the manuscript as a grammar and spelling mistakes corrector and to help improve the readability.

Contents

List of symbols & abbreviations

ϵ	Strain
ν	Poisson's ratio
σ	Stress
E	Young's modulus
E'	Storage modulus
E"	Loss modulus
tanδ	Loss factor
T_g	Glass transition temperature
T_v	Freezing topology temperature
V_f	Fiber volume fraction
V_p	Porosity volume fraction
AFM	Atomic force microscopy
BPA	Bisphenol-A
CAN	Covalent Adaptable Network
CFRP	Carbon fiber reinforced polymer
CC	Cyclic Carbonate (except Chapter 6)
CC	Climate Change (Chapter 6)
CLT	Classical Laminate Theory
CSBO	Carbonated soybean oil
DBU	1,8-Diazabicyclo(5.4.0)undec-7-ene
DFT	Density functional theory
DGEBA	Diglydicyl ether of bisphenol-A
DMA	Dynamic mechanical Analysis
DMAP	4-Dimethylaminopyridine
DMSO	Dimethyl sulfoxide
DSC	Differential scanning calorimetry
EI	Environmental Impact
EP	Epoxy
EU	European Union
FRP	Fiber reinforced polymer
FTIR	Fourier Transform Infrared
GC	Gel Content
GEC	Glycerol polycarbonate
GHG	Greenhouse gas
GPGE	Glycerol polyglycidyl ether
GWP	Global warming potential
HCl	Hydrochloric acid
IPDA	Isophorone Diamine
LCA	Life Cycle Analysis

The abbreviation list continues on the next page →

MDA	Methylene diphenyl diamine
MDI	Methylene diphenyl diisocyanate
MFA	Cellulose microfibril angle
mXDA	m-xylylene diamine
NF	Natural fiber
NFC	Natural fiber composite
NIPU	Non-isocyanate polyurethane
NMR	Nuclear magnetic resonance
PA	Polyamide
PE	polyethylene
PEC	Pentaerythritol polycarbonate
PEPGE	Pentaerythritol polyglycidyl ether
PET	Polyethylene terephthalate
PHU	Polyhydroxyurethane
PLA	Poly(lactic acid)
PU	Polyurethane
RDGE	Resorcinol diglycidyl ether
REACH	Registration, Evaluation, Authorisation and Restriction of Chemicals
RTM	Resin tranfer molding
SBC	Sorbitol polycarbonate
SEM	Scanning electron microscopy
SPGE	Sorbitol polyglycidyl ether
SI	Swelling Index
TBD	1,5,7-Triazabicyclo[4.4.0]dec-5-ene
TGA	Thermogravimetric analysis
TMPTC	Trimethylolpropane tricarbonate
TMPTGE	Trimethylolpropane triglycidyl ether
UD	Unidirectional
UN	United Nations

General introduction, hypothesis & scope of the work

1 Contextualization

There is a global consensus on the necessity to reduce the human environmental footprint on Earth. A relevant example is related to the 2015 Paris Agreement in which most countries committed to mitigate climate change with a maximum temperature of 2 °C compared to the pre-industrial level by 2100 and to adapt policies and economic paradigms to meet future needs. The last GIEC reports foreseen a drastic cut of CO_2eq emissions by half by 2030 and achieving net zero emissions by 2050 as the only solution to stay within these limits. In other words, it is critical to ensure humanity's future by adopting more sustainable practices. Such practices must be applied to all aspects of our production and consumption habits, particularly in developed countries, by reducing the production of unnecessary goods, enhancing energy and structure efficiency, and minimizing the impact of raw materials use. To achieve such ambitious changes, a bold economic shift is required. This primarily implies modifying the design of materials so they can fit into this future. Several economists have advanced the concept of a circular economy instead of the current linear one as a beneficial approach to follow.

The European Parliament recognizes the circular economy as: "a model of production and consumption, which involves sharing, leasing, reusing, repairing, refurbishing and recycling existing materials and products as long as possible. In this way, the life cycle of products is extended, including a reduction of waste to a minimum. When a product reaches the end of its life, all of its constituents are recycled and kept within the economy ideally forever. As a result, these can be productively used in a perpetual manner, thereby creating further value". The European Union's (EU) target is to build a circular and climate-neutral economy by 2050.

Given such a definition and ambitious goals, one can understand the pivotal role of materials

in this perspective. The circular economy will be inapplicable without advanced materials that sustain this model. More importantly, one cannot limit oneself to recycling but must consider all aspects, including sourcing more renewable materials, such as biomass waste and CO_2, and reducing energy consumption during production and use. In some of these aspects, fiber-reinforced polymers, or composites, are often seen as main assets thanks to their outstanding properties, particularly their lightweight. However, high-performance composites suffer from limited renewable sourcing and recycling options. The sustainability of current production and use of composite materials can be rightfully questioned.

As composites are composed of at least two distinct materials, they are much more complex than traditional metallic materials, and advancing their sustainability cannot be limited just to the selection of biobased building blocks or the investigation of recycling methods. Ideally, a comprehensive approach must be used to embrace all aspects of composite properties and ensure the results are transferable to the industry. Moreover, one cannot limit itself to sustainability assumptions, and an environmental assessment should support new developments in an ideal case. In this regard, natural fibers have been demonstrated as a relevant, sustainable alternative to unsustainable glass fibers in many applications. If the interest in natural fibers is established, the limitations of the resins remain. Indeed, composite matrices have been mainly developed over the last 70 years in conjunction with carbon and glass fibers and their sizing agents to optimize their properties. The usage of natural fibers (NF), whose physicochemical composition significantly differs from synthetic fibers, opens the door to new research opportunities through the exploration of new matrices specifically designed for such fibers.

2 Main objectives of the work

Natural fibers hold many promises to achieve sustainable composite materials. NF, such as flax or hemp, offer low environmental footprints, high mechanical properties, reasonable costs, and can be easily cultivated in Europe. Unlike synthetic fibers and most polymers, natural fibers are hydrophilic. This results in poor interfacial adhesion with most polymer matrices without specific treatments. Epoxy-amine thermosets, more polar than (unsaturated) polyesters and polyolefins, demonstrate a better affinity with NF, but the decommissioned composite must be landfilled or incinerated. Despite being more sustainable, NF composites remain not completely

applicable in the frame of a circular economy.

In this context, the EU financially supports various multidisciplinary and multicultural scientific projects, especially our Non-Isocyanate PolyUrethanes European Joint Doctorate (NIPU-EJD), with the general objective to progress on alternative polyurethane chemistries under the Horizon Europe program of Marie Skłodowska-Curie Actions (MSCA). Our project gathers twelve Early Stage Researchers (ESR) from seven academic partners, five industries, and one innovation center, to develop more sustainable polyurethanes and expand their range of applications. Polyurethanes are the sixth most-produced polymer, mainly used in foams, coatings, and adhesives. The main concerns with polyurethane rely on the sourcing of their building blocks from oil, the recycling challenges, and, more importantly, the toxicity of their isocyanate precursors. Isocyanates are subject to increasingly strict regulations in Europe and their future banishment due to their carcinogenicity, nephrotoxicity, and sensitizing effects. The main objective of our NIPU-EJD project is to develop isocyanate-free routes to polyurethanes by covering various aspects around traditional polyurethane materials and beyond within 12 individual ESR projects such as monomer synthesis from renewable resources, polymerization, self-blowing foams, adhesives & coatings, and recycling. My role was herein exploring the potential use of polyhydroxyurethanes (PHUs) in composites, mainly to replace epoxy resins when used with natural fiber, as they represent the most advanced class of NIPU.

Our main approach was based on the presence of pendant hydroxyl in the PHU backbone, offering several key features. In particular, the polarity of hydroxyurethanes is viewed as a potential asset to strengthen the fiber/matrix interface, thus increasing the mechanical properties of NFC. In addition to the potential for bio-CO_2 sourcing of PHUs, dynamic hydroxyurethane leverages novel recycling options for these resulting composites, such as mechanical recycling, welding, and reshaping. However, the current literature on PHUs does not yet support the effective design of matrices for composites.

A literature review (Chapter 1) was thereby performed to contextualize the current advancements in sustainable composites and their potential within a circular economy. The focus was on current composite solutions and the most promising emerging ones, considering the sourcing of fibers and matrices, the implications of material selection, and the impact of processing and recycling. The literature review enabled a multidisciplinary overview of the

market and research efforts to highlight the research gaps and market needs.

Given our hypothesis that PHU could be relevant, sustainable matrices for natural fiber composites, the present work aims to respond to the following questions:

- Can PHU or derivative chemistry be exploited for composites, property- and process-wise?
- Can H-bond strength, through macromolecular engineering, enhance the fiber/matrix interface, and consequently, does PHU offer the hypothesized enhanced properties?
- Are PHUs-based composites sustainable?

The first two questions are developed and addressed in Chapters 2 and 3, respectively. In answering the aforementioned questions, strategies to enhance the results are developed to advance PHU chemistry and resolve the identified drawbacks in Chapters 4 and 5, respectively. Finally, the last question is discussed in Chapter 6.

Chapter I

Sustainable structural fiber-reinforced polymers in the frame of a circular economy: a literature review

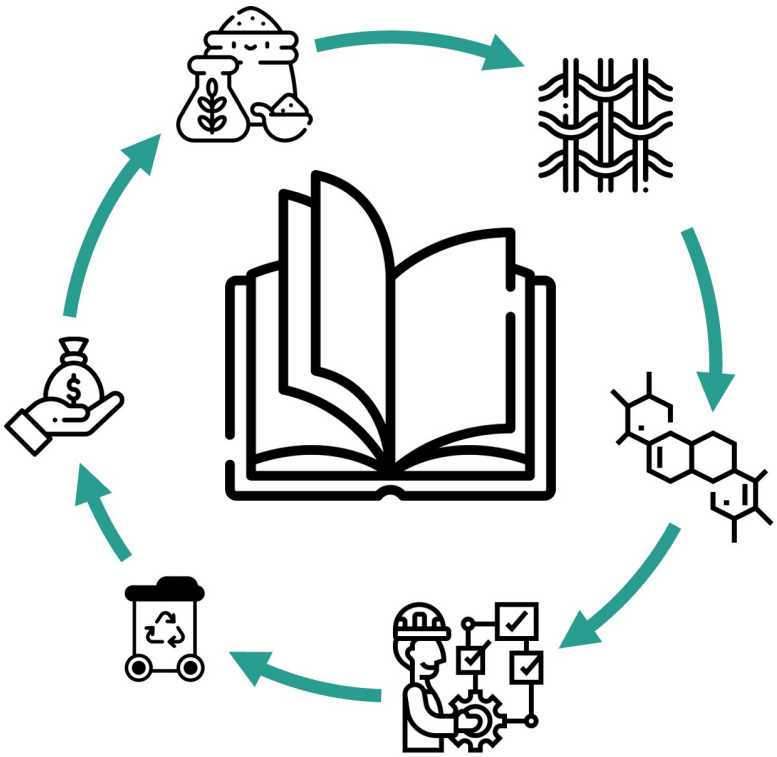

Adapted from: G. Seychal, G. Perli, A. Goldberg, H. Sardon, N. Aranburu, and J.M. Raquez, En route to the rational design of circular and sustainable structural fiber-reinforced polymers, *Submitted to Advanced Composites and Hybrid Materials.*
External contributions:*A.G. provided valuable comments and reference suggestions in the composite market and circular economy sections. G.P. provided valuable comments and suggestions in the matrix section and helped on Fig.1 (revised).*

Contents

I.1 Introduction

The first principle of thermodynamic laws states that energy cannot be created or destroyed in an isolated system. From a material perspective, A. Lavoisier, one of the fathers of modern chemistry, was attributed to the maxim: "Nothing is lost, nothing is created, everything is transformed". If the former deals with energy and the latter matters, one must admit that our actual mode of production and consumption of materials, ruled out by these fundamental paradigms, does not follow these principles. The additional entropy augmentation due to the irreversibility of our system forecasts a limit to the economic growth [1]. The (actual) linear production of materials consists of a series of value-added steps, consuming (fossil) energy and resources towards a final point of discarding, following a "make, use, dispose of" motto. This leads to the (definitive) loss of energy and matters in the ecosystem [2]. To pursue a more sustainable approach, both academia and industry must consider sourcing materials from renewable resources, including waste. They should prioritize the principles of "reduce, reuse, and recycle" in that order, focusing on eco-design to facilitate the integration of materials into a circular economy. [3].

The History of Mankind has always been intimately linked to materials. From stone to bronze, later to steel, the advances in materials science and technologies intensely followed humanity's evolution, alongside the access to dense and accessible energy [4]. The significant metallurgy progress on steel in the 18^{th} century, followed by aluminum in the 19^{th}, allowed new infrastructures and advances, to the extent of structures "heavier than air" to fly. One could say that we entered the era of plastic in the middle of the 20^{th} century. Although natural polymeric materials have been used for thousands of years, as old as ancient Egypt [5], it was in 1907 that Leo Baekeland developed the first synthetic polymers. Twelve years later, Nobel laureate Hermann Staudinger emitted the concept of macromolecules [6], opening the doors to unlimited advances in that field since then. The idea of reinforcing polymers with fillers, i.e., composite materials, concomitates with Baekaland's first works, using asbestos to reinforce his bakelite. However, it is the developments of glass fibers (first patent in 1880) and carbon fibers in the '50s [7], boosted by the world wars and Cold War, that brought a whole new kind of materials, able to overpass metallic structures: structural fiber-reinforced polymers (FRP) [8]. While metallic materials are inherently recyclable and relevant in a circular economy, their higher density has pushed toward their replacement by FRPs, but doing such has lead to a step back in recycling and circularity.

FRPs enabled exceptional strength-to-weight ratio materials with a wide range of properties at competitive costs. The developments in the last 50 years have seen substantial advances, and a deep understanding and mastery of knowledge and techniques have allowed significant gains in structure

performances. Tremendous efforts have been made to extend polymer matrices to various applications and markets depending on the manufacturer and end-user requirements, costs, and used fiber. Among them, unsaturated polyesters (UPR), epoxides (EP), and polyurethanes (PU) represent the vast majority of matrices in FRP [9], while glass fibers largely dominate the market. Nowadays, FRPs are seen as essential assets in a more sustainable future to diminish fuel consumption in transportation through weight savings, high-pressure vessels, renewable energy production equipment, and more [10].

Ultimately, the exponential growth of FRP use poses a significant challenge in the frame of a sustainable and circular economy. The production of fibers requires access to high quantities of energy at competitive costs. It also causes the depletion of non-renewable resources (sand and oil mainly) while releasing large amounts of greenhouse gases (GWP) in the atmosphere [11]. The production of matrices also requires significant amounts of energy and fossil resources and yields hazardous waste. Additionally, thermoset polymers are usually considered non-recyclable and cause downgraded composite structures to be lost in the ecosystem at their end-of-life (EoL), either through landfill or incineration, making the recirculation of their constituents in the economy unreachable so far [12]. Moreover, manufacturing composite parts generates a vast amount of additional waste [13]. The high embodied energy and environmental footprint prevent the true environmental benefits of using FRPs instead of conventional metallic structures to be effective [14]. The problems of the EoL arise nowadays with the first generations of large composite structures now reaching replacement time and the continuous growth of the composite market [9]. Major efforts are now put into improving the eco-design of FRPs in a frame of a circular economy through better sourcing of the building blocks, process evolution, and EoL scenarios.

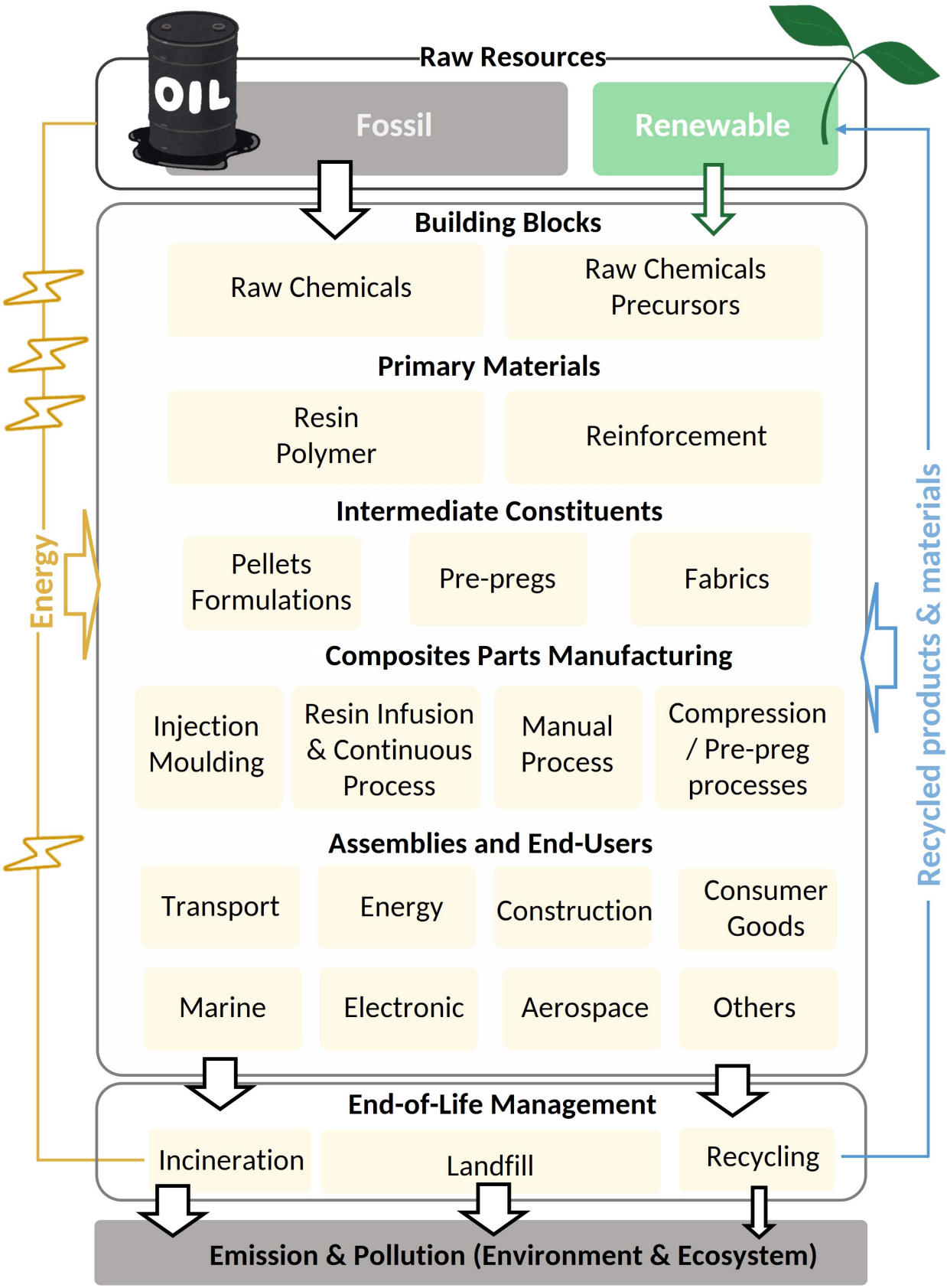

Figure I-1 – Schematic overview of the composite market value chain.

Exploring the sustainability of FRPs demands a wide range of scientific competencies, as there are numerous ways to tackle this subject. While new systems are quickly being developed in academic

laboratories, including bio-based polymers and dynamic networks [15,16], they often struggle to achieve a well-established and competitive maturity level. Implementing these innovations in an industry characterized by inertia and significant past investments is difficult, hindering the willingness to embrace disruptive changes [17,18]. Moreover, significant efforts are still needed to develop streamlined and economically viable pathways tailored to the existing FRP structures, including the recycling of "old" chemistry, such as UPR or EP. Reaching recyclable FRP that could embrace a circular economy requires mobilizing competencies and knowledge to address the complexity of FRP across various fields: organic chemistry (building blocks synthesis), polymer chemistry (polymerization and depolymerization), processing, materials science, and mechanical engineering. Addressing all the aspects of FRPs, between fibers and polymer matrices, from the sourcing of raw materials to the EoL, including production, processing, and supply chains, is essential to ensure the development of global and relevant solutions [10,19]. Circularity should be at the heart of eco-design for composites to ensure their seamless integration into a sustainable economy and a lasting future.

The future of circular economy for FRP lies in optimizing these technologies to balance environmental impact, cost-effectiveness, and material recovery rates. Progress in these areas will be crucial for reducing the overall carbon footprint of industries heavily reliant on composite materials. Achieving net-zero goals will force the composite sector to tackle sustainability challenges within its supply chain (see Fig.I-1). Until now, limited attention has been given to the role of chemistry in enhancing the sustainability of composites.

There are numerous reviews reviews discussing sustainable polymers [20], thermosets [21],epoxy resins [15],covalent adaptable networks [22], natural fibers [23], composites [24,25], and to some extent recycling [13,26–28]. However, to the author's best knowledge, none have provided a critical overview of the whole composite value chain, from sourcing to end-of-life, in a frame of a circular economy. In particular, the critical role of chemistry in composites, regarding its influence on processes, properties, and end-of-life considerations, must be discussed to a larger extent. Access to renewable feedstocks and monomers to design sustainable composites with advanced properties is critical.

This state-of-art aims to provide a multidisciplinary overview, with a priority on chemistry about the recent advances in the realm of structural composites for a future circular economy, while considering market needs and research developments. After briefly introducing the current composite market, the concept of circular economy, as applied to polymer chemistry and FRP, is discussed. The role, properties, and limitations of fiber reinforcements, as well as the pivotal role of matrices in the eco-design of FRP, are addressed. In the case of matrices, how sustainability has evolved over time will be discussed in

relation to each chemistry, from established ones to emerging ones, with a particular emphasis on emerging Non-Isocyanate Polyurethanes (NIPU), specifically poly(hydroxyurethane). This will include sourcing, scale-up, production, performances, end-of-life, and whenever possible the environmental, economic, societal, and industrial needs are also considered. Our work intends to provide an all-around overview and future perspective to, ultimately, reach truly sustainable structures in a durable and circular economy.

I.2 Current composite market situation, trends and needs

In 2023, around 13 Mt of composite materials were produced worldwide, valued at 41 bnUS$ [9]. When extended to composite manufactured parts, the market represents 105 bnUS$. The COVID-19 pandemic caused a slowdown in 2020-2021 of the composite market. However, it fully recovered and resumed its precedent growth trajectory in 2022, driven by various sectors such as construction, energy, and electronics. This growth was particularly notable in Asia (47% of the global volume), with China developing its renewable energy sector exponentially [9, 29, 30]. North America and Europe follow, with 26% and 19% of the market volume, respectively, focusing more on high-added-value applications like aerospace and transportation. The rising demand for renewable energy, electric vehicles, and hydrogen storage pushes forward the need for composite materials. Despite the ongoing global uncertainties that recently affected the market, including Covid-19 economic crisis, Boeing 737 max crashes, energy supply issues, and the wars in Ukraine and Middle-East, the market still forecasts a 5-10% compound annual growth rate (CAGR) up to 2030 [9]. For comparison, the global structural steel market represents 117 bnUS$ with a 5-6% CAGR, and the total aluminum market weight 162 bnUS$ with a projected 3-4% CAGR in the same period. The overall plastic (including FRP, thermosets, and thermoplastic) turnover in 2023 was estimated to be 624.8 bnUS$ with a projected 4% CAGR; the total volume is around 416 Mt. The global plastic trade mainly depends on single-use plastics (disposable) and commodity thermoplastic polymers such as polyethylene (PE), polypropylene (PP), polyvinyl chloride (PVC), polystyrene (PS), poly(ethylene-terephthalate) (PET), and polyurethane (PU, mostly thermosets) [31, 32]. More importantly, while FRPs represent only around 3% of the total plastic market volume, they account for around 16-20% of the total plastic market value. This makes FRPs a well-established key sector in structural materials and the global economy, yet a niche sector in the plastic industry.

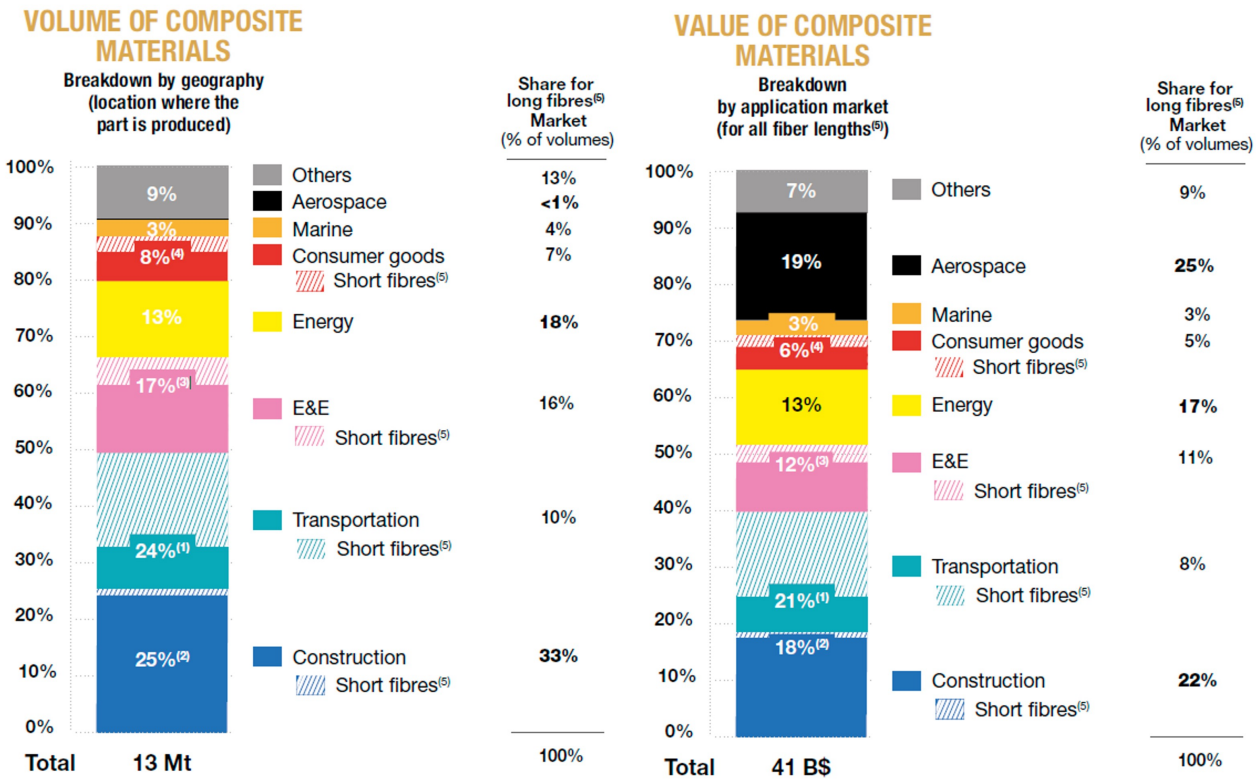

Figure I-2 – Composite market breakdown in 2023 in volume and value per application [9]. Copyright 2024 JEC. Long fiber relates to continuous, and short fiber to discontinuous.

The strict distinction in fibers for composite differentiates discontinuous and continuous fibers, with discontinuous being short (<1 mm) or long (> 1 mm). However, we consider the similarity in behavior and applications for all types of discontinuous fibers compared to continuous fibers, particularly for structural applications. Short fibers refer to discontinuous fibers in this work, and long fibers are deemed to continuous ones.

Construction (25%), transportation (24%), electronics (17%) and energy (13%) represent the largest segments of the market (see Fig. I-2). However, the requirements for these sectors are vastly different in terms of matrices (thermoset vs thermoplastic), fiber type (glass or other), and length. While the transportation sub-segment largely uses short fibers and thermoplastics (Glass/PA6, Glass/PP) to match production rates and cost requirements, the energy, electrics, marine, and aerospace sectors predominantly use long (continuous) fibers. Due to costs, equipment size, and property requirements, the energy sector (mostly wind turbine) primarly uses unsaturated polyester resin and long fibers. In general, the FRP market remains mainly dominated by glass fibers, short and long [9], representing more than 90% of the global volume (for 77% of the value) thanks to their competitive strength-to-price ratio. Natural fibers represent the second largest reinforcement, with 7-8% of the total volume and about 4% of the value. They are especially used in the transportation segment as short fiber reinforcements

due to their low cost, low density, damping properties, and environmental benefits. Conversely, the aerospace sector requires high-performance materials and prioritizes performance over cost, making the sector the first consumer of carbon fibers and epoxy. This translates into a 19% market share in value for only 1% of the market volume. Carbon fibers are approximately 14 times more expensive than glass fibers [33].

The long fiber-reinforced composite (LFRC) market is more nuanced and evenly shared than the global composite market. LFRC combines the strength of long fibers with the flexibility of polymer matrices, providing superior mechanical properties, reduced weight, and excellent corrosion resistance compared to traditional materials such as steel or aluminum [34]. The global LFRC market was valued at approximately 25–30 bnUS$ in 2023 and is projected to grow at a CAGR of 8-10%, potentially reaching USD 50–60 bnUS$ by 2030. Construction and energy (including electric & electronic) applications account for about 33% of the market each, with composites being used for infrastructure reinforcement, renovation, and building materials (rebars, beams...). Large-scale wind turbine blades are predominantly made of glass fiber composites [29]. Aerospace, marine, and transportation follow with 15-20% of the market, driven by the need for materials with high strength-to-weight ratios to improve fuel efficiency and reduce emissions. Glass fibers still account for 50–55% of global fiber use in structural composites, again due to their cost-effectiveness and good mechanical properties. Carbon fibers make up 25–30% of the market and are mainly used in aerospace and high-performance automotive sectors, sports, and leisure. In these applications, strength-to-weight ratios are crucial, making the higher costs of carbon fibers secondary. Aramid fibers contribute 5–7% of this fiber market, mainly used in applications requiring impact resistance, such as defense and aerospace. Meanwhile, natural fibers such as flax, hemp, and jute are gaining ground, representing about 5–10% of the fiber consumption, particularly in automotive and construction, in which eco-friendly solutions are in growing demand.

The market is evolving with the increasing use of carbon fiber composites for larger, more efficient blades in wind turbines or hydrogen storage, boosted by price reductions. Many efforts are being made to decrease the cost of carbon fiber, such as the technology developed by the Canoe Technology Centre, allowing an outstanding 40% cost reduction on carbon fiber (8€/kg in 2018) [7, 35]. Moreover, the extra costs related to metal corrosion boost the demand for composite in construction (including gas & oil pipelines). Recently, traditional metallic and cement-based bridges have been replaced by FRP-based structures, decreasing the need for maintenance, structural health monitoring, and heavy equipment (Smart Circular Bridges project, Flax pedestrian bridge by FiberCore and TU/e, Almere, The

Netherlands). Besides, natural fibers are quickly expanding as a sustainable alternative to glass fibers. Thermosetting resins like epoxy, polyester, and vinyl ester account for 80–85% of the LFRC market due to their higher affinity with the fibers and inherent stability. Thermoplastics, including polyamide, polypropylene, and PEEK become increasingly popular due to their recyclability and toughness, representing 15–20% of the market, but face severe limitations related to their processability [36]. Higher process temperature and pressure are usually required to melt the thermoplastic and allow the shaping and welding of the laminate, generating further CO_2 emissions. Additionally, the wetting of fibers with thermoplastic is challenging, limiting the exploitation of the full fiber potential [37].

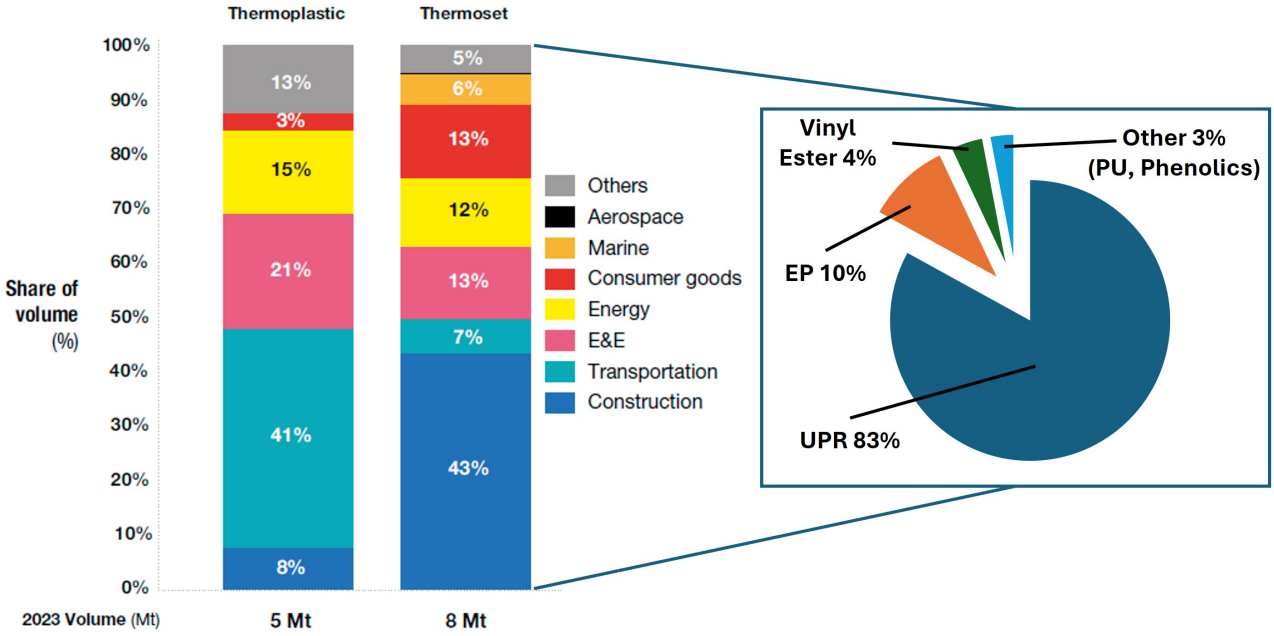

Figure I-3 – Resin market breakdown for composite by applications [9, 38]. JEC Copyright

Thermoset polymers remain the preferred matrices for composites, representing 60% of the market (see Fig. I-3). They offer good stability over time, are required for long service life, have easier tooling and lower energy than thermoplastic, and are more versatile to adjust properties and constituents in various markets [39]. Among them, unsaturated polyesters (UPR) possess the largest market share, with 83% of the total of thermosets used, followed by epoxy (10%), vinyl ester (4%), and others (polyurethanes, phenolics, bismaleides, polyimides...). The strong domination of UPR is due to their low cost, low viscosity (simplifying processes and giving access to large-scale structures), and versatility. However, their poor environmental stability, fire resistance, and mechanical properties make the epoxy more relevant in demanding applications [9, 40].

Thermoplastics (TP) matrices have seen significant growth over the last decades to stabilize to around 40% of the market volume [9]. Thermoplastics are mainly considered for their recyclability,

flexibility, and cost-effectiveness, particularly in automotive (41%) and electronics (21%). As discussed earlier, the vast majority of these thermoplastics are in combination with short glass and natural fiber in order to improve their properties at lower cost [36].

The choice of thermoset or thermoplastic matrices and the related chemistry remain strongly dependent on the targeted applications and, therefore, certain requirements. The most significant limiting parameters are mainly cost and properties. They influence all the steps of the industry, from sourcing to the manufacturing process and final application [41]. Thermosets are preferred for long fiber structural applications because of their effectiveness in wetting the fiber and their durability. Thermoplastic-based materials are ideal choices for low-cost, mass, and high-speed production.

The choice of composite constituents affects not only the final properties and total costs but also the manufacturing process [42]. The manufacturing process also plays a key role in the possible attainable properties, costs, and final applications. For instance, manual processes, such as hand lay-up, pre-preg, and thermo-compression, have lost their dominant position due to the high labor cost engaged, requiring numerous highly qualified workers. Their market share decreased from 52% in 2018 to 35% in 2023 [9]. Conversely, fast and automated processes have experienced rapid growth. Injection molding, which uses short fibers, now represents 40% of the composite market (Fig. I-4) due to the extensive increase in thermoplastic use and continues to be a growing field. The share of injection molding was only 13% in 2018 [9]. For thermosets, out-of-autoclaves are the most promising processes [43] as they offer faster production rates, less energy, and less labor. Out-of-autoclave includes continuous processes (pultrusion, pull-winding, continuous sheet, filament winding...), and infusion processes (resin transfer molding, liquid infusion...). They represent 25% of the market, with a 5-10% predicted CAGR up to 2030 [9].

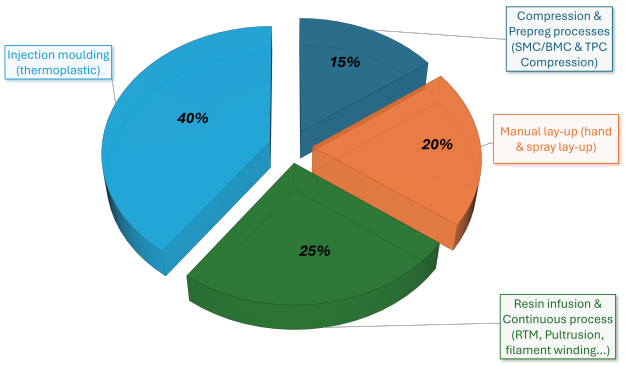

Figure I-4 – Composite manufacturing processes - market breakdown 2023, data from [9].

As previously seen, the main difficulty in obtaining sustainable material is its large portfolio of solutions that make each material distinct and, somehow, unique. This results in a highly diversified

market with extremely complex EoL management. To date, there is no unique solution, and EoL remains the least developed part of the composite value chain [27]. Only a few actors have actively offered solutions to recover and valorize decommissioned composite structures. Although many SMEs and start-ups are flourishing in that segment, they remain underdeveloped and not fully suited to the current market needs. Currently, EoL primarily involves landfill incineration (with or without energy recovery) and grinding for downgraded use (cement fillers, clinker, composite filler, etc.). Progress in developing standards and integration of recycled materials will be essential for market growth. [10, 30]. Nowadays, only 4 countries worldwide (Germany, Finland, The Netherlands, and Austria) have legislated on composite EoL to ban landfills and encourage recycling [44], but still tolerate some exceptions due to the lack of reliable solutions.

In the coming years, the LFRC market is expected to continue its strong growth trajectory, fueled by technological advancements in material processing, increasing demand for lightweight and durable materials, and the push toward sustainability. Improvements in thermoplastic composites, recycling technologies, and automation in manufacturing are likely to further propel this market, making LFRCs more cost-effective and accessible across a wider range of industries.

I.3 Sustainable structural materials in the frame of a circular economy

I.3.1 About the concept of circular economy

In a linear economy, the current model, an economic value, is created during the extraction of resources and increases through the subsequent production/transformation steps into manufactured goods and their final consumption by end-users. The value of goods becomes negative once they are discarded as waste (see Fig.I-5) [2].

Since the latter half of the 20^{th} century, many economists have identified some issues with the current economic model. The economist K.E. Boulding introduced the idea of an (economic) isolated system, by analogy to thermodynamics. In what he called the "spaceship Earth," resources are not unlimited and should be considered as capital stock. To ensure the spaceship's future, the main goal of the inhabitants should be to maintain this capital, i.e., preserving the resources [45]. The economist N. Georgescu, who pioneered the concept of "ecological economics" [1], more precisely formulated the deep connection between the economic model and thermodynamics. As the economy is deeply dependent on

energy and matter transformation and consumption, Georgescu suggested visualizing the economic sphere as a system that will reach maximum entropy; and human activities accelerating this process. Accordingly, he proposed the terminology of "low-entropy" for renewable resources and "high-entropy" for waste and pollution. In other terms, for Georgescu, low-entropy is transformed irreversibly into high entropy. Because such a pathway is irreversible, the resources are scarce (over humanity's time frame).

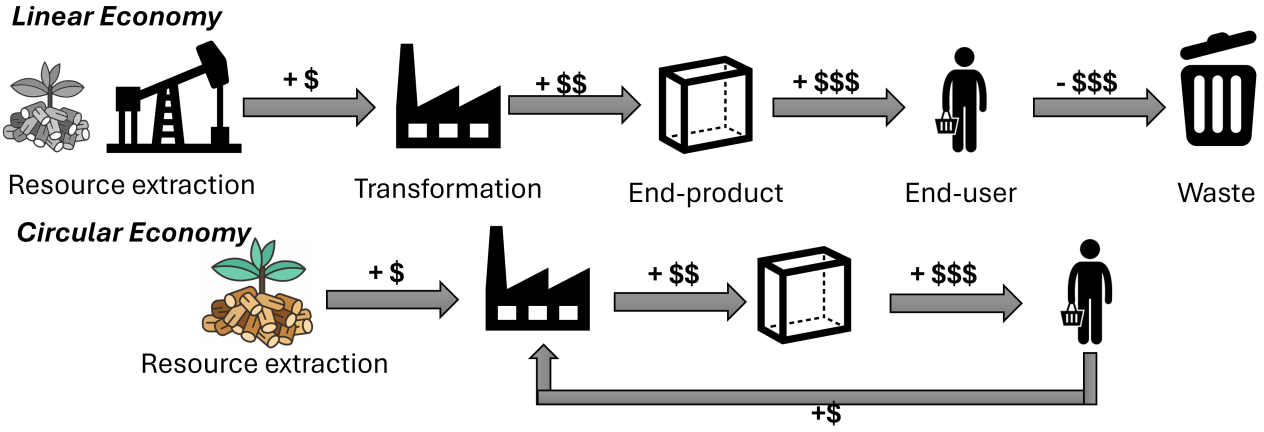

Figure I-5 – Simplified overview of an idealized linear and circular economy value chain.

Later, the concept of circular economy was formally introduced by Pearce and Turner [46]. The limits of the continuous exploitation of finite resources and the increasing waste production were exposed. They proposed, to tackle that problem, to re-incorporate end-of-life products as raw resources for new materials production, referred to as cradle-to-cradle, creating a closed-loop economy. Importantly, they stated out that the main goals were to reduce waste and build more resilient systems. Unlike the linear economy's "make, use, dispose", the circular economy first relies on the 3R's "reduce, reuse, recycle", i.e. firstly by mitigating the consumption of goods, secondly, extending the service life, and finally processing materials to recover their components/constituents. The 3R concept finally grew to 10Rs, as summarized in Fig. I-6. In a so-called circular economy, matter and energy are no longer deemed as an irreversible flow but rather as an isolated system with a finite amount of resources preventing their depletion. Later, architect R.B. Fuller defended the concept that waste "is nothing but resources we are not harvesting because we have been ignorant of their value" [47], which is particularly relevant to the composite industry.

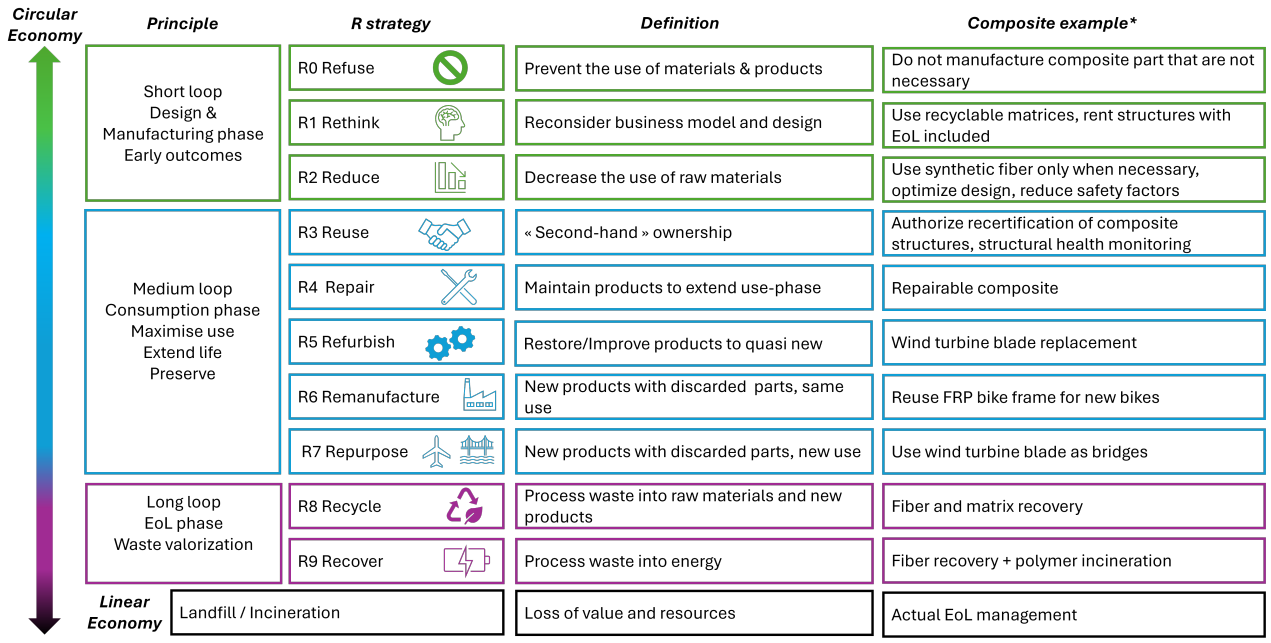

Figure I-6 – 10Rs strategies in the frame of an idealized circular economy. *Representative examples are given and might not be legally or economically viable.

In 2017, Kirchherr et al. [48] identified 114 different definitions of circular economy and proposed a unified definition: "circular economy describes an economic system that is based on business models which replace the 'end-of-life' concept with reducing, alternatively reusing, recycling and recovering materials in production/distribution and consumption processes, thus operating at the micro level (products, companies, consumers), meso-level (eco-industrial parks) and macro-level (city, region, nation and beyond), with the aim to accomplish sustainable development, which implies creating environmental quality, economic prosperity, and social equity, to the benefit of current and future generations."

It is clear how important materials and energy streams are in this context and the role that chemistry and the chemical industry can play in the realm. More specifically, composite materials, particularly made of glass fibers and carbon fibers, should be designed to fit the requirements of a circular economy. This includes the design of polymeric matrices able to be repaired, recycled, and depolymerized, with the view to ideally retrieving both fibers and matrix or monomers. The main goal should be to transform large composite waste into resources and valuable compounds [2]. They should be conceived to fulfill this definition and help designers and engineers achieve the full recirculation of waste.

From the above definition, materials embedding the principle of circular economy must fulfill the following:

- Sourcing from renewable resources: biomass, by-products, post-consumer waste...
- Limit energy consumption at all stages
- Be easily repairable to extend its service life
- Be able to be easily deconstructed and separated from the entire structure
- Be able to be repurposed to a new function
- Ultimately be able to be recycled
- Avoid the use or release of toxic and hazardous compounds

I.3.2 Materials in circular economy, from lab concept to market reality

The current global economic system is intricate, involving numerous actors, i.e., public institutions, governments, and industries at different scales (local, regional, and international). Therefore, to globalize a circular economy, it is essential to engage both States and governments as well as companies and industries.

The rising awareness of environmental challenges has significantly increased our insights about the recycling of materials, its economy, and the associated challenges [47]. The United Nations is pushing towards goals such as net zero carbon. Stricter environmental regulations [17], along with treaties promoting and regulating trades, encourage the reuse and recycling of materials and wastes [49, 50]. Although the current efforts are still insufficient, there is a consensus on the need for cooperation toward a global circular economy [4]. Industries should adopt a business model where the economic system mimics Nature, with flourishing interdependent actors [3]. However, such an ecosystem must be encouraged and supported by strong policies [47, 49].

Only few countries have already engaged programs to promote a circular economic system. China has widely invested and legislated to support the industrial recycling of by-products and waste. They created circular economy industrial parks that saved 14 million tons of GWP in 2016 [17,49]. Economical simulation plans trillions of dollars of savings if these strategies are extended nationwide [17]. Pushed to an extreme, the Club of Rome projected in a multiple-case scenario [51] from 6 European countries (Finland, France, the Netherlands, Spain, and Sweden) that shifting to a circular economy through energy efficiency, material efficiency, and renewable sourcing would cut carbon emission up to 70% with 1.5-2% increase in the Gross National Income (GNP) and reduce unemployment by nearly a third. It is

clear that the change from our current linear business model to a circular one is a monumental challenge with significant risks for the private sector. This would include the establishement of long-term common strategies among different actors, creating interdependence that can be beneficial but also present risks for investors [50, 52]. This is the reason why it requires strong support from the government through financial support, tax incentives, and regulations [49].

Implementing global circular strategies for materials would lead to substantial economic and environmental benefits but also secure supplies for industries [47]; including high-demand sectors, such as aeronautics. As an example, aircraft engine manufacturer Rolls-Royce developed the Revert program [47]. Aircraft engines require high-quality and high-performance alloys (so-called superalloys), based on titanium and/or nickel, including some minor elements like vanadium, rhenium, and cadmium [53]. The Revert program allowed Rolls-Royce to secure the supply chain by recovering alloys from production waste, dismantling decommissioned turbines, and sending back sorted alloys to their supplier. By doing such, the supplier has easier and guaranteed access to low-cost "raw" materials, while Rolls Royce secured aero-grade alloys at a lower cost. Around 60-70 jobs have been created while increasing the profits of Rolls-Royce and its business partners as well as lowering the environmental footprints of their products [47]. Other successful examples include carpet manufacturer Desso, which recovers old carpets from customers to recycle [3] or tire manufacturer Michelin, which rents transporter truck tires by the mile [2].

In polymer chemistry, recirculating carbon offer significant environmental benefits [19] as well as economic gains through the creation of local employment [2] and the value maximization at each stage. Recycled plastics are generally cheaper even though common recycling technologies (mainly thermo-mechanical) lead to a reduction of their properties [54]. Many studies have demonstrated the interest in sourcing chemicals from renewable feedstocks, in particular, C1-chemicals, to promote a circular carbon and plastic economy [19, 55]. Vidal et al. [19] proposed a bold system change to align with GIEC recommendation and limit CO_2eq emissions [56] by proposing the "full" recirculation of "carbon". They highlighted that recycling alone cannot sufficiently reduce emissions but also estimated that renewable feedstocks as raw materials cannot be the sole source; carbon capture and utilization (CCU) [57] must be developed to provide new building blocks. Renewable and cheap energy remains a crucial parameter, along with population sensitivity to such issues. In addition, smarter design of polymer-based materials is essential, particularly by maximizing service lifespan and recoverability. By doing so, they estimate 85-90% of CO_2 savings in construction sectors, a major consumer of composite materials.

I.3.3 Complexity and strength of the specialized composite market, can composite enter a circular economy

Both energy and matter are vital to material sciences, even more so to composites. Up to now, the recovery of energy, or matter, from polymers and composites is still to be addressed. According to the current situation, the composite market is inherently linear and unsustainable. Efforts must be made to recirculate the large amounts of waste in this sector. In particular, these wastes still possess an important value, embodied energy, and potential that are highly relevant for a more circular economy.

Each year, an exponential number of composite structures are decommissioned with limited recycling possibilities, mostly ending up in landfills. Even whether some interesting works have been performed in the academic literature to tackle this problem [13] (see section I.7), to the author's best knowledge, the full circular ecosystem of composite does not yet exist. Only a handful of start-up companies started to develop such strategies by developing the recycling of carbon or glass fibers and the valorization of these recovered fibers (Composite Recycling, Switzerland; Nova Carbon, France), a few years ago. Other focus on repairable composites to extend service life (CompPair, Switzerland), new resins (Mallinda Inc, USA; Recyclamine, India), and sustainable fibers (EcoTechnilin, France; Bcomp, Switzerland; Isomatex, Belgium).

However, the potential for structural composites to lead high-performance materials in a circular economy remains uncertain. Unlike commodity (single-use) plastics, structural composites are designed with dedicated processes to have long service life (>20 years), and specialized actors that can gather and recycle more efficiently as aforementioned [58]. Composite materials are primarily used in high-performance technical applications, such as transportation (aeronautics, naval...), sports and leisure, or construction [9]. These sectors are characterized by the complexity of their products and their high-performance requirements, where materials must not only meet strict safety standards and be optimized for weight, durability, and cost. The complexity of these industries has a direct influence on the sourcing and manufacturing of composites, challenging the recycling of these materials [29, 59]. The development of custom-tailored solutions, such as thermal, chemical, and mechanical recycling methods, to handle the different fibers and matrices used in composites is required. Such approaches must also integrate new design philosophies, such as modularity and disassembly, to enable easier repair, reuse, and recycling. However, their specificity limits the number of actors and ensures continuity between suppliers and clients, making the recovery of decommissioned structures easier than that of consumer goods, as exemplified by the Rolls-Royce initiative for aeronautics alloys.

There is still a challenge in conciliating performances, durability, and end-of-life. Composites'

presence in aircraft, like those from Boeing or Airbus, has substantially increased over these years, and their eventual decommissioning constitutes a significant challenge. As a result, the circular economy in aerospace must focus on optimizing disassembly and reusability, which can only be achieved through highly specialized, market-driven recycling methods [13, 35].

Similarly, in the wind energy sector, the extensive use of fiber-reinforced composites in turbine blades and the need for wind turbines to operate efficiently over 20–25 years has spurred innovation in composite materials. Yet, the complexity of recycling these blades at their EoL, given their size and multi-material compositions, requires a tailored approach [29, 30]. Wind turbine blades are a prime example regarding the complexity of the demand for specialized composites, as decommissioned blades must be recycled in ways that ensure they remain profitable for reuse or repurposing in new applications [33]. Despite the challenge, 90% of wind turbine mass is already recyclable/recycled from the metallic components, making the process of disassembly and sorting already efficient. Several millions of tons of composite materials will need to be recycled from wind blades in the coming years [60]. In response, new recycling methods are being explored to more efficiently separate fibers and matrices, with processes like thermal and mechanical recycling being considered for different types of composites [30]. Recycling strategies are increasingly being integrated into digital platforms that optimize the reuse of materials, reducing waste and improving resource efficiency [61].

Other market sectors for composites, such as construction and transportation, that represent a non-negligible part of the market volume could benefit from this high-value market, promoting sustainability and close-loop recycling in composites. However, due to the specialized nature of these markets, circular economy strategies cannot adopt a one-size-fits-all approach. As already observed by Vidal et al. for all polymers [19], multiple parallel and complementary pathways must be developed to preserve and recirculate resource capital.

The composite sector highlights the need for adaptable and complementary circular economy strategies. The materials must perform at peak levels during their service life, while their end-of-life management requires market-driven solutions that address their unique characteristics and preserve their value (Fig. I-7). In that sense, fibers, matrix, and their interactions should be advanced and selected to best suit the circularity concepts.

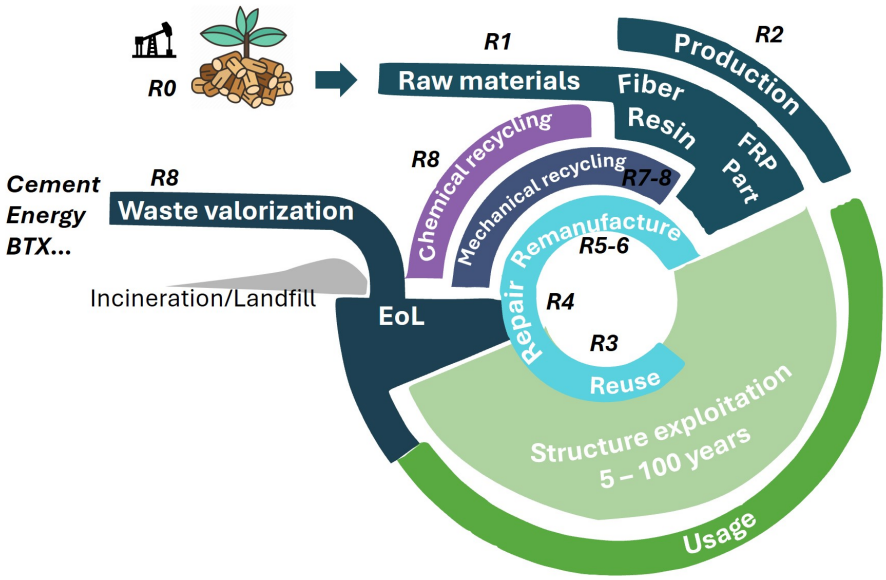

Figure I-7 – Implementation of the R's into the composite economy, a figure inspired from [10].

I.4 Fibers and Reinforcements - Drivers for properties and environmental footprint

Structural composite properties are largely determined by the fibrous reinforcement, which commonly represents 60-80% of the total mass. The type of fibers imparts the main properties of these composites as well as their costs and environmental impacts.

I.4.1 Glass fibers - The unsustainable market volume

As previously seen, glass fibers widely dominate the FRP market. Their excellent strength-to-weight ratio, resistance to environmental degradation, and cost-effectiveness make them materials of choice in many applications. However, several challenges can arise with the use of glass fibers that must be addressed in the frame of a circular economy.

I.4.1.1 Sourcing & production

Glass fibers are silica-rich amorphous materials with several grades of glass fibers available depending on the final requirements (see next section). All grades possess a high silicon dioxide content (SiO_2), which constitutes 50-70% of the total composition and is responsible for the final product's mechanical strength and thermal properties. The composition is completed with other additives such as lime (calcium oxide, CaO_3), dolomite (calcium-magnesium carbonate $CaMg(CO_3)_2$), and alumina (kaolin,

Al_2O_3) as network modifiers and alternate networks formers to adjust the properties [62]. Minor oxides such as boron oxide (B_2O_3), magnesium oxide (MgO), or alkali oxide (Na, K) can also be included to enhance specific properties, such as thermal resistance or corrosion resistance, and facilitate fiberization. Although glass fiber grades meet certain content specifications, each manufacturer possesses its own (patented) recipes, making a generalization and complete circularity complex as compositions might vary from supplier to supplier.

Glass fibers are produced in an uninterrupted continuous process to limit costly pre-heating and maximize production rates (see Fig. I-8). The raw materials are kept in separate batches before being mixed in the desired composition. The homogeneous batches are first melted and vitrified at about 1500-1800°C to become glass. A second refinement step is performed at 1100-1300°C. The molten glass is then extruded through a bushing into filaments [63]. This step is critical as it determines the diameter of the fibers, which ranges from 5 to 24 μm. The molten filaments are rapidly cooled and solidified by water spraying (or air jets), forming continuous glass filaments. At this stage, chemical sizing agents (generally water-based) are applied; this can also include a thin protective coating. The sizing agents reduce the abrasion of the equipment used to process the fibers (waiving, chopping...), protect the fibers, and enhance the adhesion with the future matrix. Typical sizings include silanes, epoxy-based compounds, and polyurethanes, which are tailored to the resin type (e.g., polyester, epoxy, or vinyl ester) used as the matrix in the final composite. A supplementary thermal step is commonly applied to cure and stabilize the sizing [63]. Finally, the continuous glass fibers are processed in desired forms (chopped, rovings, yarns, mat...). Rovings (continuous strands) are commonly used in structural composites, while mats and chopped strands are employed in applications where flexibility and moldability are important, such as in automotive or marine parts.

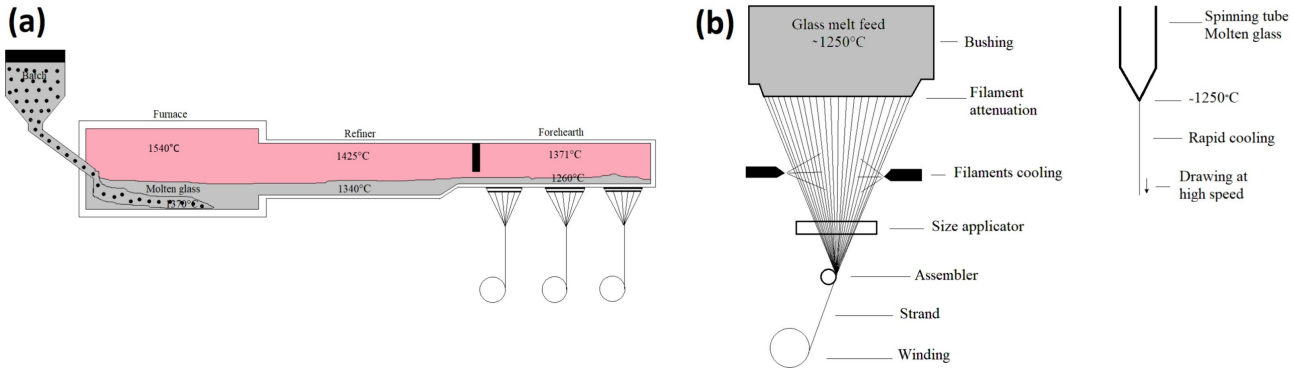

Figure I-8 – Schematic representation of glass fiber production. a) vitrification of glass in furnace, and b) GF continuous filament forming process. Reprinted from [25] Copyright 2024, with permission from Elsevier.

I.4.1.2 Properties, advantages and limits, applications

Various types of glass fibers can be produced, each with distinct compositions and mechanical properties. A-glass (Alkali-) is the oldest glass fiber type with a composition similar to glassware and lower properties than other types. They are mainly used in low-reinforcement and insulation applications [64]. E-glass (Electrical-) is the most widely used glass fiber type, known for its high tensile strength, cost-effectiveness, and suitability for general-purpose applications. E-glass is composed mainly of silicon oxide, alumina, and calcium oxide. S-glass (Structural-) fibers have higher tensile strength and modulus compared to E-glass, making them ideal for high-performance applications such as aerospace and defense. S-glass has fewer impurities (more controlled composition) than E-glass, with magnesium oxide used instead of calcium to bring more strength and stiffness (20-40 wt%). However, their compositions present more elevated melt viscosity requiring higher energy inputs and more scarce and pure raw materials. This makes S-glass fibers more expensive and environmentally impactful [25, 65]. Other glass fiber grades such as C-glass (Chemical-), AR-glass (Alkali-Resistant-), and D-glass (Dielectric-) exist for specific applications but represent a small volume and will not be discussed further. All glass fibers possess a pure elastic brittle behavior, with tensile strengths ranging from 2000-4500 MPa, modulus in the range 70-90 GPa, and 4-6% of elongation at break. Compared to other structural fibers, they have a relatively high density, between 2.4-2.6 g/cm^3, making them too heavy for some lightweight applications [66]. Except for specific grades, glass fibers are sensitive to strong oxidative, acids, alkalines, and salty environments and possesses a large operating temperature range, between -50 and 300 °C [66].

Table I-1 – Overview of reinforcement properties and eco-environmental impacts range (typical values), *Indicate approximation (old data or extrapolation), the negative GWP of NF was accounted to 0.5 for relative properties calculus.

Material			Carbon Fiber (HS)	Carbon Fiber (HM)	E-Glass	S-Glass	Basalt	Flax (elementary)	Hemp (bundle)
Absolute properties	Density	$g.cm^{-3}$	1.80	1.90	2.57	2.53	2.6-2.8	1.53-1.56	1.4-1.6
	Tensile Modulus	GPa	200-300 (250)	350-600 (500)	70-76 (72)	80-90 (85)	90-100 (92)	30-70 (53)	15-40 (28)
	Tensile Strength	MPa	4000-6000 (4800)	3000-5000 (4000)	3300-3700 (3400)	4300-4900 (4500)	3100–5000 (4800)	600-1500 (970)	300-1100 (800)
	Elongation at break	%	1.0-2.0 (1.8)	0.4-1.5 (1.2)	4.0-5.0 (4.8)	4.0-6.0 (5.2)	3.1-6.0 (4.5)	1.6-3.6 (2.15)	0.8-3.3 (2.3)
	Embodied Energy	$MJ.kg^{-1}$	100-1500 (1170)	500-1500 (1450*)	30-50 (44)	30-50 (54)	12-52 (24)	3-10 (4.4)	3-10* (4.4*)
	GWP	$kgCO_2eq.kg^{-1}$	30-80 (72)	50-100 (85*)	2.65	3.14	0.02-1.0 (0.955)	-1.4 (0.5)	-1.4* (0.5)
	Cost	$€.kg^{-1}$	25-50 (35)	50-130 (65*)	1.1–2.8 (1.8)	2.0-3.5 (3.3)	2.5-3.0 (3.0)	6-10 (9.08)	0.5-10* (9.08*)
Specific properties	Specific modulus	$GPa/g.cm^{-3}$	139	263	28	34	35	35	20
	Specific tensile strength	$MPa/g.cm^{-3}$	2700	2100	1320	1779	1811	634	571
EcoImpact	Modulus/(GWP*Density)	$GPa/kgCO_2eq.kg^{-1}g.m^{-3}$	2	3	11	11	35	70	40
	Strength/(GWP*Density)	$MPa/kgCO_2eq.kg^{-1}g.m^{-3}$	37	25	500	566	1897	1268	1143
	Modulus/(Cost*Density)	$GPa/€.kg^{-1}.m^{-3}$	4	4	16	10	11	4	2
	Strength/(Cost*Density)	$MPa/€.kg^{-1}.m^{-3}$	76	32	735	539	604	70	63
References			[33, 67–69]	[33, 67–69]	[62–64, 70–72]	[62–64, 70–72]	[70, 72–75]	[23, 76, 77]	[23, 76–78]

I.4.1.3 Environmental footprint & values for recycling

The extraction of raw materials for glass fiber production raises environmental concerns, especially regarding silica and limestone mining. Sand mining is widely recognized as a major ecological issue [79]. Sand is required in massive quantities for construction, resulting in overconsumption that surpasses natural renewal rates [80] and augments the pressure on the mined ecosystems through water depletion, landscape destruction, wildlife habitat destruction, and pollutant emission [81]. Additionally, during the production process, high-energy inputs are required to melt and extrude the glass fibers. The embodied energy of glass fibers is typically around 25-50 MJ/kg [71, 82], with associated CO_2 emissions at around 3-5 kgCO_2eq/kg. Typical furnaces use natural gas, which emits large quantities of greenhouse gases, including nitrogen oxides, carbon monoxide, dioxide, methane, and traces of other gas and particulate matter [83]. Sustainable practices in raw material sourcing have become a priority for most industry leaders. Strategies include developing mining protocols that reduce landscape impact and actively sourcing from regions with stricter environmental regulations [81, 84] and higher-quality ore deposits to reduce processing requirements. However, the lack of transparency in the protocols implemented by industries, along with economic interests, limits the ability to achieve truly sustainable practices.

Most efforts toward sustainable glass fiber production focus on reducing emissions, conserving raw materials, and improving energy efficiency throughout the production process. In particular, the advances in more efficient electrical furnaces, that can be alimented by renewable energies, allowed substantial energy savings and emissions reductions [71]. Moreover, the integration of digital monitoring and AI-driven control in furnace operations offers potential improvements in terms of yield and energy management [85]. Despite all the good practices that can be taken, the pressure on sand stocks may remain. In this regard, recirculating glass fibers can reduce the environmental burden of glass production [86] and secure feedstock supply to limit any eventual future costs. Techniques such as closed-loop recycling of cullet (broken or waste glass) back into the melting process could reduce the need for virgin materials and lower furnace energy requirements. Equally, recovering glass fibers from composites and re-melting could provide sustainable sourcing for glass fiber producers [87].

Additionally, research into bio-based, environmentally friendly sizings and low-emission binders might help the industry to shift towards more economically viable, sustainable pathways. The key challenge is to balance the demand for higher-performance fibers while aligning sustainability goals and maintaining competitive costs. With continued investment in sustainable practices, glass fiber production for composites is poised to meet the growing demand for lightweight, durable materials

across diverse sectors, including automotive, aerospace, and renewable energy.

Given the increasing demand for glass fibers in the wind turbine and transportation sectors, it is essential to find more eco-friendly replacements and alternatives to alleviate market pressure. This includes developing advanced recycling methods and exploring new materials that can offer similar or superior performance with a lower environmental footprint.

I.4.2 Basalt fibers, a potential direct replacement of glass fibers

Basalt fibers (BF) are mineral fibers obtained from fused volcanic rocks. Some authors classify BFs as natural fibers (from minerals), as they require much less human intervention than glass fibers. Basalt is a major constituent of the oceanic and continental crusts [88]. It is widely available worldwide and is considered as a largely accessible and renewable resource. Indeed, large quantities of basalt are generated each year due to volcanic activity. BFs were originally developed in the 50s in the Soviet Union (Moscow Research Institute of Glass and Plastic), mainly for military, spatial, and aerospace applications [89]. For this reason, the majority of the production and use remains nowadays concentrated in Russia, Ukraine, Germany, and China. However, new actors from the United States and Europe are now developing BFs as a potential alternative to glass fibers. While the glass fiber market represents nearly 30 bnUS$, the basalt fiber market is estimated to be 0.27 bnUS$.

I.4.2.1 Sourcing & Production of basalt fibers

BFs are deemed a viable and greener alternative to glass fibers, with similar properties [65]. Most BFs are obtained from the direct melting and fiberization of basalt ores. Similarly to glass fibers, basalt is mainly constituted of SiO_2 (40-55%), with high content of Al_2O_3, Fe_2O_3, MgO, and CaO [90]. The composition of BF depends on the sourcing of the basalt ores. In that sense, some ores and basalt grades are not suitable for continuous filament processing. In particular, some (crystalline) minerals such as olivine or biotite nucleate the crystallization of the cooling basalt melt, making the fiberization impossible due to fiber breaking during the spinning [91]. Specific care must be taken in the composition of the basalt ores. This could lead to the over-exploitation of basalt quarries, leading to environmental and landscape destruction. Some recent works and companies (as an example, FILAVA® from Isomatex S.A., Belgium) analyzed their basaltic ores to better control their compositions and thus their properties. This could enable the achievement of a more evenly distributed exploitation of basalt sources worldwide and the development of a new economy for structural materials [92].

Interestingly, the basalt fiber manufacturing process does not differ much from glass fibers, but

the overall process is considered slightly cheaper and less energy-intensive [93]. Knowledge transfer, equipment adaptations, and market development could benefit from that with no major investment or detrimental modifications compared to existing glass fiber plants. Basalt rocks are crushed and washed before getting loaded into furnaces. As the basalt already possesses terminal composition, a metering system is not required [88]. The raw materials are melted at 1400-1500°C and extruded into 10-20 μm fibers through a continuous spinning process. The cooling must be performed adequately to avoid any crystal nucleation, being detrimental to the fiber properties [91]. Similarly to glass fibers, sizing agents are required to protect the fibers, limit abrasion of equipment, and improve the fiber/matrix adhesion.

I.4.2.2 Properties, advantages, and modifications to move from glass fiber production to basalt fibers

BF are attractive for structural composite applications due to their high strength, corrosion resistance, and thermal stability. They are more expensive than E-glass, but the expected developments of the market and technologies, driven by high demand, are expected to lower basalt fiber costs to a similar level to glass fibers [73, 89]. They display properties similar to S-glass fibers with tensile strengths between 3000 and 4900 MPa and an elastic modulus ranging from 80 up to 100 GPa, but lower costs [72]. Interestingly, the elongation remains relatively high, ranging between 3 and 6%, which make them tougher than carbon fibers. BFs perform well under extreme temperatures and resist chemical degradation. They are more resistant to alkaline and acidic conditions [73] than glass fibers and possess a broader operative window starting from low temperatures (-200 °C) up to high temperatures (+700°C). On the contrary, glass fibers are more susceptible to chemically aggressive media and cannot sustain temperatures higher than 300-400 °C before considerably losing their mechanical properties [90]. However, they are slightly denser than glass fibers, with a density between 2.5 and 2.8 g/cm^3 (compated to 2.4-2.6 g/cm^3 fo GFs). In contrast to asbestos, another natural mineral fiber, BFs are completely inert and do not release any harmful compound [65, 72], being compliant with REACH regulations. They have an expected lifetime of 50 years, longer than glass fibers, which could further enhance the durability of structures [70]. When properly manufactured and sized, BF exhibits excellent adhesion properties with various resins, improving composite matrix integration and leading to improved load-bearing capabilities and longevity of the composite structures [94, 95].

Such inherently excellent properties position BF as a strong alternative to traditional glass fibers and a cost-effective option compared to carbon fibers. They are suitable for high-temperature applications in aerospace, automotive, and fire-resistant construction materials. They can be exploited in corrosive

environments, such as concrete reinforcement in construction and infrastructure applications. This combination of heat resistance, mechanical strength, and chemical durability makes basalt a more sustainable, reliable, and direct alternative to glass fibers. Despite the promising and growing interest, the development of the basalt fiber industry remains limited, with ongoing technical difficulties in ensuring consistent supply. Future work should focus on better control of the properties through composition and processes and optimization of the fiber-matrix interface. Specific care should be taken to ensure benefits for a circular economy and environment through job creation while avoiding the replication of glass fiber issues, such as the impact of sand extraction.

I.4.2.3 Environmental footprint & values for recycling

The environmental footprint of basalt fiber composites has been poorly investigated [75]. This could be understood from the currently low usage volume, and this point must be more extensively investigated in the future. In particular, the sourcing of basalt ores should be considered in terms of environmental burdens along with transportation.Recent works [74] have highlighted that basalt fiber bars (epoxy resin matrix) could lead to a reduction of up to 44% of the carbon footprint compared to similar glass fiber bars and a 50 to 89% reduction compared to galvanized and stainless steel respectively. The major contributor to the LCA of basalt fiber remains the energy required to melt and process the basalt ores [96]. The advances performed for glass fibers, using electrical furnaces with high efficiency and renewable energy, could also help reduce the environmental footprint of BFs further. Utilizing sun or wind-based electricity, available worldwide, basalt could be competitively produced on-site, reducing transportation needs and supporting local economies, contributing to the UN Sustainable Development Goals [81]. Importantly, the high thermal and chemical resistance of BF could be of high interest in pyrolysis and chemical recycling processes to retrieve the fiber, allowing it to separate from the matrix and reuse these fibers in a state similar to the virgin ones.

I.4.3 Carbon fibers, high structural performance but poor environmental footprint

Although carbon fibers comprise a minor share of the composite market, they represent non-negligible values and an even less negligible contribution to composites' environmental footprint. They are used for highly demanding applications where cost is secondary to performances.

I.4.3.1 Sourcing & production

Carbon fibers (CF) were initially developed out of the carbonization of cellulose fibers in the US during the early 50s [7]. However, the most advanced materials were obtained from the development of acrylic-based fibers. In particular, the key stabilization of polyacrylonitrile (PAN) discovered by serendipity by Shindo and industrially developed by Toray from the end of the 50s in Japan led to continuous developments since then [7]. Today, PAN-based CFs now represent 90% of CFs, with the remainder being pitch-based and rayon (viscose). PAN is obtained from the free radical polymerization of acrylonitrile in an inert atmosphere with other monomers such as styrene, butadiene, or vinyl acetate. The thermoplastic is then transformed into a filament by wet spinning using dimethylformamide (DMF) as solvent. Acrylonitrile is obtained from propylene through the SOHIO's process (see Fig. I-9). Pitch offers a more straightforward sourcing as it is a by-product of the coal industry and can also be bio-derived [97]. Mesophase pitch can be melt-spun to obtain primary fibers that can be later transformed into CF. However, pitch-based CFs do not match the PAN-based properties (see the section below) [98]. The final sourcing is rayon fibers (Lyocell and viscose fibers) obtained from regenerated cellulose [99].

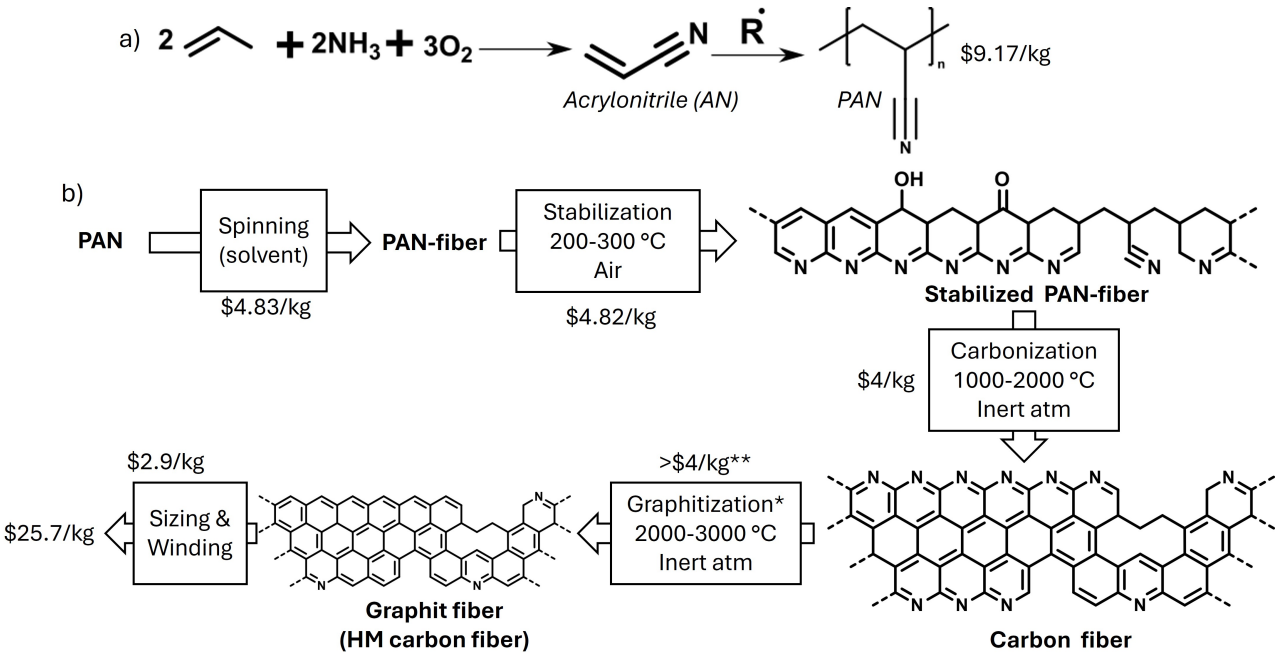

Figure I-9 – Representation of the most common pathway to obtain carbon fiber. a) Acrylonitrile synthesis by SOHIO process and PAN polymerization, b) carbon fiber manufacturing process and representative macromolecular structures. Prices are taken from [100]. *Graphitization is optional, **no data available.

In all cases, the overall process to yield CF remains consistent. The raw materials are first spun into

fibers, typically using solvents (DMF) or mechanically through dry spinning. They are then stabilized, gradually oxidized to 350°C, and finally carbonized. Carbonization is usually performed through step heating between 400 and 1600 °C. For high-modulus (HM) CF, an additional graphitization stage is performed at temperatures between 2500°C and 3500°C [101]. Surface treatment (plasma, oxidation) is generally performed to enhance the grafting of sizing agents (as for glass and basalt fibers). Finally, the continuous CFs are winded into tows, tapes, or any other reinforcement shape.

I.4.3.2 Properties, advantages and limits, applications

Inherently, CFs are highly aromatic and crystalline carbon-based materials (carbon content $> 92\%$). The high covalent energy of C=C bonds (145 kJ/mol) due to their aromatic nature results in outstanding properties. However, the process and the raw materials significantly influence the microstructure of the materials and, as a consequence, their properties. The understanding of the role of copolymerization in improving the oxidation/stabilization of PAN has led to the development of high-performance fibers after carbonization [102]. PAN-based CFs consist of highly ordered crystalline-oriented carbon layers, with amorphous regions structuring the networks and allowing efficient stress transfer between the regions, creating a "nano-carbon reinforced carbon" [103]. The crystalline domains are more refined, with less spatial separation between crystalline domains in PAN-CFs than in pitch-CFs, resulting in superior mechanical properties [104]. The defects at the surface act as crack nucleation sites, reducing the overall properties. In that sense, outstanding properties were achieved through the precise control of the microstructure together with the efforts in processing defect-free fibers, reaching 8 GPa of tensile strength for the Toray® T1200, with improved fracture toughness. Standard carbon fibers have modulus ranging from 200-500 GPa, with tensile strengths between 3 and 6 GPa. However, CFs remain brittle with low elongation (0.5-1.5%), requiring high-security coefficients and over-dimensioning CF structures to prevent catastrophic failure. Interestingly, advances in molecular dynamics [105] along with experimental works [7], such as using carbon nanotubes to nucleate the fibers crystals, forecast continuous improvements. Perspectives towards reducing the fiber size, thus defects size also predict future enhancement of CF properties [106]. These improvements could benefit other raw materials, such as pitch or lignin, to extend the portfolio of carbon fiber solutions through a better nanostructure control [103]. Along with the improvement in the engineering design of carbon laminates, CFs display a bright future for ultralightweight structures, but the sustainability of such structures must be considered (see Fig. I-10).

I.4.3.3 Environmental footprint, sustainability & values for recycling

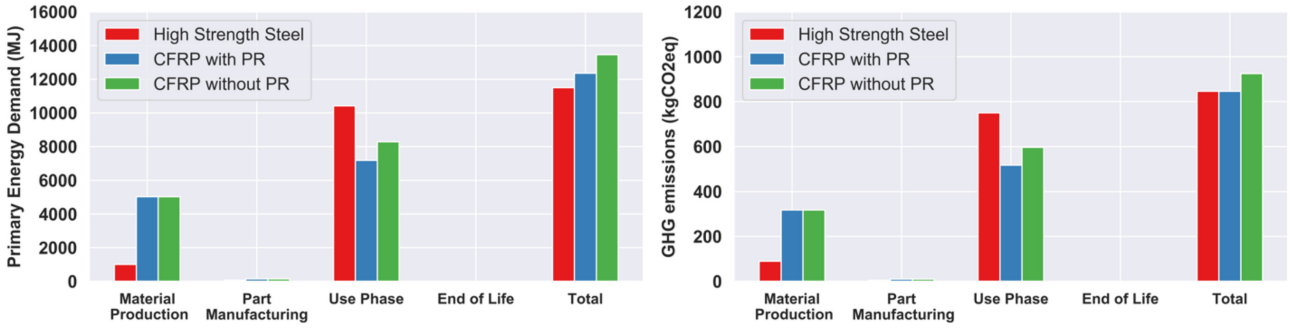

Figure I-10 – Primary energy demand (left panel) and GWP emissions (right panel) for steel and CFRP components with and without powertrain resizing (PR) with 50% secondary mass savings. Reproduced with permission from [107].

The general manufacturing process of CFs is not sustainable. In addition, the production of PAN and its monomers contribute to a substantial part of the CFs' footprints. In addition to their impactful fossil sourcing, PAN monomers are widely recognized as highly hazardous, posing problems in terms of waste, emissions, and workers' safety. Among structural materials, CFs possess the highest embodied energy and environmental footprint [68], as shown in Table I-1. Even if the weight savings in the total life cycle demonstrate the benefits of using CFs over common structural materials such as steel or aluminum [11,68], they yet do not align with net zero goals [108]. More efforts towards greener CFs are currently being made, from sourcing raw materials to processing the fibers. Producers predominantly focus on advances in process efficiency through higher energy efficiency, renewable energies, and carbon compensation. Main actors such as Toray, Hexcel, or Mitsubishi have set different goals. Hexcel targets a 30% GWP reduction by 2030, while Toray plans to become carbon neutral by 2050. Mitsubishi had the most ambitious roadmap, with its KAITEKI program in 2021 aiming to achieve carbon neutrality by 2023 and carbon positivity by 2030 [109]. They reported a 26% reduction in GHG emissions in 2022. Since then, their carbon neutrality objectives have been reviewed, but no clear date is currently set. In general, producers do not share extensive data about the sustainability advances of carbon fibers.

Other exploration routes investigated by academic researchers are being emerged, like the CO_2-sourcing of PAN [57], by utilizing algal carbon capture. In this process, algae are transformed into glycerol (and bio-diesel), methanol, propylene, and, ultimately, acrylonitrile. The authors performed a techno-economic study that showed the viability of the process, even at pilot scales. The environmental benefits were seemingly improved compared to traditional PAN synthesis routes.

Other works focus on new precursors for CFs, such as cellulose or lignins. Cellulose was one of

the original precursors of CFs; now, a small quantity of CFs is produced from regenerated cellulose, which has a more controlled composition. However, the properties of these CFs do not compete with PAN-based CFs [7]. Regarding the regenerated cellulose, rayon fibers such as viscose or Lyocell® have a poor environmental footprint. Viscose requires carbon disulfide, a highly toxic gas, in addition to hazardous solvents and the generation of large amounts of wastewater [99].

The most promising route, so far, comes from lignin [110]. After cellulose, lignin is the second most abundant organic material. Vast amounts of waste lignins are produced each year as a by-product of the wood and paper industry, with limited exploitation of its value. This makes it a relevant material for the circular economy through the use and recirculation of waste streams. Up to date, several pioneering works have demonstrated the possibility of obtaining CFs from lignin, usually with a copolymer (such as polyurethanes) to facilitate the spinning and stabilization of lignin [111]. Although not competitive with PAN, satisfactory properties were obtained, with modulus ranging from 40-80 GPa, strengths up to 1000 MPa, and elongation between 0.5 and 1.4% [98]. Importantly, LCA demonstrated lower environmental footprints of lignin-based CFRP than PAN [68, 110, 112]. Depending on the process, GWP reduction between 20 and 60% were estimated, along with lower energy consumptions.

Beyond their sourcing, the high embodied energy of carbon fibers makes them highly interesting for recycling to lower environmental impacts. Their high stability and mechanical properties forecast the potential of CFs for being reused in new applications while maintaining high performances. Although various recycling processes exist (as discussed later on), and should be adapted to the samples to be recycled (including the polymer matrix), the recovery and reuse/repurpose of carbon fibers seems to be consistently beneficial [27, 113, 114], and economically viable [115].

I.4.4 Natural fibers - The sole fully sustainable fiber for composites

Natural fibers are likely the oldest reinforcement in human history; for instance, straws were used to reinforce brick houses tens of thousands of years ago [116]. More recent examples date back to the first half of the 20th century, with the pioneering work of De Bruyne for aircraft structures [117]. During WWII, due to supply shortages, kraft paper/phenolic resins were used to replace aluminum in bombers. In 1941, Henry Ford, facing steel shortages, manufactured the conceptual "Soybean Car" made from natural fibers (Hemp & Ramie) and plastics partly made of soybean oil (among others) [118]. However, the project remains at the prototype stage. As noted in section I.2, NF currently represents 8-10% of the composite market. However, they are mostly employed as discontinuous (short) fibers and fillers. Since the early 21st century, driven by increasing environmental awareness, significant efforts have

been deployed to master NF properties and extend their use in load-bearing applications.

I.4.4.1 Sourcing and production

Natural fibers come from a wide variety of sources, including various plants (such as flax, bamboo, kenaf, etc.) and different parts of these plants (bast, straw, seed, leaf, etc.), (see Fig. I-11). Such diversity results in varying crop requirements, extraction methods, and main properties. In all cases, and unlike synthetic fibers, the length of NFs is limited by the finite size of the plants. One advantage of NF is the potential for locally sourcing natural fibers, depending on the crops available in a region (e.g., ramie in China, jute in India, and kenaf in sub-Saharan Africa...). For structural applications, bast fibers (flax, hemp, nettle, etc.) are typically the ideal candidates as they are rapidly grown and have well-known, established extraction pathways, including advantageous mechanical properties. So far, flax has been the most investigated fiber due to its broad (commercial) availability and superior properties, with hemp also emerging as a strong candidate. To simplify the readership, flax and, to a lesser extent, hemp will be primarily discussed, although other promising natural fiber exists [23].

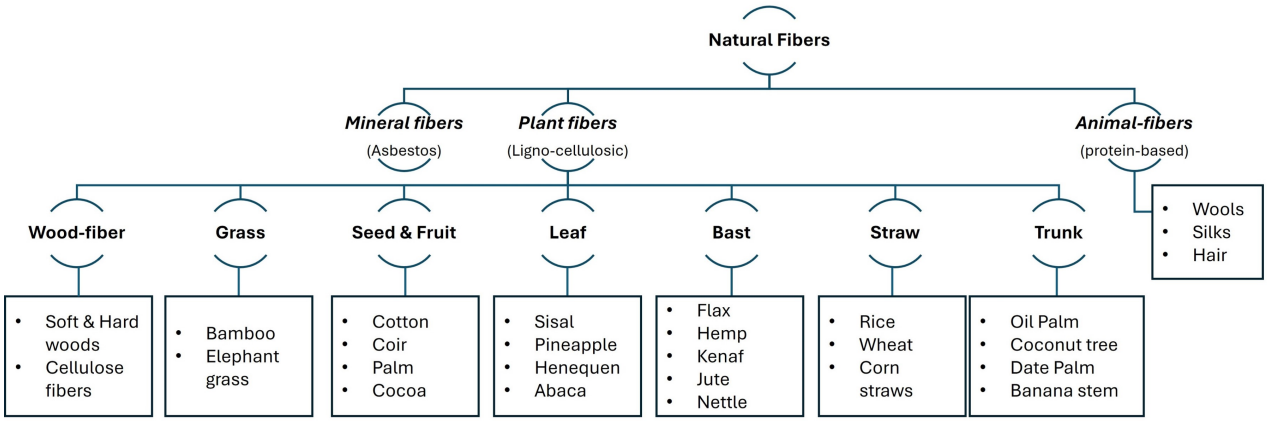

Figure I-11 – Classification of natural fibers.

Currently, Europe (France, Belgium, Netherlands) is the leading producer of flax fibers, representing two-thirds of the world's production [23]. A complete value chain that benefits textile know-how exists (specifically in Europe) and explains the rapid adoption of flax for composite over other fibers.

Significant work has been performed [119] to optimize fiber quality, properties, and economic outcomes through the careful selection of flax varieties, growth conditions, and extraction techniques. Natural fiber production can be divided into the following main stages: seeding, growth phase, harvesting (including retting), and finally, fiber extraction [23]. At each stage, various parameters influence the future properties and economic values of the fibers. Before seeding, a variety selection is

needed in accordance with the growing location and condition. Interestingly, different varieties do not significantly change the properties of elementary fiber [120]. Despite height differences, oleaginous flax and textile flax displayed similar properties, allowing for the complete valorization of flax products and their integration into a circular economy. However, this should be carefully handled as lignification of the fiber occurs during the production of the seeds, complexifying the fiber extraction process. The seeding rate plays a crucial role in future properties [119]; a high seeding rate (>1800 plants/m^2) yields thinner flax stems with lower mechanical properties due to the competition between plants. On the other hand, a low seeding rate (<1200 plants/m^2) decreases the areal fiber production, thus reducing the economic returns.

The growth stage, from seeding to harvesting, also affects the fibers' properties. As the plant naturally grows, flax (and hemp) goes through several stages: germination, growth, flowering, seed formation, and aging [119]. Climate conditions (e.g. drought, precipitation, temperatures) strongly affect the development of the plants and, consequently, the fiber properties. Drought affects the morphology and chemical compositions of the plants. Surprisingly, it has a negligible impact on the mechanical properties of the elementary fibers [121]. However, the yields were reduced, leading to variations in incomes for farmers and fluctuations in composite material prices. Hemp shows similar growth stage to flax. However, the stem tends to be longer (about 1 m for flax, 2 m for hemp), with faster growth, greater versatility in soil types, and lower requirements in fertilizers [78].

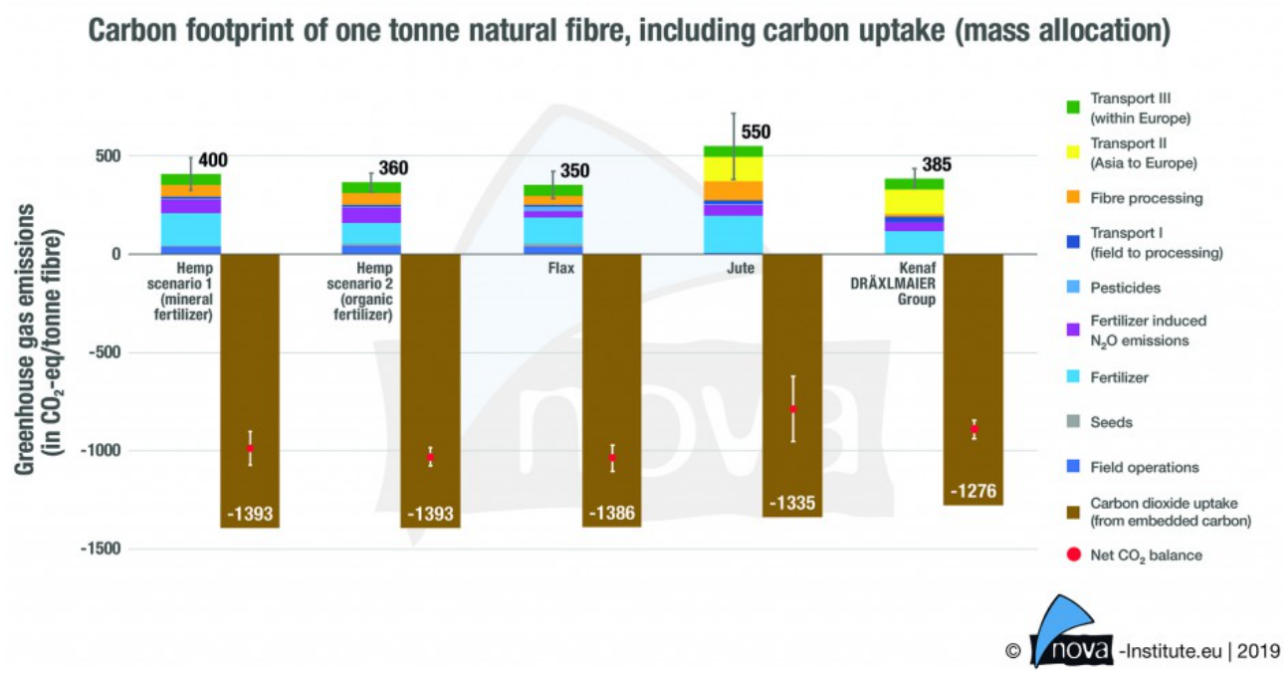

Figure I-12 – Greenhouse gas emissions per tonne of natural fiber and carbon storage by photosynthesis. Copyright 2019 Nova-Institute.eu [122].

Once the plants reach sufficiently advanced maturity, they are harvested. This includes uprooting, retting, and rolling. The most critical stage is retting, which involves fungi and microbial organisms degrading lignins and binding components by enzymes. Retting eases future fiber extraction by separating the wood from the fibers and increases the mechanical properties [123]. Retting can be performed in the open air, in the field of production (dew retting), or in a water bath with enzymes and chemicals (wet retting). Wet retting, the oldest technique is more controlled than dew retting but was progressively banned (in Europe in particular) due to the large amount of wastewater and pollution involved [23]. Dew retting is now the preferred method to obtain flax and hemp fibers. It allows the easy separation of the technical fibers from the other components, but it must be perfectly controlled. Under-retting results into higher energy input and potential damage to the fiber during the extraction, while over-retting will downgrade the fiber's properties through the degradation of the fiber cell walls [123].

Finally, the flax stems are scutched to extract the structural fibers. Proper fiber separation is critical to obtain homogeneous fiber impregnation in subsequent composite manufacturing [124]. The scutching yields long fibers, short fibers, and shives, all of them being differently valorized. An additional step, hackling, can be performed to refine the flax fiber quality. Once scutched (or hackled) fibers are obtained, they can be processed to obtain reinforcement through spinning, weaving, or unidirectional tapes.

From seeding to harvesting, these stages are also critical in the environmental footprint of natural fiber in terms of land use, eutrophication, and water consumption and wastewater generation [76], (see Fig. I-12). The energy required for seeding and harvesting is also accounted for. Scutching and hackling are major energy consumers in the production stages. Hackling is particularly energy-consuming but optional. Some works highlighted the low interest in hackle flax for composite applications, given its environmental costs [76].

I.4.4.2 Natural fibers as key materials in a circular economy

NFs, being inherently biobased, are widely regarded as sustainable materials. Up to now, the sustainability of NFs and their resulting composite materials can vary. As mentioned in the section I.4.4.1, the environmental footprint of NFs depends on the plant species, growing conditions, and treatment process. Flax and hemp are particularly promising as they require less water and fertilizers than other crops [116]. As a comparison, 600 to 1000 L of water is necessary to produce 1 kg of flax when the consumption for 1 kg of cotton is estimated to be 7000-29000 L [76]. Using fertilizers and

pesticides increases the eutrophication of water and should be limited to a minimum. Replacing GFRP by NFCs in case studies with similar mechanical performances demonstrated substantial gains in most sustainable metrics (except land use and eutrophication) [76, 86, 125]. However, it is somewhat unclear how the destruction of ecosystems and landscapes by sand extraction (glass fiber) is deemed, which could further favor NFs. The embodied energy of flax fibers is estimated to be around 10 times lower than glass fibers (4.4 vs 45 MJ/kg) [76]. From an economic viewpoint, flax benefits crop rotation and boost farmers' revenues. However, the use of flax use in composites is limited by competition with feed crops and textile use.

Hemp could further decrease the environmental burden of composites. Hemp is even considered more sustainable than flax as it requires less water and does not need fertilizers or pesticides [78]. The greater variety of hemp strains makes them adaptable to more climates, allowing hemp to be more accessible for global implementation. Hemp plants are taller than flax (2-4 m vs 1-2 m), resulting in higher fiber yield. In addition, different hemp parts can be valorized through multiple uses and markets (including pharmaceuticals) to ensure the full exploitation of its value and competitive cost of its fibers [78]. However, hemp fibers are less developed than flax ones, and further developments are still needed. Other fibers, such as nettle [126], could also provide sustainable alternatives without competition for arable land.

I.4.4.3 Properties, advantages, and limits to their applications

Natural fibers are characterized by a complex ultrastructure that generates intricate behaviors and challenges in the design of natural fiber composites (NFC) [127]. They are highly anisotropic [23]. More importantly, the plant type greatly affects the chemical composition (lignin, cellulose contents), cellulose crystallinity fraction, and morphological structure (microfibrillar angle, cross-section shape), thus affecting the final mechanical behavior. The ultrastructure of plant fiber is shown in Fig. I-13.

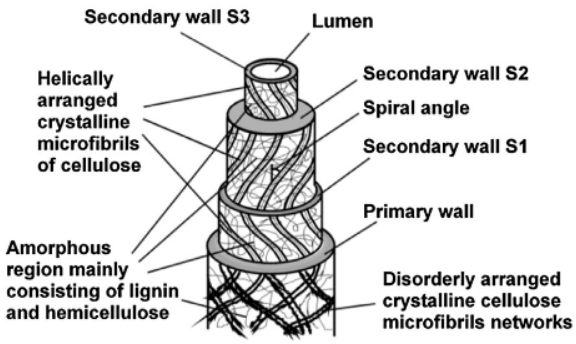

Figure I-13 – Ultrastructure of a natural vegetable fiber cell, in which the secondary wall S2 makes up to 80% of the total thickness and thus acts as the main load bearing component. Reproduced with permission from [128].

While cellulose crystallinity is crucial for providing strength and stiffness to the fiber, the microfibrillar angle (MFA) also plays a critical role. MFA represents the relative angle between the constitutive cellulose microfibrils and the fiber on its own. To improve the mechanical properties of NFs, the MFA must be as close as possible to 0°, allowing the cellulose microfibrils to bear loads in their preferential directions. Typical MFA for flax range 2-7° [129] while hemp range 7-11° [23], with both 60-90% of cellulose (of which 60-70% crystalline). As a comparison, cotton possesses a higher content of cellulose (82-98%, including crystalline one) but a higher MFA (15-25°), resulting in a lower modulus (5-13 GPa).

As the mechanical properties of NF vary upon plant species, Baley et al. [23] proposed a hierarchization to simplify NF selection for composite design, as represented in Fig. I-14. With a modulus ranging 30-70 GPa (average 53 GPa) and strength of around 1000 MPa, flax is usually considered to have the best mechanical properties, followed by ramie and alfa fibers [23, 120]. Hemp presents slightly lower mechanical properties (around 20-45 GPa in modulus and 800 MPa in strength), but the recent progress in the processing of hemp fibers, driven by European-funded programs (H2020 and CBE-JU, Ssuchy project) has shown promising results using hemp reinforcement [130]. While glass, basalt, and carbon fiber behave like pure linear elastic materials with a brittle behavior, natural fibers notably possess a non-linear visco-elasto-plastic behavior [131, 132]. This visco-elastic behavior gives NFC better damping properties than synthetic fiber composites and metallic materials [133], which is an advantage in some applications requiring insulation and vibration damping. A bilinear behavior (with two apparent moduli, E1 and E2) is typical in tensile loading. A stiffening effect, reported for flax [134] and hemp [131], exists when subjected to repeated load. Although well known, its pure origin is still debated in the scientific community but is mainly attributed to the MFA reorientation under

load [132, 134, 135].

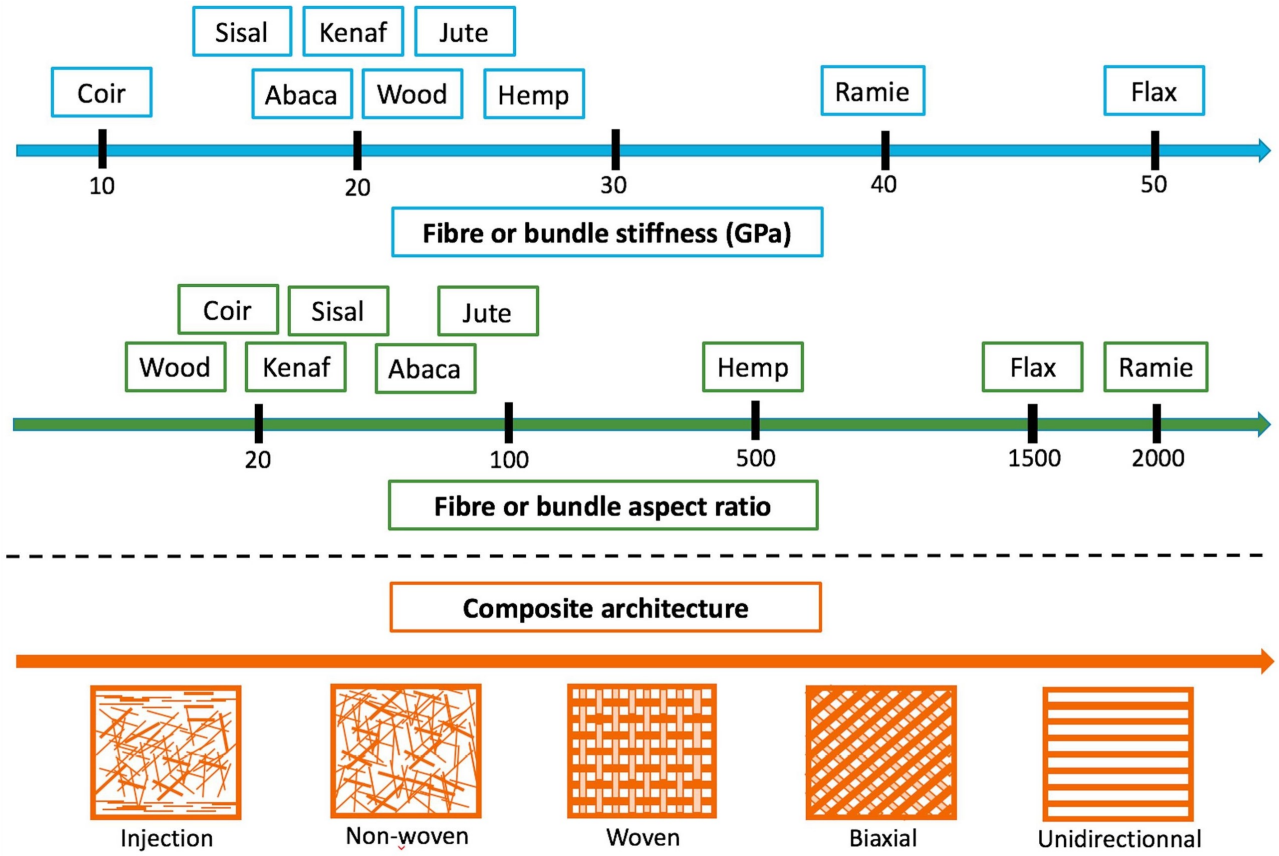

Figure I-14 – Panorama of plant reinforcement's mechanical or morphological specificity and composite's architecture diversity. Reproduced with permission from [23].

Although the mechanical properties are significantly lower than those of glass fibers, their specific properties (i.e., relative to density) are competitive [136]. Specific properties are commonly used metrics for designing sustainable structures as they directly relate to the strength (or stiffness)-to-weight ratio. In the frame of a circular economy, other metrics should be considered in the design of materials, such as the strength-to-GWP ratio or embodied energy/GWP-related metrics [71]. To help such design, Shah proposed an Ashby approach for composite, including specific properties (see Fig. I-15, and eco-impact related to processes (see Section I.6). The normalization of mechanical properties to eco-impact data is given in Table I-1.

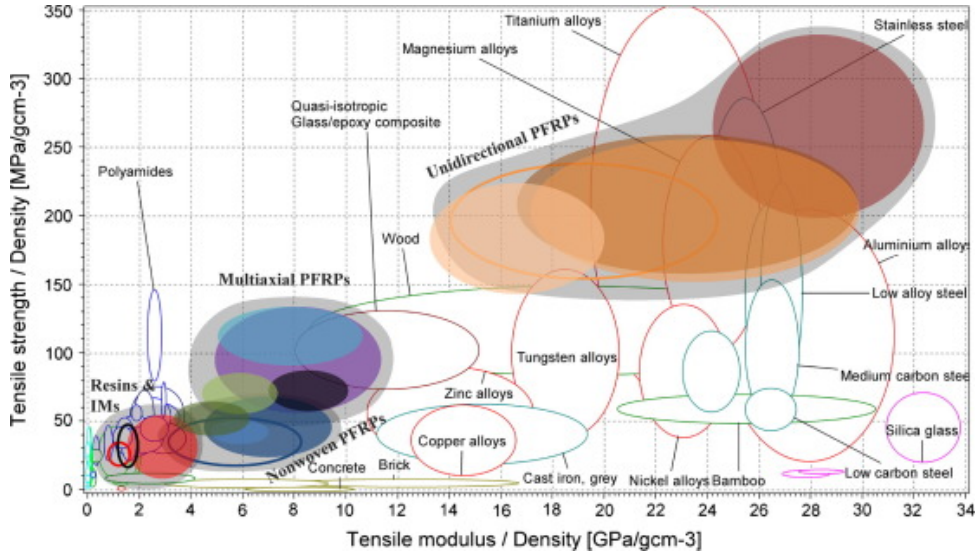

Figure I-15 – Ashby plot comparing the specific tensile modulus and specific tensile strength of NFC (filled balloons) with various other engineering materials (unfilled balloons). Reproduced with permission from [137].

Some specific behaviors and properties of NFs further influence the design of structural natural fibers. The organic composition of natural fibers, primarily consisting of carbon and oxygen from sugar-based cellulose, hemicellulose, along with aromatic lignin, makes them susceptible to fire. [138]. Additionally, their thermal stability is lower than that of synthetic fibers, as their degradation starts at temperatures above 200°C [139, 140]. NFs are generally considered for applications under temperatures below 100°C [141]. Additionally, the high number of hydroxyl functions makes them sensitive to moisture, leading to undesirable weight gains, fiber swelling, and some plasticization effects [142]. However, in the case of flax, it was shown that moisture saturation did not reduce the fiber tensile strength or fatigue properties in the longitudinal direction [143] but decreased the stiffness. Moisture can also significantly reduce the transverse properties through the weakening of the interfacial strength [144]. Hydrothermal and hygrothermal aging, particularly cyclic processes, can significantly degrade both static and fatigue properties. This was attributed to composition changes within the fiber but, more importantly, to the cyclic swelling of the fibers that generate cracks within the matrix (whose swelling is much less pronounced than NF) and the debonding of the fiber-matrix interface (Fig. I-16). These factors should be considered when designing natural fiber composites, including the importance of fiber-matrix adhesion in NFCs. Moreover, designing matrices able to withstand such swelling-shrinking cycles and maintain cohesion over time could benefit long term behavior.

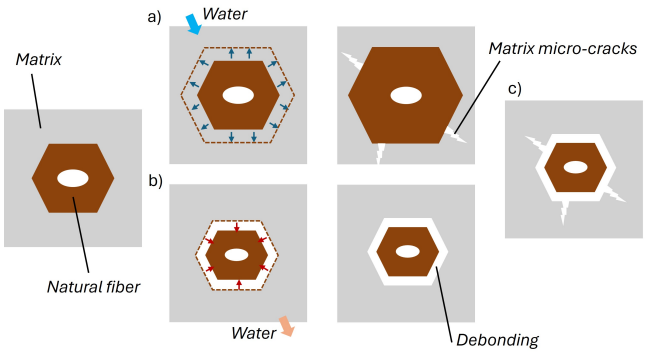

Figure I-16 – Influence of NF hygroscopic behavior on the interface and composite integrity [145]. a) Micro-cracks due to moisture swelling, b) decohesion caused by moisture desorption and shrinkage, and c) combined mechanism through aging and cyclic sorption-desorption.

I.4.4.4 The complex interface of natural fibers

The fiber/matrix interfacial adhesion is critical in FRPs, but it is probably the most complex aspect to apprehend.

Various physical and chemical phenomena influence the interface (Fig. I-17). Covalent or ionic bonds [146, 147], intermolecular bonds such as hydrogen bonding, Van Der Waals interactions, or molecular entanglements but also interdiffusion, electrostatic interactions, and mechanical interlocking affects the interfacial strength. [148, 149]. Good interfacial adhesion between the fiber and the matrix allows the efficient transfer of external loads to the fibers [150]. Through an efficient stress transfer, the fibers responsible for most of the high performances of FRPs can be exploited to their full potential, maximizing the composite properties. The interface, particularly its shear strength and toughness, governs failure mechanisms of composites [151]. Higher interfacial strength yields an increase in strength in all types of solicitations. The improvements are more pronounced in the off-axis directions, where the interface is directly solicited. High adhesion leads to a shift from interface-dominated to matrix-dominated failure modes [151]. In addition, poor interfacial adhesion can facilitate the nucleation and propagation of (micro)cracks that drastically degrade fatigue properties [25]. It is important to note that "too-strong" adhesion is not necessarily beneficial as it leads to brittle failure of the materials, while fiber pull-out and partial delamination can facilitate increase the toughness of FRPs [93, 152]. Therefore, designing a high-strength interface with improved toughness is pivotal in composites. Through chemical sizing, physical modifications, and processing steps, the interface of synthetic fibers has been extensively optimized to reach the best properties [153].

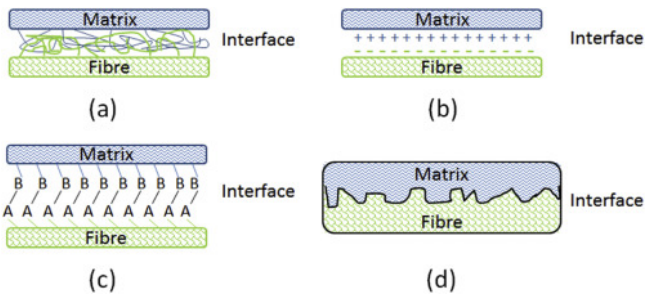

Figure I-17 – Fibre-matrix interfacial bonding mechanisms: (a) molecular entanglement following interdiffusion, (b) electrostatic adhesion, (c) chemical bonding, and (d) mechanical interlocking. Reproduced with permission from [154]. Copyright 2016 Elsevier.

By comparison with synthetic FRPs in which their structure is more controlled, the interface properties in NFCs are even more problematic to investigate and tailor. The intricate geometry of natural fibers leads to greater variability and less reliable results. Moreover, the poor interfacial compatibility between NF, generally hydrophilic, and the polymer matrix, often hydrophobic, hampers the maximization of NF properties.

Most chemical modifications of NFs induce lignin or hemicellulose removal by alkaline or acidic treatments [155, 156]. Additionally, chemical grafting can enhance fiber and matrix compatibility. For instance, thanks to the reactivity of the -OH groups of cellulose, silane treatment can yield amino-terminated or epoxy-terminated functions on the fibers, making them more compatible with epoxy resins [157]. Carboxylic acids or anhydrides, acetylation, and esterification can enhance compatibility with polyester resins and polyolefin thermoplastics. It increases roughness and mechanical interlocking, decreases the water uptake of NFs, and increases the dimensional stability [156]. Other chemical treatments have also been explored by reacting through isocyanates, acrylonitriles, peroxides, and benzoylation [158, 159]. Improvements ranging 10-30% of strength increase and a diminution up to 50% in water uptake are typically reported.

However, these results should be taken with care as most of the studies are performed on short fibers (<20 mm) or non-woven randomly oriented reinforcements where even a slight increase in the adhesion strength can lead to improvements [160]. Additionally, the sustainability and relevance of such treatments from economic and environmental viewpoints have been poorly discussed [161] but were shown to severely affect the environmental footprint. The toxicity of the compounds involved and waste chemicals might hamper the obtained benefits. NFs are mainly investigated to reduce the environmental footprint of composites. To ensure competitiveness with GF, cost must be minimized [159]. Therefore, the interest in applying additional chemical steps should be investigated, and avoided whenever possible.

I.4.4.5 Natural fibers in structural composites - reaching their full environmental potential

The reinforcement represents generally 50-75% of the mass in structural composites (continuous). In this regard, it is evident that most work mainly focuses on the sourcing, design, and reinforcement process to improve the composites' environmental score. NFs appear to be one of the most promising reinforcements for most composite applications, offering the potential to efficiently replace glass fibers with promising ecological benefits.

Many works have explored fully or partially bio-based matrices with NFs to ensure sustainability when using NFCs. Both thermosets and thermoplastics have been investigated. Thermoplastics offers several advantages. By nature, thermoplastics are recyclable, which simplyfies the EoL scenario through direct thermo-mechanical recycling and provides lower LCA over multiple cycles [162]. However, thermo-mechanical recycling involves the decrease of fiber length and the degradation of the properties between the original continuous fiber composite, meaning that the recycled one must be only used in non-structural applications [163]. Solvolyse could help separate the fibers from the thermoplastic, but it has been poorly investigated, and the use of (hazardous) solvents is debatable. Polylactic acid is biobased and bio-compostable, making it an ideal candidate for biobased composites [145, 164]. However, in all cases, the poor interfacial adhesion between non-polar thermoplastic polymer and polar NFs leads to unsatisfying properties compared to the potential of NFs [165]. In addition, thermoplastic processing requires high temperatures to reach satisfying melt viscosity to impregnate the fibers that complexifies the processing. Starting from thermoplastic monomers such as lactide to PLA [166], or methyl methacrylate to PMMA (Elium® by Arkema, [163]) offers some processing advantages while keeping the recyclability aspect of thermoplastics. However, their properties remain less competitive compared to thermoset matrices.

Thermosets, and in particular epoxy resins, provide improved wetting of the fiber and, hence, better properties [167]. Several works have exploited partially bio-based epoxy [168–170], some of them being already commercially available such as the Sicomin GreenPoxy® [59, 167]. Compared to glass fibers, similar specific properties were obtained, with environmental benefits in cradle-to-gate scenarios. Yet the recyclability of thermosets is an issue, often resulting in the landfill or incineration of biobased composite once decommissioned.

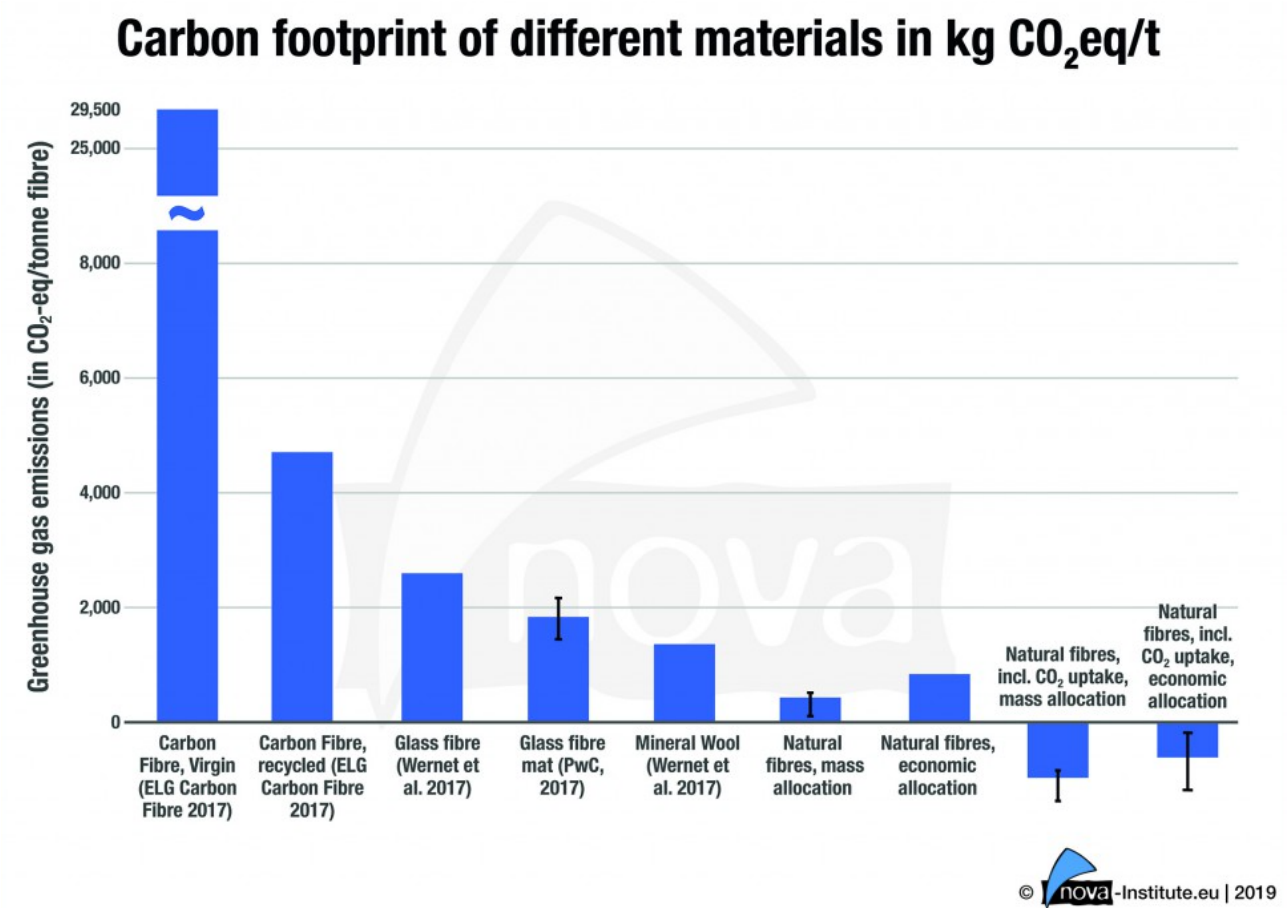

Figure I-18 – Greenhouse gas emissions per tonne of fiber used for composite application. Copyright 2019 Nova-Institute.eu [122].

Finally, it is important to note the wide diversity in sourcing and properties of fibers suitable for structural FRPs. This diversity allows the selection of different fibers adapted to the applications. To date, the most important criteria are either costs, or performances, favoring the use of glass fiber in the former and carbon fiber in the latter. However, they possess the highest environmental impacts (Fig. I-18). Other criteria such as embodied energy, resource depletion and GWP should ideally be considered by engineers to design more sustainable structures. Regulations and tax incentives policies could trigger the designing criteria to foster the production and use of plant and basalt fiber, that display competitive properties when properly used. The far superior properties of carbon fiber make them, currently, challenging to replace in their main applications. In that sense, the first R's strategies (Refuse, Rethink, Reduce) and the last (Reuse, Repurpose, Recycle) should be prioritized, i.e., limit the use of carbon fibers as a last resort, maximize use, and ensure recycling. For most applications, natural fibers are the most sustainable pathways in Europe with negative GWP and could help reach carbon-neutral goals. However, efforts are still required to match the fiber advantage with the matrix footprint.

I.5 Matrix - The key towards sustainable composites in a circular economy?

The need to shift from a linear to a circular economy requires thinking more globally about the design of composite materials. The macromolecular engineering of resins is critical for ensuring the implementation of composites in a circular economy. In an ideal case, resins must be sourced from renewable feedstocks (bio-CO_2-derived and/or post-consumer waste), scalable, and adaptable to existing composite manufacturing processes (drop-in), all while delivering the expected properties. In addition, integrating recyclable by-design systems would facilitate the recovery of valuable compounds at the EoL, ideally all of them, i.e., fiber and polymer building blocks. This comprehensive approach would not only reduce the consumption of fossil resources but also enhance the durability of structures and create value at the end of their service life by transforming them into new resources for materials with properties similar to virgin materials.

Table I-2 – Overview of matrices composition, properties and applications for composites

Resin Chemistry	Part A	Part B	Catalyst	T_g °C	Modulus GPa	Strength MPa	Elongation %	Advantages	Drawbacks	Applications	Biobased potential	Recycling	Ref
Unsaturated Polyesters	Unsaturated polyester prepolymer	Styrenic (Styrene, Vinyl Toluene) & Methacrylic diluent	Mandatory: Radical initiator (peroxides), optional: accelerator (cobalt, amines)	80-250	2.5-4.0	60-100	2.0-8.0	Low cost, easy processing, moisture resistant, chemical resistance, fast cure	VOCs, Brittle, high shrinkage, fire sensitive, limited performances, thermal stability	Marine, Construction, Energy	Everything except styrene	Polyol and acid. Styrene rich compounds are challenging	[171, 172]
Epoxy	Epoxy monomer	Amines, Anhydrides, Thiols, Acids	Not necessary in majority. Required for anhydrides, thiols...	60-150	2.0-3.5	40-80	1.0-5.0	High strength, low shrinkage, good adhesion, Chemical & Thermal resistance	Long curing time, expensive, brittle, hazardous constituents, burning behavior, Bisphenol A	Aerospace, automotive, marine, energy	Potentially 100%. Biobased amine are the most challenging	Challenge to valorize products	[15, 40, 173]
Polyurethanes	Polyester polyols, Polyether polyols	Isocyanates	Preferably, Tin catalyst, strong base	50-120	0.5-3.0	30-70	5.0-20.0	Toughness, curing speed, versatility, adhesion	Hazardous consitituents (isocyanates), UV sensitive, thermal stability, moisture sensitive process, burning behavior	Flexible composites, elastomers, automotive	Polyol. Isocyanates are challenging	Feasible, challenge in purifications	[174, 175]
Vinyl Ester	Vinyl ester prepolymer (Epoxy + Methacrylic acid, Polyol+MA)	Styrenic & Methacrylic diluent	Mandatory: Radical initiator (peroxides), optional: accelerator (cobalt, amines)	90-180	3.0-4.0	70-100	3.0-7.0	Chemical resistance, adhesion, mechanical performances	VOCs, cost (vs UPR), Bisphenol-A	Chemical tanks, marine structures	Epoxy & polyol precursor. Styrene and methacrylate difficult	Potentially, cleavage of ester groups	[176, 177]
Phenolics	Phenolic prepolymer (Novolac, Resole...) (Phenol + formaldehyde)	Formaldehyde Hexamethylene tetramine	Acid or base	150-350	3.0-4.0	40-70	1.0-3.0	High thermal resistance, burning behavior, dimensional stability	Brittle, lower mechanical strength, curing time & temperature, hazardous constituents	Fireproof structures, electrical parts	Phenol & formaldehyde	Challenging, pyrolysis	[178]

I.5.1 Toward a complementary and sustainable value chain for polymer building block sourcing

Matrices for structural materials are mainly polymers containing heteroatoms (through the ether, amine, ester linkages). Some identical challenges can be identified, particularly from the sourcing for these matrices. Epoxy, polyesters (linear and unsaturated), polyamides, and polyurethanes require either (poly)amines, diols/polyols, or carboxylic acids.

For example, bisphenol A (BPA) is a typical component of epoxy, benzoxazines, phenol-formaldehyde, and vinyl ester resins and can also be used in polyurethanes. 4,4'-Methylenedianiline (MDA) is a typical hardener in epoxy resins and is used to produce methylene diphenyl diisocyanate (MDI). All these substances are petro-sourced and are currently under scrutiny due to their toxicity, carcinogenicity, and neurotoxicity. Identifying better sourcing for polyols, phenols, and amines is vital to achieve more sustainable building blocks. Their hazardousness should also be considered to avoid health accidents similar to those experienced in the past [179].

The importance of sourcing chemicals from renewable resources has already been mentioned. Two main strategies are essential. The first one aims to switch from petro-based sourcing to renewable sourcing of the same chemicals [18, 180]. This strategy focuses on efficient chemical pathways to obtain competitive biobased compounds. The customers can readily use them as they remain the same compounds as the petro-based version. This is, for example, the case of bio-aniline and bio-phenol to obtain MDA and BPA, among others. However, this does not address health considerations. Industries mainly deploy this strategy. Moreover, the processes can adversely affect the actual environmental benefits, which are often undisclosed by sectors.

The second strategy consists of finding biobased alternatives to existing compounds. Most of these researches are performed by academics and typically have lower TRL, making it more complex to implement in the industry as the value chain does not necessarily exist. However, it is often the most advantageous strategy as it contributes to the valorization of waste products such as lignin and can help reduce the toxicity of the chemicals used [181].

For both strategies, certain resources and pathways are of particular interest in the fields of polymers (and, subsequently, composites) as they might provide relevant and steady quantities through industrialization processes (keeping in mind the reduced consumption associated with a circular economy) [55, 182]. Namely, lignins, non-edible (or mass-produced) carbohydrates (cellulose and starch), and CO_2 are promising chemical platforms for sourcing monomers that are suitable to replace existing petro-based monomers. Additionally, terpenes, vegetable oils, and miscellaneous agricultural

waste fermentation can provide valuable chemicals for the polymer industry [54].

I.5.1.1 Lignin, from waste to valuable phenols and amines

Lignin is a plentiful biopolymer produced in large quantities by the paper industry. It is the most abundant source of aromatic chemicals [183]. About 100 Mt are produced annually, with the most being used as a low-grade fuel [184]. The depolymerization of lignin into valuable compounds and their separation is challenging [185]. Different processes exist, such as kraft lignin or soda lignin; but discussing the different depolymerization processes, while critical, is beyond the scope of this work [184].

Several phenolic compounds have been obtained from lignin that can effectively serve as platform chemicals, as schemed in Fig. I-19. Lignin is principally constructed of syringyl, guaiacyl, and hydroxyphenyl primary compounds. However, depending on the lignin source and the extraction process, there is a too large variety of compounds extracted [186]. Extraction yields are generally low and produce considerable quantities of by-products [187]. The catalytic fractionation of lignin is valuable through the efficient valorization of these products [188] while reducing GWP emissions. Innovative pathways have emerged to stabilize the depolymerization of lignin and promote high yields and well-defined chemicals through in-situ functionalization [185,189]. This strategy produced biobased polyamides with a reduction of GWP and economic advantages compared to conventional PA-6,6 [190].

From lignin, guaiacol, is an exciting compound [181, 191, 192]. Guaiacol is analogous to phenol substituted by a methyl ether in the ortho position. Guaiacol can efficiently replace BPA [181,193], but can also be aminated to replace MDA and MDI [192] (see Fig. I-19). Other phenolic compounds, such as vanillin [194] or eugenol [195], demonstrate promising potential for producing sustainable materials.

In addition to phenols, amines can also be produced from lignin [191,196]. As previously mentioned, phenolic can be aminated through Williamson etherification and Smiles rearrangement [192] to obtain aromatic amines. The group from Barta explored the use of Raney Nickel to catalyze both the hydrogenation of phenol into cycloaliphatic alcohols and their subsequent amination in the presence of ammonia [197, 198]. Despite being potentially biobased, no environmental assessment was found using ammonia, which might hamper benefits [199], due to the fact that ammonia production is one of the most polluting chemical processes [200]. Nevertheless, the direct fabrication of primary amines from alcohol is promising for polymers and composites, as they are the most challenging compounds to replace for epoxy resins.

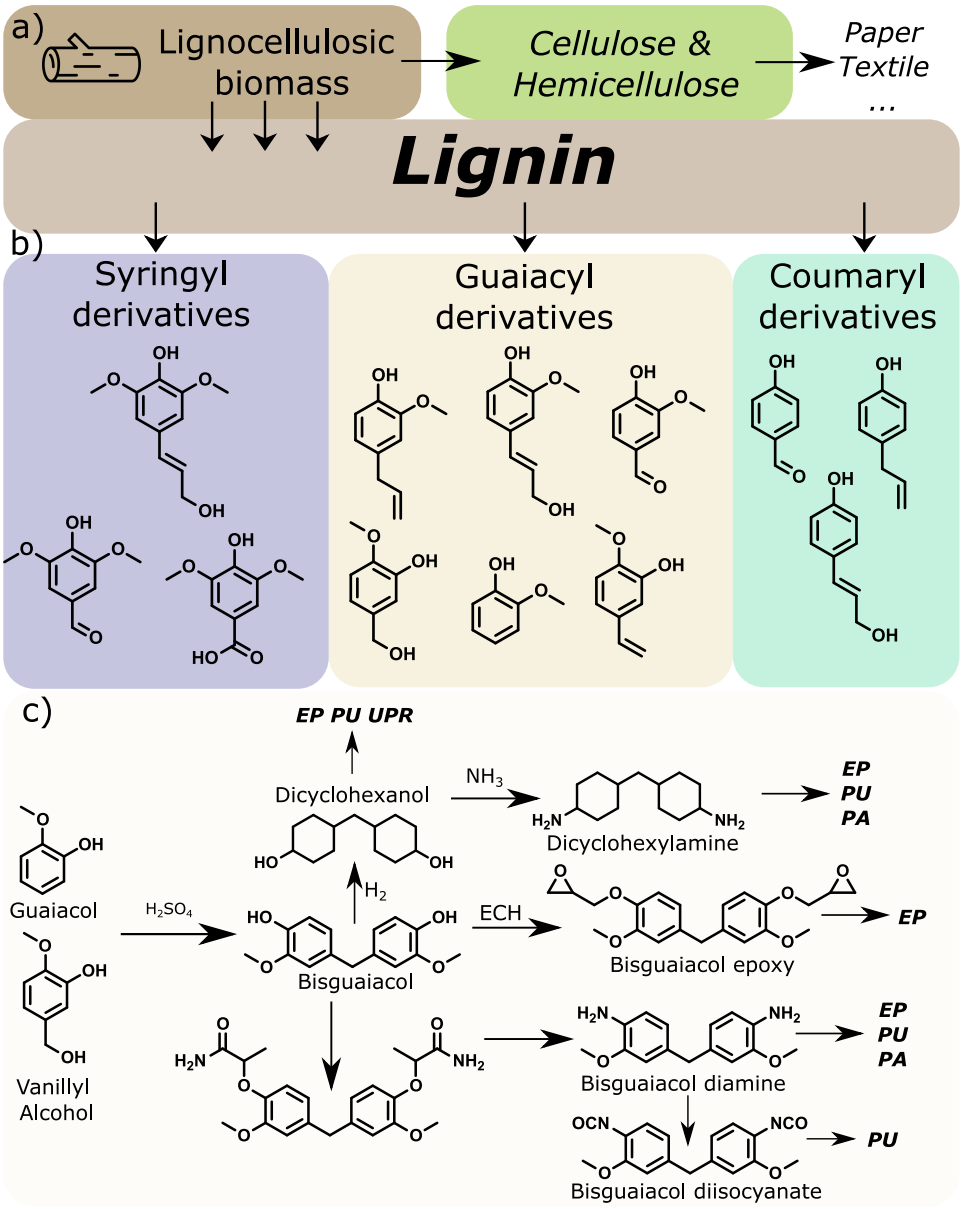

Figure I-19 – Lignin valorization into key building blocks for composite applications. a) Schematic representation of the lignocellulosic value chain, with lignin as a major by-product, b) Typical lignin constituents and small phenolic compounds, c) catalytic valorization of guaiacol compounds into key monomers for composite and polymer applications. The bisguaiacol pathways are summarized from [192, 201, 202]

I.5.1.2 Carbohydrates and polysaccharides, easy access to precious building blocks

Polysaccharides (cellulose, hemicellulose, starch, chitin) are the most abundant biopolymers on earth, accounting for 70-80% of the total biomass. They are the primary source of energy for living organisms but also offer a renewable feedstock for the polymer industry.

Typically, the use of such resources begins with the depolymerization of polysaccharides into simple

sugars such as glucose/fructose (from starch and cellulose, Fig. I-20) or xylose (from hemicellulose, Fig. I-21). Subsequently, these sugars are transformed into more valuable compounds for industries. All these transformations can be developed through bio-fermentation (in the presence of bacteria, yeast, etc.), enzymatic, or chemical pathways. Common challenges are related to scaling and managing by-product generation. The toxicity of produced compounds to fermenting organisms typically imposes highly dilute media that increase energy consumption and lower yields [203]. It is also crucial that competition with food production is avoided on a large scale perspective. Moreover, many crops, such as maize, have detrimental environmental footprints due to the use of large quantities of water, fertilizers, and pesticides.

Over the last 20 years, numerous chemical compounds have been obtained from glucose, and some are industrially produced or at pilot scale. The most famous example is the production of polylactide (PLA), from the fermentation of starch to lactic acid [204]. PLA is employed as a bio-compostable (and sometimes biodegradable) composite, often combined with flax [145].

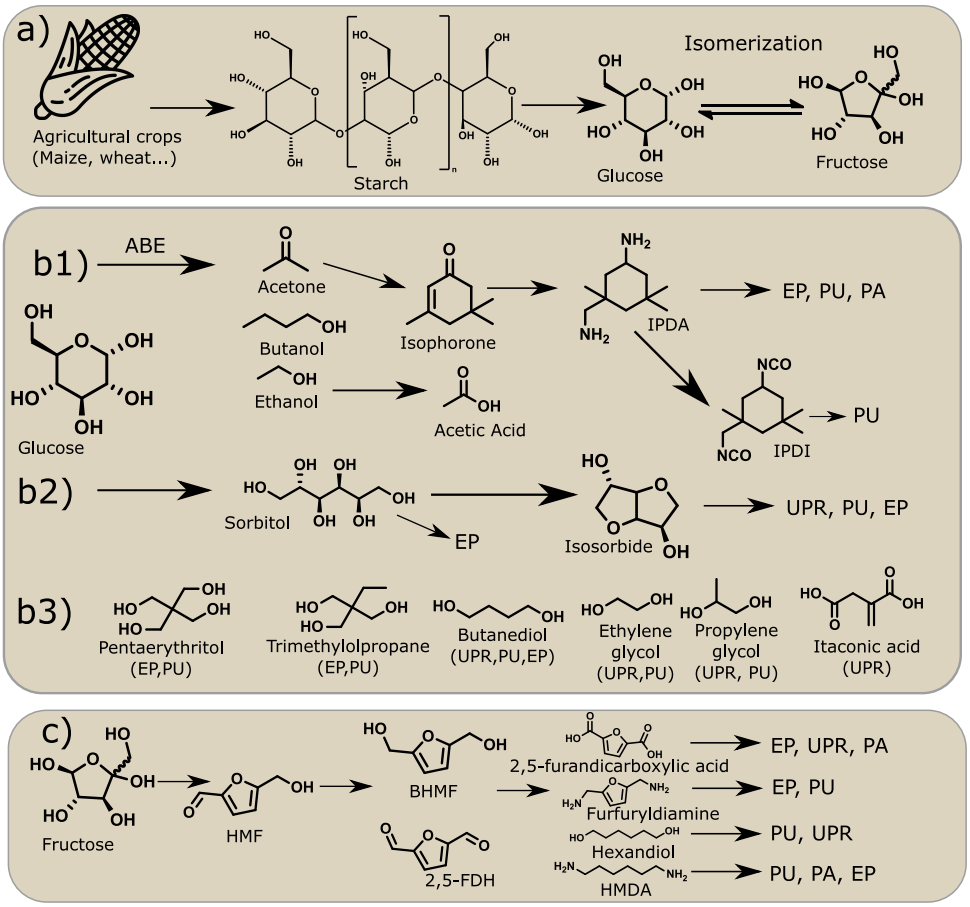

Figure I-20 – From crops to valuable compounds. a) Starch fermentation to glucose and fructose, b) glucose route, b1) Acetone-Butanol-Ethanol (ABE) process to isophorone diamine, b2) sorbitol route, b3) various compounds from glucose, and c) fructose route to furanic compounds.

Sorbitol [205] and isosorbide [206] are also promising building blocks to provide polyol and amines used in epoxy, polyurethane, and polyester resins. Various polyols are obtained through the fermentation of starch by bacteria, leading to trimethylolpropane, pentaerythritol, and butanediol [203]. These are standard components for epoxy resin and polyurethanes. Biobased butanediol is produced on a large scale and represents an important fraction of partially biobased epoxy resins. The long-time known acetone-butanol-ethanol (ABE) fermentation process is also regaining industrial interest [207]. From bio-acetone, Evonik Industries AG is now producing bio-isophorone, a mass-produced precursor of isophorone diamine and diisocynate, typical crosslinkers in epoxy and polyurethanes.

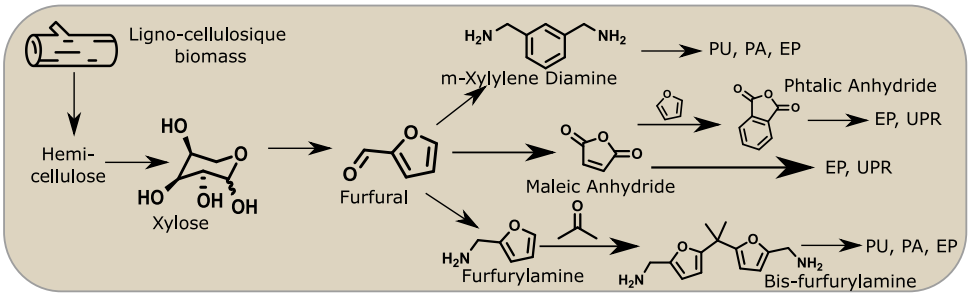

Figure I-21 – Hemicellulose route to furanic compounds.

Phloroglucinol and resorcinol, which are potential aromatic alternatives to BPA are also produced from glucose (see Fig. I-22). They have already shown significant promise in the preparation of epoxy resins [170] and other high performances resins [208,209]. However, the carcinogenicity of these phenolic compounds remains a major concern [210].

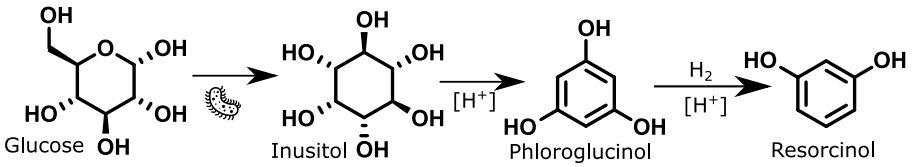

Figure I-22 – Phloroglucinol and resorcinol production from glucose, adapted from [211]

Aniline, a multimillion-ton produced aromatic amine, mainly for epoxy and polyurethane resins, has been successfully produced and commercialized by Covestro AG from the fermentation of glucose [212] (see Fig. I-23). The GWP was shown to be reduced when compared to traditional petro-based aniline [213].

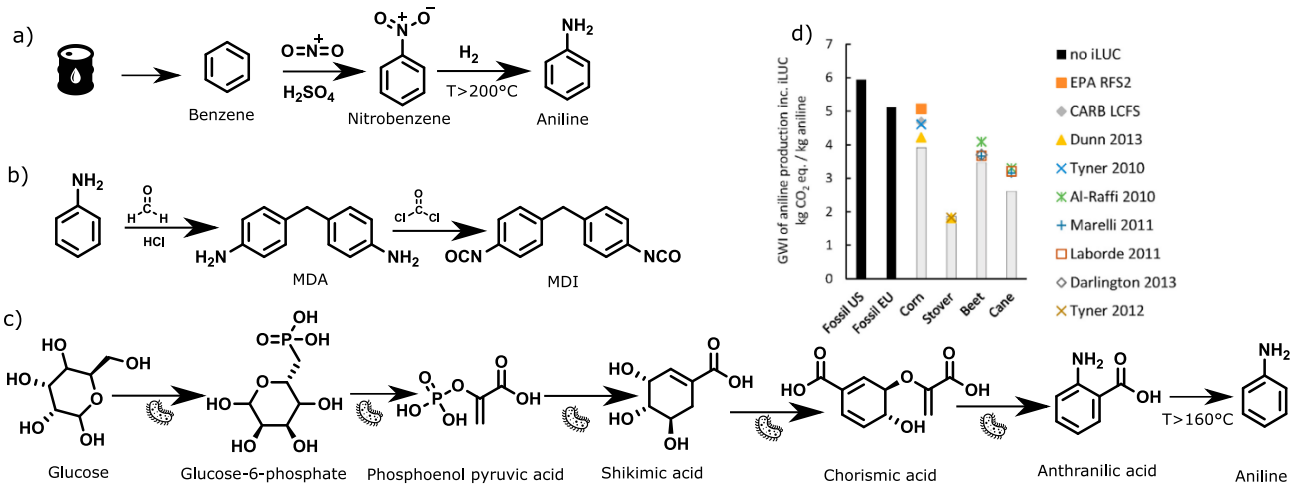

Figure I-23 – a) Conventional petro-based pathway for aniline, b) transformation of aniline to typical polymer building blocks, c) fermenting process from glucose to anthranilic acid (simplified from [212], and d) GWP comparison of petro-based aniline and biobased one [213].

Finally, furanic compounds are emerging as a versatile platform for various applications as they can provide numerous building blocks. Alternative pathways to petro-based existing compounds, such as m-Xylylene diamine (mXDA) [214], maleic and phthalic anhydride [215], and hexamethylenediamine (HMDA) [216] were demonstrated. However, these pathways may include multiple steps and may not be industrially or environmentally relevant. The overall yields of mXDA and the 5-step process from furfural may hinder the practical applicability [214]. The synthesis of HMDA from fossil resources was demonstrated to be more economically and environmentally friendly than from biomass [216], and it is currently produced at pilot scales by Coverstro AG and Genometica.

Furan compounds can also provide new chemical structures with lot of promise. For instance, 2,5-furan dicarboxylic acid (FDA), an aromatic diacid that brings stiffness and thermal stability to polyester [217], has shown to be advantageous compared to its petro-based counterparts, terephthalic acid [218]. FDA provides high thermal stability as a replacement to BPA in epoxy [219]. Amine crosslinkers can also be obtained to replace conventional aromatic diamines [220, 221].

I.5.1.3 Pyrolysis by-products valorization

Complete recirculation of organic compounds is not feasible. Vidal et al. [19] have already acknowledged that some polymers cannot be recycled. Moreover, certain waste materials might not be environmentally or economically viable to recirculate. In these cases, pyrolysis could be a realistic ultimate solution.

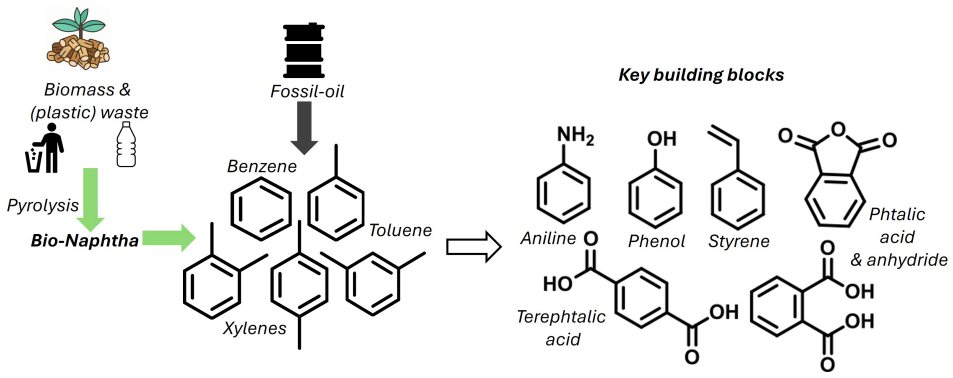

Figure I-24 – Biomass & waste valorization by pyrolysis to bio-naphtha and key building blocks for composite matrices.

The thermal decomposition of biomass and organic waste in an inert atmosphere has emerged as a promising pathway for producing BTX (Benzene, Toluene, Xylene) from renewable sources (see Fig I-24). The technique effectively converts lignocellulosic biomass into aromatic hydrocarbons [180]. By exploiting pyrolysis to recover valuable aromatic compounds (and small molecules of gas), the process can complement chemical extraction and waste management efforts [19]. Notably, the production of bio-naphtha and bio-BTX from renewable feedstocks has been successfully developed by Neste Oyj, a Finnish oil refiner with several patents to control the composition, even in the presence of nitrogen and oxygen impurities [222, 223]. From this bio-BTX, bio-phenol was produced and applied by Covestro for BPA-derived plastics [224].

I.5.1.4 Carbon Capture and Utilization, exploring CO_2s a valuable chemical

The use of carbon dioxide in chemistry has a long history [225], and is used for a variety of compounds, some of them being commercialized (see Fig. I-25). CO_2 is a key element in urea production from ammonia, representing nearly 75% of the 150 Mt produced annually [226]. Other chemicals such as salicylic acid (50%), methanol, dimethyl carbonate, and ethylene carbonate are industrially produced from CO_2, albeit on a smaller scale [226]. The detrimental overproduction of CO_2 has pushed policies to encourage industries and academics to increase efforts in efficient Carbon Capture and Utilization (CCU). Significant progress has been made towards the capture of CO_2 either from industrial processes or from open-air, using biotechnologies, amines, and covalent organic frameworks among others [227,228]. CO_2 is remarkably stable (-394 kJ/mol), which makes its activation complex and economically difficult without strong governmental policies [227]. Despite this, CO_2 remains a promising chemical that could help partially decarbonize the composite industry.

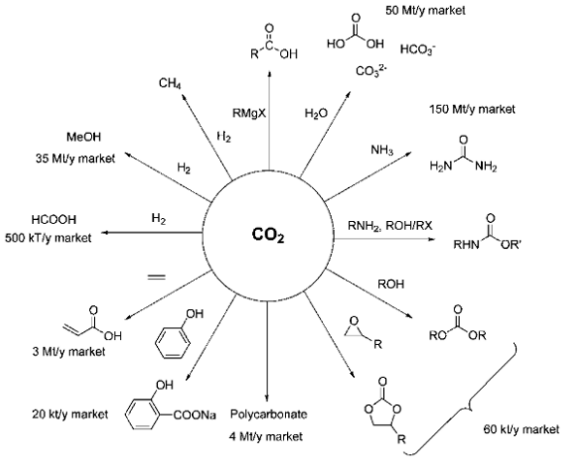

Figure I-25 – Chemical transformation of CO_2 into commodity chemicals and market volumes. Reproduced with permission from [229].

Although mainly limited to academia, CO_2 has been proven to be a valuable compound for the production of building blocks in advanced polymers [230]. High molar mass linear polycarbonates were produced from CO_2 and oxides, presenting advantageous properties when compared to BPA-phosgene derived polycarbonate [231,232]. Acrylic acid and methacrylic acids, key components for the preparation of unsaturated polyester and vinyl ester, were also reported, but the results demonstrate discrepancies in the reproducibility [233–235].

One of the most promising strategies can be related to the synthesis of cyclic carbonates [230, 236]. Cyclic carbonates can be obtained from the cyclo-additions of CO_2 into epoxides [237]. The process can be quantitatively performed in solvent-free conditions using supercritical CO_2. These cyclic carbonates are valuable for producing Non-Isocyanate Polyurethanes (see Section I.5.6). Other intermediates to provide more reactive cyclic carbonates (such as exovinylenecarbonate) were also developed [238] in order to obtain high-performance polymers such as polycarbonate [239], and polyurethane [240], that can even be recycled more efficiently than traditional ones. Recently, CO_2-derived oxazolidones (cyclic urethanes) have been demonstrated to be a versatile polymer with easy recyclability and suitable for manufacturing composites with natural fibers [241]. However, the development of cyclic urethanes remains at a very low TRL and is not yet suited for rigorous investigations aimed at composite applications. They remain potential future solutions if production is scaled to a few kilograms.

I.5.2 Unsaturated Polyesters - The low-cost large scale resin

Unsaturated polyesters (UPR) are the most commonly used thermoset matrices for composites. They represent 87% of thermosets resins and 65% of the total composites production. Despite their

widespread use in various composite applications, UPRs pose several issues arising from their sourcing and end-of-life perspectives.

I.5.2.1 Backgrounds of UPR, composition, polymerization, and properties.

Unsaturated polyesters consist of polyester oligomers or prepolymers containing reactive unsaturations, a reactive diluent that often plays the role of crosslinker, and a free-radical initiator (see Fig. I-26). The prepolymer is prepared from unsaturated dicarboxylic acids or their anhydride equivalents, polymerized with a diol. Maleic (cis) acid/anhydride or fumaric acid/anhydride (trans) as unsaturated dicarboxylic acids or its anhydride equivalent are preferred unsaturated diacids, with fumaric acid being more reactive for free-radical crosslinking [172]. Glycols such as ethylene glycol, propylene glycol, butanediol, and cyclohexyl dimethanol are used in various proportions to tailor the properties and prepare the prepolymer [172]. In addition, aromatic saturated diacids/anhydrides are used to improve chemical resistance, strength, or toughness, particularly with isophthalic acid/anhydride and adipic acid that are commonly used for such.

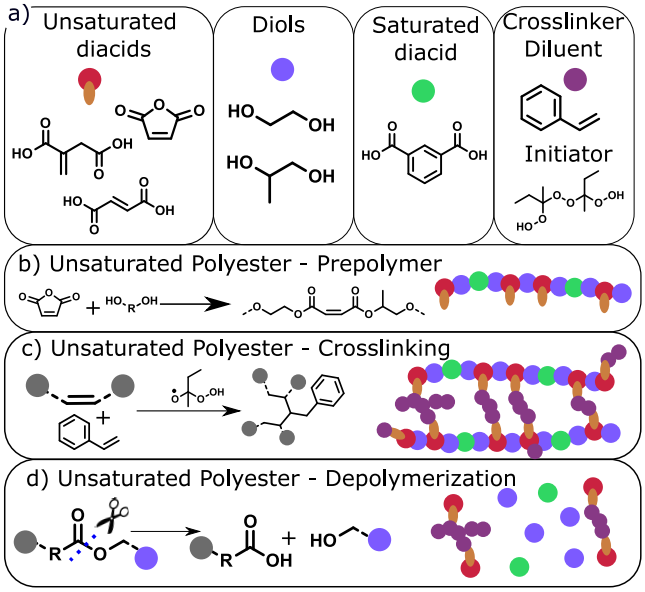

Figure I-26 – Unsaturated polyesters. a) Typical monomer precursors, b) pre-polymerization from diacid and diols to unsaturated polyester, c) crosslinking of UPR, and d) representative hydrolysis of UPRs.

Maleate and fumarate cannot be homopolymerized efficiently. Due to their molecular weight, polyester prepolymers have relatively high viscosity. Therefore, reactive diluents, typically styrene or methyl methacrylate, are used to lower the viscosity and crosslink the network [242]. Typical UPR formulations have viscosities ranging from 0.5-2 Pa.s, making them ideal candidates for infusion

processes at low temperatures.

UPRs undergo crosslinking through a free radical polymerization process. Typically, peroxides such as methyl ethyl ketone peroxide (MEKP) or benzoyl peroxide (BPO), are used to initiate the free radicals when heated. An accelerator (cobalt-based) can lower the free radical initiation temperature and accelerate the curing process [243]. Room temperature curing is feasible by employing MEKP and cobalt accelerator [243]. The initiator and catalyst composition play a significant part in the polymerization conditions as well as the future properties and stability of the network over time. During free radical polymerization, the unsaturated polyester bonds are consumed, forming new stable C-C bonds and crosslinking the polyester chains. Due to the nature of the bonds formed, UPRs are inherently stable and difficult to depolymerize. Particular attention must be brought to ensure the total consumption of the crosslinker (styrene) and the initiator to prevent the release of these (hazardous) compounds in the environment [171].

The low viscosity of UPR formulations, their versatility, and the ability to cure at room temperatures have fostered their use in large composite structures. Marine applications and infrastructures (construction and wind energy) are the most prominent consumers of UPRs. They are mostly combined with GF for producing low-cost composite materials [164] but are also investigated as matrices for natural fibers [244]. UPRs present moderate resistance to hydrolysis and solvent for general purposes but poor resistance to weathering and UV aging in outdoor applications. They tend to yellow and degrade under UV exposure. To avoid these undesirable effects, stabilizers and modifiers should be used. UPR is suitable for applications with service temperatures up to 80°C, with glass transitions generally ranging from 70-110°C. Typical mechanical performances of UPRs are reported in Table I-2. UPRs are relatively brittle materials and are prone to fire [245]. Flame retardants, often containing toxic halogen compounds, are used to mitigate this issue [246]. Despite their prevalence in fiber-reinforced plastics (FRPs), there is ongoing research to enhance the sustainability of UPRs, aligning with circular economy principles.

I.5.2.2 Routes to greener UPRs in the frame of a circular economy

The sustainability of UPRs depends primarily on sourcing components and designing polymers that are easier to deconstruct through macromolecular engineering. While UPRs represent nearly 90% of the market, it is important to emphasize that they are not investigated upon the corresponding contribution. Since 1997, less than 173 papers have been published using "bio-based" and "unsaturated polyester" as keywords, and fewer than 300 on "recycling" (Scopus database). In contrast, bio-based

epoxy have been present in nearly 2000 papers since 1996, with more than 100 papers published annually since 2017 and 227 papers in 2023 alone. More than 2000 papers on epoxy recycling have been published since 1996, with more than 300 papers in 2024. Most of the works on the sustainability of UPR-containing composites has focused on the type of natural fibers, the process parameters, and the modifications of the fibers to improve the interfacial adhesion [244].

Even though some independent transversal work on the synthesis of monomers could be relevant to UPR, it appears that the sourcing of UPR monomers from biobased and renewable sources has only been partially investigated. Much more extensive research and effort are needed in that area. Comprehensive solutions addressing both sourcing and recycling have yet to be addressed.

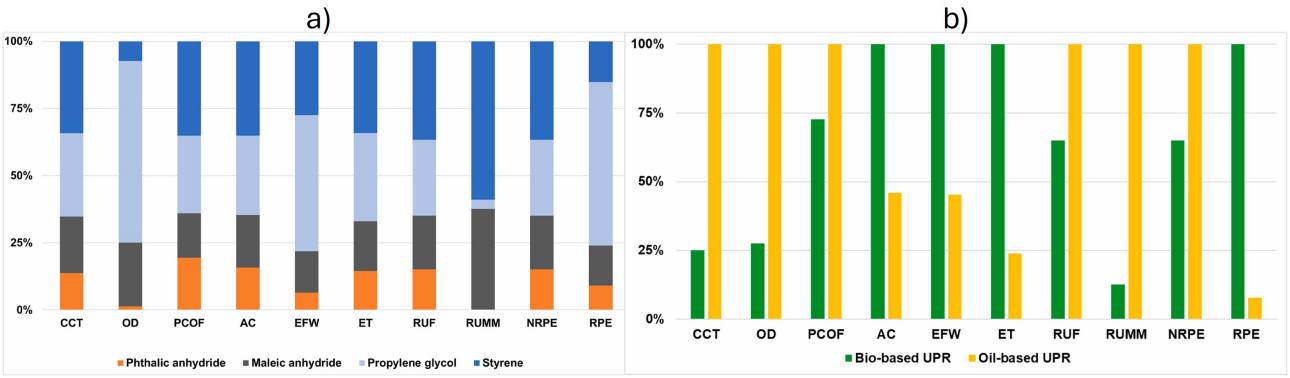

Figure I-27 – a) Environmental contribution of various components of oil-based UPR, and b) comparison of the environmental performance of bio-based and oil-based UPRs for each impact category (100% corresponds to the highest impact in each category). Reproduced with permission from [247].

Still, some works have progressed in developing renewable alternatives to existing systems, but challenges remain. For instance, petro-based compounds such as isophthalic acid can be replaced with FDA [248]. Biobased diols, including ethylene glycols and polyols like isosorbide, have also shown promising results recently [248,249]. However, sourcing biobased unsaturated dicarboxylic acid remains difficult due to limited options. Biobased routes to obtain maleic acid (MA), typically obtained from the catalytic oxidation of benzene [250], have been developed from butanol [251] or furfural [252]. LCA analyses highlight that the furfural route is more environmentally favorable than bio-butanol [253], including pilot-scale feasibility. However, valorizing by-products must be performed to diminish the footprint and E-factors, a common issue in biomass chemical transformations. Fumaric acid, the trans isomer of MA, is naturally occurring and can be easily obtained from fermentation [254]. From an economic perspective, most fumaric acid is still produced from the catalytic isomerization of MA [250].

Itaconic acid [171] and muconic acid [255] are other unsaturated dicarboxylic acids showcasing

promising potential for UPRs whether their production can be scaled to industrial quantities. Notably, if the interest in exploiting bio-based UPR has been demonstrated in some cases [247], the pathway to obtain biobased compounds should be systematically discussed. Moreover, a recent LCA on bio-based UPR by Shahid et al. [247] demonstrated the dominant role of styrene in the environmental footprint (see Fig. I-27). This reactive diluent represents the most problematic compound to urgently replace [256]. In this regard, current solutions are based on bio-based methacrylates such as isosorbide (di)methacrylate [245], bio-phenol grafted methacrylates [242, 256], and terpenes [256]. Yu et al. [242] investigated several sustainable aromatic analogs to styrene, such as veratrol and guaiacol derivatives. The reactivity and final properties are suited for considering them as alternatives. However, the viscosity of these alternatives was consistently too high to compete with styrene-based formulations, making them unsuitable for composite infusion. Moreover, the costs of lignin-derived aromatic vinyl were not discussed, but they are not competitive up to now.

I.5.2.3 About the recycling of unsaturated polyesters

As previously mentioned, the recycling of UPR has been poorly investigated. While linear polyesters are among the most advanced polymers in terms of recycling with existing pilot plants, exploiting enzymatic [257] or catalytic [258] pathways, strategies for crosslinked UPR are much less developed [259]. Some authors have investigated chemical recycling, primarily through hydrolysis of the ester bonds [260, 261], to recover some valuable diols and dicarboxylic acid (isophtalic acid). However, the MA/styrene adduct is difficult to valorize due to the stable nature of the C-C bond formed. Pyrolysis was also employed to retrieve carbon or glass fibers, by thermally degrading the matrix [262, 263]. In all reported cases, MA and styrene are wasted, further highlighting the urgence to find renewable alternatives to styrene and MA. Direct pyrolysis of UPR-based composites remains, to date, the most realistic pathway. Pyrolysis management and perspectives for composites are discussed later on in the dedicated section I.7.2.

I.5.3 Epoxy resins - Versatile, competitive, and problematic

Epoxy resins (EP) account for about 10% of the composite market. They are often the preferred choice when high performance and stability are required. EPs are highly reactive and versatile and can be used in many applications. The curing process of epoxy can easily be tuned by playing on hardener chemistry, (macro)molecular structure, and catalyst. EPs are probably the most investigated thermoset resins for composites, particularly NFC.

I.5.3.1 Basic principles of epoxy resins, monomers, curing agents and common properties for targeted applications

Epoxy resins are two-component formulations consisting of (a) low molecular weight epoxy precursors containing oxirane moieties and (b) a hardener. Depending on the hardener and some specific requirements, a catalyst might be necessary. Epoxy precursors are produced from organic compounds containing hydrogen active sites, such as hydroxyl or primary/secondary amines, that are reacted with epichlorohydrin (ECH) (see Fig. I-28), leading to glycidyl ethers. The production of epoxy monomers has high atom efficiency (generating only NaCl and water as by-products) and requires a base catalyst (typically NaOH) at a moderate temperature (below 120 °C). Although ECH is a volatile and highly toxic compound, it is extremely economical [179]. They can also be produced by the oxidation of unsaturation, such as unsaturated fatty acid, triglycerides [264], and terpenes [265]. Bisphenol-A is the prefered precursor for epoxy resin. Diglycidyl ether of bisphenol-A (DGEBA) is economical and widely available. The resulting resins derived from DGEBA have good properties (mechanical, thermal, stability to UV). Depending on the manufacturing process and applications, reactive diluents, such as aliphatic epoxies, and tougheners can be used to adjust the formulations [266]. EPs generally have higher viscosities than UPR, but viscosity as low as 250 mPa.s can be achieved for infusion processes.

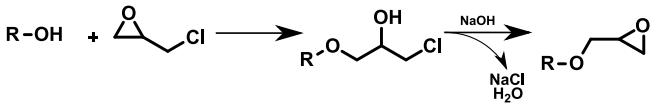

Figure I-28 – Conventional pathway to obtain glycidyl ether.

Epoxy resins are highly reactive compounds due to their strained three-membered ring structure. Substituting the oxirane ring with electron-withdrawing groups (e.g., carbonyl, aromatic...) or donating groups (ether, amines...) strongly influences EP's reactivity, creating a very versatile and convenient toolbox for adjusting EP formulations to the complex requirements of composite manufacturing. The ability to tune the reactivity of epoxy resins by choosing specific curing agents and adjusting the curing conditions. allows them to be used in various applications, ranging from construction to electronics under diverse forms like adhesives, coatings, and composite materials. This tunable reactivity is the key factor explaining the widespread use of epoxy resins in industry. The oxirane ring is more susceptible to nucleophilic attack [267], making it very reactive with various curing agents like amines, thiols, anhydrides, phenols, and acids (see Fig. I-29). The reactivity of epoxy resins depends on the type of hardener used, its structure, and reaction conditions, such as temperature and the presence of catalysts. Primary amines are the most commonly used hardeners due to their low viscosity, fast reactivity, and

wide availability. Aromatic amines such as MDA are largely used as they possess low reactivity at low temperatures and provide high T_g, mechanical properties, and stability. However, high temperatures are required to fully cure the system since secondary aromatic amines are less reactive than primary amines. Aliphatic primary and secondary amines present similar reactivity [15]. Due to concerns about the toxicity and hazards associated with primary aromatic amines [268], there is a growing interest in alternatives such as (cyclo)aliphatic amines. The most commonly used EP precursors are displayed in Fig. I-30, along with health hazards related to each one.

Anhydrides are the second most frequently used hardener for epoxy resins. They require an initiator, such as Lewis bases, to start a chain-step copolymerization [15]. Such polymerization requires higher temperatures than with amines and is considered as a latent formulation. However, most anhydrides are solid and must be solubilized or melted with the epoxy to be processed. This can limit its exploitation in certain composite processes [269]. Different fiber sizing agents might be required for epoxy-anhydride and epoxy-amine formulations as well.

Catalysts like tertiary amines, imidazoles, or metal salts can modify the reaction rate and the properties of the final product. These catalysts enhance the epoxy group's reactivity, allowing them to cure faster and at lower temperatures. However, these catalysts can also cause the yellowing of cured resins, diminish the environment's stability, and are often hazardous, with a risk of leakage from the matrix. When possible, avoiding catalyst is preferred [267].

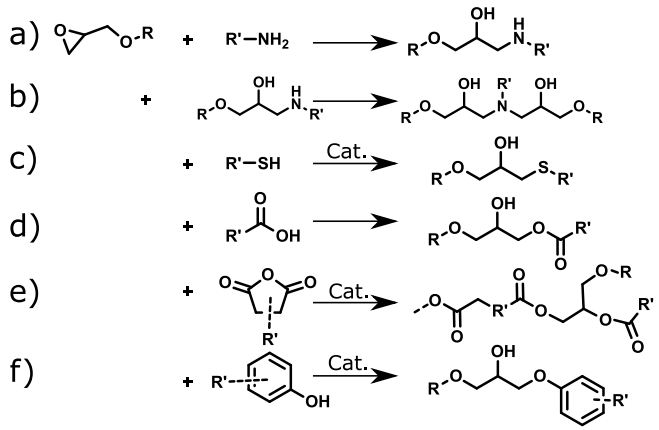

Figure I-29 – Curing agent reactions for epoxy resin. a-b) Aminolysis, c) thiol-epoxy, d) epoxy-acid, e) epoxy-anhydride, and f) epoxy-phenol.

EP resins possess excellent mechanical properties, chemical resistance, adhesion, and thermal stability, representing solid assets for structural composites. Upon curing, EPs form a hard, densely cross-linked structure, which enhances their rigidity and structural integrity. This network imparts high mechanical strength and durability, allowing epoxies to withstand significant stress and maintain

good toughness [15]. Furthermore, epoxy resins exhibit good thermal stability, performing well under heat and even high temperatures, especially when cured with appropriate hardeners like anhydrides or aromatic amines. EPs also offer excellent insulation properties, making them suitable for use as encapsulants and insulators in electronics and electrical applications [270]. Additionally, epoxy resins offer excellent chemical resistance, particularly to alkalis and solvents, which is valuable for protective coatings in harsh environments. EP tends to swell with strong acids but can withstand common acidic conditions [271].

Polar functional moieties formed during curing play a crucial role in enhancing the interfacial interactions with fibers during the fabrication of FRP composites [272]. They particularly improve interfacial strength and toughness, leading to high performances. The initial low viscosity also helps improve fiber and surface wetting for all types of fibers. Significant efforts in the field of sizings aimed first to enhance the interface of epoxy using either amine or epoxy silane agents [273]. The polar functions at the surface of NF have made EP resins the best matrix for NF, with unidirectional laminates commonly reaching a modulus of 30 GPa, and tensile stress above 320 MPa [167, 169, 274].

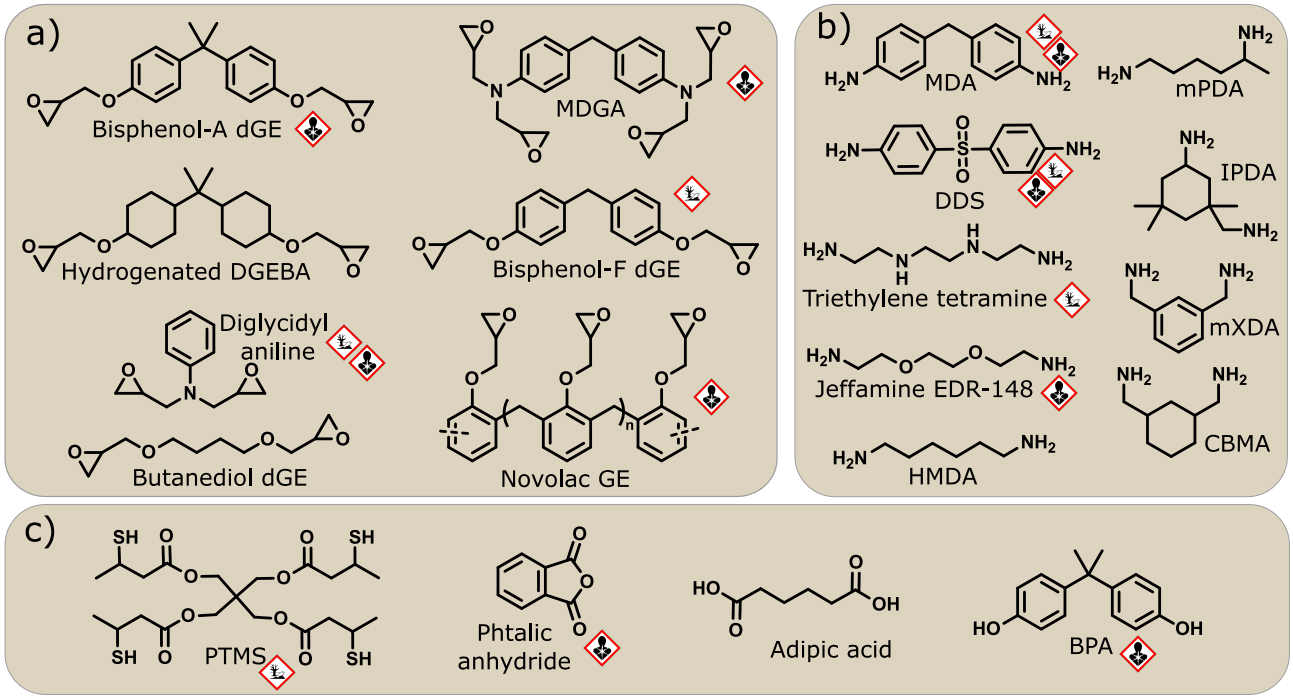

Figure I-30 – Typical EP constituents and potential health hazards. a) EP monomers, b) typical amine hardener, and c) other common hardener. Acronyms: GE, Glycidyl Ether; MDA, 4,4'-Methylenedianiline; MDGA, 4,4'-Methylenebis(N,N-diglycidylaniline); PTMS, Pentaerythritol tetrakis(3-mercaptopropionate); CBMA, cyclohexanebis(methylamine), DDS, diaminophenyl sulfone; mPDA, methylpentane diamine.

The properties of epoxy resin are significantly influenced by its structure, molecular weight, and chain length. Additionally, the number of epoxy functional groups, or oxirane rings, is critical for the crosslinking reaction, which in turn affects the performance of the epoxy thermoset. Therefore, the clever design of the epoxy monomers through careful selection of starting compounds is paramount to perfectly control epoxy-derived compounds. Anhydride acids have seen a surge as hardeners for epoxy because they are not reactive at room temperature, allowing one-pot formulations with extended working times [205]. They provide hard epoxy resins with high weather stability; however, they are more brittle [269]. Alternatively, the curing process can be conducted via UV-triggered polymerizations by using thiols-epoxy, as a base catalyst can trigger fast curing, suitable for fast light-induced designs such as 3D printing. They are highly transparent, with strong adhesion and good water resistance. Their mechanical properties are lower than amine-hardened epoxies, and their commercial availability and diversity are much lower.

I.5.3.2 Pathways towards more sustainable epoxy - a not so impossible bio-sourcing?

Significant scientific and industrial efforts have been made to improve the sustainability of epoxy resins. These efforts focus on two main aspects: (i) finding bio-based and non-toxic alternatives to commonly used DGEBA and aromatic amines and (ii) developing recycling pathways to break down the matrix and recover fibers as well as valuable building blocks.

For the past 50 years, the main route for ECH production was through the propene chlorination to allyl chloride, further oxidated to dichloropropanol (DCP) (see Fig. I-31a). DCP was then ring-closed using sodium hydroxide. This was a particularly competitive pathway because of the low cost of the reagents and process efficiency despite the high toxicity of all involved compounds (chlorine, allyl chloride) [275]. In the late 2000s, a more sustainable pathway was developed, starting from glycerol to epichlorohydrin (GTE process) [275, 276]. This process is more straightforward, with the chlorination of glycerol by hydrochloric acid (see Fig. I-31b) using a carboxylic acid catalyst (typically caproic acid) at moderate temperature (70-120°C) to obtain the key DCP intermediate. DCP can then be closed to ECH in the same manner as starting from propene.

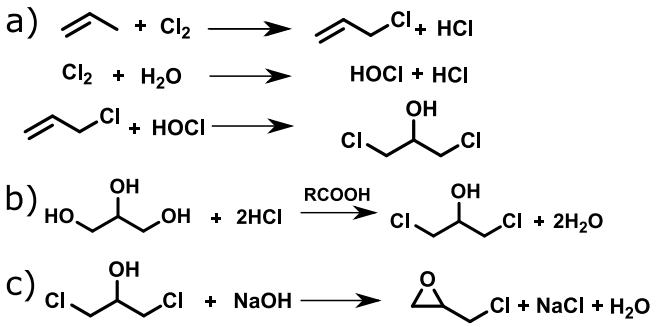

Figure I-31 – Routes to synthesize epichlorohydrin. a) petro-based pathway to dichloropropanol, b) (bio-)glycerol route to dichloropropanol, and c) final synthetic step from dichloropropanol to ECH.

This process was patented and commercialized by Solvay under the brand name Epicerol® with a production capacity of about 100 kt/yr [277]. They claim a 60% GWP reduction compared to the traditional process, consistent with the available literature data [278, 279]. Moreover, the global production of glycerol has jumped since the beginning of the 21st century due to the increase in biofuel production and the generation of glycerol as a by-product. The valorization of this waste is a good example of creating complementary value chains in a circular economy and providing additional revenue streams for bio-fuel producers [277].

Current efforts now focus on finding alternatives to BPA, through renewables routes and reducing risk for health [280]. The possibilities of sourcing bio-derived phenols and amines have been discussed in section I.5.1.

To the author's best knowledge, there is no commercialized bio-derived phenol epoxy. Partially biobased epoxy is, however, commercialized, such as Greenpoxy® or Fairpoxy® with biobased contents ranging 20-56%. This bio-content only includes the epoxy part and not the hardener, that is, amines are still petro-sourced. The final biobased contents range from 14-45%. The most common formulations include bio-based butanediol diglycidyl ether as a reactive diluent, largely available with DGEBA. For the highest bio-content, bio-ECH is used to produce DGEBA, leading to 33% of bio-carbon in it.

Scientific literature has extensively explored alternatives to replace BPA. Indeed, BPA is an endocrine disruptor that mimics estrogen and has anti-androgen capacities, causing damage to different tissues and organs, including the reproductive system, immune system, and neuroendocrine system [280].

Recently, Witthayolankowit et al. [193] proposed a comprehensive study on developing a biobased epoxy derived from bis-guaiacol. The guaiacol was extracted from birch bark. The epoxy was cured with a bio-derivable anhydride and used as matrices with hemp reinforcement, providing a fully biobased composite. They demonstrated no endocrine activity for the epoxy. They investigated the

environmental footprint (see Fig. I-32) and demonstrated the benefits of their strategy but highlighted the importance of valorizing all compounds of the lignin treatment to create an economical and environmentally beneficial value chain [187].

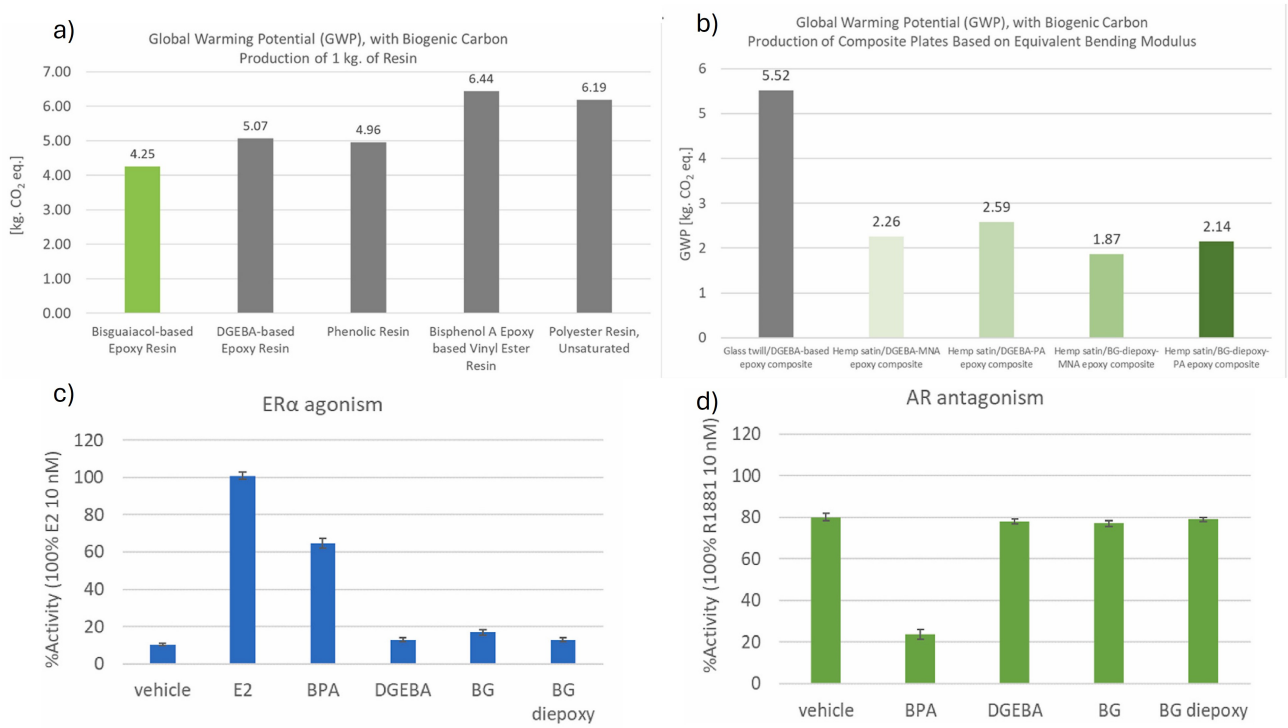

Figure I-32 – GWP as determined by an LCA for a) production of 1 kg of bis-ethylguaiacol epoxy (BG) and other benchmark resins, b) production of one hemp fibre reinforced composite plate and compared to a glass-fibre reinforced epoxy composite plate, all with an equivalent bending stiffness. c) Oestrogen receptor agonistic activity of chemicals, and d) androgen receptor antagonistic activity of chemicals. Vehicle is DMSO. Reproduced with permission from [193].

Other strategies have been deployed to develop bio-based epoxy resins that are easily depolymerized. Wu et al. [219] developed a system based on epoxidized FDA and a lignin-derived cyclo aliphatic diamine [197], thus avoiding the use of BPA and MDA (see Fig. I-33). By this approach, it remains a conventional epoxy-amine system with high T_g (around 170 °C), low sensitivity to water, and satisfying mechanical properties, suitable to manufacture glass fiber and flax fiber composites. More importantly, the incorporation of ester moieties in the presence of tertiary amines allowed the internally catalyzed depolymerization by methanolysis of esters at low temperatures (70 °C, 48 h). The process was selective and enabled the recirculation of all compounds after purification. No LCA was performed, but positive results might be expected as FDA in polyethylene furan dicarboxylate (PEF) was reported beneficial compared to petro-based compounds [218, 281], as well as lignin catalytic depolymerization [189]. However, these should be confirmed through dedicated cradle-to-cradle analysis, considering the

recycling steps and yields.

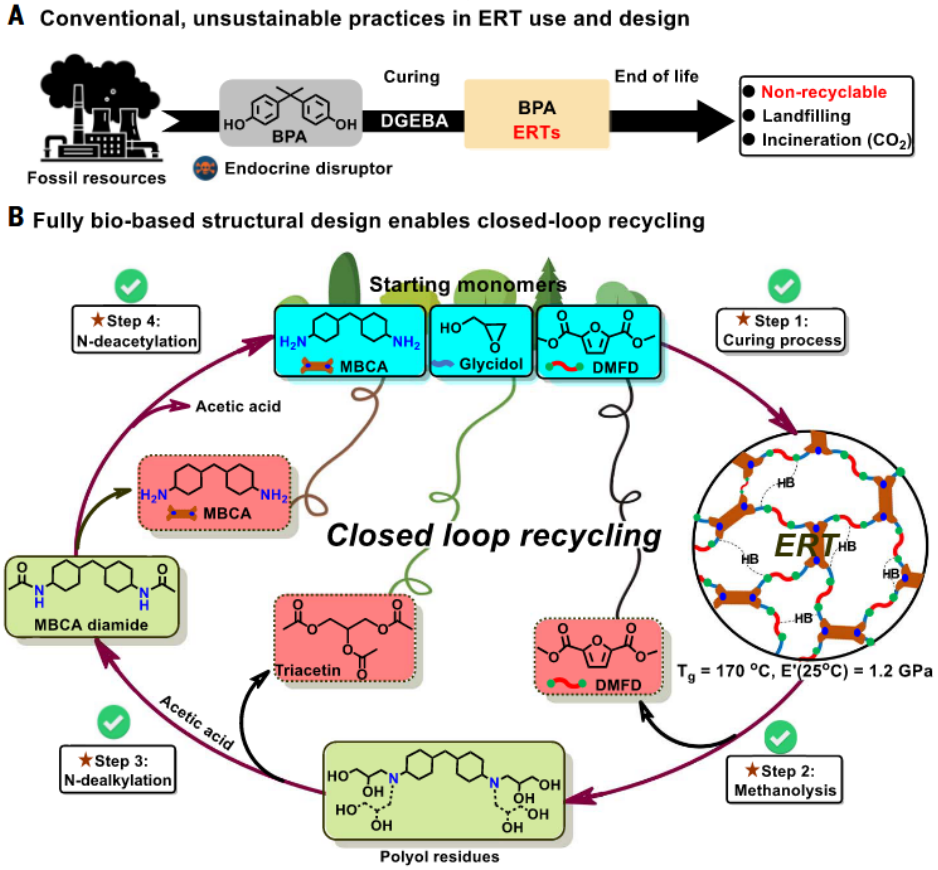

Figure I-33 – Schematic representation of the closed-loop of epoxy materials developed by Wu et al. as compared to the conventional BPA route. (A) The unsustainable status quo of BPA-based thermosets sourced from fossil resources. (B) Synthesis and closed-loop recyclability of a fully biomass-derivable epoxy resin. From [219]. Reprinted with permission from AAAS.

A parallel approach was developed by Rorrer teams, named PECAN (polyester covalently adaptable network) [205]. This interesting strategy is based on already commercially available building blocks. By reacting biobased epoxy derived from sorbitol and butanediol with methylhexahydrophthalic anhydride (MHHPA), a liquid anhydride, they obtained fully biobased epoxy-based polyesters. The properties are similar to benchmark epoxies with glass transitions of about 100 °C, modulus 1-3 GPa, and elongation of about 3-4%. The formulations have low viscosity, below 0.5 Pa.s, suitable for composite manufacturing. They demonstrated positive environmental results compared to epoxy anhydride with a GWP reduction of about 35% (see Fig. I-34). Although an increase by 25% of costs was estimated, and could represent an economic burden for some industries, it remains commercially relevant. The technology was successfully implemented into a GFRP wind-blade [282]. They demonstrated creep resistance and advanced weathering resistance compared to DGEBA epoxy and the thermoplastic

Elium®.

Using methanol and a base catalyst (K_2CO_3), they successfully depolymerized the network within 7 days at 50 °C or within 6 h at 225 °C by batches of 500 g. The recovered glass fibers were of high quality. The polymer matrix was degraded into a polyol that was subsequently used as a crosslinker for polyurethane (open-loop) and a methylated diester, which was reconverted to the initial hardener (close-loop). Unfortunately, the LCA was not performed on the recycling of the composite nor the matrix, and the temperature and solvent proportion might hamper true benefits. Despite this, their work pioneered the exploitation of competitive bio-derived epoxy through a drop-in approach within existing manufacturing techniques. This opens the door to the recycling of large composite structures. Their approach should be extendable to many epoxy-anhydride systems with minimal adjustments.

Other bio-based epoxy and alternatives to BPA have been investigated over the last two decades [283], exploring bio-phenols [181], such as vanillin [284], resorcinol or eugenol [285] and cyclic polyols, such as isosorbide [286]. These results demonstrated similar properties to DGEBA, but characterizations were not thorough enough regarding the applicability of these materials. Parameters such as viscosity and curing behavior, weathering, and environmental durability were often missing. Despite their importance, LCA and techno-economic analyses are not often conducted due to the complexity of implementing such work alongside the chemical developments of new resins.

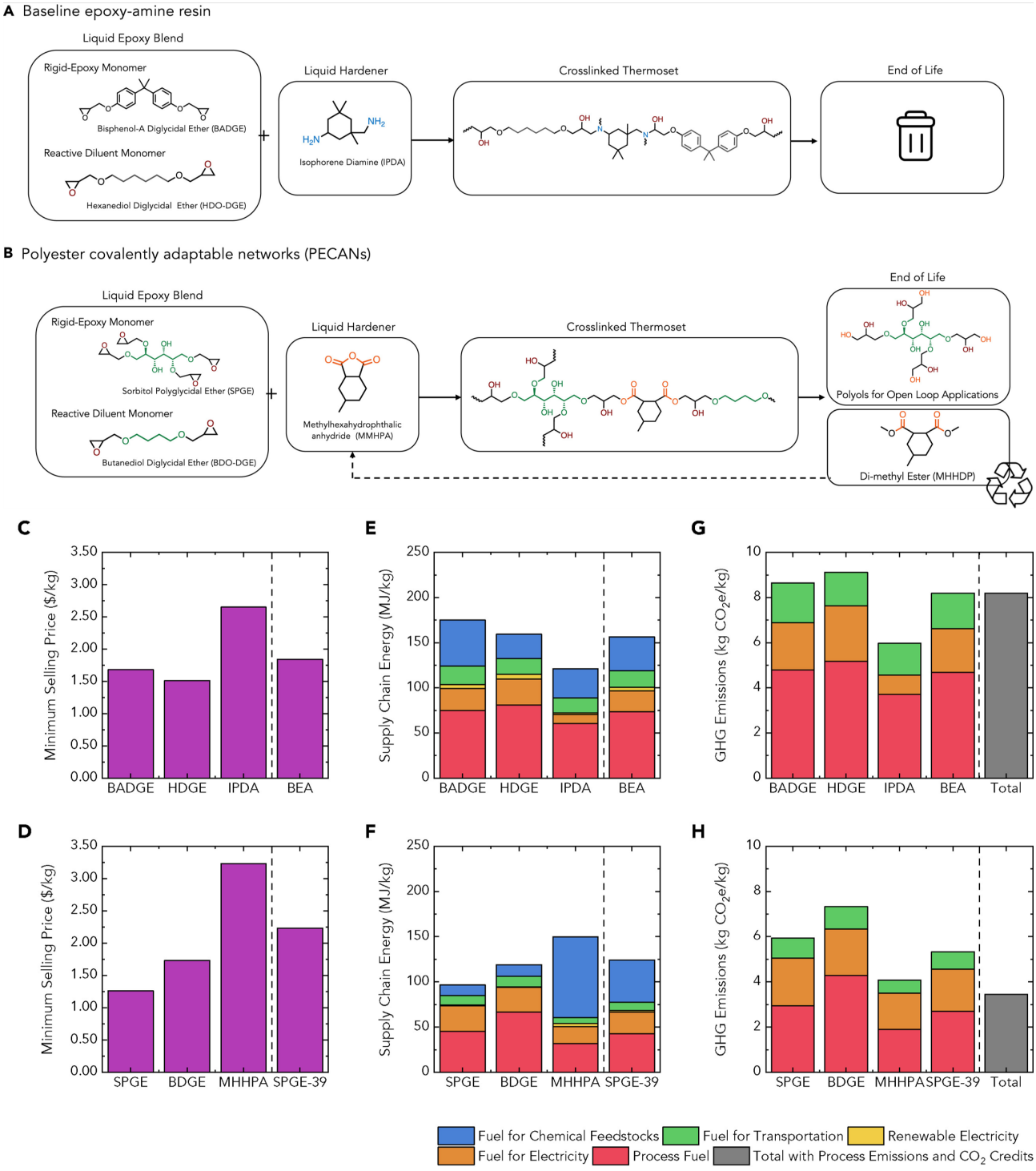

Figure I-34 – Polyester Covalent Adaptable Network (PECAN) strategy to obtain cost-competitive biobased epoxy network with low environmental footprint. a) Benchmark DGEBA-based epoxy resin, b) PECAN constituents and depolymerization (methanolysis) route, c-d) Minimum selling price estimation for the constituents and resin, e-f) cumulative energy demand for the resin production, and g-h) estimated greenhouse gases (GHG) emissions, including curing, for DGEBA-IPDA and PECAN resins respectively. Reproduced and adapted with permission from [205].

I.5.3.3 Towards recyclable epoxides - Between cheap yet not selective and expensive yet full recovery

Aside from the few mentioned works that developed a comprehensive approach to tackle the issue of epoxy-based composites by designing the resin, the EoL of these stable thermosets (epoxy-amine) remains an issue. The Recyclamine® commercialized by Aditya Birla (previously sold by Connora) incorporates acetal linkages in the amine hardener. Under acidic conditions (acetic acid), these linkages are cleaved, allowing the recovery of the fibers on one side and a thermoplastic on the other side [287]. The LCA on the recycling processwas shown positive [288], but the chemical synthesis of the Recyclamine® is not taken into account, while it can involve several steps and the use of toxic reagents [289, 290].

Epoxy-specific depolymerization protocols have been developed over the last decade towards two main strategies. The first one focuses on unselectively depolymerizing the EP under mild conditions to retrieve the fiber efficiently, often exploiting oxidative procedures. The second one is the selective catalytic cleavage of specific bonds to retrieve valuable compounds in addition to the fibers.

Unselective oxidative cleavage has been achieved with several strategies. In general, an oxidant such as hydrogen peroxide or tert-butyl hydroperoxide (TBHP) is used with a solvent and sometimes a catalyst. The pathways involved the formation of radicals that can cleave aryl-ethers and C-N bonds in the network [291]. A suitable solvent is required to swell the epoxy network, thus facilitating the penetration of the solution and the solubilization of the degraded products. Acetone [291], DMF [292], and acetic acid [293] were efficiently exploited with hydrogen peroxide to recover carbon fibers. In all cases, depolymerization took place at ambient pressure, temperature from 50-100°C, and time between 0.5-6 hours. The recovered CF did not show any signs of degradation, with limited surface oxidation. However, the degraded matrix can hardly be valorized, and no LCA was performed. Recently, Wang et al. [294] used $FeCl_2$, with acetonitrile (ACN) and TBHP to depolymerize epoxy resins; the degraded product was exploited as an adhesive with medium shear strength. Again, no LCA was performed. If the interest in recovering carbon fibers seems obvious, comparing the different approaches and reagents would help in designing industrial strategies.

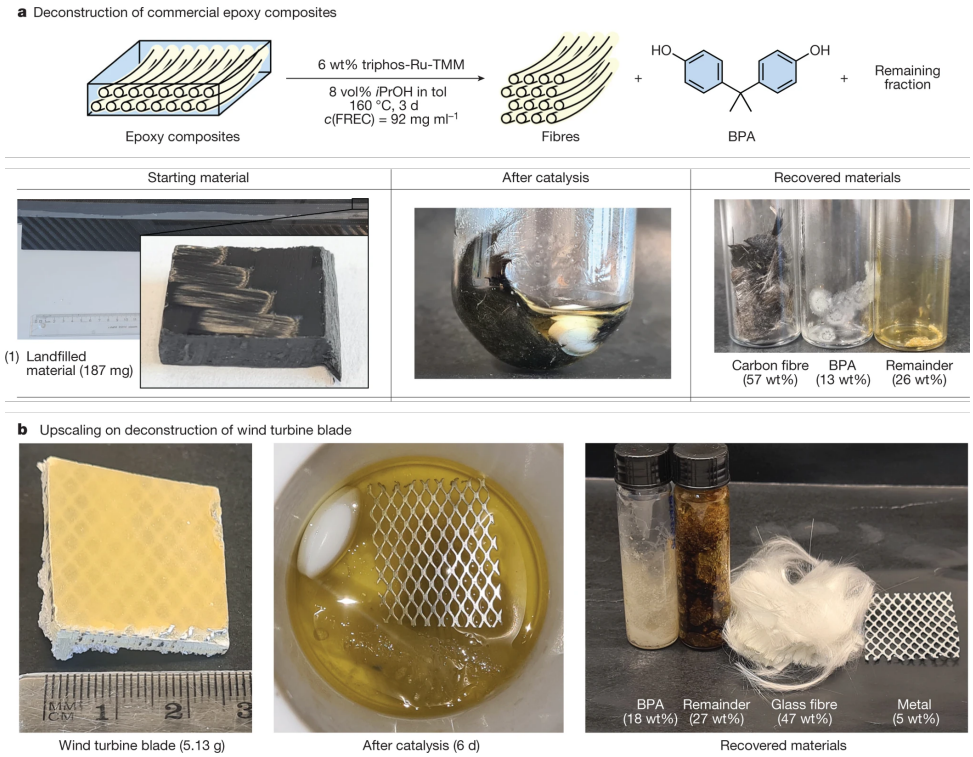

Figure I-35 – Recovery of BPA and fibers from commercial epoxy composites using Ru catalysis by Skrydstrup et al. a) Schematic of the strategy and example of a CFRP previously landfilled subjected to catalysis, b) Upscaling of deconstruction conditions on wind turbine blade. Reproduced and adapted with permission from [295].

The selective cleavage of covalent bonds is particularly challenging. Cleaving ester moieties is "easy" because they are labile [296]. However, the C-O-C and NR3 bonds in epoxy amine thermosets are much more challenging. Lately, the catalytic cleavage of C-O bonds was reported by Skrydstrup et al. [295]. Using a ruthenium catalyst with isopropanol as a hydrogen donor in toluene, they recovered BPA, with a yield of around 80% in model systems and of about 50% in epoxy resin. The procedure was extended to other (bio)phenolic resins. The fibers and aluminum parts were also recovered from turbine blade samples (see Fig. I-35). The remaining resin was considered wasted. This work is the first to provide well-defined compounds from the depolymerization of epoxy. However, the conditions used (24 h at 160°C) and the reagents, in particular the availability and cost of the ruthenium catalyst, may limit the approach to the lab scale. The environmental footprint of virgin petro-based BPA and the recovered one should also be considered.

Overall, the depolymerization of epoxy resin and the recovery of synthetic fibers have shown to be feasible. However, the optimization, as well as economic and environmental relevance, still needs to be addressed. It is important to note that to date, except for using Recyclamine [297], the recovery of natural fibers has not been achieved. NFs would require much milder conditions as they are less

chemically stable, and pyrolysis is not suitable.

I.5.4 Polyurethanes- Rising use and concerns

Polyurethanes (PU) rank as the sixth most produced polymer worldwide. Depending on the starting monomers, PU can also have a wide array of properties, from elastomeric to rigid, but they are mostly used as thermosets for cellular materials (soft and rigid foams).

I.5.4.1 A large thermosets market but marginal in composites with potential outcomes?

Despite their elevated volume produced and low cost, PUs represent only a negligible share of the composite market. However, PUs exhibit many advantages and potential for use in composites, including low cost, high reactivity, and versatile properties. They can have properties ranging from elastomeric to rigid with T_g up to 120 °C and showcase higher toughness than epoxy, with similar strength and stiffness [175]. They are also more resistant to abrasion and crack propagation than epoxy resins [298].

The limited use of PU in composites can be traced back to the traditional methods of composite processing. Historically, most of the composites were produced handcrafted by hand lay-up [41] either using prepreg or by manual impregnation of dry reinforcement. These manual processes were made in an open environment, with workers easily exposed to volatile compounds. This method is still a common practice used in sports, leisure, and aerospace. Polyurethanes result from a step-growth polymerization between polyols and polyisocyanates [299]. Isocyanates have been known for a long time as potent sensitizers and classified as carcinogenic, mutagenic, and reprotoxic [300]. For instace, methyl isocyanate was involved in the Bhopal disaster in 1984, causing thousands of dead, injured, and permanent disabilities with long-lasting effects; the decontamination efforts took 15 years [301]. They are now facing stricter REACH regulations, with a strong push towards their ban [302]. Additionally, typical isocyanates have low vapor pressure, facilitating the risk of worker exposure. Isocyanates are also sensitive to water, which hydrolyzes the isocyanate into amine, thus requiring dry working conditions (see Fig. I-36). Considering such issues, PUs have not been an ideal choice for facile composite manufacturing.

However, the increasing use of injection techniques, like resin transfer molding, has changed the game. The implementation of composites in automotive also pushes towards fast curing procedures. In that sense, the workers are much less exposed to the resins, and bi-component resins, can be mixed

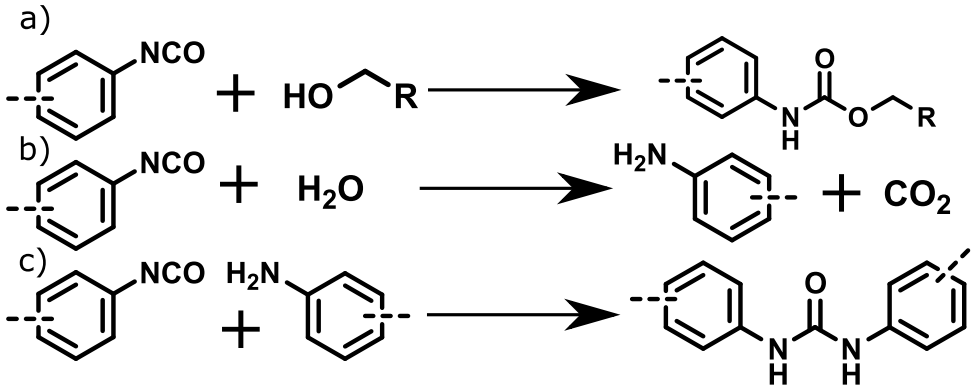

Figure I-36 – Polyurethane polymerization and main isocyanates side reaction. a) Principal urethane formation from isocyanate and alcohol, b) isocyanate hydrolysis to amine and carbon dioxide, c) urea formation from isocyanate and amine reaction.

automatically during the injection process and cured within minutes [303]. In such processes, PUs showcase advantages over other resins. Polymerization can be achieved within several hours at a temperature between 60-100°C. Using a catalyst (typically a Lewis acid), the time can be reduced to minutes or curing can take place at room temperature [299]. PUs suppliers such as Henkel or Huntsmann are now selling low-viscosity formulations suitable for Resin Transfer Molding (RTM, see section I.6), and some studies demonstrated promising results, even with natural fibers, particularly considering moisture resistance [304]. Faster production cycles intend to offer potential energy and production savings while generalizing low-cost, high-performance composites, which would help reduce service life footprint by weight savings.

I.5.4.2 The problem of the building blocks - Sourcing &toxicity

The rise in exploiting PUs in composite structures does not reduce the problems initially mentioned, i.e., the fossil sourcing of the monomers and the toxicity of isocyanates. Catalysts needed for rapid curing, typically tin-based, such as dibutyltin dilaureate (DBTDL) are also highly toxic [299]. Interestingly, stricter regulations concerning PU and the demand for renewable raw materials in typical PU applications have already paved the way for more sustainable alternatives.

For instance, rigid PU thermosets usually require molecular diols and polyols such as ethylene glycol, cyclohexyl dimethanol, and glycerol. Routes towards the bio-sourcing of these compounds already exist, with pilot and industrial scale implementations all over the world [299].

The industrial production of isocyanates is typically performed by phosgenation of amines [305]. The most common isocyanates are MDI, toluene diisocyanate (TDI), isophorone diamine (IPDI), and hexamethylene diamine (HMDI). Access to bio-based amines, particularly bio-aniline, which leads to

bio-MDA, has already been discussed, representing a current need and effort for many industries. The second compound for isocyanate production is phosgene. Phosgene is a highly toxic gas that causes acute respiratory distress syndrome. It was used as a chemical weapon during WWI. Phosgene is still the preferred way to produce isocyanates due to of its high efficiency and low cost. The phosgenation process, highly reactive, does not necessarily require a catalyst, but the solvents commonly used during the process, like o-dichlorobenzene, are toxic. Intense efforts are being made to develop phosgene-free routes to obtain (bio)isocyanates [299, 305, 306], exploring dimethyl carbonate or urea reactions with amines or thermal decomposition of carbamates [305]. So far, these strategies are still at the laboratory and exploratory levels.

Caillol et al. successfully synthesized a fully bio-derived aromatic isocyanate from bis-guaiacol, through a phosgene-free method [192]. The resulting PU exhibited properties similar to those of analogous petro-based MDI. However, the environmental strategies developed to obtain bio-based and/or phosgene-free isocyanates have not been enough discussed. Even if phosgene has to be avoided regarding its toxicity, the efficiency and the atom economy of its process, which only generates HCl, will make it difficult to replace. However, the LCA studies using biobased polyols and petro-based isocyanates have highlighted the benefits of bio-sourced PU and the important contribution of isocyanate in the global footprint [307, 308].

Despite the numerous possibilities to avoid the use of phosgene and source monomers from renewable resources, the toxicity of isocyanates will remain a concern. Therefore, new strategies to obtain PU while preventing the use of isocyanates have been explored over the last decade. They may offer decisive advantages in the realm of composites and will be discussed in section I.5.6.

I.5.4.3 Potential for recycling

PUs are widely used for foams, coatings, and fibers (e.g. Spandex ®). PUs are formed of carbamate moieties that can be cleaved upon appropriate conditions. Therefore, the recycling of PUs is relatively advanced [309], as summarized in Fig. I-37.

Most recycling strategies have been developed for PU foams, representing 65% of the market. Mechanical recycling remains the most widespread strategy through crushing and compaction of PU foams resulting into downgraded products [310, 311] but is poorly relevant for composites.

Catalytic chemical depolymerization has been conducted at the laboratory level, but scaling-up is still limited [312]. Depolymerization can be performed by hydrolysis, glycolysis, alcoholysis, and aminolysis. A catalyst, typically a base such as KOH or 1,8-Diazabicyclo[5.4.0]undéc-7-ène (DBU), is

required to activate the stable carbamate.

Hydrolysis of PUs releases CO_2 from the carbamate, leadsing to the recovery of the polyol and the amine. The challenge relies on the depolymerization conditions, often harsh, and the separation of these products. Hydrolysis commonly requires temperatures superior to 150°C [311] for extended periods (5-24 h), leading to high energy consumption. The separation of amines and polyols usually demands multiple purification steps, such as liquid-liquid extraction, which are both time- and solvent-consuming.

Glycolysis is the most developed PU depolymerization process, widely exploited in industries [309,313]. Glycolysis is traditionally performed by exploiting base-catalyzed transcarbamoylation in the presence of ethylene glycol. This generates short carbamate molecules and the recovery of the polyol. The two compounds are not miscible and lead to an in-situ phase separation [312] into polyol-rich and carbamate-rich phases. This process still requires high temperature and energy that can hamper its benefits, with some LCA analyses demonstrating a negative impact compared to virgin petro-based PUs [314] due to the higher isocyanate content need to compensate for properties depletion.

Alchoholysis, using methanol, may also offer solutions towards milder depolymerization processes [315]. In general, hydrolysis, alcoholysis, and glycolysis allow high depolymerization yields, but separation and purification showcase low purification yields. Recently, an acidolysis process developed by Bech et al. [316] has allowed the direct recovery of the amine and polyol in high yield (90%).

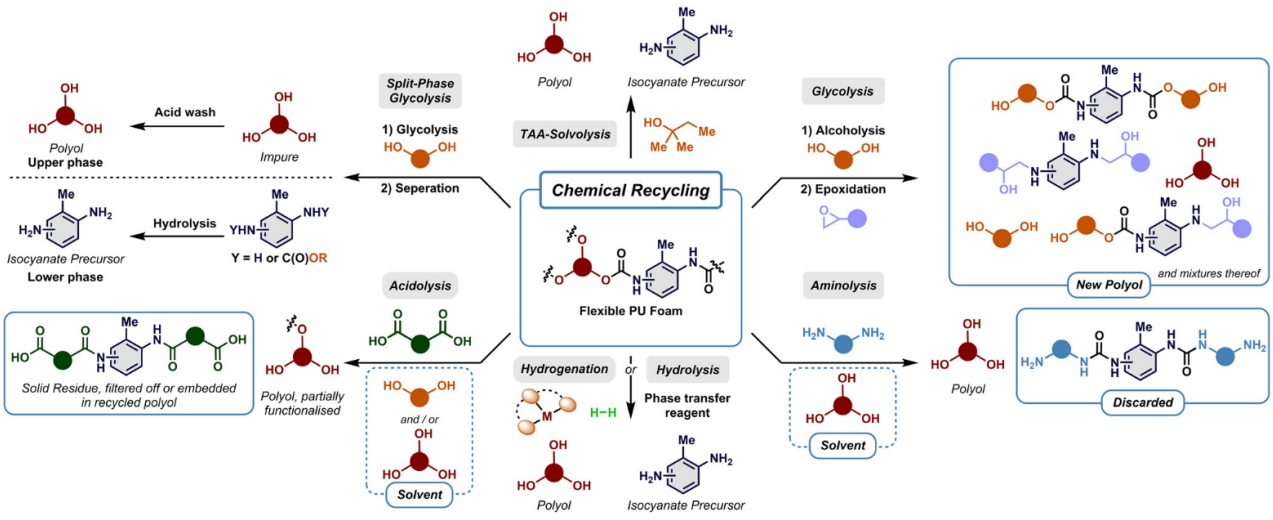

Figure I-37 – Chemical recycling methodologies for PU foam. TAA: tert-amyl alcohol. Reproduced with permission from [316].

In some cases, urethanes can be enzymatically degraded [309]. This is only possible under specific conditions and in the presence of specific enzymes such as urethanase [257], and the process should not be expected to occur naturally in the environment within a reasonable time frame. Moreover,

PU bulk thermosets may be resistant to enzymatic degradation due to the low contact between the enzyme's active site and the urethane function [317]. Other strategies could also rely on the integration of enzymes during the polymerization to trigger the depolymerization when needed [318]. Up to now, with scientific advances, urethanase and bacterial degradation could offer an alternative pathway to recirculating PU-based composites.

I.5.5 Covalent Adaptable Networks - Bridging thermosets and thermoplastics, but still a lab curiosity rather than a market reality

Thermoset matrices offer the best properties for structural composites. They can efficiently wet fibers through several processes, particularly infusion-based, and provide improved interfacial adhesion, key parameters towards high performance. In addition, they offer satisfying longevity and environmental resistance, ensuring a long service life and reducing the need for maintenance and replacement. On the other hand, their stability makes the treatment of decommissioned structures problematic. Thermoplastics offer better options for EoL, but wetting of the fibers is more complex than with thermosets, and thus, the quality of the interface is poorer, resulting in lower performances [36].

Another approach that potentially gathers the advantages of both thermosets and thermoplastic is based on Covalent Adaptable Networks (CAN). They are crosslinked polymer networks, similar to thermosets, but they possess dynamic crosslinking nodes that can be triggered on-demand. This allows the network to be reworked, even after gelation [319].Consequently, CANs display the reprocessability characteristics of thermoplastics (see Fig. I-38).

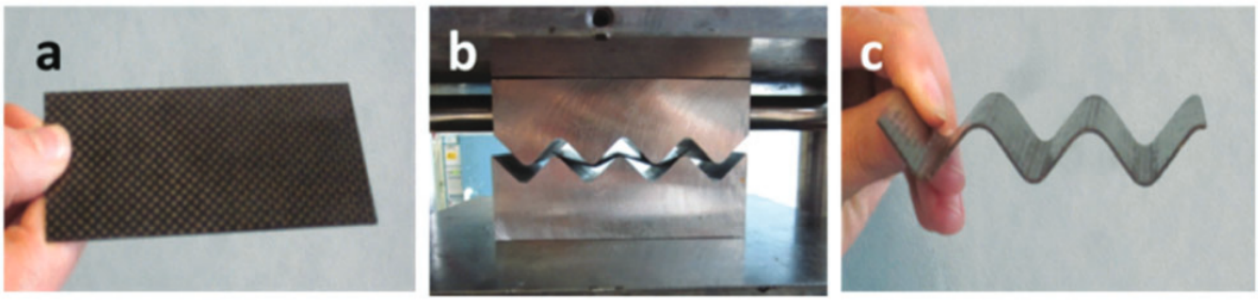

Figure I-38 – Thermoformation of cured composite laminate exploiting epoxy CAN with dynamic disulfide. A 2 mm thick carbon fiber reinforced dynamic epoxy laminate (a) was compression-molded in a zig-zag-shaped mold (b), rendering a thermoformed wavy 3D part (c). Reproduced with permission from [320]. Copyright 2016 Royal Society of Chemistry.

I.5.5.1 Historical and fundamental background of CANs,

The concept of bond exchange in crosslinked polymers dates back to the late 50s [321]. Reversible gels and polymers were reported in the 80s [322] and 90s [323–325], in particular by Rubinstein group, but they faced limited possibilities and applicability. In 2002, Wudl et al. [326] developed a polymer network that can "re-mend" itself by exploiting the reversible Diels-Alder addition reactions. Such networks are known self-healable polymers. An other work led by Lehn explored reversible covalent networks such as "dynamers" [327]. Bowman and co-workers introduced the concept of CAns [328, 329]. In parallel, Montarnal et al. exploited transesterification in epoxy through the curing of epoxy with carboxylic acid and a Zn-based catalyst to obtain a permanent crosslinking that can be reprocessed [330]. This specific class of CANs so, so-called "vitrimers," possess a temperature-viscosity relationship following an Arrhenius relationship by analogy to vitreous glass.

From a mechanical viewpoint, CANs differ from thermosets through their ability to relax stress above a specific temperature, usually called vitrification temperature or topology freezing temperature (T_v) [331, 332]. If the glass transition is superior to Tv, the chain mobility is not sufficient to allow relaxation within a realistic timeframe. Typically, CANs, particularly those with a high glass transition, are characterized under small deformations to remain within their linear viscoelastic region [333]. In that case, a Maxwell model can be adequate (see Fig. I-39). However, many complex chemical and physical mechanisms can take place at the same time. Therefore, more sophisticated models, such as the generalized Maxwell model (Wiechert model) or stretched exponential models, are sometimes used to better represent the mechanisms that take place. There is still no recognized standard for the characterization of CANs, nor unique methods. The most accepted method remains the stress relaxation experiment, mostly under shear (in a rheometer) or tension (in a DMTA apparatus), to demonstrate the ability of the crosslinked polymer to release internal stress through rearrangement of its internal structure. However, this stress relaxation ability makes CANs more sensitive to creep [334], in contrast to thermosets. Creep must be considered when designing load-bearing structures, which could be detrimental to long-term performances [335].

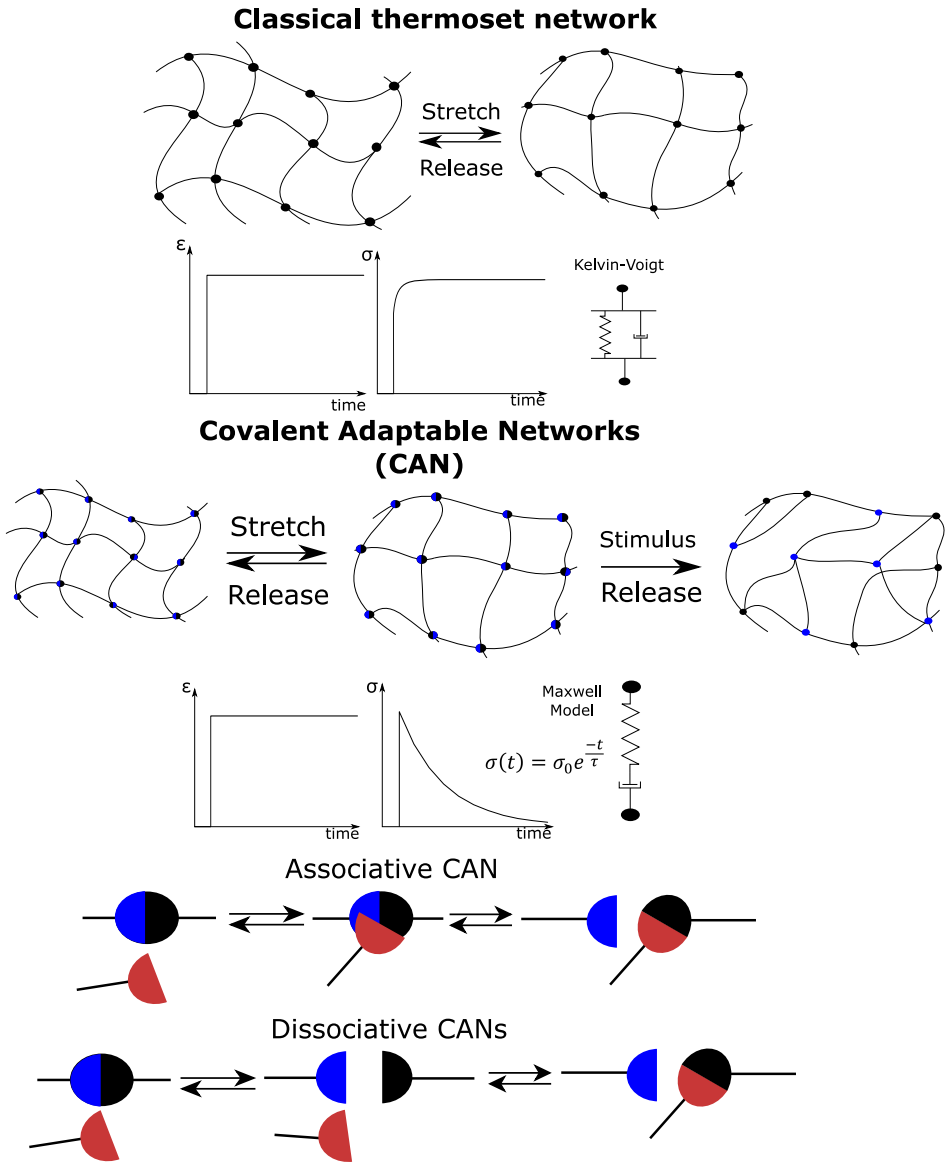

Figure I-39 – Schematic representation of thermoset upon applied for strain/release and CAN upon strain/release in the presence of an external stimulus to trigger exchange reactions. Figure inspired from [336].

I.5.5.2 The diversity of CANs and their relevance in composites

The most common classification of CANs distinguishes dissociative and associative CANs. In dissociative CANs, the dynamic moieties are temporally dissociated to react with the free functional groups [331]. The network connectivity is thus partly reduced. In associative CANs, also called vitrimers, the free reactive functions connect as initial bonds break, maintaining a permanent crosslinking density [331]. It is important to note that if associative and dissociative networks tend to differ in rheological behavior, both can showcase a "vitrimer-like" behavior. The most meaningful point is that upon certain conditions, such as swelling in a good solvent, the equilibrium of dissociative CANs can be switched

towards dissociation and thus allow the dissolution of the network [241]. Associative CANs are more stable and cannot be simply depolymerized. Several dynamic moieties can undergo both associative and dissociative exchange reactions, particularly playing on reaction conditions and catalysts [337]. For the sake of simplicity, the distinction between associative and dissociative will not be made in the rest of this state of art. However, it might imply significant changes in chemistry, applications, and limitations. In particular, many dynamic moieties can exhibit both associative and dissociative behavior [337], and the apparent behavior is often close as the kinetics and thermodynamics of dissociation is not sufficient to observe a sol-gel transition [331].

Ushered by high scientific interests, numerous CAN chemistries, strategies, and materials have been unveiled within the last decade (see Fig. I-40), with extensive literature reviews [270, 338–340], including bio-based [16, 22, 341], and composites [24]. Therefore, this section only intends to briefly reposition CANs in the frame of more sustainable structural composites.

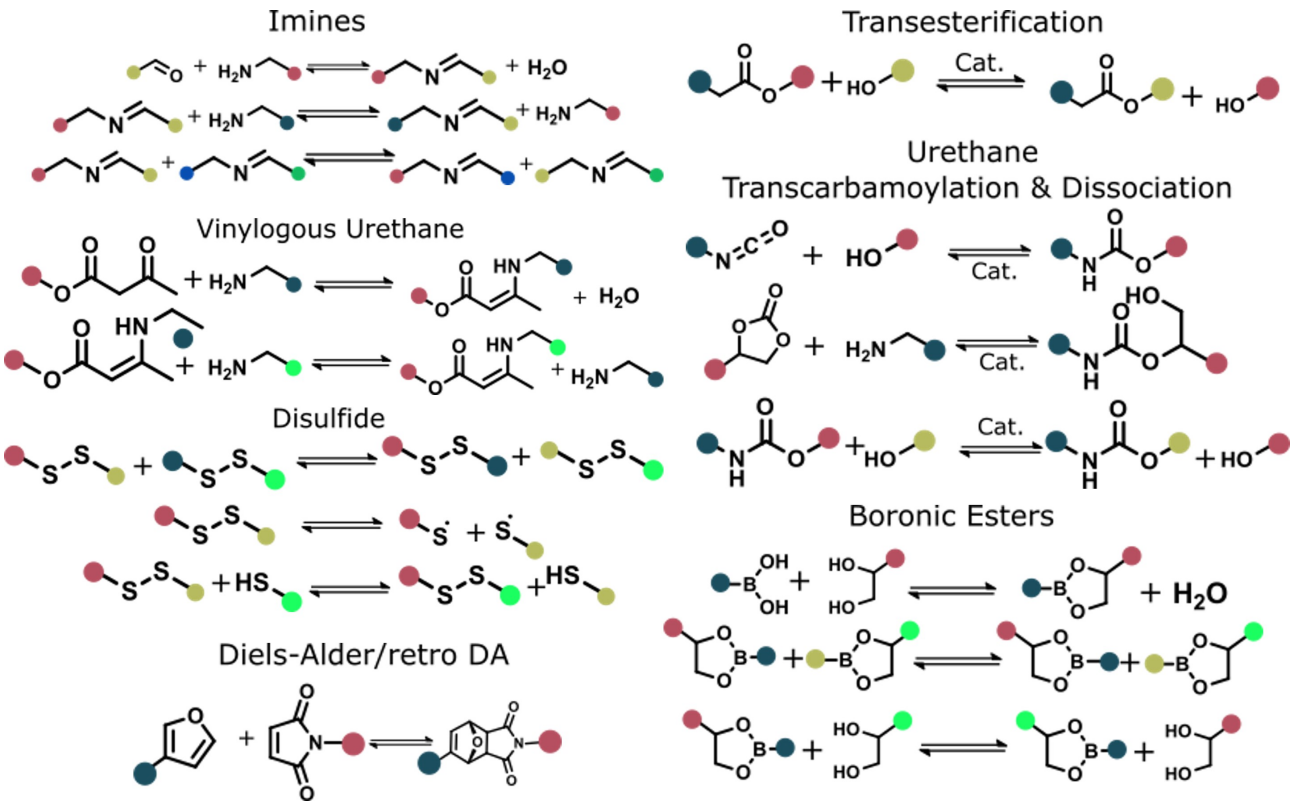

Figure I-40 – Most important dynamic chemistries exploited in composites and exchange reactions.

CANs remain very scarce and at low TRL for industrial applications, probably due to their limited availability on the market and the associated costs. To date, only Mallinda®, an American start-up, commercializes dynamic EP for composites. LCA has been almost not performed for CANs, with only Vora et al. [342] who assessed the environmental footprint of polydiketoenamines. However, their cost

and GWP were yet to meet the results of commodity polymers. By modeling a more efficient and industrial process, they showcase that circular polydiketoenamines can match benchmark polymers. This work highlights the importance of developing LCA-assisted strategies to assess the accurate environmental footprint and cost of CANs, which is severely lacking in the literature.

We propose herein to discuss only two main strategies regarding composites: a) new dynamic networks with potential in composites and b) transforming existing thermosets (i.e., UPR, EP, and PU) into CANs.

I.5.5.3 New dynamic networks for structural composites

The development of new chemistries can leverage significant potential for composites. However, mastering building block synthesis, polymerization kinetics, and properties is complex and usually requires several years of work and increments before achieving a partially optimized form. Moreover, such new chemistries must be scaled before being considered in composites.

This is the case with polyimines, formed from the condensation of (poly)aldehydes and (poly)amines. They were among the first applied to composites [343] thanks to the wide availability of multifunctional monomers. The network is also soluble in an excess of amine, allowing the fibers to be recovered. High mechanical performances were even obtained. Interestingly, imines are highly dynamic and can be processed through transamination in the presence of free amines or through metathesis [344]. The exchange is fast, allowing quick welding processes [343]. However, the implementation of large-scale composites exploiting polyimines is complex, and their sustainability is questionable, although it has not been assessed up to now. The network proposed by Taynton et al. [343] was composed of terephtaldehyde, a toxic aromatic dialdehyde; tris (2-aminoethyl)amine (TREN), a highly toxic polyamine; and several diamines, including ethylene diamine, a volatile and toxic diamine. The condensation of amines and aldehydes occurs spontaneously and generates 1 equivalent of water. To allow the impregnation of the matrix, ethanol was used, which needed to be evaporated, and the formed water also needed to be removed to advance the curing. The formation of imine is reversible; this signifies that in the presence of excess water, they can go back spontaneously to the aldehyde and amine, thus affecting the material integrity. Such questions are fundamental for considering composite applications and hydrolytic stability, and weathering should be investigated if polyimines are to be considered for composites.

Vinylogous urethanes/ureas (VU) were introduced by Du Prez's group as a potential replacement for imine and ester, owing to favorable thermodynamics [345]. VUs are formed through the condensation of

(poly)amine and (poly)acetoacetate (AA). Acetoacetate synthesis is fully scalable and can be considered green as no solvent is required, and purification can be performed through simple distillation. AA can be obtained from any polyols, including biobased like isosorbide [346], accessing a wide array of sustainable building blocks. Like imine, it forms water that need elimination for composite manufacturing. However, the thermodynamics strongly favored the formation of the VU adduct, and thus, water does not affect the extent of polymerization. They are much less sensitive to hydrolysis [345]. The exchange reaction requires an excess of amine but no catalyst; full reprocessing can be obtained within minutes at a temperature below 150°C. The authors demonstrated that they could completely control the dynamicity through the use of an organic catalyst [347]. VU (urea-based) was successfully applied to GFRP by manual impregnation [348] and the welding of cured prepregs was feasible, featuring comparable mechanical properties to epoxy benchmark (E = 40 GPa, σ = 800 MPa). However, two issues might hamper the widespread adoption of VU in composites. The first issue is process-related. The addition reaction between amines and AA is extremely fast and occurs at room temperature; thus, the injection of liquid resin might be challenging to perform in a reasonable time frame before gelation [345], especially impossible for large structures. As aforementioned, the water removal also needs to be implemented in the process. The second issue relates to the highly dynamic nature of VU. TAn excess of amine is needed for the exchange reactions to take place, but they can occur (at a slow rate) at room temperature. This leads the VU to creep, a common issue to many highly dynamic CANs [334]. To deal with such, Du Prez et al. developed several strategies. Eliminating the excess of amines while inserting secondary amines in the vicinity of the enamine defined so-called "masked primary amines", allowing the fast rearrangement at an elevated temperature while suppressing creep [349]. Another approach has been recently developed that consisted of the control of the topology by intermolecular hydrogen bonding of hybrid vinylogous urethane/urea network to control the dynamicity [350]. Finally, the design of switchable catalysts [351] also helps obtain low creep at service temperature and high dynamicity at recycling temperatures. Investigating and characterizing such strategies in applied composite materials could bring substantial benefits to structural materials sustainability, but still, an environmental assessment is yet to be performed.

Boronic esters were first introduced as self-healing polymers [352]. Since then, they have been exploited to provide healable and dynamic CANs, mostly elastomeric [353–355]. Boronic esters are typically used as crosslinkers for linear polymers or oligomers by reacting with pendant vicinal diols [356]. The reaction also generates water that requires elimination procedures. Little information is provided concerning the applicability of this chemistry in composite materials, or their sustainability. Boronic

esters are sensitive to hydrolysis, which can again decrease the stability of the matrix in a humid environment.

Recently, Raman et al. [357] introduced a new strategy to tailor the interface of composites. They inserted dynamic boronic ester functions at the fiber/matrix interface. They created covalent bonding between the fiber and the matrix by functionalizing the CF with a vicinal diol (see Fig. I-41) and modifying a commercial styrene-butadiene linear polymer with boronic functions. A highly efficient stress transfer within the material was achieved, while maintaining its toughness. Through this strategy, they increased the strain and stress of the resulting CFRP by 50% compared to a conventional DGEBA-based matrix, with and 84% improvement in toughness. Importantly, as all crosslinking nodes were derived from these boronic esters, the network was degradable in pinacol, to retrieve the CFs. However, the requirement of solvents (THF and DMF) to manufacture these composites and the complex synthetic steps needed might make this strategy not ready for large-scale composites. In any case, it could be a promising approach to unify the recyclability, properties, and toughness issues of composite.

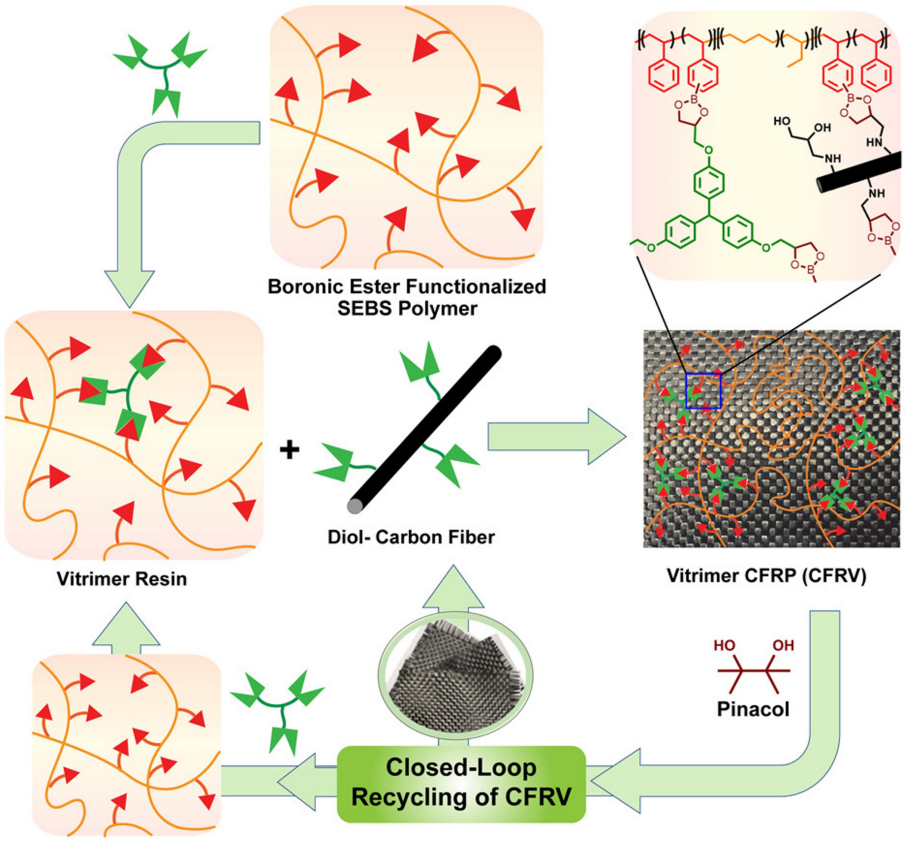

Figure I-41 – Design of CAN with implementation of dynamic boronic ester moieties at the fiber/matrix interface to achieve recyclable mechanically robust CFRP composite. Reproduced with permission from [357].

Many other dynamic networks exist, in particular those arising from click chemistry, such as thiol-enes, acetals [241,358], or β-amino esters [359]. However, access to these novel chemistries remains extremely limited due to the complexity of scaling monomer synthesis to the minimum quantities required for lab-scale composite manufacturing. Additionally, there is limited data available on the truly sustainable aspects of what is sometimes referred to as "green" chemistry, particularly when using hazardous solvents and catalysts. Besides, the characterization of the materials is often insufficient, with a lack of discussions, which further complicates and slows the selection of potential candidates for composite applications. Therefore, the most advanced dynamic networks rely on modifying well-known thermosets.

I.5.5.4 Switching existing thermosets to CANs

A crucial strategy consists of inserting dynamic linkages into existing thermosets, ideally with minor changes. This approach facilitates the implementation of CANs into existing processes and known chemistries. The most prevalent dynamic linkages include esters, urethanes, disulfides, and imines.

Unsaturated polyester resin (UPR) CANs have been poorly investigated, with only 5 articles published so far on this topic. Supposedly, the presence of ester groups should facilitate the transformation of UPR thermosets into CANs, by, for instance, introducing free hydroxyl moieties and a catalyst to enable transesterification. However, this might also affect the properties by plasticizing the UPR. Rizzo et al. proposed a straightforward approach by including a Titanium-derived catalyst, a cheap, non-toxic metal catalyst, into a commercial UPR formulation [360]. Titanium-catalyst efficiently activates the intramolecular ester metathesis. The resulting vitrimer showcased minimal property modifications compared to the benchmark and good properties retention, with 50% modulus recovery after reprocessing. The strategy was successfully applied to a CFRP [361], allowing the healing of the composite. This could help the direct thermo-mechanical recycling of these composites, which is of high interest for EoL management of marine and wind turbines.

The carbamate moieties in polyurethane are also dynamic and they can be involved in transcarbamoylation reactions [362]. However, to adequately perform these exchange reactions, PU CANs require an excess of free hydroxyl groups and a catalyst [362]. Tin-based catalysts are the most efficient but are highly toxic. Interestingly, they also help the polymerization, limiting the multiplication of compounds. The excess of polyol leads to a lower gel content of the polymer decreasing in the stability and properties of the networks. Aromatic amines containing dynamic disulfide were successfully implemented into PU-based GFRP, allowing reshaping and welding of the composite [363].

However, the process is solvent-based and appears not suited for large-scale composites. Other dynamic functions such as imines and esters were also implemented into PU networks [364] but are not relevant for the industrial scale of composites.

Finally, dynamic moieties have been largely implemented into EP resins. Ester dynamic moieties were first introduced by Montarnal et al. [330]. Free hydroxyls and dynamic esters can be directly formed from the reaction of epoxy and carboxylic compounds, creating a CAN in the presence of a catalyst (Zn-derivative). Using epoxidized diamines and a carboxylic acid curing agent, the catalyst can be avoided, exploiting the internal catalytic effect of the amine [365]. The latter was successfully implemented into CFRP and could be depolymerized in the presence of ethanolamine.

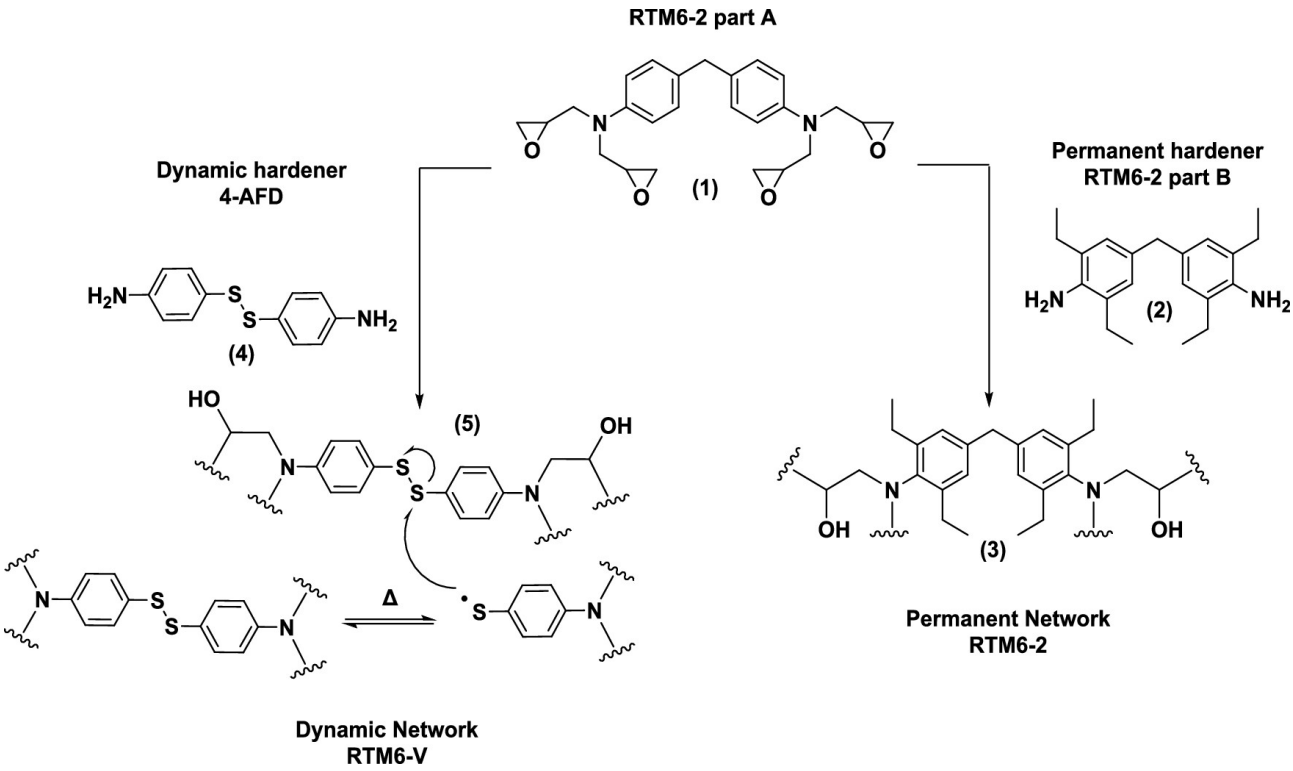

Figure I-42 – Aerograde epoxy-disulfide CAN for Resin Transfer Molding of CFRP. Reprinted with permission from [366]. Copyright 2023 American Chemical Society.

Disulfide metathesis is widely exploited to obtain dynamic EP [320]. They are probably the most advanced for composites [24, 320]. Amine crosslinkers containing disulfides such as aminophenyl disulfide (APDS, aromatic) or cystamine (CSTA, aliphatic, biobased) can be easily incorporated into EP resins. Recently, Schenk et al. [366] demonstrated that APDS can be used to successfully prepare high-performance aero-grade CFRP by resin transfer molding (Fig. I-42), with a glass transition of 232 °C. A time-temperature-transformation (TTT) diagram was developed to control the curing progress through infusion, representing the first TTT diagram of CANs.

Based on imines that are constructed from the condensation of aldehydes (or ketones) and amines, several imine-containing epoxies have been explored for composites, primarily exploiting vanillin for biosourcing, and already containing a free-alcohol and aldehyde [367–369]. This chemistry is exploited by Mallinda ®, with T_g up to 130°C obtainable. However, as the formation of imines generates 1 equivalent of water, most processes are conducting by preparing an imine-containing epoxy, which is later polymerized. This strategy leads to high-viscosity monomers that often require solvents [367], representing a drawback in composite manufacturing. Nonetheless, eliminating the formed water by imine condensation is feasible, depending on the composite process, and might be of interest if properties, cost, and environmental benefits compensate the complexity of the process.

Other dynamic functions have been successfully implemented into epoxy, such as siloxane-containing diamines [370], which allow fast reprocessing of composites, including flax-reinforced one [170]. The properties were retained after reprocessing. This hardener presents very low viscosity, allowing the efficient infusion of the resin within the reinforcement. T_g up to 85°C were obtained. One drawback might arise from the need for a catalyst, 1,5,7-triazabicyclo[4.4.0]dec-5-ene (TBD), in high content (10%) needed for the process. TBD is an expensive and corrosive catalyst that is not registered under REACH regulations.

Although dynamic systems encompass many properties, no single CAN can fully meet the diverse and often competing demands for high performance and elevated dynamicity. Various dynamic bonds have been incorporated into these networks to achieve the necessary tunability. Recently, Serra et al. [371] introduced an epoxy vitrimer featuring dual relaxation mechanisms based on imine and disulfide linkages, enabling a straightforward access to a biobased epoxy network with balanced intermediate properties. However, the dual vitrimer copolymerization approach necessitates additional complex synthetic processes, posing a significant challenge to industrial scalability.

Significant efforts have been devoted to expanding the understanding and diversity of CANs, including their applications in composites. However, a fully satisfactory solution has yet to be achieved. Key challenges remain in combining competitive properties with availability, sustainability, and recyclability. In this context, investigating other emerging chemistries could prove highly valuable, particularly in the case of non-isocyanate poly(hydroxy)urethane as discussed in the forthcoming section.

I.5.6 Non-Isocyanate Poly(hydroxy)urethane, CAN between epoxy and polyurethane; an emerging pathway towards sustainable composites ?

When discussing the potential of conventional polyurethanes in more sustainable composites, the issue of isocyanates appears predominant. Their hazardous character, combined with the high toxicity of phosgene required for isocyanate synthesis and their detrimental environmental footprint [307] make their replacement appealing.

In that aim, a growing interest has surged since 2010 to develop non-isocyanate polyurethanes (NIPU) [372]. There are many routes to obtain NIPU [373]. However, only a few appear to be pertinent in the frame of a circular and sustainable economy. Among them, poly(hydroxyurethanes) (PHU), a family of NIPU, has garnered significant attention. These resins can readily derive from renewable precursors, particularly CO_2 [230], offering modular and high-performance properties, making PHUs considered viable and sustainable alternatives to traditional PU [374].

PHUs are produced through a step-growth reaction between polyamines and polycyclic carbonates (CC). One of the best promises lies in the synthesis of CC which are easily accessible from the cycloaddition of CO_2 into (bio)epoxy (Fig .I-43) [230]. The process has been demonstrated to be easily scalable, with several tens of kg already produced by laboratories [375]. Moreover, the use of CO_2 as a feedstock makes the CC synthesis promising. Besides, using supercritical CO_2, no solvent is required and easy to obtain ($T > 30°C$, $P > 73$ bar). The carbonation of epoxy was shown to give minimal waste with a low E-factor [376], as no purification is required. Cheap catalysts with low toxicity, such as ammonium halide, provide quantitative yields [230].

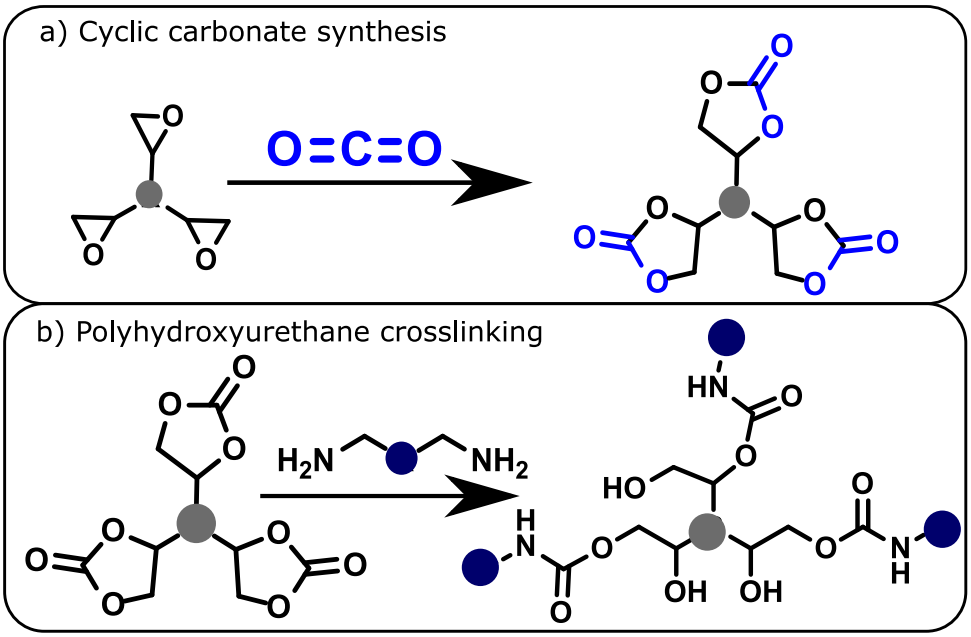

Figure I-43 – Polyhydroxyurethanes, emerging sustainable CANs. a) Obtention of cyclic carbonates from epoxy and CO_2, b) Aminolysis of cyclic carbonates to polyhydroxyurethane network.

The (macro)molecular structure of PHUs differs from PUs through the presence of hydroxyl groups pendant along the main chain skeleton. This structural feature imparts a more hydrophilic character to the resins and enhances the ability of PHU chains to form multiple hydrogen bonds [377]. The presence of these hydroxyl groups could be particularly advantageous for composite applications by providing tougher interfacial adhesion and forming intricate interactions with natural fibers.

The presence of hydroxyl groups within the PHU backbone has been shown to bring PHU thermosets with superior adhesive and mechanical properties over conventional polyurethanes (PU) [378]. PHU thermosets have shown high versatility ranging from elastomeric to stiff behavior [378,379] depending on their macromolecular structures and the degree of functionality of the CCs [380]. Fleischer et al. [381] used pentaerythritol CC (PEC) and trimethylolpropane CC (TMPTC) with a reactive aliphatic amine (HMDA) to obtain crosslinked PHUs. Their work was among the first to characterize PHU thermoset properties. The modulus of the synthesized PHUs ranged from a few MPa to 2.5 GPa, and elongation at break was superior to 3%. These properties could be suitable for high load-bearing applications. They also investigated the reactivity at several temperatures finding that temperatures higher than 70 °C were needed to obtain complete curing. The need to reach a relatively high temperature for efficient curing was also reported in other studies [372, 382] but was limited due to side reactions at temperatures over 100 °C [372, 383]. Generally, a very high discrepancy in properties was identified, even for identical formulations (see Table I-3). Such differences might come from variations in the curing

process, which has never been thoroughly studied. This highlights the appealing need to study the crosslinking behavior through rheological measurements before implementing such polymeric matrices in structural applications.

Another exciting aspect of PHUs is their ability to be reprocessed thanks to the transcarbamoylation mechanism already known in PU [362]. Monie et al. [384] were able to reprocess self-blown PHU foams, and similar results were observed for water-induced self-blown PHU foams [385]. Fortman et al. [386] studied the adaptative network properties of PHUs obtained from five and six-membered cyclic carbonates through stress-relaxation. They emphasized associative transcarbamoylation exchange reaction within the network. In the case of PHUs obtained from six-membered CCs, the thermal stability of resulting networks allows better reprocessability. In contrast, the degradation and reprocessing temperature for five-membered CC-based PHUs tend to overlap when a high degree of crosslinking is reached. Chen et al. [387] highlighted that PHUs exhibit both associative (transcarbamoylation) and dissociative (reverse cyclic carbonate aminolysis) mechanisms, although stress relaxation was not investigated. Hu et al. [388] reprocessed carbonated soybean oil (CSBO) and sorbitol ether carbonate (SEC) based PHUs, but no stress relaxation test was performed. Moreover, SEC reprocessability was poor due to the high crosslinking degree and higher glass transition temperature. In vegetable oil-based PHUs, transesterification is also considered as a possible mechanism that facilitates the reprocessability of the crosslinked network [389]. If all hydroxyurethane functions can rearrange through transcarbamoylation, the reprocessability of PHUs depends significantly on the network structure and their physical properties. Catalysts were investigated to improve the behavior [390] with DBTDL showing to be efficient to some extent but remaining an unsatisfying solution. Although CANs constitute a significant breakthrough for structural polymer applications [340, 391], the viability of PHUs for such applications must be studied to a more significant extent.

To date, PHUs have only been considered as potential replacements for PUs in their typical applications, such as foams [385, 392], coatings [393, 394], and adhesives [379, 395]. However, this can be limited by the low cost and high chemical efficiency of PUs. Alternatively, the numerous opportunities leveraged by PHUs could make them ideal candidates for more sustainable composites if developed, optimized, and characterized adequately for such applications. More than PUs, the features enabled by PHUs, such as sustainability, dynamicity, and advanced properties, could make them ideal for replacing traditional matrices, such as the aforementioned epoxy and unsaturated polyesters, while being more easily accessible than other CANs. For all the above reasons, the present dissertation focuses on this chemistry.

Table I-3 – PHU properties overview for potential composite applications

Cyclic Carbonate	Amine	Curing Protocol	Scope	GC (%)	T_g (°C)	E (MPa)	σ_y(MPa)	ϵ_y (%)	Ref
0.5TMPTGE/0.5TMPTC	MBCHA	Degassed	Adhesives	97.7	82	3300	83	8	[396]
0.25TMPTGE/0.75TMPTC		48h @80°C N_2		97.8	94	3100	93	13	
TMPTC	EDR-148	Degassed	Adhesives	96	34	14.4	10.5	130	[378]
	CBMA	12h@80°C		97	76	2370	75.100	3	
0.75TMPTC/0.25PPOBC380	CBMA	+30' @150°C		99	63	2310	77.1	3	
GGC	HMDA	Degassed @ 70°C	Cellulose	-	20	7	9	280	[381]
TMPTC		8h @70°C	nanocomposite	-	47	590	26	21	
PEC				-	51	660	33	5	
0.34TMPTC/0.66GGC				-	33	2100	68	7	
TMPTC	HMDA	mix @ 130°C and 80°C		-	50	1600	44	2.860	[380]
	0.75HMDA – 0.25GGAA	14h @80°C		-	56	2400	64	2.7	
	0.75HMDA-0.25PGAA	+ 4h@100°C		-	55	2850	60	2.1	
PGC	HMDA			-	56	2340	69	3.1	
CSBO	HMDA	mix @50°C		96.2	9.9	65	6.1	308	[379]
	MXDA	12h@70°C	Adhesives	98.6	21.3	94	7.5	227	
	IPDA	+4h@100°C		97.6	26	161	8.3	177	
CSBO	EDA	Degassed @70°C	Coating	-	20	4	6	240	[397]
	BDA	10h@70°C	& Adhesives	-	17	2	2	310	
	IPDA	+ 3h@100°C		-	40	50	5	200	
CLSO	EDA			-	55	180	18	57	
	BDA			-	45	300	17	84	
	IPDA			-	60	1460	10	1	
LDC	LupasolFG	Degassed @70°C		-	55	2400	7	1	[398]
PEC	HMDA	10h@70°C		-	51	660	33	5	
	HMDA/CAA	+ 3h@100°C		-	51	1740	63	6	
PGC	DAP	Mix @100°C		-	41	3390	70	2.5	[399]
0.9PGC/0.1LDC		16h @80°C		-	45	3860	83	2.800	
0.7PGC/0.3LDC		+ 4h @100°C		-	58	4040	88	2.490	
LDC	LUPASOL FG			-	94	4370	75	1.3	
SEC	IPDA	Mix @100°C		-	140	4000	15	0.370	[400]
	DDA	16 h @ 80°C		-	78	900	30	3.700	
	0.5IPDA/0.5DDA	+4h @100°C		-	93	2300	53	2.600	
	0.5IPDA/0.5HMDA	+ 1h@170°C		-	74	3700	40	1	
0.1STC/0.9SEC	IPDA			-	160	3900	nd	0.40	
C-St-G-SA	DETA	24h @RT + 2h@85°C	Surface coating	-	10	2500	9.480	85.3	[401]
CDGEBA		+ 0.5h @150°C	& antibacterial	-	100	5100	25.5	10.8	

I.6 Brief discussion about the importance of manufacturing technology in composites and their sustainability

The manufacturing technology plays a pivotal role in the properties and sustainability of composites. Selecting a specific manufacturing process for composite production involves several key considerations. On the one hand, the scale, shape, and production rate will dictate which processes are suitable and thereby define their overall costs. For example, autoclaves are adapted for large parts with high mechanical properties but showcase high energy consumption, high costs, and low production rates. For that reason, they are commonly used in aeronautics and aerospace [42]. The thermo-compression process, is well suited for small-scale structures with faster rates and parallel lines, such as sports and leisure [43]. On the other hand, the process will condition the matrix requirements, such as viscosity and curing time, as well as the type and form of reinforcement. Balancing these considerations and optimizing the conditions will contribute to the final quality of the material [41].

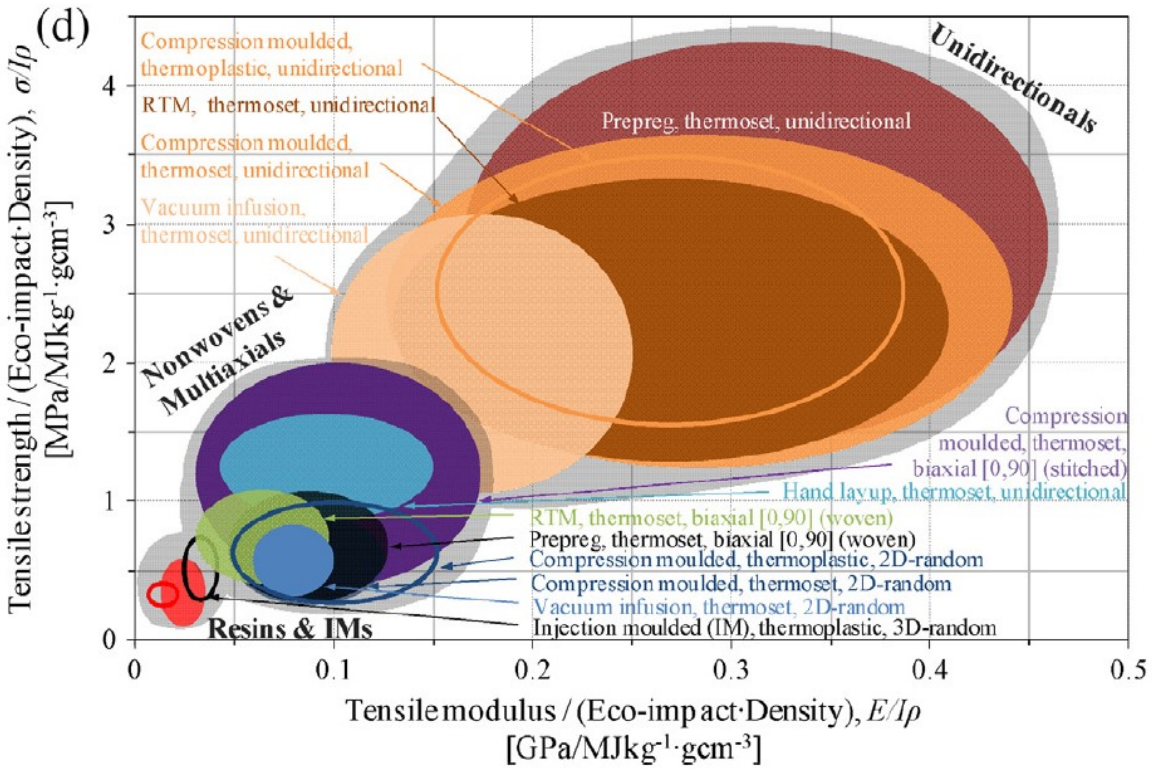

Figure I-44 – Ashby plot comparing the relative eco-impact normalized tensile modulus and tensile strength of composite processed (filled balloons) with various other engineering materials (unfilled balloons). Reproduced with permission from [137].

Historically, hand lay-up was the most employed technique. Although high quality parts can be obtained, it requires highly skilled workers (i.e., expensive labor) and limits the production rate. Nowadays, injection/infusion processes are encountering a significant growth, in particular in automotive sectors, due to the need for faster production rates [402], while maintaining high quality. Additionally, the chosen process will significantly modify the material's environmental footprint because of the energy inputs and waste outputs. Energy, in addition to ecological considerations, remains fundamental in defining production costs. All these aspects push towards the use of out-of-autoclave methods [43].

RTM is one of the most important out-of-autoclave methods. It is already largely exploited and mastered for composites, but its use is still following a substantial growth [9]. Indeed, RTM demonstrated significant energy and cost savings compared to autoclave [403, 404], see Fig. I-45. Equally, the energy savings, with less generated waste, were shown to enable the decrease of several environmental impacts, in particular, GWP [403, 404], even compared to metallic process [11]. It is important to note that these results might differ from one application to another, as well as the origin of the energy input and process parameters. Some studies also demonstrated better results for autoclave over RTM [405]. Nonetheless, with a near-net-shape process, improvement of resins towards faster curing time and lower temperature would benefit all aspects of the composite value chain.

Processing technology has led to significant investments from composite manufacturers that strongly limit the adoption to other technologies. In that sense, new chemistries, including CAN ones, must be adapted to existing procedures to be implemented by industries [24].

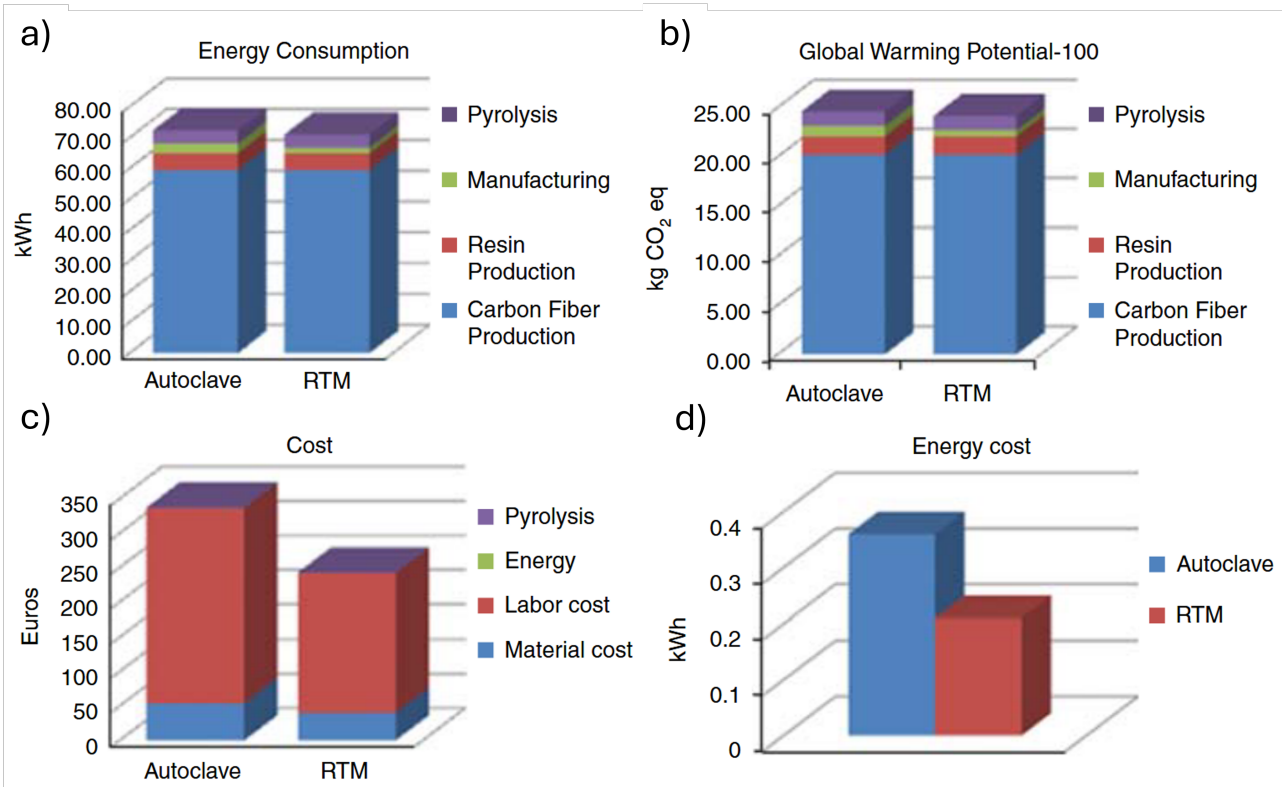

Figure I-45 – Comparison of a) energy consumption, b) global warming potential and c) total cost, and d) energy cost of an aeronautic component manufactured by autoclave or RTM. Reproduced with permission from [403].

I.7 End-Of-Life Scenario, towards nested circular economy - Environmental and Technological perspectives

There are many pathways toward more sustainable composite materials through the selection of the reinforcement, matrix, processing, and the optimized design of the structure. Even in the case of a genuinely green scenario with renewable sourcing, low energy processes, and extended service life, any composite structure will end up as waste. At this point, end-of-life management becomes crucial in the recirculation and valorization of (some) constituents and imparts non-negligible impacts on the cradle-to-grave or cradle-to-cradle balance sheet.

I.7.1 General considerations

Many waste management strategies exist (see Fig. I-46), though not all are implemented industrially. Currently, most (composite) wastes are landfilled, with some being incinerated, but the inorganic fibers still require landfill [60]. Incineration with energy recovery is sometimes considered but does not necessarily benefit the GWP, particularly in countries with low-carbon electricity (such as France, Sweden, or Paraguay).

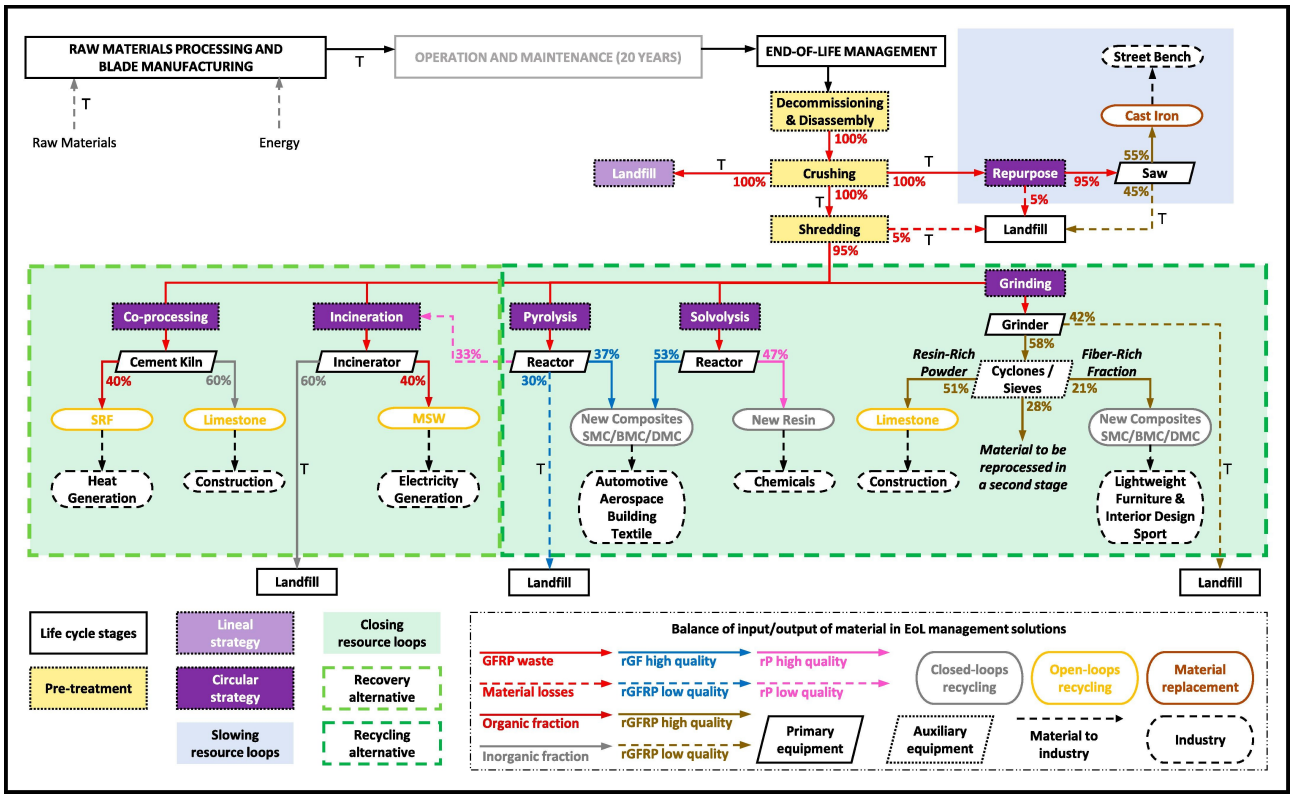

Figure I-46 – Life cycle management of composite materials, as applied here to wind turbine blades, and the different EoL strategies applicable. Acronyms: T: transport, SRF: Solid Recovered Fuel, MSW: Municipal Solid Waste, SMC: Sheet Moulding Compound, BMC: Bulk Moulding Compound, DMC: Dough Moulding Compound, GFRP: Glass Fiber Reinforced Polymers, rGF: recycled Glass Fiber, rGFRP: recycled Glass Fiber Reinforced Polymers, rP: recycled Plastic (epoxy resin). Reproduced with permission from [406].

A small proportion of composites is reused or recycled. However, landfilling of composite structures is progressively banned worldwide through tax incentives or new regulations, like in Germany in 2009 [44], due to land occupation and long-term pollution [30]. However, landfilling is still, to date, the most economic EoL scenario with an estimated 200-300 €/ton (including transportation, waste management, and gate fees) [407]. Direct repurposing of composite structures also exists, such as

converting wind blades into bridges [408], but is marginal. Mechanical recycling is the most advanced and industrially applied recycling strategy, but it only provides low-grade materials because of the reduction of the reinforcement length [409]. This method is generally limited to thermoplastic FRP, which can be melted and reinjected into new applications. Thermosets-based FRPs are reduced to low-quality fillers. Again, the process of grinding tends to make the fillers not even competitive in prices and performance compared with conventional fillers such as carbonates or silica [33]. Nevertheless, mechanical recycling could still be viable through the use of CANs in order to enable higher properties of the recycled products using simple reshaping and welding [24]. The wear of grinding equipment should also be considered for large-capacity plants.

More promising strategies have been envisioned over the last two decades through the developments of direct reuse/repurpose value chains, pyrolysis techniques, and chemical recycling. All of them impart different environmental burdens and economic potential, and the same level of maturity is not achieved for all. No recycling technique was demonstrated to possess both low cost and low environmental footprint [410]. Moreover, the matrix chemistry, reinforcement type, form, and initial/final application types severely affect and dictate the economic and environmental viability of each EoL scenario.

In composite recycling, retrieving the fibers is the most critical aspect. They commonly represent 40-80% in weight of the laminate and about 60-95% of the economic value [25, 44]. They also convey the majority of the environmental score. Accordingly, fibers drive the environmental and economic interests of recycling (see Fig. I-47). Virgin carbon fibers possess a high cost, ranging from 30-60€/kg (2018) [411], and a high environmental footprint (100-1500 MJ/kg), which makes them particularly interesting to recover. It was estimated that recovered CF by pyrolysis could range between 5 and 15€/kg to be profitable [410, 411] while grinding costs range between 0.3 and 5 €/kg [410]. As glass fibers typically range between 1-3€/kg for low grade and 3-30€/kg for high-performances [410], the cost of most recycling methods is challenging to make recovered GF cost-competitive with virgin ones. Cement kiln was considered to be one of the best valorization strategies for GFRP by Hagnell et al. [33]. For both GF and CF, retrieving the fiber helps reduce the footprint compared to virgin materials by 20-90% [113, 410]. However, this value strongly depends on the fibers and process. Supposedly, glass and basalt fibers could be re-melted into virgin continuous fibers, but these have not been considered so far.

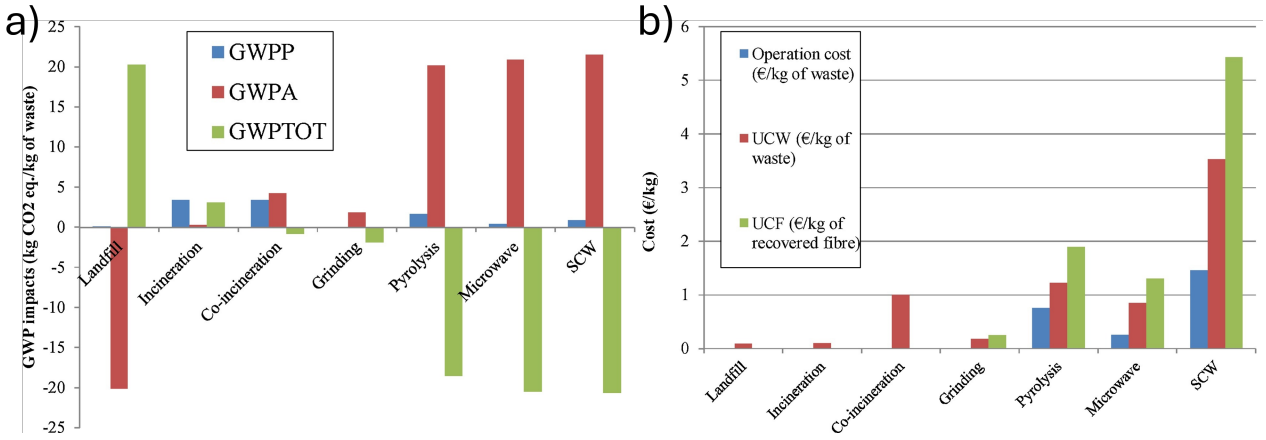

Figure I-47 – a) GWP, and b) Cost implications of the EoL management of CFRPs. Acronyms: SCW, Supercritical water; GWPP, GWP impact of the process; GWPA, GWP impact of substituted products; GWPTOT, GWP total of the system; UCF, the average unit cost per mass unit of recovered fiber; UCW, the average unit cost per mass unit of waste. Reproduced with permission from [410].

Apart from the mechanical recycling of thermoplastic/natural fiber composites [412], and the biodegradation of PLA/NF composites [413–415], the recycling of NFC has been poorly addressed or discussed. In NFCs, the matrix contributes a significant part of the total environmental footprint; therefore, the recovery of the matrix could be critical. Moreover, recycling methods involve harsh conditions such as aggressive chemical reagents, long times, or temperatures higher than 150°C that cannot be considered due to the lower stability of NFs when compared to CFs or GFs.

Moreover, most studies focus on composite structures and pure composite materials; the importance of material identification, sorting, and the presence of other constituents such as metallic grids and manufacturing waste (uncured pre-preg cuts...) might require specific waste streams [11, 33].

I.7.2 Pyrolysis - balancing energy inputs and recovery quality

Pyrolysis is one of the most advanced emerging recycling techniques. Before pyrolysis, composite are first collected and shredded (see Fig. I-48). The pyrolysis process itself involves heating between 350-700°C in an inert atmosphere; the process degrades the organic matrix into char, gas, and oil (potentially). The inorganic fiber recovered generally needs to be washed, and treated for further use [263]. Pyrolysis can be advantageous as it does not necessarily require the removal of other chemical compounds, such as coatings or paint, that could be damageable in another process. It can be adapted to most matrices, although the temperature for some might differ; UPR can be degraded below 400°C

while high-performance resins such as EP or PEEK requires higher temperatures [33, 87]. However, pyrolysis requires high energy input and can significantly degrade the fiber properties. Temperatures higher than 400°C can lead to a 50% reduction of GF mechanical properties [64]. The pyrolysis process is currently cost-effective only for high-value fibers, such as carbon fiber. It is already implemented commercially for CFRP (Gen2 Carbon—ELG Group), and some Start-Ups are now implementing new pyrolysis equipments for pilot scale (Composite Recycling, Switzerland), using a mobile pyrolysis unit able to recover glass fibers. The details of the start-up technology, including economic or environmental benefits, are not disclosed. They recently signed a partnership with Veolia Recycling (2024) for pilot-scale pyrolysis recycling with a capacity of up to 2 ton/day.

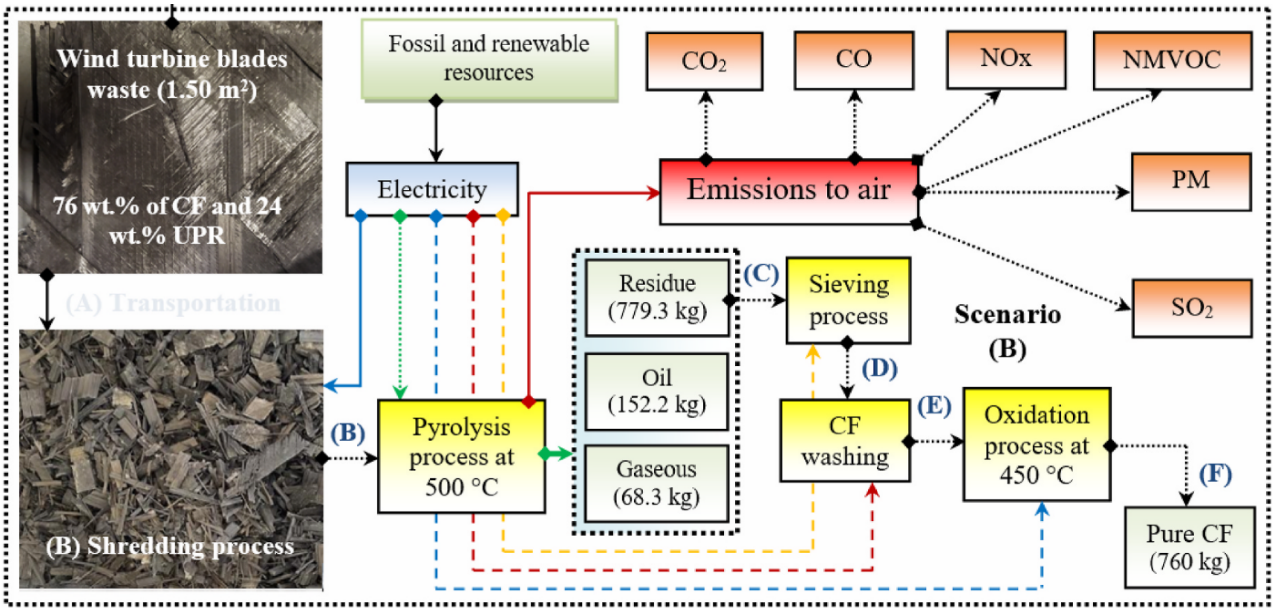

Figure I-48 – Schematic representation of conventional pyrolysis of FRP and its outputs. Reprinted from [263] Copyright 2024, with permission from Elsevier.

In all cases, pyrolysis demonstrates more economic potential than incineration for energy recovery as it allows for the retrieving of materials. The oil produced from the degraded polymer might be expected to be valorized in the future [97, 416]. Additionally, using an oxygen-free environment prevents combustion, reducing air pollution.

A new generation of pyrolysis procedures is rapidly being developed [82]. In the latter, a bed of silica sand is fluidized by hot air to rapidly heat the FRP materials, facilitating the recovery of fibers through the erosion of the polymer matrix. Similarly, microwave-assisted pyrolysis is an advanced technique that heats FRP scrap materials by rapidly transferring thermal energy in an inert atmosphere, breaking down the polymer matrix into fuels.

From an environmental aspect, Yousef et al. [263] discussed the environmental and economic

benefits of recovering carbon fibers from UPR composites through pyrolysis. They highlighted the potential to reduce several parameters such as climate change and fossil resources scarcity (see Fig. I-50). However, the exceptionally high energy consumption (around 2500 kWh/ton of composites) led to detrimental outcomes on other criteria, such as terrestrial acidification and ozone depletion. Using catalytic pyrolysis and artificial neural networks, they successfully obtained aromatic chemicals that could benefit such strategy [262, 416].

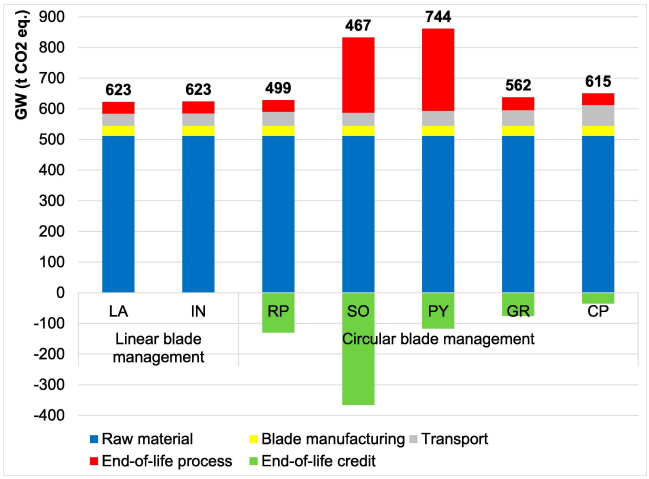

Figure I-49 – Influence of the EoL management on the global warming potential of GFRP wind turbine blades. Acronyms: LA: landfill, IN: incineration with electricity recovery, RP: repurposing, SO: solvolysis, PY: pyrolysis, GR: grinding, CP: co-processing in cement kiln. Reproduced with authorization from [406].

I.7.3 Chemical recycling

The chemical recycling of thermosets and their composites is appealing, yet it is not as well-developed as other strategies. It generally provides the highest fiber quality [417]. It can be divided into four main strategies: selective catalytic depolymerization, mild oxidative depolymerization, sub-critical solvolysis, and supercritical solvolysis. In all cases, solvents are necessary to dissolve the degraded product and ease the cleaning of the fiber. The solvent cost and environmental score severely affect the relevance of the process but also its efficiency [418]. Ideally, toxic and halogenated solvents must be avoided (e.g., DMF, dichloromethane/chloroform, hexane...), while non-toxic (biobased) solvents (ethyl acetate, ethanol, methanol, water...) with a low boiling point can support the recirculation [419].

The selective catalytic pathways target degradable bonds for high recovery yields. Conditions are typically expected to be below 200°C; a pressurized step might be necessary if low boiling point reagents and solvents are required. However, the depolymerization conditions severely differ from

polymers, catalysts, and solvents [291, 295, 420]. Effective selective depolymerization protocols have been developed for thermoplastics such as polyesters, polyurethanes, and polycarbonates, and are still to be implemented for thermosets. They require the use of an organic catalyst (commonly base, acids, organic salts) [258, 421] or a metallic catalyst [295, 422], and a nucleophile (alcohols, glycols, amines). In some cases, the nucleophile can also play the role of the solvent, as in the case of the depolymerization of ester-containing epoxy by methanol [205, 219]. Selective recycling strategies depend on the polymer chemistry and thus require sorting or multiple steps for mixed composite waste.

Unselective oxidative depolymerization has been developed for epoxy-amine-based composites. Interestingly, the fiber can be retrieved within few hours at ambient pressure and a temperature below 80°C. As such, it was successfully applied to glass and carbon fibers but it has never been tried with natural fibers [293, 294]. Both selective and unselective depolymerization strategies were discussed in the specific section corresponding to each type of polymer.

Currently, there is no data on the economic or environmental benefits of these two emerging strategies. This is most probably because they are still at low TRL (2-3) and thus not enough established and generalized. Most of the LCA and DEA investigations for EoL management of composites are performed on sub- or super-critical solvolysis.

Sub-critical solvolysis is generally a hydrolysis strategy where water is below its critical point (200 °C < temperature < 374 °C and pressure < 221 bars). Other solvents (ethanol, methanol) can also be used. Supercritical solvolysis is performed above the critical point, is more efficient, has faster rates, and has higher recovery quality. They are still at the research stage, but their TRL is slightly higher than catalytic depolymerization, with pilot plants being implemented [27]. Difficulties in scaling up such a process could appear, but it remains beneficial for the overall results with optimized conditions [423]. The energy input for the process imparts the most economic and environmental cost. In all case studies, solvolysis was beneficial by comparison with incineration or landfill for carbon fibers [115, 410, 423]. Compared to pyrolysis, the results are somewhat unclear; some authors claimed better results of supercritical solvolysis over pyrolysis [406, 410, 423] (Fig. I-49), while others position pyrolysis as more efficient [424]. From an economic viewpoint, pyrolysis remains more competitive at the current development stages [407, 410]. Glass fiber recovery from pyrolysis and solvolysis is not competitive with virgin glass fibers [33, 410]. Pillain et al. [423] took into account the fiber quality in their analysis. Indeed, pyrolysis can significantly decrease CF properties and make them only suited to replace GF. They show that the substitution of GF by pyrolyzed rCF is not relevant when the decrease is superior to 40% (Fig. I-50a). On the other hand, supercritical water does not alter the properties

and provides significant environmental benefits. If the fiber quality is not differentiated, similar outcomes are obtained (Fig. I-50b). The different recycling strategies should be, however, considered as complementary to best mitigate environmental footprints and maximize product valorization.

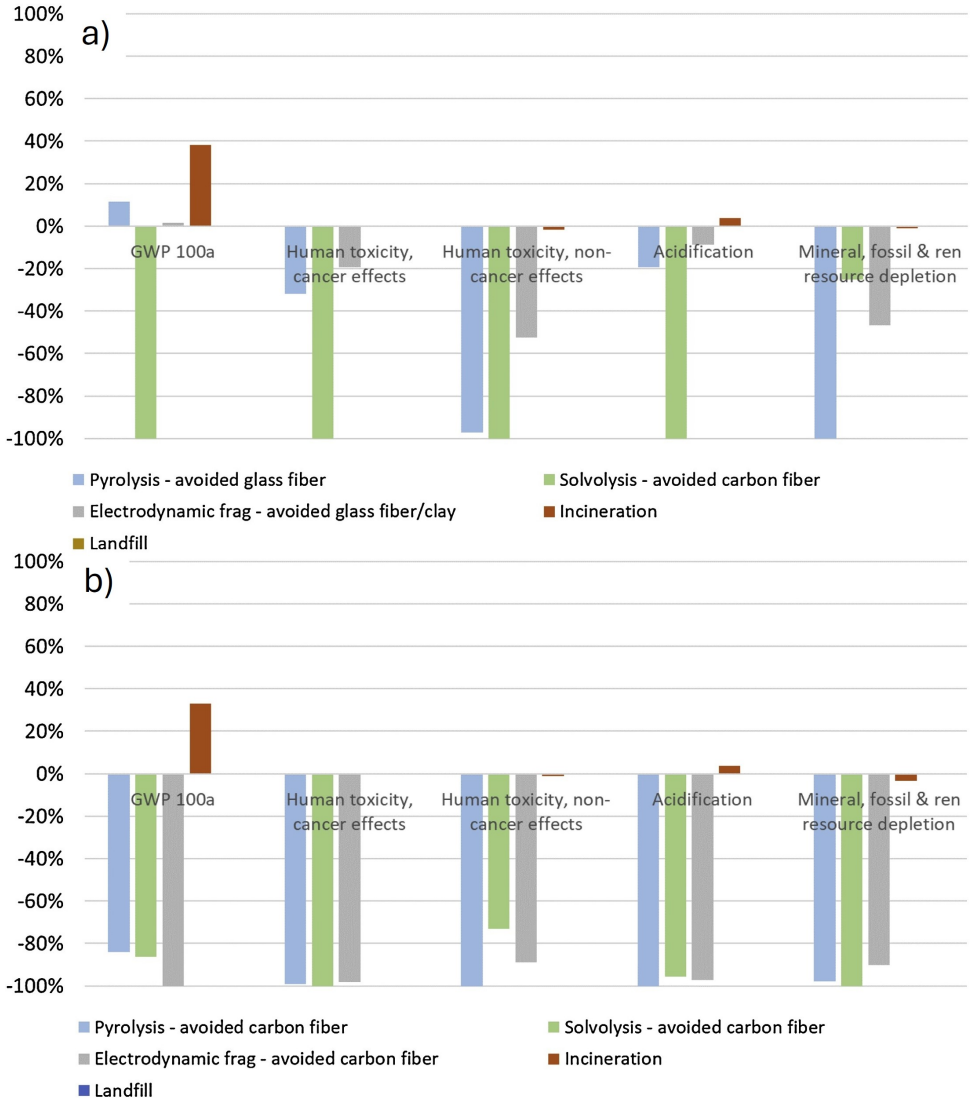

Figure I-50 – Environmental impacts comparison between pyrolysis, supercritical hydrolysis, electrodynamic fragmentation, incineration, and landfilling, a) considering the fiber degradation and thus different substitution product, and b) considering the same quality of carbon fiber (predictions upon optimization).Reprinted from [423] Copyright 2019, with permission from Elsevier.

None of these processes have been applied to natural fibers (except for acidolysis of Recyclamine derived epoxides). Similar to pyrolysis, the conditions for supercritical solvolysis are not suitable for NF. Mild depolymerization conditions could be valuable but should be discussed environmentally (and economically). The environmental footprint of NF is much lower than that of synthetic fibers, and prices are only slightly higher than that of GF. The viability of recovering natural fibers might be

questioned, in addition to the existing technological challenges. Upon those considerations, scientific efforts might be more valuable toward the design of fully biobased resins with extended durability and low GWP emissions.

I.7.4 Ideal valorization of recovered products

The valorization of the matrix-degraded products has been chiefly foreseen as non-viable [425]. The full recirculation of the products into a virgin polymer is not realistic if current developments are considered, albeit certain authors have succeeded at lab-scale [219]. However, the reagents involved and the successive purification steps make the economic and environmental aspects irrelevant. To date, a sustainable 100% recirculation of composites has not been demonstrated nor seems attainable despite significant efforts and breakthroughs. Up to now, unrecoverable organic compounds could be valorized through pyrolysis to recirculate carbon in naphtha and syngas (see Fig. I-51), as claimed by Vidal et al. [19].

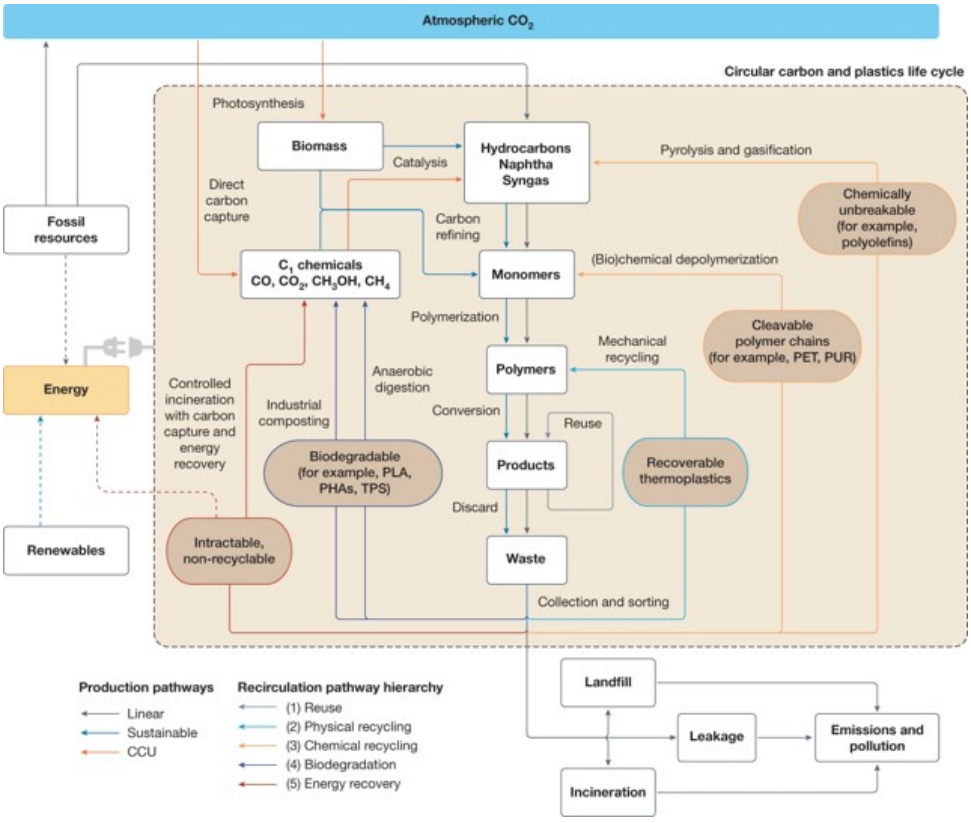

Figure I-51 – The global circular carbon and plastics life cycle as proposed by Vidal et al. to replace the current linear flows (represented in black). Acronyms: PET, poly(ethylene terephthalate); PHAs, poly(hydroxy alkanoates); PLA, poly(lactic acid); PUR, poly(urethane); TPS, thermoplastic starch. Reproduced with permission from [19]. Copyright 2024 Springer Nature.

The fibers hold more promise for recycling. Composite properties are highly dependent on the form of the reinforcement. As reclaimed fibers will be necessarily discontinuous, conventional manufacturing of randomly oriented mat can provide low-medium grade reinforcement [426]. Woven fabrics can retain the weave depending on the process and can thus be used as such [27]. However, obtaining aligned discontinuous fibers in continuous tape would be profitable for higher performance of the recycled composites. This process allows fiber to be realigned, woven, or transformed into thin isotropic mats. Notably, a sizing agent can be reapplied during this step as it is lost during the recycling [27]. Various techniques utilizing electrical, magnetic, and pneumatic methods have been explored in the past to align discontinuous fibers in a preferred direction, but most of them face limitations to the type of fibers, quality, length, and production rate [427].

To present one promising example widely studied, the University of Bristol developed the HiPerDiF equipment (High-Performance Discontinuous Fibre) [427]. The process explores the fiber suspension in water going through parallel plates with a water jet to obtain highly aligned fibers. About 65% of the fibers were in the ±3° range. The resulting unidirectional tapes exhibited a tensile modulus of 115 GPa and a tensile strength of 1509 MPa, with a fiber volume fraction of 55%. The technology was successfully applied to a yachting demonstrator [428]. The research team also investigated the hotspot to lower the environmental footprint of the technology, mainly caused by electricity power [429].

Another research team in Bordeaux patented a mechanical equipment to unweave and realign carbon fibers [430]. From woven carbon reinforcement, a continuous tape with 95% of fibers in a ±14° range is obtained. High performances were also obtained [431]. The technology is now under commercial development by the Start-Up Nova Carbon®, in Bordeaux (Southwest France).

I.8 Summary and conclusions

Despite being known for many decades, the continuous depletion of resources and the exponential increase of the human footprint on the environment have raised awareness on the need to rethink the economic paradigm. The amounts of waste and rapid resource attrition due to our existing linear economy cannot be sustained for much longer than a few decades. The UN global objectives of limiting global warming to +1.5°C by 2100 impose new strategies. Earth is a closed system, so limiting entropy imposes the use of renewable resources and the recirculation of waste. Efficiency must be improved at all levels through higher energy yields, lower material use, and eco-design.

Fiber-reinforced polymers (FRP) will be critical in achieving ambitious goals. Their exceptional strength-to-weight ratio allows to obtain much more performant structures. FRPs have become an

irreplaceable asset in many applications. Nonetheless, FRPs cannot be considered sustainable materials. Carbon and glass fibers contain high embodied energy and high GWP while causing the attrition of critical resources such as sand and oil. The fossil-based thermoset matrices significantly hamper the recovery of decommissioned composite structures. It is critical to rethink the composite industry from raw material extraction to end-of-life management and valorization. This review reports the current existing solutions to foreseen composites in a sustainable circular economy model.

Many academics have explored different strategies to lower the impact of composites, such as the use of natural fibers and thermoplastics, including the recycling possibilities. Using alternative fibers to glass fibers provides substantial environmental and economic benefits. Flax, hemp, and basalt are promising. Natural fibers are the only ones that demonstrate high properties when considering sustainable criteria, and NFCs are close to fulfill net zero carbon goals. Carbon fibers' sustainability seems to rely on the obtention of biobased PAN. Lignin-based CFs could also be beneficial but are not competitive so far.

The pivotal role of chemistry in the realm of composite has often been occulted or forgotten. Many biobased substitutes for petro-based polymer building blocks have been reported in the literature but rarely developed following the requirements of the composite industry. Only a few investigated the actual environmental benefits of these compounds, while the chemical steps involved sometimes imply highly toxic or polluting reagents, solvents, and catalysts. An optimized valorization of feedstocks to different products and markets is often required to compete with highly atom-efficient and cost-effective petro-chemical processes. Still, bio-based resins, particularly epoxy ones, seem to be promising in reducing environmental impacts and toxicity compared to conventional ones. The complex interface between fiber and matrix, crucial to the final composite properties, is often not considered when developing new resins, particularly for natural fiber.

Some emerging chemistries could benefit more through other complementary sourcing, such as CO_2-derived polymers and Covalent Adaptable Networks. Recyclable by-design thermosets are advancing but should also be developed and characterized to better suit the composite industry requirements. This includes the need to develop resins that are implementable into efficient manufacturing processes such as RTM. Developing low-viscosity resins that can be cured in a short and controlled time at low to moderate temperatures remains the main threshold for their potential implementation. Again, the evaluation of environmental impact and economic worth should be addressed to a larger extent, as only one LCA has been reported for CANs up to now.

The recycling of composites remains complex despite the development of various strategies. The

economic and environmental benefits rely on the recovery of the fibers, as the recovery of matrices or functional building blocks is too complex and worthless. Considerable efforts must be conducted in this direction, and new catalytic pathways developed for commodity polymers could benefit the composite industry, but they still need to be validated.

Not all processes lead to the same fiber quality, environmental score, and economic value. The different processes must be developed in a complementary manner to mitigate current drawbacks. Mechanical recycling is the simplest method, but it downgrades the composite to low-value use. Pyrolysis and solvolysis are the most advanced emerging technologies for recycling as they can provide higher quality fiber, but optimization of conditions is essential to ensure relevant outcomes. The recovery of CFs is, so far, the only valuable one because of its extremely high cost and environmental footprint. The current recycling costs make the recovery of glass fibers not competitive with virgin ones. Improvement in the processes' efficiency, the rise of energy and resource prices, taxes, and regulations could boost the interest in recirculating glass fibers. Natural fiber recycling has almost not been studied, apart from biodegradation and mechanical recycling (limited to some thermoplastic matrices). The recycling of NFC with thermoset matrices is still to be established and discussed.

Finally, considering all the requirements about composites, there are some polymeric matrices with significant promises. Among them, polyhydroxyurethanes (PHU) could play a pivotal role in the realm. From an environmental perspective, PHUs are an interesting, sustainable alternative to isocyanate-derived polyurethanes due to their CO_2 sourcing, the wide availability of biosourced substrates for carbonation and their low-cost production. Furthermore, they could present strong interactions with NF thanks to the high adhesion properties of PHUs arising from their pendant hydroxyl moieties. When EoL is considered, their dynamic nature could bring promising features such as reshaping, welding, and, finally, mechanical or chemical recycling as ultimate revalorization steps. However, as PHUs are still in their infancy, they have not been investigated for such applications. Especially, there is a lack of comprehensive data available from the literature to demonstrate the applicability of PHUs in composites within the context of a circular economy.

Chapter II

Investigating the structure-properties relationship of polyhydroxyurethanes for potential composite applications.

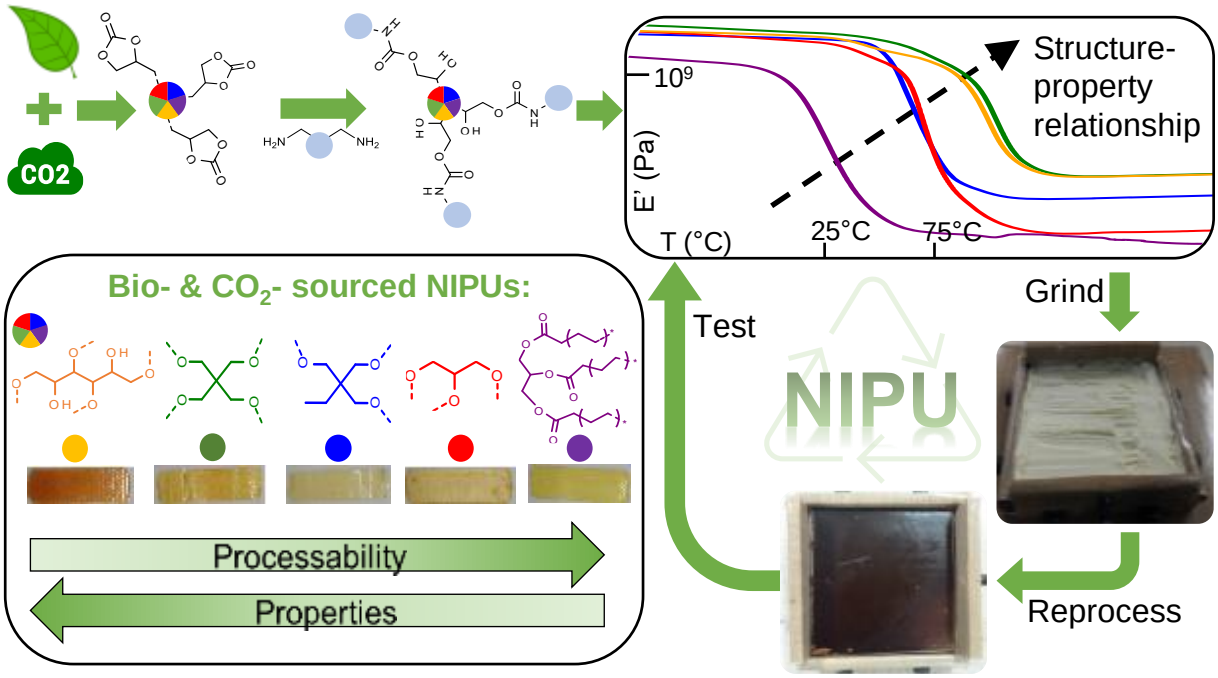

Adapted from: Seychal, G.; Ocando, C.; Bonnaud, L.; De Winter, J.; Grignard, B.; Detrembleur, C.; Sardon, H.; Aramburu, N.; Raquez, J.-M. Emerging Polyhydroxyurethanes as Sustainable Thermosets: A Structure–Property Relationship. ACS Appl. Polym. Mater. 2023, 5 (7), 5567–5581. `https://doi.org/10.1021/acsapm.3c00879`.

External contributions: *J.D.W. performed the mass spectrometry measurements. B.G. performed the synthesis of TMPTC at the kg scale (throughout the manuscript). SEM images were performed by Materia Nova.*

Contents

II.1 Introduction

As understood from the previous state-of-art, sustainability has become a key challenge in material science over the last twenty years. Polymer-based structural materials can assess such challenges, particularly fiber-reinforced ones. However, polymers adapted for such materials remain scarcely limited. Most biobased polymers suffer from unsatisfying properties to compete with conventional petroleum-based materials despite the important development and perspective in the field [21, 432]. In that sense, material scientists need to focus on new emerging polymers to meet both sustainability and high-performance goals to fulfill future industrial requirements. Polyhydroxyurethane (PHU) thermosets, a type of non-isocyanate polyurethanes (NIPU), are considered a new alternative to polyurethanes and epoxides thermosets, thanks to the bio- and CO_2-based cyclic carbonates used monomers [372].

PHU thermosets have shown high versatility ranging from elastomeric to stiff behavior [378, 379]. However, as previously discussed, an important scattering in properties and behavior has been observed in the literature. Moreover, up-to-date, only a few rheological studies have been conducted on thermoset PHUs [379, 433, 434] and to the authors' best knowledge, none have focused on potential load-bearing PHUs.In particular, polymers used as matrices for fiber-reinforced composites require such characterization to assess whether they meet the process requirements. Rheological measurements provide useful processing parameters such as the viscosity over time and temperature, the pot life (time before the mixture becomes unprocessable), and the gel time (time before the mixture acts as a solid). These parameters are preponderant in many industrial processes when curing must be implemented [41]. Although the low reactivity of five-membered CCs and the significant increase in the viscosity of epoxy monomers after carbonatation are widely recognized, they have not been thoroughly examined.

The potential and characteristics of PHU thermosets have not been fully explored, which limits the selection of appropriate matrices for composites. More specifically, the relationship between the processability, the final properties, and the recyclability of PHU thermosets as a function of the macromolecular structure of the CCs, as much as their level of functionalization, must be assessed.

In this chapter, we investigate the opportunities offered by several PHU formulations, their potential applications, and operating windows. Particularly, we propose to evaluate five potentially biobased five-membered CC of different degrees of functionality (TrimethylolPropane - TMPTC, Pentaerythritol -PEC, Glycerol -GEC, Sorbitol -SBC, and Carbonated Soybean Oil -CSBO) cured with an aromatic amine (m-Xylylene diamine - MXDA) to design high-performance sustainable PHU thermosets. The selected epoxy precursors in this study were chosen for their potential biobased origin, their ability to

crosslink once carbonated, and their low initial viscosity. TMPTC has been used in several studies and was considered as the reference system. The fully biobased and highly functional PEC and SBC make them of particular interest to achieve high-performance thermosets but their high viscosity could be problematic. On the other hand, GEC is a liquid CC monomer, which, regarding the manufacturing process of structural materials, could allow a better flow of the curing thermoset. Finally, fatty acid CSBO-based PHUs can increase ductility and decrease reactivity thanks to their long aliphatic chains.

The synthesized cyclic carbonates were structurally characterized using mass spectrometry and ^{1}H-NMR. The rheological behavior during the curing of PHU thermosets was investigated and compared with the viscosity of the starting cyclic carbonates as a first approach. The final properties of fully cured neat matrices were then evaluated followed by their adaptable network properties and ability to be reprocessed in the case of the most interesting formulations.

II.2 Results and discussion

II.2.1 Synthesis and characterization of cyclic carbonates for PHU thermosets

All cyclic carbonates, as represented in Fig. II-1a, were synthesized using CO_2 under supercritical conditions and fully characterized, and the results are summarized in Table II-1. ^{1}H-NMR, mass spectrometry, TGA, and DSC curves can be found in the appendix.

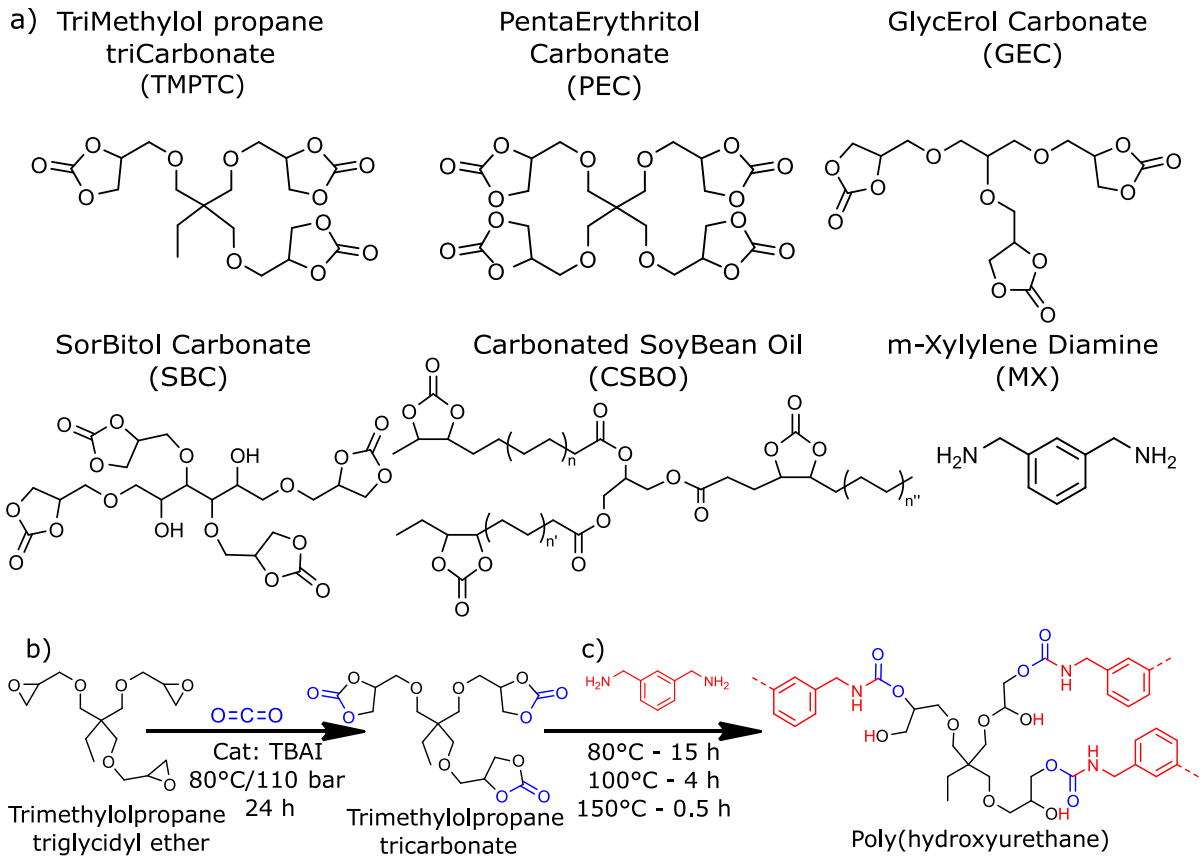

Figure II-1 – a) Idealized (macro)molecular structures of the resins precursors and b) model reaction from TMPTGE epoxy monomer to TMPTC cyclic carbonate to c) p(TMPTC-MX) PHU thermoset

Table II-1 – Characteristics of the synthesized cyclic carbonates

Name	Ref	CEW	M_n	#CC	$T_{d_{5\%}}$	T_g	$\eta_{25°C}$	$\eta_{50°C}$
		g/eq	g/mol		°C	°C	Pa.s	Pa.s
Trimethylol propane tricarbonate	TMPTC	175	530	2.9	236	-19	148	6
Pentaerythritol carbonate	PEC	180	709	3.9	232	-7	863	30
Glycerol carbonate	GEC	170	495	2.9	224	-25	30	2.4
Sorbitol carbonate	SBC	260	-	-	239	3	65000	2050
Carbonated soybean oil	CSBO	310	1083	3.5	336	-23	120	7

The full conversion was confirmed by ^{1}H-NMR through the full disappearance of epoxy peaks between 2.9 and 3.2 ppm and the appearance of carbonate signals between 4.3 and 4.9 ppm, as shown in the appendix (Fig. II-A1 to II-A5). The complete conversion was further confirmed by mass spectrometry (Fig. II-A6 to II-A10). Being consistent with the insertion of CO_2, the quantitative

conversion of epoxy to cyclic carbonate derivatives was observed by the complete shift of the ionized entities as ascribed to starting materials to a higher 44 mass unit per epoxy function converted [375]. All mass spectra are characterized by a distribution of different ionized entities, highlighting the presence of different molecules in both starting and resulting materials. This distribution is related to the presence of halohydrin formed during the polyol epoxidation as observed by Camara et al. [435]. For both ESBO and CSBO, the distribution of mass is related to the different aliphatic chain length of triglycerides in soybean oil as reported by Poussard et al. [375], and to the number of unsaturated bonds epoxidized. Several studies have shown that the best molar ratio between CCs and primary amine functions for PHUs synthesis was 1:1 [399, 436]. For these reasons, the effective determination of carbonate content has to be performed accurately. More specifically, CEW was evaluated using an internal standard (toluene) to determine the average number of carbonate per gram of products [378]. Thanks to this method, average functionality can be estimated from molar mass and CEW (Table S1). All CCs have a functionality superior to 2.5, making them suitable for thermoset matrices.

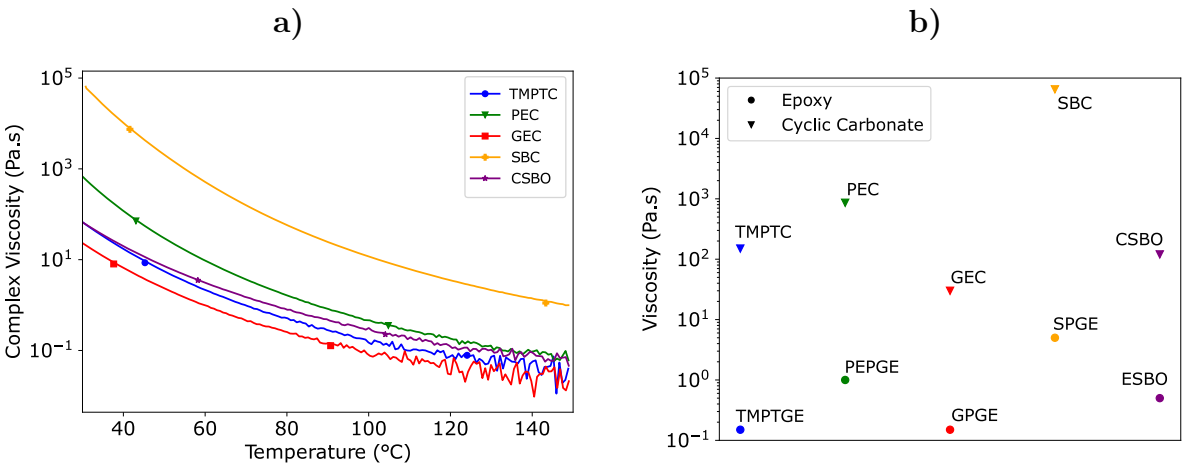

Figure II-2 – a) Viscosity evolution of the cyclic carbonates over temperature, and b) comparison of viscosity of epoxy and carbonate monomers at 25 °C

In most thermoset industrial applications, the viscosity and the thermal stability of products are important parameters. For these reasons, TGA and rheological measurements were applied to the synthesized carbonates. TGA analyses (Fig. II-A11) evidence no major degradation before 200 °C. Fig. II-2a depicts the evolution of the viscosity with temperature and Fig. II-2b allows the comparison of the viscosity of each CC with respect to the starting epoxy monomer. Carbonating epoxy monomers drastically increases the viscosity of the medium by a 200 to 1000 factor. However, no clear relationship can be observed, complicating the prediction of the final carbonate viscosity. For example, while

TMPTGE and GPGE have similar initial viscosity, the resulting TMPTC shows higher viscosity than the GEC. SBC was found to be almost solid at room temperature. Still, it remains that the number of CC functions in the monomer is responsible for the viscosity of the mixture. While these low-viscosity epoxy precursors are commonly used as a reactive diluent for diglycidyl ether of bisphenol A [40], in some cases (SBC and PEC mostly), they become too viscous to be processable within an industrial process such as liquid resin infusion or resin transfer molding. In these techniques, viscosities between 0.5 and 1 Pa.s are desirable [41]. However, the viscosity of the obtained CCs can be adapted through the use of low-viscosity difunctional CCs to meet industrial requirements [381, 400].

II.2.2 Study on the relationship between CC structure and the rheological curing behavior of polyhydroxyurethane formulations

Rheology is an interesting tool to investigate the crosslinking behavior of thermosets, particularly pot life and gel time. Pot life can be directly related to the processability of a mixture, highlighting the time when the viscosity remains low enough to be processable. Gel time refers to the beginning of gelation, where the formation of the polymer network starts due to the cross-linking of the polyfunctional monomers. The curing kinetics of the PHU thermosets were evaluated through rheological measurements to determine the processing window of the formulations and the effect of the CC structure on the curing behavior.

II.2.2.1 Non-isothermal rheology

First, the effect of temperature was assessed through non-isothermal analyses. Complex viscosity and modulus are represented in Fig. II-3a-b respectively, and important values are reported in Table II-2. Our first observations reveal an important variation in the initial viscosity from one formulation to another, being obviously highly influenced by the viscosity of the CC. However, while GEC monomer is less viscous than CSBO, it must be noted that the lowest viscosity at room temperature was achieved for the CSBO-MX mixture with 15 Pa.s compared to 29 Pa.s for GEC-MX. The CEW of CSBO being more important than for GEC, this cannot be attributed to the amount of curing amine in the mixture, being almost twice less in the CSBO mixture than with GEC. Therefore, the difference in viscosity could be attributed to the higher reactivity of the low molecular weight CCs obtained from glycidyl ether [437] compared to the carbonate in the fatty acid backbone [375]. That is, the reaction starts earlier in the case of GEC, implying higher initial viscosity. Complex viscosity follows a small

decrease with increasing the temperature up to 80 °C for TMPTC-MX, PEC-MX, SBC-MX, and GEC-MX formulations, and up to 130 °C for CSBO. For the sake of comparison, the melt-viscosity of the curing formulations was reported at 80 °C, whereby such temperature was considered during the curing methods, enabling a good compromise between processability and curing time. At this temperature TMPTC-MX, GEC-MX, and CSBO-MX have comparable viscosities from 4 to 7 Pa.s and 14 Pa.s for PEC-MX. However, at this temperature, the melt-viscosity of SBC-MX remains too high to be considered easily processable. At temperatures higher than 90 °C, the viscosity increases drastically, and a gel point is observed. Gel point was reached for all the formulations, highlighting effective crosslinking for all PHUs. Just after, storage and loss modulus curves reach a plateau and do not evolve significantly. However, the gelling temperatures are superior to the limit in which side reactions can occur [373].

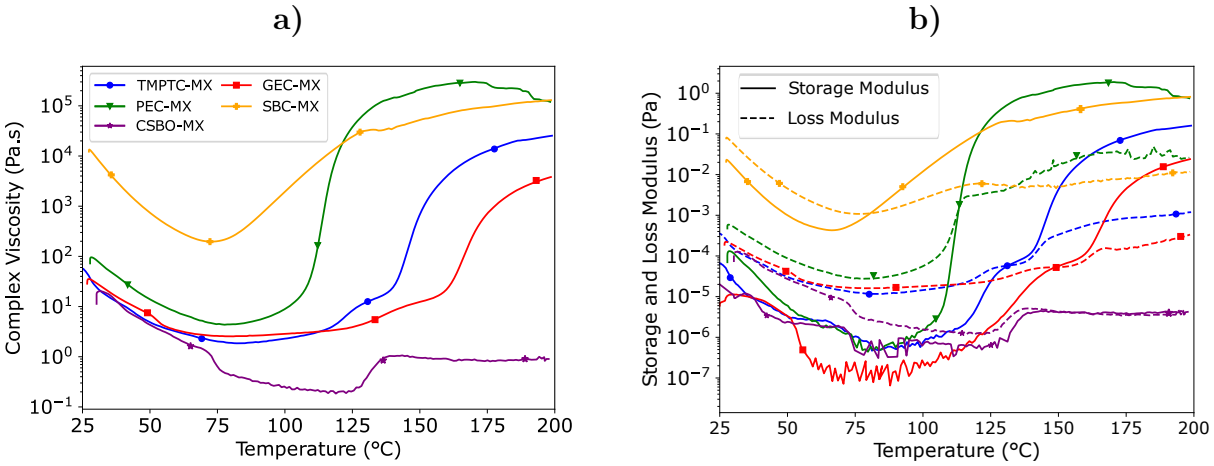

Figure II-3 – a) Viscosity evolution, and b) Storage and Loss Modulus evolution during non-isothermal curing rheological analyses.

The differences in terms of behavior can be attributed to several factors. First, the number of CC functions plays a significant role in this behavior. Indeed, higher functionality was already observed to increase the viscosity of the monomer. Herein, it also leads to faster gel point and a more crosslinked network [438]. Accordingly, if highly functional CCs can be used to obtain fast and dense crosslinking, they drastically affect the processability of the mixture. Secondly, for each formed hydroxyurethane function, the density of hydrogen bonds increases, leading to less mobility in the network and, consequently, an increase in the bulk steric hindrance, lowering the reaction rate [439]. While a higher temperature tends to break hydrogen bonds, it also eases the ring-opening of the CC by the primary amine [381, 435], leading to a faster network formation. Hence, the system is facing

opposite effects between the decrease of the viscosity and the increase of reactivity and crosslinking with temperature. Such observations were already highlighted in thermoplastic PHU where hydrogen bonds were shown to drastically affect the polymerization [377]. Finally, the optimal curing temperature of the PHU thermosets must be adapted to limit side reactions while ensuring full curing. For these reasons, we proposed here a three-step curing protocol for our formulations with an initial curing stage at 80 °C.

Table II-2 – Rheological results of the PHU formulations for non isothermal tests

Formulation		TMPTC-MX	PEC-MX	GEC-MX	SBC-MX	CSBO-MX
$\eta_{25°C}$	Pa.s	53	75	29	12209	15
$\eta_{50°C}$	Pa.s	5	14	7	728	4
T_{gel}	°C	131	113	149	80	149

II.2.2.2 Isothermal rheology

Isothermal rheological analyses were performed at 80 °C. The viscosity and moduli evolution for the five formulations is presented in Fig. II-4c-d and numerical values are summarized in the second part of Table II-3. As can be seen in Table II-3, the initial viscosity of the PHU formulations differs drastically from each other, depending on CC functions and CC reactivity as observed previously. CSBO-MX stands as the less reactive monomer with a long pot life of 138 min and a low initial viscosity. Such results are in agreement with non-isothermal results and can be attributed to the less reactive CC in the aliphatic backbone [437]. TMPTC-MX and GEC-MX have similar properties with an initial viscosity of around 3 Pa.s and a pot-life of 23 and 30 min, respectively, that can be considered sufficient for processing in many applications. The main drawback is the gelation time being superior to one hour for TMPTC-MX and even 4 hours in the case of GEC-MX. However, as it can be found in Fig. II-A13, the gelation was reached when the temperature increased up to 100 °C. This can be attributed to the CC in the middle of the GEC backbone being less accessible than the CC moieties, leading to higher energy required to fully react, as highlighted by Cornille et al. in their model reaction [439]. As observed in non-isothermal analyses, the highly functional PEC leads to a higher initial viscosity of 10 Pa.s as well as a too-short pot life (7 min) and gelation time (12 min). The same statements can be drawn from the highly functional SBC-MX where an initial viscosity superior to 1000 Pa.s, no pot-life, and a gel time of 1 min were observed highlighting the importance of the number of CCs in the curing

properties of PHUs.

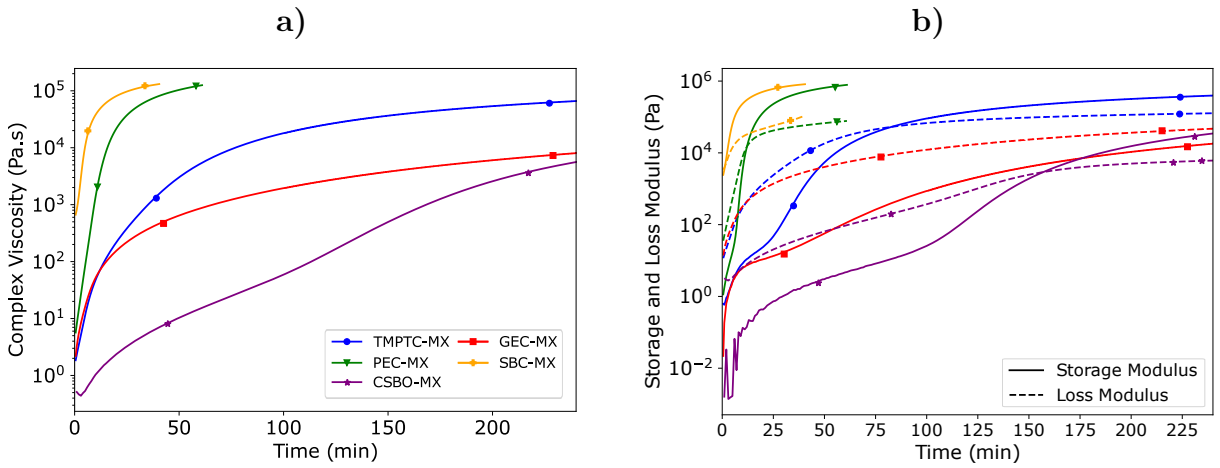

Figure II-4 – a) Viscosity evolution and b) Storage and Loss Modulus evolution during isothermal curing

However, if the properties are affected by the number of CC functions and their structure, the general behavior of all formulations appears to be similar. A continuous logarithmic increase of both viscosity and storage modulus can be seen from the beginning. Soon after the gel point is reached, a plateau is observed, and no significant changes can be noticed. The origin of the plateau can be explained by the completion of the reaction as well as by an elevated hydroxyl group density during the curing of PHU. These hydroxyl groups can participate in additional H-bonding within the mixtures, resulting in a higher viscosity while lowering the accessibility of remaining moieties (amine and/or CC) to crosslink. These observations are in accordance with Blain et al. [377], who highlighted that these additional hydrogen bonds can affect the progress of polymerization in the case of linear PHUs. This behavior is in accordance with the non-isothermal analyses previously reported in this work. In order to obtain a balance between easy processing, fast curing, and enhanced properties, the use of CC monomer mixtures could be considered [440]. For instance, attending to their relatively low viscosity and reactivity, GEC and CSBO could be of interest to tune the viscosity of highly reactive and viscous PEC.

Table II-3 – Rheological results of the PHU formulations for non isothermal tests

Formulation		TMPTC-MX	PEC-MX	GEC-MX	SBC-MX	CSBO-MX
η_{init}	Pa.s	2.8	10.6	4	1045	0.44
Pot Life	min	22.5	7	29.5	-	138
Gel Time	min	82.5	12	nd	1	157

II.2.3 Characterization of the polyhydroxyurethane thermosets

As previously mentioned, all formulations were cured in a three-step protocol in order to determine their overall performance. The protocol was designed to obtain the best properties while minimizing the need for long-time and high temperatures. The protocol was chosen on the basis of the rheological analyses. A long curing step (i.e., 15 hours) at 80 °C was necessary to obtain a good extent of curing while avoiding side reactions related to the nucleophilic attack of the remaining amine groups onto the hydroxyurethane function [373]. Even though the crosslinking stage was first conducted at 80 °C, the network was not fully cured, requiring an additional curing step at 100 °C and a short 30-min post-curing at 150 °C in order to obtain the highest degree of crosslinking and best properties. The obtained PHU thermoset samples are depicted in Fig. II-5.

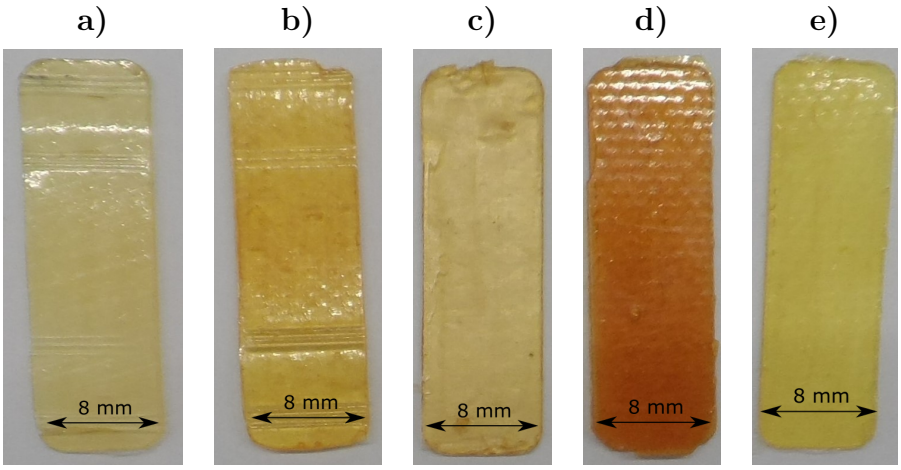

Figure II-5 – Photos of polymerized PHUs a) p(TMPTC-MX) b) p(PEC-MX) c) p(GEC-MX) d) p(SBC-MX) and e) p(CSBO-MX)

II.2.3.1 Confirmation of the curing extent and thermal behavior

At first, FTIR spectra (Fig. II-A14 to II-A18) confirmed the conversion of cyclic carbonates to hydroxyurethane linkage with the disappearance of the carbonyl group of carbonate at 1780 cm^{-1} and the appearance of a urethane signal at 1690 cm^{-1}. A small residual peak of CC was found in all formulations, revealing that some CCs were still unreacted. These observations are in accordance with DSC results in Fig. II-6a where a slight shift between 1 to 6 °C of the T_g of the thermoset was observed between the first and second ramps.

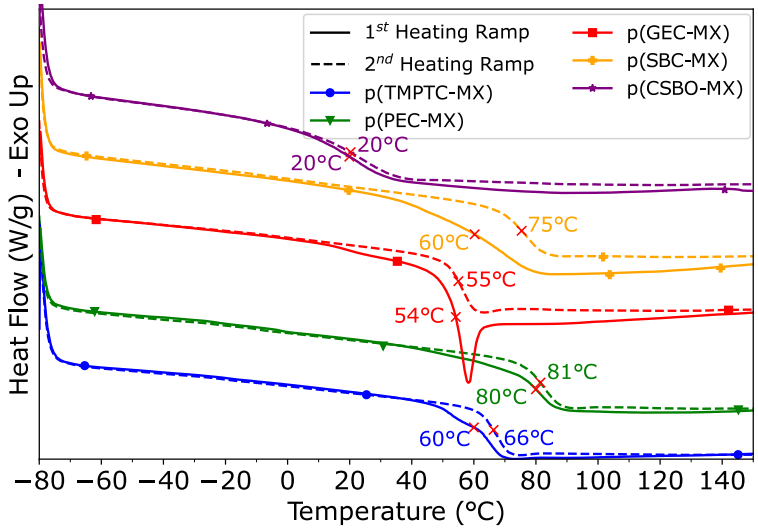

Figure II-6 – DSC heating ramps of the cured PHU formulations.

When considering thermoset polymers, a sufficient level of curing must be reached to ensure optimal properties and stability for the manufactured parts. DSC is a powerful tool as it gives the T_g of the system as manufactured in a first heating ramp. A potential lack of curing can then be identified through a second scan by a shift of the T_g. The DSC thermograms are presented in Fig. II-6. DSC curves highlight the broad range of results from one formulation to another on both levels of curing and T_g. The highest T_g was obtained for p(PEC-MX) polymer with 80 °C while for p(TMPTC-MX), p(SBC-MX), and p(GEC-MX) glass transition temperatures ranged between 55 °C and 60 °C. p(CSBO-MX) formulation has the lowest T_g, at 20 °C. The glass transition temperature is a function of the crosslinking density of the network, i.e. the number of CC functions in the carbonated precursors, and of the macromolecular structure of the precursors (e.g., a long aliphatic chain provides higher mobility, thus lowering the T_g) [378]. In this case, the high T_g of p(PEC-MX) is explained by the high degree of functionality leading to a highly crosslinked thermoset. On the opposite, p(GEC-MX) and p(TMPTC-MX) bearing three carbonates, exhibit a slightly lower T_g. Neither formulation presented any residual exothermic peak, and only a limited shift of T_g is observed

for p(TMPTC-MX) and p(GEC-MX).

An exception can be raised with p(SBC-MX) since it possesses a lower initial T_g than that would be expected, considering its high functionality. An important shift in T_g from 60 °C to 75 °C is also observed. This results from the numerous hydroxyl functions in the backbone of SBC, increasing the steric bulk hindrance and lowering both reactivity and diffusion of the amines in the curing network [377]. It can be noted that a good level of curing and interesting glass transition temperatures were obtained for all studied PHU thermosets making them suitable for structural applications [441].

II.2.3.2 Chemical resistance and moisture sensitivity

Swelling index (SI) and gel content (GC) were measured in a polar and a non-polar solvent (THF and toluene, respectively) in order to determine the crosslinking degree of the network. The results are summarised in Table II-4. All PHUs swell more in THF than in toluene due to their polar character [442]. p(TMPTC-MX), p(PEC-MX), p(GEC-MX), and p(SBC-MX) present a high gel content (superior to 98%) and low swelling index (inferior to 5%), except for TMPTC which showed a SI of 56.6% when immersed in THF. On the other hand, p(CSBO-MX) presents a higher swelling index and a lower gel content in both THF and toluene. This higher SI can be explained by the low crosslinking density induced by the macromolecular structure of CSBO, which consists of a long and flexible aliphatic backbone. The higher SI can also be explained by a lack of reactivity of CCs in the middle of the aliphatic chains of CSBO compared to CCs obtained from glycidyl ether [372]. By contrast to p(CSBO-MX), p(PEC-MX) and p(SBC-MX), presenting the highest crosslinking density, did not swell significantly, remaining below 1%. The poor reactivity of CSBO was further confirmed by the easiness of extracting the remaining precursors after swelling in both solvents. Indeed, mass spectrometry revealed the presence of saturated triglycerides in CSBO (m/z 685.4) in the supernatant, which cannot be epoxidized nor carbonated. The SI and GC results are similar to those of other studies on similar formulations [378, 381].

The sensitivity of PHUs to water is a key point for structural applications. Indeed, the ability of materials to absorb water is usually considered as a major drawback for aging. In the case of PHU thermosets, the high hydrophilicity of the hydroxyurethane moiety has been reported in several studies [381, 398, 433]. This water absorption can lead to a decrease of the T_g [384, 385]. This phenomenon is highly dependent on the chemical structures of both cyclic carbonates and curing amine and their ratio [397]. Similar observations can be made from this study. p(CSBO-MX) presents a low (5%) water uptake (WU) due to the hydrophobicity of the carbonate backbone and

the low hydroxyurethane content (that can be expressed through the higher CEW compared to other monomers), while p(GEC-MX) and p(PEC-MX) present significant WU of respectively 47 and 25%. The p(TMPTC-MX) formulation is slightly lower (13%) due to the presence of methyl groups in the backbone. The WU must be considered for further applications as it could be detrimental in structural applications but of interest for specific applications such as hygromorph materials [443].

Table II-4 – Gel content and swelling index of the PHU thermosets

Formulation	SI_{THF} %	$SI_{Toluene}$ %	GC_{THF} %	$GC_{Toluene}$ %	MU %	WU %
p(TMPTC-MX)	56.6 ± 1.73%	0.14 ± 0.12%	99.76 ± 0.44%	98.43 ± 0.8%	2.6 ± 0.1%	13 ± 1%
p(PEC-MX)	0.72 ± 0.16%	0.87 ± 0.61%	98.24 ± 0.17%	98.62 ± 0.65%	3.5 ± 0.4%	25 ± 1%
p(GEC-MX)	3.14 ± 0.88%	0.76 ± 0.16%	99.76 ± 0.41%	98.88 ± 0.8%	2.5 ± 0.5%	47 ± 2%
p(SBC-MX)	0.81 ± 0.66%	0.44 ± 0.56%	99.03 ± 0.39%	98.76 ± 0.46%	3.3 ± 0.3%	30 ± 4%
p(CSBO-MX)	239.28 ± 18.04%	54.04 ± 1.03%	74.59 ± 1.6%	93.67 ± 0.97%	1.1 ± 0.7%	5 ± 1%

II.2.3.3 Thermal stability

The thermal stability of the cured PHUs was evaluated through TGA under inert gas (N_2). Curves are presented in Fig. II-7, and values of interest are summarised in Table II-5. p(TMPTC-MX), p(PEC-MX), p(GEC-MX) and p(SBC-MX) formulations present comparable thermal stability and good performance. Indeed, in all cases, the $T_{d_{5\%}}$ is superior to 260 °C. The maximum degradation peak is observed at temperatures superior to 290 °C. Residual char was found between 12 and 20% for the four previously cited PHU thermosets. By contrast, although it has comparable $T_{d_{5\%}}$ and T_{max}, p(CSBO-MX) exhibits a very low (4%) residual char. This can be attributed to the aforementioned lower crosslinking density of CSBO, as well as to its long aliphatic structure and the presence of unreacted fatty acid and triglycerides. As a general observation, it must be noted that a higher degree of crosslinking favors the thermal stability and the charring of the thermosets. Both degradation temperature and residual char are in the range or slightly higher than those of epoxy resins [444], highlighting reasonable resistance to thermal degradation and sufficient stability to be used in thermoset applications.

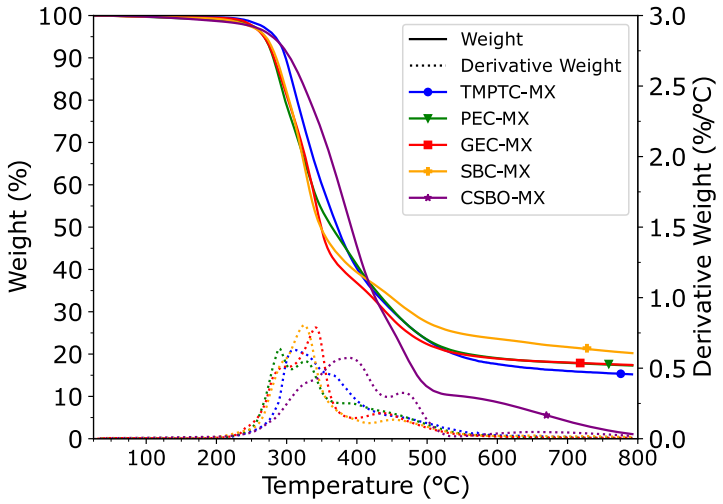

Figure II-7 – TGA under N_2 flow

II.2.3.4 Thermo-mechanical and mechanical properties

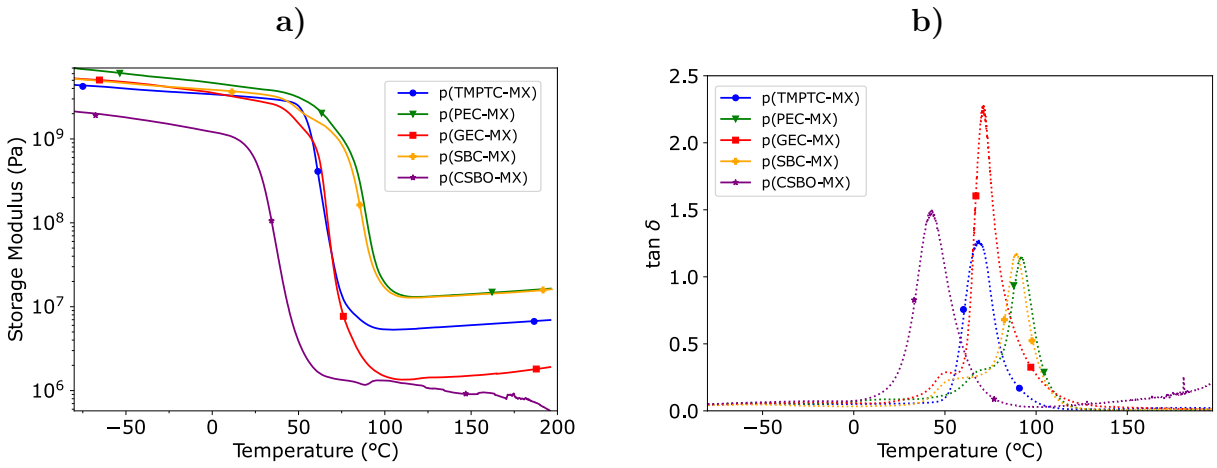

Figure II-8 – Dynamical Mechanical Analysis of the PHU formulations. a) Storage modulus, and b) tan δ as a function of temperature.

Thermo-mechanical properties of synthesized PHUs were assessed through DMA. Storage modulus and tanδ are represented as a function of temperature in Fig. II-8a-b and values can be found in Table II-5. The transition between the vitreous to the rubbery domain is defined at the maximum of the tanδ curve when chains are activated in large motions and named T_α [445]. This α transition appears within the same range as the glass transition determined by DSC. From the decrease of storage modulus between the glassy and rubbery domain, the crosslinking density can be evaluated and used to compare the different networks [445]. p(TMPTC-MX), p(PEC-MX), p(GEC-MX), and p(SBC-MX)

present similar behavior with a high storage modulus superior to 3 GPa in the glassy domain and a rubbery plateau superior to 1 MPa. p(CSBO-MX) presents the lowest storage modulus and T_α with 1210 MPa and 42 °C respectively, owing to the more flexible backbone. Moreover, it can be noted that the rubbery storage modulus drops with the temperature, highlighting a lower level of crosslinking and stability, as already highlighted through gel content and TGA analyses. p(PEC-MX) and p(SBC-MX) formulations have the highest crosslinking density, as expected due to the high content of CC moieties. p(TMPTC-MX) presents a slightly lower crosslinking density than p(PEC-MX) and p(SBC-MX) but remains quite high when compared to literature [378]. Surprisingly, even though p(GEC-MX) could be expected to have similar behavior and crosslinking density than p(TMPTC-MX) if their comparable glass transition temperatures and glassy moduli are considered, it was found to present a lower crosslinking density, comparable to that of p(CSBO-MX). This can be explained by the lower mobility of the CC in the middle of the GEC backbone, being less accessible to react with the amine, as already considered during rheological analyses. In other terms, the p(GEC-MX) network is less built than the other formulations. On the other hand, the shape of the peak in tanδ curves is known to be representative of the homogeneity for the polymer [445]. p(CSBO-MX) and p(TMPTC-MX) have a narrow and symmetric peak, highlighting a good homogeneity of the network. p(PEC-MX), p(SBC-MX), and p(GEC-MX) also have a narrow peak, but a small shoulder can be found at the onset of the α transition. This emphasizes a relatively good homogeneity of the network in general but some phase separation could have been achieved within the network [378, 446].

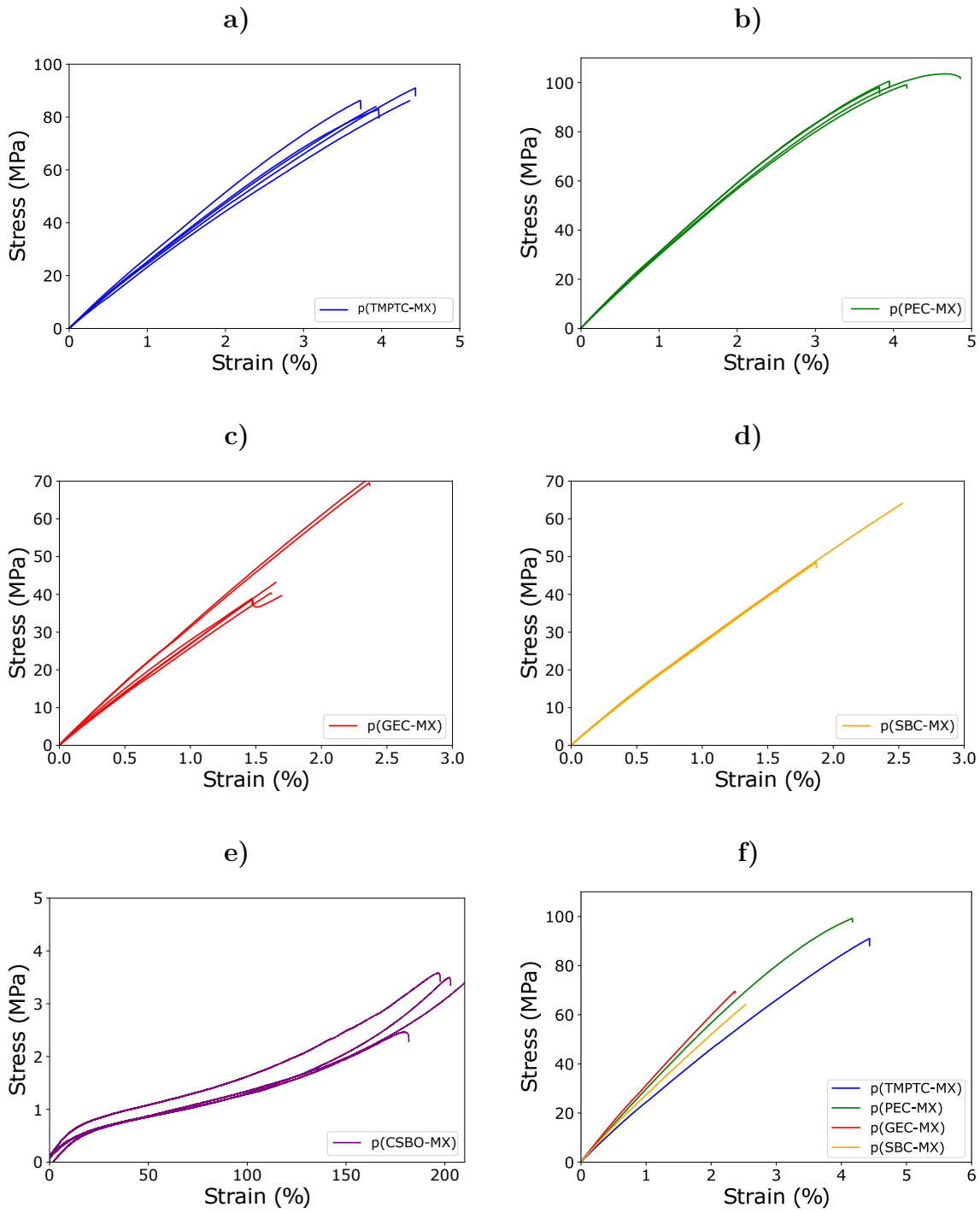

Figure II-9 – Tensile strain-stress curves of the PHUs formulations. a) p(TMPTC-MX), b) p(PEC-MX), c) p(GEC-MX), d) p(SBC-MX), e) p(CSBO-MX), and f) representative tensile curves of the different PHU formulations.

Considering future structural applications, the mechanical properties of the PHUs were characterized by monotonic tensile tests. Strain-stress curves are presented in Fig. II-9. Young's modulus, maximum strength, and strain at break are summarized in Table II-5. p(TMPTC-MX), p(PEC-MX), p(GEC-MX), and p(SBC-MX) present equivalent mechanical behaviors with a high Young's modulus between 2.4

GPa and 3.0 GPa. p(TMPTC-MX) and p(PEC-MX) thermosets display an outstanding balance of mechanical properties, with a strain at break superior to 4% and tensile strength of 89 and 100 MPa respectively, making them among the strongest PHU thermosets available in literature [378,380,381,399]. It must be noted that p(CSBO-MX) possesses an elastomeric behavior with low modulus and tensile strength (7 and 3 MPa respectively) and high ductility (200%). Thus, p(CSBO-MX) could be of interest to toughen other PHU formulations. As a general observation, the properties and the behavior of the formulated PHU thermosets appear to be suitable to compete with epoxy systems [447] as a greener alternative.

Table II-5 – Physical properties of the tested formulations (mean ± standard deviation)

Formulation			TMPTC-MX	PEC-MX	GEC-MX	SBC-MX	CSBO-MX
DSC	T_g	°C	60	80	54	60	20
TGA	$T_{d_{5\%}}$	°C	284	268	267	270	280
	$T_{d_{max}}$	°C	311	290	341	325	387
	Char	%	16	17.9	18.0	21.7	4.1
DMA	T_α	°C	68	92	70	88	42
	E'_{glassy}	MPa	3020	3650	2940	3690	1210
	$E'_{rubbery}$	MPa	5.33	13.10	1.60	15.30	1.40
	$\nu'_{E'}$	mol/m^3	559	1335	142	1580	139
Tensile	E	MPa	2472 ± 227	2999 ± 46	2780 ± 225	2658 ± 16	7 ± 2
Test	σ_{max}	MPa	88.8 ± 5.1	100.4 ± 2	50.6 ± 14.5	51.3 ± 9.6	3.3 ± 0.5
	ϵ_{max}	%	4.2 ± 0.6	4.15 ± 0.32	1.87 ± 0.38	1.99 ± 0.4	200.26 ± 15.49

II.2.4 Assessment of PHUs as Covalent Adaptable Networks

II.2.4.1 Stress relaxation properties

Even though they are derived from natural resources, the end-of-life of thermosets remains a major drawback when considering the environmental footprint of such materials. As an alternative, CAN polymers appear as a greener pathway to afford the recycling of so-often discarded materials [391]. PHUs are deemed promising candidates to efficiently replace non-reprocessable epoxy thermosets because they possess such dynamic network behavior. Previous works [22, 362, 386, 388] highlighted two main mechanisms in the exchange reaction of PHU networks: the associative transcarbamoylation, represented in Fig. II-10a have been reported to be the main mechanism, but dissociative reverse cyclic

carbonate aminolysis, represented in Fig. II-10b, has also been reported. Associative mechanisms induced a constant crosslinking density during rearrangement, while the dissociative mechanism is related to the breaking of reversible bonds, enabling the polymer to flow.

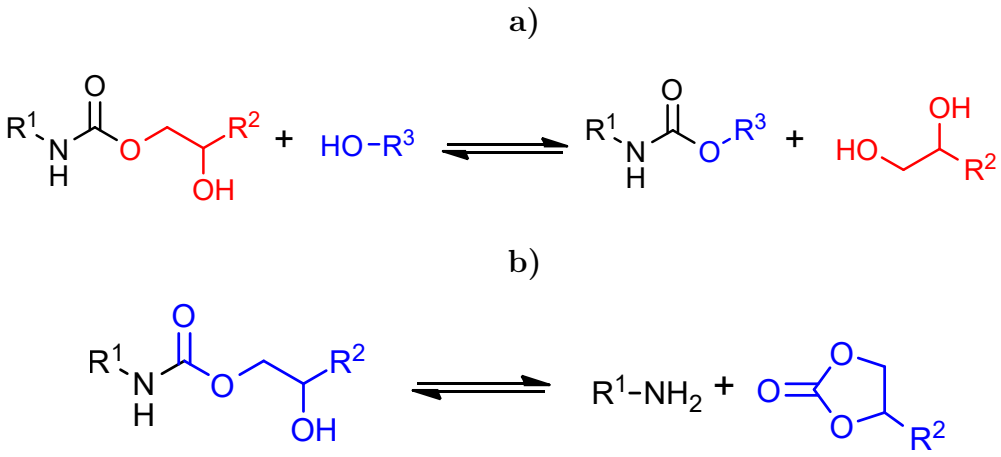

Figure II-10 – Polyhydroxyurethane potential rearrangement mechanisms. a) Transcarbamoylation (associative) b) Reverse cyclic carbonate aminolysis (dissociative)

The stress relaxation has been investigated for all formulations on a DMA in tensile mode to assess their reversible nature. All PHU formulations show stress relaxation ability as can be seen in Fig. II-11a-e and through Arrhenius law in Fig. II-11f, highlighting the ability of the hydroxyurethane moieties to rearrange. The activation energy (E_a), the square residual (r^2) of Arrhenius fitting, and the freezing temperature (T_v) are summarised in Table II-6.

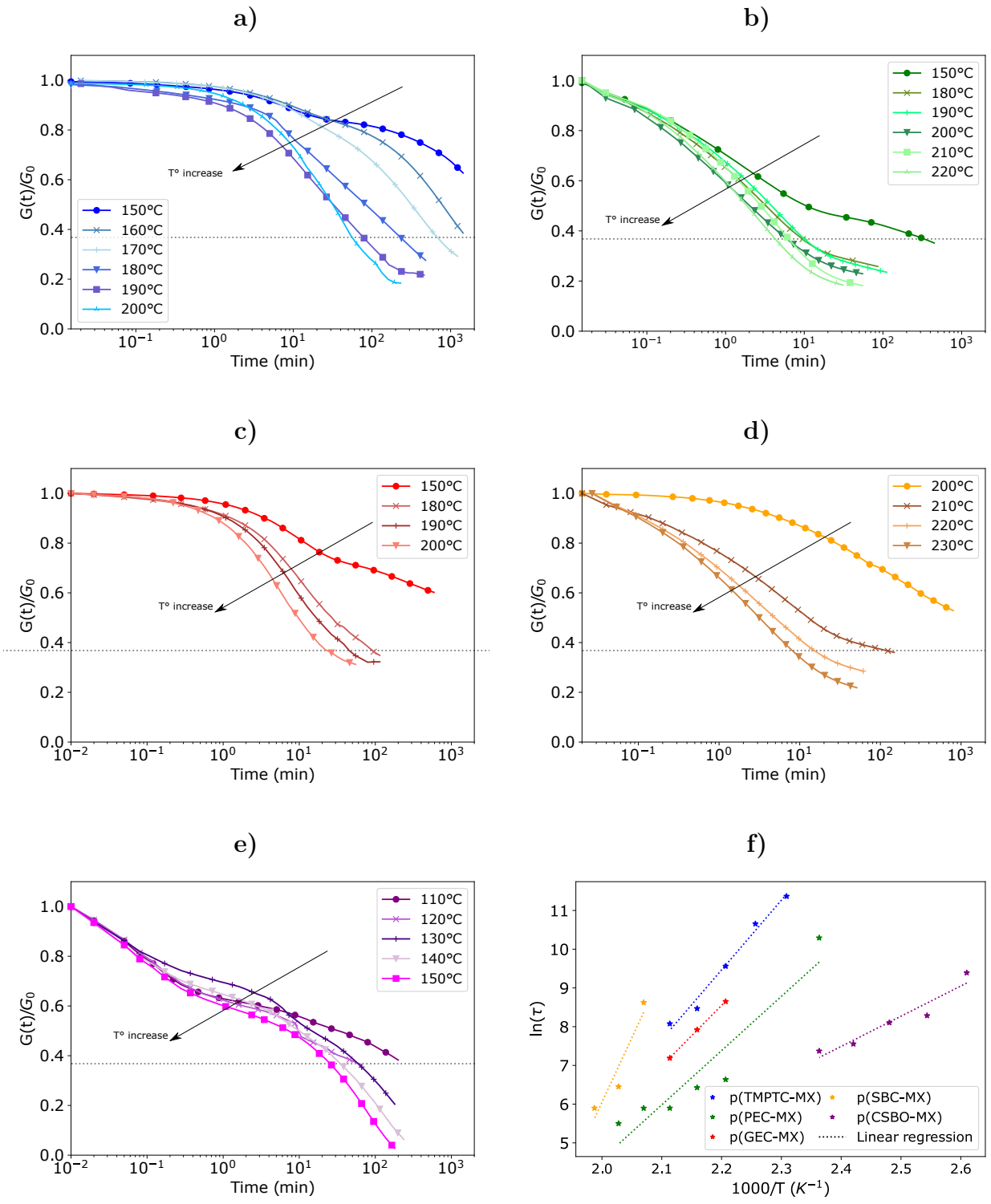

Figure II-11 – Stress relaxation of a) p(TMPTC-MX), b) p(PEC-MX), c) p(GEC-MX), d) p(SBC-MX), e) p(CSBO-MX), and f) Arrhenius plot of the PHUs.

The stress relaxation analyses highlight that p(CSBO-MX) formulation differs in behavior when compared to p(TMPTC-MX), p(PEC-MX), p(GEC-MX), and p(SBC-MX) systems due to the important difference in the network structure. p(CSBO-MX) presents the lowest activation energy (65 kJ/mol)

with stress relaxation starting at low temperature (110 °C). The same observations were made by Hu et al. [388] highlighting that lower temperature and processing time were required for CSBO-based PHUs due to transcarbamoylation, reverse aminolysis, and transesterification mechanisms when compared to a denser network. p(TMPTC-MX), p(PEC-MX), p(GEC-MX), and p(SBC-MX) appear to be less sensitive to stress relaxation with longer time and higher temperature required. A relaxation effect was already observed in p(TMPTC-MX) at 150 °C but requires time superior to 1000 minutes, making it not suitable nor competitive with other CAN polymers. Temperatures higher than 180 °C were required to relax in a reasonable amount of time even though the relaxation started at a lower temperature. At 180 °C, stress relaxation was reached after 4 h for p(TMPTC-MX), 1 h 30 for p(GEC-MX), and 12 min for p(PEC-MX). It must be noted that no catalyst was used to promote transcarbamoylation and reverse aminolysis.

Noticeable differences can also be found in activation energy among the formulations. p(SBC-MX) did stress relax but requires high energy, with the risk to get overlapped with thermal degradation events. p(TMPTC-MX), p(PEC-MX), p(GEC-MX), and p(SBC-MX) possess closer properties with activation energy between 123 and 150 kJ/mol, remaining comparable to other studies on PHUs [386, 448, 449]. Indeed, Fortman et al. [386] reported activation energies between 110 and 140 kJ/mol for six-membered CC-based PHUs with T_g around 50 °C. Chen et al. [448] synthesized five-membered CC-based PHUs with T_g around 20 °C, and also observed high activation energy between 135 and 155 kJ/mol. However, the rearrangement in the PHU networks remains of high complexity when compared to more known dynamic functions such as disulfide bonds [320, 449] and must be studied to a larger extent. As highlighted by Bakkali et al. [362], different mechanisms can take place, and each one is activated at different temperatures. Moreover, the hydroxyl functions within the PHU backbone can be either primary or secondary functions with a competition between reactivity and steric hindrance [442].

The topology freezing temperature (T_v) was also estimated. This temperature estimates the minimum temperature required for exchange reactions to occur [450]. The obtained values are consistent with the observed relaxation behavior and identified E_a of the formulated PHUs. In particular, T_v of p(TMPTC-MX), p(PEC-MX), p(GEC-MX), and p(SBC-MX) is ranging between 115 °C for p(GEC-MX) and p(TMPTC-MX) to 185 °C for p(SBC-MX), explaining the quicker relaxation obtained for p(GEC-MX) and p(PEC-MX) at a lower temperature than for p(TMPTC-MX) and p(SBC-MX). On the contrary and in addition to the low E_a, p(CSBO-MX), possesses a T_v of 29 °C, only slightly superior to its T_g, in accordance with values found in the literature for transesterification mechanisms [451] and underestimating that transesterification is the main mechanism in p(CSBO-MX)

network.

Nonetheless, it should be highlighted that although their performance cannot be compared to other systems such as siloxane [370], Schiff Base [452] or disulfide bond [320, 449], the PHU formulations, even when catalyst-free, can behave as CANs. In order to increase the transcarbamoylation rate and, therefore, the potential of PHUs in recycling, the use of catalysts should be considered. A more intensive investigation should be conducted to better understand and improve this high-potential behavior.

Table II-6 – Activation energy of PHUs through Arrhenius law fitting

Formulation	E_a	r^2	T_v
	kJ/mol		°C
p(TMPTC-MX)	149.6	0.992	142
p(PEC-MX)	116.4	0.944	118
p(GEC-MX)	130.3	0.998	115
p(SBC-MX)	276.6	0.950	185
p(CSBO-MX)	64.8	0.957	29

II.2.4.2 Reprocessing of polyhydroxyurethane thermosets

As a proof of concept, p(TMPTC-MX) and p(PEC-MX) were reprocessed (Fig. II-12) using the protocol shown in Fig. II-13a. Isothermal TGA in air was performed at 160 °C for 15 h to ensure that no significant degradation occurred during reprocessing. Less than 5% of weight loss was observed during the TGA analysis as shown in Fig. II-A19. Besides, in Fig. II-13b-c the SEM micrographs of the cryogenically fractured cross-sections of the reprocessed p(PEC-MX) and p(TMPTC-MX) are presented. They demonstrate the obtention of fully consolidated homogeneous materials. No porosity or microcracks can be observed.

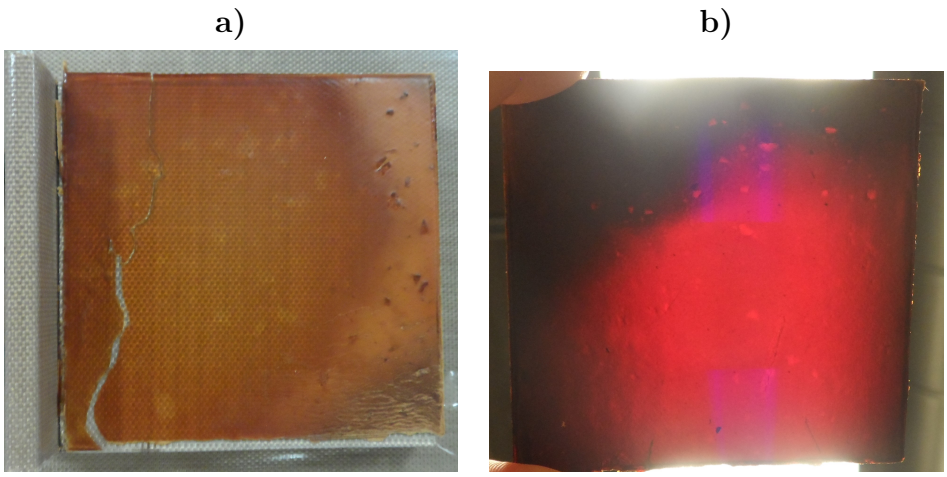

Figure II-12 – Reprocessed PHU a) p(TMPTC-MX), b) p(PEC-MX)

Both films obtained were homogeneous and translucent with only one hazy area due to the welding close to the edge of the mold. This is the first indication of the efficient network rearrangement of these thermosets, which is believed to happen via chemical rearrangement. In order to fully assess the chemical and not physical bonding, samples were immersed into THF for 3 weeks as reported in Fig. II-A20. After 3 weeks, no segmentation of the polymer was observed, indicating that the rearrangement happened through exchanges of reversible bonds [453]. The storage modulus and $tan\delta$ curves of the reprocessed films, obtained by DMA, are presented in Fig. II-13d-e, and numerical values are reported in Table II-7. Additionnally, IR spectra of virgin and reprocessed PHU polymers are shown in Fig. II-13f-g. IR results highlight no change in spectra that could be related to side reactions, degradation, or any changes in the chemical structure. The DMA curves highlight a thermoset behavior with a high storage modulus at a temperature below the glass transition and a loss of two orders of magnitude after, and the $\tan\delta$ peak is unique and sharp. This confirms the homogeneity of the reprocessed sample. Storage modulus at 25 °C was almost fully recovered for the reprocessed p(PEC-MX) and of about 50% for p(TMPTC-MX) formulation. This result is in agreement with stress relaxation analyses where p(PEC-MX) was found to relax faster than p(TMPTC-MX). T_v of p(TMPTC-MX), being 142 °C, a higher temperature is necessary to obtain comparable properties restoration as p(PEC-MX), having a T_v of 118 °C. Surprisingly, the α transition was higher for both reprocessed formulations while comparable crosslinking densities are observed (slightly higher for p(TMPTC-MX), slightly lower for p(PEC-MX)). This increase in the α transition can be partly attributed to a post-curing effect, in particular for p(TMPTC-MX) due to the combined effect of pressure and temperature [368, 453]. No rigid urea linkage that could further explain such behavior in the α transition [454] seems to have been formed during reprocessing since no peak at 1650 cm^{-1} was observed; however, it cannot be completely

ruled out. In both cases, reprocessing appears feasible, with good mechanical properties recovered; however, the reprocessing operating window is narrow to prevent thermal degradation.

Table II-7 – Thermo-mechanical properties of reprocessed p(TMPTC-MX) and p(PEC-MX) formulations

Sample		T_α	$E'_{glassy}25°C$	$E'_{rubbery}$	$\nu'_{E'}$	Recovery
		°C	MPa	MPa	mol/m^3	%
p(TMPTC-MX)	original	68	3120	5.3	559	-
p(TMPTC-MX)	reprocessed	81	1600	7.2	712	51.3
p(PEC-MX)	original	92	3996	13.8	1335	-
p(PEC-MX)	reprocessed	107	3921	11.1	1036	98.1

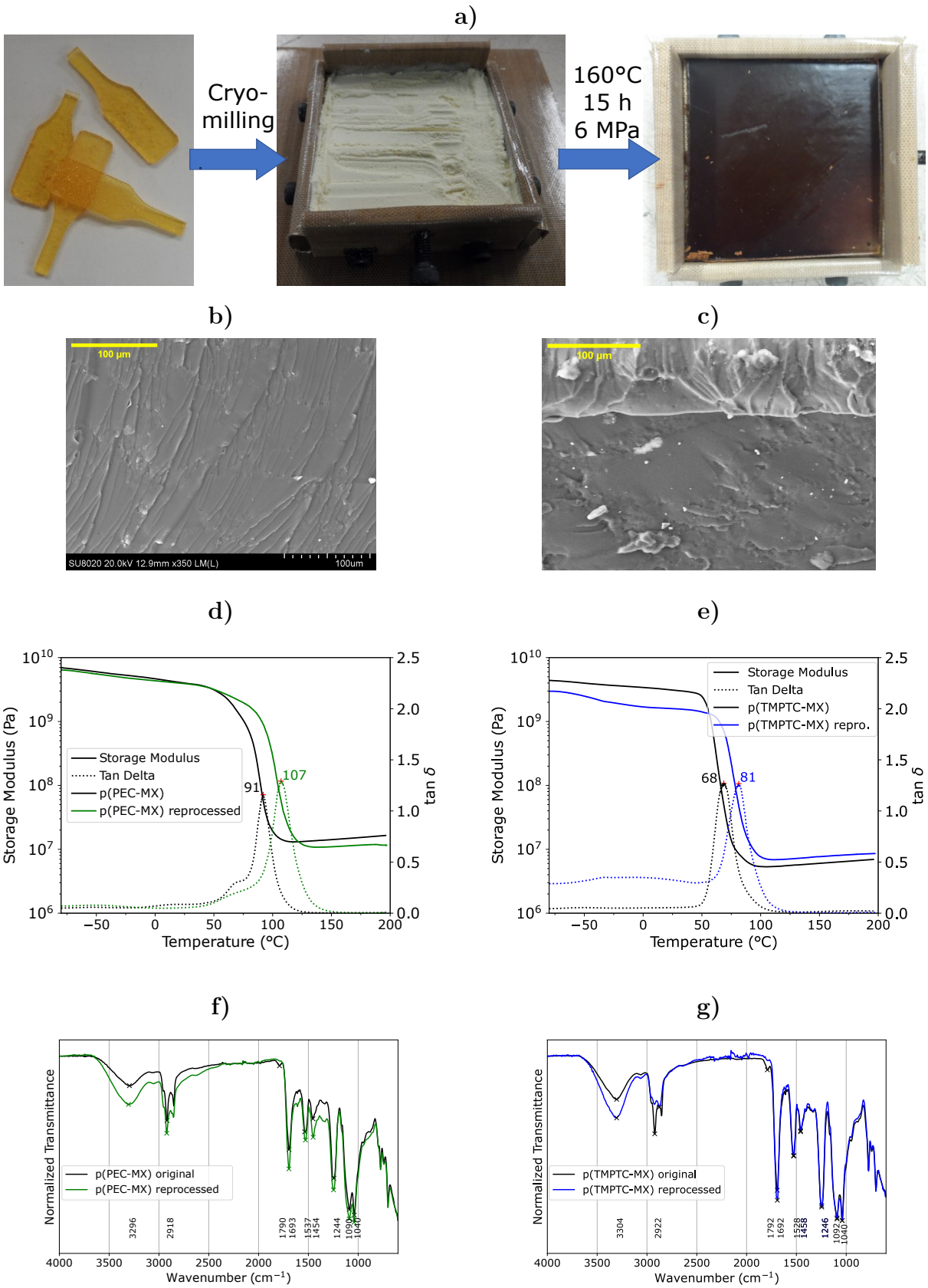

Figure II-13 – Reprocessing of PHUs. a) General protocol and reprocessed p(PEC-MX), b-c) SEM picture of cryo-fractured cross-sections of p(PEC-MX) and p(TMPTC-MX), d-e) DMA curves of p(PEC-MX)and p(TMPTC-MX),- and f-g) FTIR of p(PEC-MX)and p(TMPTC-MX)

II.3 Conclusions

Addressing green chemical processes, bio-based building blocks, enhanced polymer properties, and improved end-of-life options for the final structure remains a significant challenge in material sustainability. Among the numerous sustainable polymers developed over the last decades, polyhydroxyurethanes (PHU), from bio- CO_2-based precursors, arise as versatile, safer, and greener alternatives to conventional polyurethanes in many applications. In particular, the high hydrogen-bonding ability of PHU thermosets can pave the way to enhanced properties.

Up-to-date, no study on the relationship between the degree of functionality, the carbonate macromolecular structure, and the properties (processability, thermo-mechanical, reprocessability) has been conducted on PHU thermosets. As a consequence, a gap of knowledge was found, altering the vast implementation of PHUs to engineered applications. This chapter investigated this relationship, from the cyclic carbonate synthesis to the reprocessing of the crosslinked network, considering the CC's structure and degree of functionality. Five potentially biobased cyclic carbonates were synthesized from their epoxy precursors with CO_2 in solvent-free conditions and cured with an aromatic diamine.

The processability was investigated through rheology. The curing behavior of PHU thermosets is highly dependent on functionality, quickly reaching a non-processable state due to hydrogen bonding. The properties of the cured networks display high modulus, stress, and strain, together with good thermal stability. The thermo-mechanical properties of the PHU thermosets are comparable to those of conventional polyurethanes and epoxies, making them promising and competitive candidates for structural applications. Moreover, the vitrimeric behavior of the formulated PHUs was investigated. All formulations exhibit the ability to stress relax in catalyst-free conditions, and the reprocessed PHUs show similar thermo-mechanical behavior as the original ones. However, further work needs to be done in order to take advantage of such features, as reprocessing requires high temperature, high pressure, and a long time, rendering this ability hardly suitable in such conditions.

From the overall obtained results, the trimethylolpropane-based formulation appears as the most promising candidate to act as a composite matrix since it has relatively adequate viscosity that would allow processing using standard equipment (below 15 Pa.s at 80 °C), with interesting properties.

To further explore the prospective application of PHUs in composite materials, a thorough comparison with the epoxy counterpart should be performed for both pristine polymers and composites. Hybridizing PHUs with other chemistries, such as epoxy, methacrylate, and thiol-ene, may be considered to enhance their processability, final properties, or end-of-life scenario based on the eventual fabrication process and requirements of the final applications.

Chapter III

Exploiting PHU/Flax strong interfacial interactions to bring new opportunities in natural fiber composites

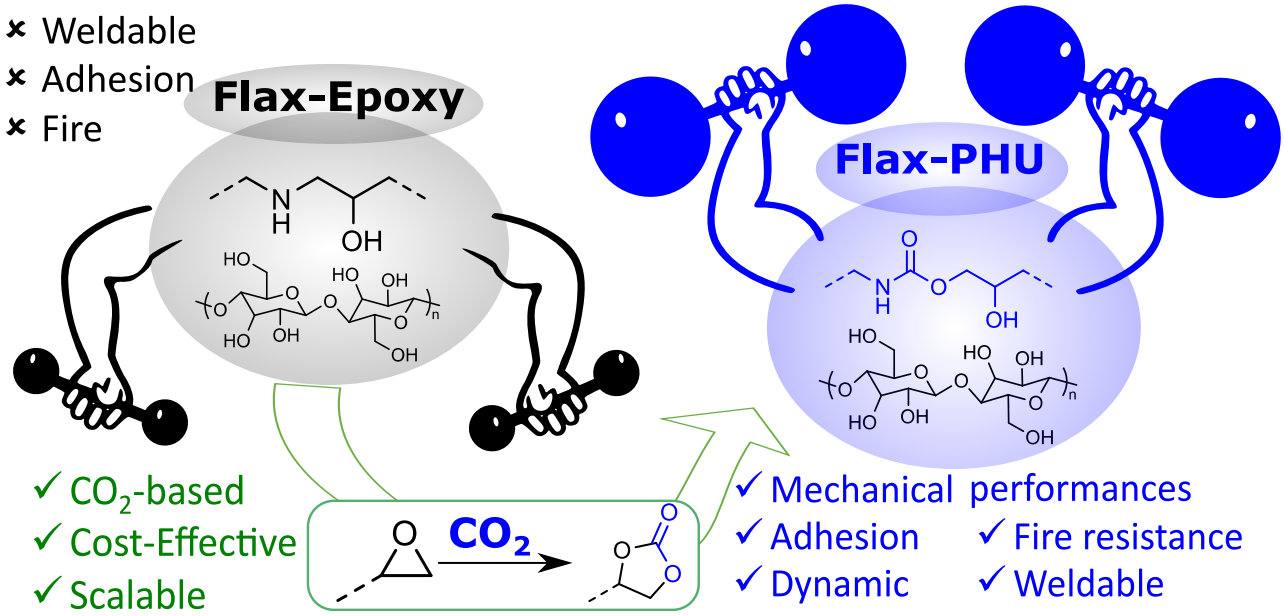

Adapted from: Seychal, G.; Nickmilder, P.; Lemaur, V.; Ocando, C.; Grignard, B.; Leclère, P.; Detrembleur, C.; Lazzaroni, R.; Sardon, H.; Aranburu, N.; Raquez, J.-M. A Novel Approach to Design Structural Natural Fiber Composites from Sustainable CO 2 -Derived Polyhydroxyurethane Thermosets with Outstanding Properties and Circular Features. Composites Part A: Applied Science and Manufacturing 2024, 185, 108311. https://doi.org/10.1016/j.compositesa.2024.108311.
External contributions: *P.N. performed the AFM measurements. V.L. performed the atomistic simulations. SEM images were performed by Materia Nova.*

Contents

III.1 Introduction

As previously stated in the literature review, natural (cellulosic) fibers (NF) such as flax, hemp, or sisal possess the potential to replace glass fibers in many composite applications. The combination of epoxy-amine (EP) resins with NFs has delivered structural composites whose remarkable performances [455] result from the presence of H-bonds and the potential reaction between oxirane and hydroxyl moieties [456].

As already observed in the previous chapter, PHU formulations, at the current development stage, possess viscosity and require long curing times, which limit their use in the realm of composite manufacturing. Yet they remain promising platforms with many advantages. Structurally, PHUs differ from PURs by the presence of hydroxyl moieties pendant along the main chain skeleton, providing hydrophilicity to the resins [372]. We hypothesized that this specific structure could favor the ability of PHU chains to form multiple hydrogen bonds, which is of particular interest for NFCs. This could also lead to a viable end-of-life recycling scenario by allowing the repurposing of structural composites through compression molding. Capitalizing on the intrinsic PHU features, a new generation of sustainable and recyclable composite materials could be designed, offering remarkable thermo-mechanical properties.

In this chapter, we propose the use of this unique PHU chemistry to manufacture unidirectional flax-based laminates by thermocompression. The neat PHU thermoset was characterized and compared to an epoxy counterpart made from trimethylolpropane triglycidyl ether. Notably, as CCs are obtained from epoxide monomers, the latter can also be polymerized by aminolysis, enabling the direct comparison between the material properties made from either epoxy or CC precursors. The reaction schemes are presented in Fig.III-1. Unidirectional flax laminates were then manufactured, and their morphology and mechanical performance were characterized. The study was completed by Atomic Force Microscopy and quick atomistic simulations to better understand the interactions between PHU and flax at the interface. Their fire behavior was also assessed, as this is a major requirement in structural applications. Finally, taking advantage of the dynamicity of the hydroxyurethanes in PHU networks, single-ply flax-PHU sheets were cured and later welded as pre-preg materials.

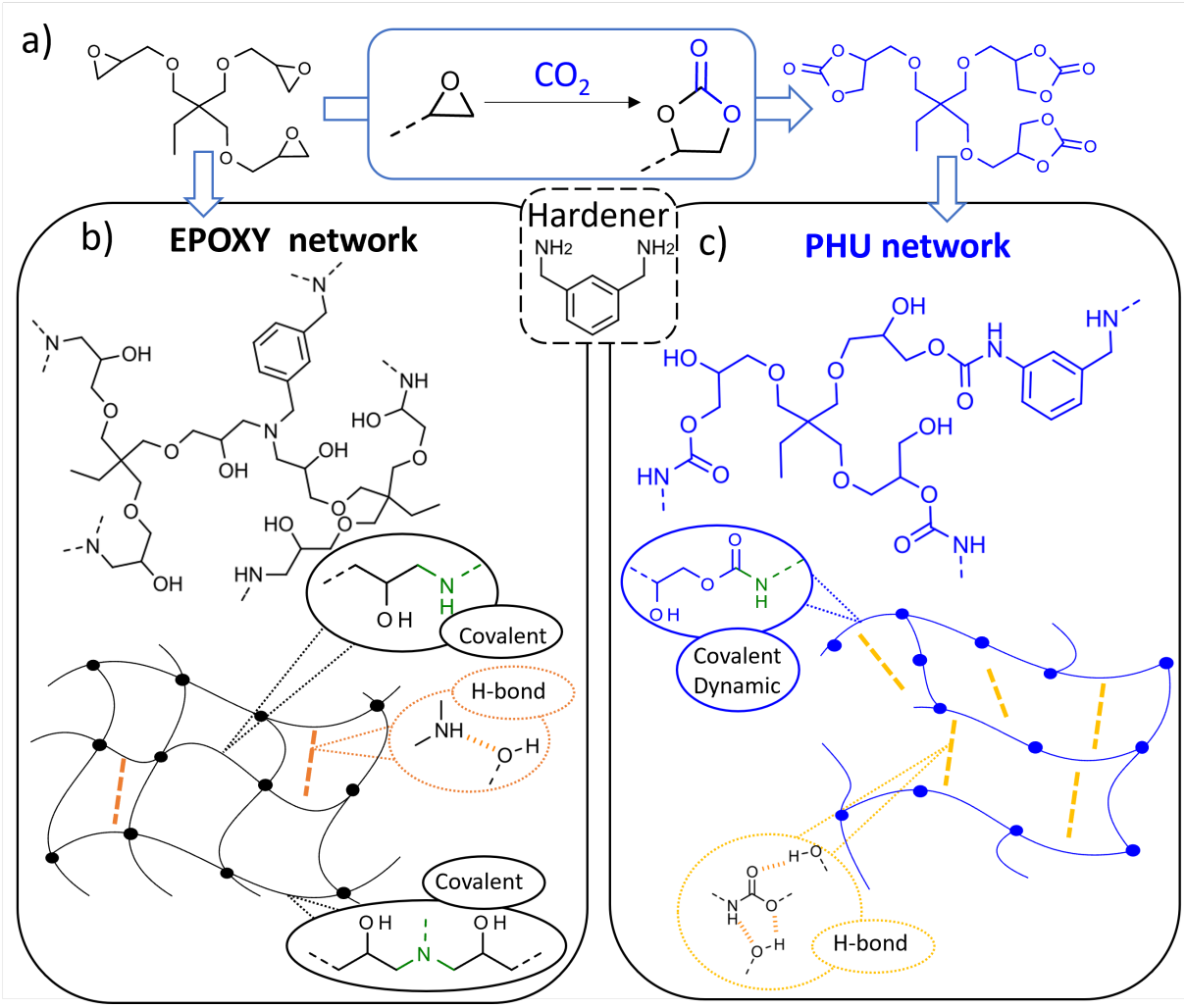

Figure III-1 – a) Formation of cyclic carbonate by addition of CO_2 to epoxy, b) Epoxy-amine representative network, and c) PHU representative network. (Full line insets represent the network crosslinking node, and dotted line insets represent the potential inter-/intra-molecular H-bond formed.)

III.2 Results and Discussion

III.2.1 Optimization of the PHU matrix

Before delving into composite manufacturing, the PHU formulation was optimized by adding different types and amounts of catalysts. Considering composite manufacturing processes, catalysts can enhance the curing time but can also drastically decrease the processability [41]. For each catalyst, 1 mol%, 5 mol%, and 10 mol% were considered with respect to CC functions. Isothermal rheological tests during the curing were performed at 80 °C. Results are summarized in Table III-1. The viscosity, storage, and loss modulus evolution over time can be found in Fig. III-4 and Fig. III-3. Overall results highlight the importance of the catalyst and the catalytic load over the curing of these mixtures. By adding

only 1 mol % of DMAP or DBU, the curing was positively affected. To reach the gel point, 49 and 51 min at 80 °C were necessary compared to the original 83 min, representing a decrease of about 40%. Interestingly, the pot life was not significantly affected, with 20 and 19 min, respectively, compared to 23 min for the non-catalyzed system. Surprisingly, a higher amount of DMAP did not lead to any important changes in the curing behavior, as no observable changes were found in the pot life, and the gel time dropped down to 41 min with 10 mol% of DMAP. Therefore, a threshold effect could be considered in the case of DMAP, and higher amounts are not required. The catalytic effect was reported to be greatly influenced by hydrogen bonding during polymerization [372, 377]. Consequently, this behavior could be related to the increase of the H-bonding that can decrease the catalytic effect of DMAP not being strong enough to act when the viscosity becomes too high [457]. Contrary to DMAP, DBU amount was shown to significantly modify the curing behavior. If 1% of DBU shows the same trends as DMAP, the reaction occurs much faster at room temperature with 5% of load. The faster start of the reaction was highlighted by the increase in the initial viscosity, reaching 83 Pa.s with 10% of DBU. Along the initial viscosity, the pot life was decreased up to 4 min and the gel time was reduced to 20 min. The improved catalytic effect of DBU on the catalysis of PHU polymerization was previously reported in literature [372]. However, it should be noted that in the mentioned work, PHUs were investigated for their potential use as adhesives, and the requirements on catalyst effect differ from composite manufacturing [41]. In any case, the DBU high catalytic activity appears to be detrimental for the processing window. Such behavior reflects the importance of the catalyst type and amount on the processability.

The amount of catalyst could also play an effect on the mechanical properties. In this work, it was assumed that the catalyst could act as a plasticizer and therefore decrease the glass transition or the glassy modulus [458]. For these reasons, the effect of catalyst was studied by DMA for 10% of DMAP or DBU. The extracted values are reported in Table III-1 and the graph can be found in Fig. III-4a. Infrared spectroscopy was also performed and depicted inFig. III-4b. With 10% of catalyst load, the FTIR reveals the appearance of urea signals at 1650 cm^{-1}. The formation of these urea linkages is the result of side reactions promoted by the catalyst, as previously reported in literature [373, 377]. The presence of catalysts also led to a decrease of about 20% of the storage modulus. However, the alpha transition (T_α) and the crosslinking density were unaffected by the presence of catalyst. With 10% of DMAP, the evolution of $\tan\delta$ exhibits two peaks that could be related to the presence of the urea linkage and potential phase separation [459]. Considering the effect of the studied catalyst on the processability and the final properties, 1% of DMAP was selected for the rest of the present study.

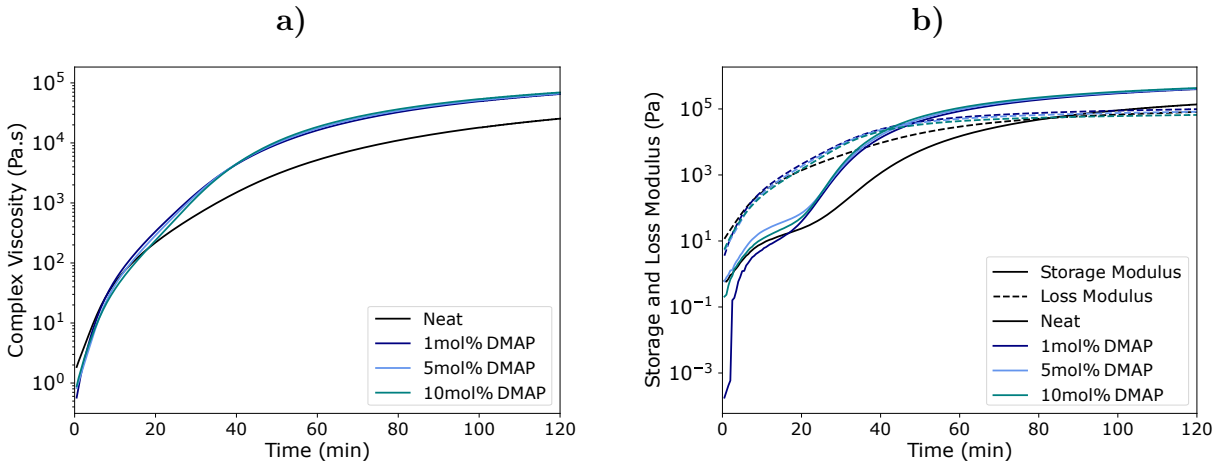

Figure III-2 – DMAP catalyst effect on a) Viscosity evolution of the TMPTC-MX formulations, and b) Modulus evolution during curing rheological behavior at 80 °C

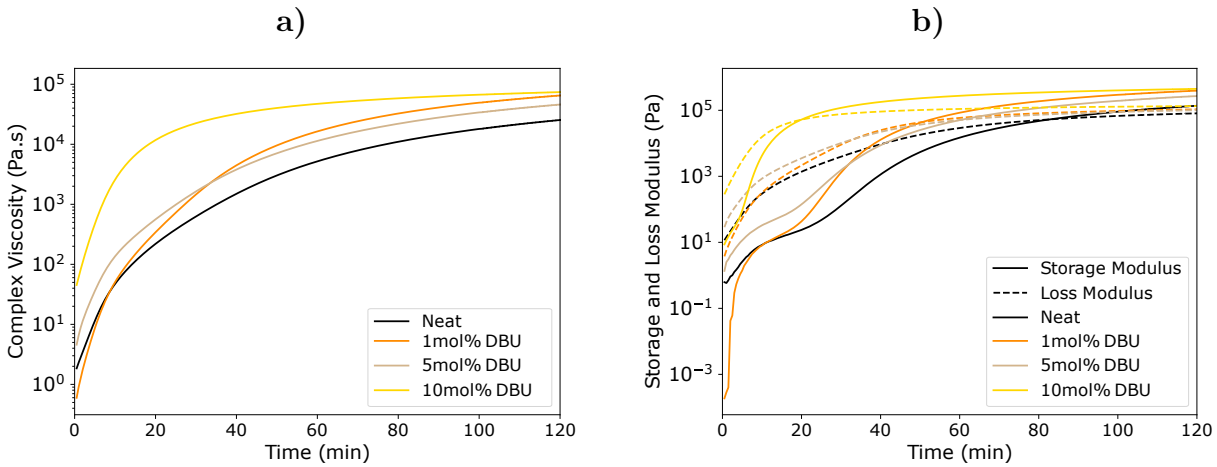

Figure III-3 – DBU catalyst effect on a) Viscosity evolution of the TMPTC-MX formulations, and b) Modulus evolution during curing rheological behavior at 80 °C

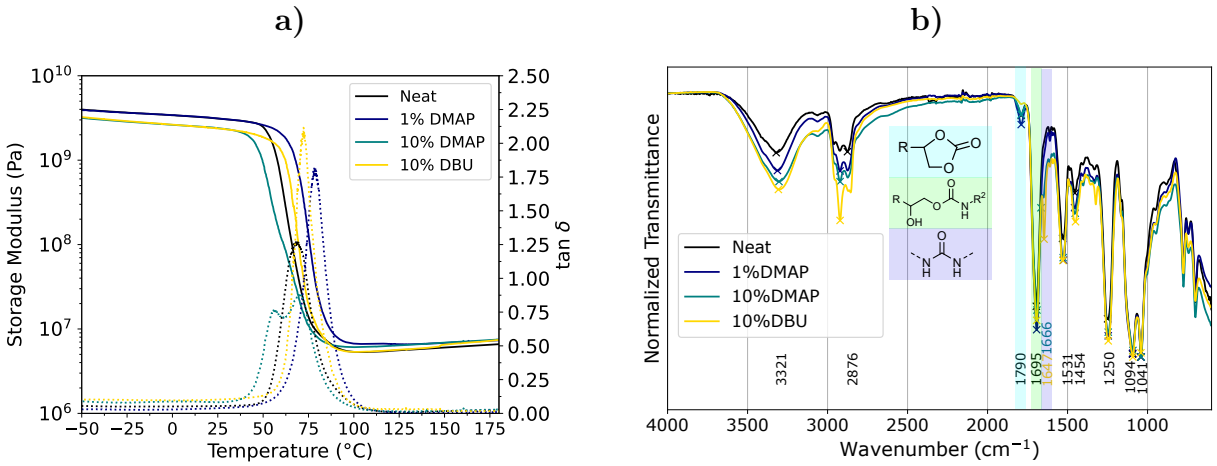

Figure III-4 – a) Effect of catalyst on thermo-mechanical properties, and b) FTIR of the cured TMPTC-MX thermosets with catalyst load

Table III-1 – Effect of catalyst on curing and thermo-mechanical properties of PHUs

			Neat	1% DMAP	5% DMAP	10% DMAP	1% DBU	5% DBU	10% DBU
Isothermal	η_{init}	Pa.s	2.8	1.3	1.4	1.6	1.3	8.9	82.5
rheology	Pot Life	min	23	19	20	21	19	15	4
	Gel Time	min	83	49	45	41	51	60	20
DMA	T_α	°C	69	78	-	70	-	-	72
	$E'_{25°C}$	MPa	3121	3129	-	2405	-	-	2374
	$E'_{rubbery}$	MPa	5.5	6.58	-	6.3	-	-	5.6
	ν'_e	mol/m^3	559	657	-	642	-	-	569

III.2.2 Comparison of the properties of PHU and epoxy thermosets

Before preparing NFCs based PHU resins, benchmarking of the thermo-mechanical performances of neat epoxy and PHU matrices was carried out. To date, unidirectional NFCs with the highest thermo-mechanical properties are commonly achieved with epoxy-amine systems [160, 460]. Switching from epoxides to cyclic carbonates implies a substantial change in terms of polymerization features, composite processing, and microstructure of the resins [461]. Consequently, and with the aim of assessing the interest of PHU chemistry over epoxy systems for NFC fabrication, the effect of the precursors on the processability and the final physical properties of the crosslinked polymers was studied.

III.2.2.1 Differences in resin flow and curing of epoxy and PHU

It was previously reported that the CC conversion from epoxide led to a significant increase in the viscosity [462], likely altering its processability. To investigate this, we analyzed the curing behavior and viscosity evolution through isothermal rheology at the curing temperature of 80 °C, as shown in Fig. III-5. Data are summarized in Table III-2. The rheological behavior of the PHU and the epoxy formulations show notable differences. The PHU displays a continuous increase in viscosity followed by a plateau with conversion progressing at a slower rate. Conversely, the low viscosity of the epoxy resin does not show any significant changes at the very beginning of the test and gelation occurs rapidly, resulting in a steady increase of the viscosity after a few minutes. It is worth noting that the initial viscosity of the PHU mixture was significantly higher than that of the epoxy formulation by a factor of 10. With a viscosity of 0.1 Pa.s, the epoxy possesses a very low viscosity making it a commonly used reactive diluent and suitable for most infusion processes [160]. On the opposite, the PHU formulation presents an initial viscosity of 1.3 Pa.s, which rapidly increases to reach a plateau. Such particular behavior can be explained by secondary H-bonding generated during PHUs curing. These newly formed bonds result in higher viscosity, and lower reactivity due to the steric bulk hindrance effect [377]. Even though such resin can lead to elevated viscosity during curing, their curing behavior remains satisfactory for small-scale thermo-compression [41, 160].

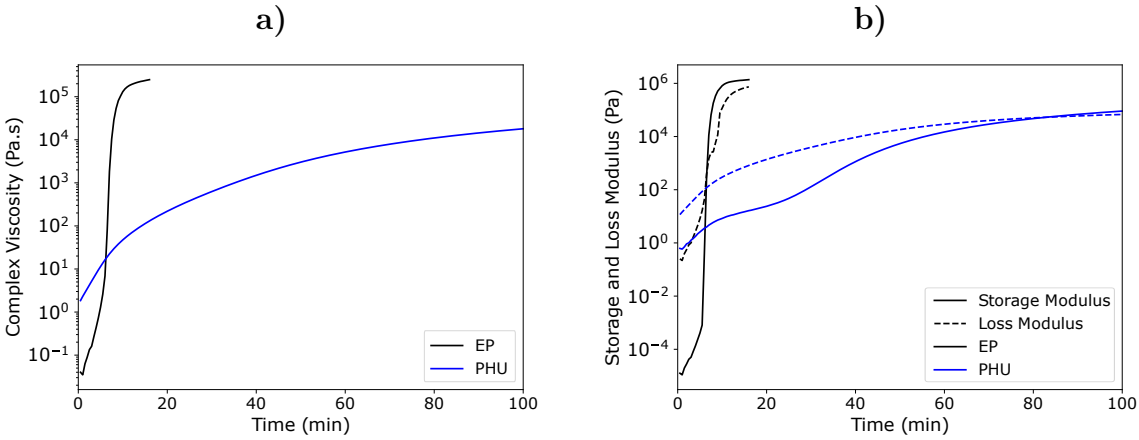

Figure III-5 – Isothermal curing (80 °C) of epoxy and PHU in rheometer.a) Viscosity evolution, and b) Modulus evolution over time

III.2.2.2 Thermo-mechanical properties

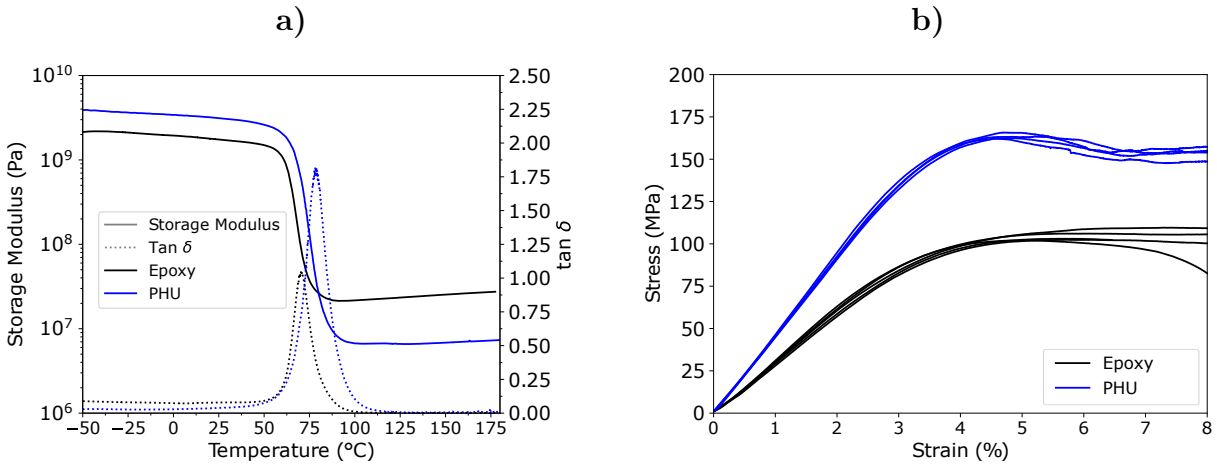

Figure III-6 – a) Thermo-mechanical behavior, and b) three-point monotonic bending strain-stress curves of the epoxy and PHU neat matrices used for composite impregnation.

Mechanical and thermo-mechanical properties of the fully cured thermosets were assessed through Dynamical Mechanical Analyses (DMA) (Fig. III-6a), three-point bending (Fig. III-6b), and tensile tests (Fig. III-A2). All values are reported in Table III-2. Interestingly, the PHU thermoset displays a notable improvement regarding the thermo-mechanical properties. DMA highlights a superior glassy modulus at room temperature, from 1.7 GPa for the epoxy up to 3.1 GPa for the PHU. The α transition relaxation (T_α), relative to the glass transition, marks the change from the glassy domain to the rubbery domain. This transition, as determined at the maximum of the $\tan\delta$ curve, occurs at a slightly higher temperature in the case of the PHU. In particular, the PHU shows an 8 °C higher transition temperature, rising from 70 °C for the epoxy to 78 °C for the PHU. Moreover, the sharp and narrow peak in the $\tan\delta$ curve indicates a homogeneous network structure. The large intensity of the $\tan\delta$ peak of the PHU compared to the epoxy reveals drastic changes in the thermo-mechanical behavior. This heightened intensity, alongside the lower crosslinking density of PHUs, highlights the excellent damping capacity of the material [133].

Table III-2 – Comparison between epoxy and PHU neat matrices properties used for composite impregnation (mean ± standard deviation)

			Epoxy	PHU
	GC_{THF}	%	98 ± 1	99 ± 1
	ρ	g/cm^3	1.19 ± 0.01	1.26 ± 0.02
Isothermal	η_{init}	Pa.s	0.10	1.30
rheology	Pot Life	min	6.5	19.0
80 °C	Gel Time	min	6.5	49.0
TGA	$T_{d_{5\%}}$	°C	315	284
	$Char_{800°C}$	%	13.3	15.2
Tensile	E	GPa	2.5 ± 0.1	2.5 ± 0.2
	σ_{yield}	MPa	55.1 ± 2.0	88.8 ± 5.1
	ε_{yield}	%	2.9 ± 0.1	4.2 ± 0.6
3Pt	E	GPa	2.7 ± 0.2	4.4 ± 0.1
bending	σ_{yield}	MPa	104.6 ± 2.7	163.5 ± 1.4
	ε_{yield}	%	5.8 ± 0.5	4.8 ± 0.3
DMA	T_α	°C	70	78
	$E'_{25°C}$	MPa	1746	3129
	$E'_{rubbery}$	MPa	23.0	6.6
	ν'_e	mol/m^3	2346	657

This change is mainly related to the difference in the macromolecular structure of the network. Indeed, in addition to the effect of the precursor structure (aromatic, aliphatic...), it has been demonstrated that the thermo-mechanical properties of amorphous thermosets are significantly affected by the crosslinking density [463] and the hydrogen bonding [464]. Herein, the ring opening of oxirane by amines leads to secondary (primary amine reacting) and tertiary amines (secondary amines reacting) with free pendant hydroxyl groups [465]. Consequently, the resulting network is highly crosslinked with a density of 2346 mol/m^3. In contrast, for PHUs, only primary amines react with CC [437], and lead to a hydroxyurethane moiety [466]. This results in a significantly lower crosslinking density, with 657 mol/m^3. Hence, the two macromolecular structures are relatively close due to the precursor's similar structures but differ in linkage nature, crosslinking, and H-bonds density and type. These differences explain the superior thermo-mechanical properties of PHUs over epoxide counterparts at room temperature. Both H-bonds and macromolecular structure contribute to a high glassy modulus and an elevated T_α while the presence of numerous weak hydrogen bonds maintains a ductile behavior and an elevated

modulus. After reaching the rubbery state, the H-bond density and strength significantly decrease and its total strength becomes insufficient, making the thermo-mechanical properties of the PHU only dictated by covalent bonding. Together with a crosslinking density of 2346 mol/m^3, the epoxy exhibits a higher rubbery storage modulus than the PHU. This behavior is also observed in both monotonic tensile and three-point bending tests. In tensile, a similar Young's modulus of 2.5 GPa is obtained for both thermosets. However, the PHU exhibits a significant increase of 61 % and 47% of the stress and strain at break, respectively, over the epoxy counterpart. In three-point bending, both modulus and stress are increased in PHU by 63 and 56 %, respectively, while maintaining a comparable level of ductility. It is worth noting that even though the strain at yield was similar for both polymers, PHU did not break during the bending test.

The different trends in tensile and bending behavior can be likely explained on the basis of other organic materials. The presence of H-bonds has been shown to increase the shearing properties of organic materials [467], explaining the higher modulus and stress during bending of the PHU compared to the epoxy counterpart. Although three-point bending tests are not supposed to exhibit shear in the Euler-Bernoulli beam theory, we cannot completely avoid it during our tests. In tensile testing, this shearing effect is not present and the lower crosslinking density of the PHU can be counterbalanced by H-bonds leading to a similar modulus. However, the macromolecular structure allows the PHU to reach higher stress and strain at break than the epoxy counterpart [464] thanks to its stronger H-bond interactions even though the crosslinking density is lower (see the modeling section below).

The thermal stability was evaluated by thermogravimetric analysis (TGA) under N_2 gas (Fig. III-A1). TGA results show that the thermal degradation is almost the same with a slight increase in the char yield of the PHU over the epoxy counterpart. Overall, the study shows a significant improvement in the thermo-mechanical properties when moving from epoxy chemistry to polyhydroxyurethane chemistry. These improvements highlight the substantial advantages of utilizing carbonate derivatives as a means to readily enhance the properties of thermosets. Furthermore, the obtained thermo-mechanical properties were found to align perfectly with the requirements of NFC in the frame of high-performance matrices [160].

III.2.3 Evaluation of flax-PHU (F-PHU) and flax-epoxy (F-EP) structural composites

III.2.3.1 About the impregnation quality, fiber content, and porosity levels

Unidirectional flax fiber laminates were manufactured using the two studied matrices. The obtained laminates and the Scanning Electron Microscopy (SEM) images of their transversal cross-sections are depicted in Fig. III-7. The density, fiber volume fraction (V_f), and void content (V_v) were calculated for each specimen and summarized in Table III-3.

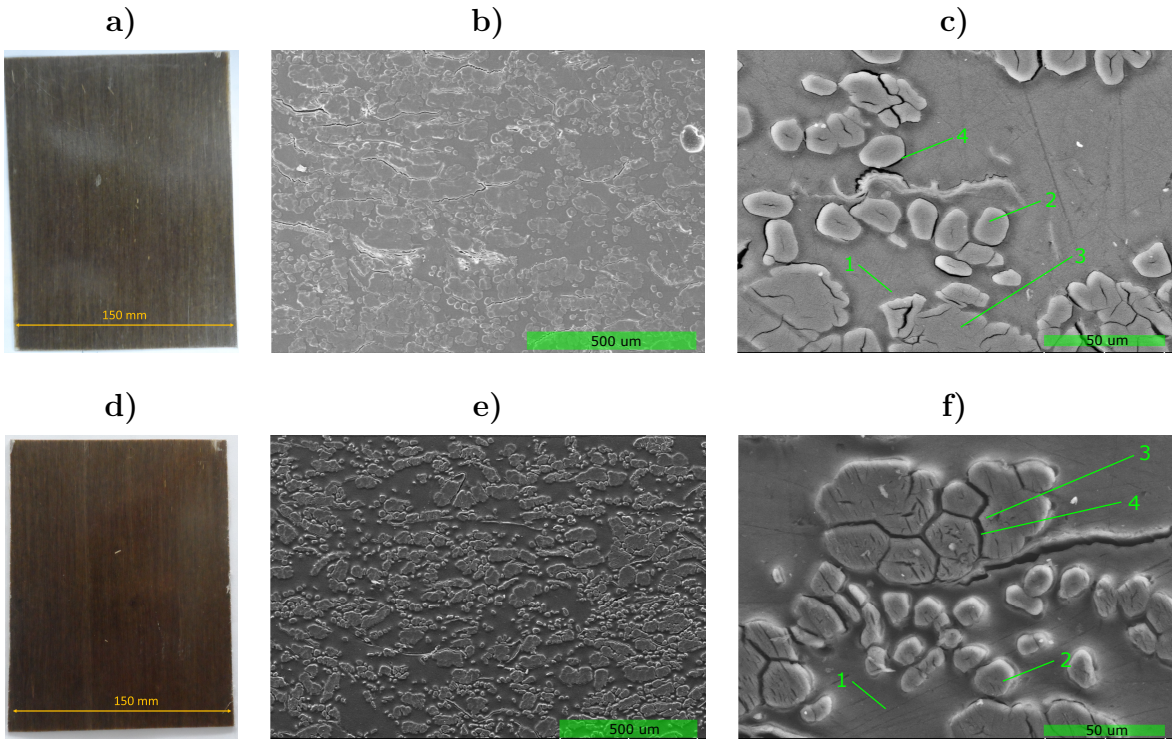

Figure III-7 – Pictures of the manufactured laminates, SEM cross-section images with x80 magnifications and x700 magnifications (left to right) for a-c) F-EP, and d-f) F-PHU. 1: Matrix, 2: flax fiber, 3: fiber bundle, 4: adhesion discontinuity

All laminates exhibit high V_f, which are consistent with reinforcements, resulting in 50% for F-PHU, and 48% for F-EP. These values are typical for flax composites obtained through thermocompression [167, 460]. V_v is between 0.2% for F-EP and 1.1% for F-PHU, in the lower range of flax fiber composites, demonstrating the high quality of the fiber impregnations [160]. The SEM images reveal well-impregnated materials with no significant differences between each other and no significant defects detected. Notably, the F-EP appears to have better-impregnated fiber bundles (Fig. III-7c) due to its lower viscosity, consistent with the low porosity level. However, the SEM images reveal closer proximity

at the interface in PHU-based laminates compared to epoxy-based one, suggesting a better affinity between PHU and natural fibers [455].

III.2.3.2 Investigation of the fiber/matrix interface, observation and rationalization

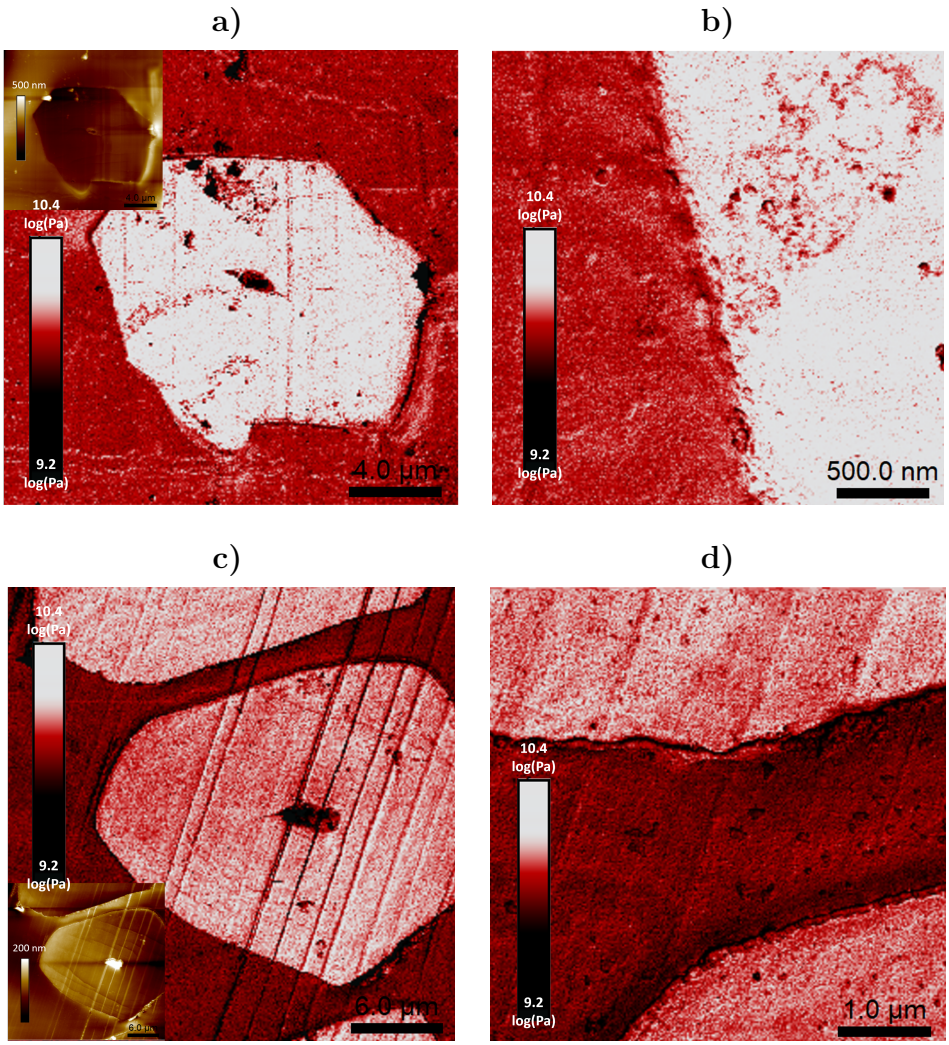

Figure III-8 – a) AFM-PFT rigidity modulus (log scale) of cryo-microtomed F-PHU sample (Inset: corresponding topographic image).b) zoom of a). c) AFM-PFT rigidity modulus (log scale) of cryo-microtomed F-EP sample. (Inset: corresponding topographic image). d) zoom of c).

To investigate the interface at the microscale, Atomic Force Microscopy (AFM) was performed, and the results are displayed in Fig. III-8. Noteworthy, AFM images revealed superior wetting of the flax with the PHU matrix compared to the epoxy one. This was evident from the continuity of material observed between the flax and the PHU matrix at the interface. Despite good impregnation, the F-EP

reveals discontinuity at the interface, revealing a lower affinity between the fiber and the matrix. To the author's best knowledge, it is the first time that such results have been observed in the case of NFC. Such images are consistent with the previously observed SEM images and highlight the improved affinity between PHUs and natural cellulosic fibers due to their hydrophilic character.

To gain atomistic insights into the enhanced affinity of PHUs with natural fibers compared to epoxy matrices, a modeling study combining a classical approach (molecular mechanics and molecular dynamics) and quantum calculations (Density Functional Theory, DFT) has been conducted. The calculations reveal higher complexation energies for PHUs with natural cellulose (-23.4 kcal/mol) in contrast to epoxy matrices (-21.2 kcal/mol). Despite the fact that both complexes feature three stabilizing hydrogen bonds, the larger complexation energy observed for PHUs with natural cellulose is attributed to the formation of these hydrogen bonds with three distinct atomic sites of cellulose, whereas in the case of epoxy matrices, the H-bonds are localized to only two atoms as shown in Fig.III-9. The increase in the number of contact points on cellulose for PHU systems is a consequence of the chemical characteristics of PHU, wherein the amine and alcohol functional groups are more spatially separated compared to those in epoxy matrices. This structural difference favors increased interactions between PHUs and cellulose. Natural fibers are complex hierarchical structures composed by celluloses (crystalline and amorphous), hemicelluloses, pectins, lignin, and others [23]. Therefore, for the sake of simplicity, the flax was modeled as a single repeating unit of cellulose in the atomistic simulations. As a consequence, the model should not be considered an accurate representation but an insight into the complex interactions occurring at the fiber/matrix interface. The results support the original hypothesis that implementing stronger H-bonds in the polymer backbone through this novel PHU chemistry would lead to a more intimate relationship between hydrophilic fibers and the matrix. However, a better understanding of the true interfacial interactions - chemically and physically - remains required in the future of natural fiber composite to embrace their potential fully. Such work should include more detailed and representative modeling of the fiber structure.

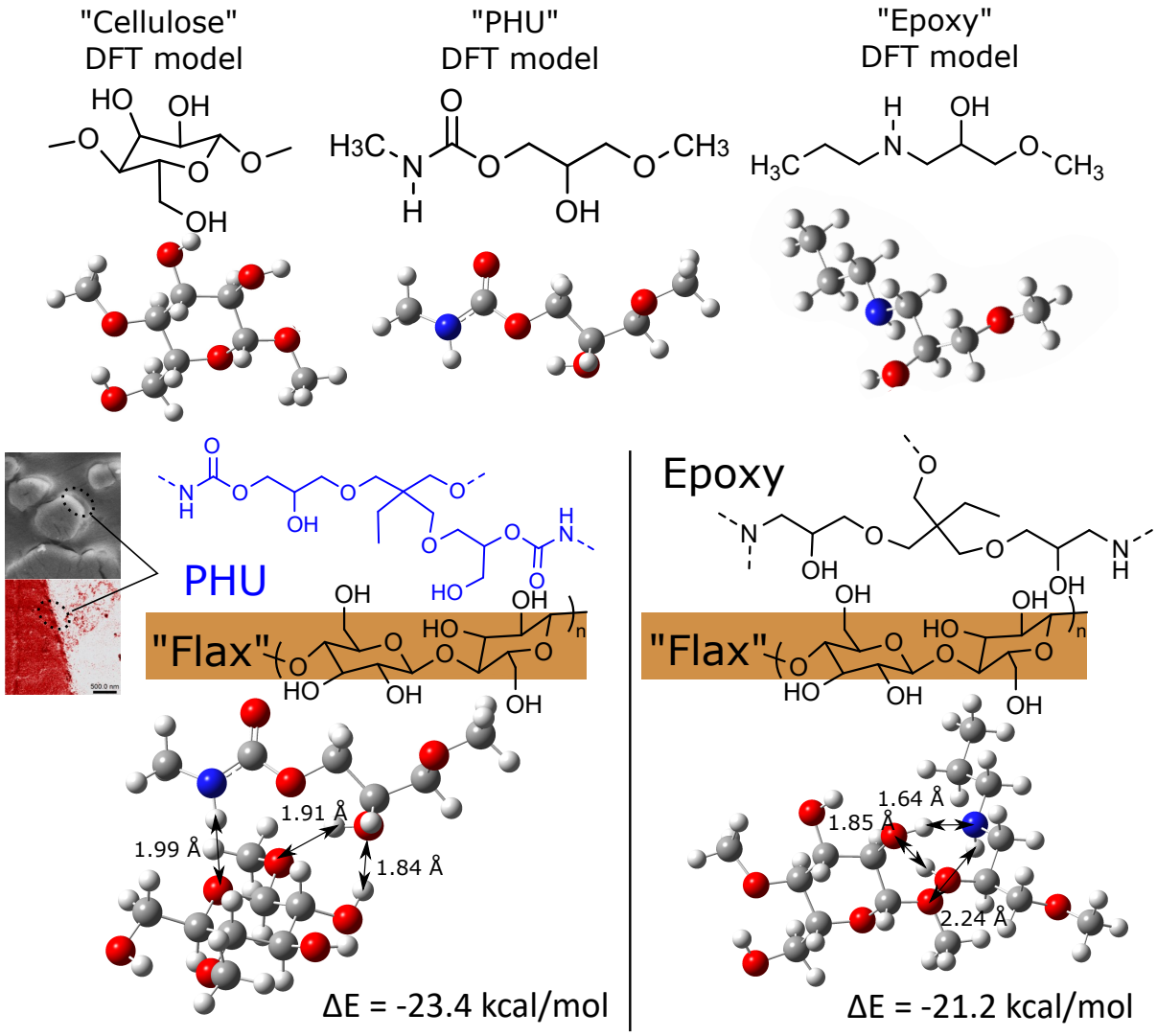

Figure III-9 – Schematic representation of the interface of the composites with the DFT-optimized structure of the F-PHU (left) and F-EP(right) complexes. The numerical values correspond to the lengths of the H-Bonds between PHU or EP and the cellulose and to the energies for F-PHU and F-EP

III.2.3.3 Mechanical behavior of the flax/PHU and flax/EP laminates

The mechanical properties of the unidirectional laminates were assessed by three-point bending tests in the two main orthotropic directions: one with the load parallel to the fibers (referred to as F0), and one with the load perpendicular to the fibers (referred to as F90). The bending stress-strain curves of these materials are presented in Fig.III-10 and a summary of their properties is shown in Table III-3. It is important to note that the bending behavior is affected by the material's tensile, compressive, and shear properties. Accordingly, the failure is initiated by the weakest of these three constituents [468]. All tests consistently exhibited low dispersion and low scattering of the results,

confirming the effectiveness of the processing method and the reliability of the results.

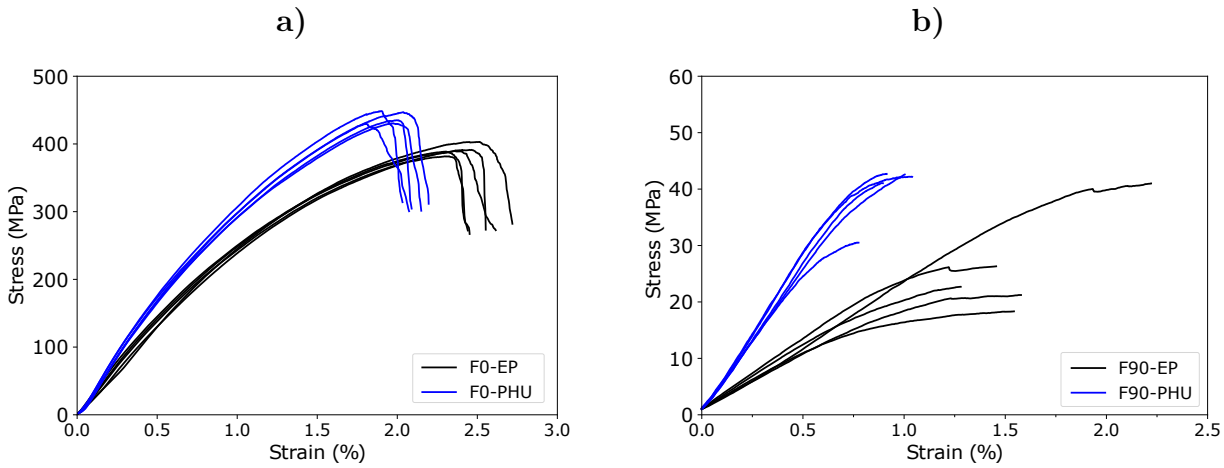

Figure III-10 – Three-point bending strain-stress of F-EP and F-PHU in a) longitudinal and b) transverse directions.

In the longitudinal direction, high bending properties were achieved for all materials, with a modulus of 28 GPa for F0-EP and an even more impressive 35 GPa for F0-PHU. Additionally, these materials displayed impressive ultimate stress values, with F0-EP reaching 391 MPa and F0-PHU achieving an even higher 438 MPa. Interestingly, the F0-PHU material exhibits remarkable modulus and admissible stress, surpassing its epoxy counterpart as well as previous studies in the literature involving similar materials [169, 274, 455, 469, 470]. In this loading direction, the matrix acts as a transferring agent of external forces to the load-bearing fibers. Therefore, it is expected that the better the interfacial adhesion, the higher the bending properties will be [455]. The strain at break of the laminates was slightly lower for PHU-based laminate (2.39% for F0-EP, 1.94% for F0-PHU). This reduction is also attributed to the improved affinity between the fibers and the matrix. In the case of lower adhesion, fiber pull-out tends to occur, resulting in a slight increase in the strain [456]. On the contrary, efficient load transfer to the fibers leads to a sharp break of both the fibers and the matrix [471]. This observation is further confirmed by the SEM images of the fractured samples, as depicted in Fig. III-11 where the fibers are seen to be broken at the very failure facies for F0-PHU, while pulled-out fibers are visible on the F0-EP. Hence, these initial results provide further support for the strong affinity between PHUs and flax attributed to H-bonds, as previously stated through atomistic simulations and SEM and AFM analyses.

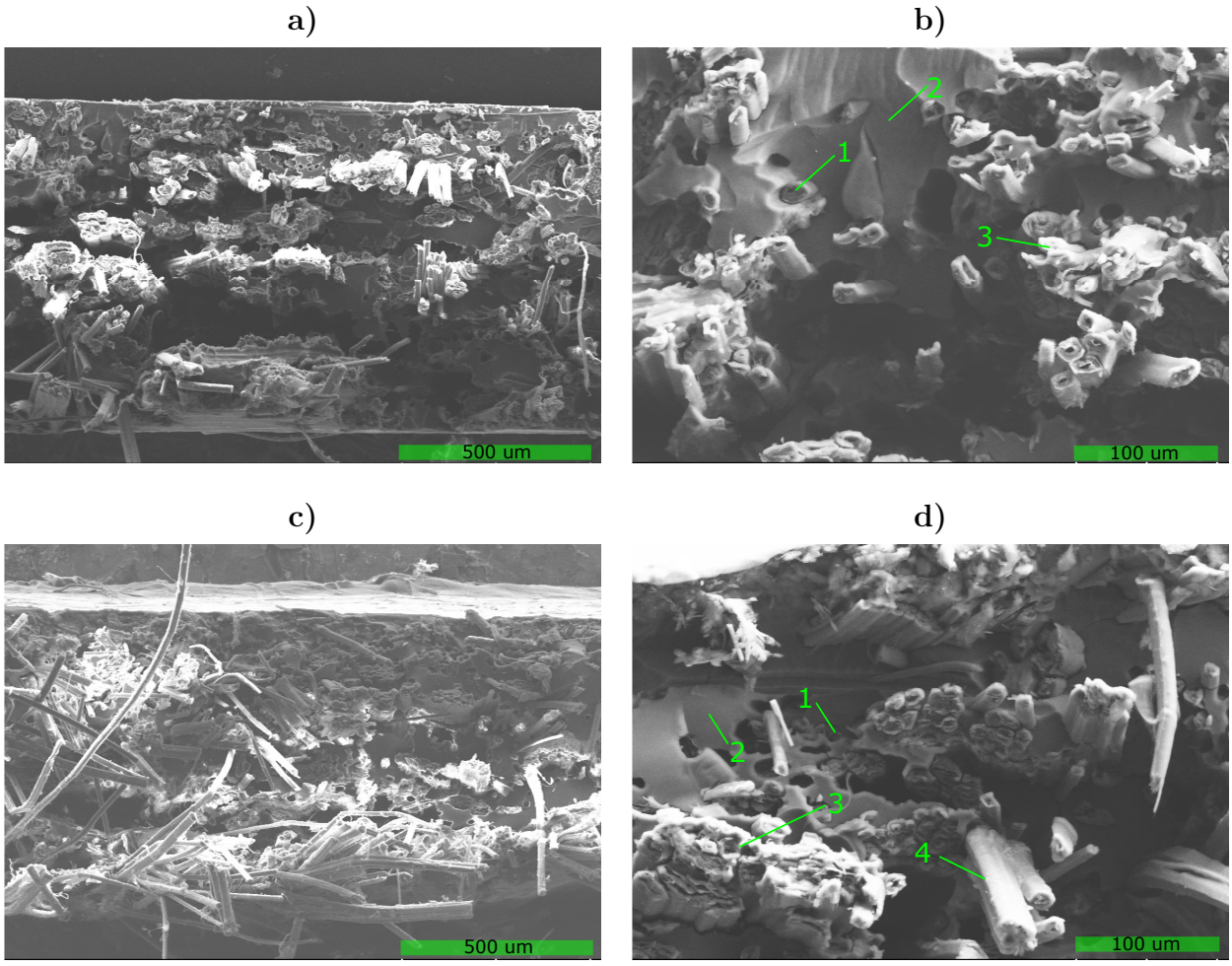

Figure III-11 – Representative SEM images of the three-point bending broken samples. F0-PHU with a) x80 and b) x300 magnifications, and F0-EP with c) x80 and d) x300 magnifications. 1: Fiber break, 2: Matrix break, 3: Fiber short pull-out, 4: Fiber long pull-out.

Despite the remarkable superiority of the F0-PHU laminate in terms of modulus and stress when compared to F0-EP, it is important to note that similar behavior and high properties were achieved for all laminates. In the longitudinal direction, the behavior is mainly governed by the reinforcement [455]. As a result, no significant differences can arise. On the opposite, in the transverse direction, the behavior is mainly brought by the matrix, and the fibers tend to act as defects [160]. Moreover, since the interfacial adhesion is directly submitted to the load in tension and compression, the transverse properties give a good insight into the interfacial strength [274]. In this transverse orientation, PHU-based laminate exhibits high-performance behavior with a bending modulus exceeding 5.0 GPa and a stress of 40 MPa. The obtained properties appear to be significantly superior to those of F90-EP, which shows a bending modulus of 2.2 GPa and a bending stress of 26 MPa. The properties obtained for F-PHU laminates are superior to equivalent materials found in literature, which exhibit

properties similar to F90-EP [169, 274]. This increase in performance can likely be attributed to the improved interfacial adhesion, as previously elucidated through atomistic simulations, AFM, SEM, and longitudinal bending analyses. Importantly, these observations reveal that flax-PHU composites exhibit high mechanical properties in both orthotropic directions, rendering them interesting candidates for the NFC market.

Table III-3 – Flax fiber reinforced polymer properties in three-point bending (mean ± standard deviation)

Load direction	Matrix	ρ g/cm^3	V_f %	V_v %	E GPa	σ MPa	ϵ %	E_{th} GPa	E/E_{th}
Longitudinal	EP	1.30 ± 0.01	48.4 ± 0.7	0.2 ± 0.1	27.9 ± 0.7	390.9 ± 6.9	2.39 ± 0.09	29.0	0.96
	PHU	1.31 ± 0.01	50.1 ± 3.8	1.1 ± 0.4	35.2 ± 0.6	438.2 ± 8.1	1.94 ± 0.08	30.7	1.15
Transverse	EP	1.30 ± 0.01	48.7 ± 0.4	0.2 ± 0.1	2.2 ± 0.2	25.9 ± 8	1.62 ± 0.32	5.0	0.43
	PHU	1.31 ± 0.01	51.5 ± 2.7	1.3 ± 0.3	5.4 ± 0.4	39.8 ± 4.7	0.93 ± 0.09	6.5	0.83

III.2.3.4 Normalization of results and adhesion efficiency using micromechanical model

In many studies, it has been found that both V_f and porosity content significantly impact material properties [23, 160]. For these reasons, Chamis' micromechanical model was applied to compare normalized moduli. The normalized value gives therefore an efficiency coefficient of adhesion [472]. Interestingly, the theoretical longitudinal modulus is comparable in all cases, with values around 30 GPa. When normalized, the ratio of the F0-EP material is 0.96. In this reference case, the ratio of moduli already highlights high compatibility and wettability between this low-viscosity amine-epoxy resin and the fiber. F-PHU laminate exhibits a ratio of 1.15, revealing important improvements in adhesion efficiency compared to the epoxy systems. These results corroborate the enhanced adhesion observed through mechanical tests and AFM analyses. For transversal properties, where the adhesion significantly affects the results, similar trends are observed. The adhesion efficiency of PHU-based materials significantly outperforms that of the epoxy-amine system. F90-EP exhibits an efficiency of 0.43, which is aligned with literature findings [160]. As observed in the longitudinal direction, the PHU matrix exhibits a significant increase in adhesion efficiency with a ratio of 0.83 for F90-PHU. These results, in addition to the first observations and mechanical results back up the original hypothesis that hydroxyurethane in the matrix would generate a stronger H-bond than epoxy amine. Such improvement

leads to higher mechanical properties without requiring any fiber treatment. Therefore, the PHU matrix not only leads to an increase in both the apparent mechanical properties and calculated ones but also an increase in the adhesion strength.

Theoretically, micro-mechanical models like Chamis' assume perfect adhesion between fiber and matrix, representing an ideal material. Comparison to experimental data should lead to values lower than 1 [160]. However, the properties of natural fibers are dependent on many parameters such as the year of production, variety of flax, and fiber extraction methodology, leading to notable scattering of their properties, in particular modulus and density [23]. Therefore, the chosen values for the micromechanical model might slightly underestimate the real properties of the reinforcement. Regardless, these values still allow for meaningful comparison, especially considering that the reinforcement remains within the same range and should be taken for internal comparison within this study.

III.2.3.5 Comparison and discussion in the case of carbon fiber composites

Carbon fiber composites, employing fibers specifically sized for epoxy matrices (as bought), were manufactured for comparative purposes with the NFC. They allow to compare the adhesion efficiency and extend the discussion about the use of PHUs as matrices. Their pictures and cross sections can be found in Fig. III-12, and properties are summarized in Table III-4. When observing the impregnation quality, the higher viscosity of the PHU matrix appears to play a significant part. Indeed, higher porosity content and apparent lack of impregnation were revealed. In particular, the lower diameter and, thus, higher aspect ratio of carbon fiber makes their proper wetting challenging when viscous and polar matrices are employed. Such issues were not detected in the case of natural fibers.

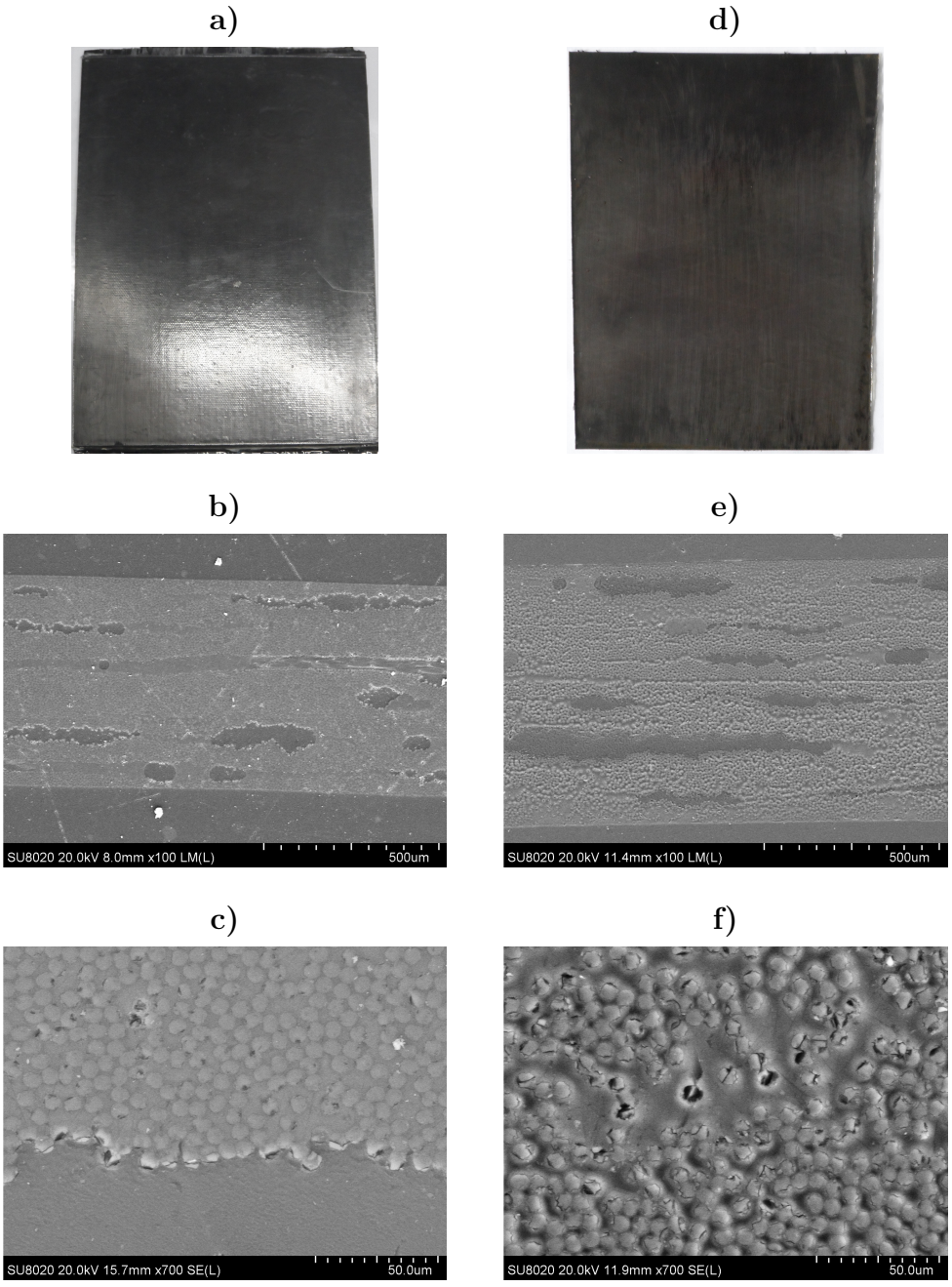

Figure III-12 – Pictures of the manufactured laminates, SEM cross-sections images with x80 magnifications and x700 magnifications (top to bottom) for a-c) C-EP, and d-f) C-PHU

Interestingly, the epoxy matrix leads to significantly better mechanical properties in both orthotropic directions when compared with the PHU matrix, as highlighted by the stress-strain curves shown in Fig. III-13. Moreover, in that case, the application of Chamis's model and the adhesion efficiency ratio highlights better results for epoxy-based composites. This particularly highlights the interest of PHUs to obtain high-performance NFCs without sizing agents due to the intrinsic compatibility of NF and PHUs. The theoretical model, along with monotonic bending tests, SEM images of broken samples, and AFM analyses, highlight the improved interfacial strength of PHUs with flax fibers due to better

chemical and physical affinity, in addition to the good wettability with natural fiber.

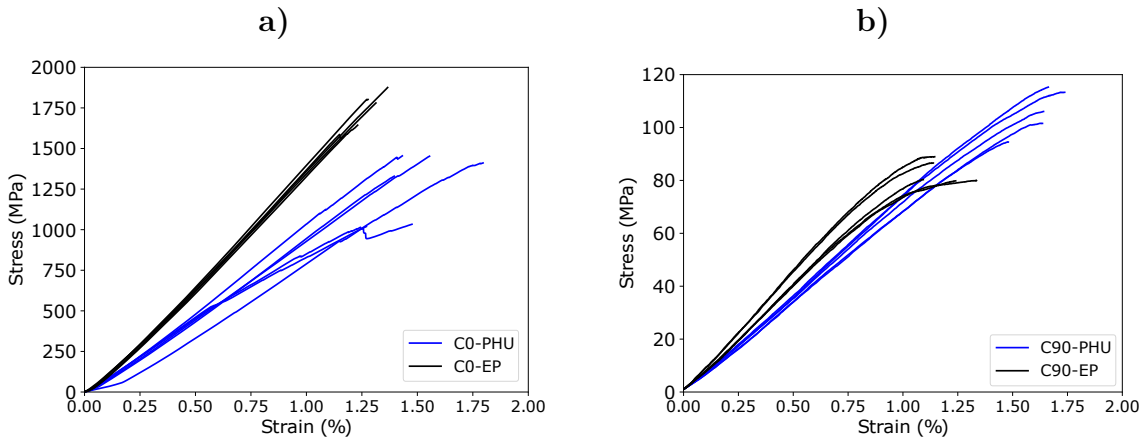

Figure III-13 – Three-point bending of the carbon fiber reinforced polymers for the laminates a) $[0]_6$ b)$[90]_6$

Table III-4 – Carbon fiber reinforced polymer properties in three-point bending (mean ± standard deviation)

Load direction	Matrix	ρ g/cm^3	V_f %	V_v %	E GPa	σ MPa	ϵ %	E_{th} GPa	E/E_{th}
Longitudinal	EP	1.46 ± 0.02	52.4 ± 1.5	2.1 ± 0.2	132.4 ± 2.5	1738 ± 106	1.27 ± 0.07	127.1	1.04
	PHU	1.42 ± 0.01	46.2 ± 2.0	3.5 ± 0.2	92.6 ± 7.0	1283 ± 186	1.49 ± 0.16	113.3	0.82
Transverse	EP	1.46 ± 0.02	56.6 ± 2.2	2.6 ± 0.2	8.7 ± 0.5	83.1 ± 3.9	1.19 ± 0.09	7.4	1.18
	PHU	1.42 ± 0.01	46.3 ± 2.4	3.5 ± 0.3	7 ± 0.2	106.2 ± 7.6	1.63 ± 0.08	8.9	0.79

III.2.3.6 Insights about the fire behavior of PHU-based NFC

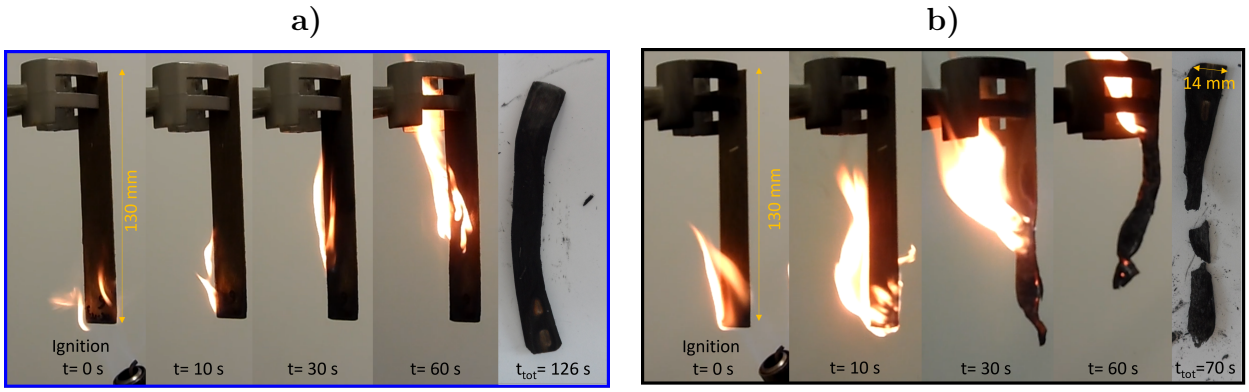

Figure III-14 – Pictures of composite samples during UL94 vertical burning test. a) F-PHU, and b) F-EP laminates

Flax-epoxy systems are known to have poor fire resistance [473]. This limitation leads to several challenges when considering their use in applications such as transportation. Typically, the incorporation of halogenated or phosphorated compounds is required to meet fire safety standards, but this approach is questionable in terms of sustainability. Hence, we proposed here a straightforward evaluation of the flammability of flax-PHU composites following the vertical UL-94 standard. F-EP and F-PHU were tested, and the results were compared. Pictures of the tests are presented in Fig.III-14. Notable differences between the two materials were observed. The F-EP materials exhibit a typical behavior of flax-epoxy material when no fire retardant is used, where large flames catch up at the ignition and propagate quickly throughout the sample, accompanied by significant smoke generation. Within less than 70 seconds, the material was entirely consumed by the flames, leaving behind the residual char that was too brittle to be handled, indicating the complete loss of the material's integrity during the burning test. On the opposite, Flax-PHU exhibits a smoother fire behavior. Samples required more than two minutes to burn, with slower flame propagation and no significant smoke generation. The residual char was stable and cohesive in a single piece, revealing the retention of some material properties and the formation of a stable protective char layer. This observation was also corroborated by TGA (Fig. III-15). Although the flax-PHU material does not meet the criteria for self-extinguishing properties and is not classified as such in the test, the behavior remains enhanced when compared to the epoxy counterpart. Potential dehydration and aromatization of the network could explain such behavior and should be investigated in depth to fully understand the involved mechanism.

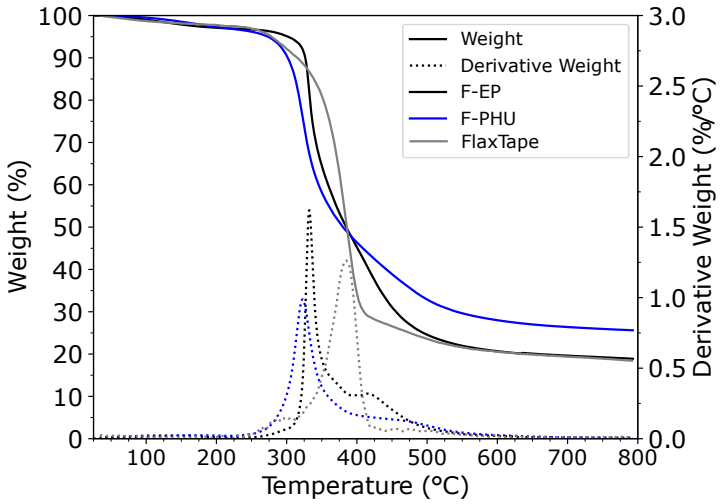

Figure III-15 – TGA under N_2 flow of the flax laminates

In general, the combination of high thermo-mechanical properties, the enhanced affinity between the fibers and the matrix, and the enhancement of the fire behavior through the simple addition of CO_2 to bio-epoxy resins open an interesting new sustainable platform for natural fiber composites. These composites occur to be of high interest to the transportation industry as they offer the potential to replace petro-based polymers and improve the sustainability of composite materials with improved properties.

III.2.4 Welding of pre-preg PHU composites

Reprocessable thermosets constitute a significant breakthrough in the composite industry as they can provide many opportunities such as welding, reshaping, and recycling of such materials, or recovery of the fibers [24]. Upon heating, hydroxyurethane functions are subjected to transcarbamoylation and dissociative reactions [362]. In transcarbamoylation, bond exchanges between hydroxyl and urethane functions allow the reprocessing of such thermosets under specific conditions without loss of crosslinking density [387]. The dissociative reaction reforms the cyclic carbonate and amine, thus leading to a decrease in the crosslink nodes [387]. These two reactions give PHU thermosets the ability to be catalyst-free reprocessed at elevated temperatures [462]. Exploiting this unique feature, single-ply F-PHU laminates were manufactured. These F-PHU sheets were then welded by thermo-compression as represented in Fig. III-16a.

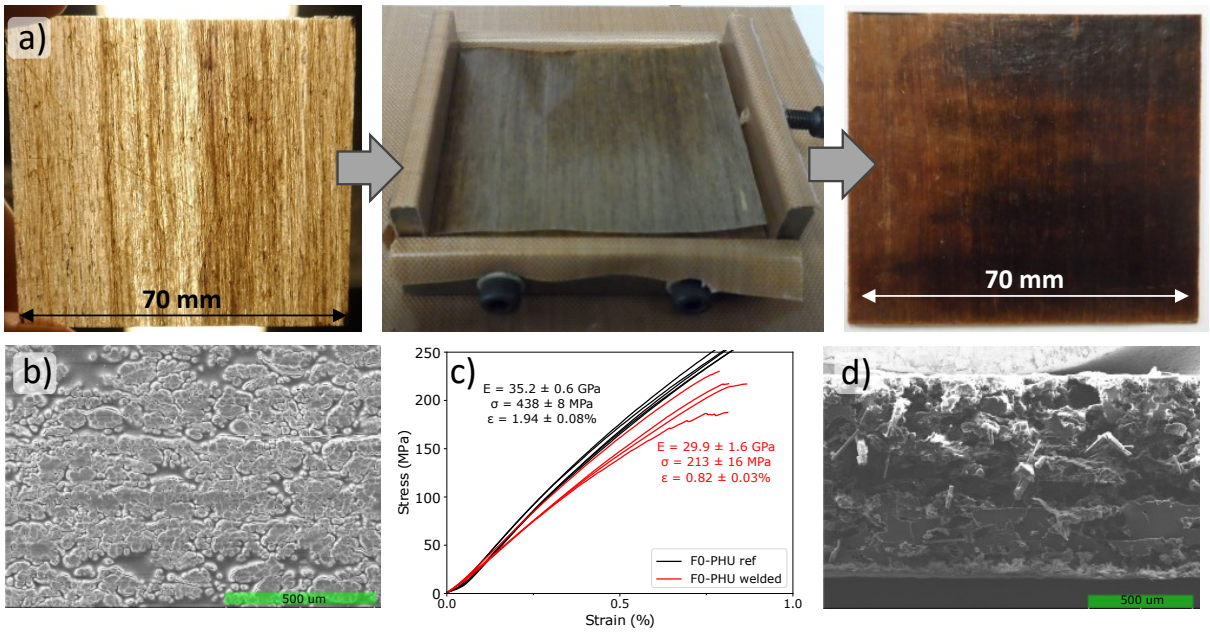

Figure III-16 – a) Welding process of flax-PHU laminate. From left to right, single-ply cured sheet, stacking in the mold and cured plate. b) SEM of the welded composite cross-section, c)Three-point bending strain-stress curves of the welded F-PHU composite in the longitudinal direction, c) failure facies of the three-point bending specimen with x70 magnification.

The obtained material was smooth and homogeneous despite the harsh conditions required to weld the plies efficiently. The SEM picture presented in Fig. III-16b depicts efficient welding without any observable welding line nor significant longitudinal discontinuity. When compared to the non-reprocessable epoxy material (Fig. III-17), which exhibits porosities, and identifiable ply lines, the SEM highlights the good welding of the plies thanks to PHU dynamic networks. Three-point bending was applied to assess the properties of the welded laminate. The curves are presented in Fig. III-16c, alongside the F0-PHU manufactured in the previous section as a reference. The welded composite exhibits a modulus of 30 GPa, a stress of 213 MPa, and a strain at break of 0.82%. The results are only slightly scattered, revealing the overall material homogeneity and the reliability of the process. The high modulus emphasizes the effectiveness of the welding process [474]. Moreover, the failure facies presented in Fig. III-16d disclose neat and brittle failure of the fibers, leading to the catastrophic failure of the entire material with no delamination observed. This further highlights the efficacy of the welding process [474].

It is important to note that despite the rather good ultimate properties obtained compared to other works in the literature [460] and the effectiveness of the welding, the laminate experienced a significant drop in the ultimate properties, approximately 50%, compared to the original material. This decrease can be attributed to the thermal degradation of the fibers, as stated in literature [23].

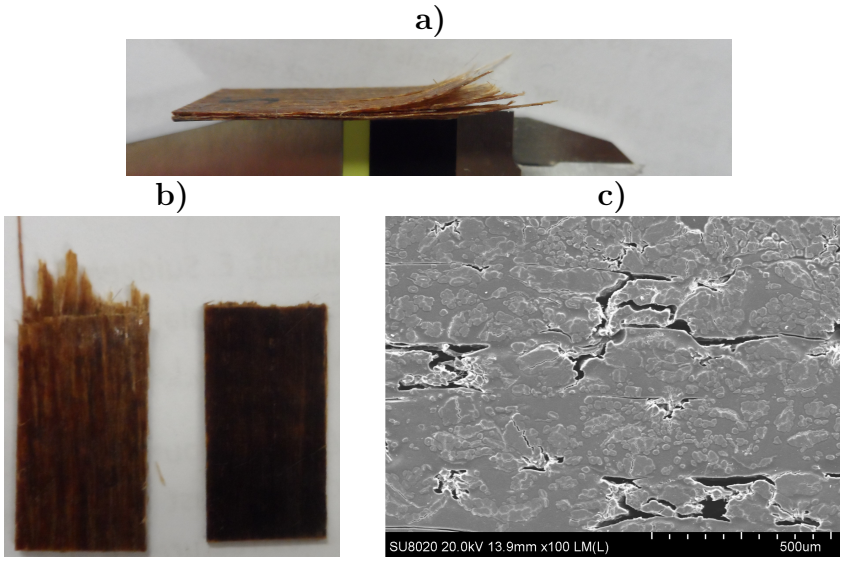

Figure III-17 – a) Broken "welded" F-EP laminates with delamination b) comparison of the broken welded samples epoxy matrix (left) and PHU matrix (right), and c) SEM image of the F-EP laminate

Prolonged exposure to elevated temperature leads to a drastic change in the microstructure of the fibers and their chemical composition, and thus embrittlement.

However, the welding of the flax-PHU composite must be seen as a proof-of-concept, showcasing a specific added feature derived from the shift of chemistry from epoxides to polyhydroxyurethanes. Here, the materials were processed under catalyst-free conditions. Further exploration of optimized reprocessing conditions, catalysts, formulations, and recycling methods [390] are expected to yield even more promising outcomes. Such features open doors to the implementation of bio-based recyclable structural composites with improved properties.

III.3 Conclusions

In this chapter, we explore the possibility of advantageously employing interfacial hydrogen bonding between natural fibers and sustainable polymer to design high-performance natural fiber composites.

Specifically, polyhydroxyurethanes (PHU) were synthesized from bio- and CO_2- derived cyclic carbonates and diamine. The physical properties of the neat PHU were measured and compared to a similar epoxy network. PHUs exhibit superior thermo-mechanical properties with a glass transition temperature above 78 °C and a bending modulus exceeding 4 GPa. The obtained properties were found to align with the requirements for structural natural fiber composites.

For the first time, PHU was used to manufacture flax fibers' unidirectional laminates. The results

indicated homogeneous impregnation and enhanced wetting of the fiber with PHU compared to epoxy, as confirmed by AFM measurements and rationalized via atomistic simulations. The bending properties were among the highest reported in the literature, with a modulus of 35 GPa, and ultimate stress and strain of 440 MPa and 1.94% respectively. Interestingly, when normalizing results through Chami's micromechanical model, PHU-based composites outperform epoxy ones by nearly 30%. Such an increase was found to be specific to the natural fiber-PHU material as carbon fiber composites were superior using epoxy resins. Taking advantage of the inherent dynamic urethane linkages, we successfully manufactured cured pre-impregnated laminates that were further welded to create the final material. Although this welding process has potential, further optimization is necessary because the slow relaxation behavior of PHU, even at high temperatures, leads to the degradation of natural fibers.

Polyhydroxyurethanes appear as a new sustainable platform suitable for the composite industry, particularly for applications in the transportation market. PHUs, however, remain an emerging polymer, and comprehensive studies regarding durability, aging, and environmental conditions should be performed to facilitate the widespread adoption of PHU-Natural fiber composites. The reprocessing and recycling of the final material should also be investigated in depth, and new routes should be explored to make PHU competitive with other dynamic chemistries. The observed viscosity may pose a potential limitation for scaling up the manufacturing of such sustainable materials, a challenge that could be overcome through the exploration of a hybridization strategy, using reactive diluents and compatible chemistries.

Chapter IV

Overcoming PHU limitations through a simple hybridization strategy for cutting edges opportunities

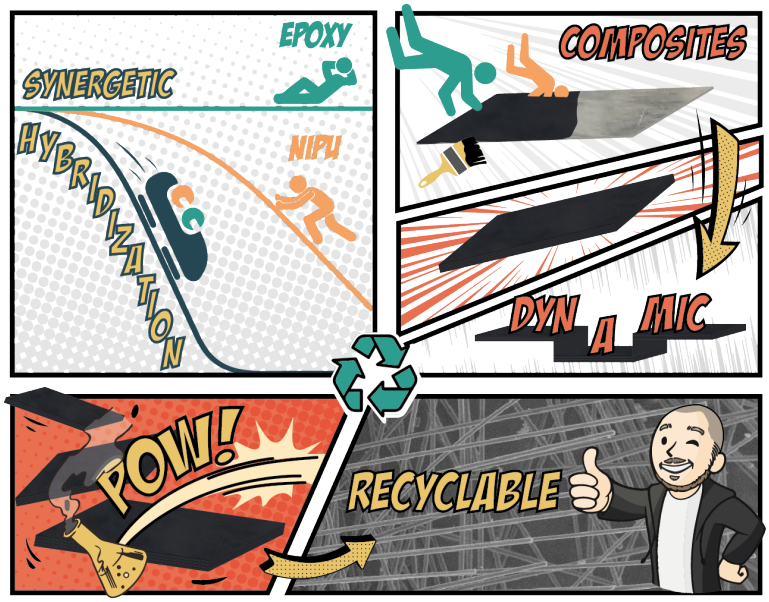

Adapted from: Seychal, G.; Ximenis, M.; Lemaur, V.; Grignard, B.; Lazzaroni, R.; Detrembleur, C.; Sardon, H.; Aranburu, N.; Raquez, J. Synergetic Hybridization Strategy to Enhance the Dynamicity of Poorly Dynamic CO 2 -derived Vitrimers Achieved by a Simple Copolymerization Approach. Adv Funct Materials 2024, 2412268. https://doi.org/10.1002/adfm.202412268.

External contributions: *The figures from the article are the work of M.X.; V.L. calculated the DFT analyses. XPS measurements were performed by SGIker of UPV/EHU.*

Contents

IV.1 Introduction

The precedent chapter has demonstrated that PHU might offer a strong alternative to epoxy resin in natural fiber composites. They displayed high thermo-mechanical properties and strong affinities with the natural fibers resulting in enhanced properties compared to composite benchmark. Yet, several issues arise when considering PHU for composites. First, the high viscosity and long curing times predict difficulties in implementing such chemistry in "large"-scale composite manufacturing. Second, one of the advantages of PHU lies in their dynamic behavior, making them covalent adaptable networks (CAN). However, this dynamicity is poorly efficient. Catalysts showed limited efficiency in improving the dynamicity [390]. Additionally, considering the results from the previous section, it would also limit the processability of PHU through the fastening of early reactions, reducing the operating window, already narrow enough.

Therefore, finding a solution that could fasten the exchange mechanism in PHUs while easing the processability (i.e., lower viscosity, longer pot life at room temperature, and faster gel time at elevated temperature) is the key to seriously considering PHU in the composite industry.

Copolymerization is a well-known toolbox in the polymer field to finely tune properties. In most cases, the resulting copolymer possesses properties in between both respective materials [475, 476]. In only a few rare cases, a synergetic effect is achieved and leads to outstanding performances exceeding any expectation [232, 357]. This synergetic effect is widely spread in natural materials and organisms through millennia of evolution to obtain sophisticated materials with outstanding performances and efficiency, such as spider silk [477] or mussel collagen [478] but hardly predictable in man-made materials. Synergetic engineered materials are sometimes obtained from a biomimetic approach to reproduce natural behavior like hygromorph metamaterials [479]. Recently, Chen et al. [480] exploited such a synergetic copolymerization approach to unify polymerizability, recyclability, and performance properties of linear polymers. By this means, they obtained outperforming polymers with facile polymerization at room temperature with controlled structures, high performances, and fully controlled depolymerization.

To the author's best knowledge, such a synergetic approach through simple copolymerization has not been exploited in the realm of CANs. Inspired by these natural examples, we hypothesized that highly efficient dynamic networks could be obtained through simple copolymerization of easily accessible building blocks. Such a strategy would open the door to more unrestricted CANs for industrial applications, especially composite materials, and allow closed-loop structural materials. More precisely, thanks to this novel approach, we design a highly efficient dynamic network made of two

distinct polymers, in which each corresponding chemistry would smoothly operate as the counterweight to the other. In such an approach, a polymer can bring dynamic linkages that normally require activation (i.e. catalyst), in a synergetic manner with the other polymer that provides this catalytic effect.

It was recently observed that dynamic networks could be highly influenced by the presence of an internal catalyst that enhances relaxation times substantially [481]. In our plan to exploit this behavior efficiently, we hypothesized that copolymerizing PHUs with a polymer that could generate this internal catalyst in-situ could facilitate the exchange reaction.

One of the polymers that could generate this internal catalyst upon polymerization is the widespread conventional non-dynamic epoxy-amine thermosets (EP). Indeed their curing generates hydroxyl with secondary and tertiary amines neighboring groups that could potentially accelerate the transcarbamoylation exchange reaction, thus improving the efficiency of the dynamic network [481]. Furthermore, the low viscosity of the epoxy and wide library of available building blocks allow the implementation of large-scale composite manufacturing without requiring any change from the already existing manufacturing protocols. Additionally, both being polymerized by amines, the formulation would be one-pot and one-step, without any new scarcely accessible reagents nor catalyst, valorize CO_2, and be industrially relevant.

To delve into this synergetic hybridization strategy (Fig. IV-1), in this work, several hybrid epoxy-PHU are synthesized with different epoxy/urethane ratios to demonstrate the auto-catalytic effect of the epoxy-derived amino-alcohol for the transcarbamoylation of hydroxyurethanes. Firstly, we perform some model reactions and atomistic simulations to understand the difference between conventional transcarbamoylation and the synergetic hybridization autocatalytic approach. Later on, we investigate the (re)shapability, weldability, and recyclability of this hybrid copolymer which exhibits a fast catalyst-free adaptable behavior in comparison to the conventional epoxy and PHU network. Furthermore, we compare the properties of the hybrid systems with the analogous pristine epoxy and we show that the attained properties are similar or even superior to the traditional epoxy resin. We also demonstrate that this network can be cleaved under mild conditions allowing the recovery of the high-added value carbon fibers. The recovered fibers were characterized and re-used for manufacturing a new composite material fully closing the loop of such an innovative approach.

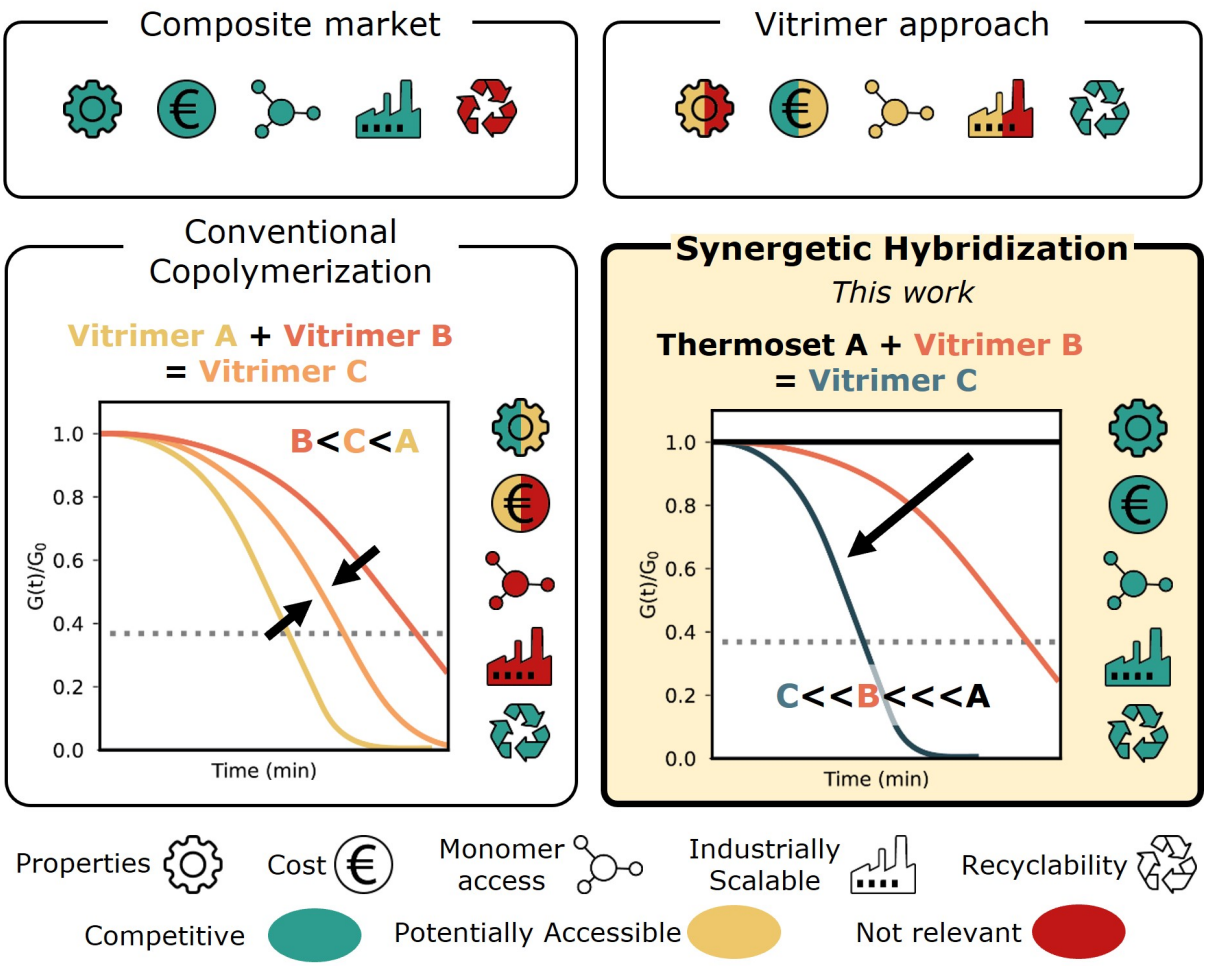

Figure IV-1 – General scheme of the synergetic hybridization approach compared to previous work and market limitations.

IV.2 Results and discussion

IV.2.1 Synergetic effect of hydroxyurethane-epoxy for self-catalyzed transcarbamoylation

IV.2.1.1 Hypothesis validation through model reactions

To highlight that the amino-alcohols formed by the epoxy network could efficiently take part in a fast transcarbamoylation exchange reaction, models were investigated. Firstly, to have a better understanding about the system and its feasibility, a simple atomistic simulation was conducted. Two secondary alcohols of very similar structures, but one incorporating a neighboring amine were used, respectively called reaction A and reaction B as presented in Fig. IV-4. The amino-alcohol mimics the product obtained from epoxy aminolysis. Atomic charges of the hydroxyl incorporating the amine,

determined by fitting of the electrostatic potential (ESP) of the DFT-optimized isolated fragments, are found to be more negative (-0.66 e) compared to those of the secondary alcohol (-0.63 e), thus revealing higher nucleophilicity by the hydrogen bonding and the electron-withdrawing effect of the neighboring amine [482]. Furthermore, the difference in free enthalpy of the amino-alcohol-based transcarbamoylation was lower (ΔG_0 = -6.70 kJ/mol) than the conventional transcarbamoylation (ΔG_0 = -3.16 kJ/mol), see technical details in the methodology chapter 9.2.1. This first result indicates that if the transcarbamoylation is feasible, a catalyst is required to fasten the exchange rate. In the case of the epoxy-based network, the formed amino-alcohol could be expected to play as the catalyst and the reactant and promote the network's dynamicity.

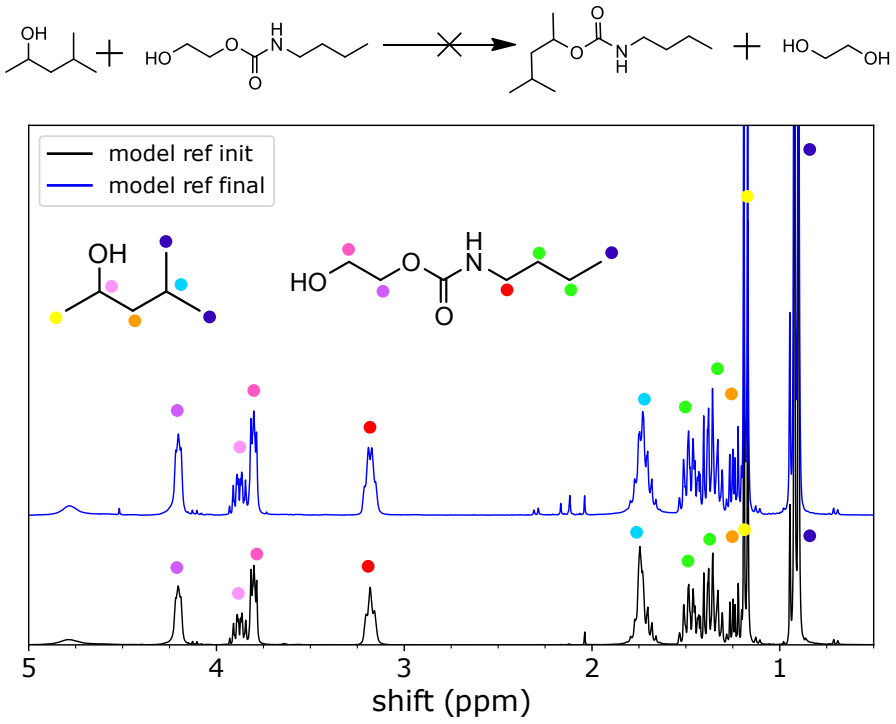

Figure IV-2 – ^{1}H-NMR in $CDCl_3$ of the 2-hydroxyethyl n-butylcarbamate model compound with 4-Methyl-2-pentanol before and after 24 h at 120 °C

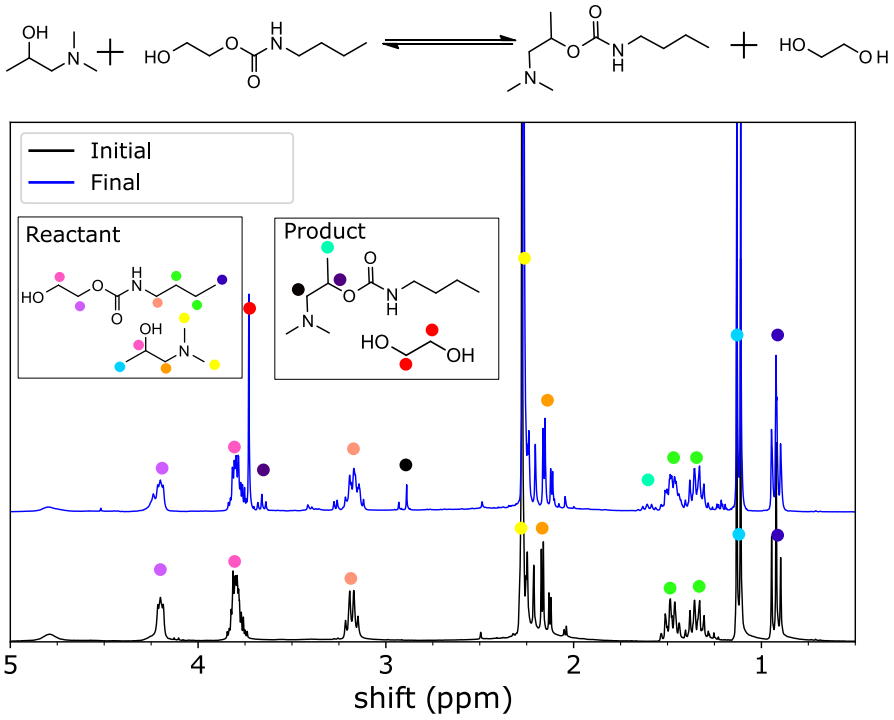

Figure IV-3 – ^{1}H-NMR in $CDCl_3$ of the 2-hydroxyethyl n-butylcarbamate model compound with 1-dimethylamino-2-propanol mimicking the epoxy compound before and after 24 h at 120 °C

Based on these promising preliminary results, model exchange reactions were conducted as illustrated in Fig. IV-4. No ethylene glycol (EG) generation, that would reveal the exchange reaction, was observed in the case of uncatalyzed alcohol-carbamate transcarbamoylation (reaction A, Fig. IV-2), in agreement with previous work in literature [390]. This first confirmed the impossible use of transcarbamoylation in mild conditions (temperature lower than 150 °C) without any catalyst. When the amino-alcohol compound was used (reaction B, Fig. IV-3, and Fig. IV-A1-IV-A5), however, EG release was quickly observed at temperatures as low as 100 °C demonstrating the positive effect of this autocatalytic system and the improvement of the exchange rate. An activation energy of 123.6 kJ/mol was calculated, correlating a previous work on catalyzed transcarbamoylation [362]. Mass spectra analysis (Fig. IV-A6) confirmed that the amino-alcohol was reacting with the carbamate moieties forming the new product (m/z= 203.17) but also, to a more limited extent, was able to catalyze the primary alcohol of the hydroxyurethane and thus, forming a difunctional urethane (m/z= 283.16). Base catalysts (like triethylamine, or guanidine derivatives) are commonly used for transcarbamoylation by deprotonation of the reacting alcohol thus increasing the nucleophilicity [362]. The amino-alcohol used has a pKa around 10.5-11, similar to triethylamine, explaining the observed product. This is particularly important, as an external catalytic effect of the tertiary amine would probably be hindered in the copolymer network

due to steric hindrance and hydrogen bonding, while the internal activation of the neighboring hydroxyl group will be encountered in the bulk material. The model reaction demonstrated the internal catalysis of epoxy-derived alcohol to act efficiently in the transcarbamoylation reaction allowing us to go on to the material scale.

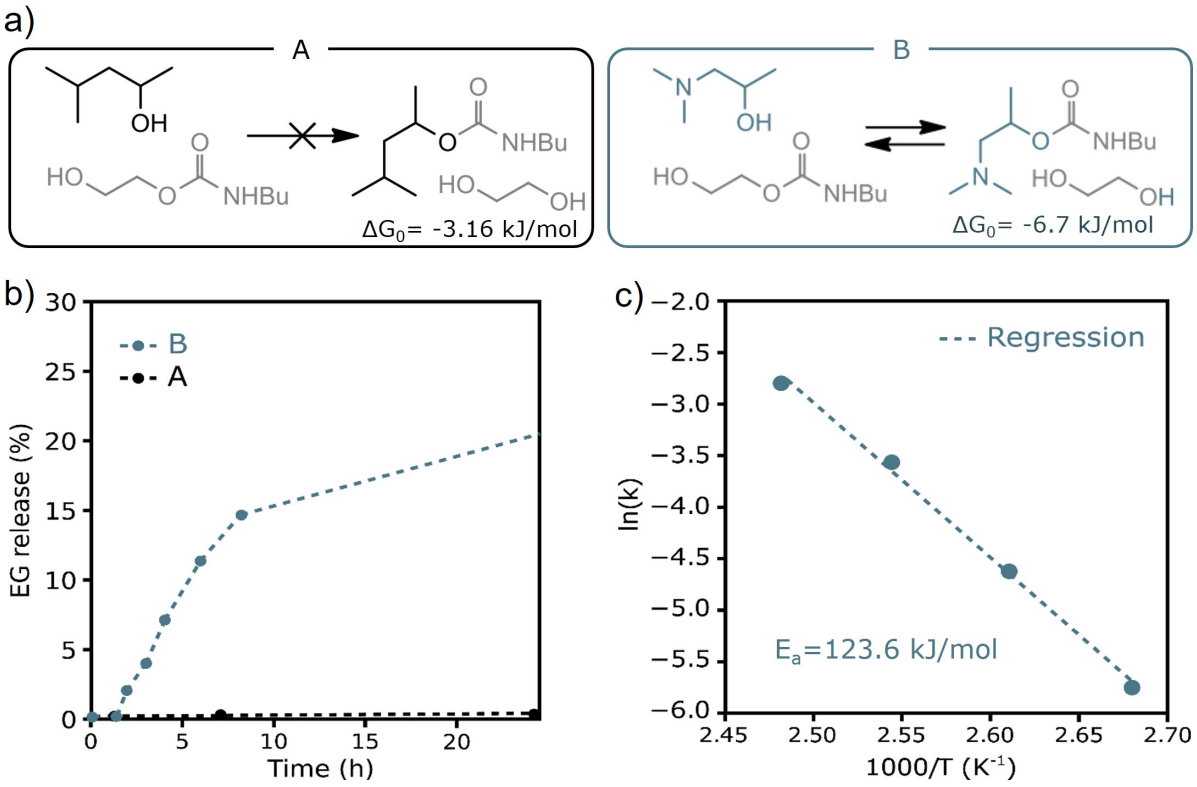

Figure IV-4 – Design of catalyst-free efficient transcarbamoylation reaction. a) Model reaction A: Conventional uncatalyzed transcarbamoylation. Model reaction B: Internally-catalyzed amino-alcohol transcarbamoylation. b) Kinetic of the release of ethylene glycol (EG) during the exchange reaction, and c) Arrhenius plot of the internally catalyzed exchange

IV.2.1.2 Design of the dynamic hybrid networks

The epoxy-based CAN was built by the facile incorporation of cyclic carbonates in the starting epoxy monomer (Fig. IV-6a). A diamine was used as the same crosslinking agent by reacting with both epoxy and cyclic carbonates. The cyclic carbonate aminolysis leads to a hydroxyurethane moiety (Fig. IV-5a), while the aminolysis of epoxy leads to secondary and tertiary amines with pendant free-hydroxyl (Fig. IV-5b). The hydroxyurethane moieties act as the dynamic linkage while the epoxy-derived hydroxyls act as the internally catalyzed alcohols to perform transcarbamoylation as represented in Fig. IV-6a. In this work, the trimethylolpropane triglycidyl carbonate (TMPTC) was chosen as a trifunctional cyclic carbonate for its low viscosity, crosslinking ability, and potential biobased origin [462] as well as

being the most widely used precursors of PHU in literature, which facilitates comparison. Resorcinol diglycidyl ether (RDGE) was chosen as a potential bio-derived epoxy monomer [444] that has proven to be a suitable replacement for the hazardous Bisphenol-A [170]. m-Xylylene Diamine (MXDA), a potential furfural-derived aromatic diamine was chosen as the hardener [214] to bring stiffness and stability to the network, compatible with high-performance materials.

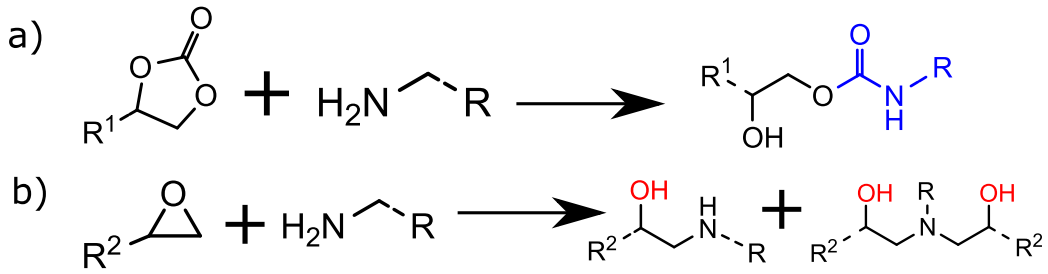

Figure IV-5 – Aminolysis reaction scheme. a) Aminolysis of cyclic carbonates to hydroxyurethane moiety, and b) aminolysis of oxirane to secondary and tertiary amino-alcohol.

Several formulations of TMPTC-RDGE with different mass content of cyclic carbonates were investigated in stress relaxation (Fig. IV-6b). Interestingly, only 10% of cyclic carbonates can already lead to some (slow) stress relaxation while the range 25%-75% seems to be the most promising with relaxation times within 20 min, demonstrating the expected synergistic behavior in this range. Although previous work has highlighted that pure PHU could stress relax in catalyst-free conditions [462], it required several hours at a temperature superior to 180 °C, leading to partial thermal degradation [483]. Herein, we report the fastest relaxation for a PHU-based dynamic network, thanks to this copolymerization strategy. The 50% content of cyclic carbonates leads to the fastest relaxation time at 180 °C in only 7 min. This can be understood as the network needs a good balance between activated hydroxyls and dynamic hydroxyurethanes to perform adequately. The higher content of epoxy favors the network dynamicity as it provides a sufficient number of activated hydroxyl groups. No thermal degradation during the relaxation process was observed by isothermal dynamic mechanical analysis (DMA) and thermogravimetric analysis (TGA) over 1 h at 180 °C (Fig. IV-A10), with less than 0.6 wt% loss.

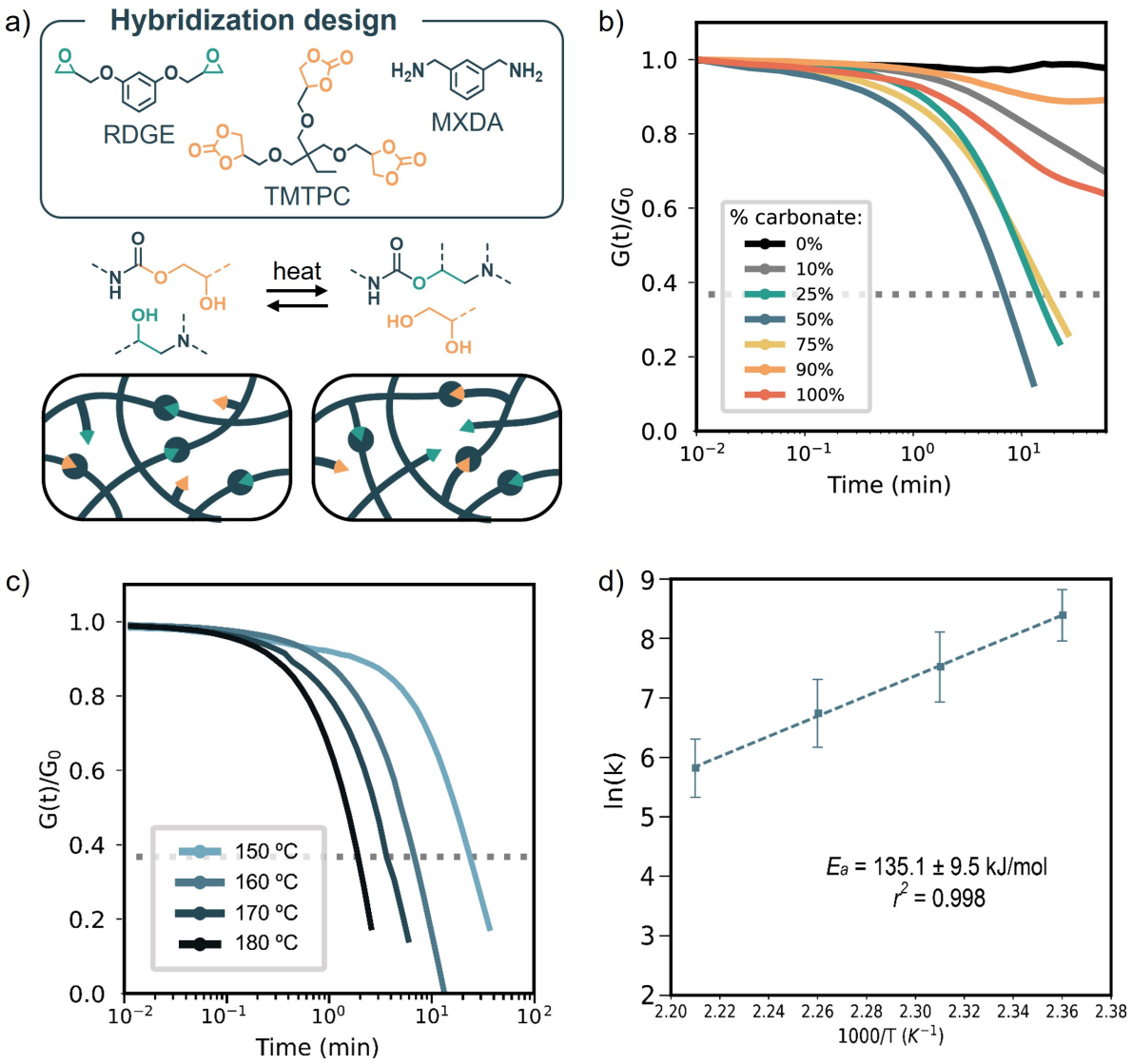

Figure IV-6 – Design of epoxy-hydroxyurethane hybrid covalent adaptable networks. a) (Macro)molecular structure of the constituent to build the synergetic hybrid polymer with transcarbamoylation reaction, b) Stress relaxation at 180 °C of the network with a different mass content of cyclic carbonates, c) Stress relaxation of the 50/50 formulation at different temperatures, and d) Arrhenius temperature-time plot from c).

The networks obtained prove to be competitive with many other systems previously reported in the literature. For instance, epoxy-disulfide-based vitrimers, one of the most efficient dynamic chemistry developed so far, were obtained by different teams [484, 485] with glass transition around 120 °C. They reported relaxation times of about 10-15 min at 180 °C, analogous to the one obtained in this work. Compared to a closer chemistry, i.e. transesterification-based system, relaxation times of around 15 min at 180 °C in the presence of zinc catalyst [330, 451] are commonly obtained. More recently, exploiting an internal catalysis strategy, equivalent times were reported [486]. A benchmark comparison graph

and table can be found in the appendix (Fig. IV-A17 and Tab. IV-A3).

Table IV-1 – Thermomechanical properties and stress relaxation of the dynamic epoxy (RDGE-TMPTC-mXDA) with different carbonate content.

%Carbonate	T_α ($°C$)	ν'_e (mol/m^3)	$\tau_{180°C}$ min
0	97	1519	-
10	98	1577	nc (>60)
25	87	663	18
50	94	664	7
75	85	613	15
90	90	1095	nc (>60)
100	78	657	237

The vitrimeric behavior was assessed for the aforementioned formulation (i.e. 50%RDGE-50%TMPTC) at several temperatures in three replicates (Fig. IV-6c, and Fig. IV-A9). Although the dynamic behavior of the urethane linkage is due to both associative (transcarbamoylation) and dissociative (reverse cyclic carbonates aminolysis) mechanisms [362], the main mechanism in the present work was assumed to be associative and a single decay Maxwell model stands for a sufficient approximation [332]. A good fit (r^2> 0.998) was obtained with a single decay Maxwell model in the time-temperature Arrhenius plot (Fig. IV-6d) confirming the formation of a fast relaxing catalyst-free dynamic network. Relaxation can be obtained within minutes at a temperature as low as 150 °C. The Arrhenius plot highlights a strong time-temperature dependence and thus the easy control of the relaxation through the simple temperature triggering without any catalyst side effects. The activation energy (135.1 kJ/mol) is consistent with the value obtained in the model reaction study and with literature on transcarbamoylation [362].

Several other monomer combinations were tested to demonstrate the versatility and efficiency of the approach thanks to the facile access to a wide library of epoxy systems suitable for many applications, including potential biobased monomers. Detailed results are presented in Fig. IV-7-IV-8 and summarized in Tab. IV-2. It is worth noting that the approach is extremely versatile and offers a wide range of properties that can be adapted to the targeted application from low glass transition (about 25 °C) to high glass transitions (about 120 °C). All formulations exhibited fast stress relaxation in catalyst-free conditions even in the case of the high glass transition and highly crosslinked network arising from the aerospace-grade epoxy 4,4'-methylenebis(diglycidylaniline). The glass transition and

crosslinking density with different carbonate content but the same constituents (i.e. RDGE-TMPTC, Tab. IV-1) were similar while changing the constituents led to very different crosslinking densities. In all cases, fast stress relaxations were obtained thus showing that chain mobility has only a limited role in the overall behavior. Additionally, the rate and efficiency of the exchange reaction can be tuned through the content of cyclic carbonates. For the sake of comparison, the rest of the study focused on the 50/50 formulation out of RDGE and TMPTC.

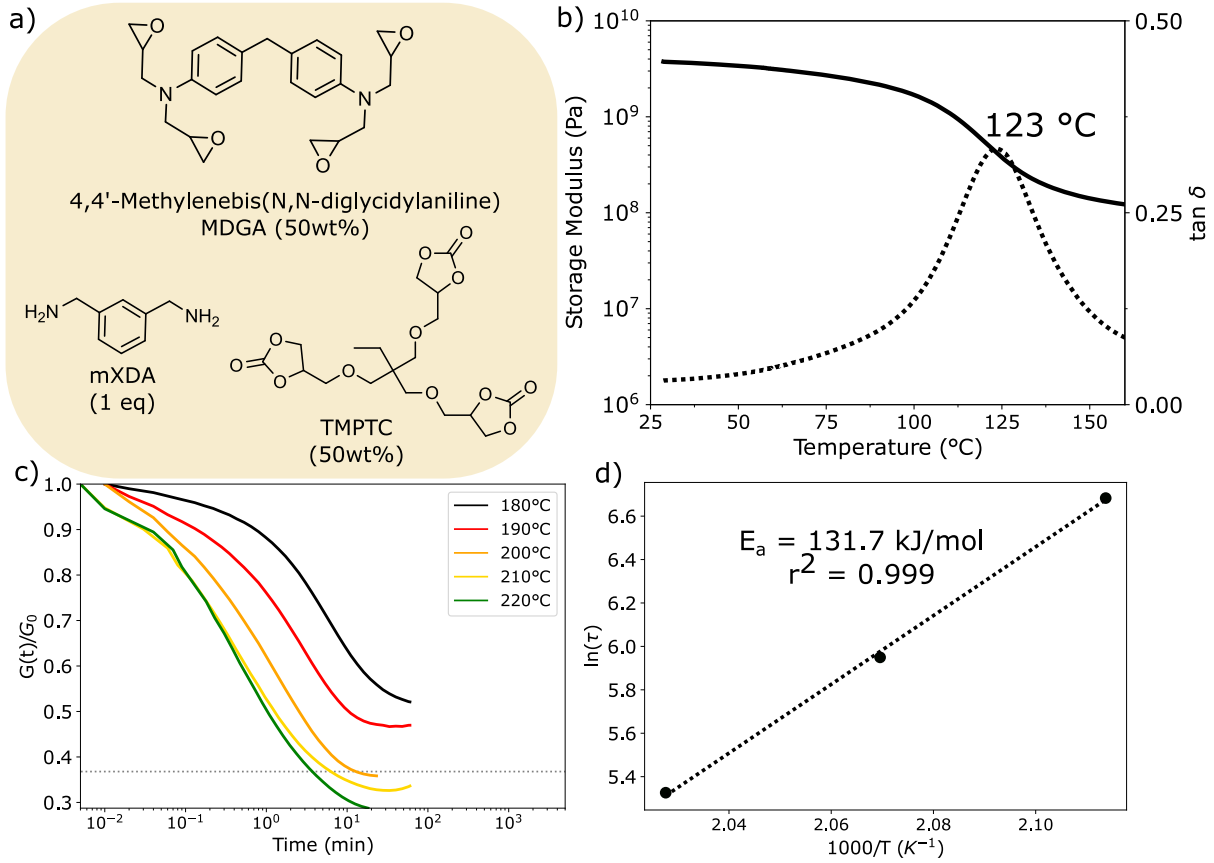

Figure IV-7 – Additional formulation with high glass transition, referred to as MTX. a) Monomer structure and formulation, b) DMA of the hybrid dynamic network, c) stress relaxation of the samples, and d) Arrhenius plot.

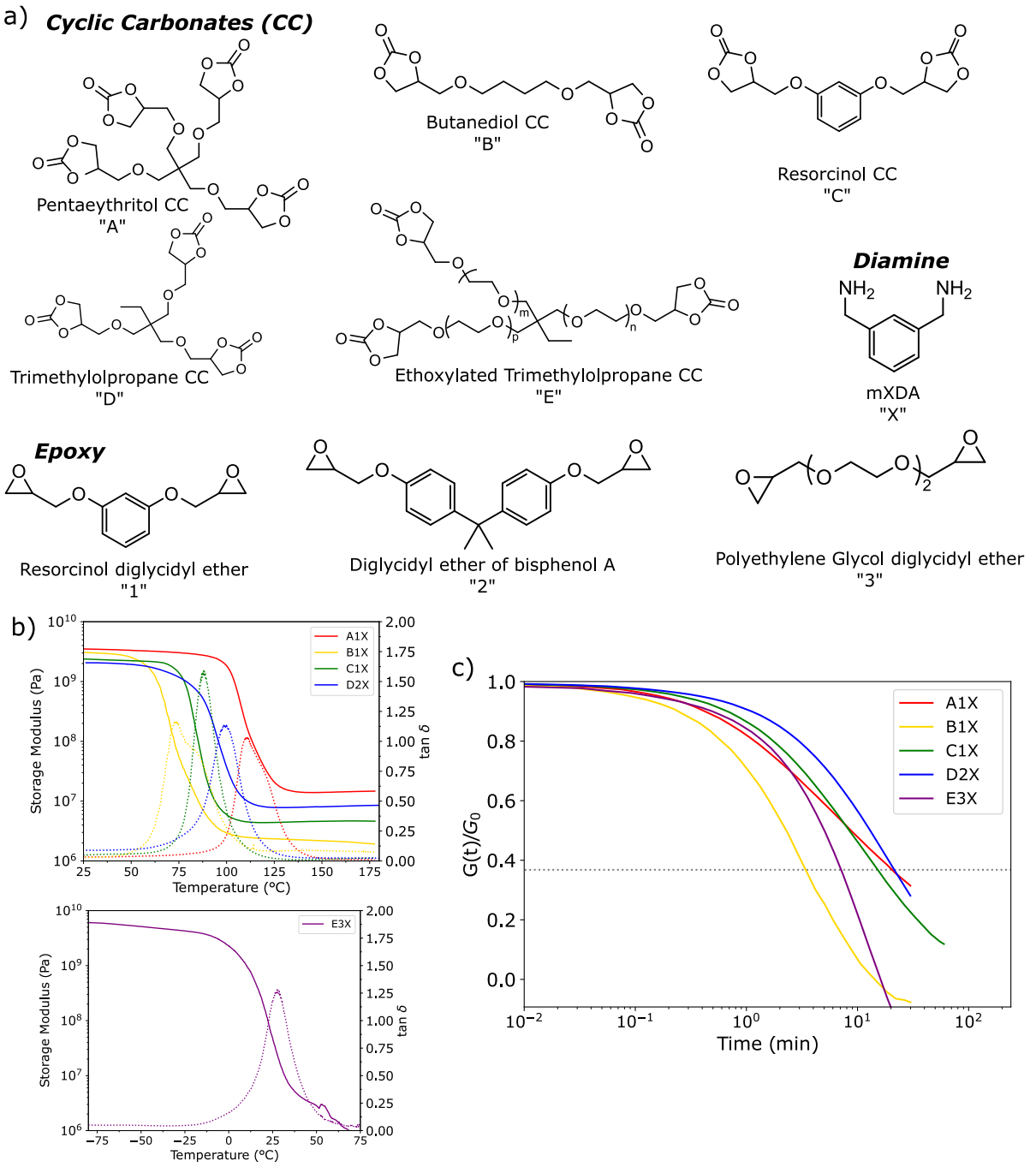

Figure IV-8 – Additional formulation. a) Monomer structure, b) DMA of the hybrid dynamic networks, and c) stress relaxation of the samples at 180 °C except A1X at 200 ° C.

Table IV-2 – Other hybrid formulations' thermomechanical and stress relaxation properties

	DMA				Stress Relaxation
	T_α	$E'_{25°C}$	$E'_{rubbery}$	ν'_e	τ (T°C)
	°C	MPa	MPa	mol.m^{-3}	min
MTX	123	3752	106	9526	13 min (200°C)
					6 min (210°C)
					3.4 min (220°C)
A1X	110	3506	14	1321	22 min (200°C)
B1X	73	2915	2.40	237	3.5 min (180°C)
C1X	88	2379	4.50	441	15 min (180°C)
D2X	99	2058	8.03	762	22 min (180°C)
E3X	27	48	2.72	311	7 min (180°C)

The formulated networks exhibit fast and efficient stress relaxation confirming our first hypothesis, and demonstrating the interest in the copolymerization approach for epoxy to reach high dynamicity of the network through the synergy between the activated alcohols and the (hydroxy)urethane moieties. The network dynamicity being demonstrated, the material was then investigated in depth to ensure no significant modification of the properties was caused by the hybridization.

IV.2.2 Dynamicity, physical properties, and reprocessability of hybrid EP-PHU

IV.2.2.1 Thermo-mechanical characterization of the hybrid network

The pristine epoxy, consisting of RDGE-mXDA, and the dynamic epoxy, consisting of RDGE-TMPTC-mXDA, were compared. Firstly, the mechanical properties were tested under tensile loading. The representative stress-strain curves are presented in Fig. IV-9a-b and the results are summarized in Tab. IV-3. No detrimental modifications of the properties were observed. The newly formulated dynamic copolymer exhibits superior mechanical properties compared to the pristine epoxy with a high Young's modulus of 3.0 GPa (vs 2.9 GPa), admissible stress of 103 MPa (vs 89 MPa), and an admissible strain of 4.0% (vs 3.3%). The modification of the network led to an increase of the modulus by 4% and by 16% and 19% for the strain and stress, respectively. These increases represent an improvement of 42% of the toughness for the new network from 1.6 MJ/m^3 to 2.3 MJ/m^3. This was ascribed in several works [487, 488] to the stronger H-bond arising from the carbamate moieties, thus maintaining a high level of stiffness while allowing more ductility within the networks.

Table IV-3 – Neat Epoxy and Hybrid dynamic network properties (mean ± standard deviation)

				DMA				Tensile		
	ρ	SI (THF)	GC	T_α	$E'_{25°C}$	$E'_{rubbery}$	ν'_e	E	σ	ϵ
	g/cm^3	%	%	°C	MPa	MPa	mol/m^3	GPa	MPa	%
Pristine EP	1.24 ± 0.01	28.1 ± 2.1	99.8 ± 0.3	97.3	2560	15.60	1519	2938 ± 98	88.8 ± 9.9	3.34 ± 0.47
Dynamic Hybrid EP	1.26 ± 0.01	5.7 ± 0.4	99.7 ± 0.3	93.6	4491	6.76	664	3061 ± 71	102.9 ± 6.8	3.99 ± 0.32

Equally, in a recent work [489], we highlighted the interest of pure PHU over pristine epoxy with a similar macromolecular backbone due to these stronger H-bond interactions. Lower crosslinking density PHU leads to comparable to superior thermo-mechanical properties and higher toughness than equivalent epoxy. Such can be extrapolated herein in the case of the dynamic hybrid EP where similar thermo-mechanical properties are obtained with significantly lower crosslinking density (1519 mol.m^{-3} for the pristine EP vs 664 mol.m^{-3} for the dynamic EP). For a better visualization, the internal macromolecular structure schematic representation of the dynamic EP can be found in Fig. IV-A7. This favors the potential durability of such materials by limiting the nucleation and propagation of micro-cracks [490], in addition to the perspectives of repairability due to the dynamic nature of the newly developed copolymer network [490].

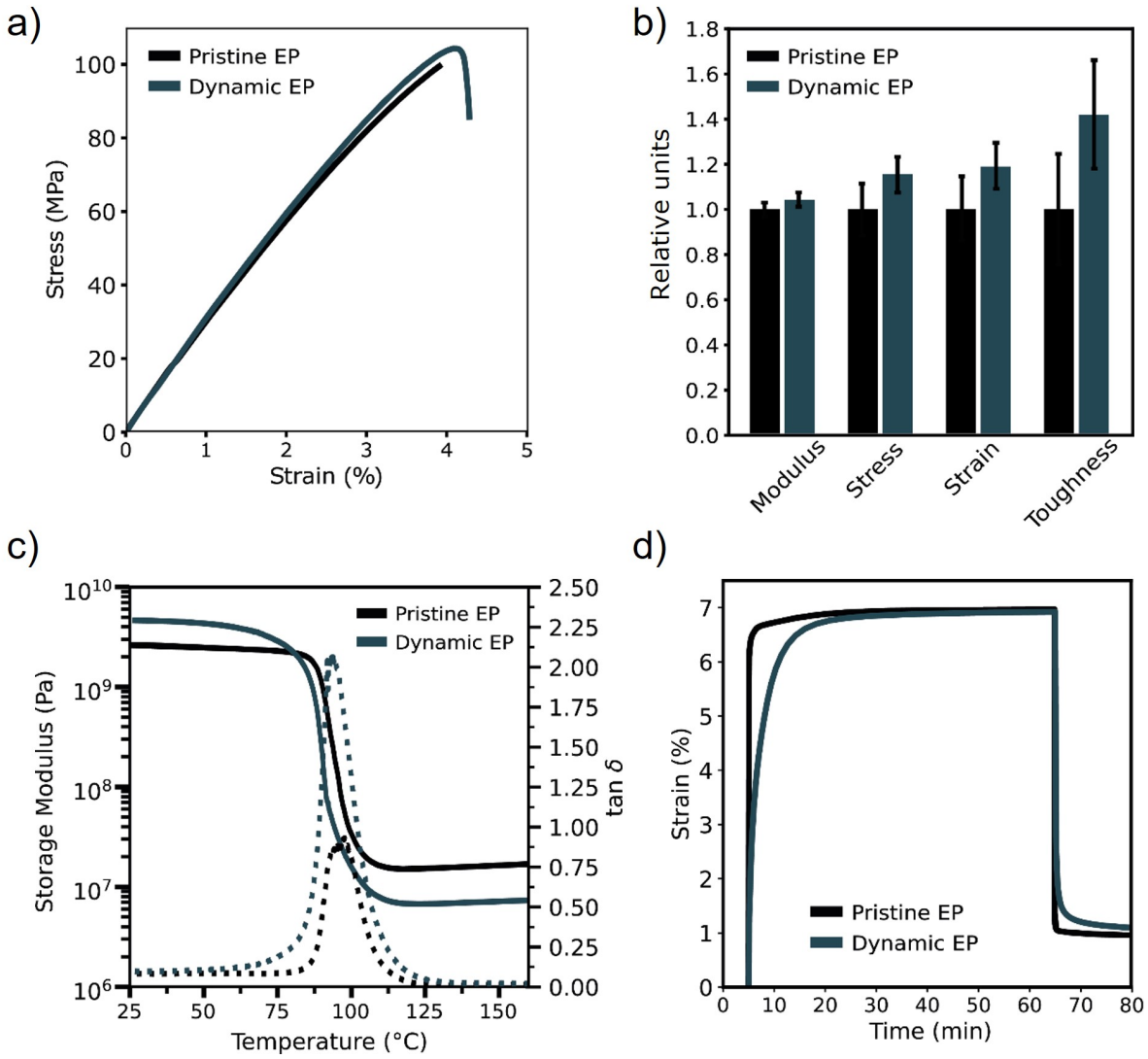

Figure IV-9 – Mechanical and thermo-mechanical behavior of the epoxy and hybrid dynamic polymers. a) Representative tensile stress-strain curves, b) Comparative mechanical properties, normalized to the pristine epoxy, c) DMA curves, and d) Tensile creep behavior at 90 °C

The thermo-mechanical properties were also assessed by Dynamical Mechanical Analysis (DMA) and creep testing. The DMA (Fig. IV-9c) displayed similar glass transitions between the pristine epoxy and the dynamic one with 97 °C and 94 °C respectively, showcasing no alteration of the network and proving suitable for similar applications. Interestingly, the glassy modulus was increased for the dynamic copolymer with 4416 MPa compared to the 2314 MPa of the pristine epoxy. In addition, the crosslinking density of the dynamic copolymer was found to be substantially lower than the pristine epoxy. This is due to the implementation of the hydroxyurethane moieties through the trifunctional cyclic carbonate that lowers the crosslinking density. In the third chapter, we reported that such lower crosslinking density in the presence of hydroxyurethane leads to stronger H-bonds of high interest. The H-bonds were shown to be stronger in PHUs than in epoxy networks [462]. H-bonds are secondary

bonds more flexible than covalent bonding, thus, they conduct an increase of the glassy modulus while allowing more motion of the macromolecular backbone. This finally permits more ductility and toughness of the system. DMA results confirmed this trend related to our copolymerization strategy, as previously observed in tensile testing, between PHU and epoxy and the successful implementation of this toughening strategy to achieve more resilient dynamic epoxy-based materials.

Creep is a known problematic side effect of CAN as the ability of the network to flow leads them to be subjected to creep behavior like thermoplastics, contrary to thermosets [491]. This behavior is strongly dependent on the chemistry involved, the design of the monomer, and the thermal sensitivity of the exchange mechanism. A highly dynamic mechanism will lead to important creep while poor dynamicity involves negligible creep [492]. Interestingly, as the transcarbamoylation is strongly dependent on the temperature and shows little dynamicity at low temperatures, it can be expected that no creep will happen in the operating window of our formulated network. Indeed, thermosets for composite applications are expected to be used at temperatures lower than the glass transition. Therefore, creep experiments (Fig. IV-9d) were conducted at 90 °C, only a few degrees before the alpha transition. The viscous behavior of the CAN was somehow more pronounced than the pristine epoxy with an observable delayed deformation to the applied stress. Interestingly, the strain and recovery were identical to the epoxy one, highlighting no creep sensitivity of the dynamic copolymer up to its glass transition.

Overall, the copolymerization approach through the implementation of dynamic hydroxyurethane implies no alteration of the properties with even some improvement in the epoxy network and is thus attractive to implement CAN in market applications quickly. Additionally, the results in this work were compared to other dynamic chemistries as a function of dynamicity versus properties (see Tab. IV-A3). The approach was shown to be competitive regarding relaxation speed and properties while providing easier access to the starting building blocks.

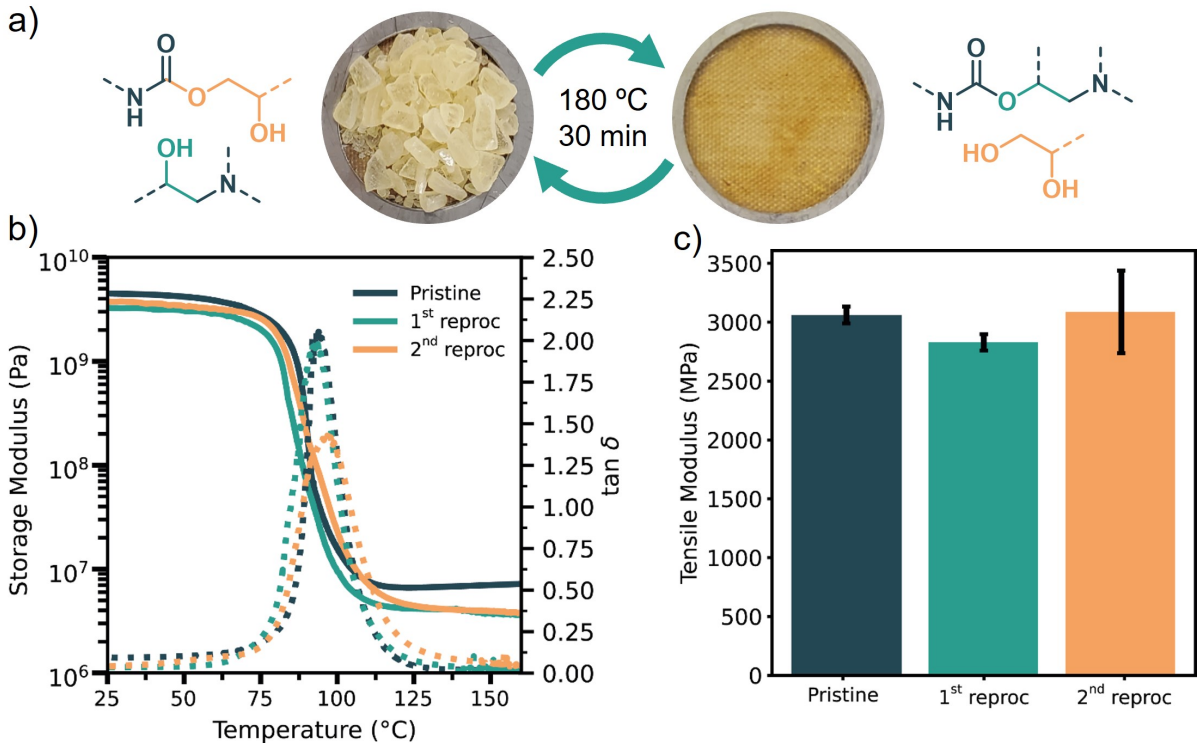

Figure IV-10 – Thermo-mechanical recyclability of the hybrid dynamic network. a) Closed-loop thermo-mechanical recycling, b) DMA curves, and c) Tensile modulus of pristine and reprocessed hybrid dynamic networks.

IV.2.2.2 Investigation of the reprocessability of the network

The reprocessability of the dynamic copolymer was therefore assessed. The polymer was thermo-mechanically reprocessed twice and tested by DMA and tensile testing. Homogeneous samples were obtained as shown in Fig. IV-10a, underlining the ability of the material to be efficiently reprocessed. The recycled sample was dived into THF solvent for 6 weeks (Fig. IV-A11), after which no destruction or cleavage of the network was observed, highlighting the formation of covalent bonding during the reprocessing. SEM micrograph of the cryogenically-fractured cross-section of the reprocessed hybrid epoxy network (Fig. IV-A12) demonstrates the efficient welding of the material, even at the core of the polymeric network. The thermomechanical behavior was similar between pristine and reprocessed samples. DMA curves (Fig. IV-10c) were comparable after two reprocessing steps with no change in the glass transition, behavior, and glassy modulus. The rubbery modulus was, however, found to be lower, representing a slight decrease of the crosslinking density, consistent with the mechanical grinding of the polymer that leads to some irreversible damages in the dynamic copolymer [493] (potential breaking of C-C bonds). Moreover, it is important to note the transcarbamoylation between amino-alcohol and hydroxyurethane leads first to a urethane and a pendant vicinal diol. It was shown in section 2.1

that the amine in the networks can catalyze alcohols to some extent, such as forming vicinal diol. In that sense, an equilibrium is formed and no further change in crosslinking density is observed between the first and second recycling steps. However, this slight change in the structure can also explain the partial loss of crosslinking density. As already observed by DMA, the tensile Young's modulus was almost fully recovered with an efficiency of 92% on the first recycling cycle and 100% on the second one. The strain and stress at break were more significantly affected by the recycling process, with a recovery of around 40% (Fig. IV-A13) due to the irreversible damages induced by the mechanical grinding and potential defects linked to the reprocessing and sample preparation methodology. In particular, the recovery of properties for hard, dynamic polymers with high modulus and admissible strength is known to be much less efficient than in the case of elastomeric CANs due to the sensitivity of the material to local defects, lower ductility, thus toughness, and the high force and energy involved within the materials [494].

Table IV-4 – Reprocessing of the hybrid dynamic network

	DMA				Tensile		
	T_α	$E'_{25°C}$	$E'_{rubbery}$	ν'_e	E	σ	ϵ
	($°C$)	(MPa)	(MPa)	(mol/m^3)	(GPa)	(MPa)	(%)
1^{st} reprocess	93.2	3262	4.12	396	2.8 ± 0.1	31.9 ± 3.2	1.1 ± 0.1
2^{nd} reprocess	96.8	3765	4.18	399	3.1 ± 0.3	37.5 ± 2.0	1.4 ± 0.1

The dynamic copolymer exhibits promising potential for future applications with the ability to be healed, reshaped, and reprocessed. In particular, it opens many doors in the realm of composite manufacturing where welding and reshapability are particularly beneficial.

IV.2.3 Application of Hybrid Epoxy-PHU polymers in high-performance composites: fabrication, properties, and features provided by the dynamicity.

IV.2.3.1 Carbon fiber composite manufacturing and testing

CANs represent a breakthrough in the composite industry as they allow high-performance materials to be reshaped and welded, impossible with conventional thermosets. Thus, prepregs and semi-finished parts can be manufactured by infusing reinforcement using conventional tooling. Complex shapes and final parts could be later obtained by exploiting the fast exchange mechanism.

In that sense, carbon fiber-reinforced composites were manufactured by thermo-compression using the investigated epoxy CAN. The composite impregnation was possible with high quality as translated through the high fiber volume fraction (V_f=63.8 ± 0.8%) and the low porosity content (V_p= 1.0 ± 1.0%).

The monotonic tensile test assessed the static mechanical performances as shown in Fig. IV-11. Extremely high mechanical performance of the CFRP was obtained with 133 GPa in modulus, and 1700 MPa of stress at break. Such outstanding results were ascribed to the successful adhesion of the resin to the fibers [151]. The matrix depicts good compatibility with commercial fibers that incorporate a conventional sizing for epoxy matrix and were used without any further modification. The obtained properties were similar to typical equivalent materials in literature and industry (see benchmark in Fig. IV-A18 and Tab. IV-A4) showing once again that this simple copolymerization approach is a suitable path to reach industrially and economically relevant dynamic matrices for high-performance materials. In particular, PHUs have shown outstanding adhesion capabilities on many substrates [394], including natural fibers [489], that enhances even further the interest of the copolymerization approach to finely tune and improve the interfacial strength of composites.

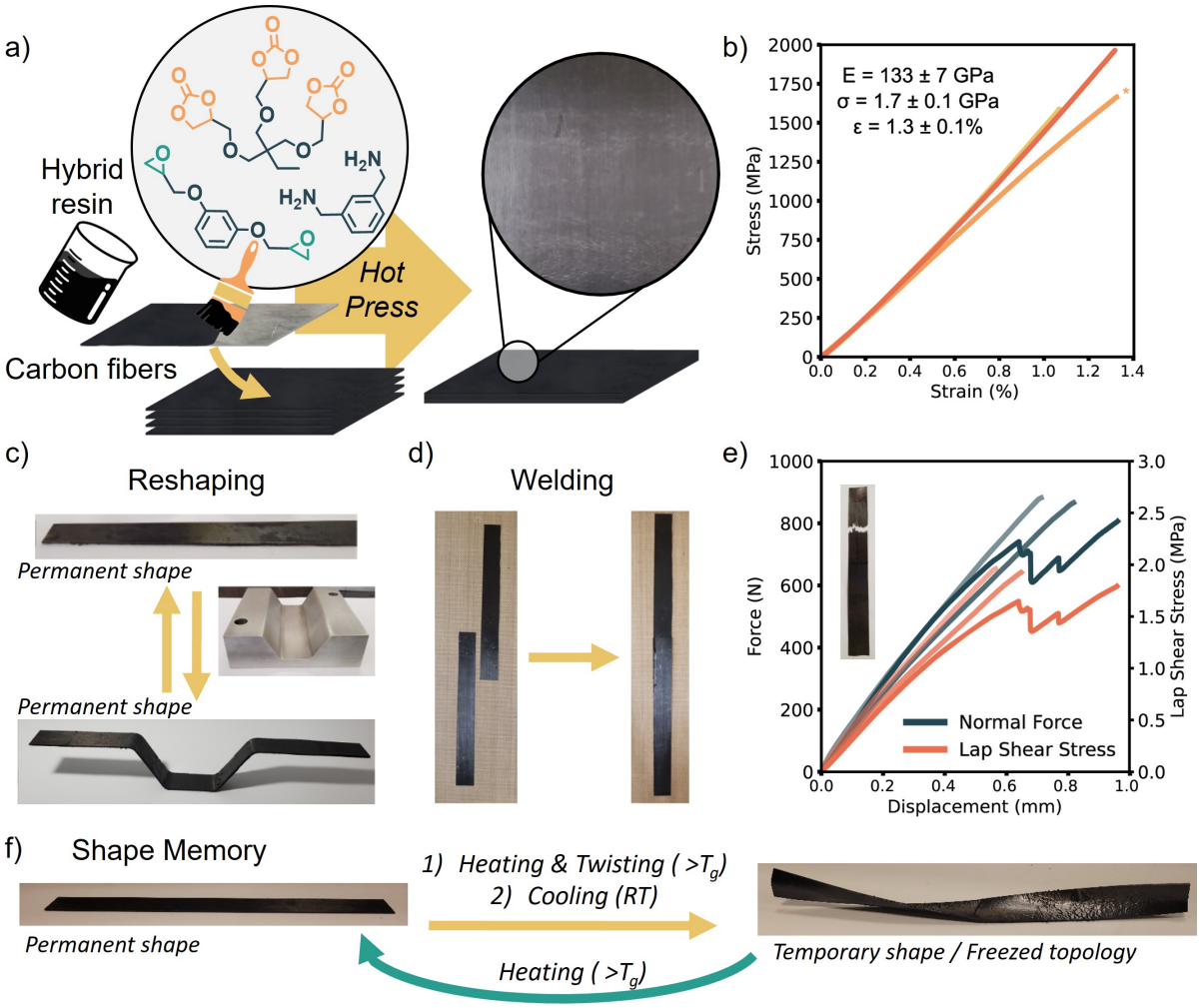

Figure IV-11 – Carbon Fiber Reinforced Vitrimer. a) Schematic representation of the impregnation process, b) Tensile stress-strain curves of the manufactured composites (*sample did not break), c) Reshaping of the carbon composites, d) Welding of single-ply composites, e) Adhesion strength of the welded composites (Inset: representative broken sample), and f) Shape-memory ability of the carbon composite.

IV.2.3.2 Exploiting the dynamic network for reshaping high-strength carbon fiber composites

The (re)shapability is illustrated in Fig. IV-11c, where the already fully cured flat laminate was reshaped in a complex geometry within 30 min at 180 °C. The newly obtained shape was smooth and defect-free with no buckling at the edges or surface that would be indicative of a detrimental delamination. The fibers' orientation was kept. This demonstrates that the system can be extended to new shaping and manufacturing processes, such as composite forging. In that sense, an easy-to-store and stable, flat pre-preg composite can be manufactured on a large scale and then shaped and welded into the final part with desired orientations within a few minutes. This would thus open the door to

fast high-performance composite manufacturing processes that were up to date inaccessible due to the long time needed to cure epoxy. Additionally, it would lead to the reshaping of end-of-life structures (such as plane wings) to new second-life structures with outstanding performances and limited cost and environmental footprint. Besides, the weldability was investigated (Fig. IV-11d-e) where two single-ply cured sheets were self-welded together by thermo-compression thanks to the exchange reaction. This was only possible with the dynamic copolymer formulated where the -OH functions can thus form covalent bonding through the transcarbamoylation mechanism at the interface between the two plies. The adhesive strength was evaluated. Adhesive strength values of about 2 MPa were obtained, in the range of similar materials and conventional adhesion of CFRP [474]. Interestingly, the failure did not happen in the welded area but was initiated at the welded edge due to stress concentration, and propagated by splitting within the laminates. This illustrates that the welding was strong and efficient, and additionally opened the door to cured pre-impregnated laminates that could be shaped and welded in a fast process. This is of particular interest for the automotive industry, where fast processes are expected and CFRP could help reduce weight and thus energy consumption. In addition to the outstanding properties of the composite material, the dynamic matrices provide the key features to allow the efficient reshaping and welding of semi-finished parts even incorporating a high content of stiff carbon fibers with no apparent damage or structural integrity decrease. Moreover, shape memory behavior can be achieved for other specific applications such as passive actuation (Fig. IV-11f).

IV.2.4 End-of-life scenarios and recyclability

Reshaping and welding of CFRP offers many advantages in the realm of composite structures. However, their end-of-life is a rising concern as more and more structures are reaching the end of their planned service life.

IV.2.4.1 Thermo-mechanical direct reprocessing/recycling

Taking advantage of the thermally activated network, the CFRP was first recycled through a simple thermo-mechanical process (Fig. IV-12). The chips were cut in parts and then pressed 30 min at 180 °C. The material obtained was tested in three-point bending tests. With a modulus of 3.7 GPa and a maximum stress of 28 MPa, the material displays mechanical properties consistent with random blocks of aligned fibers that lead to an integral material. However, the material properties are quite poor for CFRP due to stress concentration, high fiber volume fraction thus low matrix quantity to be strongly welded, and no control of the fiber orientations. It remains an open door for low-cost fast re-use of

existing structures that cannot be obtained with conventional EP-based composites.

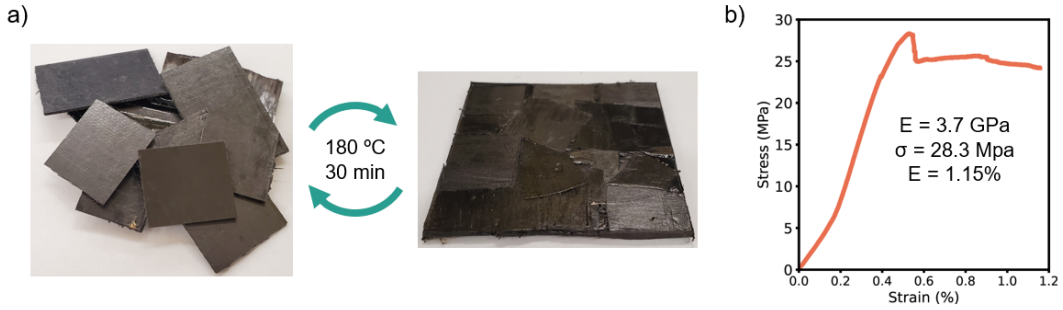

Figure IV-12 – Thermomechanical recycling of the carbon fiber reinforced composites with the hybrid dynamic matrix.

More generally, it can be expected that the structures and the composite materials at their end of first service life do not reach a sufficient safety trust level and should be downgraded. If the composite material integrity can be questioned and thus the thermo-mechanical recycling is not adapted, the carbon fiber could still have sufficient properties for many other applications, including semi-structural and structural ones. Moreover, the cost of carbon fibers and their detrimental environmental footprint make them the most valuable product to recover in composites with a real environmental and economic interest [13].

IV.2.4.2 Mild chemical recycling for the recovery of carbon fibers

In that sense, another option was investigated through chemical recycling. This pathway is more promising as it allows the recovery of the high-value carbon fibers [495]. The CFRP chips were introduced in an 80:20 mixture of (glacial) acetic acid and hydrogen peroxide (30 wt% in water). This solution generates in-situ peracetic acid that can cleave the epoxy-amine linkage [293]. The solution with CFRP chips was heated to 60 °C under constant magnetic agitation. The oxidative solution destroyed the polymer integrity within 4 h, and the CFs were simply recovered by filtration, dried, and reused. Starting from 10 g of the CFRP, 6.75 g of carbon fibers were recovered, consistent with the estimated weight fraction (68-70 wt%, from both calculus and TGA analysis), and highlighting no noticeable loss of fibers in the process. The acetic acid mixture was recovered by rotary evaporation and reused for a new recycling batch (Fig. IV-A16). 220 mL of the slightly diluted acetic acid solution were recovered, as already mentioned in previous studies [293], and unveiled an 85-90% recovery of the solvent.

This way, high-value carbon fibers were retrieved under mild conditions. The recovered fibers were analyzed by SEM (Fig. IV-13c), XPS (Fig. IV-13f), TGA (Fig. IV-13e), and FTIR (Fig. IV-A14).

The surface of the fibers was removed off from any polymer residues as observed by SEM and FTIR, as no characteristic peak of the polymer matrix was observed. Additionally, the sizing agent was removed, which is typical for the chemical recycling of CF [13]. XPS displays the appearance of a new peak located at 288.7 eV revealing the partial oxidation of the carbon fiber surface by the oxidative treatment. The oxygen content at the CF surface increased from 19.9% to 23.8%. Such observations were already addressed by Das et al. [293]. This slight oxidation at the carbon fiber surface did not lead to detrimental effects on the fibers, and, overall, the integrity of the fibers was maintained. Further, this local oxidation could be interesting in forming new bonds with amine-based matrices and act as adhesion promoters for further use [496]. The TGA confirms the similarity between virgin and recycled CF.

To prove the possibility of valorizing such reclaimed CF in new high-added-value applications, the fibers were re-used as a non-woven mat with the dynamic copolymer matrix and tested in three-point bending (Fig. IV-13d). The recycled material exhibits outstanding properties with a modulus close to 50 GPa, a stress at break of almost 500 MPa, and an admissible strain superior to 2.1%. The properties obtained indicate that the reclaimed fibers can be efficiently used for many applications, particularly in transportation as they exhibit properties similar to aluminum with a higher strength-to-weight ratio, promising carbon footprint, and low cost. The mild conditions used to recover the fibers are of particular interest as they are economically relevant with low-cost, easily accessible, and recoverable reagents. Thus, a new generation of recycled carbon fibers at a competitive price and interesting environmental footprint [497] could join the market again.

Regarding the chemical recyclability of the hybrid epoxy-PHU vitrimer, it is important to note that the matrix was cleaved in a (mild) oxidative process. Although extremely efficient, this process is not selective and leads to many potential side reactions, and therefore does not conduct a straightforward recovery of chemical building blocks. Previous works have used oxidative processes or other more selective chemical recycling paths [292, 293, 295, 498]. In most cases, the identification, separation, and purification of valuable building blocks lead to low yield and a highly intensive process that can be questioned in terms of sustainability and industrial scalability. The oxidative process leads to the easy recovery of the high-value carbon fibers but also to the potential loss of the polymeric matrix.

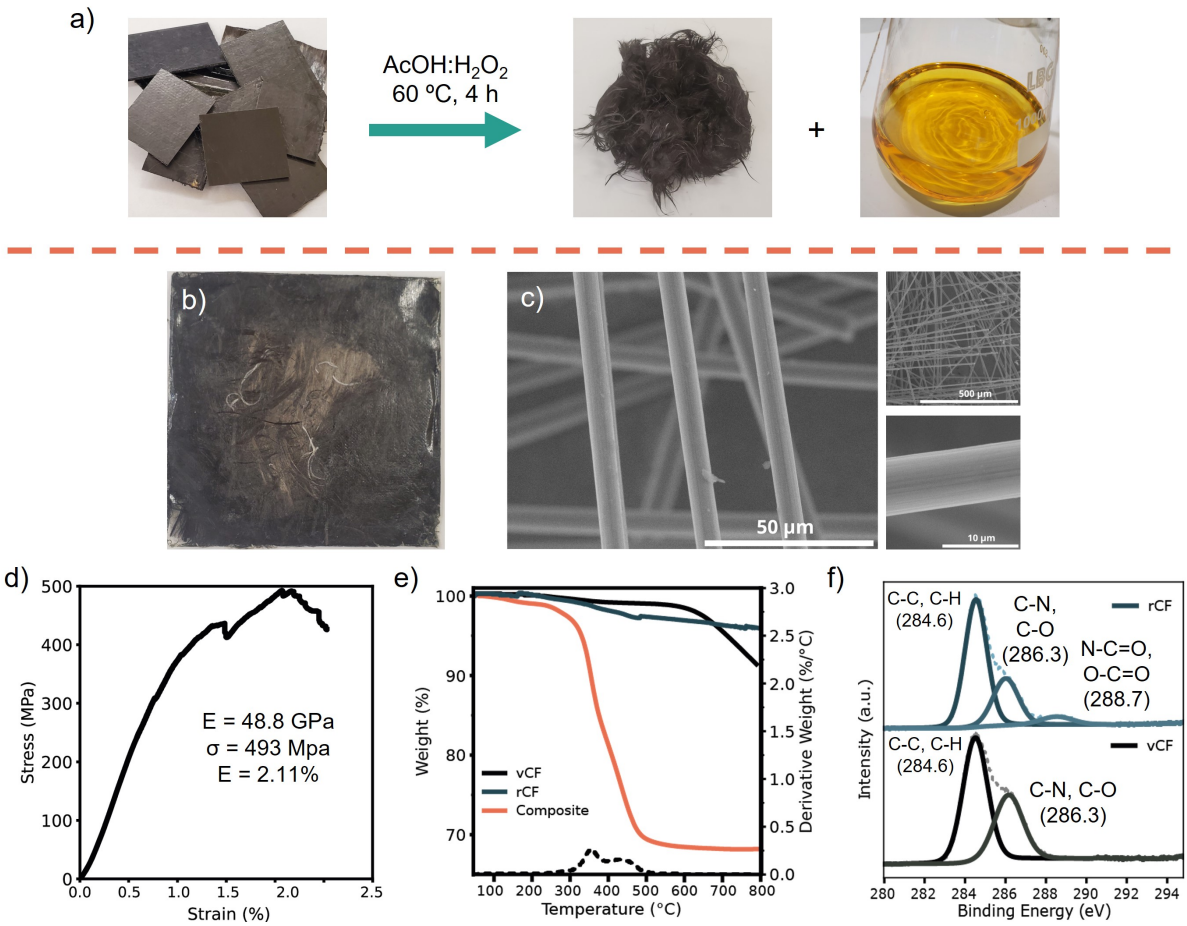

Figure IV-13 – Recycling of CFRP. a) Chemical recycling of the composites by resin oxidation and fiber separation, b) Non-woven carbon composites fabricated from recovered fibers, c) SEM images of the recovered fibers, d) Three-point bending strain-stress curves of the chemically recycled composites, e) TGA of the composite, virgin CF and recovered CF, and f) XPS analyses of the virgin and recovered fibers.

IV.3 Conclusions

A new strategy is proposed to obtain a highly scalable and efficient covalent adaptable network through a synergetic copolymerization approach. Non-dynamic, widely spread thermosets, e.g. epoxy-amine, and a poorly dynamic polyhydroxyurethane network can be used to form a new highly efficient network. The resulting copolymer exhibits a fast catalyst-free adaptable behavior allowing the novel network to be recycled in mild conditions. The synergetic behavior was demonstrated to arise from the amino-alcohol formed by the epoxy-amine reaction while the dynamic hydroxyurethane is obtained from the aminolysis of cyclic carbonates. The copolymer displays high tunability and promising properties, similar or superior to the pristine epoxy. The dynamic copolymer was used to manufacture carbon

fiber composites that exhibit strong adhesion at the fiber/matrix interface leading to outstanding mechanical properties suitable for structural applications in conventional carbon composite uses. The cured composite could be easily reshaped from flat plates to complex geometries within half an hour and equally welded. Such scalable and efficient copolymers are extremely promising for transportation applications where large volumes are produced in intensive production lines. Finally, the copolymer can be cleaved in an oxidative process in mild conditions to recover the high-added-value carbon fibers efficiently. The carbon fibers were shown to be only slightly affected by the chemical recovery and were reused for a new composite part with remarkable properties. This innovative copolymerization approach is a promising step towards globally available epoxy-based materials with high performances in a closed-loop circular economy. It will also help foster PHU chemistry in the realm of composite materials. Yet, the processability of such matrices should be investigated to ensure their applicability in traditional composite manufacturing processes. It should be extended to natural fiber composites, and the recovery of these more sensitive fibers should be explored.

Chapter V

Upscaling of hybrid EP/PHU matrices to industrially relevant processes: curing, properties and recycling of RTM-made natural fiber composites

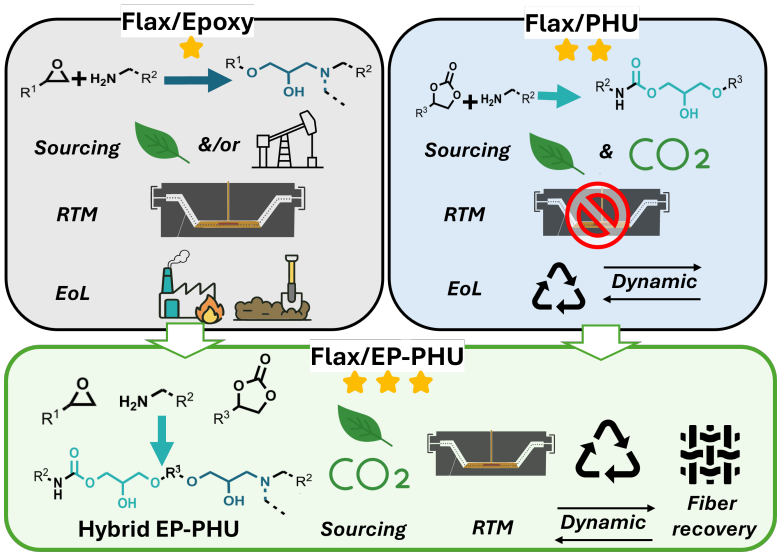

Adapted from: G. Seychal, B. Miranda Campos, G. Perli, V. Placet, B. Grignard, G. Bonnet, C. Detrembleur, H. Sardon, N. Aranburu, and J.M. Raquez, Implementing recyclable bio- and CO_2-sourced synergetic dynamic matrices via precise control of curing and properties for natural fiber composites within industrially relevant resin transfer molding, *Accepted in Chemical Engineering Journal*
External contributions: *V.P. performed and analyzed the tensile properties of the flax yarns. EDX and SEM images were performed in Materia Nova, XPS measurements were performed by SGIker of UPV/EHU.*

Contents

V.1 Introduction

The first two chapters have demonstrated that PHUs, as initially hypothesized, display a strong affinity with natural fibers but exhibit high viscosity and long curing times that limit the manufacturing of larger composite samples with limited formulation options. The dynamicity of PHU was not sufficient to be considered in composites. The last chapter has demonstrated that the synergetic hybridization strategy between EP and PHU leads to a significant increase in the dynamicity and that CFRP can be efficiently reshaped and welded, while the matrix can also be cleaved to retrieve the fibers. Considering this synergetic hybrid in real-case composite manufacturing chains might be pertinent, but there is still a lack of understanding to ensure their relevance.

The preliminary results obtained in the previous chapter need to be confirmed for natural fibers, which are much more sensitive to chemicals and external conditions.

We have seen in the literature review that out-of-autoclave systems present considerable growth among the possible processes for manufacturing FRPs due to the lower tooling and energy consumption cost, higher production rates, and improved versatility [43]. Resin Transfer Molding (RTM) is one of the essential out-of-autoclave processes as it allows fast curing rates, high fiber volume fraction, and high impregnation quality for parts up to a few meters in size with good surface finish [43]. However, to meet RTM requirements, the curing behavior of the matrix must be precisely controlled so that low viscosity for fast reinforcement impregnation (ideally below 1 Pa.s) and fast curing (within 1 h at low to moderate temperature) are needed.

To the author's best knowledge, dynamic chemistries for resin transfer molding of natural fiber composites have never been explored, and even less targeting large-scale, low-cost production with potential for fiber-matrix separation. Only very recently, Schenk et al. [366, 484] explored aerograde disulfide-based EP dynamic networks for RTM of carbon fiber composites. Although efficient, the high temperatures required in their systems would lead to the deterioration of NF, and no fiber recovery was studied. Such a research gap may result from the challenge of developing innovative and more environmentally friendly materials on a large scale and at a cost suitable for composite manufacturing processes. The synergetic hybrid EP-PHU could thus be a solution.

In this chapter, we propose to develop and investigate this novel hybridization strategy to achieve efficient and sustainable NFC, displaying recyclability potential and meeting RTM requirements. First, model reactions were performed to investigate the mutual catalytic effect between EP and PHU by improving the aminolysis reaction rate. Then, hybrid formulations with viscosities suitable for RTM were investigated, as shown in Fig. V-1.

The curing was then studied through rheological and calorimetric methods, particularly the EP/CC content ratio effect. Friedman's isoconversional model was exploited to obtain the activation energy evolution and understand the curing behavior. Flax composites with different EP/CC ratios were then manufactured by RTM. The impregnation quality was evaluated, and their properties were assessed. The results were rationalized by ANOVA analyses and the Classical Laminate Theory. The capacity of these dynamic flax-based composites to be efficiently reshaped was demonstrated. Finally, the flax fibers were recovered using a mild process to cleave the matrix and reused as reinforcing fibers into a new composite. The effect of the acidolysis on the flax fiber was deeply investigated.

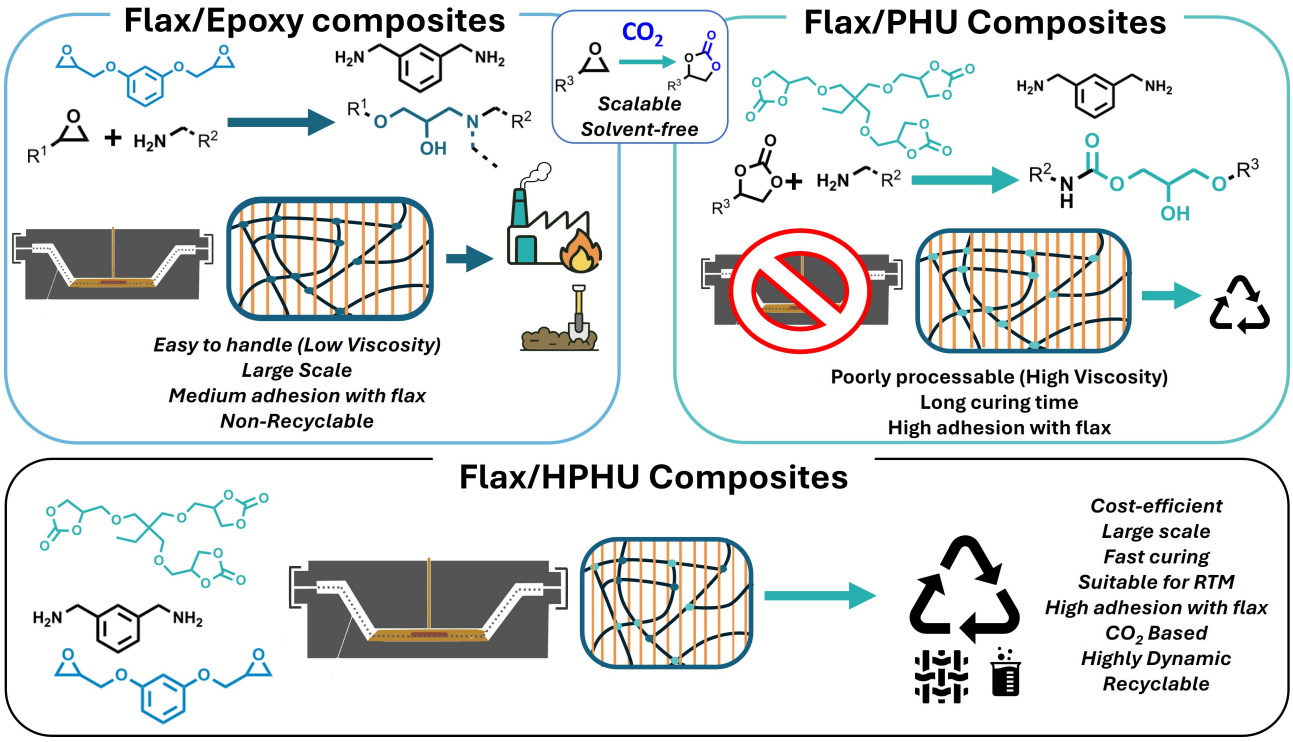

Figure V-1 – General scheme of the hybridization approach to introduce PHU in the composite industry.

V.2 Results and discussions

V.2.1 Mutual catalytic effect on the aminolysis of cyclic carbonates and epoxy compounds

For industrial applications, a rapid curing process is essential to minimize tooling requirements and improve the overall manufacturing speed, ensuring ongoing industrial relevance. Despite their advantageous properties, certain matrices, like PHU, pose a significant challenge due to their prolonged

curing times and high viscosity [499]. Similarly, epoxides also require prolonged curing, even at temperatures higher than room temperature [500]. An intriguing question arises regarding how the synergetic hybridization strategy affects the overall curing process. In particular, the competition between epoxy and cyclic carbonates toward aminolysis must be first addressed.

In this respect, the aminolysis of a cyclic carbonate mimicking the actual polymer building block (herein butyl carbonate - BGC) by a primary amine (benzylamine - BzA) was first studied at 25 °C. In the reference scenario, only the BGC and BzA were used (Fig. V-A1). In the second scenario, 0.5 eq of an opened epoxy model (mEP, see Fig. V-2,Fig. V-A2) was added to see a potential catalytic effect from the formed epoxy compound within the formulation. The evolution of the BGC conversion is depicted in Fig. V-2a. The aminolysis of the cyclic carbonate occurred spontaneously at room temperature with the quick conversion of 60% of the cyclic carbonate compound within 1 h. This is ascribed to the reported catalytic effect of amines that act as both reactant and catalyst [501]. However, the conversion rate significantly decreases after 2 h of reaction. 85% of conversion is reached after 5 h, and an asymptotic behavior is observed with a low extent of conversion, requiring 24 h to reach more than 99% conversion. This trend has been reported in the literature [439] and has been attributed to the effects of steric hindrance and hydrogen bonding, limiting the overall conversion of the cyclic carbonates. Additionally, the depletion of free amines reduces the initial catalytic effect, resulting in a slower reaction completion. Interestingly, a catalytic effect is observed when mEP is added. After 1 h, 75% of CC conversion was reached, and 91% after 5 h, showing a positive effect of the presence of amino-alcohols in the reaction media (Fig. V-2a). Even if somewhat unexpected, this positive effect can be understood as these bases and alcohols/protic species are known to catalyze the aminolysis kinetics of cyclic carbonates [390, 434]. The amino-alcohols obtained through aminolysis of oxirane have a pKa around 10-11, providing this base-catalyst effect in addition to hydrogen bonding [382, 502]. It was also reported that basic compounds (such as triethylamine and guanidine derivatives...) stabilize the intermediary ammonium alkoxide [503] and, similarly, mEP compounds may serve as a proton-transfer (Fig. V-2d). Likewise, in the case of CC aminolysis, the pendant hydroxyl group acts as a hydrogen donor and stabilizes the intermediate alkoxide together with the N-H of the urethane. Ultimately, the alkoxide deprotonates the ammonium to form the final adduct.

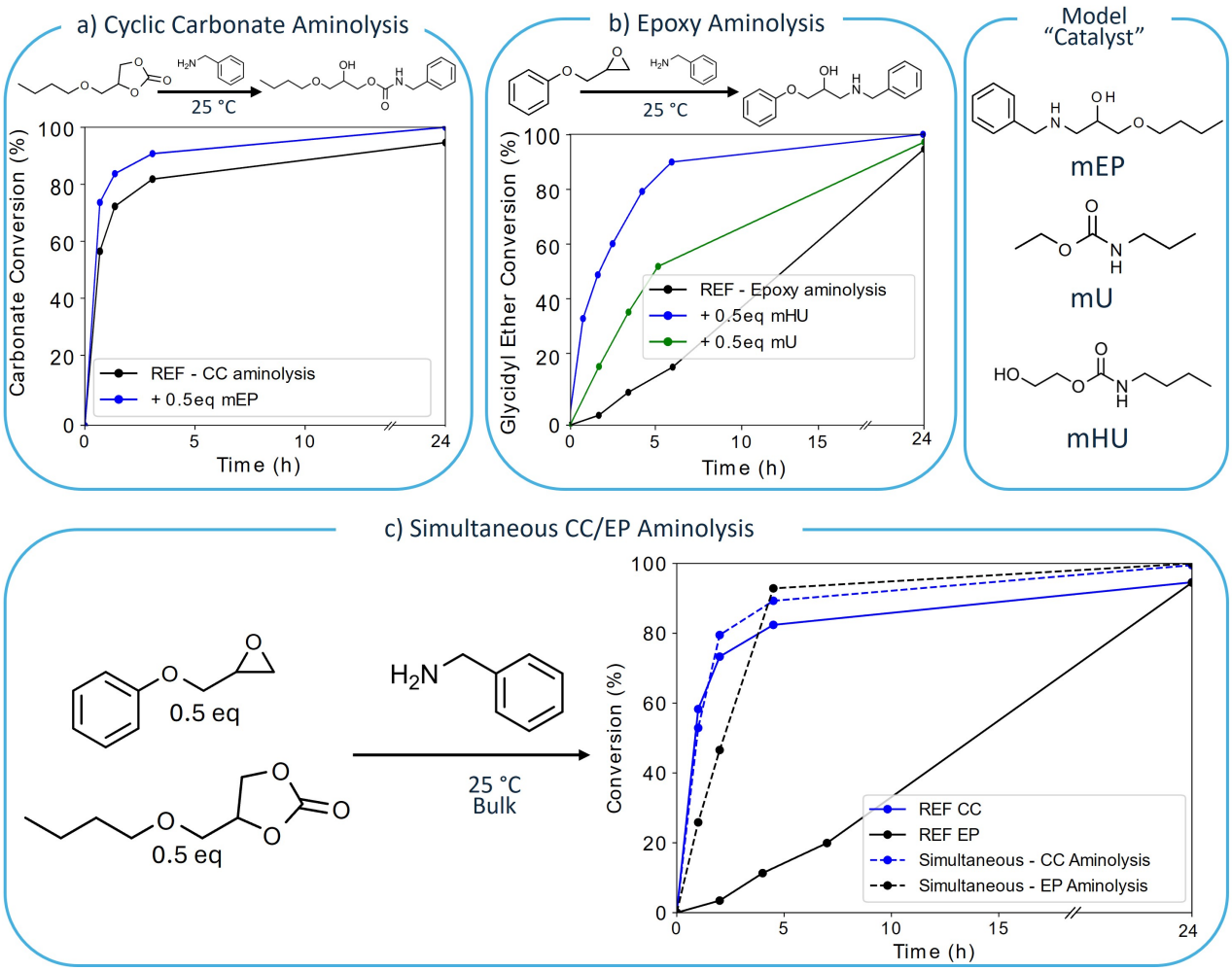

Figure V-2 – Model reaction kinetic study of the catalytic effect of presential epoxy and urethane compound. a) Aminolysis of cyclic carbonate, b) aminolysis of epoxy, and c) simultaneous aminolysis of epoxy and cyclic carbonate.

A similar reaction was conducted between a model epoxy (Phenyl Glycidyl Ether – PGE) and the same BzA curing amine at 25 °C (Fig. V-A3). The reference uncatalyzed reaction showed a typical behavior for epoxy-amine compounds with a prolonged reaction in the early stage, reaching only 20% after 7 h but quickly evolving up to 95%. Epoxides exhibit exponential curing behavior due to the autocatalytic effect of amino-alcohols during the aminolysis. Early stages are slow, with limited spontaneous reactions happening. Still, the formation of hydroxyl compounds favors the reactions [458], thus generating a cascade effect that accelerates the curing rate [392].

Unlike epoxy aminolysis, the aminolysis of CCs is catalyzed by the presence of free primary amines, facilitating early hydroxyurethane formation. Based on this observation, we hypothesized that the formed hydroxyl compound could fasten the epoxy aminolysis. To demonstrate this, a model hydroxyurethane (mHU) was introduced into the reaction media (Fig. V-A5). As initially hypothesized,

a significant positive effect was detected with more than 90% conversion in 7 h, representing a reaction four times faster. In the presence of mHU, the catalytic hydroxyurethane is already present, activating the epoxy and accelerating the reaction. To discriminate the importance of the urethane moiety in the system and its role compared to the hydroxyl moiety derived from hydroxyurethane, a similar urethane compound (mU, Fig. V-A4) was also tested, i.e., not bearing any alcohol moiety. Interestingly, an intermediate behavior was found at around 60% conversion within 7 h, representing a reaction 3 times faster than the reference but slower than when using mHU. However, the catalytic effect was still noticeable. The catalytic effect of mU confirms that it is not solely the hydroxyl moiety that contributes significantly to the catalytic action of mHU but urethanes also play a role in accelerating the epoxy aminolysis, more likely through hydrogen bonding.

While these initial separated kinetic model reactions show promise, a final experiment was performed through the simultaneous aminolysis of epoxy and cyclic carbonate compounds. This approach acknowledges that competitive reactions may take place, limiting the catalytic behavior of each compound on the other. Thus, PGE, BGC, and BzA were mixed directly, and the hydroxyurethane and epoxy formation were monitored. The results are presented in Fig. V-2c and Fig. V-A6. Interestingly, we observed that the CC aminolysis is similar to the reference at the early stage, with about 60% conversion within an hour. Even if the catalytic effect is not as pronounced as in the case of the mHU-catalyzed reference that displayed a conversion of 37% in 1 h, the epoxy aminolysis in the EP/CC system was significantly faster than in the case of the reference EP (20% conversion in 1 h vs. 3%) This can be understood through the need to generate a sufficient amount of hydroxyurethane moieties to achieve a notable catalytic effect on the epoxy, therefore delaying the reaction slightly. However, after 5 h of reaction, both CC and EP reached more than 90% of conversion while the reference cases were at 80% and 15%, respectively. As a result, although some competition could have been anticipated between the aminolysis of epoxy and CC, thus hindering the full completion of one compound, a mutual catalytic effect was observed. This allowed each system to help the others in achieving higher conversion degree more quickly. These unexpected observed features enable the future application of PHU chemistry in rapid curing processes such as RTM. We can anticipate a similar behavior at the polymer scale with the quick reaction of cyclic carbonates increasing the opening of the epoxy, thus leading to faster curing at lower temperatures.

V.2.2 Curing behavior of EP/CC formulations and final properties of EP-PHU copolymers

In composite manufacturing, it is essential for reactive resins to display low viscosity to efficiently impregnate the reinforcement used, ideally at room temperature. Additionally, the curing should be as fast and controlled as possible to minimize manufacturing costs, energy consumption, and thermal degradation when heating is required for curing. Although the mutual catalytic effect of EP and CC in the aminolysis reactions was effectively proven in the previous section, the situation may differ in the case of the bulk polymers. Therefore, EP/CC formulations of various compositions were prepared, in addition to the reference EP and PHU homopolymers, and their curing behavior was analyzed by DSC and rheology.

To achieve physical properties that align with market expectations (low viscosity, glass transition temperature of 90-100 °C, high strength...), trimethylolpropane tricarbonate (TMPTC) was selected as the cyclic carbonate monomer. The trifunctionality of the starting molecule facilitates a sufficient degree of cross-linking within the polymer network. The resorcinol diglycidyl ether (RDGE) was selected as the epoxy monomer. RDGE is a potential lignin-derivative replacement for the widespread bisphenol-A diglycidyl ether [211]. RDGE is an aromatic epoxy; therefore, it will also bring sufficient rigid substructures within the backbone. Furthermore, RDGE possesses low (melt) viscosity at room temperature to act as a reactive diluent in the formulation of the hybrid PHU. Finally, m-Xylylene Diamine (MXDA), a potential furfural bio-derived amine [214], was selected as a co-reagent between RDGE and TMPTC to further bring more aromaticity into the network, improving the mechanical and thermo-mechanical properties of the resulting material.

The viscosity of the EP/CC mixtures was measured to determine the optimal amount of epoxy diluent needed to obtain viscosity values below 5 Pa.s, which is a typical value for epoxide formulations dedicated to RTM processes. For the formulation under study, an amount superior to 25 % in mass is required (Fig. V-A7). Although the viscosity of neat TMPTC is high (150 Pa.s), limiting its application in many processes, adding just a small amount of epoxides can drastically lower the viscosity of the formulation by an order of magnitude. This emphasizes the effectiveness of hybrid EP-PHU by appropriately adapting and spreading the use of PHU in advanced manufacturing processes.

V.2.2.1 Non-isothermal DSC curing - Assessing the curing behavior evolution

Non-isothermal curing was performed on the hybrid polymer formulations to investigate the aforementioned potential catalytic effect as a function of the epoxy content. The non-isothermal

curves obtained with 0, 25, 50, 75, and 100% epoxy content at 5, 10, and 20 K/min from 25 to 220 °C are presented in Fig. V-3. Extracted data are reported in Table V-1. Interestingly, the presence of hydroxyurethane led to a significant decrease in the maximum temperature peak, curing enthalpy, and offset temperature compared to neat epoxy. Additionally, the onset temperature was significantly lower and the conversion rate increased, highlighting the improvement in the curing rate compared to neat epoxy or neat PHU. PHUs are known to have a slow curing rate with a strong dependence on the temperature to reach a sufficient amount of conversion [436]. This appears evident through the conversion plot (Fig. V-3) of the non-isothermal DSC with two distinct phases of curing: one between 25 °C and 130 °C with only 50% of conversion and a second phase between 150 °C and 200 °C to finally reach full completion. This is particularly problematic for advancing PHU chemistry in composites, especially when used with biobased fibers. This highlights that prolonged curing time and high temperatures are necessary. However, when increasing the epoxy content, conversions higher than 80% are reached at temperatures lower than 80 °C. This can be understood through the catalytic effect reported earlier in this work as well as the high exothermic behavior of epoxy. The latter can generate a sufficient amount of energy to push the aminolysis forward [392].

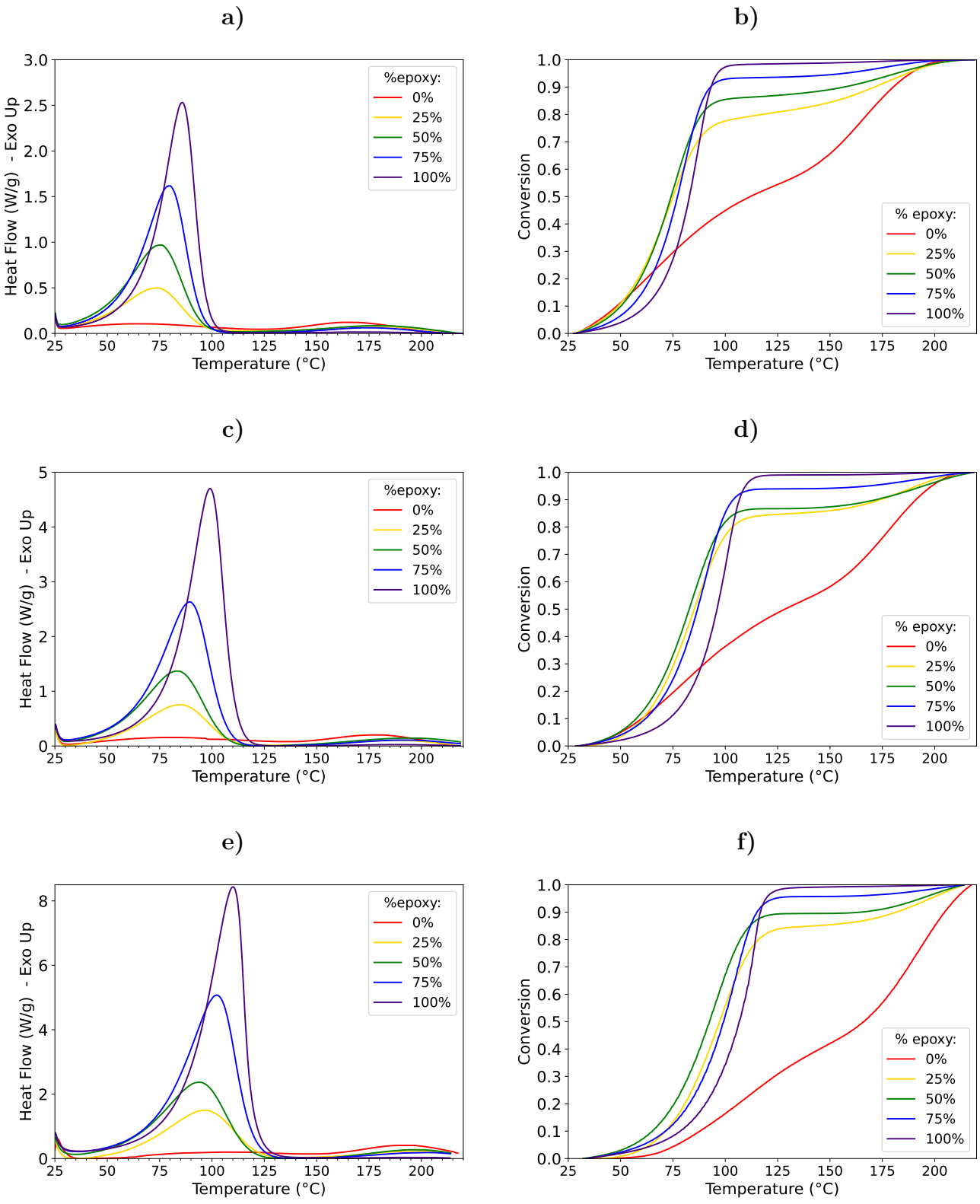

Figure V-3 – Non-Isothermal DSC curing analyses. a) Thermograms, b) conversion at 5 K/min, c) Thermograms, d) conversion at 10 K/min, e) Thermograms, and d) advance curing at 20 K/min.

Exploiting Friedman's iso-conversional model (Fig. V-4), the activation energy of the different

systems was obtained as a conversion function as reported in Fig. V-4f. Friedman's iso-conversional model was preferred to Ozawa's and Kissinger's models as it does not assume a constant E_a throughout the whole reaction. Instead, the activation energy depends on the extent of the reaction and thus provides a more accurate representation of reality. Given the observed behavior through the non-isothermal curing, particularly for the PHU, a constant E_a cannot be assumed. As expected from the previous observation, the activation energy of the neat PHU was much lower than that of the other formulations (26.5 kJ/mol vs 68.4 kJ/mol for the pure epoxy). The pure PHU shows, however, a significant and continuous increase of the activation energy after reaching 30% of conversion. This highlights a known issue with PHUs: the curing process slows down as the conversion increases. This significantly limits complete curing and necessitates higher curing temperatures, resulting in increased energy consumption This behavior is ascribed to the reduction in the amount of the catalyzing free amines and to a change in the curing mechanism, which becomes controlled by diffusion mechanism rather than kinetics [504]. This is coherent with previously reported behavior on the polymerization of thermoplastic PHUs, which was hindered by hydrogen bonds [377]. Additionally, the higher temperatures required to push the polymerization forward will promote uncontrolled and undesirable side reactions [373, 437]. The hybrids show an activation energy of 59.5, 82.2, and 73.5 kJ/mol from 25 to 75% of epoxy content, respectively. This result seems to contradict the expected trends as lower activation energy compared to epoxy would have been expected, given that the reaction rate is faster at the initial stage. This could be due to the limitations of Friedman's model in accurately estimating the activation energy of a complex system such as EP/CC mixtures, where different mechanisms take place and overlap with each other. However, the augmentation of the activation energy, as observed in pure PHU, resumed after 70% conversion, consistent with the decrease in the conversion rate and the further need to increase the temperature to obtain a higher curing level.

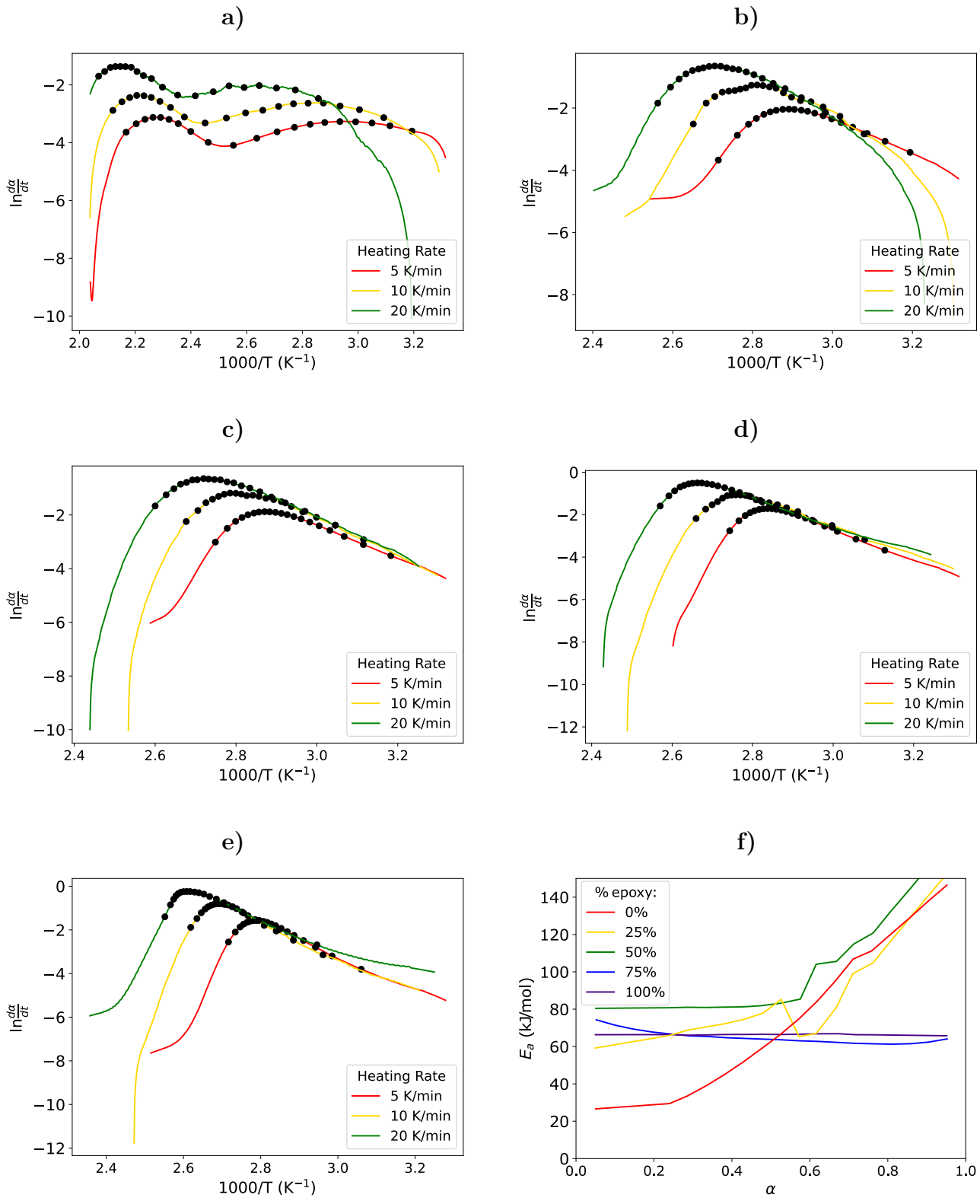

Figure V-4 – Friedman isoconversional plots. a) neat PHU (0%EP), b) hybrid 25%EP, c) 50%EP, d) 75% EP, e) neat EP, and f) calculated activation energy (E_a) as a function of the conversion.

V.2.2.2 Designing a curing protocol for RTM

Based on the observed non-isothermal curing behavior, a temperature of 80 °C was selected as a suitable temperature for a fast and controlled curing of the hybrid formulations, limiting side reactions and reaching a high level of conversion.

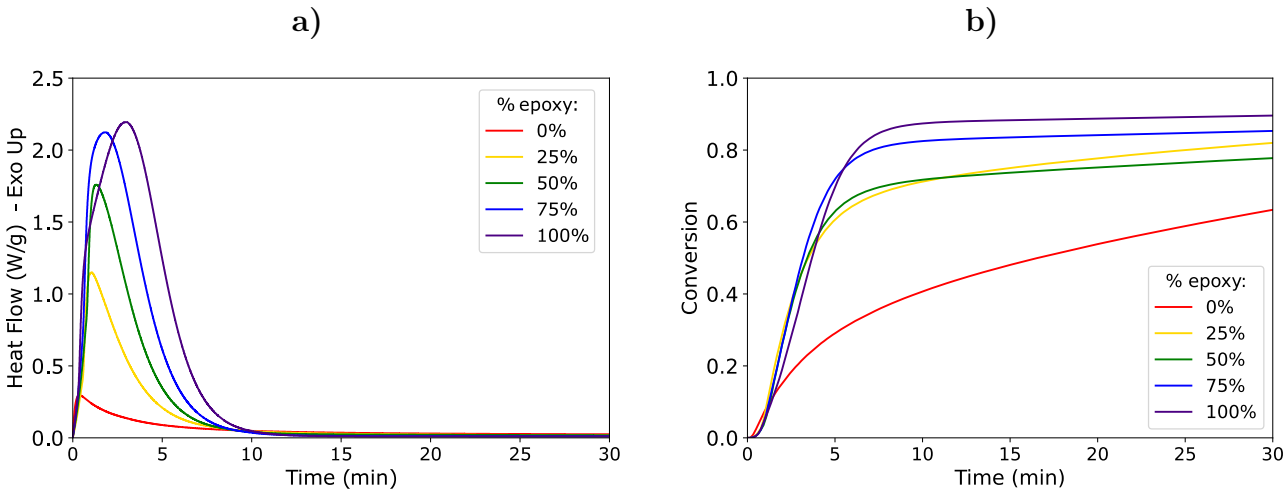

Figure V-5 – Isothermal DSC curing analyses at 80 °C. a) Thermograms, and b) conversion.

The isothermal curing of the formulation was also monitored by DSC. The curves obtained regarding heat flow and curing degree as a function of time are presented in Fig. V-5, and key data are reported in Table V-1. The maximum heat peaks appear earlier in the case of hybrid formulations compared to pure epoxy. Additionally, the offset appears much earlier, and the conversion of the resins significantly increases in the case of the hybrid EP/CC formulations compared to PHU. The PHU only reached 65 % of curing extent, consistent with previous literature work [382, 462]. Conversions superior to 80% were obtained for the hybrid formulations, highlighting the positive effect of this synergy between EP and PHU chemistries. Yet, it also demonstrates that there is no need for a long curing time at 80 °C. At the same time, a post-curing step is essential to ensure the complete formation of the polymer network and, thus, structural stability. Finally, the hybrid EP/CC formulations appear to cure faster than neat PHU at potentially lower temperatures with a superior extent of curing. This makes the approach much more promising for composite manufacturing.

Table V-1 – DSC and rheological curing properties of the hybrid formulations

%EP			0	25	50	75	100
DSC	E_a	kJ/mol	26.5	59.5	82.2	73.5	68.4
Non-Isothermal	Tpeak	°C	66.4	74.1	75.7	79.8	85.6
5 K/min	Q_{max}	W/g	0.18	0.50	0.97	1.62	2.53
	ΔH_T	J/g	169	287	456	581	701
	Onset	°C	30.2	41.3	45.7	54.6	65.8
DSC	Peak Time	min	3.35	3.31	3.35	4.03	5.49
Isothermal	Q_max	W/g	0.29	1.15	1.76	2.12	2.19
80 °C	Offset	min	33.30	20.96	16.63	13.26	13.86
	ΔH_T	J/g	110	235	363	496	628
	Conversion (α)	%	65.0	81.8	79.6	85.4	89.5
Isothermal	η_{init}	Pa.s	44.4	6.0	4.7	4.6	6.0
Rheo	Pot Life	min	nc	2.3	7.0	11.0	12.0
25°C	Gel Time	min	>60	>60	>60	>60	36
Isothermal	η_{init}	Pa.s	2.80	0.35	0.13	0.05	0.10
Rheo	Pot Life	min	4.5	3.3	3.3	3.3	3.5
80 °C	Gel Time	min	83	41	15	5	5

Besides the DSC thermograms, the curing behavior was assessed through rheological experiments at 25°C (Fig. V-6a-b) and 80 °C (Fig. V-6c-d). The primary goal was to assess that the formulations provide sufficient time at room temperature for efficient processing and infusing through RTM while confirming the fast curing once the impregnation is performed. Values are summarised in Table V-1. At 25 °C, viscosities below 6 Pa.s were obtained for epoxy content superior to 25%, which makes them particularly suited for RTM [41]. The observed rheological behavior at 25 °C agrees with the previous model reactions and DSC results. When a high content of cyclic carbonates is present, the reaction starts immediately, as observed by the continuous increase of the viscosity. The formulations containing 50 and 75% of EP are particularly noteworthy due to their low viscosities (4.6 Pa.s), extended pot life (>10 min), which allows enough time before the viscosity becomes too high to remain processable. This seems particularly adapted to allow moderate to high PHU content in the network while still remaining processable. This study at 25 °C was particularly appealing to ensure the suitability of the formulations for future impregnation processes. Notably, over an hour at 25 °C did not lead to any gelation of the hybrid formulations. Interestingly, developing pre-preg composites that are more stable at room temperature than pure epoxy pre-preg could offer significant advantages [505], especially given the dynamic behavior of such systems [506].

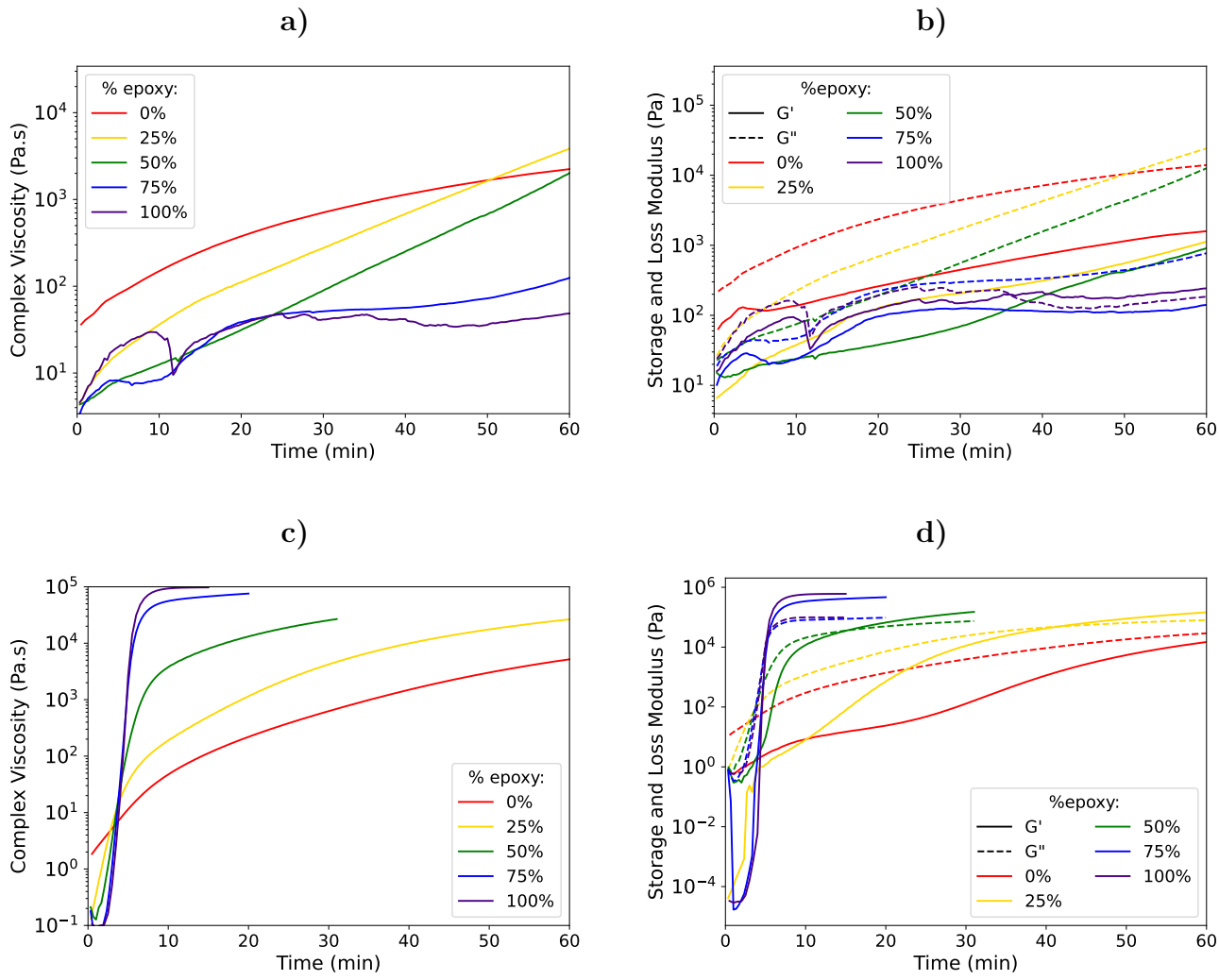

Figure V-6 – Curing rheological behavior. a) Viscosity Evolution, and b) Modulus plot at 25 °C, c) Viscosity Evolution, and d) Modulus plot at 80 °C.

Finally, the curing behavior was studied at 80 °C. Similar trends to the DSC are observed, with a high curing rate for the hybrid. At 80 °C, the gel time was significantly reduced for the hybrid formulation compared to that of the pure PHU, requiring only 15 min instead of 83 min. The gel point was consistent with the DSC results where conversion higher than 60% is obtained after 10 min. This confirms that time ranging between 15 and 30 min should be enough to reach a sufficient level of curing for such hybrid systems and be further post-cured at higher temperatures, significantly reducing processing time and equipment use.

V.2.3 Mechanical behavior of synergetic EP-PHU hybrids as a function of the hybridization level.

In continuous fiber-reinforced polymers, the reinforcement primarily sustains the load [507]. Yet, the matrix is critical in transferring it to the fibers. Additionally, the matrix protects the fibers and binds them together. Hence, it is essential to maintain high mechanical properties and good thermal stability in the matrix. The influence of the hybridization strategy on the pure polymer properties was therefore assessed.

First, the thermo-mechanical properties of the thermosets were assessed by DMA in tensile mode at different epoxy contents (Fig. V-7c). Surprisingly, the hybrid materials' storage modulus was superior to pure epoxy or pure PHU thermosets. We demonstrated in chapter 3 the superior thermo-mechanical properties of PHU over a similar epoxy counterpart [489]. This was attributed to stronger H-bonds in PHU. In epoxides, the high crosslinking density plays a significant part in the mechanical properties in addition to the macromolecular backbone [463]. However, these permanent and strong covalent interactions lead to high stiffness and thermal stability but lower ductility. Herein, we do not observe any increase in the crosslinking density compared to PHU due to the use of primary amines in the network. Yet, the PHU brings the aforementioned strong and ductile H-bonding ability. Importantly, the glass transitions are significantly increased compared to the pristine PHU, reaching values similar to the epoxy. This confirms the positive effect of the hybridization strategy through the engineering of the macromolecular structures, bringing together different types of bonds (covalent and H-bonds) that interact jointly. As such, an increase in thermal stability and stiffness can be achieved while boosting toughness.

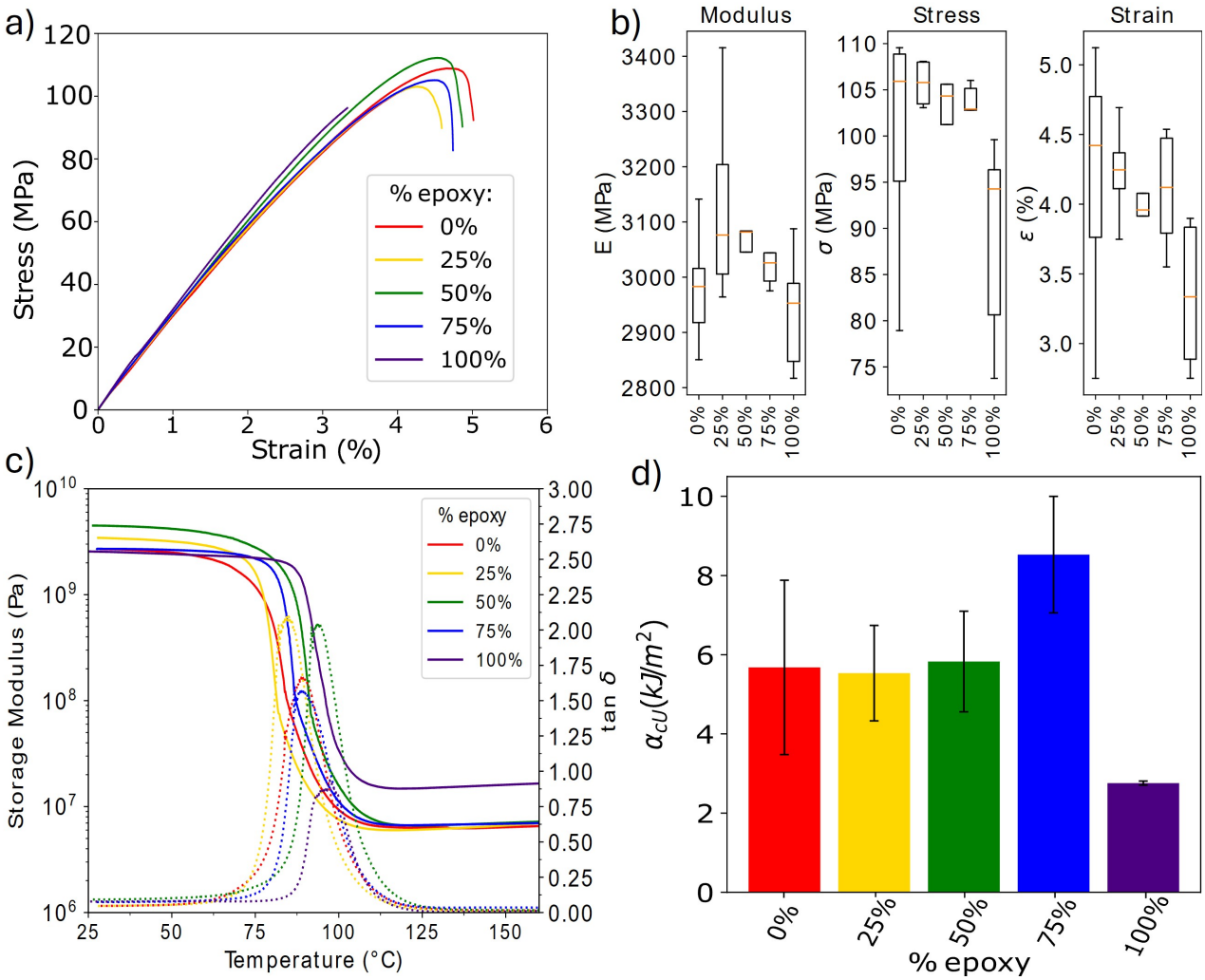

Figure V-7 – (thermo)Mechanical properties of the hybrid epoxy-PHU. a) Representative tensile strain-stress curves, b) boxplot of the tensile properties, c) DMA, and d) Charpy's impact results.

The quasi-static monotonic mechanical properties were assessed by tensile tests (Fig. V-7a-b), and extracted properties are summarized in Table V-2. As already observed by DMA, a slight increase in Young's modulus was unveiled, highlighting the positive effect of this hybrid material on tuning the processability without decreasing the final properties. In polymers, an increase in modulus or glass transition temperature often results in decreased ductility, which can negatively impact the durability of future structures. In the proposed hybridization strategy, as already discussed, the resulting material incorporates "weak" H-bonds. This leads to equivalent or superior strain at break but also higher ultimate stress as the material possesses a better ability to absorb mechanical deformation with a higher stiffness [146]. This combined increase in the strain and stress is related to a higher work in the material, i.e. the toughness is increased. Therefore, the impact toughness of the material can be expected to increase in the hybrid materials. For this reason, the impact toughness was evaluated

through unnotched Charpy impact tests Fig. V-7d. The results confirmed the observed trends with a positive hybridization effect on the toughness with similar toughness between pure PHU and hybrid and an increase close to 100% compared to the pure EP, in agreement with previous findings [487]. This is highly interesting as one of the issues about composite materials is their poor impact damage behavior, and is mainly driven by the matrix [274, 508]. In that sense, increasing the toughness of such structural materials through this simple hybridization process seems industrially relevant and greener than other processes, such as the addition of impact modifiers and toughgeners that usually leads to a decrease of other key properties [509].

However, considering the slight variations in all mechanical properties, an ANOVA was conducted to assess their significance (see Fig. V-A8), which showed no significant statistical differences. Even if partly surprising, it remains a major result. Indeed, the primary objective was to substantially improve the processability and curing protocol, thus allowing the implementation of PHU chemistry on a large scale. As the tensile results remain similar to pure EP or PHU, it discloses minor, although positive, modifications that could simplify future implementation in industries comparable to marketed EP systems. In impact toughness, only the hybrid containing 75% of EP was considered statistically different with an impact toughness of 8.5 kJ/mol, much higher than the pure EP (2.8 kJ/mol), other hybrids ranging in between EP and PHU.

Based on all the above, hybridization can be considered a straightforward approach to exploit PHU chemistry in conventional epoxy-based materials. The overall results confirm that if pure PHUs do not fulfill the requirements of the composite industry, particularly process-wise, the hybridization strategy offers a simple yet efficient approach to overcome their limitations and can be directly implemented without compromising existing processes. It is particularly interesting that this approach not only maintains but also slightly enhances the material properties. The resulting PHU hybrid formulations align with the RTM process requirements, showcasing promising properties for composite applications.

Table V-2 – Physical properties (mean ± deviation) of hybrid EP-PHU formulations

		DMA				Tensile			Impact
% Epoxy	ρ	T_α	$E'_{25°C}$	$E'_{rubbery}$	ν'_e	E	σ	ϵ	α_{CU}
	g/cm^3	°C	MPa	MPa	mol/m^3	GPa	MPa	%	kJ/m^2
0	1.29 ± 0.01	78	3129	6.6	657	2.9 ± 0.1	100.3 ± 11.3	4.19 ± 0.81	5.7 ± 2.2 ab
25	1.27 ± 0.01	85	3441	6.1	613	3.1 ± 0.2	105.7 ± 2.4	4.23 ± 0.33	5.5 ± 1.2 ab
50	1.26 ± 0.01	94	4491	6.9	664	3.1 ± 0.1	102.9 ± 6.8	3.99 ± 0.32	5.8 ± 1.3 ab
75	1.25 ± 0.01	87	2704	6.8	663	3.0 ± 0.1	102.6 ± 3.5	4.09 ± 0.38	8.5 ± 1.5 b
100	1.25 ± 0.01	97	2560	15.9	1519	2.9 ± 0.1	88.8 ± 9.9	3.34 ± 0.47	2.8 ± 0.1 a
p-value	-	-	-	-	-	0.204	0.063	0.109	0.0003
significant	-	-	-	-	-	No	No	No	Yes

V.2.4 RTM manufacturing of flax-EP-PHU composites

Given the satisfying results obtained from the synergetic hybrid EP-PHU approach, with low viscosity, fast curing, and satisfying thermo-mechanical properties, RTM-made composite samples were manufactured (Fig. V-8). Composites with an engineered lay-up of 11 plies were manufactured by RTM using unidirectional woven flax as the reinforcement. 25, 50, 75, and 100% of epoxy content were used as formulations. A curing protocol for RTM was developed consisting of the injection of the reaction mixture (co-monomers and hardener) for 10 min at room temperature in a 60 °C preheated mold, followed by a 30 min curing at 80 °C. An out-of-mold post-curing step was finally conducted at 160 °C for 1 h to ensure complete curing.

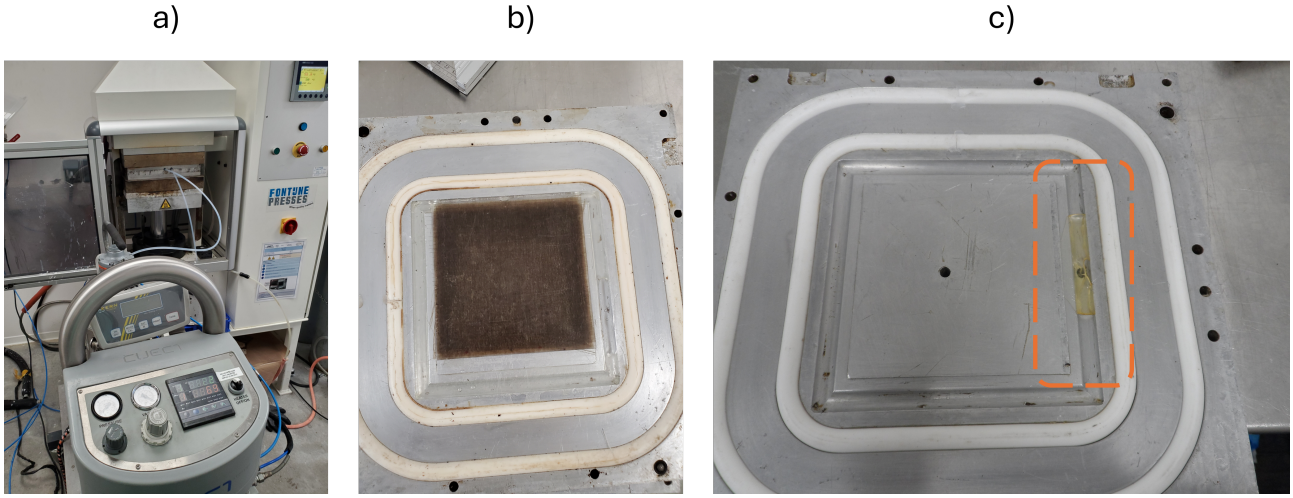

Figure V-8 – Resin Transfer Molding of Composites. a) RTM apparatus, b) Mold used with freshly made composite plate, and c) failed attempt to use 100% PHU as matrices for RTM injection.

The obtained composites were satisfyingly impregnated, with no apparent surface defect or fiber misorientation (Fig. V-9a-d). The impregnation quality was evaluated by SEM. The "between-plies" impregnation (Fig. V-9e-h) and interpenetration of the matrix within the yarns (Fig. V-9i-l) were investigated. The 25%EP demonstrated significantly high viscosity, which hindered complete impregnation under the current injection parameters, as indicated by the presence of a fully non-wetted area (Fig. V-9a).

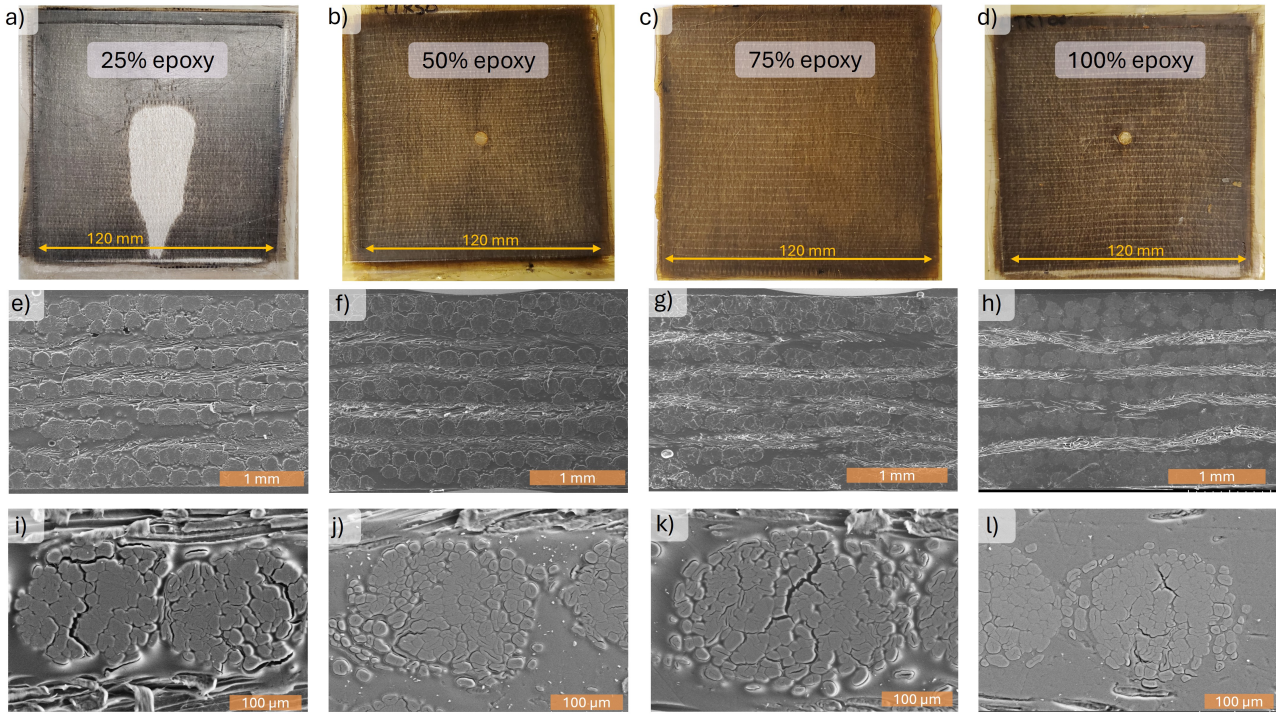

Figure V-9 – Resin Transfer Molding of flax reinforced hybrid EP-PHU composites. a-d) Photographs of the composite plates, e-h) SEM micrographs of crosscut sections with x30 magnifications, and i-l) SEM micrographs of crosscut sections on tows with x300 magnifications for 25,50,75 and 100% of epoxy (from left to right).

With 50% or higher contents of EP, the impregnation at the laminate scale is of high quality, homogeneuos, and defect-free. All plies are perfectly impregnated and bonded together. SEM analyses reveal high-quality impregnations for the 50%-100% EP formulations. Some issues with the fluidity and the tight twist of the fiber roving can lead to some heterogeneities in the yarn's impregnation, although they remain infrequent and do not affect high standards for flax reinforcement [499]. This could be improved in the future through simple adjustments of the formulation, components, and parameters optimization. Lower twisting of the flax yarns could also facilitate their internal wetting, further improving mechanical properties [510]. For all systems, high fiber volume fractions (V_f) ranging between 57% and 62% were obtained (Table V-3), in the highest range of reported achievable V_f [160].

Notably, while high V_f has been reported to lead to high porosity content (V_p) [511], extremely low Vp were obtained, with 1% for the 25% EP system and below 0.5% for the other ones, consistent with SEM images, and showing the high suitability and consistency of hybrid EP-PHU formulations for RTM manufacturing process.

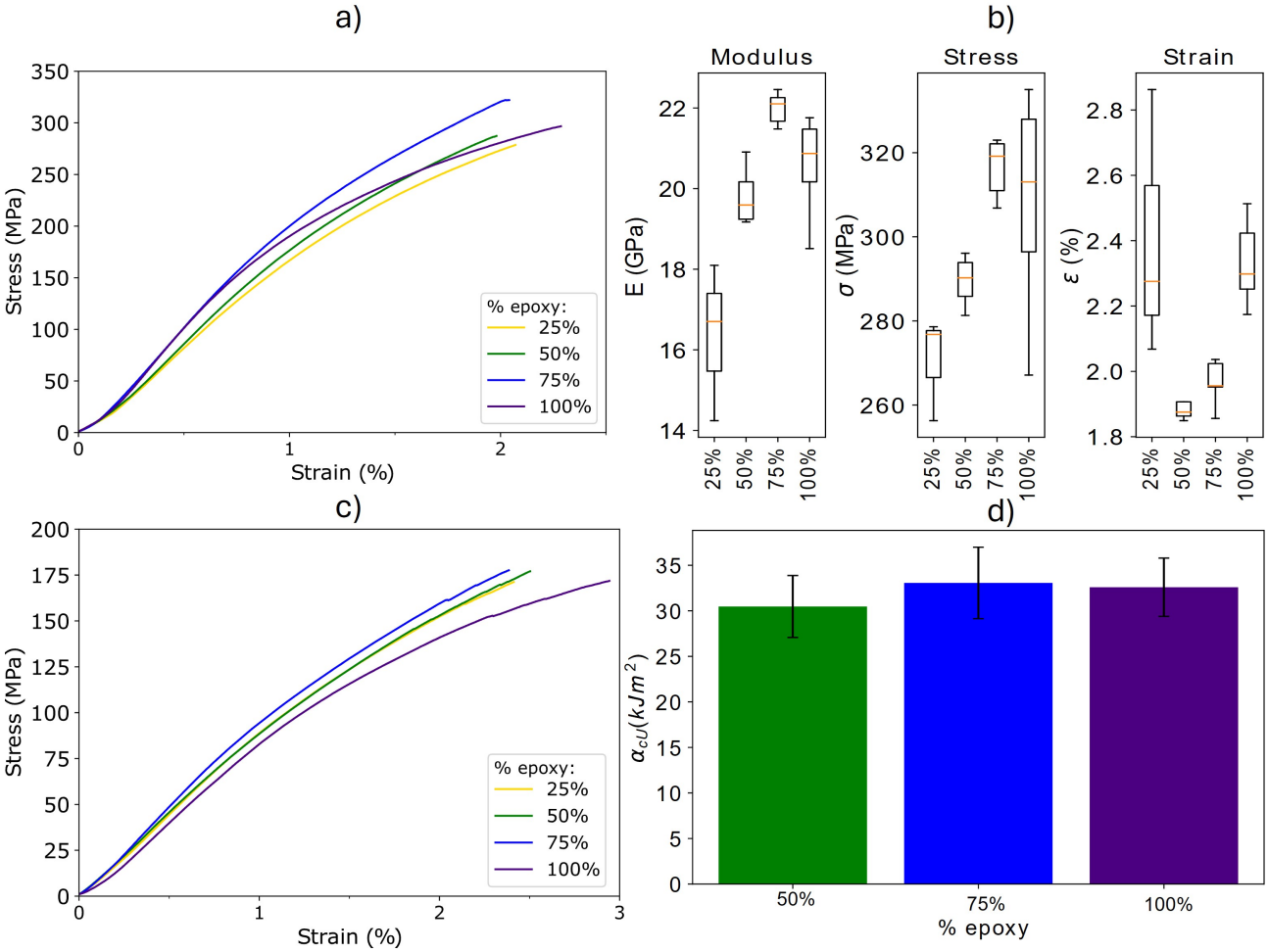

Figure V-10 – Mechanical properties of the RTM-manufactured flax/epoxy-PHU. a) Representative three-point bending curves in the principal direction, b) boxplot of the bending properties in the main composite direction, c) Representative three-point bending curves in the transverse direction, and d) Charpy impact results in the principal direction. (25% plate did not provide enough sample to be tested).

The three-point bending mechanical behavior in the two main orthotropic directions was evaluated. Representative strain-stress curves are presented in Fig. V-10a-c. The lower modulus was obtained for the 25%EP composite, with 16.3 GPa due to the lower impregnation quality obtained. ANOVA was also performed (Fig. V-A11 and V-A12). 50% EP was considered statistically similar to the reference EP-based composite with 20.1 and 19.0 GPa, respectively. The formulation containing 75% EP was considered statistically improved with 22.0 GPa. The admissible strain was not affected by the different

matrices. The slightly lower strain observed for 50% and 75% EP could be explained through strong interactions at the fiber-matrix interface, limiting pull-out and debonding and privileging fiber breaking. As the internal yarn impregnation is not complete, the load transfer to all fibers is limited, thus decreasing slightly the admissible stress. The ultimate stress is similar between the reference EP and the PHU-75%EP hybrid with 325 and 316 MPa, respectively. As expected, 25% of EP decreased the stress with 270 MPa due to the lower impregnation quality. As strong interactions between PHUs and cellulosic fibers were previously reported [489], the difference between the different formulations appears to be mainly process-related due to the observed lack of internal yarns impregnation, limiting efficient load transfer between the fibers. Although the interfacial adhesion between flax and the EP-PHU is expected to improve, the complexity of the reinforcement used here could lead to a counterproductive effect, potentially diminishing the anticipated benefits of the PHU chemistry. This can also corroborate the observed trends in the transverse directions. High modulus between 9.0 and 9.6 GPa are obtained, without any statistical significance, despite the differences in impregnation quality. Again, the stress at break was slightly diminished when a low epoxy content was used. To effectively compare the results within this study and with other works, the Classical Laminate Theory (CLT), homogenized with Chami's model, was employed to compute the global laminate stiffness matrix and determine the theoretical modulus, as reported in Table V-3. The method can be found in the method chapter (Chapter 8, section 9.1.1). A good agreement between theoretical and experimental results was obtained, with a ratio between 0.8 for the 25% EP hybrid and superior to 0.9 for the others, confirming the quality of the resulting composite. The results are in the highest range of the literature [512, 513]. Toughness was also assessed in the main composite direction. High toughness was obtained for all formulations, superior to 30 kJ/m^2.

In general, high mechanical properties are obtained. There are no statistical differences that could be detrimental to the reliability of hybrid EP-PHU as an alternative to existing market matrices. Additionally, further improvements can be anticipated, optimizing process parameters and formulations during industrialization.

Table V-3 – Properties (mean ± standard deviation) of RTM-made flax composites in the main lay-up and transverse directions.

					Bending			CLT		Charpy
%EP	LayUp	ρ	V_f	V_v	E	σ	ϵ	E_{CLT}	E/E_{CLT}	α_{CU}
		g/cm^3	%	%	GPa	MPa	%	GPa		kJ/m^2
25	$[0/(0/90)_2/\bar{0}]_S$	1.36 ± 0.01	57.7 ± 0.6	1 ± 0.6	16.3 ± 1.6 b	270.5 ± 10.1 b	2.40 ± 0.34	20.3	0.80	-
50	$[0/(0/90)_2/\bar{0}]_S$	1.37 ± 0.01	57.9 ± 0.4	0.2 ± 0.8	19.0 ± 0.3 a	294.8 ± 10.2 b	1.99 ± 0.12	21.1	0.90	30.5 ± 3.4
75	$[0/(0/90)_2/\bar{0}]_S$	1.37 ± 0.02	62.4 ± 0.9	0.4 ± 1.1	22.0 ± 0.4 c	316.3 ± 6.4 a	1.96 ± 0.06	22.1	0.99	33.1 ± 3.9
100	$[0/(0/90)_2/\bar{0}]_S$	1.36 ± 0.01	58.8 ± 0.4	0 ± 0.1	20.1 ± 0.4 a	325.5 ± 15.1 a	2.26 ± 0.19	21.1	0.95	32.6 ± 3.2
p value	-	-	-	-	0.0003	0.001	0.356	-	-	0.550
significant	-	-	-	-	Yes	Yes	No	-	-	No
25	$[90/(90/0)_2/\bar{90}]_S$	1.36 ± 0.01	57.7 ± 0.6	1 ± 0.6	9.0 ± 0.2	167.1±6.9 b	2.4±0.01	9.9	0.91	-
50	$[90/(90/0)_2/\bar{90}]_S$	1.37 ± 0.01	57.9 ± 0.4	0.2 ± 0.8	9.0 ± 0.5	166.1±10.9 b	2.35±0.18	9.0	0.84	-
75	$[90/(90/0)_2/\bar{90}]_S$	1.37 ± 0.02	62.4 ± 0.9	0.4 ± 1.1	9.4 ± 0.6	172.3±5.6 a	2.38±0.19	9.4	0.87	-
100	$[90/(90/0)_2/\bar{90}]_S$	1.36 ± 0.01	58.8 ± 0.4	0 ± 0.1	9.6 ± 0.1	190.1±3.5 a	2.47±0.05	9.3	0.91	-
p-value	-	-	-	-	0.240	0.007	0.736	-	-	-
significant	-	-	-	-	No	Yes	No	-	-	-

V.2.5 Perspectives towards the reshaping and recycling of natural fiber composites

The end-of-life of FRPs remains a well-known and yet ongoing issue. Despite several sustainability advantages of NFC, their EoL remains problematic. The current EoL management for NFC consists of incineration, landfill, or, in the best cases, grinding them down for use as fillers in low-quality materials. Interestingly, the exploration of PHU chemistry presents opportunities in the realm. The hybrid epoxy-PHU was found to be reprocessable thanks to the dynamicity of the polyhydroxyurethane networks. Initially, PHU stood out as a poorly dynamic system, requiring harsh conditions for dynamicity [462]. This leads to the partial degradation of the natural fibers [489] and low economic or environmental interest.

Interestingly, the hybridization of PHU with EP led to a network containing both dynamic hydroxyurethane moieties and easily accessible internally catalyzed hydroxyl moieties. As such, a much faster and more efficient dynamicity materializes, preserving the flax fiber integrity upon reshaping. This is not accessible through conventional epoxy. As shown in Fig. V-11, an RTM-manufactured sample was heated to 180 °C and reshaped in a press using copper bars to control pressure points. From a small, flat sample, a wave-shaped composite was obtained. The fiber orientation and material integrity were kept, and no debonding or delamination was generated, contrary to the epoxy-based

reference (Fig. V-A13).

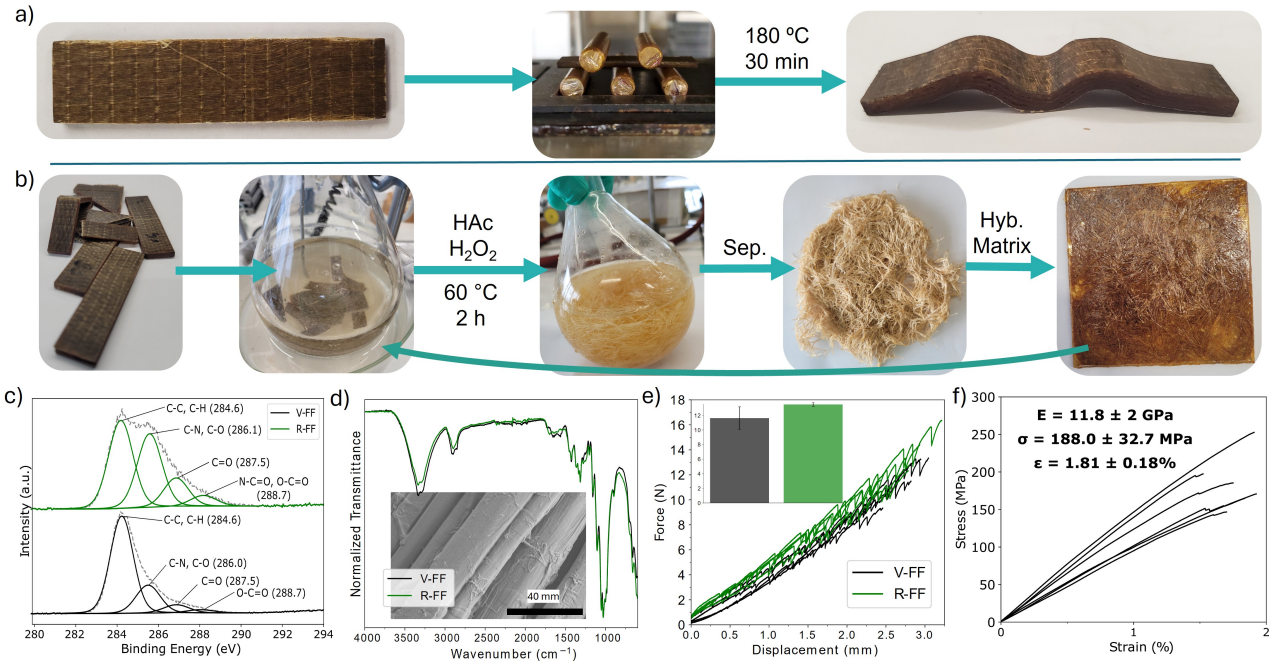

Figure V-11 – Exploiting the dynamic behavior of the hybrid formulations for advanced opportunities and recycling. a) Thermo-mechanical reshaping of the flax composite, b) chemical recycling and flax yarns recovery and reuse, c) XPS, d) FTIR (inset SEM of R-FF), e) tensile analyses of the virgin and recovered flax yarns, and f) bending of the manufactured composite using recovered flax yarns.

Chemical degradation of the polymer matrix under mild conditions can be an ideal solution to retrieve fibers or yarns and repurpose them in new applications. However, the severe conditions and catalysts needed to depolymerize epoxy thermosets are not suitable for natural fibers [295]. Indeed, the organic nature of such fibers makes them sensitive to strong chemical reagents and temperature. In the case of our synergetic hybrid approach, oxidative acidolysis was employed as a gentler method, avoiding the use of harsh or expensive reagents during the chemical degradation process (Fig. V-11b). A solution of acetic acid and hydrogen peroxide (80:20) was prepared, and the composite samples were broken into small pieces for immersion. When heating to 60 °C, the acetic acid - hydrogen peroxide solution generates peracetic acid, a selective oxidant that effectively cleaves amine and aryl-ether linkages [514]. This process could be industrially relevant, as continuously feeding the oxidative solution with hydrogen peroxide could enable the degradation of the matrix while regenerating the acetic acid in the process.

Here, the network was destroyed, and the yarns could be recovered in just 2 h. Interestingly, while peracetic acid has been reported to cleave pure epoxy [293], the reaction conditions typically require

longer times (4-8 h) and higher temperatures than here. Two mechanisms contribute to depolymerizing the networks. First, the excess in acetic acid cause the network to swell [515], leading to its partial physical breakdown. As the crosslinking density of hybrid EP-PHU is lower than that of neat EP, which relies more on hydrogen bonds, the swelling is faster and more noticeable. Additionally, the flax fibers can significantly swell in aqueous media, initiating cracks in the matrix [144], and improving the first physical mechanism. Then, hydroxyl and acyloxy radicals can more easily cleave the C-N bonds and Ar-O-C bonds, leading to the destruction and solubilization of the thermoset.

After filtration and washing using distilled water, the flax yarns were dried. 7.3 g of fibers were recovered, representing 58.8% of the total composite mass, consistent with the flax fiber mass content (around 60-62%), indicating minor losses. SEM images (Fig. V-A15) showcased no apparent presence of polymer residues and the recovery of pure flax yarns. XPS was employed to characterize the fibers' surface (Fig. V-11c). The analysis reveals a slight modification of the surface composition with a lower carbon content (67%) compared to virgin fibers (V-FF) (81%) and a higher content of oxygen (29 vs 17%). One must keep in mind that the protocol is also used in the delignification process of wood fibers [516] to obtain pure cellulose. Therefore, if some partial oxidation may occur, the main reason for this observed surface composition is the removal of lignin (carbon-rich), in favor of a more oxygen-rich cellulose. This is further confirmed by the significant augmentation of the C-O relative atomic concentration (Fig. V-A16, Table V-A1-V-A2), which is indicative of cellulose. Even if a partial oxidation of the fiber surface is anticipated with the slight augmentation of C=0 relative, the effect is limited. Moreover, XPS represents the surface composition over a few nanometers (typically 5-10 nm). Energy-dispersive X-ray spectroscopy (EDX) was also used to analyze the surface through depth (Fig. V-A17, Table V-A3), typically, about 10 μm. In that case, almost no change in the composition was observed, highlighting that the oxidation remains significantly contained at the very surface. FTIR (Fig. V-11d) and TGA analyses (Fig. V-A14) also confirmed no significant changes in the chemical structure of fibers, indicating the complete removal of the matrix. The recovered flax yarns were subjected to tensile testing to assess the retention of their mechanical properties and the results were compared to those of the virgin ones used in the reinforcement (Fig. V-11e). Interestingly, no diminution of the tensile strength or strain was unveiled. Furthermore, R-FF showcased slightly superior mechanical properties with a 16% increase in strength (13.49 N vs 11.62 N) and 2% in displacement (Fig. V-A18), which corroborate with higher relative content of cellulose in the fiber. Although these differences are not statistically significant (Fig. V-A18), this is the first time that the chemical recovery of flax reinforcement is obtained without any major degradation, allowing their future exploration for

second-life uses.

Finally, a composite was manufactured out of the reclaimed flax fibers by thermo-compression, with a fiber volume fraction of about 45%. The fibers were not realigned and were used as non-woven reinforcement. The direct comparison with the virgin materials is, therefore, not relevant. Interestingly, high mechanical properties (Fig. V-11e) were obtained with a bending modulus around 12 GPa, a stress at break of 188 MPa, and a strain of 1.81%, representing promising results in semi-structural applications. The materials remain still competitive with other NFC despite the oxidative depolymerization process [141]. For re-use perspectives, various machines for fiber realignment [428] have been developed over the last decades, enabling the enhancement of the properties of these fibers to give a second life for these realigned recovered flax fibers again in structural applications.

V.3 Conclusions

Although PHUs have limited prospects in the realm of industrial structural composites despite their promising properties and beneficial feedstocks, we demonstrate that their limitations could be overcome through a simple, scalable, and straightforward hybridization strategy. Formulating EP-PHU networks leads to on-demand modular systems with tunable properties as it opens the door to the library of epoxy monomers, cyclic carbonates, and amines. Viscosity can be tuned to meet process requirements. The formulations cure faster thanks to a mutual catalyzing effect between epoxy and hydroxyurethane, initiated by the early aminolysis of cyclic carbonates. The properties of resulting networks are maintained or even improved as new H-bonds are formed in the network, resulting in an improvement of the static mechanical properties and impact toughness. Finally, the hybrid formulations were suitable for RTM-processed flax composites with complex stacking sequences. The NFC obtained exhibited high mechanical properties comparable to those of benchmark epoxy-based composites. The dynamicity of these hydroxyurethane moieties is promoted by the amino-alcohols, allowing the reshaping of the cured flax composite. Finally, we demonstrated that mild oxidative depolymerization can be applied to natural fiber composites for the extraction of natural fibers. The hybrid matrix can easily be cleaved under mild conditions to retrieve high-quality flax fibers that can be repurposed in new applications. This opens the door to the pertinent implementation of these materials in a circular economy. This approach represents a reliable and consistent way to integrate CO_2-derived polyhydroxyurethane chemistry in the composite market, particularly in transportation, offering new opportunities and solutions in a large and growing market where the lack of satisfying solutions hampers sustainability goals.

Chapter VI

Environmental impact assessment of polyhydroxyurethanes and their derivatives composites

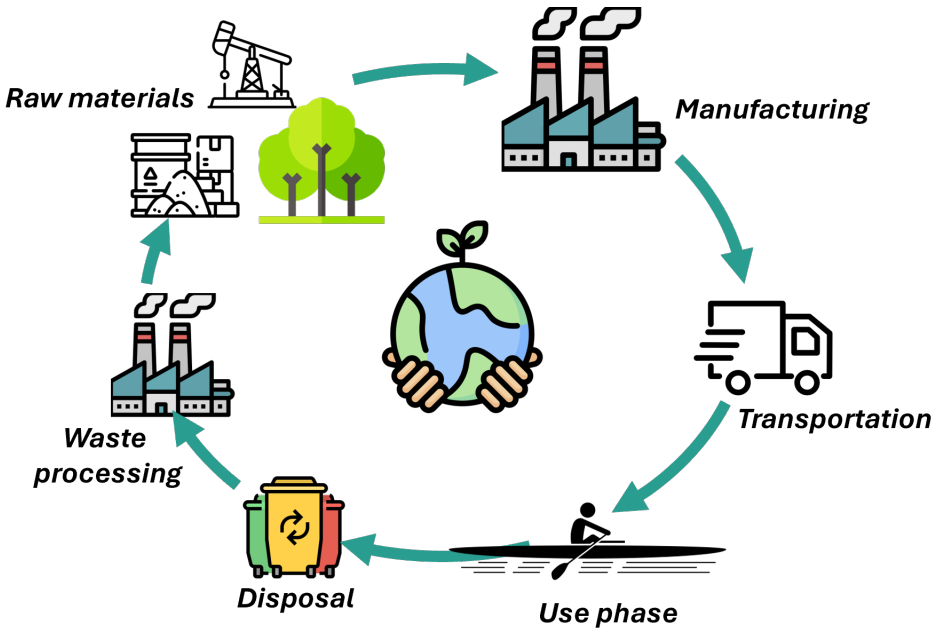

Adapted from: G. Seychal, P. Bron, O. Talon, N. Aranburu, and J.M. Raquez, Can polyhydroxyurethane Covalent Adaptable Networks, increase the sustainability of composite, a life cycle assessment, *Submitted to ACS Sustainable Chemistry & Engineering on the 11/02/2025.*
External contributions:*P.B. modeled TMPTGE, TMPTC from solvent and mXDA.*

Contents

VI.1 Introduction

Human activities are leading to dramatic changes in the Earth's climate and equilibrium [56]. The need to drastically reduce the footprint of human presence imposes to develop greener materials [56]. While fiber-reinforced polymers (FRP) offer numerous benefits to improve the performances of structures and reduce their weight, promoting energy savings during the use phase, the current FRPs cannot be deemed as sustainable [59]. Glass and carbon fibers possess high embodied energy and account for significant global warming potential (GWP) during their production [67], while (thermoset) matrices severely limit the possible end-of-life (EoL) scenarios [517].

Over the last decades, numerous new polymers and chemistries have emerged, ushering new opportunities in materials, particularly in composites [518]. By using renewable feedstocks such as natural fibers (NF) for reinforcements or bio-alternatives to petrochemicals for the matrices, significant benefits have been shown in laboratories and occasionally scaled to industrial applications. [519]. Moreover, these NFs can be combined with biobased thermoplastics to obtain potential recycling [162, 165], and eventual biodegradability [415], but the resulting NF composites usually do not show satisfying properties. By contrast, biobased thermosets, such as epoxides (EP) from plant derivatives, provide much higher stability and mechanical properties but are inherently not recyclable [141]. In this regard, the increasing interest in Covalent Adaptable Networks (CAN) that reassemble the high properties of thermosets with advanced recyclability options of thermoplastics opens new potential for the management of decommissioned composite structures [26]. Developing recycling strategies such as pyrolysis or solvolysis also enables foreseeing recirculation opportunities for the high-added-value fibers, particularly carbon fibers [424]. Natural fibers are, in most cases, significantly beneficial in view of replacement to glass fibers [76]. Pyrolysis and solvolysis were demonstrated to lead to fewer emissions than virgin carbon fiber production and, appear as viable strategies to mitigate the environmental burden of carbon fiber reinforced polymer (CFRP) structures. However, since natural fibers are more sensitive to high temperatures, pyrolysis or solvolysis cannot be applied to natural fibers.

In the previous chapters, we have demonstrated that polyhydroxyurethanes (PHU) could provide a fortunate platform for a new generation of FRPs. The hydroxyurethane moieties in the backbone enable high adhesion at the fiber/matrix interface as well as an adaptable behavior that could be reshaped and welded afterward. PHUs are shown valuable alternatives to EP resins. The literature generally considers the production of cyclic carbonates, key building blocks for PHU to be green as they are easily produced from the cycloaddition of CO_2 in EP monomers. This can even be performed quantitatively in solvent-free conditions using supercritical CO_2. However, this assumed sustainability has never been

assessed quantitatively. The additional steps to transform EP into cyclic carbonates require energy to bring CO_2 to its supercritical state and should be considered. Additionally, the polymerization protocol to obtain PHU requires a higher temperature and a longer time than epoxy. As PHUs have not been shown to be industrially relevant for the composite manufacturing industry, a hybridization strategy has been developed. This hybridization, consisting of a homogeneous PHU/EP copolymer, allowed us to reduce the viscosity to a range suitable for resin transfer molding and significantly simplified the curing protocol. Moreover, the dynamicity of the networks was enhanced, allowing faster and more efficient thermo-mechanical reshaping. Finally, we demonstrated that the networks were cleavable under mild conditions and that flax fibers and carbon fibers could be retrieved with negligible degradation.

However, all those strategies for composites and their subsequent environmental footprint largely depend on the choice of raw materials, manufacturing steps, service life, and finally, the management and valorization of decommissioned parts. Therefore, the question arising from these recent developments concerns the actual environmental footprints of PHUs and hybrids compared to epoxy in composite applications for both natural and carbon fibers. Furthermore, carbon fibers and natural fibers possess significantly different applications and environmental burdens. Therefore, one must ask whether strategies to lower the environmental footprint of one composite can be extrapolated to another. An environmental impact assessment (EIA) is herein performed with the Life Cycle Assessment (LCA) methodology to provide a simplified audit of the production and recycling of PHU-based CANs and composites. The work also aims to discuss future needs and efforts in the field of sustainable CAN composites to reduce environmental impacts (EI).

VI.2 Methods and scopes

VI.2.1 Objectives and scope definition

The main aim of the study is to evaluate the EI of sustainable structural composites that exploit CAN networks in order to highlight the potential advantages of emerging hybrid EP/PHU-based composites over EP composites. It also evaluates the synthesis steps for producing the polymer building blocks and the curing protocol for neat resins and composites. A second aim is to discuss various EoL scenarios of flax and carbon fiber composites opened by the chemistry switch and their relevance. Finally, this work aims to identify the production steps that are the most harmful to the environment and suggest ways to optimize production. Notably, the work focuses on the matrices, i.e., comparing EP resins

with PHU/EP hybrid resins and not the fibers. Therefore, carbon and flax fibers are modeled to discriminate different strategies and benefits. However, the comparison between carbon and flax fiber composites is out of the scope of this study. Moreover, the modeling of carbon fiber aimed to be representative of the order of magnitude and should not be taken for comparing carbon fiber composite EI outside of this work as it might not fully represent all impacts [67].

VI.2.2 System boundaries

The EIA was performed at different stages of the composites value chain to better understand the influence of chemistry and design choices. The first part is focused on understanding the environmental effect of a simple drop-in change from epoxy to PHU or hybrid EP-PHU and the major contributors to each material. As such, a cradle-to-gate approach was chosen. Secondly, the full life cycle (excluding the use phase) was modeled through a cradle-to-grave approach on the hybrid EP-PHU-based composite to discuss the impacts of EoL managements.

Our previous chapters have demonstrated that hybrid EP/PHU leads to a slight property improvement compared to EP. To simplify the modeling, the properties of the resins and composites were hypothesized as being equal. Therefore, there is no change in the design of the functional units (taken as 1 kg composite plates of similar stiffness). The use phase is assumed to be identical and out of the scope of our work. Equally, transportation and specific manufacturing plants are not considered. To compare the recycling process, which leads to long (>5 cm) non-oriented fibers, a quality factor of 0.7 was used, i.e., 1.0 kg of the recycled fiber composite performs like 0.7 kg virgin fiber composite. Moreover, the fibers were directly used from production as unidirectional reinforcement, so other production steps, such as weaving or sizing, are neglected.

Equally, the model represents the current development stage, i.e., at lab scale. The results might significantly differ in larger-scale facilities. Since the technology has been developed in Europe, data were chosen to fit the European market and might vary in other localizations. The representative steps of the EIA are shown in Fig. VI-1. The sequestrated carbon in flax and cyclic carbonate was not considered.

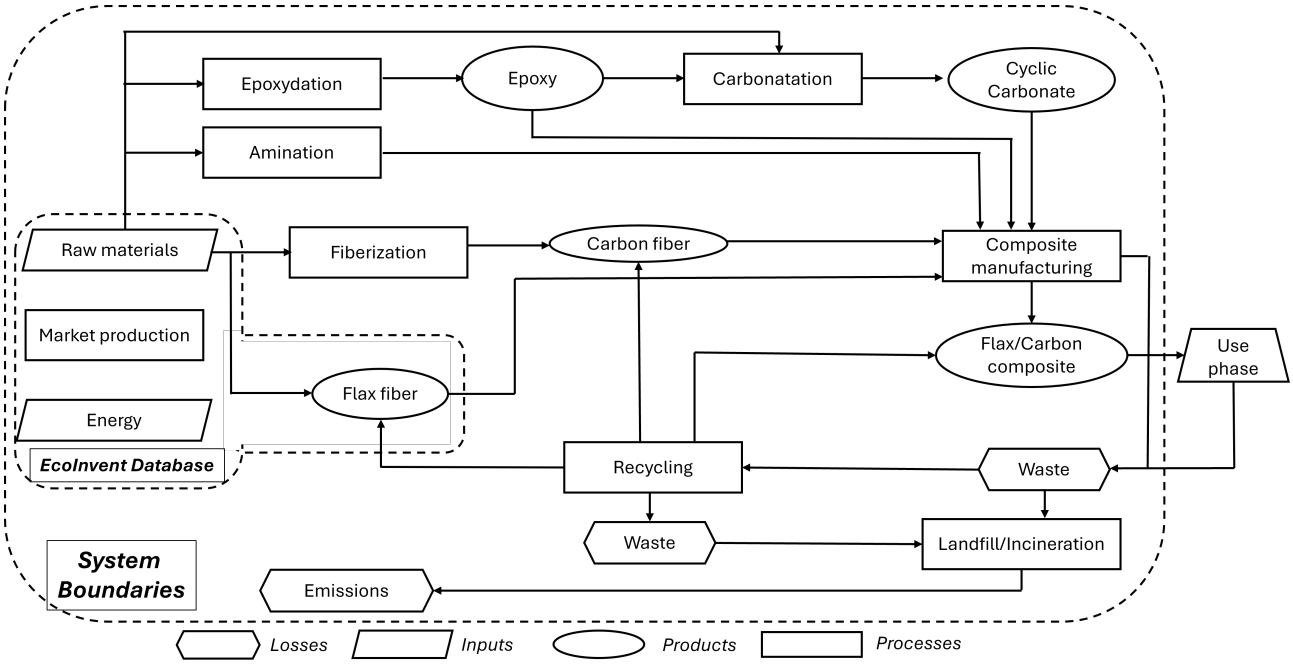

Figure VI-1 – Boundaries of the studied system and schematic representation of the overall processes and life cycle.

VI.2.3 Scenarios

The scenarios consist of three main phases. The first phase is the raw material production phase, which encompasses all the raw materials that are used in the composite and their preparation. The second phase is the composite manufacturing phase, which involves the energy consumed during the production process as well as any energy losses incurred. The final phase is the disposal phase, which includes the energy and materials required for recycling or the waste treatment of the composite. Carbon and flax fibers are studied separately. For the two first phases, a preliminary cradle-to-gate analysis is performed to compare the EIA of PHU, EP, and hybrids and the impact of the production steps. The carbonatation of epoxy is considered. Neat resins are also compared. For composites, flax-reinforced polymers are evaluated with EP, PHU, and hybrid EP-PHU matrices. Only EP and EP-PHU are deemed for carbon fibers.

To investigate the different EoL strategies and the scenarios as a whole, a cradle-to-grave LCA is performed on the hybrid EP/PHU with flax and carbon fibers. The landfill of EP-based composites is taken as a reference scenario. Four different EoL scenarios were considered:

- Landfill: For each case (flax or carbon fibers), two virgin composite materials are considered simultaneously, one of 1 kg and one of 0.7 kg. Decommissioned materials are considered to be landfilled as inert waste in the European market.

- Incineration (flax composite only): Similarly, two virgin composite materials are considered simultaneously. Decommissioned materials are considered to be incinerated with energy recovery in the European market.
- Thermo-mechanical: A virgin composite material (1 kg) for both fibers is considered and later transformed through a thermo-mechanical process into a new generation with a 0.7 quality factor. Finally, the second material is decommissioned into inert waste in the European market.
- Acidolysis: A virgin composite material (1kg) is considered. Oxidative depolymerization is employed to retrieve the fibers (flax or carbon fibers). The fibers are reused to produce a new composite with a 0.7 quality factor. The second generation is then treated in the inert waste European market.

VI.2.4 Analysis Method and environmental data

The LCA methodology is structured according to ISO standards (14040). The LCA study was performed using Simapro® 9.6 software. Ecoinvent 3.10 was used as a background database in the Cut-Off version as provided with Simapro. When unavailable in the Ecoinvent database, data were either collected from lab experiments (energy measurements, developed processes) or literature. Life Cycle Impacts were calculated with the Environmental Footprint 3.1 assessment method in the version provided by Simapro.

Background data specific to the European market were primarily selected when available (RER), otherwise, global market data (GLO) were used. Electric energy was chosen as the European mix market group. Data related to input materials were calculated at each step from the different protocols using the mass of raw materials to produce 1 kg of products. Energy-related data were directly measured using a wattmeter apparatus installed on the lab equipment with a 0.1 kWh resolution. The CO_2 credit stored through photosynthesis and the carbonatation process is not taken into account. The cut-off was chosen to zero the burden of recyclable materials (i.e. only the recycling treatment imparts the EI of subsequent uses). For analyses, all sixteen indicators listed in Table 1 were computed. However, to simplify the results and in light of the uncertainties to quantify such parameters from lab results, water use (WAT), human toxicity(HT-c & HT-NC), freshwater ecotoxicity(FWT) and land use (LU) are not graphically represented. All data are reported in the corresponding tables.

Table VI-1 – Abbreviations of EIA indicators

Acronym	Name	Unit
CC	Climate Change (GWP100)	kg CO_2 eq
ODP	Ozone Depletion	kg CFC11 eq
PM	Particulate Matter	disease inc.
IR	Ionizing Radiation	kBq U-235 eq
POF	Photochemical Oxidation	kg NMVOC eq
AC	Acidification	mol H+ eq
FE	Freshwater Eutrophication	kg P eq
ME	Marine Eutrophication	kg N eq
TE	Terrestrial Eutrophication	mol N eq
RES-f	Resources fossil	MJ
RES-m	Depletion of abiotic resources	kg Sb eq
WAT	Water Use	m3 depriv.
LU	Land Use	Pt
HT-nc	Human Toxicity non-carcinogenic	CTUh
HT-c	Human Toxicity carcinogenic	CTUh
FWT	Freshwater Ecotoxicity	CTUe

VI.3 Life cycle inventory

This section summarizes the input data exploited to model the scenarios. The inputs are summarized in the dedicated section of the chapter 8.

VI.3.1 Chemical and precursor synthesis

VI.3.1.1 Epoxy

Epoxies were modeled similarly to diglycidyl ether of bisphenol A (DGEBA), which is already available in the Ecoinvent database. Trimethylolpropane (TMP) is not present in the database and pentaerythritol was chosen as a proxy, both syntheses being closely related. Shortly, resorcinol, or trimethylolpropane, is reacted with epichlorohydrin (ECH). The reaction is commonly performed in a large excess of ECH. The excess is considered to be recycled (not modeled). Sodium hydroxide (2 eq/epoxy group) is used to close the epoxy ring. Benzyltriethylammonium chloride (TEBAC) catalyzes the reaction between TMP and ECH but is not required for resorcinol [520]. The energy requirements for the synthesis was taken identical to the one used in the Ecoinvent model for DGEBA. Resorcinol diglycidyl ether

(RDGE) has been modeled to be the epoxy, while trimethylolpropane triglycidyl ether (TMPTGE) is used as the precursor to cyclic carbonate.

VI.3.1.2 Cyclic carbonates

Cyclic carbonates are straightforwardly obtained from the cycloaddition of CO_2 within epoxy [237]. TMPTGE was used as the epoxy precursor to obtain trimethylolpropane tricarbonate (TMPTC). The typical synthesis is performed at the kg scale in a 2 L high-pressure stainless steel reactor. The epoxy is loaded with a catalyst, typically tetrabutyl ammonium iodide (here TEBAC is used in the model). CO_2 is then injected under pressure into the reactor while heating. The reactor is stabilized around 80 °C and 100 bar to reach CO_2 supercritical conditions. The reaction is typically performed between 15 and 24 h [521] with quantitative yields. No solvent is required nor purification steps.

VI.3.1.3 Amine

m-xylylene diamine (mXDA) was used as the hardener for all resins. The synthesis of amines is usually performed from the hydrogenation of nitriles [220] in the presence of a nickel catalyst. Nitriles are mainly produced from the SOHIO process. mXDA is produced from the ammoxidation of xylene, using ammonia and dioxygen to yield isophthalonitrile which is further hydrogenated to mXDA. The inputs were taken from the literature [374].

VI.3.1.4 Carbon fibers

Carbon fibers are a high source of discrepancies in literature, with several authors having reported drastically different results. The industrial secrecy around production also makes the accurate estimation difficult. Recently, Jacquet et al. [67] have proposed a justified and transparent inventory based on the Ecoinvent database. This inventory was selected as the reference. It includes acrylonitrile and vinyl acetate as the precursors to polyacrylonitrile (PAN) fibers, nitrogen, and steam to stabilize the production of fibers and electricity and heat required to carbonize the PAN fibers into carbon fibers. The results from their work highlight a global warming potential of 72 $kgCO_2eq$ and a cumulative energy of 1176 MJ per kg of carbon fibers, which is at the upper range of commonly estimated impacts for CF [522].

VI.3.2 Polymers and composite manufacturing

Detailed inputs are summarized in the dedicated LCI section of the chapter 8. All resins were cured in equimolar quantities of monomer and hardener. The EP resin comprises RDGE and mXDA. RDGE is an aromatic epoxy that is often considered an alternative to DGEBA [211, 520]. The PHU contains TMPTC and mXDA. The hybrid EP-PHU incorporates RDGE and TMPTC in a 50/50 mass ratio, cured with mXDA. Flax composites are modeled with a fiber weight fraction of 60% (around 50% fiber volume fraction), and a 70% mass fraction was used for CFRP composites (around 60% volume fraction). The curing is identical for neat resins and composites and is assumed to be performed in thermo-compression using a pressure of 4 bar. For the EP resin and the hybrid, the curing is performed for 30 min in the heating press at 80 °C followed by 1 h at 160 °C in an oven (see Chapter 5). The PHU was cured for 2 h at 80 °C, followed by 1 h at 100 °C and 1 h at 150 °C in an oven (see Chapter 3). The energy inputs were measured from our lab equipments. The energy inputs are considered to be the same for neat resins and composites and were measured to align with the requirements of the composite manufacturing. Therefore, energy inputs for the pure thermosets might be underestimated and should be taken with care. For composites, a 10% production waste was accounted.

VI.3.3 Recycling phase

Two recycling methods were considered: thermo-mechanical and chemical. The hybrid EP-PHU is a CAN. For the two methods, collecting, sorting, cleaning, and potential preliminary preparation steps are neglected.

Unlike EP thermosets, thermo-mechanical recycling can be considered to a certain extent. Two main strategies could be regarded: the first one includes the shredding of the composite and the compression into a low-grade filled polymer, similar to a short fiber reinforced thermoplastic. However, this strategy leads to a drastic downgrade in the material quality, which only enables the consideration of these as-processed materials for reuse in low-cost, low-performance applications. Moreover, the matrix weight fraction in the virgin structural composite is low, which tends to decrease the efficiency of such a method. Therefore, a repurposing approach was preferred. In that case, the laminate is collected and reshaped/welded into a new material. This approach is even more promising as it keeps the fiber length, and the thermo-compression step can consolidate the matrix, reducing porosities and cracks in the matrix generated during the first use phase [490]. The process involves a unique step of thermo-compression at 180 °C for 30 min. A quality factor of 0.7 was applied to account for the potential decrease in the material properties. This quality factor means that it is assumed that 1 kg

of recycled product would have a functional performance equivalent to 0.7 kg of virgin material. An additional 30wt% loss accounted for cuts and other preliminary preparations and finishes.

As hybrid EP-PHU was more suitable for depolymerization in mild conditions, allowing the recovery of carbon or natural fibers, chemical depolymerization was also modeled. A depolymerization mixture of glacial acetic acid (HAc) and hydrogen peroxide is prepared (80:20) and heated at 60 °C for 4 h. The network is cleaved, and the fibers can be retrieved by filtration. The HAc is recovered (90% efficiency) and re-employed. The degraded polymer solution is treated as a hazardous solvent mixture (incinerated). A new composite is prepared using 60 wt% of fibers and virgin hybrid matrix. A conservative quality factor of 0.7 is applied.

VI.4 Results and discussion

VI.4.1 Production of epoxy and cyclic carbonates

The production of cyclic carbonates for PHU resins demands the carbonatation of epoxy monomers. The synthesis only requires the use of CO_2 in supercritical conditions to play both the solvent and the reactant. However, because of the CO_2 thermodynamic stability, a catalyst and energy are required to form the desired product. Supercritical conditions are advantageous as they limit the generation of waste and purification steps, yielding the lowest E-factors [376]. Replacing epoxy resin with PHU in composite requires this additional carbonatation step, which must be first environmentally assessed.

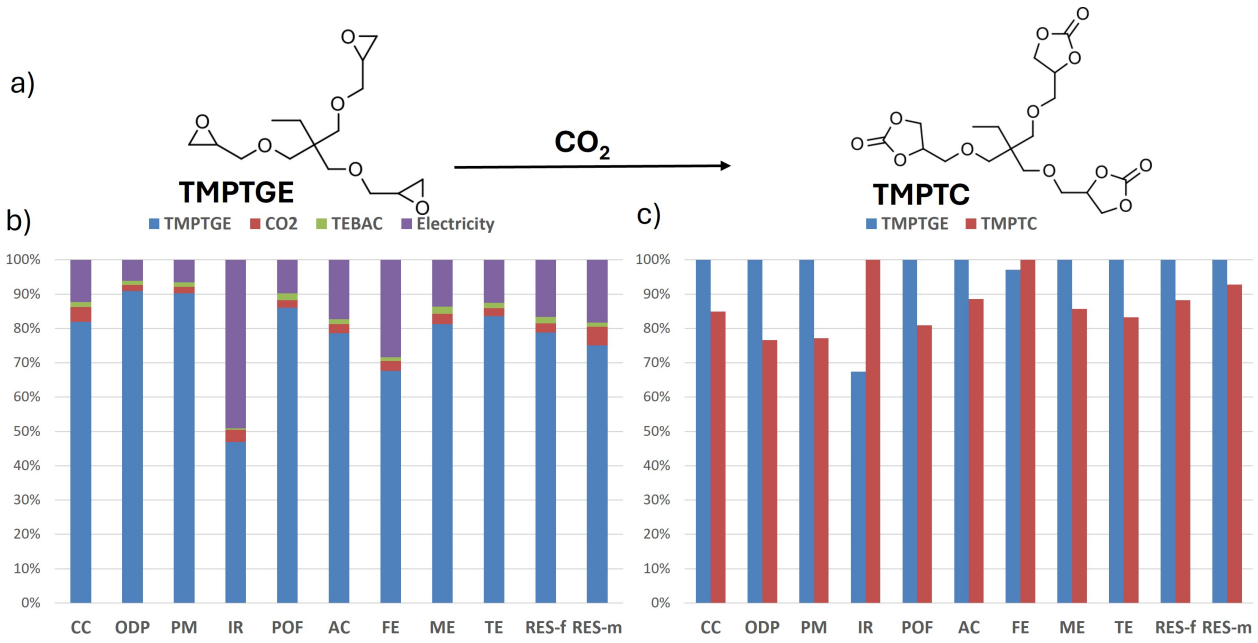

Figure VI-2 – Environmental impacts of TMPTC production. a) Contribution of each input in TMPTC, and b) Comparison of 1 kg of TMPTGE and 1 kg of TMPTC.

The contribution of each constituent in the calculated impacts of TMPTC is represented in Fig. VI-2b. The main contributor to the overall EI of TMPTC remains the epoxy monomer, accounting for 80% of the CC indicator and a major contributor to all indicators. The use of CO_2 as reactant can be almost considered as neutral, with a minor contribution to all indicators. The catalyst does not make a significant contribution either. While catalyst selection should be driven by cost, toxicity, and catalytic activity, mainly to shorten the reaction time, it does not appear to have a strong influence on EI. The energy consumption related to the reaction accounts for 12% of the CC and 17% of the resource depletion indicators. The larger contribution to the overall EI of cyclic carbonatess originates from the epoxy precursor. In that sense, the results obtained in the present work demonstrate that the supercritical carbonatation process itself does not add any detrimental environmental burden and can, to some extent, be regarded as a greener process.

The production of cyclic carbonates resulted in a mass gain for the monomers as 1.1 kg of epoxy yielded approximately 1.6 kg of cyclic carbonates. Therefore, the epoxy monomer and the cyclic carbonates were compared normalized to 1 kg of starting monomer. The results are presented in Fig. VI-2c and summarized in Table VI-A1. Interestingly, TMPTC has lower environmental impacts than its epoxy precursor owing to the efficient carbonatation process and the mass increase from CO_2 incorporation. A reduction of 15% of emitted CO_2eq is estimated. The epoxy carbon footprint is evaluated to 6.2 kgCO_2eq/kg while 5.3 kgCO_2eq/kg was attributed to TMPTC. Moreover, the overall

energy consumption is estimated to be 91 MJ/kg for TMPTC, while TMPTGE is about 103 MJ/kg, representing a 12% decrease. The values of CC indicator and cumulative energy for TMPTGE are consistent with the literature for other epoxy monomers, which are commonly estimated to be 4-8 kgCO_2eq/kg and 70-150 MJ/kg, respectively [71, 193].

Other pathways using low-pressure CO_2 have been developed [378]; however, they require the use of solvents such as ethyl acetate and a purification step, resulting in lower yields. For reference, the process was modeled (see Fig. VI-A3) and compared to the scCO_2 method. Despite lower energy consumption, the strategy led to an increase of 80% of the CC indicator, 40% of the cumulative energy, and between 20 and 40% for the other criteria. Therefore, scCO_2 currently appears to be the most promising strategy.

The results obtained from this first cradle-to-gate analysis demonstrate that the production of cyclic carbonates might be beneficial in mitigating the EI of thermosets. However, to be considered truly sustainable, the toxicity of cyclic carbonates should be addressed in the future. cyclic carbonates are commonly considered as fairly non-hazardous [437], with ethylene carbonate, a rather well-known chemical, considered safe. Yet, this should be confirmed for other carbonated monomers. Moreover, while being promising, these results need to be extended first to the material level, in accounting the process and other constituents, and finally to the entire life cycle.

VI.4.2 Comparison of epoxy, polyhydroxyurethanes, and hybrid EP/PHU resins

The previous chapter documented the lengthy curing times at elevated temperatures of pure PHU thermosets and underlined them as a problem in the production of composites. Such issues were tackled through the synergetic hybridization strategy, which facilitated and accelerated the curing process. Yet, it is important to evaluate the share of each resin's inputs into the EI, including the energy required to cure them, which might hamper future benefits. The contribution analysis of the impacts of each cured resin and the compared impacts of the three systems are presented in Fig. VI-3.

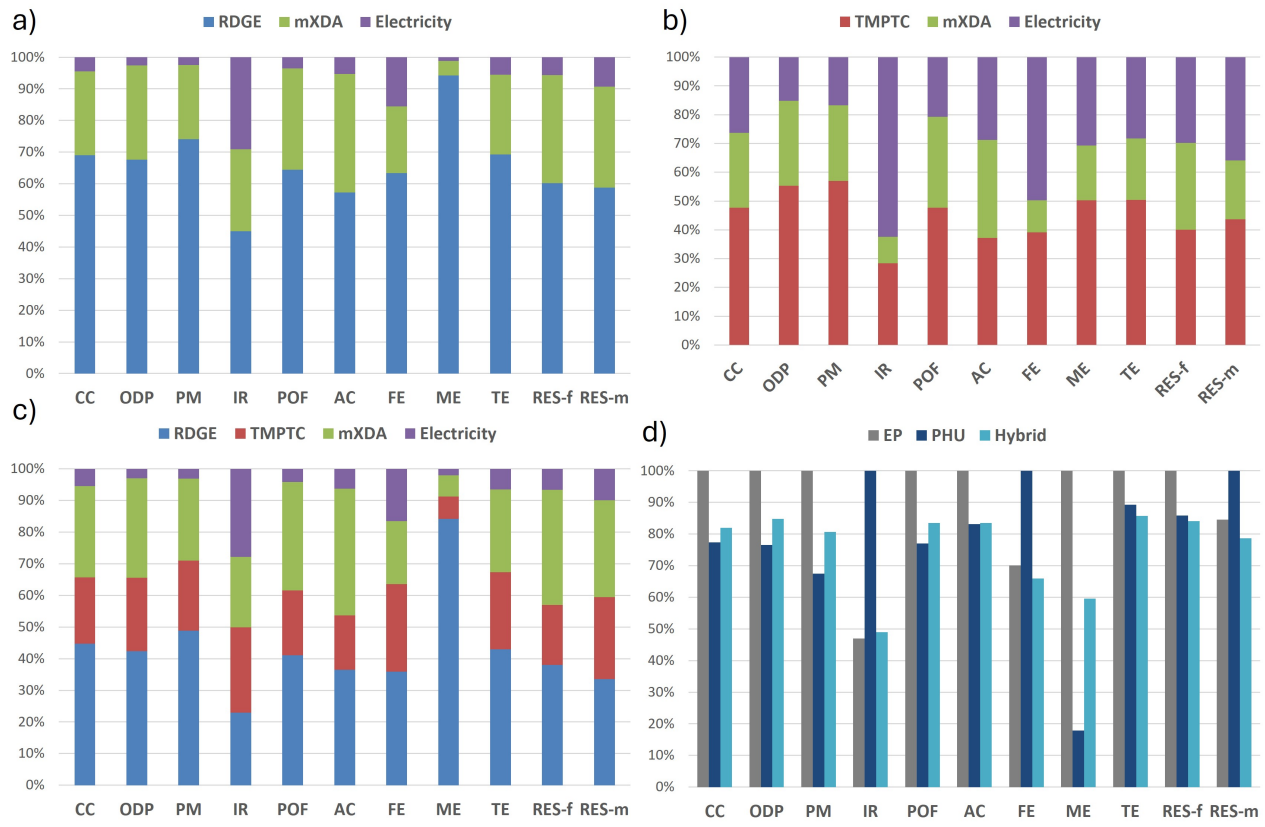

Figure VI-3 – Contribution of each constituent of the cured resins on the overall EI of the resins. a) Epoxy resin, b) PHU resin, c) hybrid EP/PHU, and d) comparison of the impacts of the different resins.

About 10.4 $kgCO_2eq/kg$ of cured epoxy resin are estimated with 10 MJ/kg required, in the upper range of typical epoxy resin [71, 193]. The main contributor in EP is RDGE, representing 70% of the CC indicator, 60% RES-f, and superior to 50% in all other categories. mXDA is the second contributor, representing about 25% of most indicators. The EI of the energy required to cure the epoxy is marginal, accounting for about 4% of emitted $kgCO_2eq$. This is sounded as the European energy mix is rather decarbonated, with about 67% coming from renewable energy or nuclear [523]. Similarly, RDGE appears as the highest contributor to the hybrid resin, representing 40-50% of the EI while only representing about a third of the mass. The influence of mXDA and electricity is similar to the one of EP with 27% and 5%, respectively. Interestingly, TMPTC represents less than 20% of the EI sources. In the pure PHU, the share of the curing energy substantially increases in all categories, becoming an important source of EI, up to 26% for CO_2eq. In that case, TMPTC represents 48% of the EI, significantly less than RDGE in the EP. The curing mXDA represents around 26% of the CC and consumed energy.

Both the hybrid and the PHU resin allowed a drastic reduction of most EI, ranging by 20% to 50%

compared to the epoxy benchmark, apart for ionizing radiation, freshwater eutrophication, and abiotic resource depletion for the PHU. The CC is reduced by 28% and 21% for the PHU and the hybrid, respectively. The PHU exhibits slightly lower CC results than the hybrid but should be considered as similar, given the potential uncertainties in modeling.

In the hybrid, the presence of RDGE possess high EI, which could be expected to impede the environmental benefit of the resin. The use of TMPTC in parallel to improving the curing protocol compared to neat PHU enables compensation for the presence of RDGE and makes the hybrid competitive with the PHU. This is promising as our previous work has demonstrated that pure PHU might not be relevant at the current development stage, but the hybrid strategy can be implemented faster while keeping the environmental benefits. The results demonstrate that PHU and their hybrids are valuable approaches to reducing the environmental footprint of epoxy-based resins.

VI.4.3 About the benefits of PHU chemistry in natural fiber composites

Natural fibers, particularly flax, have been widely demonstrated as a greener alternative to synthetic fibers [76, 125, 164]. Particularly, flax fibers have low embodied energy and account for minimal CC effects during their life cycle, sometimes resulting in negative GWP due to carbon sequestration. [76]. Therefore, in a flax fiber composite, the matrix used is responsible for a major share in the majority of indicators (apart from some exceptions such as land use or water consumption) and should be optimized to ensure the full sustainability of the resulting composite.

EP, PHU, and hybrid matrices were evaluated with scutched long fiber reinforcement in a cradle-to-gate approach. Results for individual laminates and the normalized comparison are shown in Fig. VI-4. It is assumed that the PHU or the hybrid would be used as a direct replacement for the EP resin, with no change in application. This assumption favors the benchmark resin, as the previous chapters demonstrated improvements in the properties of the PHU and the hybrid. Moreover, it must be noted that the PHU resin is considered for reference purposes only, as it might not be applicable to real-world scenarios due to economic and technological reasons.

For all composites, the flax fibers contribute to about 12-15% of most indicators. As discussed, the resin is the major contributor, which highlights the need to focus on low EI resins for NFC. The EP and hybrid resins account both for roughly 75% of the CC indicator, and 80% of the fossil resource indicator. For the flax/PHU, the low EI of the PHU resin reduced its share by about 50%. It remains rather high, considering that the resin only constitutes 40% of the mass in all composites. The PHU

point out the detrimental effects of the more energy-intensive curing protocol. In PHU, the electricity required to cure the laminate accounts for 40% of CC and is a significant contributor in all indicators.

When comparing the impacts of the three systems, using the hybrid resin demonstrates a substantial decrease in all EIs. Flax/EP showcases the highest CC indicator, photochemical oxidation, and marine eutrophication. Around 5.5 $kgCO_2eq/kq$ are estimated for the Flax/EP, with 96 MJ/kg. These values are in the upper range of the literature [193, 524], but the comparison might not be entirely feasible due to the small scale used here to model the scenarios and the reliance on mostly in-house models that commonly have higher EI than database ones. Therefore, the comparison should remain internal to the materials in the present study.

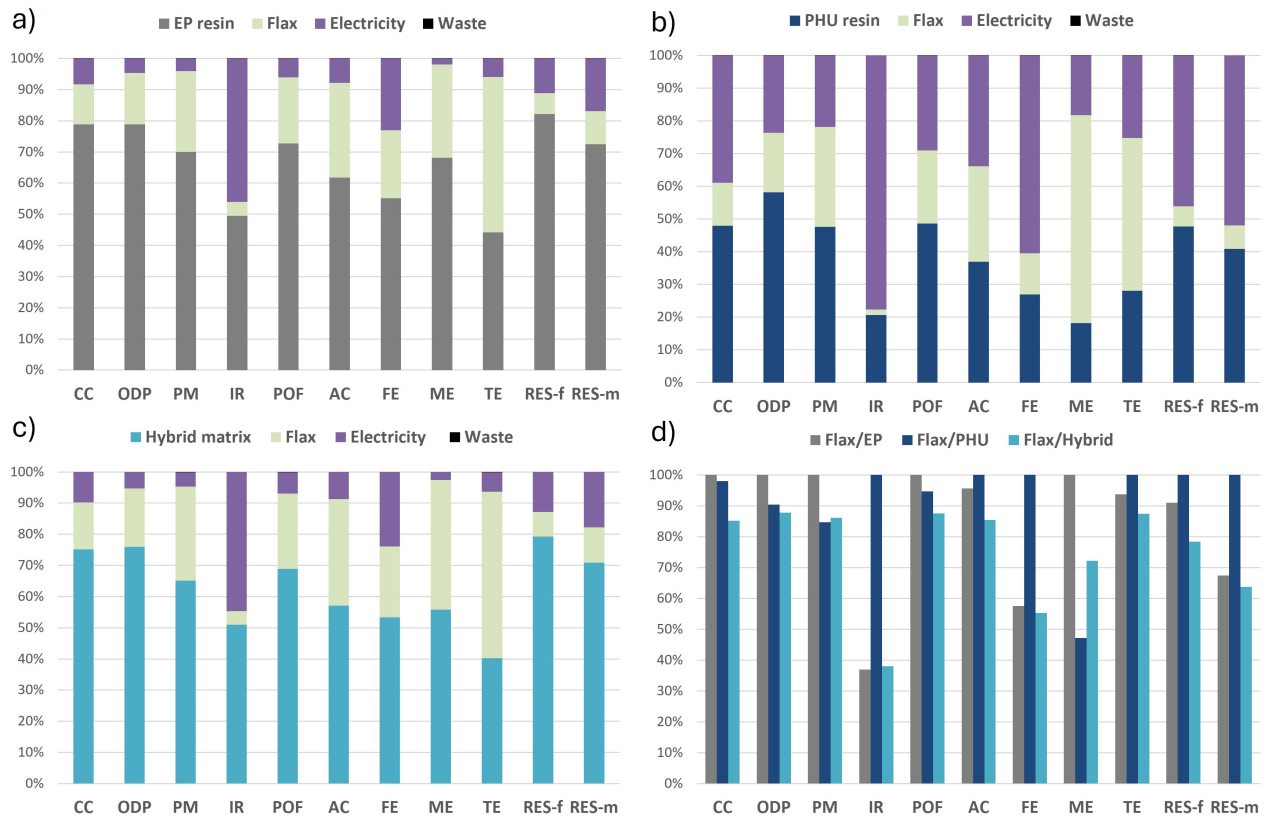

Figure VI-4 – Distribution of each constituent of the flax-based composites on the overall EI. a) Flax/epoxy composite, b) Flax/PHU composite, c) Flax/hybrid composite, and d) comparison of the different flax composite.

The flax/PHU could have been expected to be the most performing material. However, the results are totally inhibited by the detrimental amount of energy for the curing step, and no significant difference can be observed in the calculated climate change indicator with the reference. The PHU-based laminate even demonstrates the worst results in terms of ionizing radiations, acidification, freshwater and terrestrial eutrophication, and fossil energy. The fossil resource depletion indicator is estimated

to be 106 MJ/kg, which represents a 10% increase compared to flax/EP. These results showcase that using a low environmental footprint matrix might not lead to environmental benefits if the switch leads to a change in the process with higher energy consumption.

The hybrid, on the other hand, indicates more promising results. All indicators decrease compared to both PHU and EP matrices. The CC indicator and fossil resource depletion are reduced by 15% compared to the EP resin, as well as eutrophication. About 4.7 $kgCO_2eq/kg$ are estimated to be emitted during the production of flax/PHU laminates. The results demonstrate that the synergetic hybridization that was developed herein has not only opened the door to obtain efficient and easily accessible CAN, with characteristics relevant to the composite industry, but also confirmed the initial hypothesis that PHU chemistry, with optimization, represents a sustainable pathway for natural fiber composites.

VI.4.4 About the benefits of hybrid EP-PHU in carbon fiber composites

CFRPs are known for their high EI, due to the significant contribution of PAN-based carbon fiber [67]. It was demonstrated that upon careful design, the EI mainly issued from the raw materials production and composite manufacturing could be compensated by energy savings during the use phase [68] but remains not systematic [11].

We previously demonstrated that PHUs are irrelevant for CFRPs, whereas hybrids have prospects. In this regard, only the EP and hybrid resins were studied in this section. It must be noted that CFs, which represent 70% of the composite's mass, account for 93% of the CC indicator and fossil energy consumption and are the major contributors to all indicators. The results for the CF/Hybrid are shown in Fig. VI-5a. Around 50 $kgCO_2eq/kg$ of the composite was estimated with a cumulative energy of around 900 MJ/kg. The results are in the upper range of different studies but remain within the same order of magnitude [68, 525].

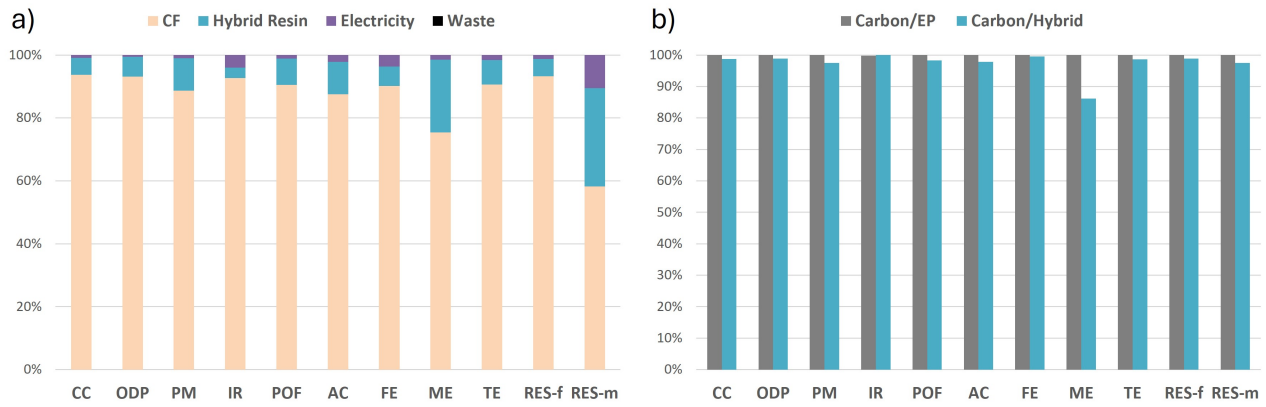

Figure VI-5 – Distribution of each constituent of the carbon-based composites on the overall EI. a) Carbon/hybrid, and b) comparison of the impacts of carbon/EP and carbon/hybrid composites.

Since CFs have the highest EI, a significant decrease in their environmental footprint cannot be expected from the resin only. The comparative results are displayed in Fig.VI-5b. The hybrid-based CFRP demonstrates a reduction in all environmental indicators. Yet, this decrease is limited to 2-5%, except for marine eutrophication, which is reduced by 15%. The differences between the two CFRPs should not be considered as sufficiently distinguishable to draw strict conclusions in this cradle-to-gate perspective.

In light of the previous results on neat resins and flax composites, a trend toward environmental impact improvements can still be highlighted. More importantly, the results strongly suggest that this emerging hybrid strategy is more promising and does not generate any detrimental environmental side effects.

VI.4.5 The end-of-life management of composites, a material-related strategy

The waste management of composites, including bio-based ones, remains a major issue [33]. The most advanced recycling technologies are so far pyrolysis [87] and solvolysis [115]. It was demonstrated that the recovery of carbon fibers (rCF) was positive on both environmental and economic aspects compared to virgin CF [410]. However, the recovery of glass fibers was, in most cases, not economically viable and not systematically beneficial for the environment [33].

The synergetic hybridization strategy developed in the present work offers an alternative to conventional epoxy resin composite materials. Firstly, the network's dynamic behavior enables the

possibility of reshaping and mechanically recycling the material. Secondly, a chemical pathway involving acetic acid (HAc) was confirmed to cleave the resin at low temperatures within a few hours. The process was effective for both flax and carbon fibers. However, the environmental benefits of recovering low EI flax fibers still need to be discussed.

The LCA was performed in a cradle-to-grave approach. A virgin material was considered at first, identical in all scenarios. In the reference scenarios, when decommissioned, the composite is landfilled or incinerated (for flax), and a new virgin material is produced. An EP-based composite with landfill EoL management was used as a reference. For the chemical recycling scenario, the first virgin material is depolymerized, and the recovered fibers are used with a virgin matrix to produce a new composite with a quality factor of 0.7. FFor the mechanical recycling scenario, we assumed that composite plates could be cut into large pieces and reshaped into semi-structural parts by welding them. As an example, a meter square turbine blade could be reshaped into sports equipment or fiberboard like materials.

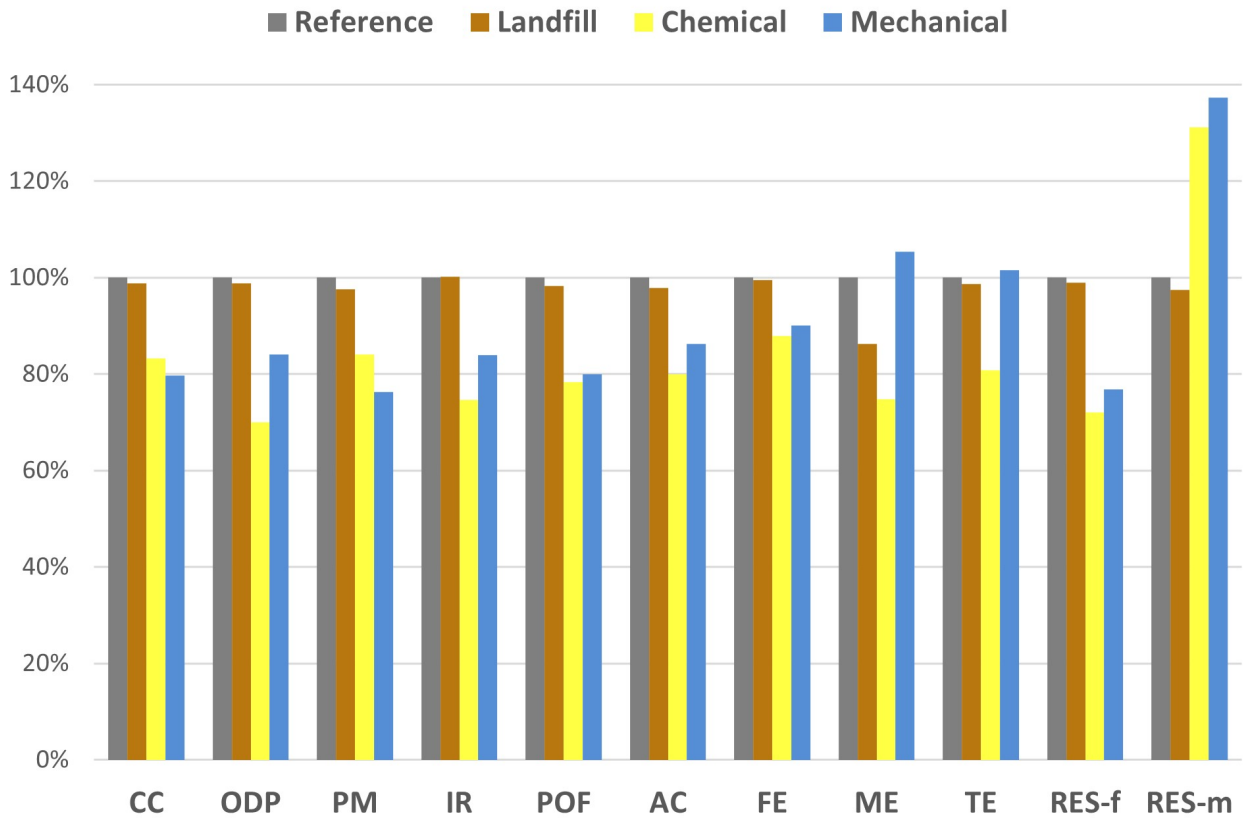

Figure VI-6 – Life cycle assessment for the different EoL scenarios exploiting the hybrid matrices with carbon fiber reinforcement. Results are normalized to the EP-based carbon composite, reference, with landfill EoL.

The LCA was first performed on the CFRP (Fig. VI-6). As observed in the previous section, a relatively positive outcome arises from the use of the hybrid instead of the EP when a conventional

landfill EoL is considered. The two scenarios were estimated to yield around 85 $kgCO_2eq$ with a fossil resource depletion equivalent to 1540 MJ. High levels of eutrophication and acidification were also caused by the landfill. Detailed results are in Table VI-A5. As expected, mechanical recycling revealed the best environmental savings with a drastic reduction of about 20-25% of all indicators except eutrophication, reducing the CC indicator to 68 $kgCO_2eq$ and the fossil resource depletion to 1186 MJ. These values for two cumulative applications are only 10% superior to the production of a single virgin material. Although some parameters such as collecting, sorting, and transportation are neglected between both applications, they give promising results towards the direct reuse of CFRP based on the hybrid resin and could justify the interest of these new matrices from the perspective of the entire life cycle.

The chemical recycling process also revealed positive outcomes compared to the landfill scenario with a reduction of the CC effect by 17% and acidification or eutrophication by about 20%. The fossil resource depletion was reduced by 28% due to the virgin CF production avoided and was also lower than that of mechanical recycling. It is important to note that the reuse of HAc was considered in the loop, which is critical for affording the benefits of chemical recycling. Further discussion on that point can be found in section VI.4.6.

Chemical recycling shows only slightly higher EI than mechanical recycling. Typically, solvolysis presents a higher environmental impact than mechanical recycling [33, 410], but it yields higher quality fibers that can be considered in advanced applications with greater economic values. The results indicate that oxidative chemical recycling can be considered an environmentally sound EoL scenario for CFRP.

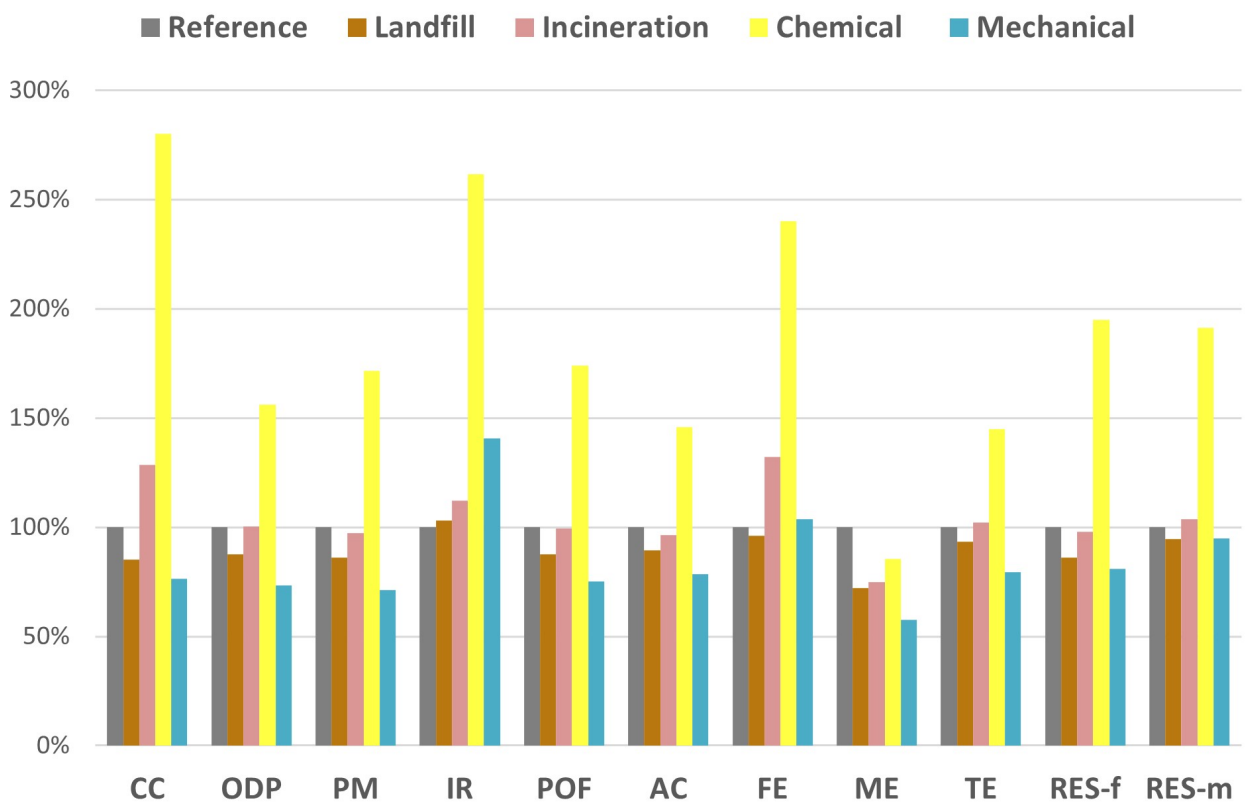

Figure VI-7 – Life cycle assessment for the different EoL scenarios exploiting the hybrid matrices with flax fiber reinforcement. Results are normalized to the EP-based flax composite, reference, with landfill EoL.

The interest in recycling materials lies in the balance between the environmental cost of producing virgin materials and the environmental cost of the recycling processes. For materials with high EI and economic value such as CFRP or metallic structures [526, 527], the recycling process tends to systematically give lower EI than virgin material production. For materials with low EI, such as natural fiber-based composite, balancing the recycling processes with the virgin materials is more challenging [528], and to date, the recovery of flax fibers remains technically difficult and has never been environmentally assessed.

The results for full life cycle scenarios for flax-composites with different EoL options are presented in Fig. VI-7. Similar to the cradle-to-gate analysis, the flax/hybrid composite demonstrates a 15% CC and RES-f decrease compared to the EP-based one. Unlike CFRP, the incineration with energy recovery was considered as the natural fibers can burn, in contrast to glass and carbon fibers, which must be removed and treated separately. The incineration can be advantageous as it is a rapid technique suitable for all types of NF/polymer matrix combinations since all materials can combust [528]. However, the results showed that the recovered energy does not balance with the total process and leads to a 28%

increase in CC and water eutrophication. Other indicators tend to be similar to the reference case scenario but are higher than the landfill of flax/hybrid composite. The higher GWP can be understood through the CO_2 and other combustion gases emitted during burning. As the European electricity mix is not a large contributor to GWP, using waste as an energy source is not advantageous. The loss of materials with only the energy recovery through a GHG emitting process does not appear to be the best choice [33].

Finally, chemical and mechanical recycling were evaluated. The chemical depolymerization to recover flax fibers is the worst scenario. The process is a low consumer of energy as the temperature required to perform the depolymerization is low (below 65 °C), and reagents are water, HAc, and hydrogen peroxide, which are typically considered as environmentally friendly [293]. Therefore, while a positive outcome might have been expected, the CC indicator increased by 180% compared to the reference. Fossil resource depletion increased by 90%. All other categories got imparted a 50% higher impact, except for marine eutrophication, but do not provide significant differences. In that sense, the chemical recycling of NFC, under the current conditions, is not sustainable. The issue lies in the use of glacial HAc and its production route (see Fig. VI-A6). About 80% of commercially available glacial acetic acid is produced from the carbonylation (carbon monoxide from syngas) of methanol under pressure (30-60 bar) and temperature (150-200 °C) in the presence of cobalt (BASF) or ruthenium (Monsanto) catalysts, and hydrogen iodide [529]. The EI of petro-based acetic acid is, therefore, elevated (3.3 $kgCO_2eq/kg$ and 62 MJ/kg). The large quantities of acetic acid required to swell and cleave the network hamper the environmental benefits of recovering natural fibers, even when recirculating 90% of HAc is considered.

Conversely, mechanical recycling appears more promising as a reduction of 24% of the CC indicator and energy demand is observed. With the exception of ionizing radiation, all impacts are reduced by about 20-30%, demonstrating that NF, using CAN matrices, can provide substantial environmental benefits in composite materials. Indeed, CAN-based composites offer properties and processes similar to traditional thermosets, while also enabling more sustainable recycling pathways.

VI.4.6 Discussions on improvement perspectives

Based on the previous results, several pathways can be drawn to further reduce the overall environmental footprint of hybrid-based composites. Gaining energy consumption and management efficiency, along with renewable electricity production, would benefit all stages. However, this is more related to state policy than research labs and will not be further discussed.

Regarding the production of cyclic carbonates, the process was considered using supercritical CO_2. When using $scCO_2$, epoxy is the major contributor to the cyclic carbonates EI, accounting for nearly 80% of all indicators. Hence, reducing the EI of the starting epoxy is the key to reducing the cyclic carbonate footprint. For epoxy, the major contributors are the epichlorohydrin and the phenol/polyol backbone. NaOH also represents a non-negligible share but will not be discussed in the current work. Depending on the backbone, ECH can be the major contributor, such as in TMPTGE (Fig. VI-A1), or second such as RDGE (Fig. VI-A2). The inputs in the current studies were taken from the current market and, therefore, petro-based. However, large efforts have been performed during the last decades to establish more sustainable pathways towards epoxy through the use of biobased epichlorohydrin [279] and renewable precursors [530] with significant benefits. The use of biobased ECH, derived from glycerol as a biofuel by-product, displayed a reduction of the CC indicator by 60% [277]. Bio-ECH is commercialized under the trademark Epicerol® and appears to be a reliable pathway to reduce the EI of both epoxy and cyclic carbonates (see Fig. VI-A5). A reduction of between 20 and 30% of the CC effect can be expected for both TMPTGE and TMPTC, as shown in Fig. VI-8.

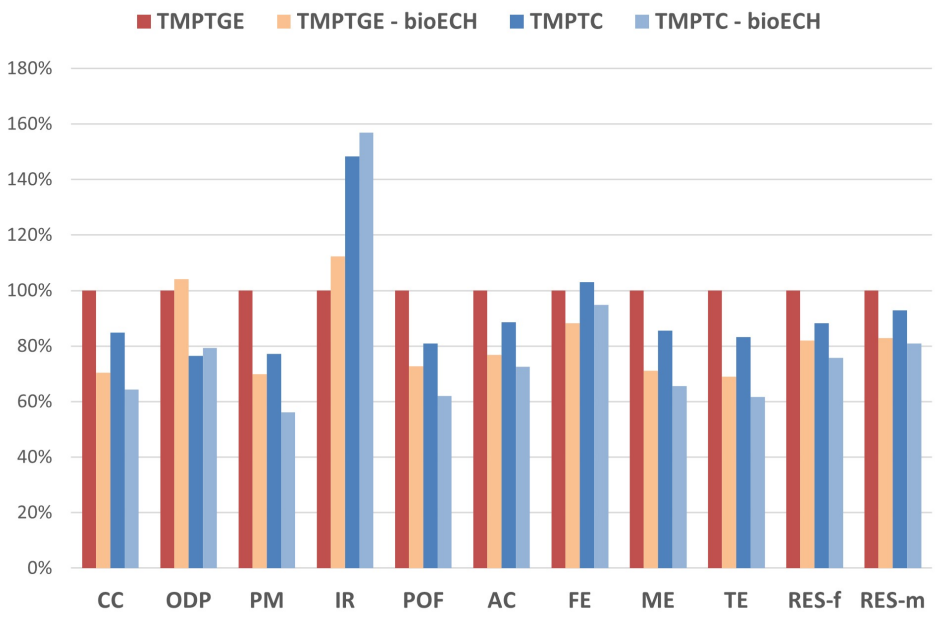

Figure VI-8 – Environmental interest of replacing petro-based ECH with glycerol-derived ECH for epoxy (TMPTGE) and cyclic carbonate (TMPTC).

It is important to note that resorcinol is a major contributor to the EI of RDGE and, therefore, the epoxy and hybrid resins. Indeed, resorcinol was chosen in the present work as it is often considered in the literature as a potential alternative to bisphenol-A (BPA) and delivers low viscosity [181,211]. Resorcinol can be bio-derived from glucose by microbial processes. However, the input data comes from the

market, where resorcinol is produced from benzene. Based on the data currently available in Ecoinvent, resorcinol EI is almost three times more significant than BPA (Fig. VI-A4). A significant reduction of the EI might be expected from bio-resorcinol but has not been assessed in the literature. The economic viability of bio-resorcinol is not ensured. Moreover, resorcinol has been recently reported as a proven endocrine disruptor and listed as a substance of very high concern under REACH classifications [531]. Therefore, future environmental improvements for synergetic hybridization should focus on low-viscosity epoxy, both phenolic and aliphatic, derived from renewable resources. The toxicity should be further considered as well. As potential substitutes, furan-derived epoxy [219], or cyclo-aliphatic alcohols derived from lignin [532] could provide less toxic precursors with environmental gains.

Equally, amines account for around 20% of resins in terms of EI. In the case of reducing the EI contribution of epoxy and cyclic carbonates, they will become major contributors. Biobased amines are facing a rising interest in both industries and academia [220]. However, to date, there is no data available on the environmental outcomes of biobased amines, to the exception of biobased aniline, proven better than its petro-sourced counterpart [213]. Reducing the EI of the curing amines through the use of biobased precursors from lignin or sugars would benefit the composite industry.

Finally, recycling was pointed out to show an important effect on the overall life cycle assessment. Mechanical recycling enabled by the hybrid's CAN nature affords substantial EI reductions compared to non-recyclable matrices. However, the significant reduction of the properties limits their application to lower-value uses. Therefore, finding ways to recover both the matrix and the fibers could still be beneficial. The relevance of recovering natural fiber, in light of the current results, must be considered from both environmental and economic perspectives.

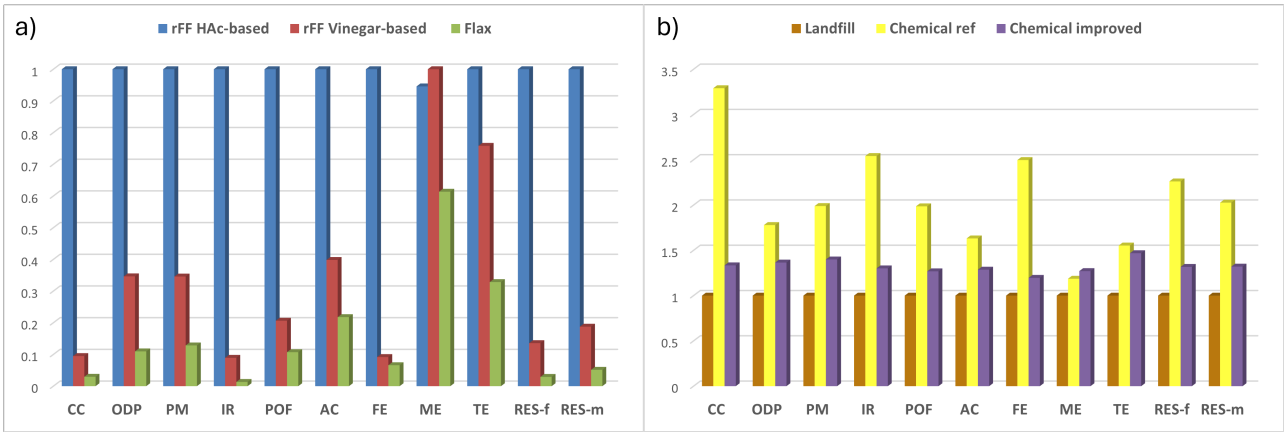

Figure VI-9 – Strategy to improve the chemical recycling through the use of vinegar to replace petro-based HAc. a) Comparison of 1 kg flax fibers from the initial chemical recycling process, the improved one, and virgin flax production, b) Comparison of the LCA outcomes from the chemical recycling of flax/hybrid composites.

The current chemical degradation process gives room for large improvements. The results indicate that market-grade HAc is not sustainable. The current process was extrapolated from lab-scale experiments. In that sense, reducing the quantity of degradation solution could help reduce the consumption of all reagents. Moreover, glacial acetic acid (>99%) is currently used. Reducing the concentration of acetic acid (HAc) below 20% would allow for the use of white vinegar, which is bio-based acetic acid derived from ethanol fermentation. To investigate this possibility, a quick experiment was performed, see Fig. VI-A7, and the EI was modeled. It is important to note that a higher amount of hydrogen peroxide was necessary. Longer times and higher temperatures were also required (15 h vs 4 h, at 70 °C instead of 60 °C). As bio-based HAc or vinegar is not available in the EcoInvent database, vinegar was replaced by a water/ethanol solution (20% concentration). The enhanced process demonstrates a reduction of 80% of CC and 70% of fossil resource depletion, as shown in Fig. VI-9. Despite the significant decrease in the EI for the chemical degradation process, which would also become more eco-friendly to recover carbon fibers (see Fig. VI-A8), the production of 1 kg of virgin flax fibers remains less detrimental to the environment than 1 kg of recycled flax fibers. Therefore, alternative pathways must be considered to design sustainable EoL scenarios for natural fiber composite. The valorization of the matrices that are currently wasted would be highly beneficial to access to an eco-friendly process for retrieving natural fibers. Moreover, directly reusing the depolymerization solution for multiple recycling batches may also be beneficial.

VI.5 Conclusions

The results in this work indicate that cyclic carbonates can provide positive environmental benefits compared to their epoxy precursors when produced from supercritical conditions. However, the resulting polyhydroxyurethane and its subsequent composites cannot be considered as environmentally beneficial compared to an epoxy network. This is ascribed to the detrimental effect of the more energy-intense protocol required to crosslink PHUs. Still, the carbonatation process does not impart environmental burden, and both EP and PHU present similar results.

The synergetic EP/PHU hybrid, whose processing and properties are more suited for the composite industry, exhibits substantial benefits. Through more efficient curing, the environmental benefit of cyclic carbonate production is retained. When combined with flax fibers, a reduction of about 15% of the global warming potential and fossil energy can be expected compared to epoxy matrices. The use of carbon fibers, which is more impactful, reduces the interest in using hybrid EP/PHU from cradle-to-gate perspectives with only 2%-5% of environmental gains.

When considering the EoL of composites, the mechanical and chemical recycling of carbon fiber composites with the synergetic hybrid is demonstrated environmentally valuable. Only marginal gain arises from mechanical recycling compared to chemical. Given the higher economic value of chemically recycled carbon fibers, oxidative chemical depolymerization could be a promising pathway to efficiently retrieve carbon fibers, provide environmental benefits, and reuse them in secondary applications, even though the polymer matrix is wasted. The recycling of natural fiber composites is more intricate to balance. The mechanical recycling, accessible through the EP/PHU covalent adaptable network is demonstrated as beneficial. The low environmental impact of the composite makes the chemical recycling process not competitive, with an increase of 300% of the climate change indicator compared to a virgin composite. This high impact is ascribed to the negative environmental footprint of acetic acid. The decrease of the acetic acid concentration opens the door to the use of biobased acetic acid (vinegar), which helps reduce the impact of chemical recycling by 90% for natural fibers. However, it remains three times more impactful than virgin flax fiber production. Through the entire life cycle assessment, the use of vinegar to chemically recycle natural fiber composites accounts for a 33% increase in the environmental impact.

For natural fiber, developing the recycling and valorization of the matrices should be investigated in the future to expect a potential positive outcome. Optimizing the dynamic behavior to enhance mechanical recycling and drastically reducing the environmental footprint of the matrix by using biobased precursors, such as bio-epichlorohydrin, appears to be a more suitable approach to

develop/create greener materials.

These preliminary results demonstrate that a synergetic EP/PHU hybrid can provide a relevant pathway toward sustainable composites by reducing the material's environmental footprint and opening new recycling strategies. Future technical and scientific work should focus on optimizing sourcing and recycling pathways to valorize all constituents and investigate long-term performances. The life cycle assessment should be later conducted on an actual engineered structure, taking into account the use phase and, therefore, the mechanical properties. A techno-economic assessment should also be performed to investigate the economic interest of such materials in the near future.

Chapter VII

Conclusion & Outlooks, future perspectives

VII.1 General conclusions

The state-of-the-art highlighted the large multidisciplinary efforts and strategies that have been and are being applied to produce more sustainable composite materials that are relevant in a circular economy. Composite materials possess exceptional properties that are essential for a durable future; however, they are not sustainable. Therefore, increased efforts are needed to focus on fibers, resins, and recycling strategies at every production stage while maintaining an interconnected approach. Unfortunately, viable industrial solutions remain scarce.

Polyhydroxyurethanes (PHU), obtained from CO_2-based cyclic carbonates (CC) and polyamines, are considered greener and safer alternatives to conventional polyurethanes (PU). Surprisingly, PHUs have only been investigated as replacements for typical PU applications without exploring other fields. The hydroxyurethane moieties along the PHU's backbone enable unexplored opportunities in adhesion and mechanical properties that could be a breakthrough in many structural applications. In particular, a special affinity between PHUs and cellulosic fibers could lead to cutting-edge properties. Furthermore, PHUs have shown thermo-mechanical recyclability arising from the ability of hydroxyurethane moieties to participate in reversible exchange reactions. However, as PHUs have never been explored for composite applications, a significant lack of understanding of their advantages and limitations exists, thus restraining development in that way. The relationship between the macromolecular structure, processability, and final properties of these materials has not been evaluated sufficiently to establish a comprehensive overview of these emerging thermosets. Without understanding the strengths and

weaknesses of such relatively new chemistry, it is not possible to advance them further in engineered applications. Throughout this work, the understanding of PHU chemistry and its derivative materials has been advanced to more applied considerations with stricter requirements, as shown in my overview.

After reviewing the current solutions envisioned in developing sustainable composites (Chapter 1), a comprehensive assessment of the curing, rheological, and thermomechanical properties of PHUs has been generated in our second Chapter. By comprehending these properties, a library of (biobased) PHUs was extended to fit various applications and help select monomers based on specific requirements. Properties comparable to average epoxy-amine formulations were obtained, with the additional benefit of the reprocessability feature. However, both viscosity and curing time were found to be a main limitation for their use in a more demanding context. These materials remain an interesting platform to investigate for structural applications, particularly fiber-reinforced polymers, that can address many sustainability challenges if their interactions with fibers are understood and limitations overcome.

In the third chapter, we confirmed our initial hypothesis that increasing the hydrophilicity of matrices would contribute to enhance the interfacial adhesion between natural fibers and their surrounding matrix. The capability of PHUs to form strong H-bonds results in outstanding mechanical properties for NFC. Exploiting this H-bond key feature, exceptional interface bonding between flax and PHU was confirmed by atomic force microscopy and rationalized by atomistic simulation. Without any treatment, an increase of 30% in stiffness and strength was unveiled compared to an epoxy benchmark, reaching 35 GPa and 440 MPa of modulus and strength, respectively. Moreover, the dynamicity of the matrix confirmed the possibility of reusing cured composite. Implementing such CO_2-derived thermosets in NFC could lead to greener high-performance materials, which is critical for a sustainable circular economy. However, the promises of neat PHU were found to be limited to the laboratory scale. Indeed, PHU monomers suitable for sufficient thermo-mechanical properties display too high viscosity and too long curing time for scaling to larger composite structures. Additionally, the dynamicity is insufficient to compete with other covalent adaptable networks.

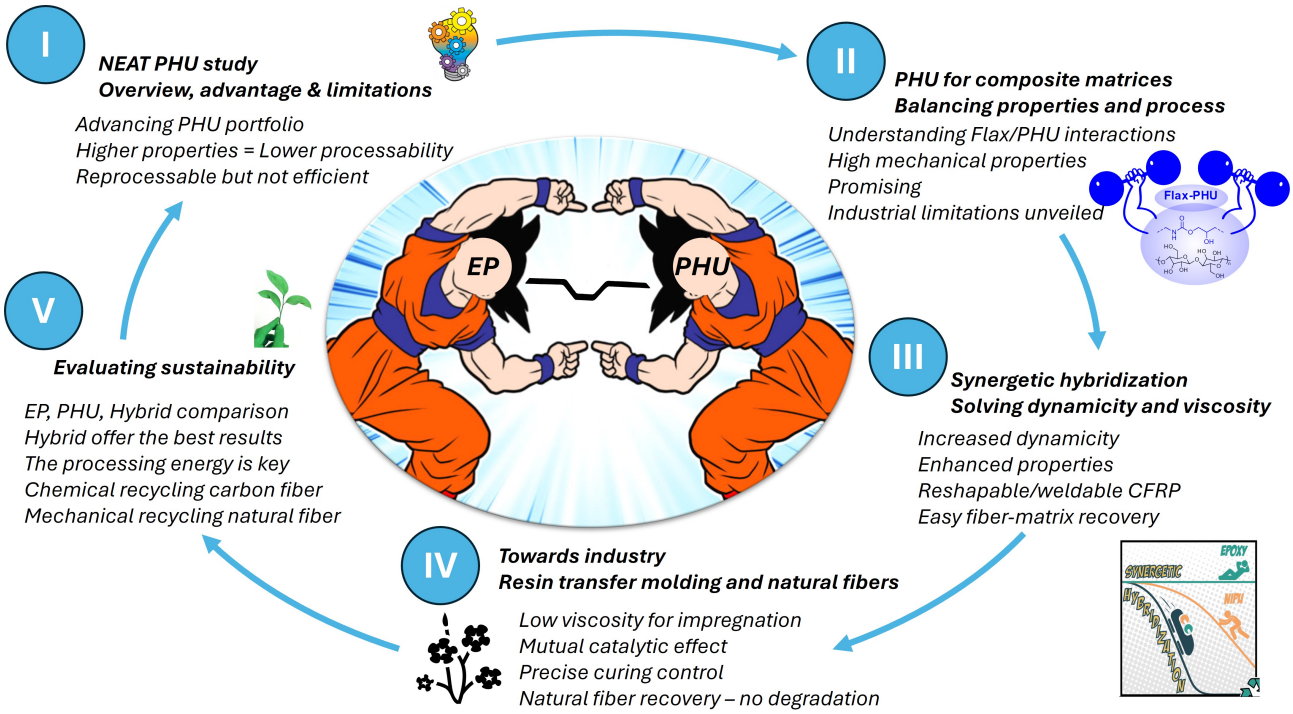

Overview of the work.

To mitigate such detrimental issues, a pragmatic strategy was developed in the fourth chapter and further developed in the fifth chapter by hybridizing PHU with compatible epoxy resins. This approach, which is also extremely simple and straightforward, provides many advantages. Firstly, it opens the door to nearly unlimited formulation options with adaptable viscosity, curing behavior, and thermo-mechanical properties. The properties were either maintained or enhanced compared to virgin homopolymers. Moreover, the high adhesion was maintained, resulting in composites with high mechanical properties. A specific formulation was investigated in depth to implement it in RTM. The hybrid matrix displays a synergetic effect that significantly increases the dynamicity, allowing faster and more efficient reshaping or welding of composite. The matrix can also be cleaved under mild conditions, allowing the fibers to be recovered without noticeable degradation. While from a material viewpoint, PHUs alone cannot be considered ideal for composites, PHU chemistry could become a major asset when hybridized with EP resin.

The sustainability of this strategy was also investigated in the final chapter by demonstrating lower impacts than EP and PHUs. Cyclic carbonates produced from epoxy using supercritical CO_2 appear interesting compared to their epoxy precursor, but their low reactivity hampers the benefits. Hybrid EP-PHU, which can be cured faster, are much more promising. The use of hybrid EP-PHU helps to reduce the environmental footprint of composites. The EoL options enabled by the network could

lead to the chemical recovery of carbon fibers and the mechanical recycling of natural fiber, ensuring positive environmental outcomes.

The life cycle analysis also confirmed the importance of evaluating so-called green chemistries, synthesis, and sustainable strategies to confirm these aspects and help develop relevant solutions for a more sustainable future. Indeed, while monomers can be found sustainable, the change in process and properties can sometimes lead to adverse effects on the material or its life cycle. Additionally, the most effective scenarios are not universally applicable to all materials. As illustrated here, while chemically recycling carbon fiber is interesting, applying this solution to natural fiber composite could harm the environment.

VII.2 Scientific perspectives

Nevertheless, the implementation of PHU chemistry for sustainable composites in a circular economy must undergo several steps before being completely realized. While our work has shown some promise, many questions have not yet been addressed, and further optimization and improvements are expected. Here, we propose to portray some future works that could have a beneficial impact on PHU chemistry, composite materials, and other related applications.

From the hybrid EP-PHU perspective, only one amine has been investigated as the curing agent in this work. However, the molecular structure of the curing amine can lead to significant differences in reactivity and final properties due to steric hindrance and basicity. This also includes the dynamicity of the network and the depolymerization efficiency. Investigating the effect of amine upon such aspects would help the understanding of the chemistry, assist in developing a more dynamic network, and facilitate better control over the rheological and curing behavior of these hybrid formulations. By achieving a comprehensive understanding, hybrid EP-PHU could unlock more applications and processes, both in composite materials and beyond. Moreover, understanding how the molecular structure of cyclic carbonate, epoxy resins, and amines interact would be highly beneficial in designing and selecting other monomers from renewable resources. Although these questions are very academic research-wise, they could later benefit many industries, providing valuable insights into the understanding of CAN chemistry, interactions, and optimization. The use of non-toxic catalysts, either for curing or reprocessing, could also be further explored. The toxicity of the involved compounds should also be assessed to definitely ensure the safety of cyclic carbonate, which remains so far an assumption.

From the composite perspective, the interactions at the fiber/matrix interface have only been investigated by macroscale tests and microscopic observations. The interface of natural fibers is intricate

and less advanced than that of synthetic fibers. In particular, the physicochemical composition of natural fibers and their irregular shape represents the main hurdle for such work. Advancing the understanding of the adhesion between natural fibers and the matrices, particularly applied to this work in the case of PHU and hybrid EP-PHU could be highly beneficial in the maximization of natural fiber composite properties and the design of adapted matrices. Exploring the interfacial strength through micromechanical tests such as fiber pull-out, micro bond, pushout, and many others, and correlating the micro-mechanical properties to the matrix chemistry and fiber/matrix physicochemical interactions would help the development of more sustainable matrices through the selection of the right functionalities and macromolecular structures. Complementing such results with mechanical models and atomistic simulations would also be helpful. However, such work would require very diverse competencies, from mechanical engineering to polymer chemistry, which are sometimes difficult to gather.

The properties of the PHU, hybrid EP-PHU, and the resulting composites have mostly been discussed based on mechanical quasi-static results. Yet, other properties are critical to predict the durability of structures and ensure their interest. The fire properties of PHUs were found to be slightly improved compared to the benchmark epoxy. A deeper investigation of this aspect should be considered and extended to the hybrid. PHUs are known to be sensitive to moisture and water, disrupting the hydrogen bonds and thus plasticizing the network. Similarly, natural fibers are prone to moisture uptake, being detrimental in many applications. However, the behavior of moistened PHU has been poorly investigated, especially with optimized curing. Again, the structure of the monomers will affect such aspects and should be discussed. Such behavior and its consequences should be interesting to investigate for PHUs, hybrid EP-PHU, and their composites. Particularly, the moisture-induced swelling of natural fibers was shown to generate cracks in the case of non-moisture sensitive matrices (relative to the NF). Exploring more moisture-sensitive matrices that can follow and adapt to the fiber swelling might limit such crack generation and thus prolong the life of the materials. Other properties, such as damping of EP-PHU composites, fatigue, aging, weathering, fracture toughness, or impact, will be needed to further advance these synergetic hybrids and could demonstrate positive outcomes based on the obtained results so far.

Finally, chemical recycling should be pushed forward. Despite numerous trials, no valuable recovery of the matrix or any compounds was achieved. Yet, retrieving the matrix could lead to an interest in recycling natural fiber composites if both fiber and resin are valorized. Selective catalytic pathways could be, therefore, explored. However, recycling, particularly for natural fiber composites, should be

supported by life cycle analysis and, ideally, techno-economic assessment to design the best strategies and support the findings from the outset. Indeed, the interest in economic and environmental recycling lies in the balance between virgin material production and the recycling process.

VII.3 Economical perspectives

PHUs have long been seen and developed as an alternative to polyurethanes to avoid using isocyanates. However, the properties of PHUs still do not match those of PUs. Moreover, one of the most important strengths of PUs is related to the raw material prices and operating costs. PU formulations can be foamed within less than a few minutes at room temperature, starting from raw materials below 5€/kg. This means that production costs (energy, equipment, labor...) are low, resulting in extremely competitive material prices. Therefore, replacing PUs with PHUs does not seem feasible without strong regulations, such as the strict interdiction of isocyanate use, which is unlikely in the near future. This challenge has prevented the industry from investigating and commercializing PHU chemistry so far. As a result, there are no large-scale cyclic carbonate suppliers worldwide, except for small-scale production available at prohibitive prices.

On the other hand, the epoxy market, in particular, as applied to (sustainable) composites, might afford a greater price flexibility. Indeed, there is a growing demand for sustainable matrices in several composite applications, particularly sports and leisure. In such applications, costs can be secondary if the properties are maintained or enhanced and the sustainability is improved, particularly the recycling aspect. In such markets, sustainability can be a selling point and justify slight overpricing. Ski, cycling, and rowing boat companies, to cite only a few of them, are increasing efforts to use recycled materials, biobased composites (natural fibers), and sustainable practices. The hybrid EP-PHU could offer the expected benefits from a lower environmental footprint, advanced properties, and recycling potential that could be highly appealing in these fields. Although EP-PHU hybrids are not the most sustainable thermosets nor the most efficient covalent adaptable networks, it could be a way for industries to familiarize themselves with these new polymer classes. Through their adoption in industries, investment could become more relevant not only in PHU production but also in other CANs. With subsequent scaling, PHUs could become more competitive with other thermosets, including PUs. Additionally, industries and scaling will necessarily leverage new challenges to overcome, thus benefiting the whole market and research world by pinpointing the most important locks and aspects to focus on.

However, for these perspectives to be realized, EP-PHU hybrids require validation at various scales. The actual Technology Readiness Level (TRL) can be estimated between 3 and 4, indicating

experimental proof-of-concept/technology validated in the lab. The production of a demonstrator is likely the next step to perform. This would help further validate the concept, offering a realistic vision to future investors or companies and highlighting the potential. As discussed earlier, sports equipment, produced either by resin transfer molding or prepregs, can be the best option to start with. For example, the manufacturing of a ski pair, a rowing seat, or a sailing foil could serve as initial projects. Small vertical wind turbine blades are sometimes manufactured by RTM and could be another valuable trial. All of these examples usually require less than 3-5 kg of resin, which is feasible considering the typical scales that were tested and the cyclic carbonate production capability. Additionally, the innocuity of cyclic carbonates has not been properly assessed. The increase in cyclic carbonate use will require compliance with health regulations such as REACH in Europe and should, therefore, be thoroughly investigated.

It is evident that there will be an economic interest in CANs and biobased polymers in the next decades. Moreover, the variability of oil prices and supply could lead countries that do not possess oil resources to push towards more stable and local raw materials from renewable resources. The initial discussion about circular economy highlighted the importance of creating an economic ecosystem where industries are not competitors but partners. EP-PHU could foster such an ecosystem by gathering various actors in the composite market that are usually more interdependent. The composite market is more a business-to-business market than other polymer ones.

Chapter VIII

Experimental, Material & Methods

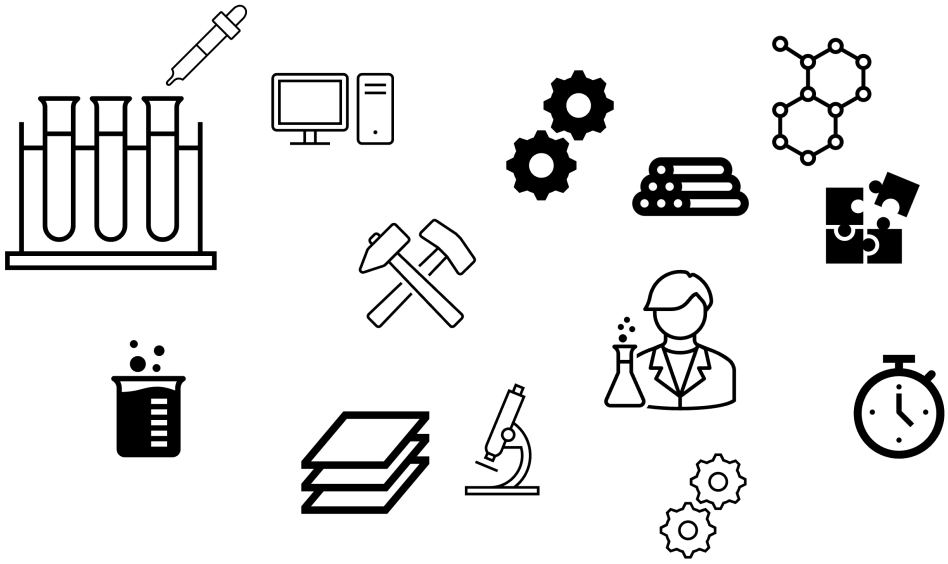

Contents

VIII.1 Description

The present section regroups all materials, methodologies, and parameters used to obtain the presented results.

Methods are regrouped by main domains (materials, synthesis, chemical characterization...). When similar methods with different parameters or slight modifications were employed, the chapter to which the method relates is specified.

VIII.2 Materials

All reagents were used as received without any further purification, except if specified.

VIII.2.1 Epoxy compounds

DENACOL NAGASE Chemtex (Japan) kindly provided trimethylolpropane triglycidyl ether (TMPTGE, DENACOL EX321, biobased grade, Epoxy Equivalent Weight EEW = 145 g/eq, $\eta_{25°C}$ = 0.15 Pa.s), glycerol polyglycidyl ether (GPGE, Denacol EX314, biobased grade, EEW= 143 g/eq, $\eta_{25°C}$ = 0.15 Pa.s), sorbitol polyglycidyl ether (SPGE, Denacol EX-614B, biobased grade, EEW= 172 g/eq, $\eta_{25°C}$ = 5 Pa.s) resorcinol diglycidyl ether (RDGE, DENACOL EX201, EEW = 117 g/eq, $\eta_{25°C}$ = 0.4 Pa.s), and polyethylene glycol (PEGGE, DENACOL EX851, EEW = 151 g/eq, $\eta_{25°C}$ = 0.03 Pa.s).

Pentaerythritol polyglycidyl ether (PEPGE, IPOX CL16eco, EEW= 163 g/eq, $\eta_{25°C}$ = 1 Pa.s), butanediol diglycidyl ether (BDGE, IPOX RD3 eco, EEW = 135 g/eq,$\eta_{25°C}$ = 0.02 Pa.s), and polyglycidyl ether of ethoxylated trimethylolpropane (EOTMPTGE, Ipox CL60, EEW = 380 g/eq,$\eta_{25°C}$ = 0.3 Pa.s) were kindly provided by Ipox Chemicals.

Epoxidized SoyBean Oil (ESBO, EEW= 240 g/eq, $\eta_{25°C}$ = 0.5 Pa.s) was purchased from Vandeputte Oleochemicals.

Diglycidyl ether of bisphenol A (D.E.R.332, Epoxy Equivalent Weight EEW = 175 g/eq), 4,4'-Methylenebis(N,N-diglycidylaniline) (MDGA, EEW = 112 g/eq), and TMPTGE (for chapter 2) were purchased from Sigma-Aldrich.

VIII.2.2 Other chemicals

1,8-Diazabicyclo[5.4.0]undec-7-ene (DBU), tetrabutylammonium iodide (TBAI), 4-(dimethylamino) pyridine (DMAP), ethylene Carbonate (EC), n-butylamine (BA), 1-Dimethylamino-2-propanol,

4-Methyl-2-pentanol, glacial acetic acid, hydrogen peroxide solution (30wt% in water), ethanol (HPLC grade), butyl glycidyl ether (BGE), phenyl glycidyl ether, benzylamine, and propyl isocyanate were purchased from Sigma-Aldrich. m-Xylylene Diamine (MXDA) was either bought from TCI or from Sigma-Aldrich, no differences were observed by NMR or on the results. Carbon Dioxide was provided by Air Liquide.

VIII.2.3 Reinforcements

Flax fiber tape (FlaxTape UD110, 110 $g.m^{-2}$) and quasi-unidirectional flax woven reinforcement (FlaxDry UD180, 180 g/m^2) were purchased from EcoTechnilin. Carbon Fiber quasi-unidirectional tape (CF-UD100, Pyrofil TR50S 15k, 100 $g.m^{-2}$, Mitsubishi) was purchased from Easy Composites EU.

VIII.3 Chemical synthesis

VIII.3.1 General synthesis of cyclic carbonate monomers

All cyclic carbonates were synthesized using CO_2 under supercritical conditions ($scCO_2$) as already reported in previous works [375, 433]. About 60 g of epoxy precursor was converted to its cyclic carbonate counterpart. TBAI catalyst (2.5 mol%) was mixed with the epoxy precursors and poured into a high-pressure 100 mL stainless steel reactor. The reactor was then filled with CO_2 and maintained under supercritical conditions at 80 °C and 110 bar for 24 h at 350 rpm, except for SPGE, which was maintained at 100 °C to avoid the solidification of the product inside the reactor. To remove unreacted CO_2, the resulting yellowish viscous products were degassed several times at 80 °C under vacuum until no bubbling occurred. The extent of the reaction was evaluated by means of ^{1}H-NMR spectroscopy following the complete disappearance of the corresponding epoxy peaks and the appearance of the corresponding carbonate ones.

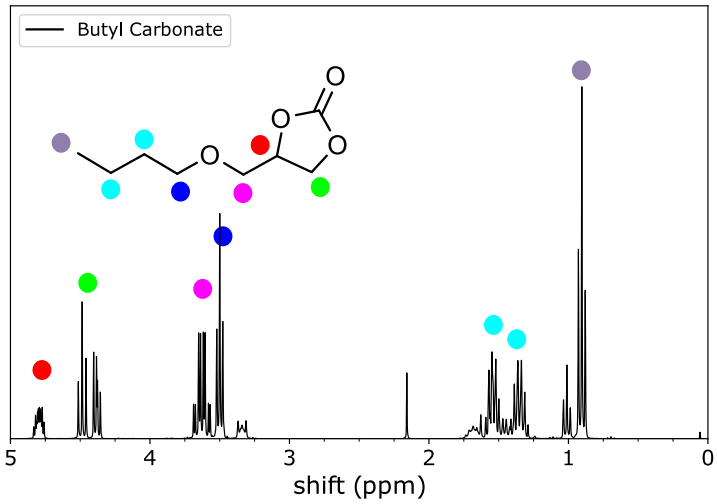

Figure VIII-1 – ^{1}H-NMR in $CDCl_3$ of the butyl carbonate compound

VIII.3.1.1 Synthesis of trimethylolpropane triglycidyl carbonate

In a typical experiment, and similarly as described before, TMPTGE (1 L, 1.157 kg) was transferred into a 2 L high-pressure reactor. Then, 35.29 g of TBAI (2.5 mol% vs TMPTE) was added before closing the cell. The cell was then equilibrated at 80 °C for 24 h, keeping a constant 100 bar CO_2 pressure and a 200 rpm stirring rate. After the reaction, the stirring was stopped, the cell was slowly depressurized at 110 °C, and the viscous product was collected and analyzed by ^{1}H-NMR in $CDCl_3$ (Supp. Fig. 1). TMPTC was produced with a yield of >98% (collected crude product >1.4 kg). The crude was collected, degassed under vacuum, and used without any purification. The obtained product was characterized by ^{1}H-NMR (Fig. VIII-2). Also, a large-scale batch was produced. Shortly, about 25 kg of TMPTGE were introduced in a 50 L high-pressure stainless steel reactor, all conditions were kept identical.

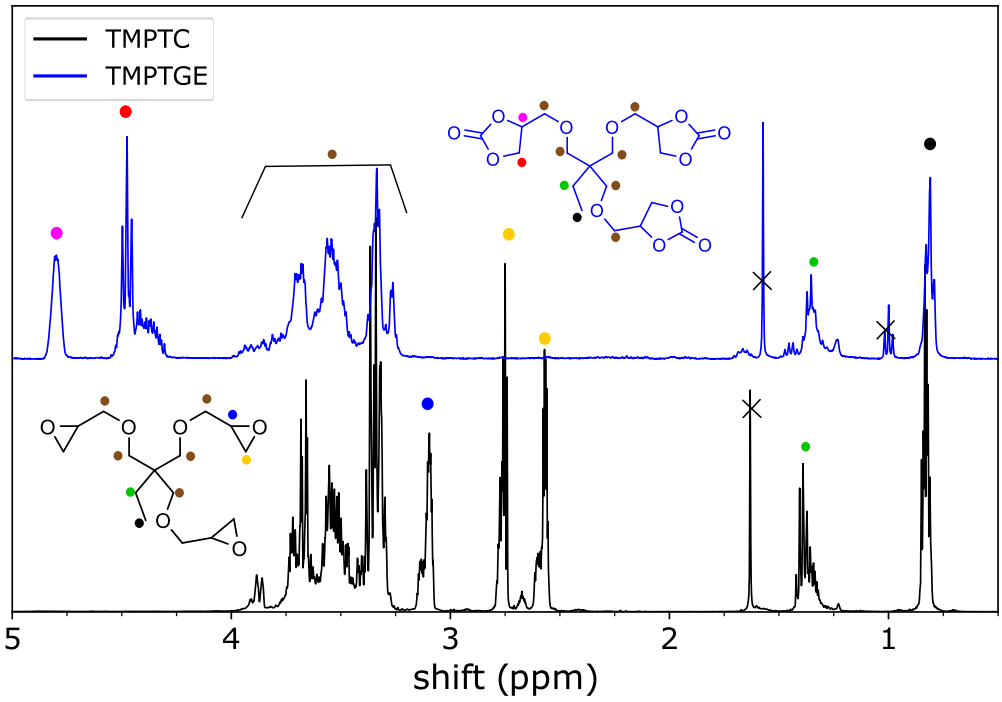

Figure VIII-2 – ^{1}H-NMR in $CDCl_3$ of the epoxy precursor (TMPTGE) and the resulting carbonate (TMPTC)

^{1}H-NMR TMPTGE ($CDCl_3$, ppm): δ = 0.84 (t, 3H, methyl group), 2.6-2.72 (m, 6H, oxirane), 3.12 (m, 3H, oxirane). TMPTC ($CDCl_3$, ppm): δ = 0.84 (t, 3H, methyl group), 4.4-4.5 (m, 6H, cyclic carbonate), 4.83 (m, 3H, cyclic carbonate).

VIII.3.2 Synthesis of the 2-hydroxyethyl n-butylcarbamate (mHU)

For chapter 4, mHU was synthesized as follows: In a 25 mL round bottom flask, ethylene carbonate (EC, 1 eq) was mixed with n-butylamine (1.1 eq) and reacted at 60 °C for 24 h under constant stirring. The crude was then dissolved in ethyl acetate and washed with water 3 times to remove the unreacted excess of amine. The product was then dried using anhydrous sodium sulfate. Ethyl acetate was then removed using a rotary evaporator. The obtained product was characterized by ^{1}H-NMR (Fig. VIII-3). 2-hydroxyethyl n-butylcarbamate ($CDCl_3$,ppm) : 4.20 (t,CH_2), 3.80 (t,CH_2), 3.20 (m,CH_2), 1.49 (m,CH_2) , 1.36 (m,CH_2), 0.92 (t,CH_3)

For Chapter 5, for the sake of a more simple process, slight modifications in the purification step were made. No difference in results could be found (except for faster workup and slightly higher yield). Ethylene carbonate (EC, 1 eq) was mixed with n-butylamine (1.1 eq) and reacted at 60 °C for 24 h under constant stirring. The crude was then dissolved in methanol and filtered through a short acidic

silica column to eliminate the excess amine. Methanol was then eliminated using a rotary evaporator.

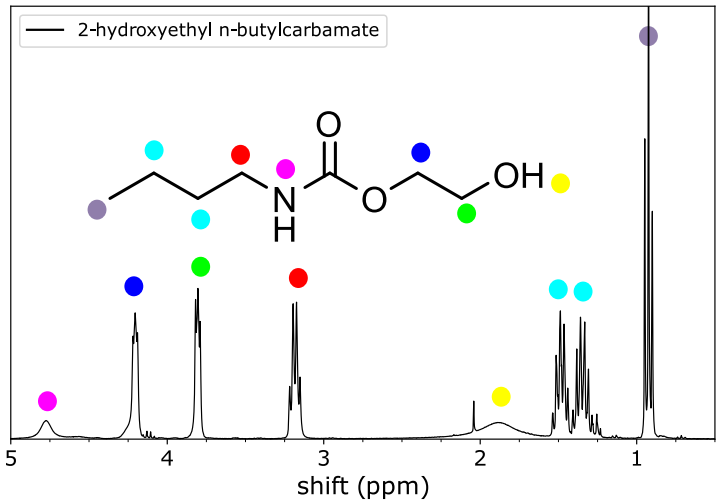

Figure VIII-3 – ^{1}H-NMR in $CDCl_3$ of the 2-Hydroxyethyl n-butylcarbamate (mHU) model compound

VIII.3.3 Ethyl n-propylcarbamate

Ethyl n-propylcarbamate (mU) was synthesized in a 25 mL round bottom flask. In a large excess of dry ethanol (10 eq) under constant stirring, propyl isocyanate (1 eq) was added dropwise and left to stir at room temperature for 1 h. The excess ethanol was then removed by vacuum evaporation. No further purification was conducted. The obtained product was characterized by ^{1}H-NMR (Fig. VIII-4).

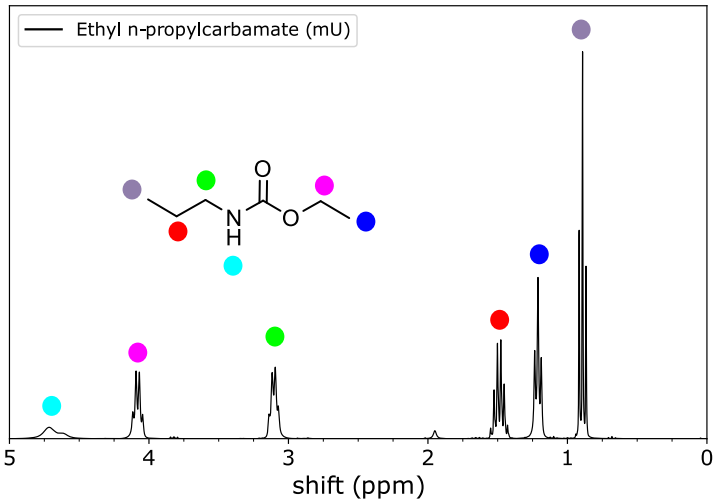

Figure VIII-4 – ^{1}H-NMR in $CDCl_3$ of the ethyl n-propylcarbamate (mU) model compound

VIII.3.4 1-Benzylamino-3-butoxy-propan-2-ol

1-Benzylamino-3-butoxy-propan-2-ol (mEP) was synthesized by mixing BGE (1 eq) with n-butylamine (1.1 eq) in a 25 mL round bottom flask and reacted at 60 °C for 24 h under constant stirring. The crude was then dissolved in methanol and filtered through a short acidic silica column to eliminate the amine excess. Methanol was then removed using a rotary evaporator. The obtained product was characterized by ^{1}H-NMR (Fig.VIII-5).

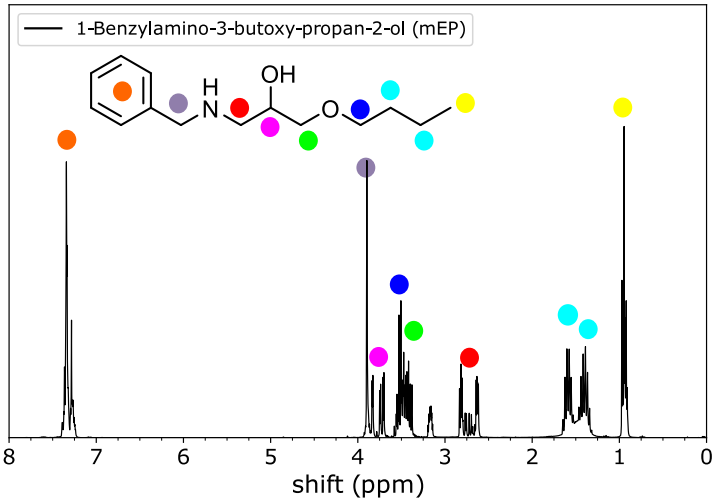

Figure VIII-5 – ^{1}H-NMR in $CDCl_3$ of the 1-Benzylamino-3-butoxy-propan-2-ol (mEP) model compound

VIII.3.5 Model reactions

VIII.3.5.1 Transcarbamoylation model reaction

Model reactions between the model hydroxyurethane compound (2-hydroxyethyl n-butylcarbamate) and model epoxy compound (1-dimethylamino-2-propanol) were carried out under various temperatures. The two components were mixed in an equimolar ratio and aliquots of the reaction mixture were sampled over time. The reactions were monitored by ^{1}H-NMR in $CDCl_3$ to determine the exchange by following the ethylene glycol signal. For the sake of comparison, the same reaction was conducted with 4-Methyl-2-pentanol which does not possess the catalyzing amine. The reaction was conducted at 120 °C for 24h.

VIII.3.5.2 Kinetic aminolysis study

The aminolysis of both BGC and PGE was monitored by ^{1}H-NMR in $CHCl_3$. For the cyclic carbonate aminolysis study, 0.5 g of BGC (2.8 mmol) was weighed in a 5 mL vial. Then, 0.307 g (2.8 mmol, 1 eq) of benzylamine (BzA) were added. In the case of the epoxy "catalyzed" formulation, 0.5 eq of mEP (0.34 g) was added. The formulation was vortexed for 30 s to ensure a homogeneous mixture. Then, the vial was let under magnetic stirring at 25 °C and an aliquot was regularly taken to be analyzed. The aminolysis rate was studied through the disappearance of both the cyclic carbonate characteristic peak (4.8 ppm) and CH2-NH2 peak (3.9 ppm) and related to the formed hydroxyurethane.

Similarly, in the epoxy aminolysis study, 0.5 g of PGE (3.3 mmol) was weighed in a 5 mL vial. Then, 0.357 g (3.3 mmol, 1 eq) of benzylamine (BzA) were added. In the case of the urethane "catalyzed" formulation, 0.5 eq of mU (0.21 g) was added. In the case of the hydroxyurethane "catalyzed" formulation, 0.5 eq of mHU (0.265 g) was added. The formulation was vortexed for 30 s to ensure a homogeneous mixture. Then, the vial was let under magnetic stirring and an aliquot was regularly taken to be analyzed. The aminolysis rate was studied through the disappearance of both the epoxy characteristic peak (3.4 ppm) and CH2-NH2 peak (3.9 ppm), and related to the formed amino-alcohol.

VIII.4 Material manufacturing

VIII.4.1 Polymerization protocol of PHU thermosets

PHU thermosets were crosslinked using a CC/amine ratio of 1:1. The amount of amine was calculated using eq.(VIII.1). The carbonate monomer was degassed under vacuum at 60 °C for one hour in order to remove any potential trapped air bubbles prior to use. MXDA was then added, and the mixture was thoroughly hand-mixed for 5 minutes at room temperature. The as-obtained mixture was then poured into 60 °C preheated PTFE mold and pressed in a Carver 4122CE manual thermopress at 80 °C and 3 bar for 15 hours. The pressure was then released and the curing was completed in an oven at 100 °C for 4 h. A post-curing step of 30 min at 150 °C was finally applied to ensure a fully cured system. Prior to any tests, samples were conditioned at 23 °C and 50% relative humidity for 2 days. Once cured, the PHU formulation is referred as p("Carbonate"-MX), p indicating that the formulation is polymerized, "Carbonate" being the used CC (TMPTC for example) and MX the curing agent (m-Xylylene diamine).

$$m_{MXDA} = m_{CC} * \frac{AHEW}{CEW} \tag{VIII.1}$$

with m_{MXDA} and m_{CC} being the mass in grams of MXDA and CC respectively. AHEW and CEW are the Amine Hydrogen Equivalent Weight and Carbonate Equivalent Weight in g/eq respectively.

VIII.4.2 Polymerization protocol of EP and PHU thermosets (chapter 3)

To expedite the curing process of PHU, 1 mol% of DMAP was used as a catalyst. The choice of catalyst and load was made based on an internal study, which revealed no alterations in the network structure or final properties but enhanced curing process. Related results from this study can be found in Chapter 3.

All epoxy and PHU thermosets were cured with an equimolar ratio of reactive functions in a similar procedure as previously explained. The precursors were degassed under vacuum at 60 °C for one hour before use. The PTFE molds were preheated at 60 °C. After adding the MXDA hardener to the monomer, the mixture was mixed manually for 5 minutes. The homogeneous mixture was poured into the mold of the wanted shape and pressed at 80 °C and 3 bar for 2 hours followed by one hour at 100 °C in an oven. A final post-curing of 1 h at 150 °C was performed to complete the curing.

VIII.4.3 Polymerization protocol of the hybrid epoxy/PHU networks

The epoxy monomer (resorcinol diglycidyl ether) and the cyclic carbonates (trimethylolpropane tricarbonate) were mixed in different weight ratios (0%, 25%, 50%, 75%, 100%) and degassed before use. The amine hardener (mXDA) was added in an equimolar ratio between reacting functions using eq.VIII.2. The mixture was manually mixed for 3 minutes. The curing was performed in PTFE molds for 30 min at 80 °C followed by a post-curing step of 1 h at 160 °C to guarantee full curing.

$$m_{NH_2} = m_{monomer} \times (\%CC \times \frac{AHEW}{CEW} + \%EP \times \frac{AHEW}{EEW}) \quad \text{(VIII.2)}$$

For chapter 4 (before curing optimization), the curing was performed for 2 h at 80 °C followed by a post-curing step of 1 h at 160 °C to guarantee full curing.

VIII.4.4 Flax and carbon unidirectional composite manufacturing (chapter 3)

Flax unidirectional hand lay-up laminates (200x150 mm^2) were manufactured by thermocompression with a $[0]_6$ stacking sequence. To impregnate the fibers, the epoxy-amine and CC-amine mixture were prepared by weighting about 1.4 times the mass of fibers. The plies were stacked in a 60 °C preheated Teflon-coated steel mold with a line of resin. This process was reported to provide high fiber volume content with fairly viscous resins and natural fibers [167]. The two axial edges were left free to allow air and matrix excess to flow out. The mold was gradually pressed to 4 bar to ensure an entire impregnation of the fibers and cured following the protocol described in section VIII.4.1, i.e. 2 h at 80 °C, followed by 1 h at 100 °C. The post-curing was conducted in an oven after unmolding for 1 h at 150 °C. The flax-PHU and flax-epoxy composite are referred to as F-PHU and F-EP, respectively. Carbon fiber composites in chapter 3 were manufactured similarly, replacing flax reinforcement by carbon tape.

Sections were precisely cut from the obtained plates using a metallic guillotine to prepare the samples. Before testing, these samples were conditioned at 23 °C and 50% RH to guarantee moisture equilibrium. The fiber mass was estimated from the reinforcement areal weight using eq.(VIII.14). Fiber volume fraction (V_f) was calculated using eq.(VIII.15) and void content (V_v) was calculated using eq.(VIII.16).

VIII.4.5 Carbon fiber composites with hybrid matrices

Unidirectional composite laminates made of 10 plies of carbon fibers were manufactured by hand lay-up and cured by thermocompression. To impregnate the fibers, the polymer mixture was prepared by weighting about 1.2 times the mass of fibers. The plies were stacked in a Teflon-coated steel mold (200x150 mm^2). Between each ply, a layer of resin was applied. The two edges in the mold length were left open to allow air and matrix excess to flow out from the mold. The mold was then placed into a heating press and a pressure of 8 bar was slowly applied to ensure an entire impregnation of the fibers. The plates were then cured under this pressure for 2 h at 80 °C. After unmolding, the post-curing was conducted in an oven at 160 °C for 1 h. Samples were precisely cut from the obtained plates using a metallic guillotine for testing. Before testing, these samples were conditioned at 23 °C and 50% RH to guarantee moisture equilibrium. The fiber mass was estimated from the reinforcement areal weight using eq.(VIII.14). Fiber volume fraction (V_f) was calculated using eq.(VIII.15) and void content (V_v) was calculated using eq.(VIII.16).

VIII.4.6 Resin Transfer Molding (RTM) of flax composites

Flax composite laminates were manufactured by RTM using a single-component CIJECT 3.0 system supplied by DIATEX. An aluminum mold of 120 x 120 x 3 mm^3 was used. A Zyvax® (Chemtrend) releasing agent was employed to coat the mold and ease the unmolding. The flax quasi-unidirectional reinforcement was precisely cut to the mold size (120 x 120 mm^2) and placed into the RTM mold. A stacking sequence of $[0/(0/90)_2/\bar{0}]_S$ (11 plies) was utilized to mimic a real case scenario with a complex lay-up and different fiber orientations. The mold was then sealed by applying 30 kN pressure in a Fontjine hydraulic press. The mold was preheated for 30 min at 60 °C. In the meantime, 150 g of co-monomers (with various ratios, see section 2.3.1) and hardener were prepared by manual mixing in a disposable steel pot. The pot containing the mixture was placed into the RTM tank and injected into the mold using a nitrogen flow through PTFE tubes. Once the co-reagents mixture was going out of the tube placed at the exit of the mold, meaning its complete filling, the PTFE tubes were clamped with a steel clamp. The mold was maintained under pressure for 30 min at 80 °C. After, the plates were cooled to room temperature and later unmolded. A post-curing step of 1 h at 160 °C was performed to ensure complete curing.

VIII.5 Material reprocessing & recycling

VIII.5.1 Reprocessing of polyhydroxyurethane thermosets

The as-cured PHU thermosets were ground into a fine powder using a cryomill's cryogenic vibratory mill. The samples used for tensile testing were first cut into small pieces and then ground three times for 3 minutes in a cryogenic vibrating chamber with 3 steel balls. The powder was then poured into a Teflon-coated 70x70 mm^2 steel mold. The mold was preheated to 160 °C in a press for 15 min. After that, a 6 MPa pressure was slowly applied and maintained for 15 h. The mold was then removed from the press and cooled down at room temperature. The as-obtained film was then removed from the mold and cut for DMA and FTIR analyses. The samples were also immersed into THF in order to evidence the welding of the samples via the formation of covalent bonds at high pressure.

VIII.5.2 Welding of flax-PHU pre-preg

Single-ply laminates were manufactured under the same condition described in section VIII.4.4. The single-ply thick sheet was then cut into 70x70 mm^2 square. Six plies were then stacked into an adapted

steel mold with a Teflon protective layer. After a preheating step of 15 min in a press, 3 kT force (around 6 MPa) was applied. Both temperature and pressure were maintained for 15 hours to efficiently weld the laminates. The obtained plate was then unmolded and cut into three-point bending test samples with a guillotine. The protocol was fixed to ensure the best results given the previously obtained conditions published in [462].

VIII.5.3 Reprocessing of the hybrid EP-PHU thermosets

The as-cured thermoset was cut into pieces. The mold was preheated to 180 °C in a press for 30 min. After that, a 6 MPa pressure was slowly applied and maintained for 20 min. The mold was then removed from the press and cooled down at room temperature. The as-obtained film was then removed from the mold and cut for analysis. The samples were also immersed into THF to evidence the welding of the samples via the formation of covalent bonds at high pressure.

VIII.5.4 Reshaping and welding of the cured composites

The reshaping of the composite was conducted in a Teflon-coated V-shaped aluminum mold in a hydraulic press. The mold was first preheated at 180 °C. A unidirectional cured CFRP panel was then put in the mold without pressure for 15 min to preheat. The pressure was slowly applied up to 5 MPa and maintained for 30 min. The press was then water-cooled and the reshaped composites unmolded.

VIII.5.5 Chemical recovery and recycling of the fibers

The degradation solution was prepared by mixing in a mass ratio of 80:20 glacial acetic acid and hydrogen peroxide (water solution 30 %wt). The composite material (10 g) was roughly cut into large pieces and put in a 250 mL round bottom flask with 250 mL of the oxidative solution. The mixture was heated to 60 °C until complete degradation of the matrix (around 4 h) under constant magnetic stirring. For flax composites, the mixture was heated to 60 °C until complete degradation of the matrix within 2 h under constant magnetic stirring.

The fibers were then recovered by filtration and washed several times with deionized water until a neutral pH was obtained. The fibers were then dried overnight in a ventilated oven at 60 °C. The reclaimed fibers were reused as a reinforcement using the hybrid matrix (50%EP-50% PHU) by impregnation under thermo-compression. For such, 4 g of fibers were compressed together to preshape the reinforcement. Then, 6 g of the hybrid resin mixture was poured into the mold. The composite was then pressed to 4 bar at 80 °C for 1 h and further post-cured one hour in an oven at 160 °C.

VIII.6 Chemical characterization

VIII.6.1 NMR spectroscopy

^{1}H-NMR was used to determine the (macro)molecular structures of chemical compounds and follow model reactions using a Bruker AMX-500 instrument. Sixteen scans were performed at room temperature at a frequency of 500 MHz. The chemical shifts are given in ppm. Around 10 mg of products were dissolved in 0.6 mL of deuterated solvents, mostly deuterated chloroform. When compounds were not soluble in $CDCl_3$, DMSO-d_6, was used (specified in that case). For chapters 4 and 5, measurements were carried out on a Bruker Advance 300 (300 MHz).

VIII.6.2 Carbonate Equivalent Weight

(CEW) was evaluated by means of ^{1}H-NMR using an internal standard following Cornille et al. work [378]. A solution of approximately 15 mg of toluene, 25 mg carbonate product, and DMSO-d6 was prepared and poured into NMR tubes. The resulting weight of these mixtures was determined by gravimetry. The CEW was calculated using eq.(VIII.3).

$$CEW(g/eq) = \frac{M_n}{functionnality} = \frac{m_{c_5} * I_{CH_3} * M_{toluene}}{(I_a + I_b + I_c) * m_{toluene}} \quad \text{(VIII.3)}$$

with m_{c_5} the mass of carbonate, I_{CH_3} the methylene integration values of Toluene (2.92 ppm) fixed at 300, $M_{toluene} = 92.138$ g/mol the molar mass of toluene, I_a, I_b, I_c, the integration of carbonate peaks at 4.29, 4.40 and 4.92 ppm respectively, and $m_{toluene}$ the mass of toluene.

VIII.6.3 Fourier-transform infrared spectroscopy (FTIR)

A Bruker FTIR Tensor 27 spectrometer was employed for FTIR in attenuated total reflectance mode with a 4 cm^{-1} resolution over 4000–600 cm^{-1} range, 32 scans were performed.

VIII.6.4 Mass spectrometry

Mass spectrometry (MS) of synthesized CCs was recorded on a Matrix-assisted laser desorption/ionization mass spectrometer (MALDI-MS) using a Waters QToF Premier mass spectrometer equipped with a Nd:YAG (third harmonic) operating at 355 nm with a maximum output of 65 μJ delivered to the sample in 2.2 ns pulses at 50 Hz repeating rate. Time-of-flight mass analyses were performed in the reflectron mode at a resolution of about 10000. All samples were analyzed using

trans-2-[3-(4-tert-butylphenyl)-2-methylprop-2-enylidene]malononitrile (DCTB) as matrix [533], which was prepared as a 40 $mg.mL^{-1}$ solution in $CHCl_3$. This solution (1 μL) was applied to a stainless-steel target and air-dried. Therefore, 1 μL of this solution was applied to the target area already bearing the matrix crystals and air-dried. The molecular weight of the synthesized carbonates was estimated using eq.(VIII.4).

$$M_n = \frac{\sum_{n=1}^{n} I_i * M_i}{\sum_{n=1}^{n} I_i} \tag{VIII.4}$$

with I_i the intensity of the identified peak as an approximation of the molar composition and M_i its respective mass.

VIII.6.4.1 High-resolution mass spectrometry (HRMS)

HRMS (chapter 4) was measured with a Waters modelo SYNAPTTM G2 HDMSTM, using a Q-TOF detector and negative electrospray ionization ESI+, and elution of the sample was done using $CHCl_3$.

VIII.6.5 X-ray photoelectron spectroscopy (XPS)

XPS measurements were performed on a Versaprobe III Physical Electronics (ULVAC) system with a monochromatic Al Kα radiation source (1486.7 eV). An initial analysis was carried out to determine the elements present (wide scan: step energy 0.2 eV, pass energy 224 eV) and detailed analyses were carried out on the detected elements (detail scan: step energy 0.05 eV, pass energy 27 eV, time per step 20 ms) with an electron exit angle of 45º. The spectrometer was previously calibrated with Ag (Ag 3d5/2, 368.26 eV). The spectra were fitted using the CasaXPS 2.3.26 software, which models the contributions after a background subtraction (Shirley).

VIII.7 Physical characterization

Before all tests, conditioning was applied for at least 48 h at 23 °C under a relative humidity of 50 ± 5%.

VIII.7.1 Rheological measurements

Rheological properties of the thermosets during curing were measured using an Anton Paar Modular Compact Rheometer MCR302. Two disposable parallel aluminum plates of 25 mm diameter, with a 1 mm air gap were used. A 2% strain was applied at 1 Hz. About 1.5 g of the investigated mixture was poured into the bottom plate.

Non-isothermal analyses were performed from 25 °C to 200 °C at a 10 °C/min heating rate.

Isothermal rheological analyses for PHU thermoset curing were performed at 80 °C with the aforementioned parameters.

The viscosity of synthesized CC, and hybrid monomers mixtures as a function of temperature was measured from 25 °C to 150 °C following the same described protocol.

VIII.7.2 Thermogravimetric Analyses (TGA)

TGA was performed on a TGAQ500 from TA Instruments. About 10 mg of the product was weighed. The analyses were conducted from 25 to 800 °C following a 20 °C/min heating ramp under a N_2 flow of 60 mL.min^{-1}.

VIII.7.3 Differential Scanning Calorimetry

(DSC) was conducted on a TA Instruments DSC Q2000. About 10 mg of product was weighed in an aluminum pan. For polymers, two heating ramps from -80 °C to 200 °C at 10 °C/min heating rate were performed under N_2 atmosphere.

VIII.7.3.1 Matrix curing analyses

The formulations' curing behavior in Chapter 5 was investigated by DSC using a TA instruments Discovery 25 apparatus with aluminum hermetic pans. About 5 mg of the uncured system was precisely weighed. Non-isothermal curing analyses were performed from 25 °C to 220 °C at 5, 10, and 20 °C/min heating rates. Isothermal curing was performed at 80 °C for 1 hour with a 10 °C/min heating ramp to reach the targeted temperature.

VIII.7.4 Dynamical Mechanical Analyses (DMA)

DMA were conducted on a TA Instruments DMA Q800 in tension mode. Rectangular samples of 20x8x0.8 mm^3 were used. The gauge length was fixed at 10 mm. The DMA analysis was performed from 25 to 180 °C at a 3 °C/min heating rate. 0.1% strain was applied at 1 Hz. The DMA results were used to determine the crosslinking density ($\nu_{E'}$) of samples using rubber elasticity theory as described in eq.(VIII.5).

$$\nu_{E'} = \frac{E'_{T_{\alpha+50}}}{3RT_{\alpha+50}} \tag{VIII.5}$$

with $T_{\alpha+50}$ being the temperature of the rubbery plateau set 50 K after the α transition taken at the maximum of the tanδ curve, $E'_{T_{\alpha+50}}$ the storage modulus in Pa at the specified temperature and R the perfect gas constant (8.314 J.mol^{-1}K^{-1}).

VIII.7.5 Monotonic tensile tests of pure polymers

The mechanical properties of the neat matrices were investigated through monotonic tensile testing on a ZwickRoell Z2.5 equipment up to failure with a 2.5 kN load cell at a 1 mm/min displacement rate according to ASTM D638 standard requirements [534]. For each formulation, five dog-bone type V samples were tested. Elastic Modulus was computed between 0.1% and 1.0% strain by linear regression.

VIII.7.6 Monotonic tensile tests of composites (chapter 4)

Composite materials were tested following the ASTM D3039 standard with a 50 kN cell at a 1 mm/min displacement rate up to failure. Samples of dimension 200 x 15 x 0.9 mm^3 were used. The strain was measured using a 50 mm extensometer. Tabs made of glass fiber composites (40x15x3 mm^3) with sandpaper were used to avoid sample slip from grips.

VIII.7.7 Three-point monotonic bending tests

The three-point monotonic bending properties of the composites as ascribed in ASTM D790, were investigated in both parallel and perpendicular to fibers' orientation load orientation. Five rectangular samples were tested with a 50.8x12.7x manufactured thickness mm^3 geometry at 1 mm/min. A 0.1 MPa preload was used to ensure perfect contact. A span length of 32 mm was used. The bending modulus was evaluated between 0.1 and 0.5% bending strain by linear regression.

The three-point monotonic bending properties for pure polymers were measured according to ASTM D790, similarly to previously described. The samples were rectangular with 50.8x12.7x 3 mm^3.

VIII.7.8 Charpy Impact Toughness

Flatwise Charpy unnotched impact tests were carried out on a Ray-Ran 2500 pendulum impact tester. A hammer of 0.668 kg with a 3.46 m/s impact speed was used to apply 2.71 J impact energy.

VIII.7.9 Stress Relaxation

Stress relaxation tests were conducted on the DMA Q800 in tension mode. Rectangular samples of 20x8x0.8 mm^3 were used. The gauge length was fixed at 10 mm. Once the specified temperature was reached, the sample was held for 5 min before applying a 1% strain. Stress relaxation of the dynamic crosslinked network is defined using a Maxwell model as described in eq.(VIII.6). The dynamic covalent behavior was highlighted using the Arrhenius relationship by plotting τ^* as a function of 1/T as shown in eq.(VIII.7).

$$\frac{G(t)}{G_0} = e^{\frac{-t}{\tau^*}} \tag{VIII.6}$$

$$\tau^* = \tau_0 e^{\frac{E_a}{RT}} \tag{VIII.7}$$

$$\tag{VIII.8}$$

with G being the relaxation modulus in MPa, τ the time constant in second, E_a the activation energy in kJ/mol, R the perfect gas constant (8.314 $J.mol^{-1}.K^{-1}$), T the temperature in Kelvin.

The hypothetical topology freezing temperature (T_v) where the material is theoretically switching from solid to liquid behavior due to the exchange mechanisms within the network was estimated at the relaxation time $\tau^*_{T_v}$ using eq.(VIII.9) and eq.(VIII.10) [319, 535].

$$\tau^*_{T_v} = \frac{3\eta}{E'_{rubbery}} \tag{VIII.9}$$

$$T_v = \frac{1000 E_a}{(\ln \tau^*_{T_v} - \ln \tau_0) R} - 273.15 \tag{VIII.10}$$

VIII.7.10 Tensile Creep

Polymer creep behavior was measured in the DMA instrument with the same sample geometry as DMA and stress relaxation. The samples were heated at the desired temperature and maintained for 5 min to ensure equilibrium. Then, a 0.5 MPa stress was applied for 60 minutes, and the strain was recorded.

VIII.7.11 Vertical UL94 burning test

According to ASTM D3801-2010, samples of dimensions of 130 mm × 14 mm x 6 plies (as manufactured) were used to assess the fire behavior of the composites. Ignition for 10 s in air atmosphere was done using a Bunsen burner.

VIII.7.12 Density measurement

Density measurements have been conducted using Archimede's principle. Small square samples (for composites) of 10x10 mm^2 were laser cut. They were first weighed in air and then weighed in ethanol. Density was then calculated using (VIII.11) Three samples have been evaluated for each configuration to average results.

$$\rho = \frac{M_{air}}{M_{air} - M_{ethanol}}(\rho_{air} - \rho_{ethanol}) + \rho_{ethanol} \tag{VIII.11}$$

with M_{air} and $M_{ethanol}$ being the weight of the sample in the air and in the ethanol respectively. Fluid densities were taken as $\rho_{ethanol} = 0.79$ g/cm^3 and $\rho_{air} = 0.0012$ g/cm^3.

VIII.7.13 Swelling Index, Gel Content and Water Uptake of PHU thermosets

To determine both swelling index (SI) and gel content (GC) of the formulations, three samples of about 20 mg were weighted (m_0) and soaked in a polar (THF) and non-polar (toluene) solvent. Samples were then collected, excess solvent was removed using absorbent paper, and then weighted (m_1). SI was calculated using eq.(VIII.12). The same samples were then dried at 80 °C under vacuum for 24 h and weighted (m_2). The GC was calculated using eq.(VIII.13)

$$SI = \frac{m_1 - m_0}{m_0} * 100 \tag{VIII.12}$$

$$GC = \frac{m_2}{m_0} * 100 \tag{VIII.13}$$

Moisture uptake (MU) and Water uptake (WU) of PHU thermosets were assessed. PHU samples of about 50 mg were weighed (m_{0a}) and dried for 24 h at 80 °C in a vacuum oven. Samples were then weighed again (m_{0b}) and dipped into demineralized water. After 24 h, samples were taken back and excess water was removed using absorbent paper and weighed again (m_1). The water uptake was calculated using the same formula as the SI measurement using (m_{0a}) for MU and (m_{0b}) for WU.

VIII.7.14 Tensile testing of the flax yarns

The tensile testing of virgin and recovered flax yarns was performed using a capstan system (Fig. VIII-6) to guarantee systematic failure within the span length. A 70 mm span length was used. The test speed was set to 1 mm/min.

Figure VIII-6 – Flax yarn tensile testing capstan set-up.

VIII.8 Optical and morphological characterization

VIII.8.1 Atomic force microscopy (AFM)

A Dimension Icon AFM with RTESPA 300 cantilevers (Bruker Corp.) was used to obtain the AFM Peak Force Tapping (PFT) measurements. The cantilevers possess a spring constant around 40 Nm^{-1} and a tip radius of 8 nm. The deflection sensitivity was determined with the help of a sapphire sample. The areas scanned were between 1.5 and 50 μm^2. The generated data were analyzed with the help of the Nanoscope Analysis software. Samples were prepared without embedding and cut with a diamond knife at -80 °C.

VIII.8.2 Scanning Electron Microscopy (SEM)

SEM images were taken out on a Hitachi's STEM FEG SU8020 instrument with 5.0 nm resolution in general mode up to 2.0 nm at 5 kV. Voltage ranged from 0.1 to 30 kV, and the magnification varied from 20 to 800k. A platinum-palladium coating of 9 nm was sprayed on samples. For Chapter 5, a tungsten coating was used. It provides a more homogeneous coating with better achievable resolution.

For Chapter 4, SEM was performed with a HITACHI TM3030Plus Tabletop Scanning Electron Microscope (SEM) at 15 kV. Polymer samples were gold-coated in an SC7620 Mini Sputter Coater (Quorum).

VIII.8.3 Fiber and porosity volume fraction

The fiber mass was calculated using eq.(VIII.14). Fiber volume fraction (V_f) was calculated using eq.(VIII.15) and void content (V_v) was calculated using eq.(VIII.16).

$$m_f = n \times A_r \times S \tag{VIII.14}$$

$$V_f = \frac{\frac{m_f}{\rho_f}}{\frac{m_f}{\rho_f} + \frac{m_c - m_f}{\rho_m}} \tag{VIII.15}$$

$$V_v = 1 - \rho_c\left(\frac{w_m}{\rho_m} + \frac{w_f}{\rho_f}\right) \tag{VIII.16}$$

in which n is the plies quantity, S is the sample's cross-section area, and A_r is the flax tape areal weight. ρ_x, m_x, and w_x refer to the density, the mass, and the weight fraction respectively. f subscript refers to fibers, m to the matrix, and c to the composite. Flax' density was chosen from the supplier technical data sheet at 1.39 g/cm^3 for flaxtape and 1.45 g/cm^3 for flaxdry.

VIII.9 Analytical, numerical models, and calculations

VIII.9.1 Chamis' micromechanical model - Modulus prediction

To normalize the experimental values and thus obtain an estimation of the adhesion efficiency, the Chamis' micromechanical model [536] was used. Chamis' model was preferred to the traditional Rule-Of-Mixture for its better estimate of the elastic properties. The dramatic effect of porosities on the properties was not considered due to the uncertainties of its measurements and the low differences between the manufactured samples. The theoretical longitudinal bending modulus was computed

using eq.(VIII.17) and the theoretical transverse modulus was calculated using eq.(VIII.18). Matrix properties were taken from the present study. Reinforcement properties are summarized in Supp.Tab.2.

$$E_{L_{th}} = V_f E_{11_f} + (1 - V_f) E_m \tag{VIII.17}$$

$$E_{T_{th}} = \frac{E_m}{1 - \sqrt{V_f}(1 - E_m / E_{22_f})} \tag{VIII.18}$$

where E_m is the matrix modulus, E_{11_f} and E_{22_f} are the fiber longitudinal and transverse modulus respectively.

VIII.9.2 Classical Laminate Theory

To allow the comparison of the present work with the literature, the classical laminate theory (CLT) was used to predict the properties of each laminate. Chamis' micromechanical model [536] was used first to predict the local properties of a single ply using eq.(VIII.17) and eq.(VIII.18) for the longitudinal and transverse modulus, respectively. Poisson ratio were calculated from eq. (VIII.19) and (VIII.20). Matrix properties were taken from the present study (subscript m), the Poisson ratio was set to 0.4. The reinforcement properties (Ecotechnilin FlaxDry UD180) were back-calculated from the technical datasheet of the supplier ($E_{11_f} = 35$ GPa, $E_{22_f} = 8$ GPa, $\nu = 0.49$).

$$\nu_{12} = V_f \nu_f + V_m \nu_m \tag{VIII.19}$$

$$\nu_{21} = \nu_{12} \frac{E_2}{E_1} \tag{VIII.20}$$

From Chami's modulus, the stiffness matrix Q is calculated in the ply local coordinates.

$$Q = \begin{bmatrix} Q_{11} & Q_{12} & 0 \\ Q_{12} & Q_{22} & 0 \\ 0 & 0 & G_{66} \end{bmatrix} \tag{VIII.21}$$

$$Q_{11} = \frac{E_1}{1 - \nu_{12}\nu_{21}} \tag{VIII.22}$$

$$Q_{22} = \frac{E_2}{1 - \nu_{12}\nu_{21}} \tag{VIII.23}$$

$$Q_{12} = \frac{\nu_{12}E_2}{1 - \nu_{12}\nu_{21}} \tag{VIII.24}$$

$$G_{66} = 0 \tag{VIII.25}$$

Each ply stiffness is then calculated in the global coordinates, following eq.(VIII.26).

$$Q' = T^{-1}QT \tag{VIII.26}$$

where T is the transformation matrix from the ply orientation angle θ.

$$T = \begin{bmatrix} m^2 & n^2 & 2mn \\ n^2 & m^2 & -2mn \\ -mn & mn & m^2 - n^2 \end{bmatrix} \tag{VIII.27}$$

with m = cosθ, and n = sinθ.

The equivalent bending stiffness matrix [D] is then calculated as follows:

$$D = \frac{1}{3}\sum_{n=1}^{N} Q'(z_k^3 - z_{k-1}^3) \tag{VIII.28}$$

with z_k being the z coordinates of the ply k from the middle axis of the laminate.

from [D], the theoretical bending modulus can be obtained:

$$E_{B_1} = D_{11}\frac{12}{h^3} \tag{VIII.29}$$

$$E_{B_2} = D_{22}\frac{12}{h^3} \tag{VIII.30}$$

with h the total thickness of the laminate.

VIII.9.3 Atomistic simulations

To estimate the complexation energies of F-PHU and F-EP assemblies and their structural characteristics, molecular mechanics and molecular dynamics simulations were first performed on

isolated PHU, EP, and a short fragment of cellulose (see structures in chapter 3) with the Dreiding force field and using the Gasteiger method to assign atomic charges, as implemented in the Materials Studio package [BIOVIA, Dassault Systèmes, Materials Studio 2022, San Diego: Dassault Systèmes, 2021]. Successive quenched dynamics at different temperatures were performed until no further improvement of the total energy of the system was found. Based on the optimized structures of the isolated fragments, F-PHU and F-EP complexes were built and submitted to quenched dynamics simulations to extract their lowest energy structures. Finally, both the lowest energy structures of the isolated fragments and the complexes were re-optimized at the DFT level using the B3LYP functional, a 6-31G** basis set, and the GD3BJ Grimme's dispersion correction [537]. The reported complexation energies correspond to the energy difference between the DFT-calculated energy of the complex and the sum of the DFT-calculated energies of the isolated fragments. The reported H-bond lengths were also extracted from the DFT-optimized complexes.

VIII.9.3.1 Transcarbamoylation free energies

The free energies of the transcarbamoylation reactions have been estimated at the Density Functional Theory (DFT) level using the B3LYP functional, a 6-31G** basis set and the GD3BJ Grimme's dispersion correction [537] as the energy difference between the sum of the free energies of the DFT-optimized isolated products and that of the reactants. The reported atomic charges have been obtained by fitting the electrostatic potential (ESP charges [538]) calculated at the same level of theory as for the reaction free energies calculations.

VIII.9.4 Friedman's isoconversional model for curing kinetics of matrices

From DSC analyses, the conversion degree can be computed through the ratio between partial enthalpy and the total enthalpy as described in eq.VIII.31. The non-isothermal DSC measurements were used to evaluate the activation energy (E_a) in the nth order kinetic model [504, 539] described in eq. VIII.32 of the systems using Friedman's model (eq.VIII.33).

$$\alpha = \frac{\int_{t_0}^{t} H_t}{\Delta H_T} \tag{VIII.31}$$

$$\frac{d\alpha}{dt} = Ae^{-\frac{E_a}{RT}}(1-\alpha)^n \tag{VIII.32}$$

$$\ln\frac{d\alpha}{dt} = \ln Af(\alpha) - \frac{E_a}{RT} \tag{VIII.33}$$

where α is the curing advance, H_T is the curing enthalpy, R is the perfect gas constant, and A the pre-exponential factor.

VIII.9.5 Statistical analyses

Analysis of Variance (ANOVA) was performed on the measured mechanical properties to evaluate potential statistical differences between formulations. A one-way ANOVA with a 95% confidence interval was chosen to discriminate the mechanical properties discrepancies. For each property, the p-value was computed. The difference is considered statistically meaningful when the p-value is lower than 0.05. When the p-value was below 0.05, a pairwise Tukey's test was conducted to discriminate the differences between each formulation. For each test case, letters a, b, and c assemble the groups of statistical similarities.

VIII.10 Life Cycle Inventory (Chapter 6)

Table VIII-1 – Life Cycle Inventory of TEBAC

Name	Process unit	Input	Output	Unit
Production of benzyltriethylammonium chloride (TEBAC)		-	0.660	kg
Benzyl chloride	Benzyl chloride (RER) market	0.390	-	kg
Triethyl amine	Triethyl amine (GLO), market	0.283	-	kg
Ethyl acetate	Ethyl acetate (GLO), market	0.006	-	kg
Acetonitrile	Acetonitrile (GLO), market	0.018	-	kg
Hazardous waste, for incineration	Hazardous waste, for incineration (Europe without Switzerland), market	-	0.053	kg

Table VIII-2 – Life Cycle Inventory the Raney Nickel

Name	Process unit	Input	Output	Unit
Production of Ni-Al Alloy	-	-	1	kg
Aluminum	Aluminum, primary, ingot (AI Area, EU27 & EFTA)	0.50	-	kg
Nickel	Nickel, Class 1 (GLO), market	0.50	-	kg
Production of Ni-Al powder 100um	-	-	0.99	kg
NiAl Alloy	nan	1	-	kg
Argon	Inert gas for discharge lamps (GLO), market	0.33	-	kg
Electricity	Electricity, medium voltage (RER), market	0.75	-	kWh
Electricity	Electricity, medium voltage (RER), market	0.79	-	kWh
Production of Raney Nickel	-	nan	0.400	kg
NiAl powder	nan	1	-	kg
Sodium hydroxide	Sodium hydroxide, without water, in 50% solution state RER, market	0.80	-	kg
Water	Water, deionised (Europe without Switzerland), market	68.20	-	kg

Table VIII-3 – Life Cycle Inventory of RDGE

Name	Process unit	Input	Output	Unit
Production of RDGE	Adapted from Ecoinvent epoxy resin	-	1	kg
Resorcinol	NPG0 - Resorcinol (GLO), market	0.50	-	kg
Epichlorohydrin	Epichlorohydrin (GLO), market	0.830	-	kg
Sodium hydroxide	Sodium hydroxide, without water, in 50% solution state (RER), market	0.730	-	kg
Water	Water, cooling, unspecified natural origin, RER	8E-3	-	m3
Water	Water, river, RER	5E-4	-	m3
Water	Water, well, RER	4E-4	-	m3
Electricity	Electricity, medium voltage (RER), market	0.224	-	kWh
Heat	Heat, district or industrial, natural gas (RER), market	1.059	-	MJ
Heat	Heat, from steam, in chemical industry (RER), market	0.117	-	MJ
Emissions in air, water	Water/m3, RER	-	0.001	m3
Emission in water, chloride	Chloride	-	0.328	kg
Emission in water, Sodium	Sodium (I)	-	.23	kg
Emission in water, water	Water, RER	-	4E-4	m3
Wastewater	Wastewater, average (CH), market	-	3E-8	m3
Wastewater	Wastewater, average (Europe without Switzerland), market	-	1E-6	m3

Table VIII-4 – Life Cycle Inventory of TMPTGE

Name	Process unit	Input	Output	Unit
Production of TMPTGE	Adapted from Ecoinvent epoxy resin	-	1	kg
Trimethylolpropane	Pentaerythritol (GLO), market	0.440	-	kg
Epichlorohydrin	Epichlorohydrin (GLO), market	0.920	-	kg
Sodium hydroxide	Sodium hydroxide, without water, in 50% solution state (RER), market	0.790	-	kg
TEBAC	TEBAC	.04	-	kg
Water	Water, cooling, unspecified natural origin, RER	8E-3	-	m3
Water	Water, river, RER	5E-4	-	m3
Water	Water, well, RER	4E-4	-	m3
Electricity	Electricity, medium voltage (RER), market	0.224	-	kWh
Heat	Heat, district or industrial, natural gas (RER), market	1.059	-	MJ
Heat	Heat, from steam, in chemical industry (RER), market	0.117	-	MJ
Emissions in air, water	Water/m3, RER	-	0.001	m3
Emission in water, chloride	Chloride	-	0.361	kg
Emission in water, Sodium	Sodium (I)	-	0.397	kg
Emission in water, water	Water, RER	-	4E-4	m3
Wastewater	Wastewater, average (CH), market	-	3E-8	m3
Wastewater	Wastewater, average (Europe without Switzerland), market	-	1E-6	m3

Table VIII-5 – Life Cycle Inventory of TMPTC

Name	Process unit	Input	Output	Unit
Production of TMPTC	-	-	1.6	kg
TMPTGE	TMPTGE	1.1	-	kg
Carbon Dioxide	Carbon dioxide, liquid (RER), market	0.50	-	kg
TEBAC	TEBAC	.04	-	kg
Electricity	Electricity, medium voltage (RER), market	3.30	-	kWh

Table VIII-6 – Life Cycle Inventory of mXDA

Name	Process unit	Input	Output	Unit
Production of m-xylylene diamine (mXDA), from [374]	-	-	1	ton
Xylene	Xylene (RER), market	1.610	-	ton
Ammonia	Ammonia, anhydrous, liquid (RER), market	0.610	-	ton
Dioxygen	Oxygen, liquid (RER), market	1.450	-	ton
Dihydrogen	Hydrogen, gaseous(GLO), market	0.071	-	ton
N-methylpyrrolidone	N-methyl-2-pyrrolidone (GLO), market	0.129	-	ton
Raney Nickel	Raney Nickel	0.011	-	ton
Electricity	Electricity, medium voltage (RER), market	40.6	-	MJ

Table VIII-7 – Life Cycle Inventory of carbon fibers

Name	Process unit	Input	Output	Unit
Production of carbon fibers [67]	-	-	1	kg
Acrylonitrile	Acrylonitrile (GLO), market	2.090	-	kg
Vinyl Acetate	Vinyl acetate (GLO), market	.02	-	kg
Nitrogen	Nitrogen, liquid (RER), industrial	11.50	-	kg
Steam	Steam, in chemical industry (RER), market	33.90	-	kg
Heat	Heat, district or industrial, natural gas (Europe without Switzerland), industrial furnace >100kW	360.20	-	MJ
Electricity	Electricity, medium voltage (RER), market	33.40	-	kWh

Table VIII-8 – Life Cycle Inventory of TMPTC, using solvent

Name	Process unit	Input	Output	Unit
Production of TMPTC at low pressure using solvent	-	-	388	g
TMPTGE	TMTPGE	300	-	g
CO_2	Carbon dioxide, liquid (RER), market	131	-	g
Ethyl Acetate (solvent)	Ethyl acetate (GLO), market	135.30	-	g
Water	Water, deionised (Europe without Switzerland), market	400	-	g
NaCl	Sodium chloride, brine solution (GLO), market	10	-	g
MgSO4	Magnesium sulfate (GLO), market	20	-	g
Ethylene bromide (catalyst)	Ethylene bromide (RER), market	9.6	-	g
Electricity	Electricity, medium voltage (RER), market	.08	-	kWh
Heat	Heat, district or industrial, natural gas RoW, market	.04	-	MJ
Solvent waste	Spent solvent mixture (Europe without Switzerland), market	-	545	g
Hazardous waste	Hazardous waste, for incineration (Europe without Switzerland), market	-	20	g

Table VIII-9 – Life Cycle Inventory of biobased epichlorohydrin

Name	Process unit	Input	Output	Unit
Production of bio-epichlorohydrin (bio-ECH) Almena 2016	-	nan	1	ton
Glycerol	Glycerine FR, treatment of used vegetable cooking oil, purified, esterification , Cut-off, U	1.250	-	ton
Methanol	Methanol (RER), market	0.235	-	ton
HCl	Hydrochloric acid, without water, in 30% solution state (RER), market	1.104	-	ton
NaOH	Sodium hydroxide, without water, in 50% solution state (RER), market	0.573	-	ton
Water	Water, well	4070	-	L
Heat (Natural Gas)	Heat, district or industrial, natural gas (RER), market	8.640	-	MJ

Table VIII-10 – Life Cycle Inventory the different resins (with curing)

Name	Process unit	Input	Output	Unit
Epoxy resin, cured	-	-	1	kg
RDGE	RDGE	0.630	-	kg
mXDA	mXDA	0.370	-	kg
Cure (press) 0.5 h 80 °C	Electricity, low voltage (RER), market	1	-	kWh
Post-cure (oven) 1h 160 °C	Electricity, low voltage (RER), market	0.40	-	kWh
PHU Resin, cured	-	-	1	kg
TMPTC	TMPTCscCO$_2$	0.720	-	kg
mXDA	mXDA	.28	-	kg
Cure (press) 2 h 80 °C	Electricity, low voltage (RER), market	5.6	-	kWh
Cure (oven) 1 h 100 °C	Electricity, low voltage (RER), market	0.6	-	kWh
Post-cure (oven) 1h 150 °C	Electricity, low voltage (RER), market	0.2	-	kWh
Hybrid Resin, cured	-	-	1	kg
RDGE	RDGE	0.335	-	kg
TMPTC	TMPTC	0.335	-	kg
mXDA	mXDA	.33	-	kg
Cure (press) 0.5 h 80 °C	Electricity, low voltage (RER), market	1	-	kWh
Post-cure (oven) 1h 160 °C	Electricity, low voltage (RER), market	0.40	-	kWh

Table VIII-11 – Life Cycle Inventory the different composites (with curing)

Name	Process unit	Input	Output	Unit
Flax fiber composite	-	-	1	kg
Resin formulation	Resin formulation (without energy)	0.440	-	kg
Flax	Fibre, flax, long, scutched (RER), market	0.660	-	kg
Curing	Electricity, low voltage (RER), market	see LCI resin	-	kWh
Inert waste	Inert waste (RER), market	-	0.1	kg
Carbon fiber composite	-	-	1	kg
Resin formulation	Resin formulation (without energy)	.33	-	kg
Carbon fiber	Carbon fiber	0.770	-	kg
Curing	Electricity, low voltage (RER), market	see LCI resin	-	kWh
Inert waste	Inert waste (RER), market	-	0.1	kg

Table VIII-12 – Life Cycle Inventory the chemical recycling

Name	Process unit	Input	Output	Unit
Chemically recycled flax fibers	-	-	0.590	kg
Acetic Acid	Acetic acid, without water, in 98% solution state (GLO), market	16	-	L
Hydrogen peroxide	Hydrogen peroxide, without water, in 50% solution state (RER), market	1.2	-	L
Water	Water, deionised (Europe without Switzerland), market	2.80	-	L
Recycled acetic acid	Acetic acid, without water, in 98% solution state (GLO), market	-14.40	-	L
Electricity	Electricity, low voltage (RER), market	0.1	-	kWh
Electricity	Electricity, low voltage (RER), market	0.30	-	kWh
Waste	Spent solvent mixture (Europe without Switzerland), treatment	-	6.1	L
Chemically recycled carbon fibers	-	-	0.670	kg
Acetic Acid	Acetic acid, without water, in 98% solution state (GLO), market	16	-	L
Hydrogen peroxide	Hydrogen peroxide, without water, in 50% solution state (RER), market	1.2	-	L
Water	Water, deionised (Europe without Switzerland), market	2.80	-	L
Recycled acetic acid	Acetic acid, without water, in 98% solution state (GLO), market	-14.40	-	L
Electricity	Electricity, low voltage (RER), market	0.1	-	kWh
Electricity	Electricity, low voltage (RER), market	0.30	-	kWh
Waste	Spent solvent mixture (Europe without Switzerland), treatment	-	6.1	L
Chemical recycling from vinegar	-	-	Same	kg
Water	Water, well	8	-	L
Biobased acetic acid	Ethanol, without water, in 99.7% solution state, from fermentation (GLO), market	2	-	L
Hydrogen peroxide	Hydrogen peroxide, without water, in 50% solution state (RER), market	4	-	L
Electricity	Electricity, low voltage (RER), market	1	-	L
Waste	Wastewater, average (Europe without Switzerland), market	-	2.50	L

Table VIII-13 – Life Cycle Inventory the recyled composites

Name	Process unit	Input	Output	Unit
Mechanically recycled composite	-	-	1	kg
Virgin composite	Carbon or flax composite	0.50	-	kg
Cutting	Electricity, low voltage (RER), market	0.30	-	kWh
Reshaping	Electricity, low voltage (RER), market	2.90	-	kWh
Waste	Inert waste (RER), market	-	0.50	kg
Composite from recycled carbon fibers	-	-	1	kg
recycled fibers	rCF	0.650	-	kg
Resin hybrid EP/PHU	Resin, without curing	0.350	-	kg
Curing	Electricity, low voltage (RER), market	1.40	-	kWh
Composite from recycled flax fibers	-	-	1	kg
recycled fibers	rFF	0.550	-	kg
Resin hybrid EP/PHU	Resin, without curing	0.350	-	kg
Curing	Electricity, low voltage (RER), market	1.40	-	kWh

Appendix

Contents

A.1 Appendix Chapter 2

A.1.1 Carbonate Precursors

H-NMR

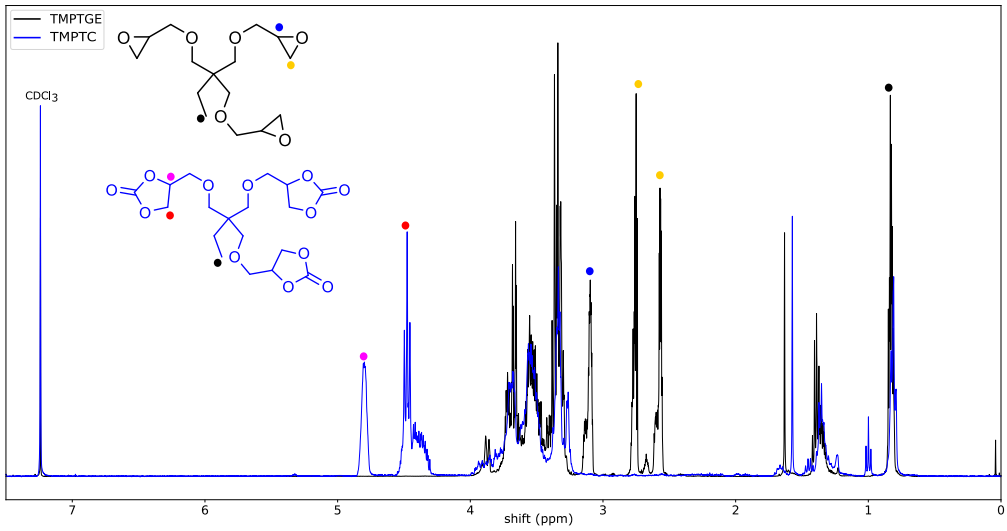

Figure II-A1 – ^{1}H-NMR of the Trimethylol Propane Triglycidyl Ether (TMPTGE) and the Trimethylol Propane Carbonate (TMPTC)

^{1}H-NMR TMPTGE ($CDCl_3$, ppm): δ = 0.84 (t, 3H, methyl group), 2.6-2.72 (m, 6H, oxirane), 3.12 (m, 3H, oxirane).

^{1}H-NMR TMPTC ($CDCl_3$, ppm): δ = 0.84 (t, 3H, methyl group), 4.4-4.5 (m, 6H, cyclic carbonate), 4.83 (m, 3H, cyclic carbonate).

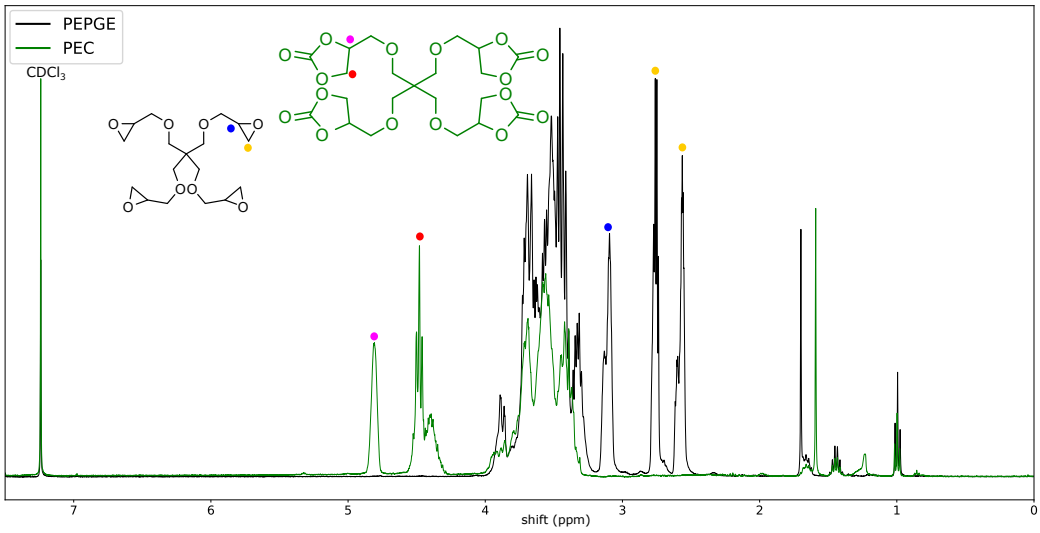

Figure II-A2 – ^{1}H-NMR of the Pentaerythritol Polyglycidyl Ether (PEPGE) and the Pentaerythritol Carbonate (PEC)

^{1}H-NMR PEPGE ($CDCl_3$, ppm): δ = 2.61-2.8 (m, 8H, oxirane), 3.14 (m, 4H, oxirane).

^{1}H-NMR PEC ($CDCl_3$, ppm): δ = 4.42-4.52 (m, 8H, cyclic carbonate), 4.85 (m, 4H, cyclic carbonate).

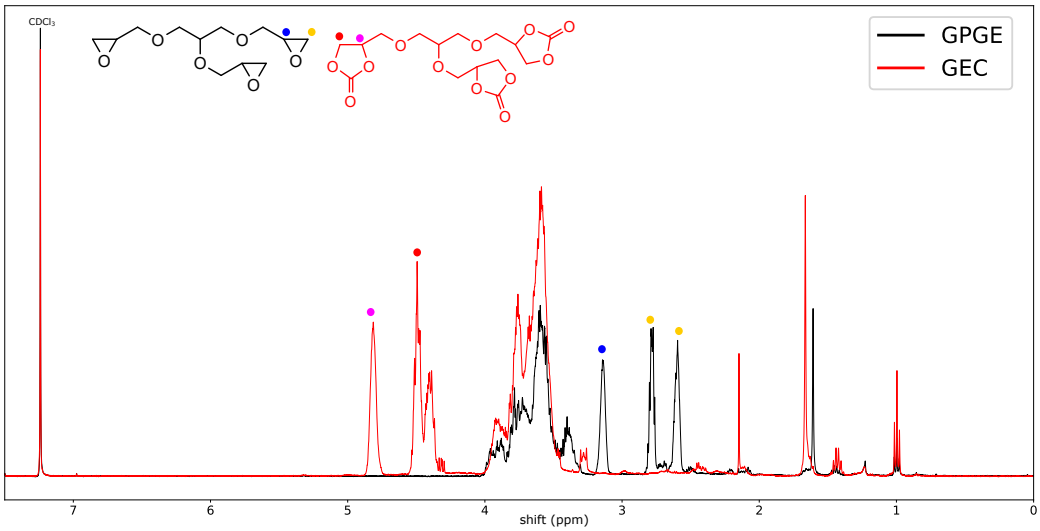

Figure II-A3 – ^{1}H-NMR of the Glycerol Polyglycidyl Ether (GPGE) and the Glycerol Carbonate (GEC)

^{1}H-NMR GPGE ($CDCl_3$, ppm): δ = 2.64-2.83 (m, 6H, oxirane),3.19 (m, 3H, oxirane).
^{1}H-NMR GEC ($CDCl_3$, ppm): δ = 4.44-4.54 (m, 6H, cyclic carbonate), 4.86 (m, 3H, cyclic carbonate).

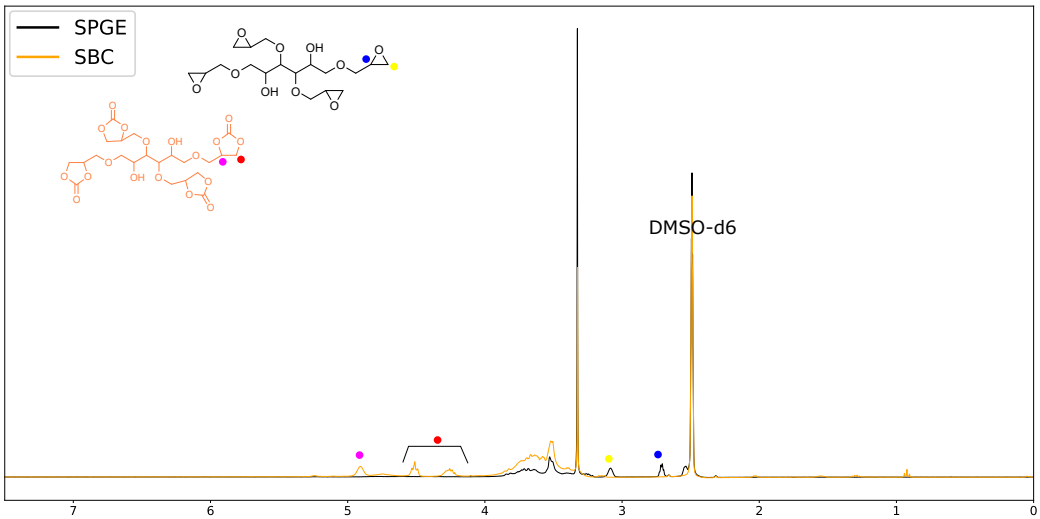

Figure II-A4 – ^{1}H-NMR of the Sorbitol PolyGlycidyl Ether (SPGE) and the Sorbitol Carbonate (SBC)

^{1}H-NMR SPGE ($DMSO_{d6}$, ppm): δ = 2.72 (m, 8H, oxirane), 3.10 (m, 4H, oxirane).
^{1}H-NMR SBC ($DMSO_{d6}$, ppm): δ = 4.27-4.53 (m, 8H, cyclic carbonate), 4.93 (m, 4H, cyclic carbonate).

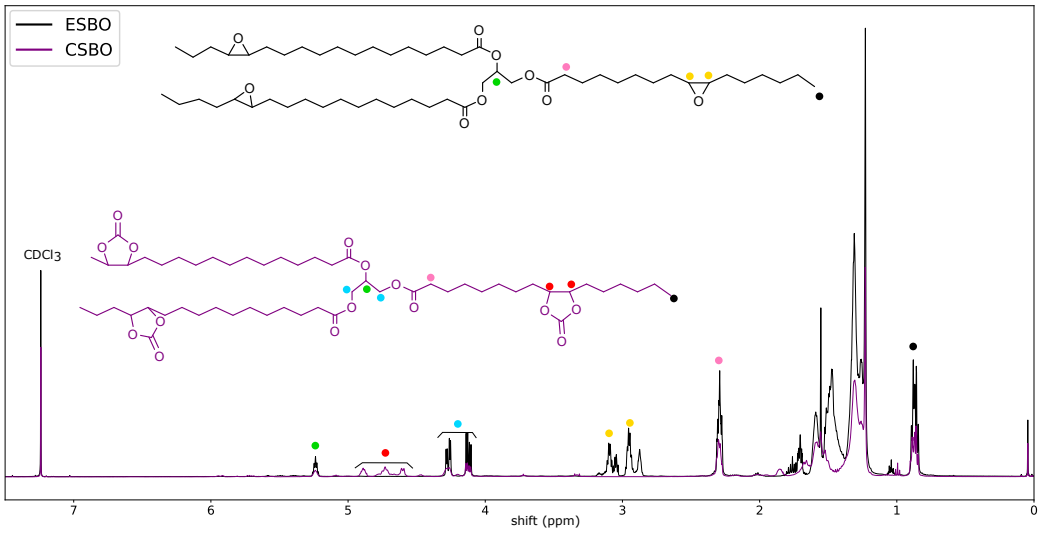

Figure II-A5 – ^{1}H-NMR of the Epoxidized SoyBean Oil (ESBO) and the Carbonated SoyBean Oil (CSBO)

^{1}H-NMR ESBO ($CDCl_3$, ppm): $\delta = 2.98$ (m, 6H, oxirane).
^{1}H-NMR CSBO ($CDCl_3$, ppm): $\delta = 4.75$ (m, 6H, cyclic carbonate).

Mass Spectrometry

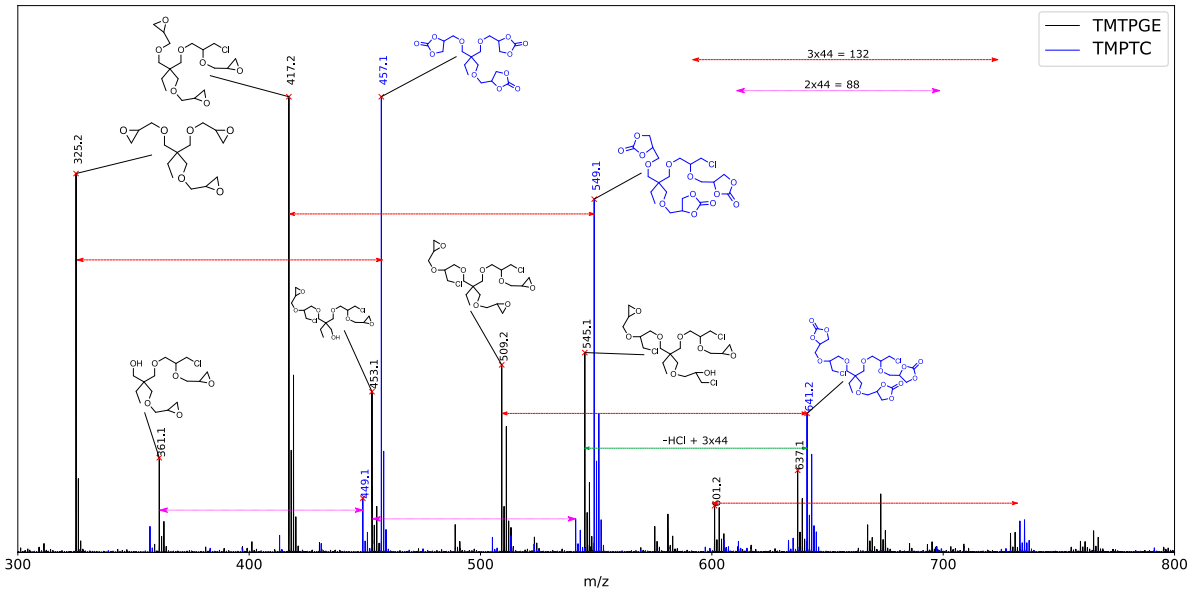

Figure II-A6 – Mass spectrometry of the Trimethylol Propane Triglycidyl Ether (TMPTGE) and the Trimethylol Propane Carbonate (TMPTC)

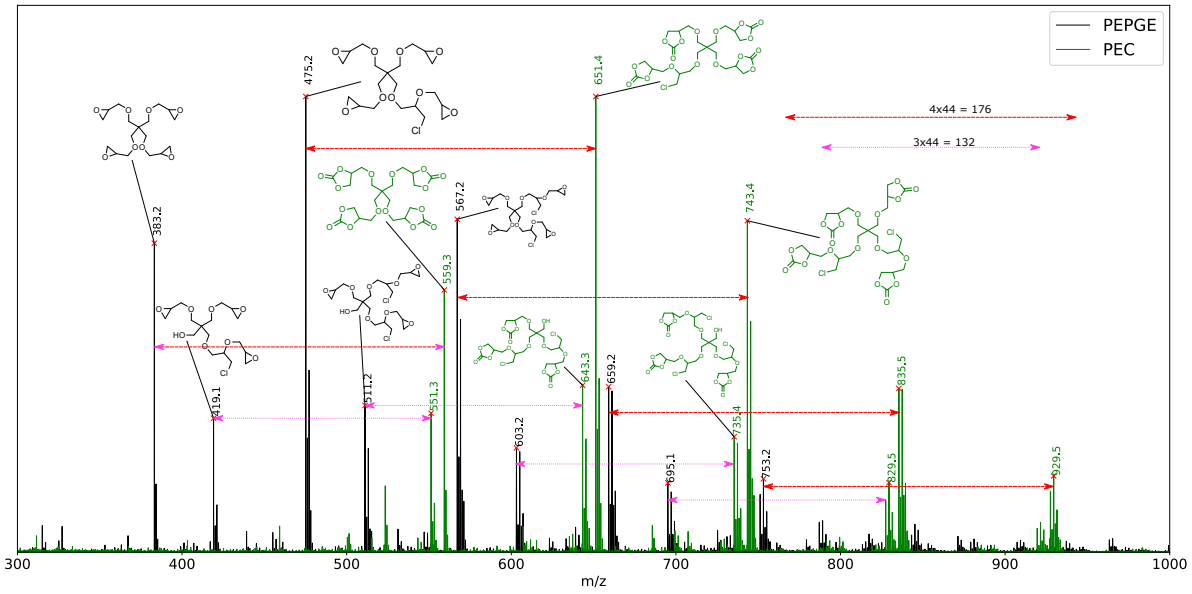

Figure II-A7 – Mass spectrometry of the Pentaerythritol Polyglycidyl Ether (PEPGE) and the Pentaerythritol Carbonate (PEC)

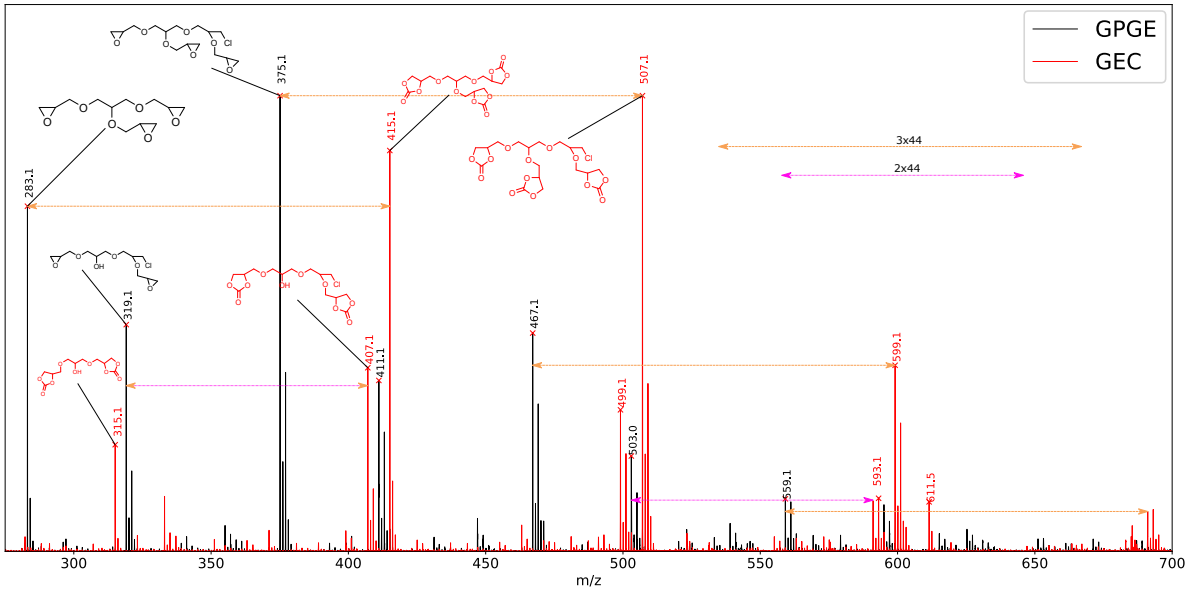

Figure II-A8 – Mass spectrometry of the Glycerol Polyglycidyl Ether (GPGE) and the Glycerol Carbonate (GEC)

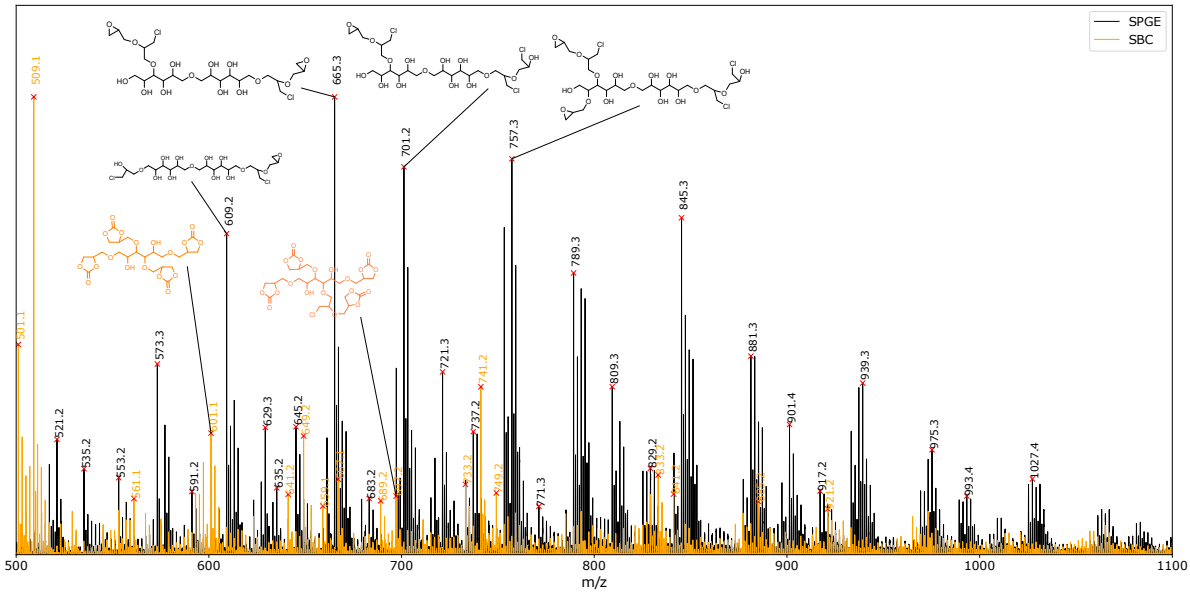

Figure II-A9 – Mass spectrometry of the Sorbitol PolyGlycidyl Ether (SPGE) and the Sorbitol Carbonate (SBC)

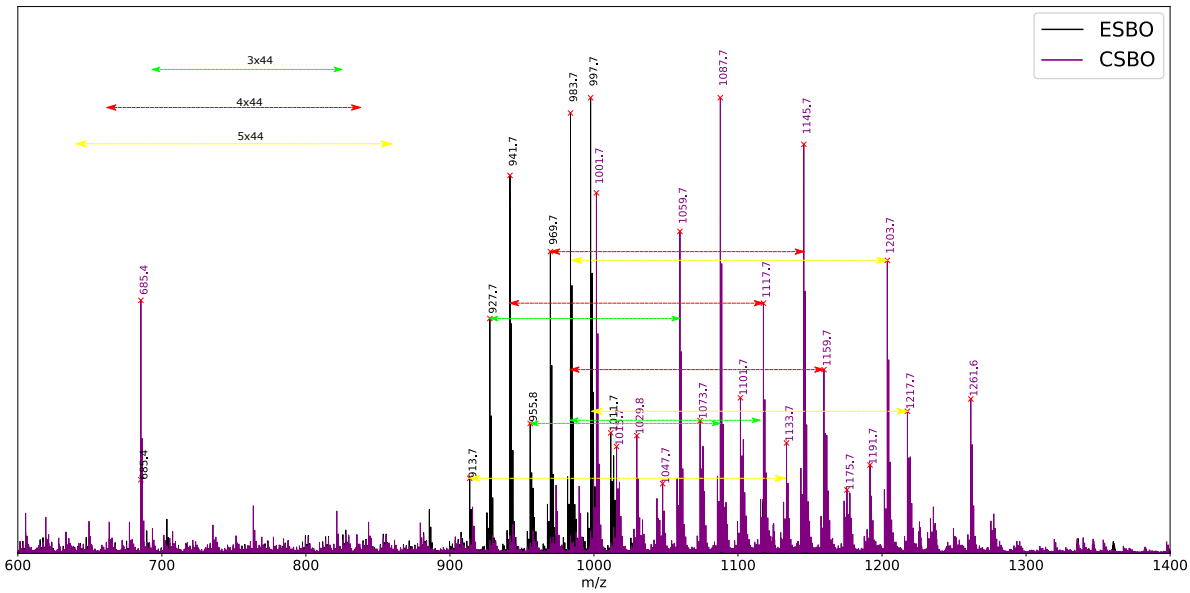

Figure II-A10 – Mass spectrometry of the Epoxidized SoyBean Oil (ESBO) and the Carbonated SoyBean Oil (CSBO)

Thermophysical properties of the carbonates

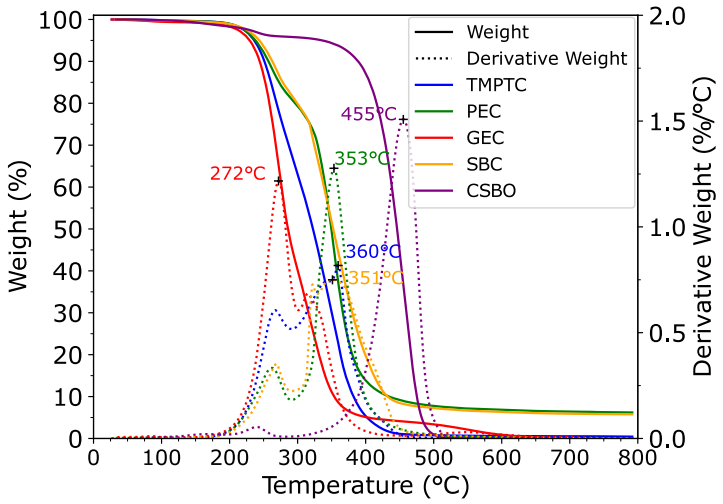

Figure II-A11 – TGA of the synthesized cyclic carbonates

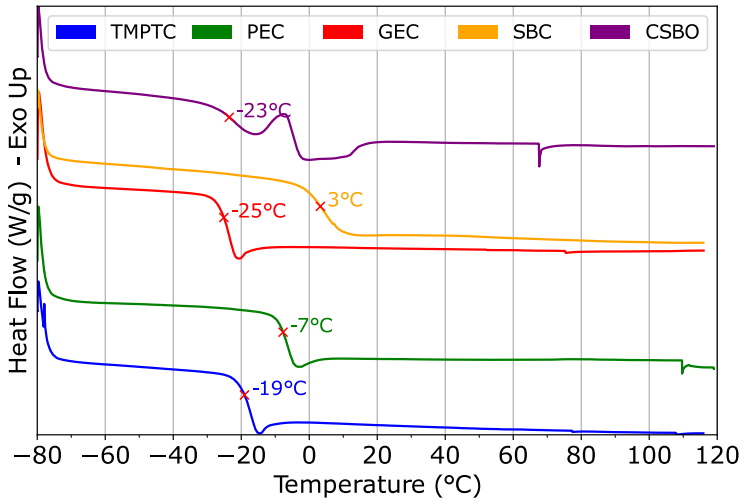

Figure II-A12 – DSC of the synthesized cyclic carbonates

A.1.2 Rheology of curing polyhydroxyurethanes

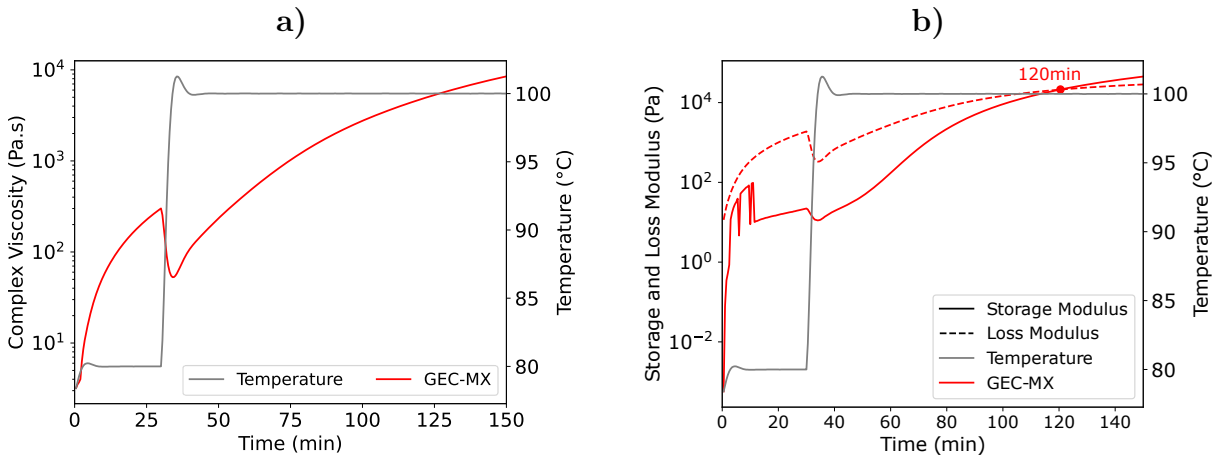

Figure II-A13 – Two step (80°C & 100°C) isothermal curing of the GEC-MX formulation. a) Complex viscosity, and b) Storage and Loss Modulus evolution with gel point

A.1.3 Cured polyhydroxyurethanes, complementary characterizations

FTIR

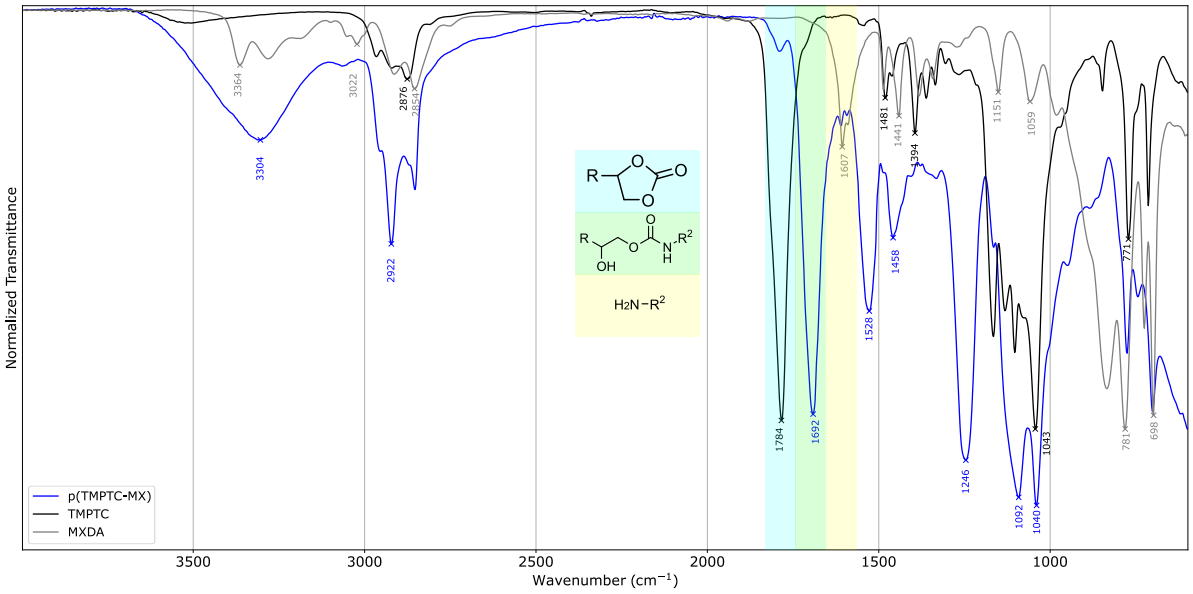

Figure II-A14 – FTIR of the p(TMPTC-MX) and its corresponding monomers

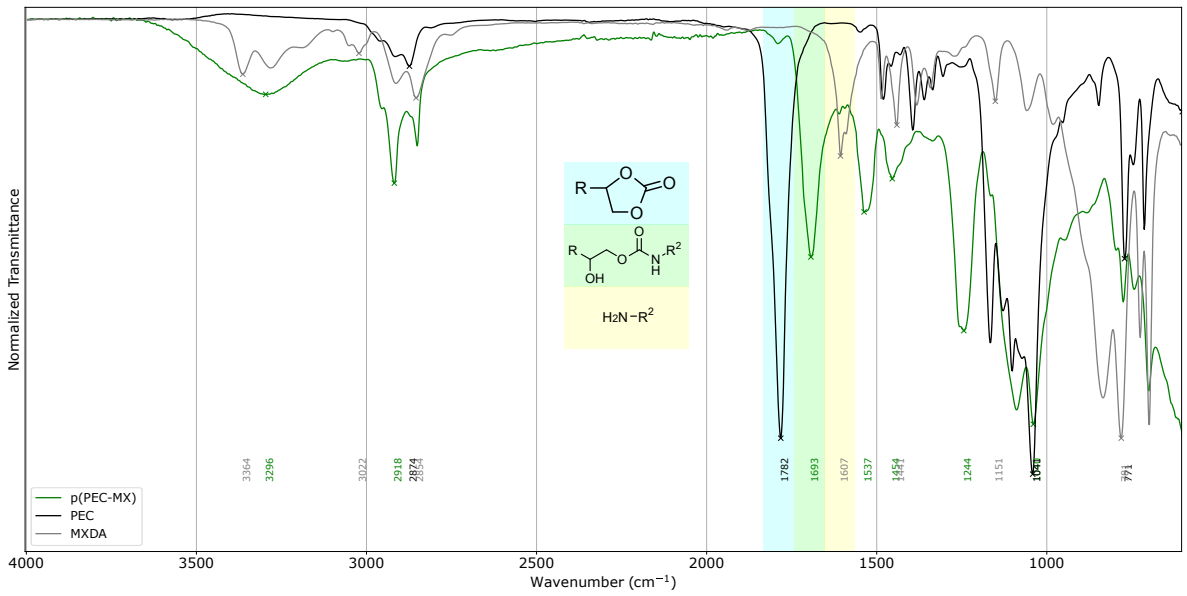

Figure II-A15 – FTIR of the p(PEC-MX) and its corresponding monomers

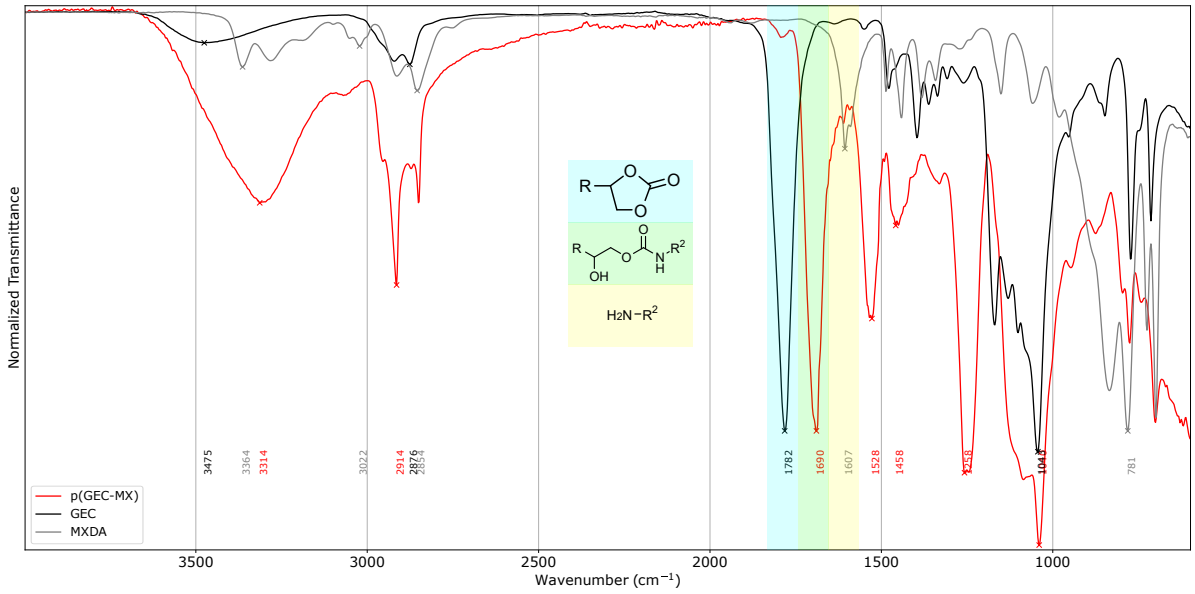

Figure II-A16 – FTIR of the p(GEC-MX) and its corresponding monomers

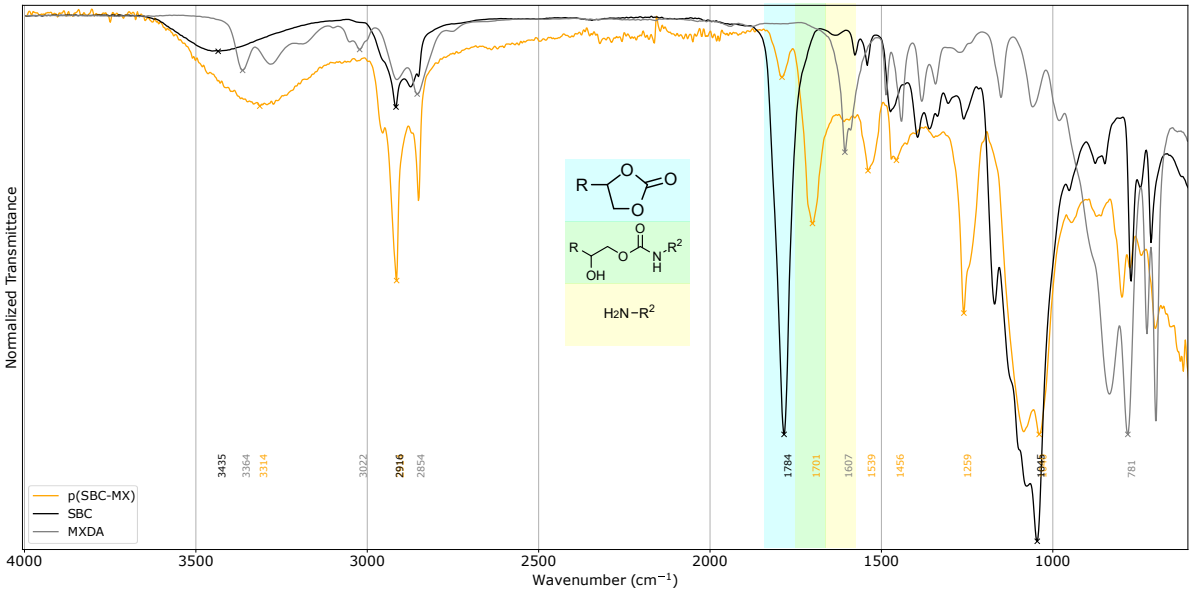

Figure II-A17 – FTIR of the p(SBC-MX) and its corresponding monomers

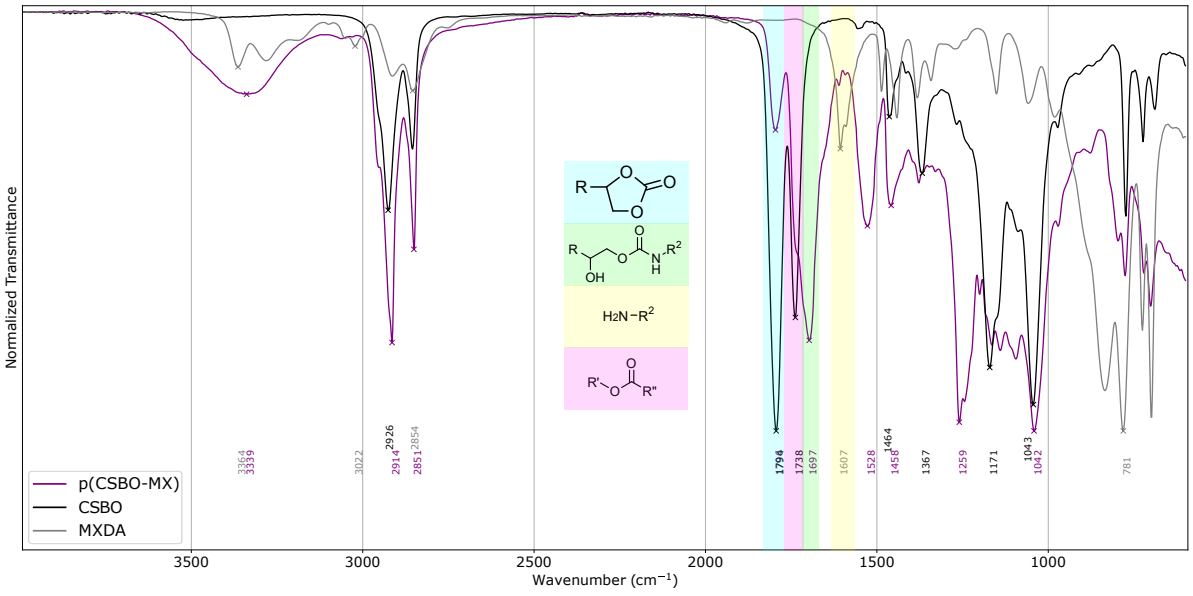

Figure II-A18 – FTIR of the p(CSBO-MX) and its corresponding monomers

Thermal stability during stress relaxation

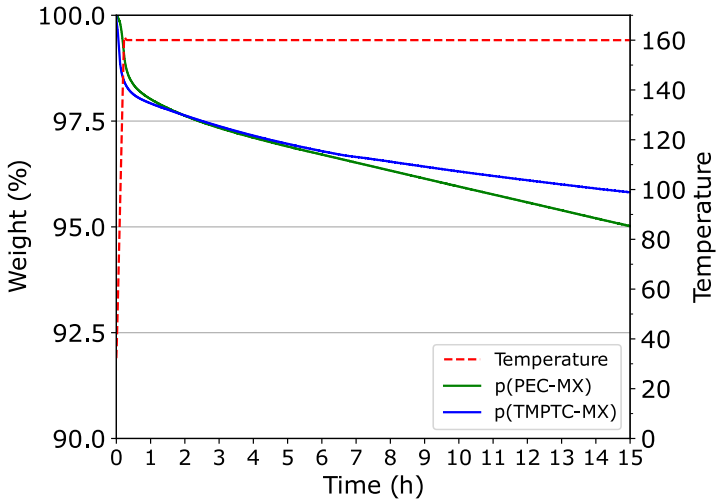

Figure II-A19 – Isothermal TGA of p(PEC-MX) and p(TMPTC-MX) thermoset at 160°C for 15h

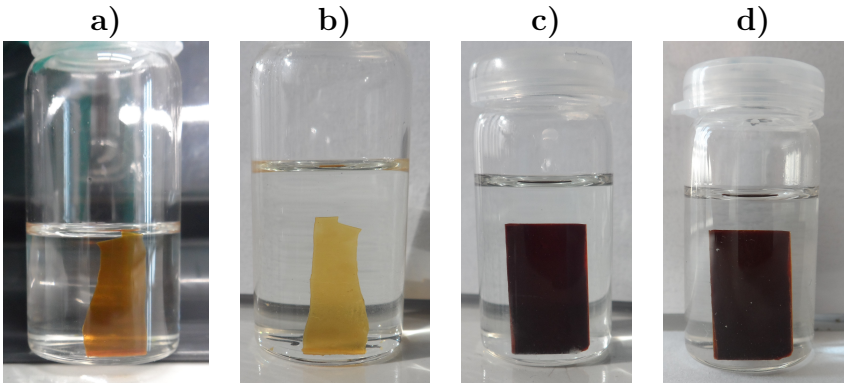

Figure II-A20 – Reprocessed PHU samples in THF solvent a) p(TMPTC-MX) t=0, b) TMPTC-MX t=3 weeks, c) p(PEC-MX) t=0, and d) p(PEC-MX) t=3 weeks

A.2 Appendix Chapter 3

A.2.1 Thermal stability of EP and PHU matrices

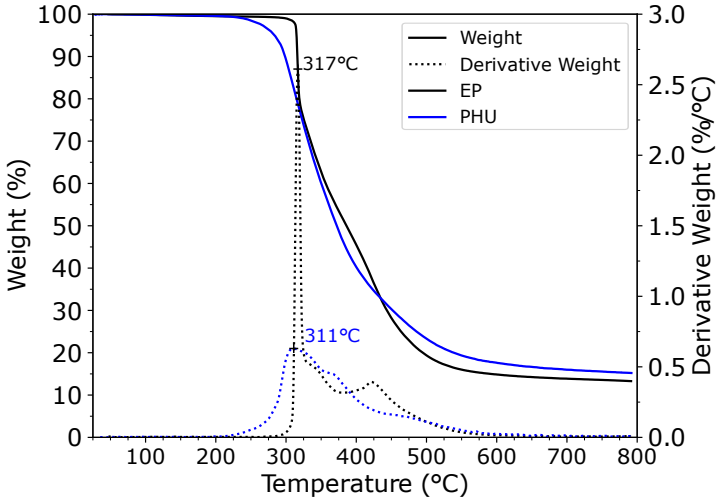

Figure III-A1 – TGA under N_2 flow of epoxy and PHU matrix

A.2.2 Mechanical properties - Tensile tests of EP and PHU matrices

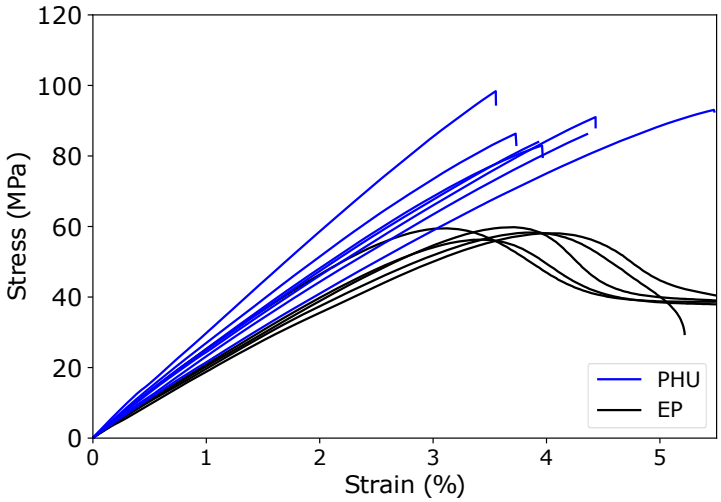

Figure III-A2 – Tensile tests of PHU and epoxy matrix

A.3 Appendix Chapter 4

A.3.1 Exchange model reactions - Mass spectra & Kinetics

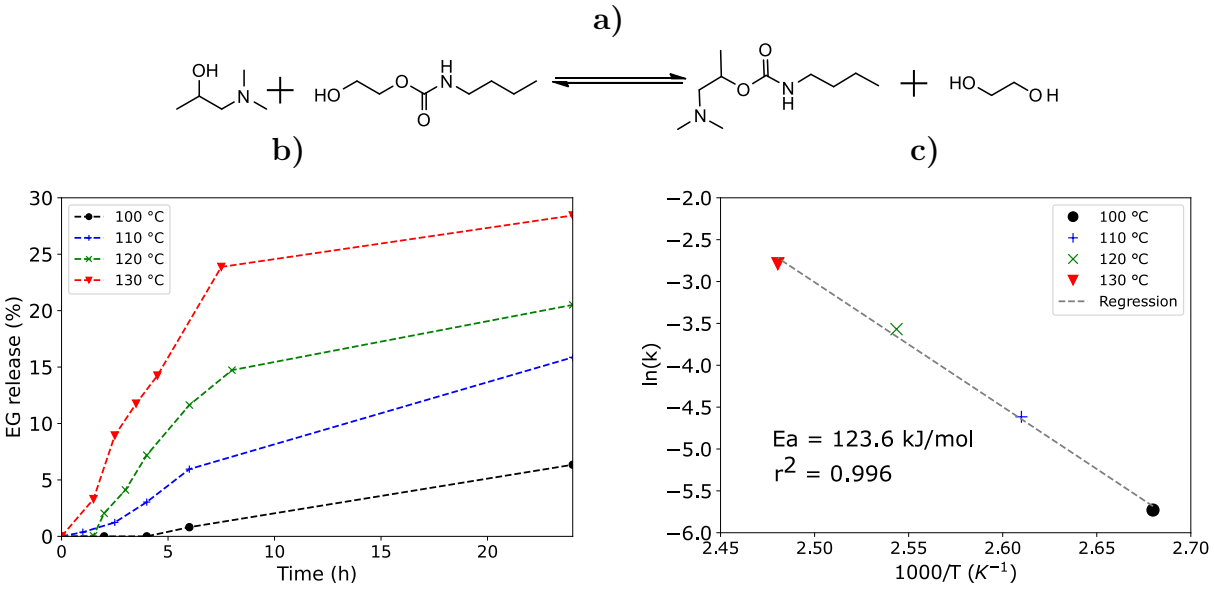

Figure IV-A1 – Kinetic of Ethylene Glycol (EG) release at different temperatures obtained by ^{1}H-NMR in $CDCl_3$ of the 2-hydroxyethyl n-butylcarbamate model compound with 1-dimethylamino-2-propanol mimicking the epoxy compound. a) Model reaction, b) kinetic plot, and c) Arrhenius graph with linear regression.

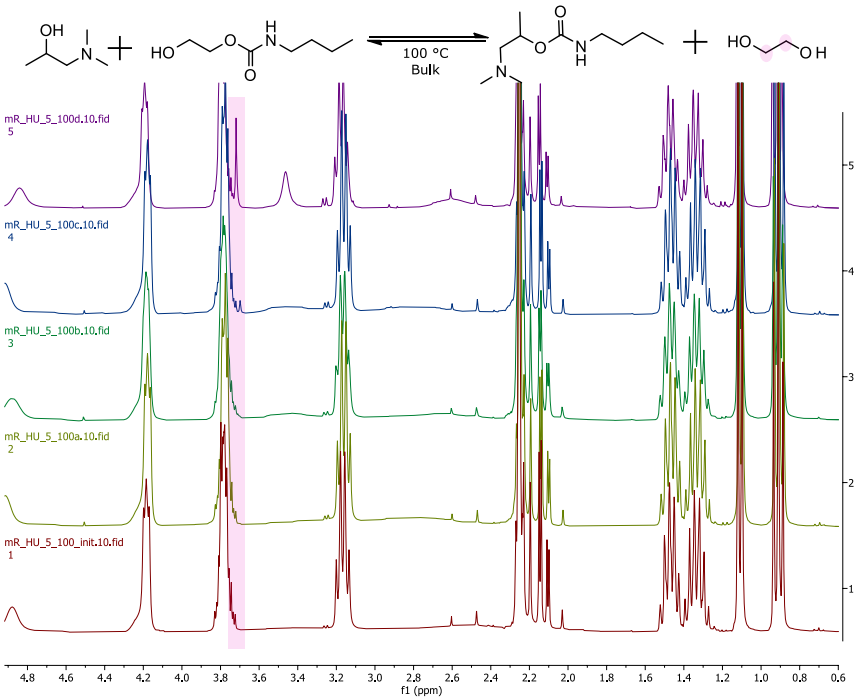

Figure IV-A2 – ^{1}H-NMR kinetic model reaction in $CDCl_3$. Ethylene Glycol (EG) release at 100 °C obtained by ^{1}H-NMR in $CDCl_3$ of the 2-hydroxyethyl n-butylcarbamate model compound with 1-dimethylamino-2-propanol mimicking the epoxy compound.

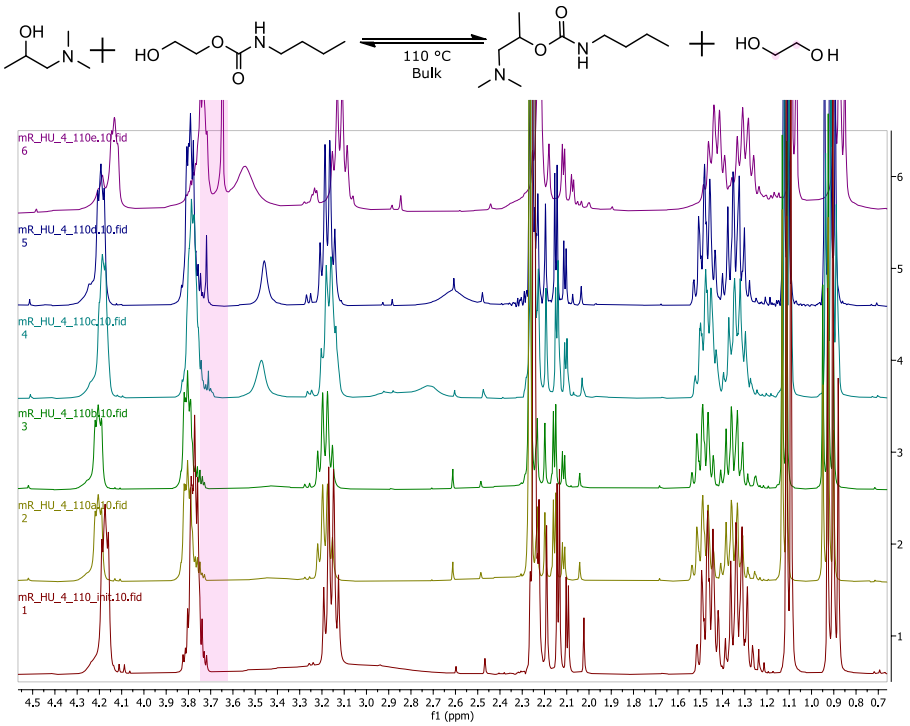

Figure IV-A3 – ^{1}H-NMR kinetic model reaction in $CDCl_3$. Ethylene Glycol (EG) release at 110°C obtained by ^{1}H-NMR in $CDCl_3$ of the 2-hydroxyethyl n-butylcarbamate model compound with 1-dimethylamino-2-propanol mimicking the epoxy compound.

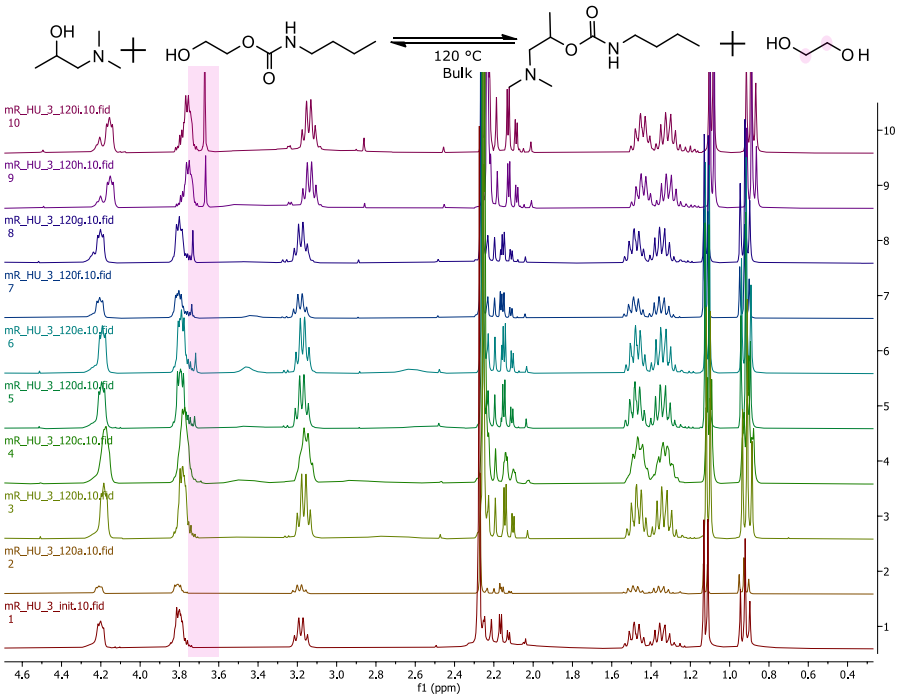

Figure IV-A4 – ^{1}H-NMR kinetic model reaction in $CDCl_3$. Ethylene Glycol (EG) release at 120°C obtained by ^{1}H-NMR in $CDCl_3$ of the 2-hydroxyethyl n-butylcarbamate model compound with 1-dimethylamino-2-propanol mimicking the epoxy compound.

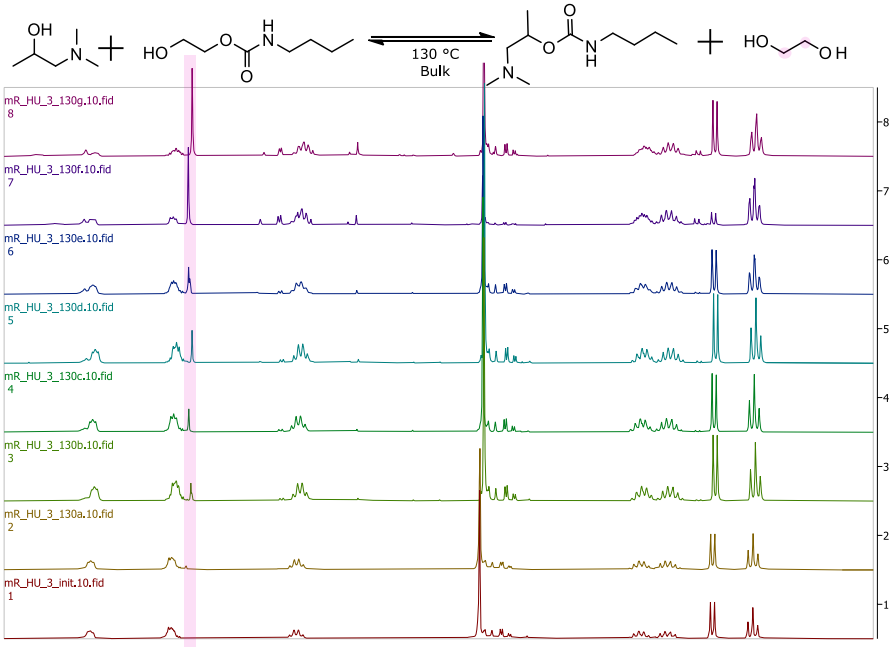

Figure IV-A5 – ^{1}H-NMR kinetic model reaction in $CDCl_3$. Ethylene Glycol (EG) release at 130°C obtained by ^{1}H-NMR in $CDCl_3$ of the 2-hydroxyethyl n-butylcarbamate model compound with 1-dimethylamino-2-propanol mimicking the epoxy compound.

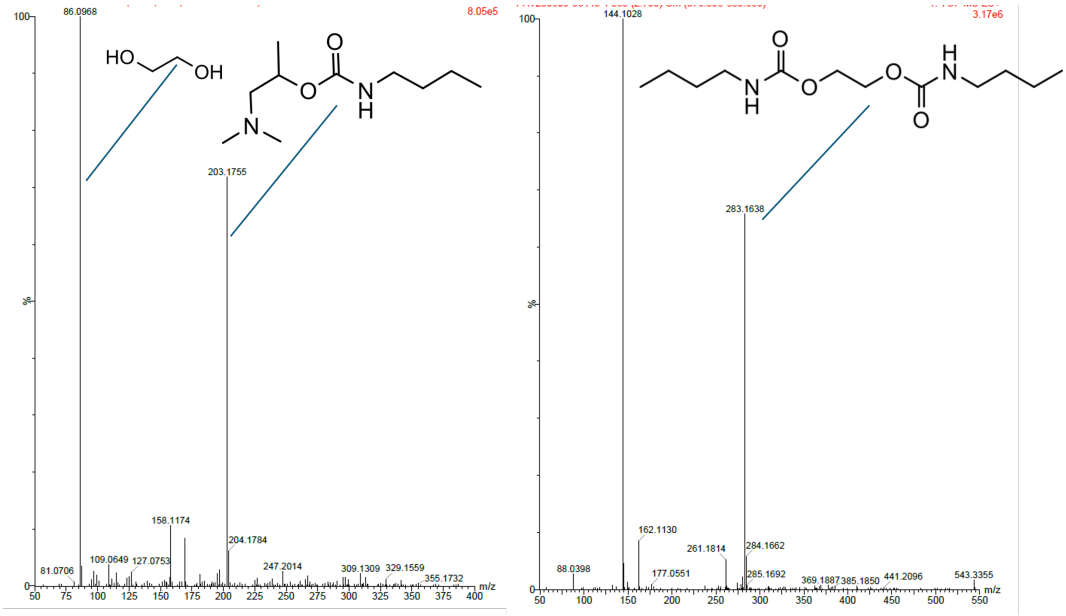

Figure IV-A6 – GC-MS of the model exchange reaction between 2-hydroxyethyl n-butylcarbamate model compound with 1-dimethylamino-2-propanol mimicking the epoxy compound.

A.3.2 Neat hybrid network properties

Hybrid Network Internal Structure

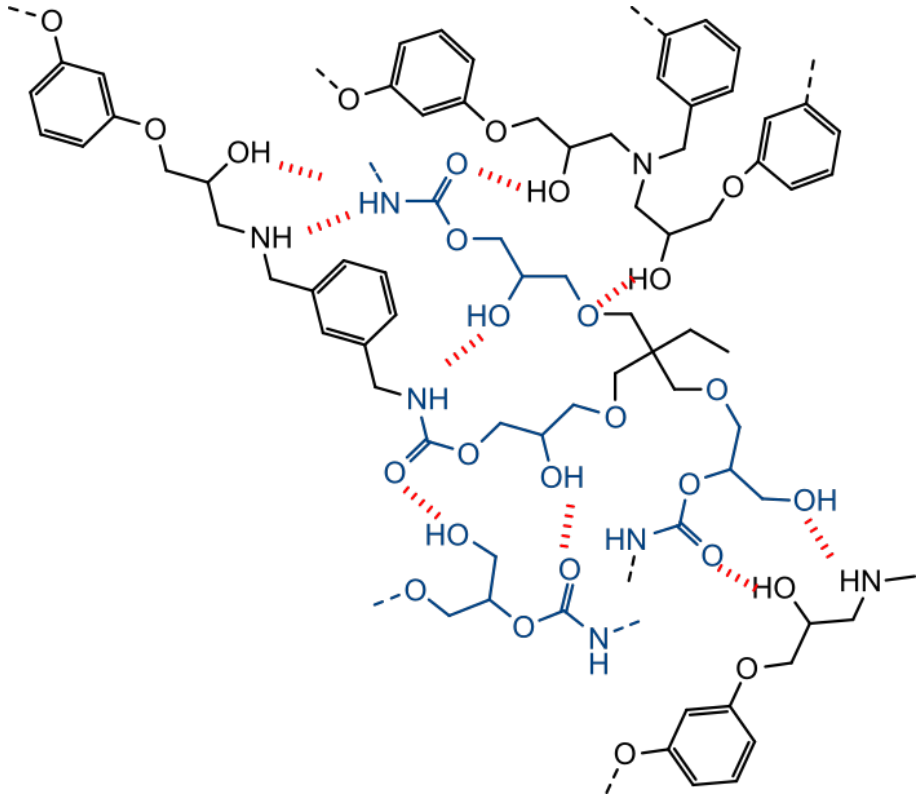

Figure IV-A7 – Dynamic hybrid EP internal structure. The blue backbones correspond to PHU segments, black to epoxy-derived moieties, and the red dotted lines correspond to H-bond potential sites.

Tensile curves and complementary results on the main formulation

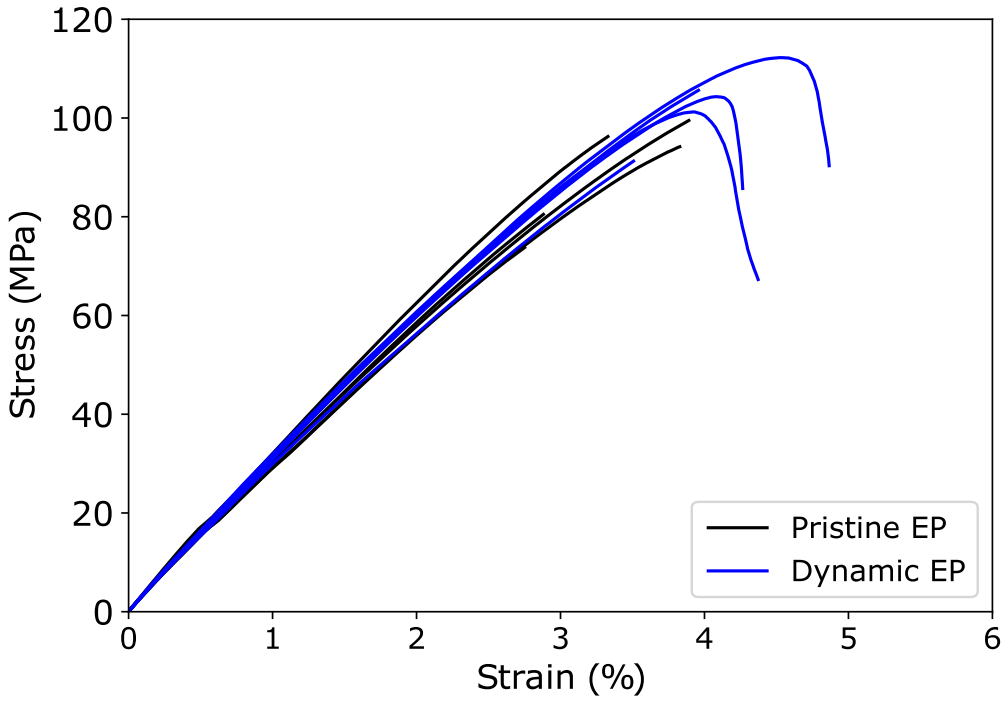

Figure IV-A8 – Exhaustive strain-stress curves obtained for the pristine and hybrid dynamic epoxides in tensile mode.

Replicates of stress relaxation hybrid EP 50/50

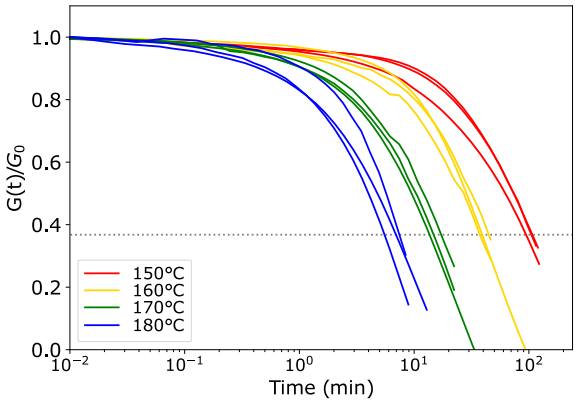

Figure IV-A9 – Stress relaxation experiments of the hybrid EP (50%RDGE-50%TMPTC) at 150 °C, 160 °C, 170 °C, and 180 °C

A.3.3 Reprocessed sample and dynamic behavior - additional results

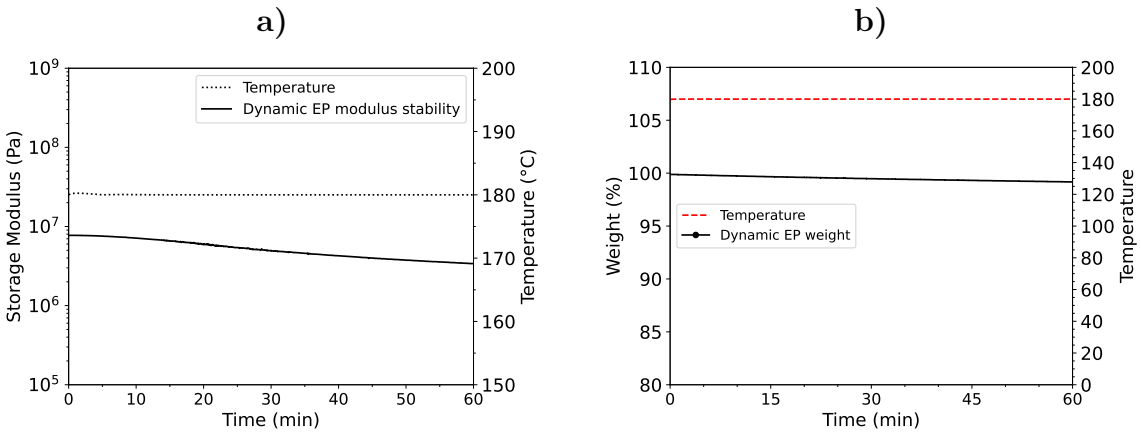

Figure IV-A10 – Thermal stability assessment of the dynamic EP. a) Storage modulus evolution at 180 °C, and b) Thermal weight stability at 180 °C.

Figure IV-A11 – Swelling in THF for 6 weeks of the reprocessed hybrid dynamic epoxy.

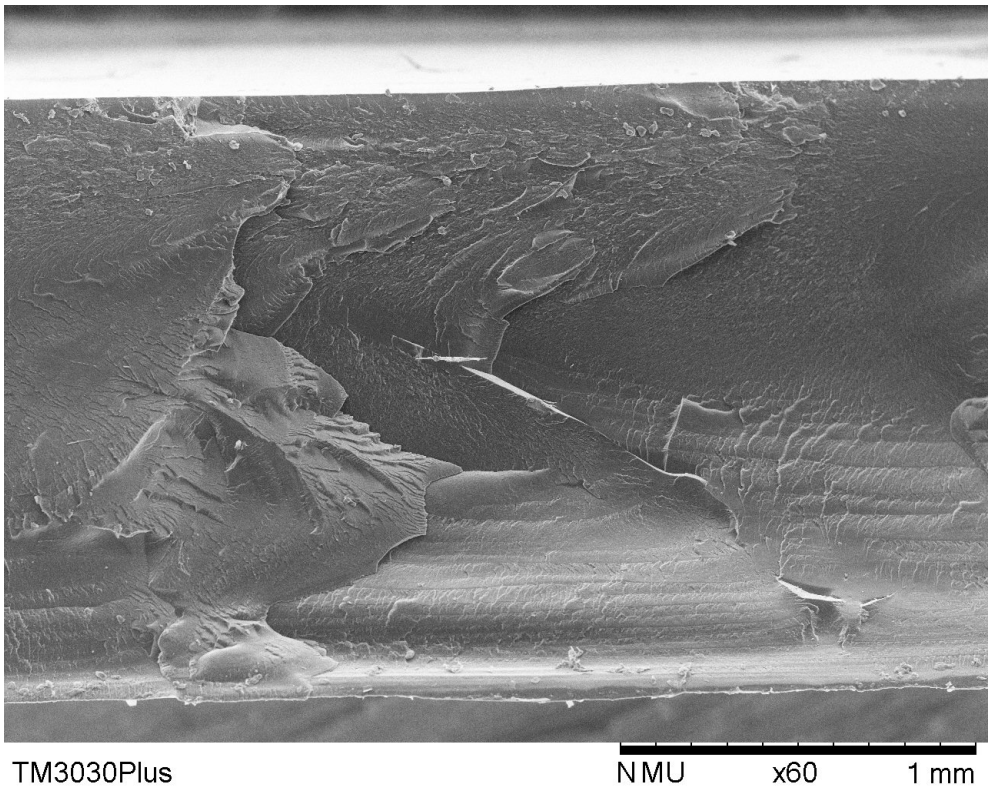

Figure IV-A12 – SEM micrographs of the reprocessed hybrid dynamic epoxy after cryobreaking.

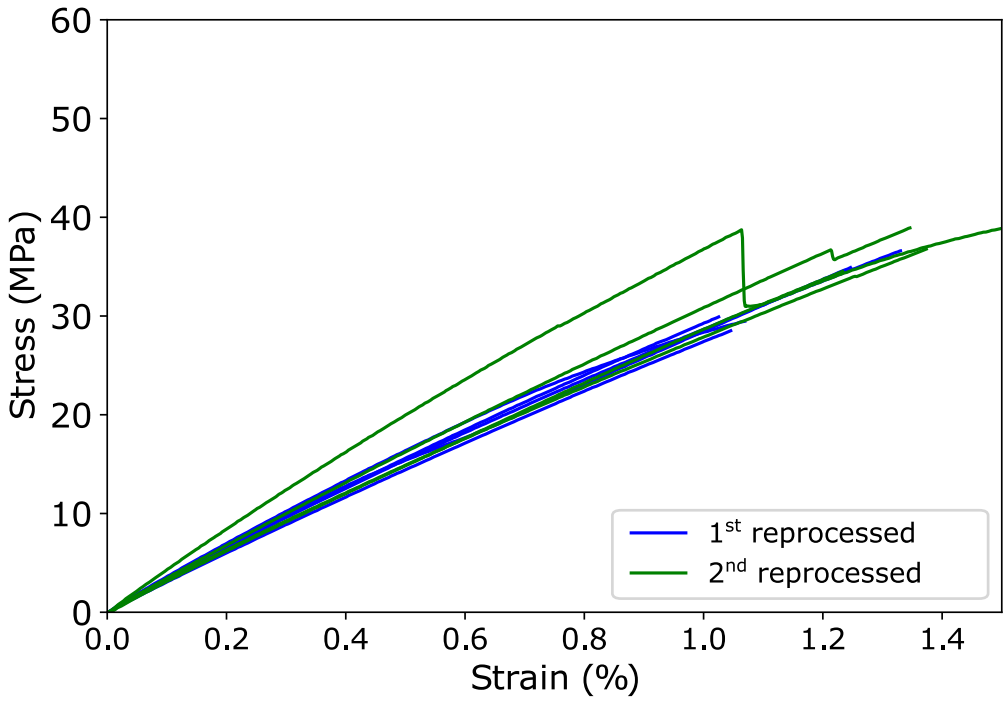

Figure IV-A13 – Tensile testing of the reprocessed pure hybrid dynamic polymer.

A.3.4 End-of-life of composites - Additional results

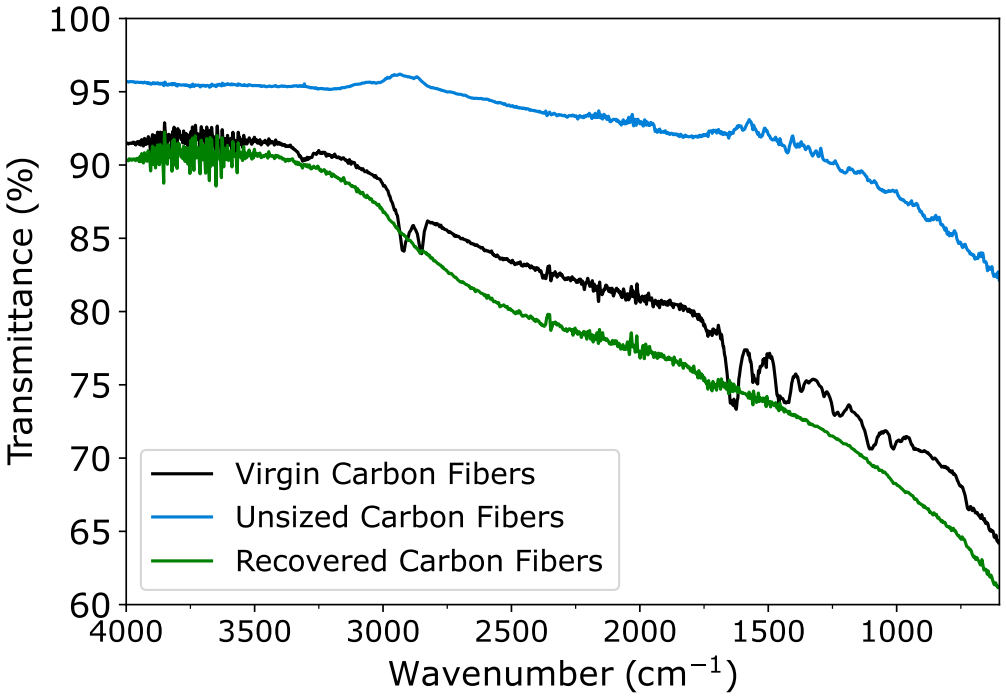

Figure IV-A14 – FTIR spectra of the virgin and recovered carbon fibers

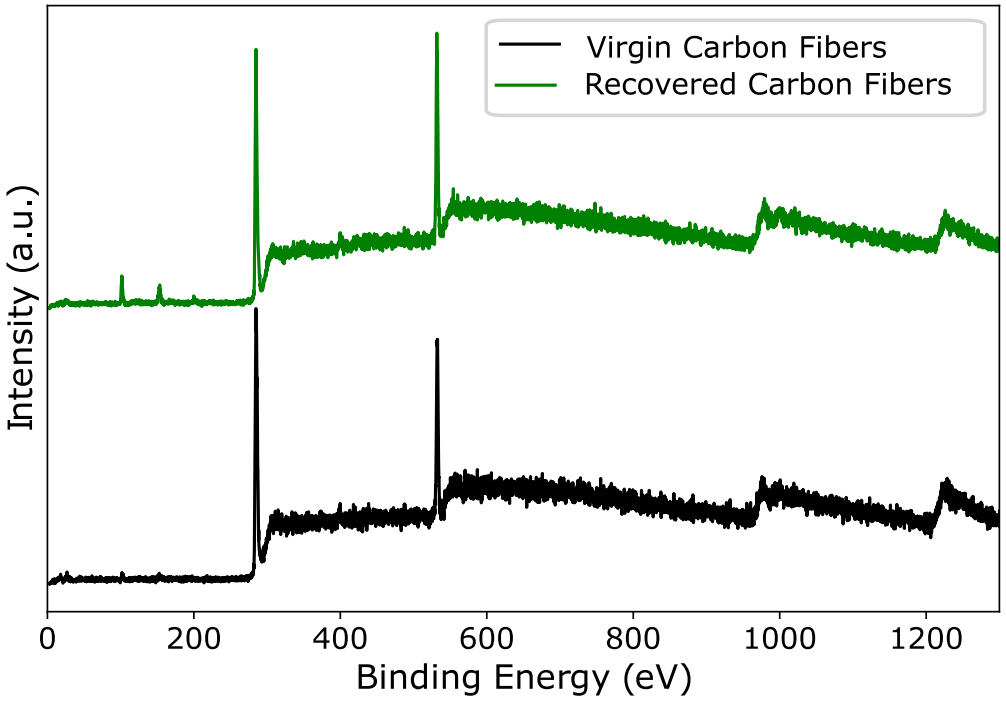

Figure IV-A15 – XPS, survey composition of the virgin and recovered carbon fibers

Element	Name	Position	FWHM	Library RSF	Raw Area	Area/(RSF*T*MFP)	%At Conc	% Atomic rel
C	C-C, C-H	284.60	1.46	0.314	3895.76	540.11	48.62	77.65
	C-N, C-O	286.26	1.67	0.314	2327.03	322.52	29.03	
O	O1s	531.03	1.77	0.733	314.76	17.86	1.61	19.89
	O1s	532.580	1.77	0.73	3579.59	203.07	18.28	
N*	N1s	399.50	2.01	0.499	241.82	20.65	1.86	1.86
Si*	Si2p	102.06	1.71	0.429	64.01	6.72	0.60	0.60

* Espectro cercano al ruido, estimación

Table IV-A1 – XPS results for virgin carbon fibers

Element	Name	Position	FWHM	Library RSF	Raw Area	Area/(RSF*T*MFP)	%At Conc	% Atomic rel
C	C-C, C-H	284.63	1.30	0.314	5835.30	809.04	45.46	68.87
	C-N, C-O	286.12	1.50	0.314	2466.41	341.86	19.21	
	N-C=O, O-C=O	288.65	1.88	0.314	539.33	74.72	4.20	
O	O1s	531.98	1.73	0.733	5710.72	324.02	18.21	23.76
	O1s	533.20	1.73	0.733	1741.43	98.79	5.55	
N	N1s	399.79	1.88	0.499	687.60	58.73	3.30	3.30
Si	Si2p	102.05	1.54	0.429	644.97	67.71	3.80	3.80
Cl*	Cl (2p 3/2)	200.28	1.340	1.08	80.94	3.31	0.19	0.280
	Cl (2p 1/2)	201.880	1.340	1.082	40.47	1.65	0.09	

* Espectro cercano al ruido, estimación

Table IV-A2 – XPS results for recovered carbon fibers

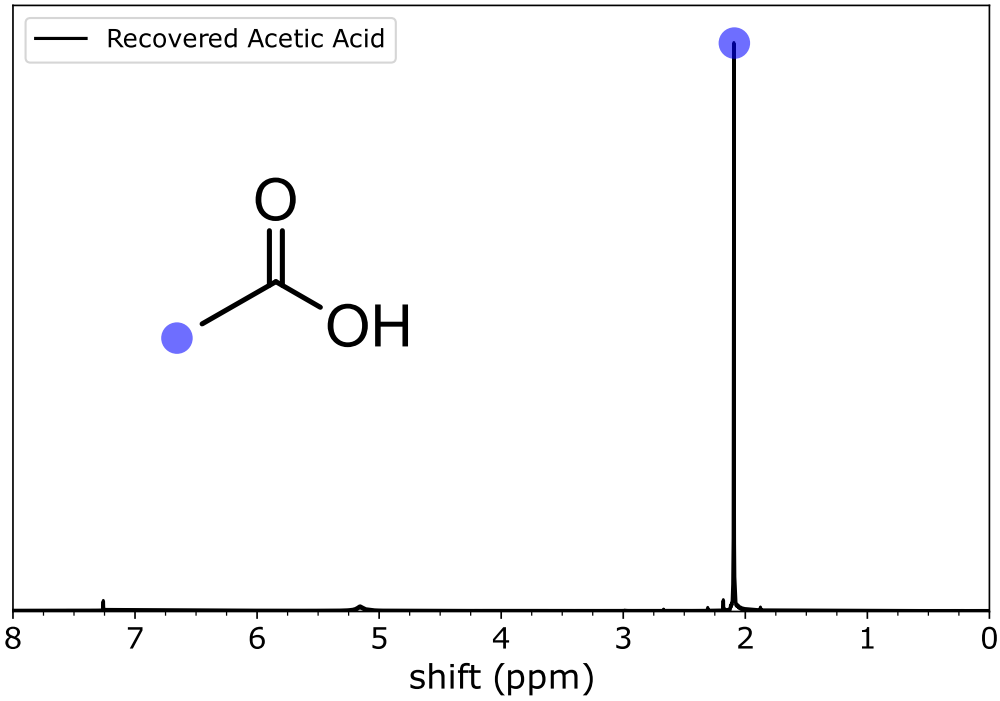

Figure IV-A16 – H-NMR in $CDCl_3$ of the recovered Acetic Acid after depolymerization, filtration, and evaporation. Acetic acid ($CDCl_3$,ppm) : 2.09 (s,CH_3)

A.3.5 Benchmark & Comparison with other CAN and CFRP

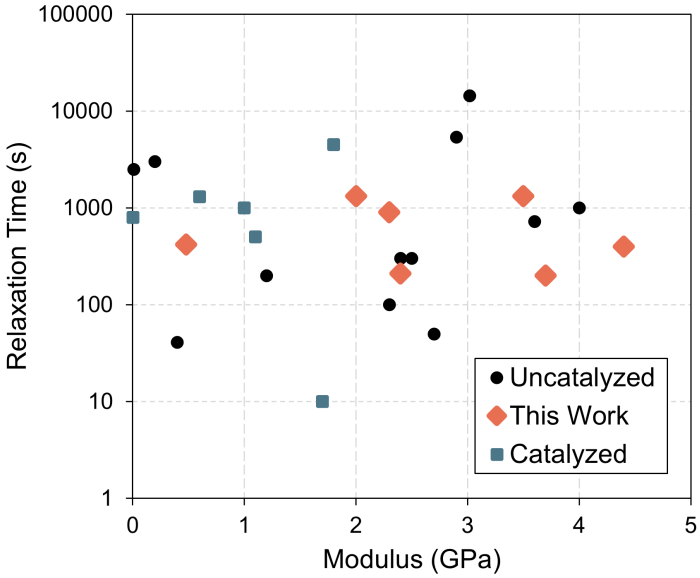

Figure IV-A17 – Comparative plot of the stress relaxation versus modulus of different CANs found in literature vs this work.

Ref	Chemistry	Catalyst	$E_{25°C}$ GPa	T_g °C	τ^* s	Rel.Temp. °C
THIS WORK	Epoxy/PHU	-	3.7	123	200	220
		-	3.5	110	1320	200
		-	4.4	94	400	180
		-	2.4	73	210	180
		-	0.5	27	420	180
		-	2.3	88	900	180
		-	2	99	1320	180
[366]	Epoxy/Amine- Disulfide	-	2.7	232	50	245
[490]	Benzoxazine/transesterification	-	-	113	2012	150
[462]	Polyhydroxyurethane (PHU)	-	3.0	60	14400	180
	PHU	-	3.6	80	720	180
	PHU	-	2.9	54	5400	180
[357]	Boronic Ester crosslink of copolymer	-	0.2	180	3000	262
[470]	Benzoxazine/transesterification	-	2.5	132	301	160
	Benzoxazine/transesterification	-	0.4	65	41	160
[345]	Vinylogous urethane	-	2.4	87	300	140
[540]	Boronic Ester	-	0.01	0	2500	160
[483]	PHU	-	1.2	54	200	180
[541]	Epoxy/amine - disulifide	-	nc	176	500	185
[542]	Epoxy/amine disulfide	-	nc	147	1000	160
[543]	Benzoxazine/transesterification	-	4	143	1000	180
[365]	Epoxy / Ester	-	2.3	86	100	180
[370]	Epoxy/Amine -Siloxane	TBD (10mol%)	nc	57	100	180
[241]	N,S-Acetal	MSA (5mol%)	1.7	44	10	75
[544]	Oxime	MSA (5mol%)	nc	-29	200	150
[545]	Epoxy Acid	TBD (5mol%)	1	18	1000	180
[546]	PU	DBTDL (1mol%)	nc	50	30	140
[390]	PHU	DBTDL (2 mol%)	0.01	10	800	160
[330]	Epoxy/Ester	Zn(ac)2 (5mol%)	1.8	57	4500	190
[360]	Unsaturated Polyester	Titanium butoxide (2.0wt%)	1.1	70	500	180
[547]	Epoxy/Ester	Zn2+ Ionomer (5mol%)	0.6	43	1300	170

Table IV-A3 – Comparison of different dynamic chemistries performance

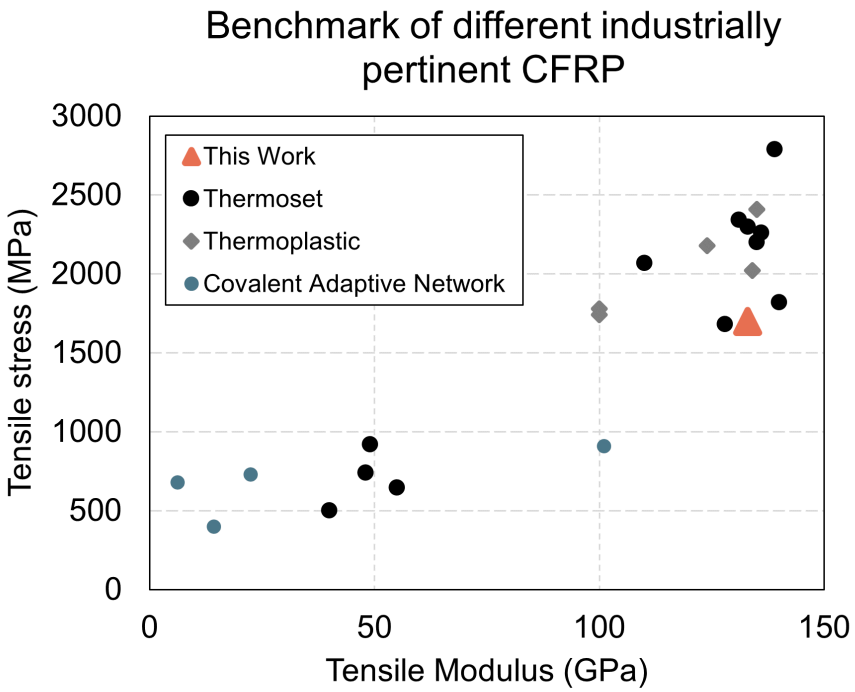

Figure IV-A18 – Comparative plot of CFRP modulus versus ultimate stress found in literature or commercially available, using thermoset, thermoplastic, or CAN as matrices.

	Name/ref	Supplier	Fibre	Matrix	T_g °C	E GPa	σ MPa	Recyclable	Catalyst
CAN	This work		Carbon	EP/PHU	27-130	133	1700	Yes	no
	[343]		Woven Carbon	Polyimine (PI)	60-145	14.2	400	Yes	no
	[548]		Woven Carbon	EP/PI	135-147	6.2	681	Yes	DMAP
	[361]		UD Carbon	UPR	150	101	910	Yes	Ti(IV)
	[357]		Woven Carbon	Modified SBpin	180	22.370	731	Yes	no
Thermoset	XC130 150 g UD Prepreg	Easy Composite	UD Carbon	Epoxy	140	55	645	no	-
	Carbon Fibre Strip	Easy Composite	UD Carbon	Vinyl Ester	80	40	500	no	-
	HexPly®8552 - AS4 Fibers	Hexcel	UD Carbon	Epoxy	200	135	2200	no	-
	HexPly®8552 - AS7 Fibers	Hexcel	UD Carbon	Epoxy	200	133	2300	no	-
	Conventional Pre-preg	Toray	UD Carbon	Epoxy	nc	49	920	no	-
	ET40	Toray	UD Carbon	Epoxy	nc	48	740	no	-
	2300 Prepreg system	Toray	UD Carbon	Epoxy	148	139	2790	no	-
	2510/P707AG-15	Toray	UD Carbon	Epoxy	146	128	1682	no	-
	T300/EP2500 Toray	Toray	UD Carbon	Epoxy	nc	140	1820	no	-
	Prepreg 316	Mitsubishi	UD Carbon	Epoxy	115	136	2260	no	-
	HMT317	Mitsubishi	UD Carbon	Epoxy	125	110	2070	no	-
	Prepreg 350	Mitsubishi	UD Carbon	Epoxy	192	131	2344	no	-
Thermoplastic	VESTAPE-PA12	Evonik	UD Carbon	PA12	40	100	1740	Yes	-
	VESTAPE-PEEK	Evonik	UD Carbon	PEEK	151	100	1780	Yes	-
	Toray Cetex®TC1320	Toray	UD Carbon	PEKK	160	135	2410	Yes	-
	Toray Cetex®TC915	Toray	UD Carbon	PA6	75	124	2179	Yes	-
	Toray Cetex®TC1200 P	Toray	UD Carbon	PEEK	143	135	2410	Yes	-
	Toray Cetex®TC1100	Toray	UD Carbon	PPS	90	134	2020	Yes	-

Table IV-A4 – Comparison of different vitrimer & commercially available carbon fiber composites

A.4 Appendix Chapter 5

A.4.1 Mutual catalytic effect on the aminolysis of CC and epoxy compounds

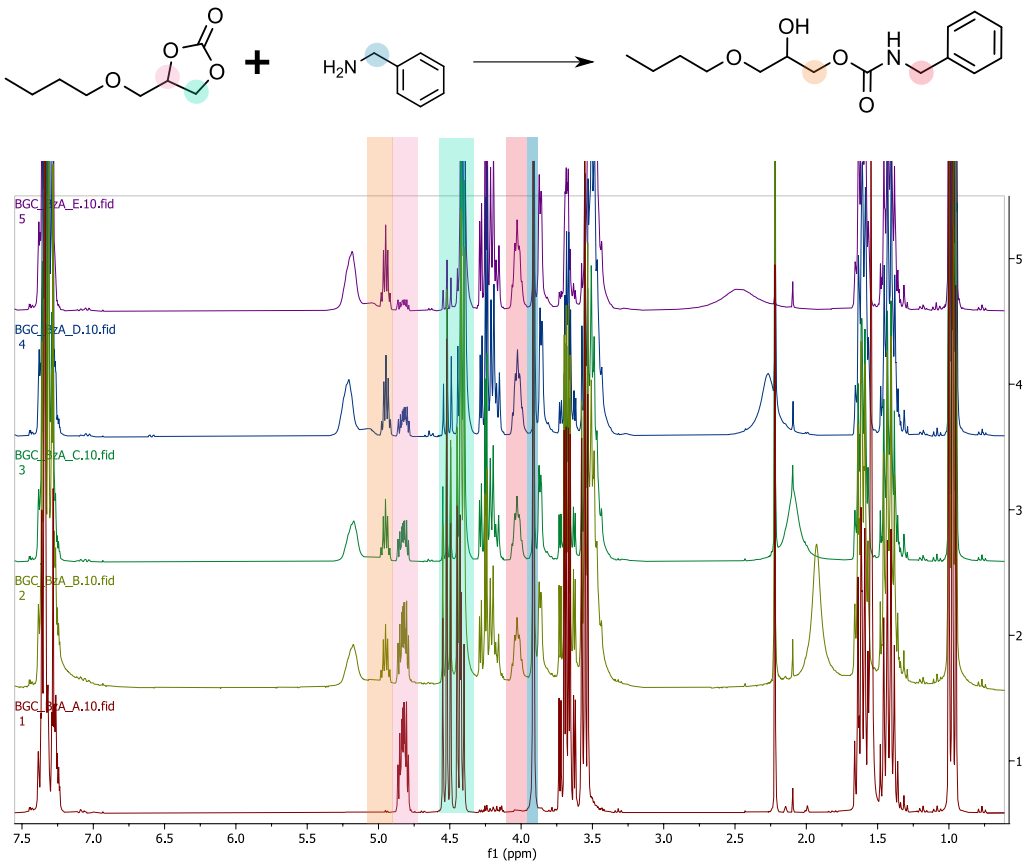

Figure V-A1 – ^{1}H-NMR kinetic model reaction in $CDCl_3$. Aminolysis of butyl carbonate by benzylamine.

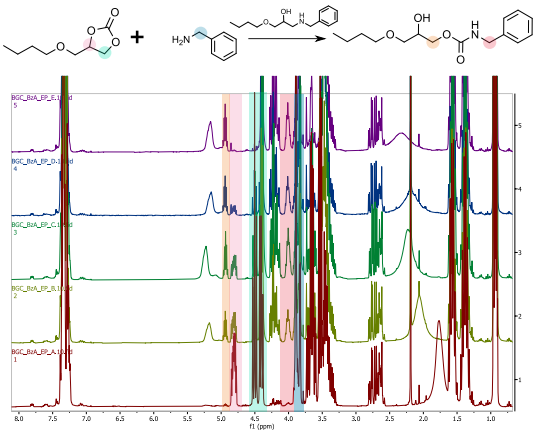

Figure V-A2 – ^{1}H-NMR kinetic model reaction in $CDCl_3$. Aminolysis of butyl carbonate by benzylamine in the presence of epoxy model compound (0.5eq mEP).

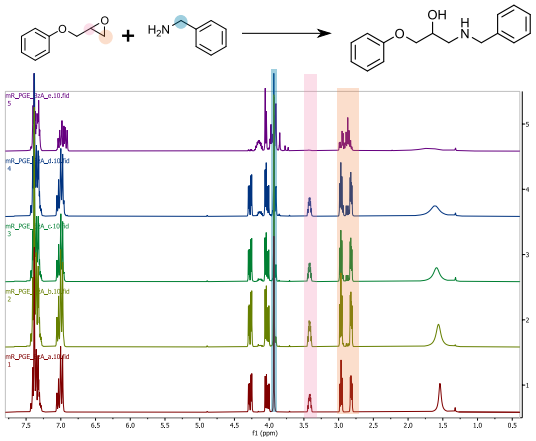

Figure V-A3 – ^{1}H-NMR kinetic model reaction in $CDCl_3$. Aminolysis of phenyl glycidyl ether by benzylamine.

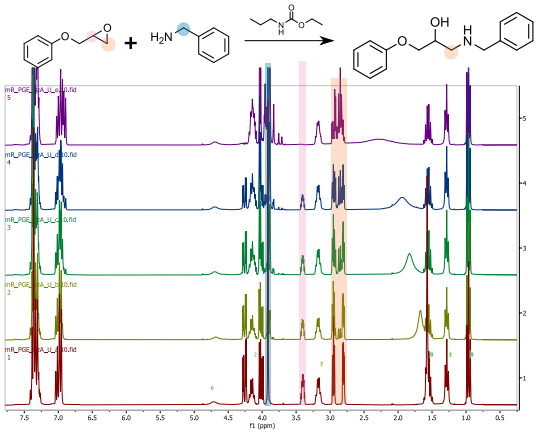

Figure V-A4 – ^{1}H-NMR kinetic model reaction in $CDCl_3$. Aminolysis of phenyl glycidyl ether by benzylamine in the presence of model urethane compound (mU, 0.5eq).

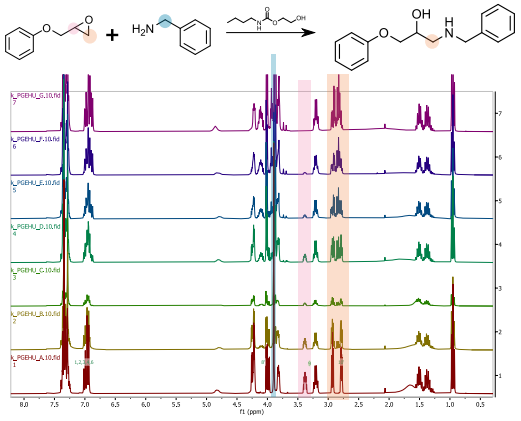

Figure V-A5 – ^{1}H-NMR kinetic model reaction in $CDCl_3$. Aminolysis of phenyl glycidyl ether by benzylamine in the presence of model hydroxyurethane compound (mHU, 0.5eq).

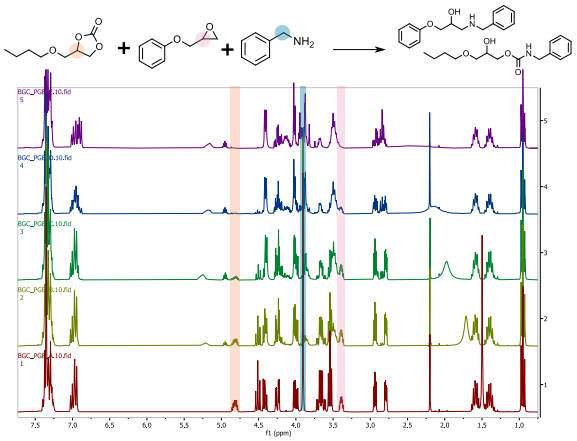

Figure V-A6 – ^{1}H-NMR kinetic model reaction in $CDCl_3$. Simultaneous aminolysis of phenyl glycidyl ether and butyl carbonate by benzylamine.

A.4.2 Hybridizing EP-PHU, effect of the EP quantity on co-monomer formulation viscosity

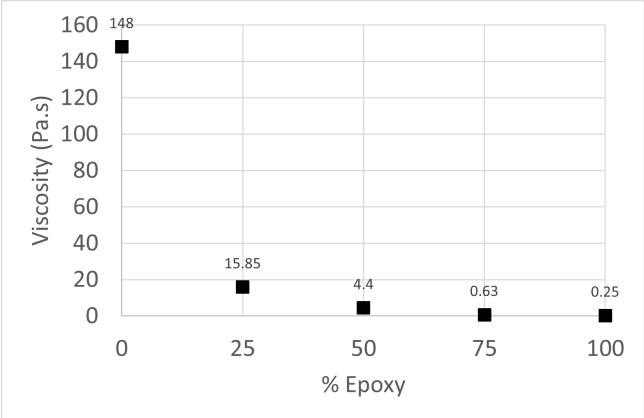

Figure V-A7 – Viscosity of the EP-CC mixture (prior to addition of amine hardener).

A.4.3 Influence of the hybridization on the properties of the neat resin

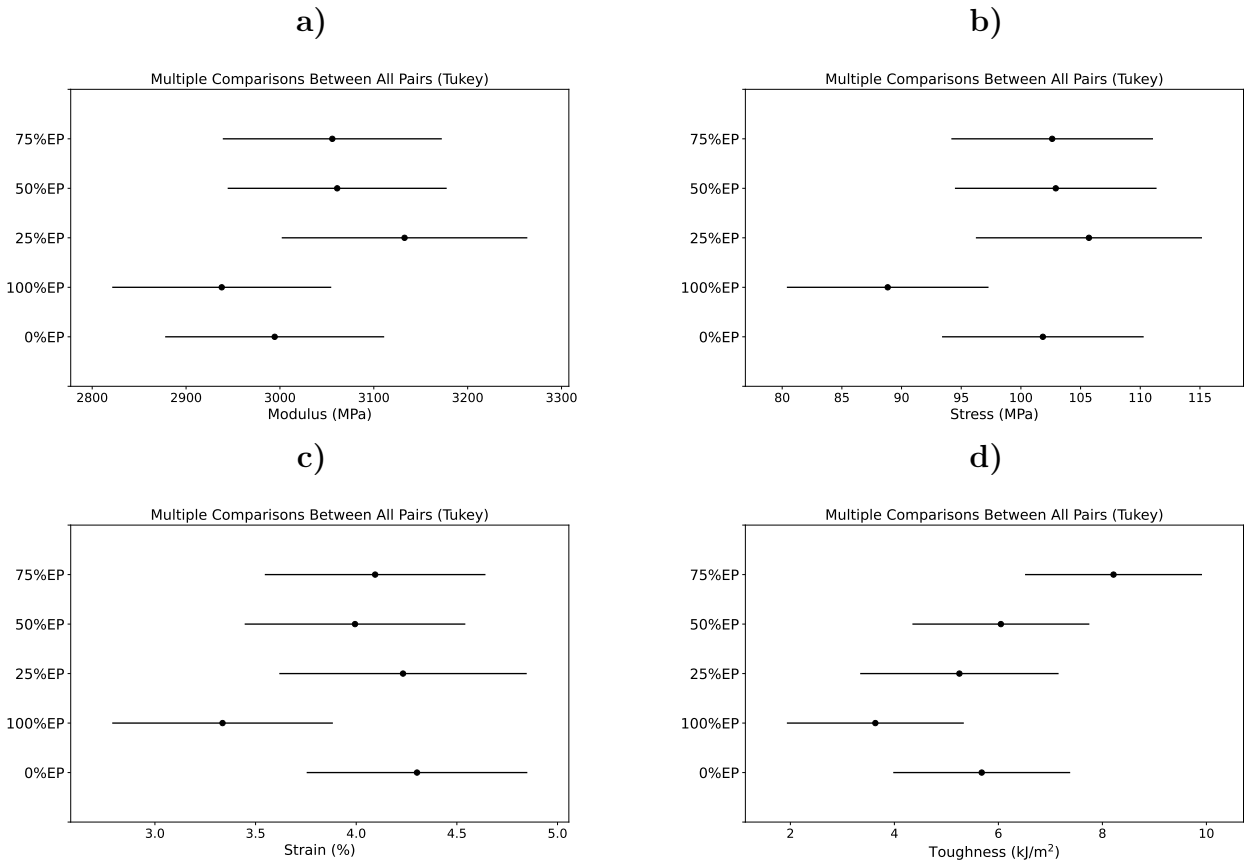

Figure V-A8 – Tukey's Test results after ANOVA for the neat resin's mechanical properties a) Tensile Modulus, b) Stress at break, c) Strain at break, and d) Charpy's impact toughness.

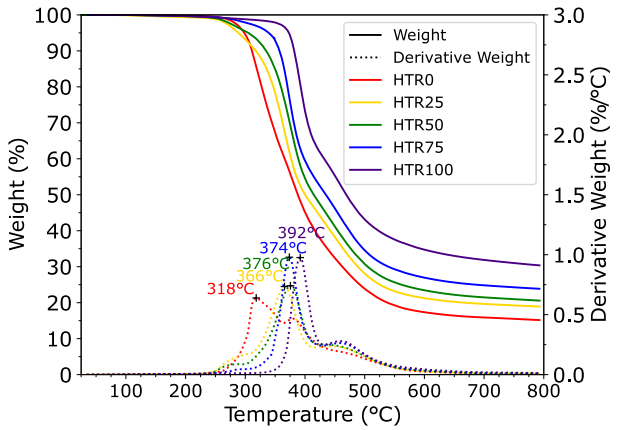

Figure V-A9 – Thermal degradation under N_2 of the matrices

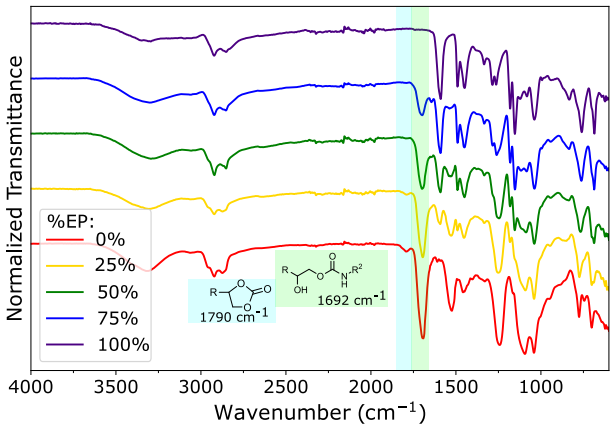

Figure V-A10 – FTIR of the matrices.

A.4.4 RTM manufacturing of flax-EP-PHU composites

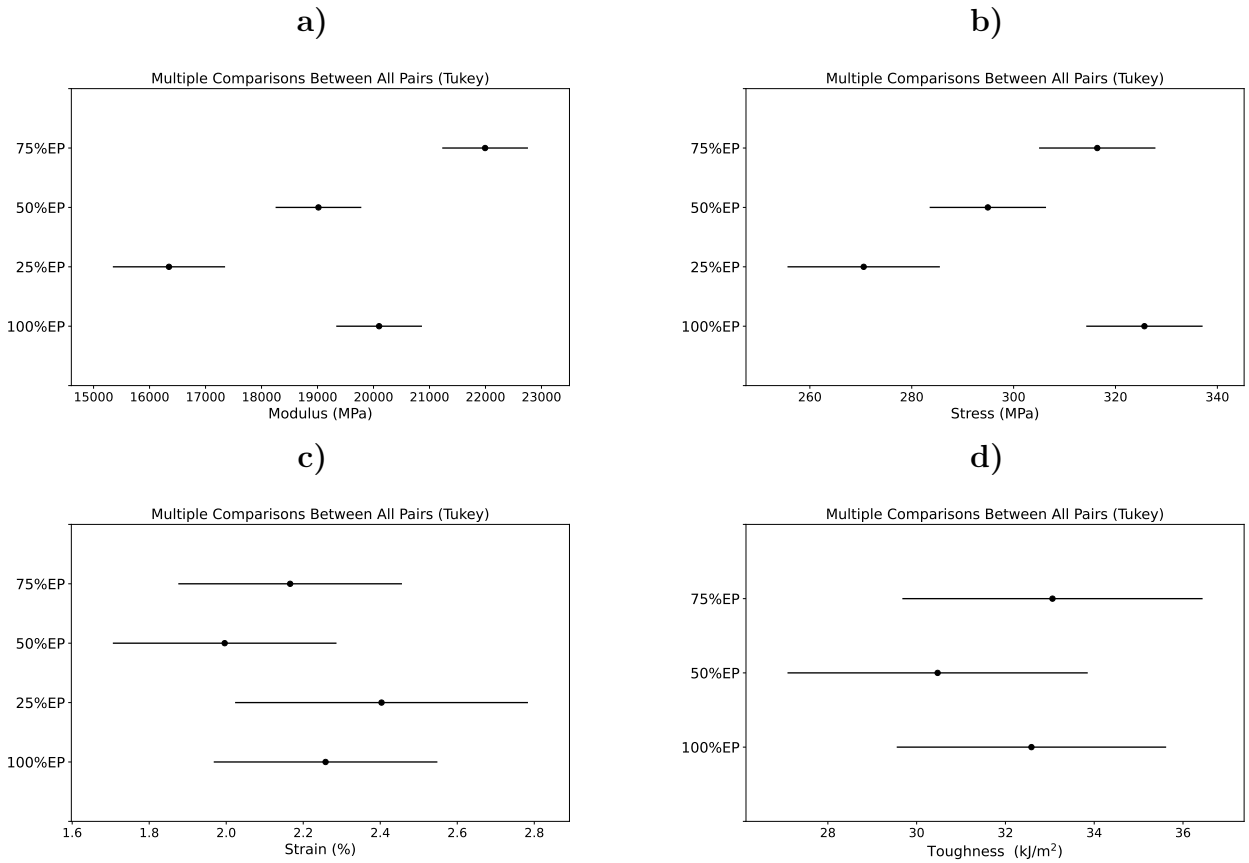

Figure V-A11 – Tukey's Test results after ANOVA for the composite's mechanical properties in the principal fiber orientation. a) Tensile Modulus, b) stress at break, c) strain at break, and d) Charpy's impact toughness.

a)

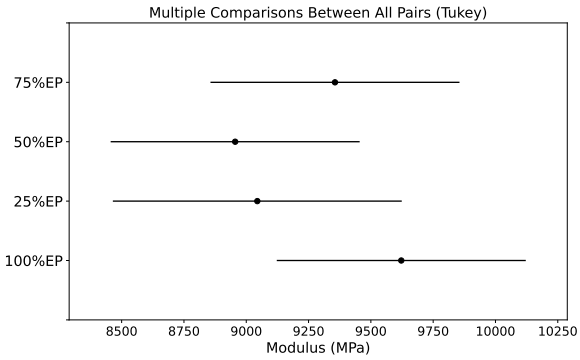

b)

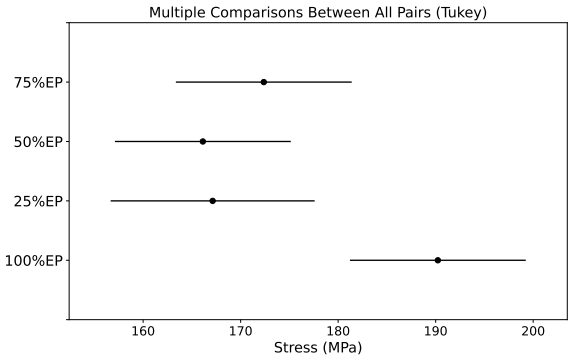

c)

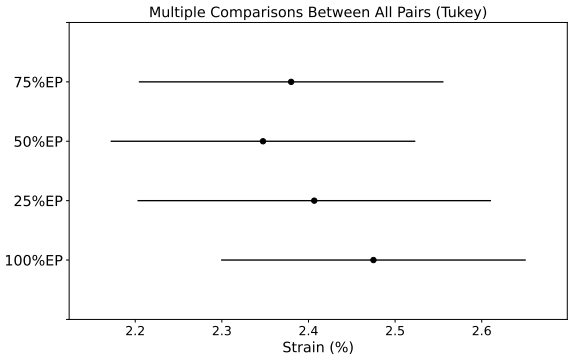

Figure V-A12 – Tukey's Test results after ANOVA for the composite's mechanical properties in the transverse fiber orientation. a) Tensile Modulus, b) stress at break, c) strain at break.

A.4.5 Perspectives towards the reshaping and recycling of natural fiber composites

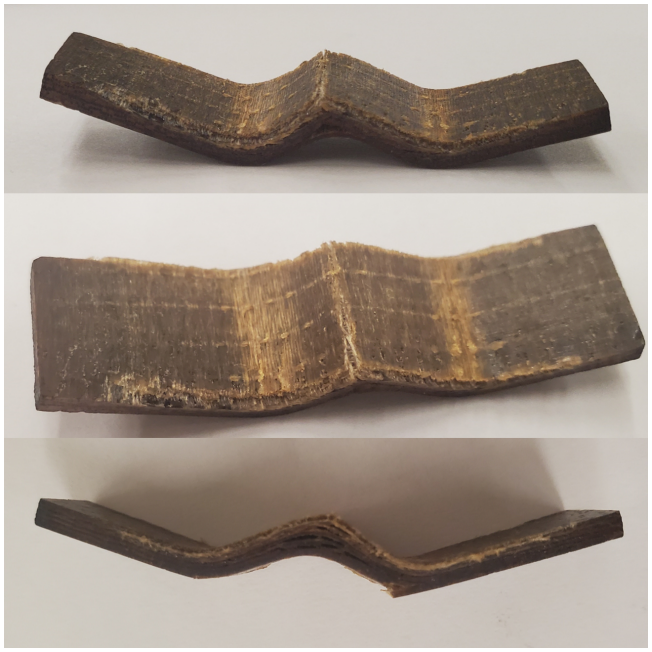

Figure V-A13 – Attempting to reshape flax-epoxy composite

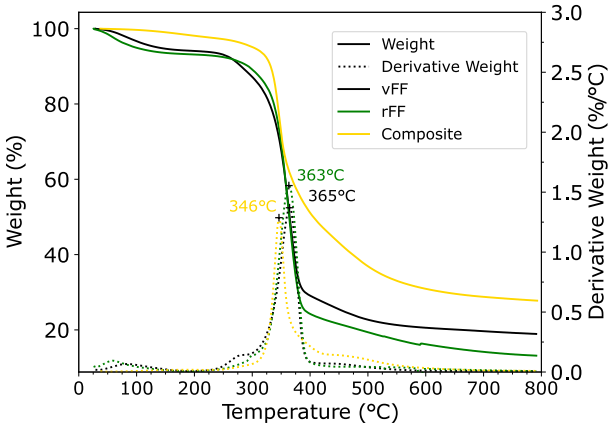

Figure V-A14 – TGA of virgin fibers (vFF), reclaimed fibers (rFF) and the initial composite.

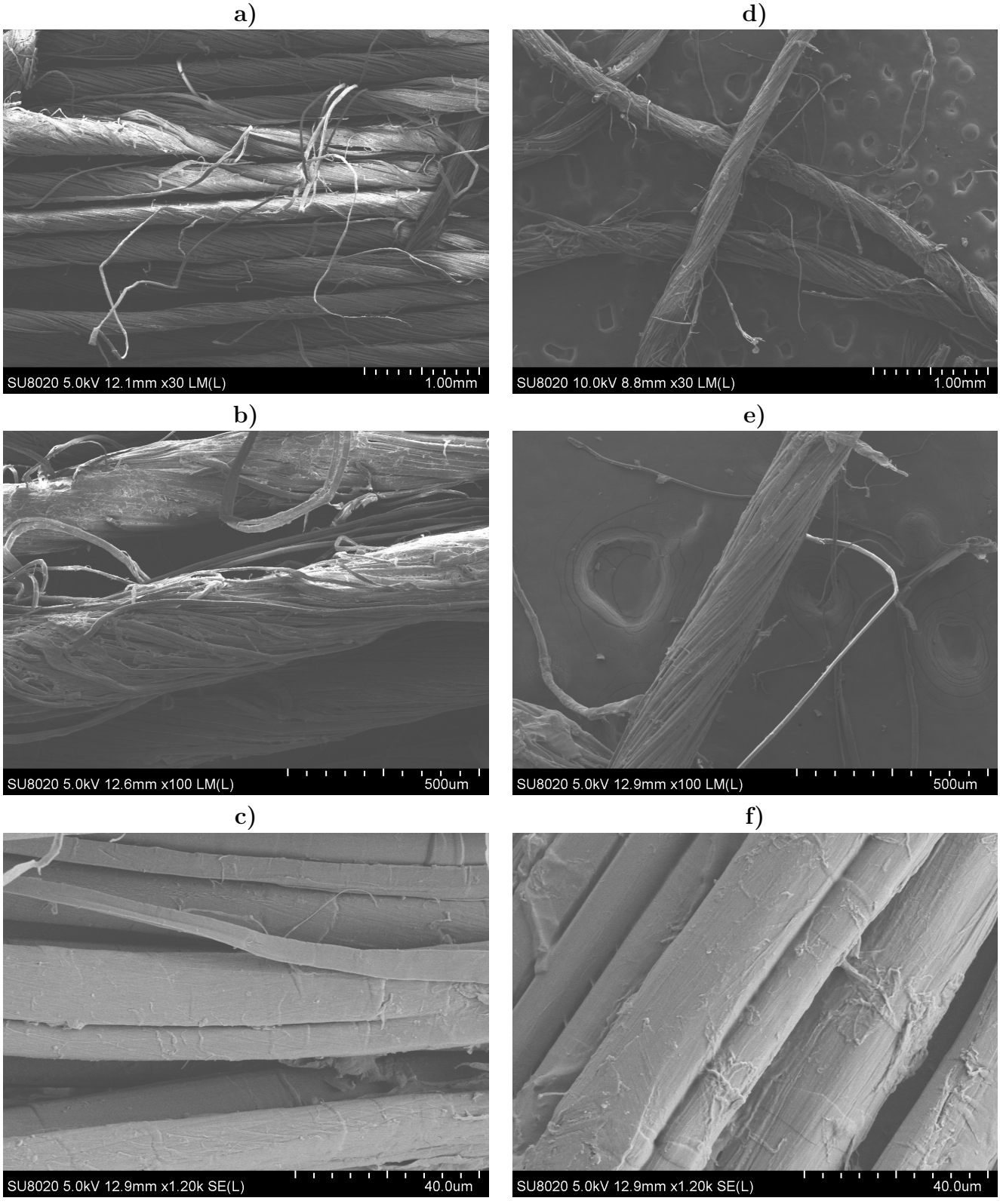

Figure V-A15 – SEM images of a-c) virgin and d-f) recovered flax reinforcement. a,d) x30 magnifications, b,e) x100 magnifications, and c,f) x1200 magnifications.

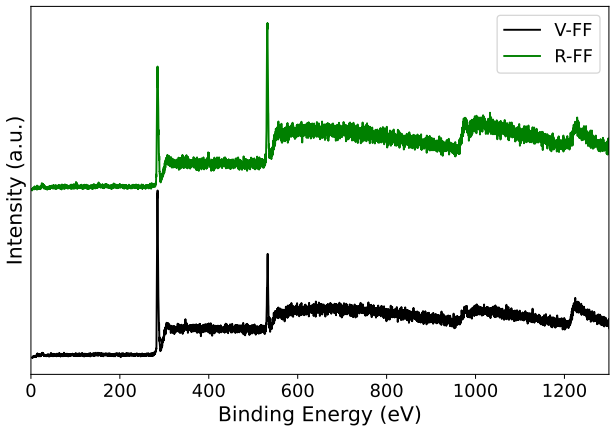

Figure V-A16 – Composition survey of the virgin and recovered flax by XPS

Table V-A1 – XPS results, surface composition for virgin flax fibers

Element	Name	Position	FWHM	Library RSF	Raw Area	Area/(RSF*T*MFP)	%At Conc	% Atomic rel
C	C-C, C-H	284.640	1.370	0.314	5103.400	707.590	56.97	81.93
	C-O	286.010	1.450	0.314	1551.430	215.050	17.31	
	C=O	287.460	1.540	0.314	484.770	67.180	5.41	
	O-C=O	288.690	1.620	0.314	201.010	27.850	2.24	
O	O1s	531.290	2.100	0.733	565.710	32.100	2.58	17.35
	O1s	532.620	2.100	0.733	3233.250	183.440	14.77	
Ca*	Ca (2p 3/2)	347.170	1.670	2.136	294.610	5.940	0.48	0.72
	Ca (2p 1/2)	350.780	1.670	2.136	147.310	2.970	0.24	

*Near noise spectrum, estimation

Table V-A2 – XPS results, surface composition for reclaimed flax fibers

Element	Name	Position	FWHM	Library RSF	Raw Area	Area/(RSF*T*MFP)	%At Conc	% Atomic rel
C	C-C, C-H	284.610	1.480	0.314	1658.270	229.930	29.290	67.06
	C-N, C-O	286.090	1.480	0.314	1384.910	191.970	24.460	
	C=O?	287.450	1.480	0.314	538.860	74.680	9.510	
	N-C=O, O-C=O	288.840	1.570	0.314	215.480	29.850	3.800	
O	O1s	532.540	2.230	0.733	4078	231.370	29.470	29.47
N*	N1s	399.860	1.960	0.499	228.620	19.530	2.490	2.49
Si*	Si2p	101.960	2.080	0.429	73.070	7.670	0.980	0.98

*Near noise spectrum, estimation

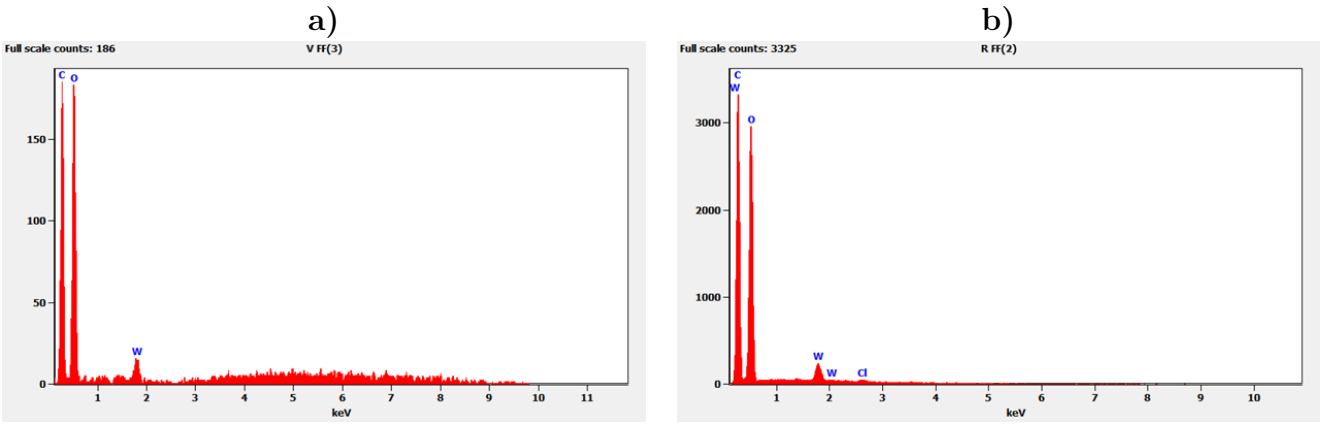

Figure V-A17 – EDX of a) virgin fibers, and b) recovered flax fibers. The tungsten element (W) is due to the conductive coating for SEM observations and EDX analysis.

Table V-A3 – Energy-dispersive X-ray spectroscopy (EDX) of virgin and recovered flax fibers

	V-FF		R-FF	
Element	Weight %	Atom %	Weight %	Atom %
C K	29.8 ± 0.6	36.1 ± 1.5	31.8 ± 0.2	38.5 ± 0.5
O K	70.2 ± 1.5	63.9 ± 2.8	66.9 ± 0.5	60.9 ± 0.8
Cl K	nd	nd	1.4 ± 0.2	0.6 ± 0.2
Total	100	100	100	100

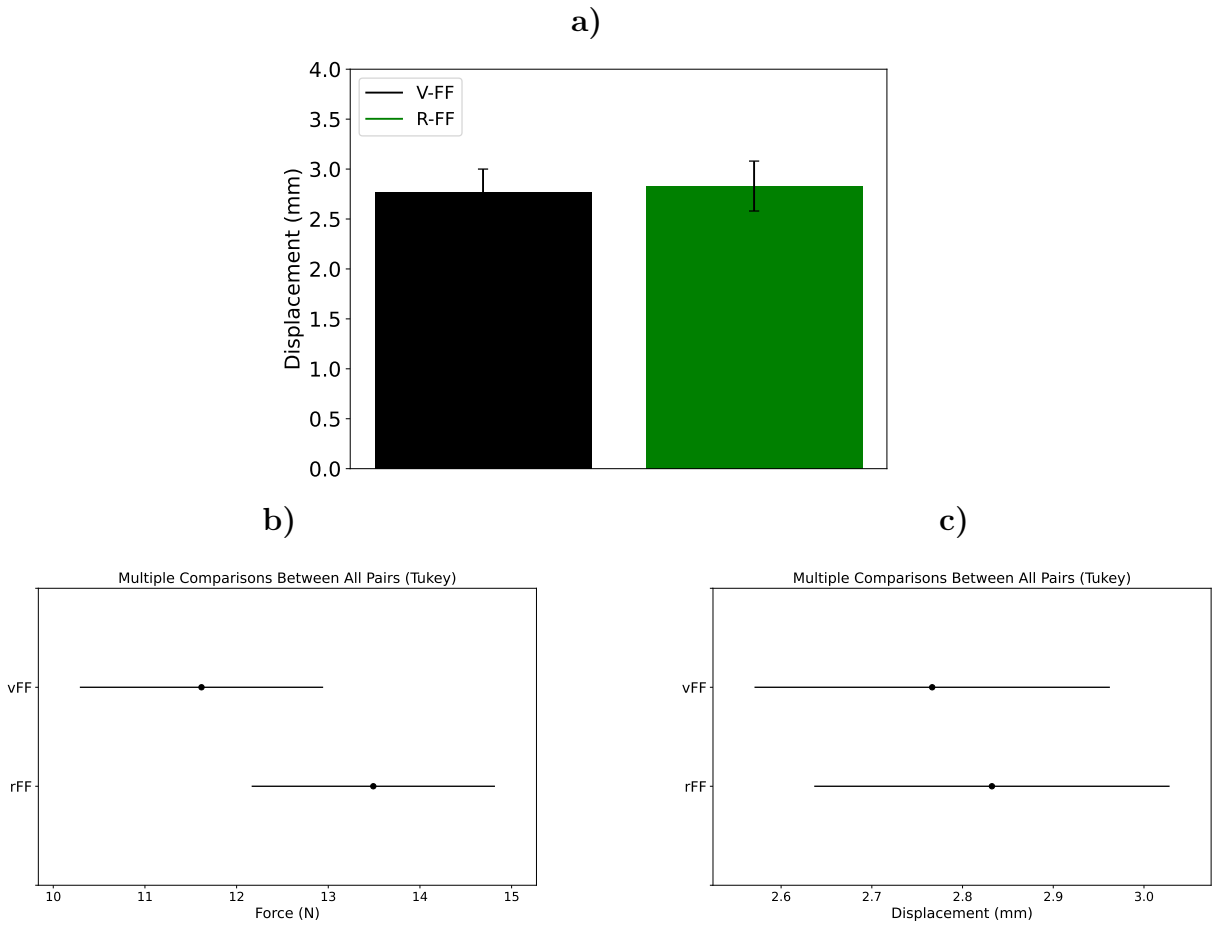

Figure V-A18 – a)Admissible displacement of the virgin and recovered flax yarns. Tukey's Test results after ANOVA for the virgin and recovered flax yarns: b) Tensile strength, and c) Tensile elongation.

A.5 Appendix Chapter 6

A.5.1 Monomer EI results

Epoxy synthesis and results

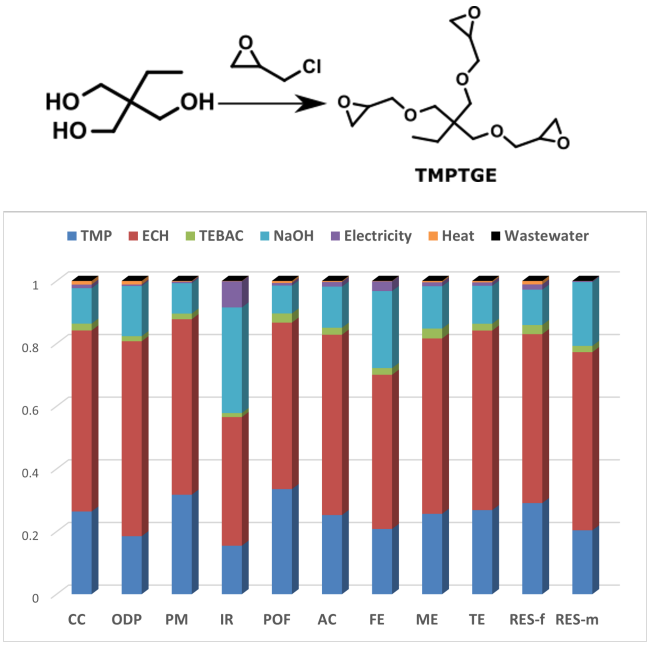

Figure VI-A1 – TMPTGE synthesis, contribution analysis

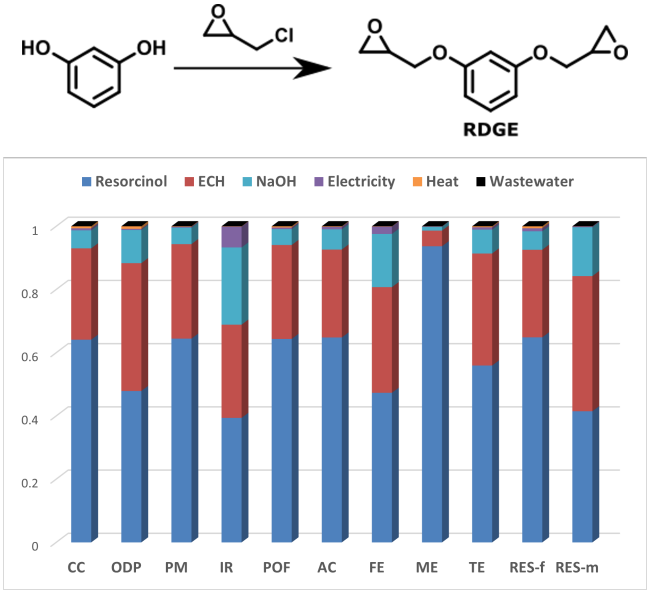

Figure VI-A2 – RDGE synthesis, contribution analysis

TMPTC synthesis

Table VI-A1 – EIA of TMPTGE, TMPTC from supercritical CO_2 and TMPTC from CO_2 in solvent. Results for 1 kg of monomer.

Indicator	Unit	TMPTGE	TMPTC ($scCO_2$)	TMPTC (solvent)
CC	kg CO_2 eq	6.2	5.3	9.1
ODP	kg CFC11 eq	$2.6x10^{-7}$	$1.96x10^{-7}$	$2.5x10^{-7}$
PM	disease inc.	$2.7x10^{-7}$	$2.07x10^{-7}$	$3.2x10^{-7}$
IR	kBq U-235 eq	0.57	0.85	0.61
POF	kg NMVOC eq	0.02	0.02	0.02
AC	mol H+ eq	0.02	0.02	0.03
FE	kg P eq	0.002	0.002	0.003
ME	kg N eq	0.005	0.004	0.006
TE	mol N eq	0.05	0.04	0.06
RES-f	MJ	103	91	119
RES-m	kg Sb eq	$5.1x10^{-5}$	$4.8x10^{-5}$	$5.5x10^{-5}$
WAT	m3 depriv.	2.1	1.7	2.4
LU	Pt	20	18	22
HT-nc	CTUh	$5.6x10^{-8}$	$5.9x10^{-8}$	$8.3x10^{-8}$
HT-c	CTUh	$3.0x10^{-8}$	$2.4x10^{-8}$	$3.0x10^{-8}$
FWT	CTUe	168	122	166

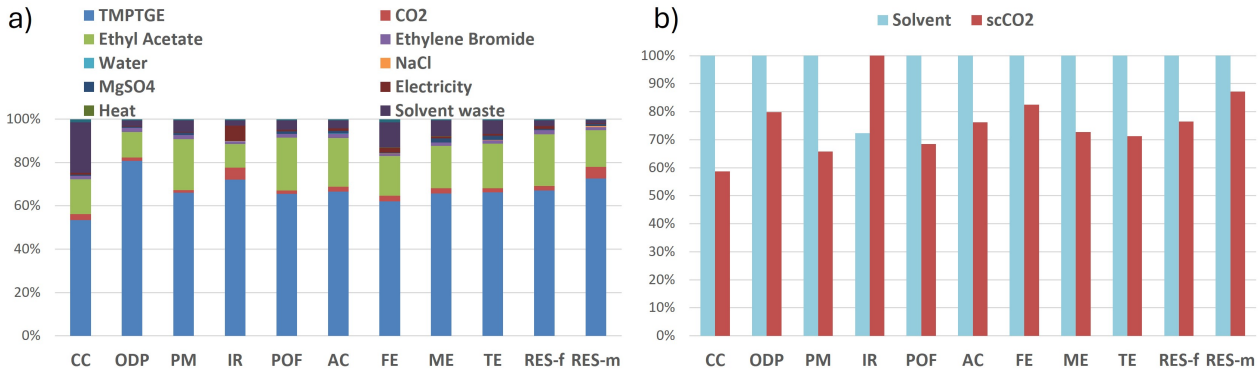

Figure VI-A3 – Comparative EI for TMPTC produced using supercritical CO_2 ($scCO_2$) and gaseous CO_2 in solvent (ethyl acetate).a) Contribution of the composition to the EI of TMPTC from solvent, and b) compared EI.

A.5.2 Resin detailed results

Table VI-A2 – Environmental impacts of the cured resins (1kg)

Indicator	Unit	EP	PHU	Hybrid
CC	kg CO_2 eq	10.4	9.0	8.5
ODP	kg CFC11 eq	3.3x10^{-7}	2.6x^{-7}	2.8x^{-7}
PM	disease inc.	3.9x10^{-7}	2.6x10^{-7}	3.1x10^{-7}
IR	kBq U-235 eq	1.0	2.2	1.1
POF	kg NMVOC eq	0.04	0.03	0.03
AC	mol H+ eq	0.05	0.04	0.04
FE	kg P eq	0.003	0.004	0.003
ME	kg N eq	0.04	0.00	0.02
TE	mol N eq	0.07	0.06	0.06
RES-f	MJ	190	163	160
RES-m	kg Sb eq	6.4x10^{-5}	7.9x10^{-5}	6.2x10^{-5}
WAT	m3 depriv.	3.9	3.5	3.5
LU	Pt	25	28	22
HT-nc	CTUh	7.2x10^{-8}	8.9x10^{-8}	6.8x10^{-8}
HT-c	CTUh	5.9x10^{-8}	2.8x10^{-8}	4.2x10^{-8}
FWT	CTUe	208	105	156

A.5.3 Composite detailed results

Table VI-A3 – Environmental impact assessment results FFRP

Indicator	Unit	Flax/EP	Flax/PHU	Flax/Hybrid
CC	kg CO_2 eq	5.5	5.4	4.7
ODP	kg CFC11 eq	1.8x10^{-7}	1.6x10^{-7}	1.6x10^{-7}
PM	disease inc.	2.4x10^{-7}	2.0x10-1	2.1x10^{-7}
IR	kBq U-235 eq	0.64	1.73	0.66
POF	kg NMVOC eq	0.02	0.02	0.02
AC	mol H+ eq	0.03	0.04	0.03
FE	kg P eq	0.002	0.003	0.002
ME	kg N eq	0.02	0.01	0.02
TE	mol N eq	0.06	0.07	0.06
RES-f	MJ	96	106	83
RES-m	kg Sb eq	3.6x10^{-5}	5.4x10^{-5}	3.45x10^{-5}
WAT	m3 depriv.	1.9	2.0	1.8
LU	Pt	222	228	221
HT-nc	CTUh	8.7x10^{-8}	1.09x10^{-7}	8.5x10^{-8}
HT-c	CTUh	3.1x10^{-8}	1.95x10^{-8}	2.4x10^{-8}
FWT	CTUe	112	70	89

Table VI-A4 – Environmental impact assessment results CFRP

Indicator	Unit	Carbon/EP	Carbon/Hybrid
CC	kg CO_2 eq	50.4	49.8
ODP	kg CFC11 eq	$1.5x10^{-6}$	$1.4x10^{-6}$
PM	disease inc.	$1.0x10^{-6}$	$9.8x10^{-7}$
IR	kBq U-235 eq	7.4	7.5
POF	kg NMVOC eq	0.11	0.11
AC	mol H+ eq	0.13	0.13
FE	kg P eq	0.012	0.011
ME	kg N eq	0.03	0.03
TE	mol N eq	0.24	0.23
RES-f	MJ	907	897
RES-m	kg Sb eq	$6.0x10^{-5}$	$5.9x10^{-5}$
WAT	m3 depriv.	11.5	11.4
LU	Pt	65	64
HT-nc	CTUh	$1.6x10^{-7}$	$1.6x10^{-7}$
HT-c	CTUh	$9.8x10^{-8}$	$9.2x10^{-8}$
FWT	CTUe	149	131

A.5.4 Life cycle assessment

Carbon fiber reinforced composites

Table VI-A5 – LCA results CFRP

Indicator	Unité	Reference	Landfill	Chemical	Mechanical
CC	kg CO_2 eq	85.6	84.7	71.4	68.3
ODP	kg CFC11 eq	$2.5x10^{-6}$	2.5x10-3	$1.7x10^{-6}$	$2.1x10^{-6}$
PM	disease inc.	$1.7x10^{-6}$	$1.7x10^{-6}$	$1.4x10^{-6}$	1.3x10-3
IR	kBq U-235 eq	12.7	12.7	9.4	10.3
POF	kg NMVOC eq	0.20	0.19	0.20	0.16
AC	mol H+ eq	0.22	0.22	0.18	0.19
FE	kg P eq	0.02	0.02	0.02	0.20
ME	kg N eq	0.06	0.05	0.04	0.06
TE	mol N eq	0.40	0.40	0.30	0.40
RES-f	MJ	1543	1526	1112	1186
RES-m	kg Sb eq	$1.0x10^{-4}$	$1.0x10^{-4}$	$1.3x10^{-4}$	$1.4x10^{-4}$
WAT	m3 depriv.	19.4	19.1	18.5	14.2
LU	Pt	111	110	97	109
HT-nc	CTUh	$2.7x10^{-7}$	$2.7x10^{-7}$	$3.3x10^{-7}0$	$2.7x10^{-7}$
HT-c	CTUh	$1.7x10^{-7}$	$1.6x10^{-7}$	$1.3x10^{-7}$	$1.74x10^{-7}$
FWT	CTUe	253	224	330	330

Flax fiber reinforced composites

Table VI-A6 – LCA results FFRP

Indicator	Unit	Reference	Landfill	Incineration	Chemical	Mechanical
CC	kg CO_2 eq	9.4	8.0	12.0	26.0	7.2
ODP	kg CFC11 eq	$3.1x10^{-7}$	$2.7x10^{-7}$	$3.1x10^{-7}$	$4.8x10^{-7}$	$2.3x10^{-7}$
PM	disease inc.	$4.1x10^{-7}$	$3.5x10^{-7}$	$4.0x10^{-7}$	$7.0x10^{-7}$	$2.9x10^{-7}$
IR	kBq U-235 eq	1.09	1.12	1.22	2.85	1.53
POF	kg NMVOC eq	0.40	0.03	0.04	0.06	0.03
AC	mol H+ eq	0.60	0.05	0.06	0.06	0.05
FE	kg P eq	0.003	0.003	0.004	0.008	0.003
ME	kg N eq	0.04	0.03	0.03	0.03	0.02
TE	mol N eq	0.11	0.10	0.11	0.16	0.09
RES-f	MJ	164	141	160	319	132
RES-m	kg Sb eq	$6.2x10^{-5}$	$5.8x10^{-5}$	$6.4x10^{-5}$	$11.9x10^{-5}$	$5.9x10^{-5}$
WAT	m3 depriv.	3.10	2.80	3.19	9.50	2.50
LU	Pt	378	376	378	256	293
HT-nc	CTUh	$1.48x10^{-7}$	$1.45x10^{-7}$	$1.57x10^{-7}$	$2.7x10^{-7}$	$1.28x10^{-7}$
HT-c	CTUh	$5.3x10^{-8}$	$4.07x10^{-8}$	$4.8x10^{-8}$	$6.6x10^{-7}$	$3.4x10^{-7}$
FWT	CTUe	191	152	213	282	120

A.5.5 Discussions about improvements

Bisphenol A and resorcinol

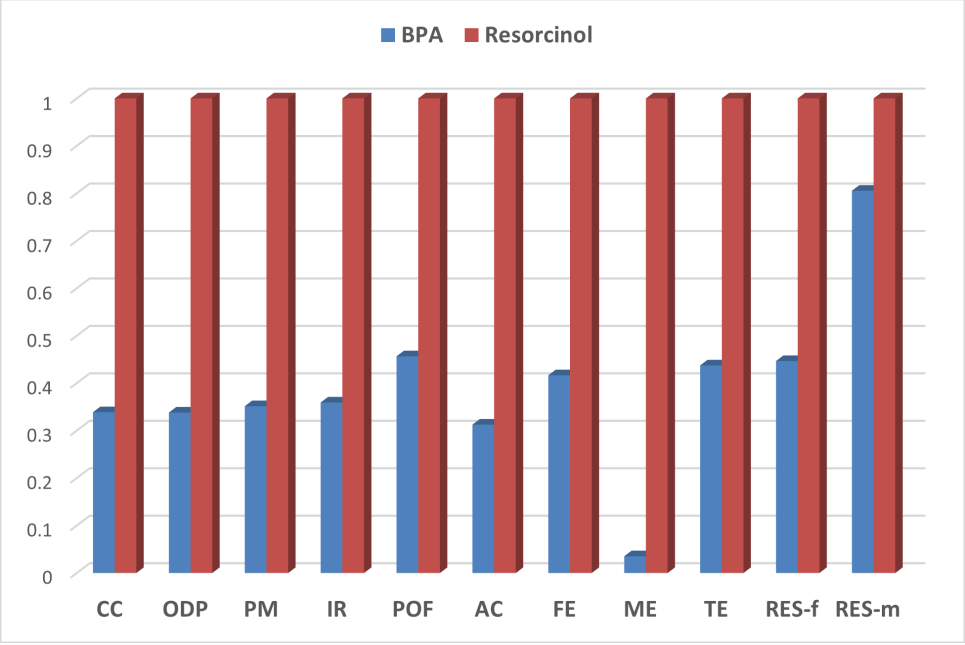

Figure VI-A4 – Comparative EI between bisphenol-A (BPA) and resorcinol for 1 kg, obtained from EcoInvent 3.4 database.

Bio-epichlorohydrin interest

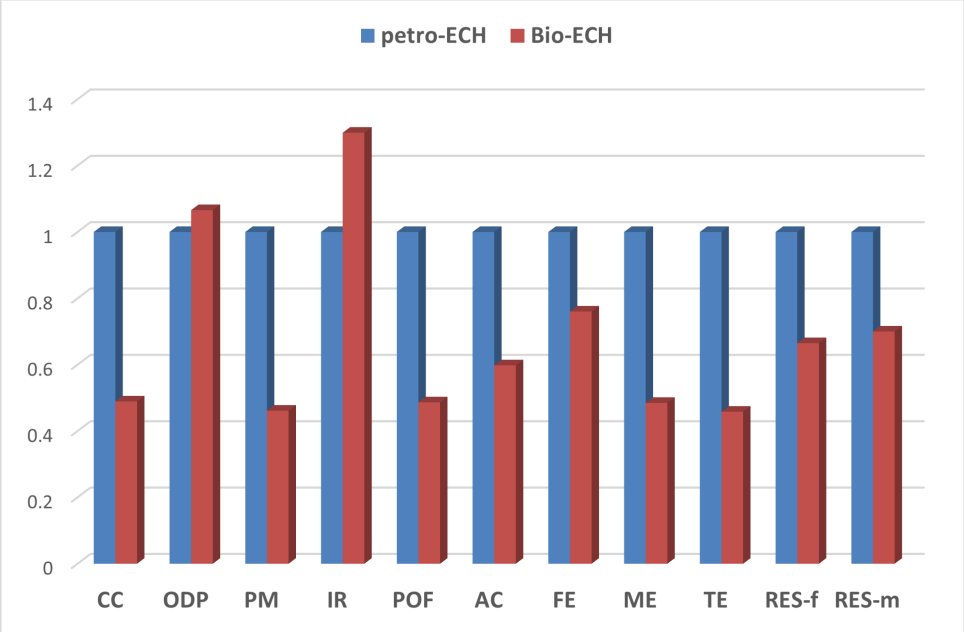

Figure VI-A5 – Comparison of EI of biobased (glycerol) and petro-based (allyl chloride) epichlorohydrin.

Impact of acidolysis and improvements

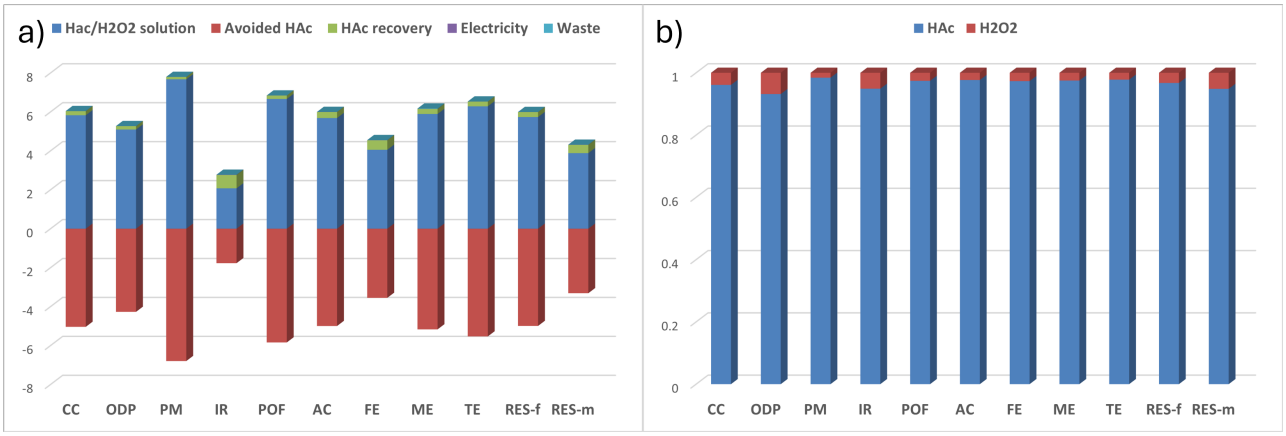

Figure VI-A6 – EI of the chemical recycling process and importance of HAc. a) contribution of each constituent in the recycling process, and b) shares of HAc in the depolymerization solution mixture.

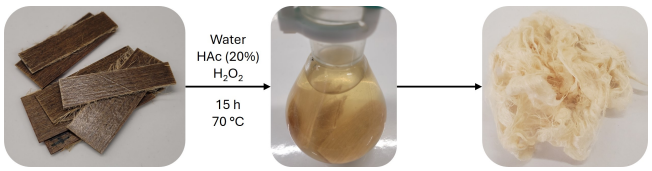

Figure VI-A7 – Pictures of the recycling of the flax/hybrid composite in 20% acetic acid.

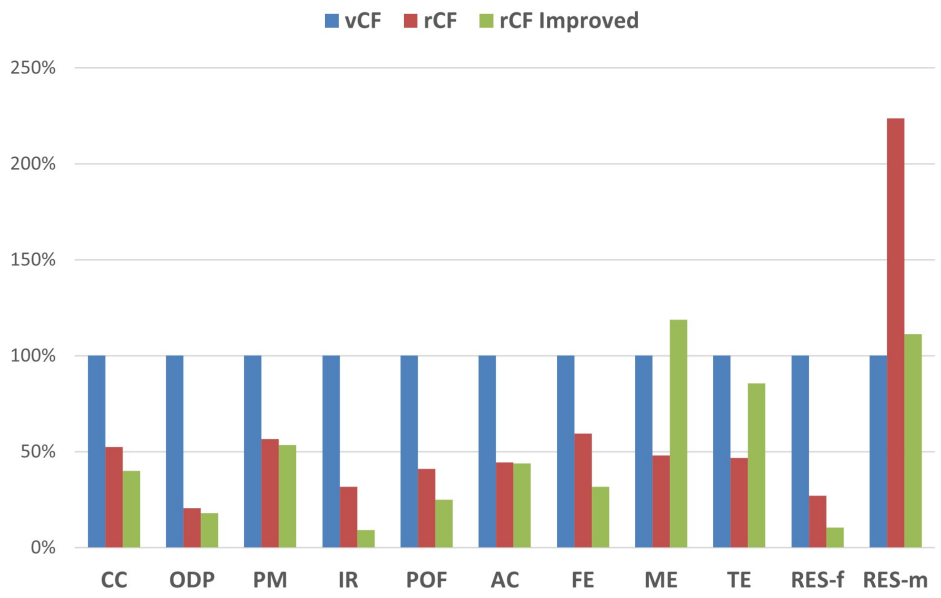

Figure VI-A8 – Improvement of the chemical recycling processes for CFRP. Comparison of the environmental footprint of virgin carbon fibers (vCF) vs the glacial acetic acid process (rCF) and the vinegar-based process.

Bibliography

[1] Georgescu-Roegen N. The Entropy Law and the Economic Process in Retrospect. Eastern Economic Journal. 1986;12(1):3-25.

[2] Stahel WR. The circular economy. Nature. 2016 Mar;531(7595):435-8.

[3] Wise C, Pawlyn M, Braungart M. Eco-engineering: Living in a materials world. Nature. 2013 Feb;494(7436):172-5.

[4] Ekins P, Domenech T, Drummond P, Bleischwitz R, Hughes N, Lotti L. The Circular Economy: What, Why, How and Where. OECD; 2020. Managing environmental and energy transitions for regions and cities.

[5] Fay PA. 1 - A history of adhesive bonding. In: Adams RD, editor. Adhesive Bonding (Second Edition). Woodhead Publishing Series in Welding and Other Joining Technologies. Woodhead Publishing; 2021. p. 3-40.

[6] Staudinger H. Über Polymerisation. Berichte der deutschen chemischen Gesellschaft (A and B Series). 1920;53(6):1073-85.

[7] Tanaka F. Pioneering the carbon fiber frontier: A half-century of industry leadership and the road ahead. Composites Part B: Engineering. 2024 Jul;281:111515.

[8] Herakovich CT. Mechanics of composites: A historical review. Mechanics Research Communications. 2012 Apr;41:1-20.

[9] Co E. JEC Observer: Current trends in the global composites industry 2023-2028. JEC Group. 2024;Special Issue.

[10] JEC T. Composite sustainability Report 2024. JEC Composites Magazine. 2024;Special Issue(2):1-72.

[11] Witik RA, Payet J, Michaud V, Ludwig C, Månson JAE. Assessing the life cycle costs and environmental performance of lightweight materials in automobile applications. Composites Part A: Applied Science and Manufacturing. 2011 Nov;42(11):1694-709.

[12] Liu Y, Yu Z, Wang B, Li P, Zhu J, Ma S. Closed-loop chemical recycling of thermosetting polymers and their applications: a review. Green Chemistry. 2022;24(15):5691-708.

[13] Zhang J, Chevali VS, Wang H, Wang CH. Current status of carbon fibre and carbon fibre composites recycling. Composites Part B: Engineering. 2020 Jul;193:108053.

[14] Duflou JR, De Moor J, Verpoest I, Dewulf W. Environmental impact analysis of composite use in car manufacturing. CIRP Annals. 2009;58(1):9-12.

[15] Auvergne R, Caillol S, David G, Boutevin B, Pascault JP. Biobased Thermosetting Epoxy: Present and Future. Chemical Reviews. 2014 Jan;114(2):1082-115.

[16] Sougrati L, Duval A, Avérous L. Biobased and aromatic Covalent Adaptable Networks: When architectures meet properties, within the framework of a circular bioeconomy. Materials Science and Engineering: R: Reports. 2024 Dec;161:100882.

[17] Geng Y, Sarkis J, Bleischwitz R. How to globalize the circular economy. Nature. 2019 Jan;565(7738):153-5.

[18] Sanford K, Chotani G, Danielson N, Zahn JA. Scaling up of renewable chemicals. Current Opinion in Biotechnology. 2016 Apr;38:112-22.

[19] Vidal F, Van Der Marel ER, Kerr RWF, McElroy C, Schroeder N, Mitchell C, et al. Designing a circular carbon and plastics economy for a sustainable future. Nature. 2024 Feb;626(7997):45-57.

[20] Mohanty AK, Wu F, Mincheva R, Hakkarainen M, Raquez JM, Mielewski DF, et al. Sustainable polymers. Nature Reviews Methods Primers. 2022 Jun;2(1):46.

[21] Raquez JM, Deléglise M, Lacrampe MF, Krawczak P. Thermosetting (bio)materials derived from renewable resources: A critical review. Progress in Polymer Science. 2010 Apr;35(4):487-509.

[22] Lucherelli MA, Duval A, Avérous L. Biobased vitrimers: Towards sustainable and adaptable performing polymer materials. Progress in Polymer Science. 2022 Apr;127:101515.

[23] Bourmaud A, Beaugrand J, Shah DU, Placet V, Baley C. Towards the design of high-performance plant fibre composites. Progress in Materials Science. 2018 Aug;97:347-408.

[24] Schenk V, Labastie K, Destarac M, Olivier P, Guerre M. Vitrimer composites: current status and future challenges. Materials Advances. 2022;3(22):8012-29.

[25] De B, Bera M, Bhattacharjee D, Ray BC, Mukherjee S. A comprehensive review on fiber-reinforced polymer composites: Raw materials to applications, recycling, and waste management. Progress in Materials Science. 2024 Dec;146:101326.

[26] Spini F, Bettini P. End-of-Life wind turbine blades: Review on recycling strategies. Composites Part B: Engineering. 2024 Apr;275:111290.

[27] Oliveux G, Dandy LO, Leeke GA. Current status of recycling of fibre reinforced polymers: Review of technologies, reuse and resulting properties. Progress in Materials Science. 2015 Jul;72:61-99.

[28] Feng Y, Zhang Z, Yue D, Belko VO, Maksimenko SA, Deng J, et al. Recent progress in degradation and recycling of epoxy resin. Journal of Materials Research and Technology. 2024 Sep;32:2891-912.

[29] Veers P, Dykes K, Lantz E, Barth S, Bottasso CL, Carlson O, et al. Grand challenges in the science of wind energy. Science. 2019 Oct;366(6464):eaau2027.

[30] Patel P. Wind turbine blade recycling picks up speed. Chemical & Engineering News. 2024 Mar.

[31] Geyer R, Jambeck JR, Law KL. Production, use, and fate of all plastics ever made. Science Advances. 2017 Jul;3(7):e1700782.

[32] Europe P. The Circular Economy for Plastics – A European Analysis 2024. Plastic Europe; 2024. 1.

[33] Hagnell MK, Åkermo M. The economic and mechanical potential of closed loop material usage and recycling of fibre-reinforced composite materials. Journal of Cleaner Production. 2019 Jun;223:957-68.

[34] Elfaleh I, Abbassi F, Habibi M, Ahmad F, Guedri M, Nasri M, et al. A comprehensive review of natural fibers and their composites: An eco-friendly alternative to conventional materials. Results in Engineering. 2023 Sep;19:101271.

[35] Zhang J, Lin G, Vaidya U, Wang H. Past, present and future prospective of global carbon fibre composite developments and applications. Composites Part B: Engineering. 2023 Feb;250:110463.

[36] Yao SS, Jin FL, Rhee KY, Hui D, Park SJ. Recent advances in carbon-fiber-reinforced thermoplastic composites: A review. Composites Part B: Engineering. 2018 Jun;142:241-50.

[37] Goda I, Padayodi E, Raoelison RN. Enhancing fiber/matrix interface adhesion in polymer composites: Mechanical characterization methods and progress in interface modification. Journal of Composite Materials. 2024 Dec;58(29):3077-110.

[38] Reux F. Overview of the global composite market. JEC Composites Magazine. 2019;Special Issue(1).

[39] Pascault JP, editor. Thermosetting polymers. No. 64 in Plastics engineering. New York, NY Basel: Dekker; 2002.

[40] Penn LS, Chiao TT. Epoxy Resins. In: Lubin G, editor. Handbook of Composites. Boston, MA: Springer US; 1982. p. 57-88.

[41] Advani SG, Hsiao KT. 1 - Introduction to composites and manufacturing processes. In: Advani SG, Hsiao KT, editors. Manufacturing Techniques for Polymer Matrix Composites (PMCs). elsevier ed. Woodhead Publishing Series in Composites Science and Engineering. Woodhead Publishing; 2012. p. 1-12.

[42] Li Y, Xiao Y, Yu L, Ji K, Li D. A review on the tooling technologies for composites manufacturing of aerospace structures: materials, structures and processes. Composites Part A: Applied Science and Manufacturing. 2022 Mar;154:106762.

[43] Ekuase OA, Anjum N, Eze VO, Okoli OI. A Review on the Out-of-Autoclave Process for Composite Manufacturing. Journal of Composites Science. 2022 Jun;6(6):172.

[44] Chatziparaskeva G, Papamichael I, Voukkali I, Loizia P, Sourkouni G, Argirusis C, et al. End-of-Life of Composite Materials in the Framework of the Circular Economy. Microplastics. 2022 Sep;1(3):377-92.

[45] Boulding KE. The Economics of the Coming Spaceship Earth. In: Environmental Quality in a Growing Economy. RFF Press; 1966. p. pp 3 14. Num Pages: 12.

[46] Pearce DW, Turner RK. Economics of Natural Resources and the Environment. JHU Press; 1989.

[47] Kiser B, Andrew C, Vickerson A, Magdani N. Circular economy: Getting the circulation going. Nature. 2016 Mar;531(7595):443-6.

[48] Kirchherr J, Reike D, Hekkert M. Conceptualizing the circular economy: An analysis of 114 definitions. Resources, Conservation and Recycling. 2017 Dec;127:221-32.

[49] McDowall W, Geng Y, Huang B, Barteková E, Bleischwitz R, Türkeli S, et al. Circular Economy Policies in China and Europe. Journal of Industrial Ecology. 2017 Jun;21(3):651-61.

[50] Corvellec H, Stowell AF, Johansson N. Critiques of the circular economy. Journal of Industrial Ecology. 2022 Apr;26(2):421-32.

[51] Wijkman A, Skånberg. The Circular Economy and Benefits for Society. Club of Rome; 2017.

[52] Royle M, Gibson EA. Championing systems thinking to create a circular economy of chemicals. Chem. 2023 Mar;9(3):543-6.

[53] Gloria A, Montanari R, Richetta M, Varone A. Alloys for Aeronautic Applications: State of the Art and Perspectives. Metals. 2019 Jun;9(6):662.

[54] Rosenboom JG, Langer R, Traverso G. Bioplastics for a circular economy. Nature Reviews Materials. 2022 Jan.

[55] Zhu Y, Romain C, Williams CK. Sustainable polymers from renewable resources. Nature. 2016 Dec;540(7633):354-62.

[56] Calvin K, Dasgupta D, Krinner G, Mukherji A, Thorne PW, Trisos C, et al. IPCC, 2023: Climate Change 2023: Synthesis Report. Contribution of Working Groups I, II and III to the Sixth Assessment Report of the Intergovernmental Panel on Climate Change [Core Writing Team, H. Lee and J. Romero (eds.)]. IPCC, Geneva, Switzerland. Intergovernmental Panel on Climate Change (IPCC); 2023.

[57] Arnold U, Brück T, De Palmenaer A, Kuse K. Carbon Capture and Sustainable Utilization by Algal Polyacrylonitrile Fiber Production: Process Design, Techno-Economic Analysis, and Climate Related Aspects. Industrial & Engineering Chemistry Research. 2018 Jun;57(23):7922-33.

[58] Colledani M, Turri S, editors. Systemic Circular Economy Solutions for Fiber Reinforced Composites. Digital Innovations in Architecture, Engineering and Construction. Cham: Springer International Publishing; 2022.

[59] Baley C, Davies P, Troalen W, Chamley A, Dinham-Price I, Marchandise A, et al. Sustainable polymer composite marine structures: Developments and challenges. Progress in Materials Science. 2024 Oct;145:101307.

[60] Mishnaevsky L. Sustainable End-of-Life Management of Wind Turbine Blades: Overview of Current and Coming Solutions. Materials. 2021 Feb;14(5):1124.

[61] Krauklis AE, Karl CW, Gagani AI, Jørgensen JK. Composite Material Recycling Technology—State-of-the-Art and Sustainable Development for the 2020s. Journal of Composites Science. 2021 Jan;5(1):28.

[62] Kolesov YI, Kudryavtsev MY, Mikhailenko NY. Types and Compositions of Glass for Production of Continuous Glass Fiber (Review). Glass and Ceramics. 2001 May;58(5):197-202.

[63] Jones FR, Huff NT. Structure and properties of glass fibres. In: Handbook of Tensile Properties of Textile and Technical Fibres. Elsevier; 2009. p. 529-73.

[64] Cevahir A. Glass fibers. In: Fiber Technology for Fiber-Reinforced Composites. Elsevier; 2017. p. 99-121.

[65] Jamshaid H, Mishra R. A green material from rock: basalt fiber – a review. The Journal of The Textile Institute. 2016 Jul;107(7):923-37.

[66] Ekşı S, Genel K. Comparison of Mechanical Properties of Unidirectional and Woven Carbon, Glass and Aramid Fiber Reinforced Epoxy Composites. Acta Physica Polonica A. 2017 Sep;132(3-II):879-82.

[67] Jacquet L, Le Duigou A, Kerbrat O. A Proposal for a Carbon Fibre-Manufacturing Life-Cycle Inventory: A Case Study from the Competitive Sailing Boat Industry. Journal of Composites Science. 2024 Jul;8(7):276.

[68] Das S. Life cycle assessment of carbon fiber-reinforced polymer composites. The International Journal of Life Cycle Assessment. 2011 Mar;16(3):268-82.

[69] Tapper RJ, Longana ML, Norton A, Potter KD, Hamerton I. An evaluation of life cycle assessment and its application to the closed-loop recycling of carbon fibre reinforced polymers. Composites Part B: Engineering. 2020 Mar;184:107665.

[70] Mancini M. The Basalt Fiber—Material Design Art. SpringerBriefs in Applied Sciences and Technology. Cham: Springer Nature Switzerland; 2023.

[71] Morini AA, Ribeiro MJ, Hotza D. Carbon footprint and embodied energy of a wind turbine blade—a case study. The International Journal of Life Cycle Assessment. 2021 Jun;26(6):1177-87.

[72] Osnos S. JEC Composites Magazine - N°108 - october 2016. JEC Composites. 2016 Oct;108.

[73] Shi FJ. A Study on Structure and Properties of Basalt Fiber. Applied Mechanics and Materials. 2012 Nov;238:17-21.

[74] Pavlović A, Donchev T, Petkova D, Staletović N. Sustainability of alternative reinforcement for concrete structures: Life cycle assessment of basalt FRP bars. Construction and Building Materials. 2022 Jun;334:127424.

[75] Ghimire A. Life Cycle Assessment of Glass Fiber or Basalt Fiber Composite Baseball Bats; A Comparative Environmental Analysis [Bachelor Thesis]. Arcada University of Applied Sciences: Mechanical and Sustainability Engineering; 2023.

[76] Le Duigou A, Davies P, Baley C. Environmental Impact Analysis of the Production of Flax Fibres to be Used as Composite Material Reinforcement. Journal of Biobased Materials and Bioenergy. 2011 Mar;5(1):153-65.

[77] allianceflaxlinenhemp E. Situation économique du marché du lin et du chanvre européen. Alliance for European Flax-Linen & Hemp; 2024. Q3-2024.

[78] Müssig J, Amaducci S, Bourmaud A, Beaugrand J, Shah DU. Transdisciplinary top-down review of hemp fibre composites: From an advanced product design to crop variety selection. Composites Part C: Open Access. 2020 Oct;2:100010.

[79] Beiser V. Sand mining: the global environmental crisis you've probably never heard of. The Guardian. 2017 Feb.

[80] Beiser V. Why the world is running out of sand. BBC. 2019 Nov.

[81] Bendixen M, Iversen LL, Best J, Franks DM, Hackney CR, Latrubesse EM, et al. Sand, gravel, and UN Sustainable Development Goals: Conflicts, synergies, and pathways forward. One Earth. 2021 Aug;4(8):1095-111.

[82] Pender K, Yang L. Glass Fibre Composites Recycling Using the Fluidised Bed: A Comparative Study into the Carbon Footprint in the UK. Sustainability. 2024 Jan;16(3):1016.

[83] Colangelo S. Reducing the environmental footprint of glass manufacturing. International Journal of Applied Glass Science. 2024;15(4):350-66.

[84] Hübler M, Pothen F. Can smart policies solve the sand mining problem? PLOS ONE. 2021 Apr;16(4):e0248882.

[85] Chahed H, Usman M, Chatterjee A, Bayram F, Chaudhary R, Brunstrom A, et al. AIDA—A holistic AI-driven networking and processing framework for industrial IoT applications. Internet of Things. 2023 Jul;22:100805.

[86] Joshi SV, Drzal LT, Mohanty AK, Arora S. Are natural fiber composites environmentally superior to glass fiber reinforced composites? Composites Part A: Applied Science and Manufacturing. 2004 Mar;35(3):371-6.

[87] Naqvi SR, Prabhakara HM, Bramer EA, Dierkes W, Akkerman R, Brem G. A critical review on recycling of end-of-life carbon fibre/glass fibre reinforced composites waste using pyrolysis towards a circular economy. Resources, Conservation and Recycling. 2018 Sep;136:118-29.

[88] Singha K. A Short Review on Basalt Fiber. International Journal of Textile Science. 2012.

[89] Fiore V, Scalici T, Di Bella G, Valenza A. A review on basalt fibre and its composites. Composites Part B: Engineering. 2015 Jun;74:74-94.

[90] Deák T, Czigány T. Chemical Composition and Mechanical Properties of Basalt and Glass Fibers: A Comparison. Textile Research Journal. 2009 May;79(7):645-51.

[91] Gao H, Jiang B, Lei S, Hu L, Dai H, Cheng Z, et al. Glass characteristic comparisons and analyses from basalt for continuous fiber and ordinary basalt. Ceramics International. 2024 Oct.

[92] Jagadeesh P, Rangappa SM, Siengchin S. Basalt fibers: An environmentally acceptable and sustainable green material for polymer composites. Construction and Building Materials. 2024 Jul;436:136834.

[93] Chen C, Ding Y, Wang X, Bao L. Recent advances to engineer tough basalt fiber reinforced composites: A review. Polymer Composites. 2024;45(15):12559-74.

[94] Khandelwal S, Rhee KY. Recent advances in basalt-fiber-reinforced composites: Tailoring the fiber-matrix interface. Composites Part B: Engineering. 2020 Jul;192:108011.

[95] K V B, Shirvanimoghaddam K, Rajan GS, Ellis AV, Naebe M. Surface treatment of Basalt fiber for use in automotive composites. Materials Today Chemistry. 2020 Sep;17:100334.

[96] Chowdhury IR, Pemberton R, Summerscales J. Developments and Industrial Applications of Basalt Fibre Reinforced Composite Materials. Journal of Composites Science. 2022 Dec;6(12):367. Number: 12 Publisher: Multidisciplinary Digital Publishing Institute.

[97] Elkasabi Y, Mullen CA, Strahan GD, Wyatt VT. Biobased tar pitch produced from biomass pyrolysis oils. Fuel. 2022 Jun;318:123300.

[98] Le ND, Varley RJ, Hummel M, Trogen M, Byrne N. A review of future directions in the development of sustainable carbon fiber from bio-based precursors. Materials Today Sustainability. 2022 Dec;20:100251.

[99] Spörl JM, Beyer R, Abels F, Cwik T, Müller A, Hermanutz F, et al. Cellulose-Derived Carbon Fibers with Improved Carbon Yield and Mechanical Properties. Macromolecular Materials and Engineering. 2017;302(10):1700195.

[100] Choi D, Kil HS, Lee S. Fabrication of low-cost carbon fibers using economical precursors and advanced processing technologies. Carbon. 2019 Feb;142:610-49.

[101] Tanaka F, Okabe T. 1.4 Historical Review of Processing, Microstructures, and Mechanical Properties of PAN-Based Carbon Fibers. In: Comprehensive Composite Materials II. Elsevier; 2018. p. 66-85.

[102] Grassie N, McGuchan R. Pyrolysis of polyacrylonitrile and related polymers—VI. Acrylonitrile copolymers containing carboxylic acid and amide structures. European Polymer Journal. 1972 Feb;8(2):257-69.

[103] Tanaka F, Okabe T, Okuda H, Ise M, Kinloch IA, Mori T, et al. The effect of nanostructure upon the deformation micromechanics of carbon fibres. Carbon. 2013 Feb;52:372-8.

[104] Harano T, Takeichi Y, Usui M, Arai Y, Murao R, Negi N, et al. Observation of Distribution of pi-Orbital-Oriented Domains in PAN- and Pitch-Based Carbon Fibers Using Scanning Transmission X-ray Microscopy. Applied Sciences. 2020 Jan;10(14):4836.

[105] Ito A, Okamoto S. Using Molecular Dynamics to Assess Mechanical Properties of PAN-Based Carbon Fibers Comprising Imperfect Crystals with Amorphous Structures. nternational Journal of Mechanical and Mechatronics Engineering. 2013;7(9).

[106] Tanaka F, Okabe T, Okuda H, Kinloch IA, Young RJ. Factors controlling the strength of carbon fibres in tension. Composites Part A: Applied Science and Manufacturing. 2014 Feb;57:88-94.

[107] Ghosh T, Kim HC, De Kleine R, Wallington TJ, Bakshi BR. Life cycle energy and greenhouse gas emissions implications of using carbon fiber reinforced polymers in automotive components: Front subframe case study. Sustainable Materials and Technologies. 2021 Jul;28:e00263.

[108] Eisenriegler S, editor. The Circular Economy in the European Union: An Interim Review. Cham: Springer International Publishing; 2020.

[109] Jommersbach K. Mitsubishi Chemical Advanced Materials to Become Climate Neutral by 2023 and Targets Climate Positivity by 2030; 2021.

[110] Obasa VD, Olanrewaju OA, Gbenebor OP, Ochulor EF, Odili CC, Abiodun YO, et al. A Review on Lignin-Based Carbon Fibres for Carbon Footprint Reduction. Atmosphere. 2022 Oct;13(10):1605.

[111] Culebras M, Beaucamp A, Wang Y, Clauss MM, Frank E, Collins MN. Biobased Structurally Compatible Polymer Blends Based on Lignin and Thermoplastic Elastomer Polyurethane as Carbon Fiber Precursors. ACS Sustainable Chemistry & Engineering. 2018 Jul;6(7):8816-25.

[112] Beaucamp A, Muddasar M, Culebras M, Collins MN. Sustainable lignin-based carbon fibre reinforced polyamide composites: Production, characterisation and life cycle analysis. Composites Communications. 2024 Jan;45:101782.

[113] Nunes AO, Viana LR, Guineheuc PM, Da Silva Moris VA, De Paiva JMF, Barna R, et al. Life cycle assessment of a steam thermolysis process to recover carbon fibers from carbon fiber-reinforced polymer waste. The International Journal of Life Cycle Assessment. 2018 Sep;23(9):1825-38.

[114] Hermansson F, Heimersson S, Janssen M, Svanström M. Can carbon fiber composites have a lower environmental impact than fiberglass? Resources, Conservation and Recycling. 2022 Jun;181:106234.

[115] Prinçaud M, Aymonier C, Loppinet-Serani A, Perry N, Sonnemann G. Environmental Feasibility of the Recycling of Carbon Fibers from CFRPs by Solvolysis Using Supercritical Water. ACS Sustainable Chemistry & Engineering. 2014 Jun;2(6):1498-502.

[116] Baley C, Bourmaud A, Davies P. Eighty years of composites reinforced by flax fibres: A historical review. Composites Part A: Applied Science and Manufacturing. 2021 May;144:106333.

[117] Bruyne NAd. Plastic Materials for Aircraft Construction. The Aeronautical Journal. 1937 Jul;41(319):523-90.

[118] Shurtleff W, Aoyagi A. Henry Ford and his Researchers - History of their Work with Soybeans, Soyfoods and Chemurgy (1928-2011): Extensively Annotated Bibliography and Sourcebook. Soyinfo Center; 2011.

[119] Baley C, Gomina M, Breard J, Bourmaud A, Davies P. Variability of mechanical properties of flax fibres for composite reinforcement. A review. Industrial Crops and Products. 2020 Mar;145:111984.

[120] Baley C, Bourmaud A. Average tensile properties of French elementary flax fibers. Materials Letters. 2014 May;122:159-61.

[121] Melelli A, Durand S, Alvarado C, Kervoëlen A, Foucat L, Grégoire M, et al. Anticipating global warming effects: A comprehensive study of drought impact of both flax plants and fibres. Industrial Crops and Products. 2022 Sep;184:115011.

[122] De Beus N, Carus M, Barth M. Natural fibres show outstandingly low CO2 footprint compared to glass and mineral fibres. Renewable Carbon News. 2019.

[123] Bourmaud A, Siniscalco D, Foucat L, Goudenhooft C, Falourd X, Pontoire B, et al. Evolution of flax cell wall ultrastructure and mechanical properties during the retting step. Carbohydrate Polymers. 2019 Feb;206:48-56.

[124] Coroller G, Lefeuvre A, Le Duigou A, Bourmaud A, Ausias G, Gaudry T, et al. Effect of flax fibres individualisation on tensile failure of flax/epoxy unidirectional composite. Composites Part A: Applied Science and Manufacturing. 2013 Aug;51:62-70.

[125] Blanchard JMFA, Sobey AJ. Comparative design of E-glass and flax structures based on reliability. Composite Structures. 2019 Oct;225:111037.

[126] Viotti C, Albrecht K, Amaducci S, Bardos P, Bertheau C, Blaudez D, et al. Nettle, a Long-Known Fiber Plant with New Perspectives. Materials. 2022 Jun;15(12):4288.

[127] Richely E, Bourmaud A, Placet V, Guessasma S, Beaugrand J. A critical review of the ultrastructure, mechanics and modelling of flax fibres and their defects. Progress in Materials Science. 2022 Feb;124:100851.

[128] Rong MZ, Zhang MQ, Liu Y, Yang GC, Zeng HM. The effect of fiber treatment on the mechanical properties of unidirectional sisal-reinforced epoxy composites. Composites Science and Technology. 2001 Aug;61(10):1437-47.

[129] Melelli A, Jamme F, Legland D, Beaugrand J, Bourmaud A. Microfibril angle of elementary flax fibres investigated with polarised second harmonic generation microscopy. Industrial Crops and Products. 2020 Nov;156:112847.

[130] Corbin AC, Sala B, Soulat D, Ferreira M, Labanieh AR, Placet V. Development of quasi-unidirectional fabrics with hemp fiber: A competitive reinforcement for composite materials. Journal of Composite Materials. 2021 Feb;55(4):551-64.

[131] Placet V, Cissé O, Lamine Boubakar M. Nonlinear tensile behaviour of elementary hemp fibres. Part I: Investigation of the possible origins using repeated progressive loading with in situ microscopic observations. Composites Part A: Applied Science and Manufacturing. 2014 Jan;56:319-27.

[132] Lefeuvre A, Bourmaud A, Morvan C, Baley C. Elementary flax fibre tensile properties: Correlation between stress–strain behaviour and fibre composition. Industrial Crops and Products. 2014 Jan;52:762-9.

[133] Duc F, Bourban PE, Plummer CJG, Månson JAE. Damping of thermoset and thermoplastic flax fibre composites. Composites Part A: Applied Science and Manufacturing. 2014 Sep;64:115-23.

[134] Baley C. Analysis of the flax fibres tensile behaviour and analysis of the tensile stiffness increase. Composites Part A: Applied Science and Manufacturing. 2002 Jul;33(7):939-48. Number: 7.

[135] Placet V, Bouali A, Perré P. The possible role of microfibril angle of Hemp fibre during fatigue tests and its determination using Wide-Angle X-ray diffraction. Matériaux & Techniques. 2011;99(6):683-9.

[136] Shah DU, Schubel PJ, Clifford MJ. Can flax replace E-glass in structural composites? A small wind turbine blade case study. Composites Part B: Engineering. 2013 Sep;52:172-81.

[137] Shah DU. Natural fibre composites: Comprehensive Ashby-type materials selection charts. Materials & Design (1980-2015). 2014 Oct;62:21-31.

[138] Ao X, Vázquez-López A, Mocerino D, González C, Wang DY. Flame retardancy and fire mechanical properties for natural fiber/polymer composite: A review. Composites Part B: Engineering. 2024 Jan;268:111069.

[139] Gassan J, Bledzki AK. Thermal degradation of flax and jute fibers. Journal of Applied Polymer Science. 2001;82(6):1417-22.

[140] Siniscalco D, Arnould O, Bourmaud A, Le Duigou A, Baley C. Monitoring temperature effects on flax cell-wall mechanical properties within a composite material using AFM. Polymer Testing. 2018 Aug;69:91-9.

[141] Malik K, Ahmad F, Yunus NA, Gunister E, Nakato T, Mouri E, et al. A Review of Flax Fiber Reinforced Thermoset Polymer Composites: Thermal-Physical Properties, Improvements and Application. Journal of Natural Fibers. 2021 Oct:1-19.

[142] Lu MM, Fuentes CA, Van Vuure AW. Moisture sorption and swelling of flax fibre and flax fibre composites. Composites Part B: Engineering. 2022 Feb;231:109538.

[143] Berges M, Léger R, Placet V, Person V, Corn S, Gabrion X, et al. Influence of moisture uptake on the static, cyclic and dynamic behaviour of unidirectional flax fibre-reinforced epoxy laminates. Composites Part A: Applied Science and Manufacturing. 2016 Sep;88:165-77.

[144] Koolen G, Soete J, van Vuure AW. Interface modification and the influence on damage development of flax fibre – Epoxy composites when subjected to hygroscopic cycling. Materials Today: Proceedings. 2020;31:S273-9.

[145] Pantaloni D, Melelli A, Shah DU, Baley C, Bourmaud A. Influence of water ageing on the mechanical properties of flax/PLA non-woven composites. Polymer Degradation and Stability. 2022 Jun;200:109957.

[146] Potaufeux JE, Odent J, Notta-Cuvier D, Delille R, Barrau S, Giannelis EP, et al. Mechanistic insights on ultra-tough polylactide-based ionic nanocomposites. Composites Science and Technology. 2020 May;191:108075.

[147] Zhou F, Cheng G, Jiang B. Effect of silane treatment on microstructure of sisal fibers. Applied Surface Science. 2014 Feb;292:806-12.

[148] Huang S, Fu Q, Yan L, Kasal B. Characterization of interfacial properties between fibre and polymer matrix in composite materials – A critical review. Journal of Materials Research and Technology. 2021 Jul;13:1441-84.

[149] Karger-Kocsis J, Mahmood H, Pegoretti A. Recent advances in fiber/matrix interphase engineering for polymer composites. Progress in Materials Science. 2015 Aug;73:1-43.

[150] Yuan X, Zhang Z, Mu X, Shan C, Gao X, Zhu B. Recent progress on interface characterization methods of carbon fiber reinforced polymer composites. Chemical Engineering Journal. 2024 Nov;499:156220.

[151] Herrera-Franco PJ, Drzal LT. Comparison of methods for the measurement of fibre/matrix adhesion in composites. Composites. 1992 Jan;23(1):2-27.

[152] Feng J, Gao C, Safaei B, Qin Z, Wu H, Chu F, et al. Exceptional damping of CFRPs: Unveiling the impact of carbon fiber surface treatments. Composites Part B: Engineering. 2025 Feb;290:111973.

[153] Zheng H, Zhang W, Li B, Zhu J, Wang C, Song G, et al. Recent advances of interphases in carbon fiber-reinforced polymer composites: A review. Composites Part B: Engineering. 2022 Mar;233:109639.

[154] Zhou Y, Fan M, Chen L. Interface and bonding mechanisms of plant fibre composites: An overview. Composites Part B: Engineering. 2016 Sep;101:31-45.

[155] Van de Weyenberg I, Chi Truong T, Vangrimde B, Verpoest I. Improving the properties of UD flax fibre reinforced composites by applying an alkaline fibre treatment. Composites Part A: Applied Science and Manufacturing. 2006 Sep;37(9):1368-76.

[156] Shenoy Heckadka S, Nayak SY, Joe T, Zachariah N J, Gupta S, Kumar N V A, et al. Comparative Evaluation of Chemical Treatment on the Physical and Mechanical Properties of Areca Frond, Banana, and Flax Fibers. Journal of Natural Fibers. 2020 Jun:1-13.

[157] Abdelmouleh M, Boufi S, Belgacem MN, Duarte AP, Ben Salah A, Gandini A. Modification of cellulosic fibres with functionalised silanes: development of surface properties. International Journal of Adhesion and Adhesives. 2004 Feb;24(1):43-54.

[158] Li X, Tabil LG, Panigrahi S. Chemical Treatments of Natural Fiber for Use in Natural Fiber-Reinforced Composites: A Review. J Polym Environ. 2007:9.

[159] Kabir MM, Wang H, Lau KT, Cardona F. Chemical treatments on plant-based natural fibre reinforced polymer composites: An overview. Composites Part B: Engineering. 2012 Oct;43(7):2883-92.

[160] Shah DU. Developing plant fibre composites for structural applications by optimising composite parameters: a critical review. Journal of Materials Science. 2013 Sep;48(18):6083-107.

[161] George M, Bressler DC. Comparative evaluation of the environmental impact of chemical methods used to enhance natural fibres for composite applications and glass fibre based composites. Journal of Cleaner Production. 2017 Apr;149:491-501.

[162] Bourmaud A, Le Duigou A, Baley C. What is the technical and environmental interest in reusing a recycled polypropylene–hemp fibre composite? Polymer Degradation and Stability. 2011 Oct;96(10):1732-9.

[163] Allagui S, El Mahi A, Rebiere JL, Beyaoui M, Bouguecha A, Haddar M. Experimental studies of mechanical behavior and damage mechanisms of recycled flax/Elium thermoplastic composite. Polymers and Polymer Composites. 2022 Jan;30:09673911221090048.

[164] Duigou AL, Davies P, Baley C. Replacement of Glass/Unsaturated Polyester Composites by Flax/PLLA Biocomposites: Is It Justified? Journal of Biobased Materials and Bioenergy. 2011 Dec;5(4):466-82.

[165] Woigk W, Fuentes CA, Rion J, Hegemann D, van Vuure AW, Dransfeld C, et al. Interface properties and their effect on the mechanical performance of flax fibre thermoplastic composites. Composites Part A: Applied Science and Manufacturing. 2019 Jul;122:8-17.

[166] Miranda Campos B, Beauvois J, Bourbigot S, Fontaine G, Stoclet G, Bonnet F. One step production from the monomer of poly(L-lactide)/flax biocomposites by thermoplastic resin transfer molding: Mechanical properties and aging. Polymer Composites. 2024;45(14):13392-404.

[167] Cadu T, Berges M, Sicot O, Person V, Piezel B, Van Schoors L, et al. What are the key parameters to produce a high-grade bio-based composite? Application to flax/epoxy UD laminates produced by thermocompression. Composites Part B: Engineering. 2018 Oct;150:36-46.

[168] Di Mauro C, Genua A, Rymarczyk M, Dobbels C, Malburet S, Graillot A, et al. Chemical and mechanical reprocessed resins and bio-composites based on five epoxidized vegetable oils thermosets reinforced with flax fibers or PLA woven. Composites Science and Technology. 2021 Mar;205:108678.

[169] Jeannin T, Gabrion X, Ramasso E, Placet V. About the fatigue endurance of unidirectional flax-epoxy composite laminates. Composites Part B: Engineering. 2019 May;165:690-701.

[170] Debsharma T, Engelen S, De Baere I, Van Paepegem W, Prez FD. Resorcinol-Derived Vitrimers and Their Flax Fiber-Reinforced Composites Based on Fast Siloxane Exchange. Macromolecular Rapid Communications. 2023 Feb:2300020.

[171] Li Q, Ma S, Xu X, Zhu J. Bio-based Unsaturated Polyesters. In: Unsaturated Polyester Resins. Elsevier; 2019. p. 515-55.

[172] Penczek P, Czub P, Pielichowski J. Unsaturated Polyester Resins: Chemistry and Technology. In: Crosslinking in Materials Science. vol. 184. Berlin, Heidelberg: Springer Berlin Heidelberg; 2005. p. 1-95.

[173] Kumar S, Krishnan S, Mohanty S, Nayak SK. Synthesis and characterization of petroleum and biobased epoxy resins: a review. Polymer International. 2018 Jul;67(7):815-39.

[174] Zia KM, Bhatti HN, Ahmad Bhatti I. Methods for polyurethane and polyurethane composites, recycling and recovery: A review. Reactive and Functional Polymers. 2007 Aug;67(8):675-92.

[175] Akindoyo JO, Beg MDH, Ghazali S, Islam MR, Jeyaratnam N, Yuvaraj AR. Polyurethane types, synthesis and applications – a review. RSC Advances. 2016;6(115):114453-82.

[176] Zhang X. High-performance biobased vinyl ester resin and its fiberglass-reinforced composite with high glass transition temperature (T g), excellent flame retardancy and mechanical properties. Polymer Degradation and Stability. 2023.

[177] Yadav SK, Schmalbach KM, Kinaci E, Stanzione JF, Palmese GR. Recent advances in plant-based vinyl ester resins and reactive diluents. European Polymer Journal. 2018 Jan;98:199-215.

[178] Basafa M, Hawboldt K. A review on sources and extraction of phenolic compounds as precursors for bio-based phenolic resins. Biomass Conversion and Biorefinery. 2023 Apr;13(6):4463-75.

[179] Lithner D, Larsson A, Dave G. Environmental and health hazard ranking and assessment of plastic polymers based on chemical composition. Science of The Total Environment. 2011 Aug;409(18):3309-24.

[180] Wegelin S, Meier MAR. Bio-based aromatics for chemicals and materials: Advances in renewable drop-in and functional alternatives. Current Opinion in Green and Sustainable Chemistry. 2024 Jun;47:100931.

[181] Tavernier R, Semsarilar M, Caillol S. Bio-sourced alternatives to diglycidyl ether of bisphenol A in epoxy–amine thermosets. Green Materials. 2024 Sep;12(3):121-67.

[182] Ragauskas AJ, Williams CK, Davison BH, Britovsek G, Cairney J, Eckert CA, et al. The Path Forward for Biofuels and Biomaterials. Science. 2006 Jan;311(5760):484-9.

[183] Bajwa DS, Pourhashem G, Ullah AH, Bajwa SG. A concise review of current lignin production, applications, products and their environmental impact. Industrial Crops and Products. 2019 Nov;139:111526.

[184] Libretti C, Santos Correa L, Meier MAR. From waste to resource: advancements in sustainable lignin modification. Green Chemistry. 2024;26(8):4358-86.

[185] Questell-Santiago YM, Galkin MV, Barta K, Luterbacher JS. Stabilization strategies in biomass depolymerization using chemical functionalization. Nature Reviews Chemistry. 2020 May;4(6):311-30.

[186] Li W, Sun H, Wang G, Sui W, Dai L, Si C. Lignin as a green and multifunctional alternative to phenol for resin synthesis. Green Chemistry. 2023;25(6):2241-61.

[187] Kumaniaev I, Navare K, Mendes NC, Placet V, Acker KV, Samec JSM. Conversion of birch bark to biofuels. Green Chemistry. 2020 Apr;22(7):2255-63.

[188] W Bartling A, L Stone M, J Hanes R, Bhatt A, Zhang Y, J Biddy M, et al. Techno-economic analysis and life cycle assessment of a biorefinery utilizing reductive catalytic fractionation. Energy & Environmental Science. 2021;14(8):4147-68.

[189] Shuai L, Amiri MT, Questell-Santiago YM, Héroguel F, Li Y, Kim H, et al. Formaldehyde stabilization facilitates lignin monomer production during biomass depolymerization. Science. 2016 Oct;354(6310):329-33.

[190] Manker LP, Hedou MA, Broggi C, Jones MJ, Kortsen K, Puvanenthiran K, et al. Performance polyamides built on a sustainable carbohydrate core. Nature Sustainability. 2024 Mar;7(5):640-51.

[191] Blondiaux E, Bomon J, Smoleń M, Kaval N, Lemière F, Sergeyev S, et al. Bio-based Aromatic Amines from Lignin-Derived Monomers. ACS Sustainable Chemistry & Engineering. 2019 Apr;7(7):6906-16.

[192] Lemouzy S, Delavarde A, Lamaty F, Bantreil X, Pinaud J, Caillol S. Lignin-based bisguaiacol diisocyanate: a green route for the synthesis of biobased polyurethanes. Green Chemistry. 2023;25(12):4833-9.

[193] Witthayolankowit K, Rakkijakan T, Ayub R, Kumaniaev I, Pourchet S, Boni G, et al. Use of a fully biobased and non-reprotoxic epoxy polymer and woven hemp fabric to prepare environmentally friendly composite materials with excellent physical properties. Composites Part B: Engineering. 2023 Jun;258:110692.

[194] Fache M, Boutevin B, Caillol S. Vanillin Production from Lignin and Its Use as a Renewable Chemical. ACS Sustainable Chemistry & Engineering. 2016 Jan;4(1):35-46.

[195] Dumas L, Bonnaud L, Olivier M, Poorteman M, Dubois P. Eugenol-based benzoxazine: from straight synthesis to taming of the network properties. Journal of Materials Chemistry A. 2015 Mar;3(11):6012-8.

[196] Wybo N, Duval A, Averous L. Benign and Selective Amination of Lignins towards Aromatic Biobased Building Blocks with Primary Amines. Angewandte Chemie International Edition. 2024 Jul:e202403806.

[197] Wu X, Galkin MV, Barta K. A well-defined diamine from lignin depolymerization mixtures for constructing bio-based polybenzoxazines. Chem Catalysis. 2021 Dec;1(7):1466-79.

[198] Wu X, De Bruyn M, Barta K. A Diamine-Oriented Biorefinery Concept Using Ammonia and Raney Ni as a Multifaceted Catalyst. Chemie Ingenieur Technik. 2022 Nov;94(11):1808-17.

[199] Gu Z, Liu Z, Yang S, Xie N, Ma K. Exergy and environmental footprint analysis for a green ammonia production process. Journal of Cleaner Production. 2024 May;455:142357.

[200] Boerner LK. Industrial ammonia production emits more CO2 than any other chemical-making reaction. Chemists want to change that. Chemical & Engineering News. 2019;97(24).

[201] Luterbacher JS, Martin Alonso D, Dumesic JA. Targeted chemical upgrading of lignocellulosic biomass to platform molecules. Green Chem. 2014 Oct;16(12):4816-38.

[202] Hernandez ED, Bassett AW, Sadler JM, La Scala JJ, Stanzione JF. Synthesis and Characterization of Bio-based Epoxy Resins Derived from Vanillyl Alcohol. ACS Sustainable Chemistry & Engineering. 2016 Aug;4(8):4328-39.

[203] Woelk HU. Stärke als Chemierohstoff — Möglichkeiten und Grenzen. Starch - Stärke. 1981;33(12):397-408.

[204] Sardon H, Mecerreyes D, Basterretxea A, Avérous L, Jehanno C. From Lab to Market: Current Strategies for the Production of Biobased Polyols. ACS Sustainable Chemistry & Engineering. 2021 Aug;9(32):10664-77.

[205] Wang C, Singh A, Rognerud EG, Murray R, Musgrave GM, Skala M, et al. Synthesis, characterization, and recycling of bio-derivable polyester covalently adaptable networks for industrial composite applications. Matter. 2024 Feb;7(2):550-68.

[206] Rose M, Palkovits R. Isosorbide as a Renewable Platform chemical for Versatile Applications—Quo Vadis? ChemSusChem. 2012 Jan;5(1):167-76.

[207] Veza I, Muhamad Said MF, Latiff ZA. Recent advances in butanol production by acetone-butanol-ethanol (ABE) fermentation. Biomass and Bioenergy. 2021 Jan;144:105919.

[208] Haida P, Signorato G, Abetz V. Blended vinylogous urethane/urea vitrimers derived from aromatic alcohols. Polymer Chemistry. 2022;13(7):946-58.

[209] Zhan Z, Yan H, Wang H, Cheng J, Ran S, Fang Z. Novel full bio-based phloroglucinol benzoxazine resin: Synthesis, curing reaction and thermal stability. Polymer. 2020 Jun;200:122534.

[210] Flickinger CW. The benzenediols: catechol, resorcinol and hydroquinone — a review of the industrial toxicology and current industrial exposure limits. American Industrial Hygiene Association Journal. 1976 Oct;37(10):596-606.

[211] Gioia C, Banella MB, Vannini M, Celli A, Colonna M, Caretti D. Resorcinol: A potentially bio-based building block for the preparation of sustainable polyesters. European Polymer Journal. 2015 Dec;73:38-49.

[212] Jaeger G, Magnus J, Moussa AS, Olf G, Lolli G, Behnken S, et al.; Covestro Deutschland AG, assignee. Recombinant strain producing O-aminobenzoate and fermentative production of aniline from renewable resources via 2-aminobenzoic acid. US10731187B2; 2020.

[213] Winter B, Meys R, Bardow A. Towards aromatics from biomass: Prospective Life Cycle Assessment of bio-based aniline. Journal of Cleaner Production. 2021 Mar;290:125818.

[214] Scodeller I, Mansouri S, Morvan D, Muller E, De Oliveira Vigier K, Wischert R, et al. Synthesis of Renewable m-Xylylenediamine from Biomass-Derived Furfural. Angewandte Chemie. 2018 Aug;130(33):10670-4.

[215] Shao X, Su L, Zhang J, Tian Z, Zhang N, Wang Y, et al. Green Production of Phthalic Anhydride from Biobased Furan and Maleic Anhydride by an Acid Resin Catalyst. ACS Sustainable Chemistry & Engineering. 2021 Nov;9(43):14385-94.

[216] Dros AB, Larue O, Reimond A, De Campo F, Pera-Titus M. Hexamethylenediamine (HMDA) from fossil- vs. bio-based routes: an economic and life cycle assessment comparative study. Green Chemistry. 2015;17(10):4760-72.

[217] Wang JG, Liu XQ, Zhu J. From Furan to High Quality Bio-based Poly(ethylene furandicarboxylate). Chinese Journal of Polymer Science. 2018 Jun;36(6):720-7.

[218] Stegmann P, Gerritse T, Shen L, Londo M, Puente A, Junginger M. The global warming potential and the material utility of PET and bio-based PEF bottles over multiple recycling trips. Journal of Cleaner Production. 2023 Apr;395:136426.

[219] Wu X, Hartmann P, Berne D, De Bruyn M, Cuminet F, Wang Z, et al. Closed-loop recyclability of a biomass-derived epoxy-amine thermoset by methanolysis. Science. 2024 Apr;384(6692):eadj9989.

[220] Froidevaux V, Negrell C, Caillol S, Pascault JP, Boutevin B. Biobased Amines: From Synthesis to Polymers; Present and Future. Chemical Reviews. 2016 Nov;116(22):14181-224.

[221] Fache M, Montérémal C, Boutevin B, Caillol S. Amine hardeners and epoxy cross-linker from aromatic renewable resources. European Polymer Journal. 2015 Dec;73:344-62.

[222] SUNTIO V, Visuri O, Lindqvist P; Neste Oyj, assignee. Method for producing renewable fuel. US20240294838A1; 2024.

[223] BYMAN O, Malm A, WAHLSTRÖM R, LEHTIMAA T, KUMAR H; Neste Oyj, assignee. Method for producing renewable hydrocarbons. US12134738B2; 2024.

[224] De Vaugelas F. Première étape dans la coopération entre Covestro, Neste et Borealis. L'Usine Nouvelle. 2020 Oct.

[225] Aresta M. Carbon Dioxide as Chemical Feedstock. John Wiley & Sons; 2010.

[226] Alper E, Yuksel Orhan O. CO2 utilization: Developments in conversion processes. Petroleum. 2017 Mar;3(1):109-26.

[227] Hepburn C, Adlen E, Beddington J, Carter EA, Fuss S, Mac Dowell N, et al. The technological and economic prospects for CO2 utilization and removal. Nature. 2019 Nov;575(7781):87-97.

[228] Zhou Z, Ma T, Zhang H, Chheda S, Li H, Wang K, et al. Carbon dioxide capture from open air using covalent organic frameworks. Nature. 2024 Nov;635(8037):96-101.

[229] MacDowell N, Florin N, Buchard A, Hallett J, Galindo A, Jackson G, et al. An overview of CO2 capture technologies. Energy & Environmental Science. 2010;3(11):1645.

[230] Grignard B, Gennen S, Jérôme C, W Kleij A, Detrembleur C. Advances in the use of CO 2 as a renewable feedstock for the synthesis of polymers. Chemical Society Reviews. 2019;48(16):4466-514.

[231] Rosetto G, Vidal F, McGuire TM, Kerr RWF, Williams CK. High Molar Mass Polycarbonates as Closed-Loop Recyclable Thermoplastics. Journal of the American Chemical Society. 2024 Mar;146(12):8381-93.

[232] Poon KC, Gregory GL, Sulley GS, Vidal F, Williams CK. Toughening CO2-Derived Copolymer Elastomers Through Ionomer Networking. Advanced Materials. 2023 Jul:2302825.

[233] Rajagopalan P, Kühnle M, Polyakov M, Müller K, Arlt W, Kruse D, et al. Methacrylic acid by carboxylation of propene with CO2 over POM catalysts — Reality or wishful thinking? Catalysis Communications. 2014 Mar;48:19-23.

[234] Darabi Mahboub MJ, Dubois JL, Cavani F, Rostamizadeh M, Patience GS. Catalysis for the synthesis of methacrylic acid and methyl methacrylate. Chemical Society Reviews. 2018;47(20):7703-38.

[235] Wang X, Wang H, Sun Y. Synthesis of Acrylic Acid Derivatives from CO2 and Ethylene. Chem. 2017 Aug;3(2):211-28.

[236] Rehman A, Saleem F, Javed F, Ikhlaq A, Ahmad SW, Harvey A. Recent advances in the synthesis of cyclic carbonates via CO2 cycloaddition to epoxides. Journal of Environmental Chemical Engineering. 2021 Apr;9(2):105113.

[237] Alves M, Grignard B, Mereau R, Jerome C, Tassaing T, Detrembleur C. Organocatalyzed coupling of carbon dioxide with epoxides for the synthesis of cyclic carbonates: catalyst design and mechanistic studies. Catalysis Science & Technology. 2017;7(13):2651-84.

[238] Ngassam Tounzoua C, Grignard B, Detrembleur C. Exovinylene Cyclic Carbonates: Multifaceted CO2-Based Building Blocks for Modern Chemistry and Polymer Science. Angewandte Chemie International Edition. 2022 May;61(22).

[239] Siragusa F, Van Den Broeck E, Ocando C, Müller AJ, De Smet G, Maes BUW, et al. Access to Biorenewable and CO2-Based Polycarbonates from Exovinylene Cyclic Carbonates. ACS Sustainable Chemistry & Engineering. 2021 Feb;9(4):1714-28.

[240] Razavi-Esfali M, Habets T, Siragusa F, Grignard B, Sardon H, Detrembleur C. Design of functional isocyanate-free poly(oxazolidone)s under mild conditions. Polymer Chemistry. 2024 May;15(19):1962-74.

[241] Habets T, Seychal G, Caliari M, Raquez JM, Sardon H, Grignard B, et al. Covalent adaptable networks through dynamic N,S-acetal chemistry: toward recyclable CO2-based thermosets. Journal of the American Chemical Society. 2023 Sep;145(46):25450-62.

[242] Yu AZ, Serum EM, Renner AC, Sahouani JM, Sibi MP, Webster DC. Renewable Reactive Diluents as Practical Styrene Replacements in Biobased Vinyl Ester Thermosets. ACS Sustainable Chemistry & Engineering. 2018 Oct;6(10):12586-92.

[243] Weatherhead RG. Catalysts, Accelerators and Inhibitors for Unsaturated Polyester Resins. In: FRP Technology. Dordrecht: Springer Netherlands; 1980. p. 204-39.

[244] Gañán P, Barajas J, Zuluaga R, Castro C, Marín D, Tercjak A, et al. The Evolution and Future Trends of Unsaturated Polyester Biocomposites: A Bibliometric Analysis. Polymers. 2023;15(15):2970.

[245] Chu F, Wang W, Zhou Y, Xu Z, Zou B, Jiang X, et al. Fully bio-based and intrinsically flame retardant unsaturated polyester cross-linked with isosorbide-based diluents. Chemosphere. 2023 Dec;344:140371.

[246] Lu Y, Zhang Y, Zhang K. Renewable biomass resources to access halogen- and phosphorus-free flame retardant thermosets with ultra-low heat release capacity. Chemical Engineering Journal. 2022 Nov;448:137670.

[247] Shahid AT, Silvestre JD, Hofmann M, Garrido M, Correia JR. Life cycle assessment of an innovative bio-based unsaturated polyester resin and its use in glass fibre reinforced bio-composites produced by vacuum infusion. Journal of Cleaner Production. 2024 Feb;441:140906.

[248] Hofmann MA, Shahid AT, Garrido M, Ferreira MJ, Correia JR, Bordado JC. Biobased Thermosetting Polyester Resin for High-Performance Applications. ACS Sustainable Chemistry & Engineering. 2022 Mar;10(11):3442-54.

[249] Li Y, Qu J, Dai Z, Jiang J, Fu J, Fu F, et al. Highly Bio-Based Unsaturated Polyester Resins with Improved Performance by Incorporating Isosorbide into the Polyester Prepolymer. Macromolecular Materials and Engineering. 2022;307(9):2200203.

[250] Lohbeck K, Haferkorn H, Fuhrmann W, Fedtke N. Maleic and Fumaric Acids. In: Wiley-VCH, editor. Ullmann's Encyclopedia of Industrial Chemistry. vol. 22. 1st ed. Wiley; 2000. p. 145-55.

[251] Pavarelli G, Velasquez Ochoa J, Caldarelli A, Puzzo F, Cavani F, Dubois JL. A New Process for Maleic Anhydride Synthesis from a Renewable Building Block: The Gas-Phase Oxidehydration of Bio-1-butanol. ChemSusChem. 2015;8(13):2250-9.

[252] Lan J, Chen Z, Lin J, Yin G. Catalytic aerobic oxidation of renewable furfural to maleic anhydride and furanone derivatives with their mechanistic studies. Green Chem. 2014;16(9):4351-8.

[253] Cucciniello R, Cespi D, Riccardi M, Neri E, Passarini F, Pulselli FM. Maleic anhydride from bio-based 1-butanol and furfural: a life cycle assessment at the pilot scale. Green Chemistry. 2023 Jul;25(15):5922-35.

[254] Roa Engel CA, Straathof AJJ, Zijlmans TW, Van Gulik WM, Van Der Wielen LAM. Fumaric acid production by fermentation. Applied Microbiology and Biotechnology. 2008 Mar;78(3):379-89.

[255] Rorrer NA, Dorgan JR, Vardon DR, Martinez CR, Yang Y, Beckham GT. Renewable Unsaturated Polyesters from Muconic Acid. ACS Sustainable Chemistry & Engineering. 2016 Dec;4(12):6867-76.

[256] Wu Y, Fei M, Qiu R, Liu W, Qiu J. A Review on Styrene Substitutes in Thermosets and Their Composites. Polymers. 2019;11(11):1815.

[257] Tournier V, Duquesne S, Guillamot F, Cramail H, Taton D, Marty A, et al. Enzymes' Power for Plastics Degradation. Chemical Reviews. 2023 May;123(9):5612-701.

[258] Jehanno C, Alty JW, Roosen M, De Meester S, Dove AP, Chen EYX, et al. Critical advances and future opportunities in upcycling commodity polymers. Nature. 2022 Mar;603(7903):803-14.

[259] An W, Wang XL, Liu X, Wu G, Xu S, Wang YZ. Chemical recovery of thermosetting unsaturated polyester resins. Green Chemistry. 2022;24(2):701-12.

[260] Zhang N, Hou X, Cui X, Chai L, Li H, Zhang H, et al. Amphiphilic catalyst for decomposition of unsaturated polyester resins to valuable chemicals with 100% atom utilization efficiency. Journal of Cleaner Production. 2021 May;296:126492.

[261] Wang B, Shen Y, Lu F, Xu N, Liu Y, Li D, et al. A closed-loop recovery strategy of unsaturated polyester composite: Bridging heterogeneous catalyst and resin by noncovalent interactions. Composites Science and Technology. 2022 Nov;230:109788.

[262] Yousef S, Eimontas J, Zakarauskas K, Striūgas N. Recovery of styrene-rich oil and glass fibres from fibres-reinforced unsaturated polyester resin end-of-life wind turbine blades using pyrolysis technology. Journal of Analytical and Applied Pyrolysis. 2023 Aug;173:106100.

[263] Yousef S, Eimontas J, Stasiulaitiene I, Zakarauskas K, Striūgas N. Recovery of energy and carbon fibre from wind turbine blades waste (carbon fibre/unsaturated polyester resin) using pyrolysis process and its life-cycle assessment. Environmental Research. 2024 Mar;245:118016.

[264] Di Mauro C, Malburet S, Genua A, Graillot A, Mija A. Sustainable Series of New Epoxidized Vegetable Oil-Based Thermosets with Chemical Recycling Properties. Biomacromolecules. 2020 Sep;21(9):3923-35.

[265] Mija A, Louisy E, Lachegur S, Khodyrieva V, Martinaux P, Olivero S, et al. Limonene dioxide as a building block for 100% bio-based thermosets. Green Chemistry. 2021;23(24):9855-9.

[266] Chen J, Nie X, Liu Z, Mi Z, Zhou Y. Synthesis and Application of Polyepoxide Cardanol Glycidyl Ether as Biobased Polyepoxide Reactive Diluent for Epoxy Resin. ACS Sustainable Chemistry & Engineering. 2015 Jun;3(6):1164-71.

[267] Vidil T, Tournilhac F, Musso S, Robisson A, Leibler L. Control of reactions and network structures of epoxy thermosets. Progress in Polymer Science. 2016 Nov;62:126-79.

[268] Gheni SA, Ali MM, Ta GC, Harbin HJ, Awad SA. Toxicity, Hazards, and Safe Handling of Primary Aromatic Amines. ACS Chemical Health & Safety. 2024 Jan;31(1):8-21.

[269] Yoon M, Lim CS. Comparative experiments on amine vs. acid anhydride curing agents for epoxy resin required for automotive parts. Journal of Polymer Research. 2022 Dec;30(1):9.

[270] Yang Y, Xu Y, Ji Y, Wei Y. Functional epoxy vitrimers and composites. Progress in Materials Science. 2021 Jul;120:100710.

[271] Lim JSK, Gan CL, Hu XM. Unraveling the Mechanistic Origins of Epoxy Degradation in Acids. ACS Omega. 2019 Jun;4(6):10799-808.

[272] Yu A, Gupta V. Measurement of in situ fiber/matrix interface strength in graphite/epoxy composites. Composites Science and Technology. 1998 Nov;58(11):1827-37.

[273] Thomason JL. Glass fibre sizing: A review. Composites Part A: Applied Science and Manufacturing. 2019 Dec;127:105619.

[274] Hallak Panzera T, Jeannin T, Gabrion X, Placet V, Remillat C, Farrow I, et al. Static, fatigue and impact behaviour of an autoclaved flax fibre reinforced composite for aerospace engineering. Composites Part B: Engineering. 2020 Sep;197:108049.

[275] Santacesaria E, Tesser R, Di Serio M, Casale L, Verde D. New Process for Producing Epichlorohydrin via Glycerol Chlorination. Industrial & Engineering Chemistry Research. 2010 Feb;49(3):964-70.

[276] Bell BM, Briggs JR, Campbell RM, Chambers SM, Gaarenstroom PD, Hippler JG, et al. Glycerin as a Renewable Feedstock for Epichlorohydrin Production. The GTE Process. CLEAN – Soil, Air, Water. 2008 Aug;36(8):657-61.

[277] Almena A, Martín M. Technoeconomic Analysis of the Production of Epichlorohydrin from Glycerol. Industrial & Engineering Chemistry Research. 2016 Mar;55(12):3226-38.

[278] Kočí V, Loubal T. LCA of liquid epoxy resin produced based on propylene and glycerin. Acta Environmentalica Universitatis Comenianae. 2012;20(20):62-7.

[279] Cespi D, Cucciniello R, Ricciardi M, Capacchione C, Vassura I, Passarini F, et al. A simplified early stage assessment of process intensification: glycidol as a value-added product from epichlorohydrin industry wastes. Green Chemistry. 2016;18(16):4559-70.

[280] Ma Y, Liu H, Wu J, Yuan L, Wang Y, Du X, et al. The adverse health effects of bisphenol A and related toxicity mechanisms. Environmental Research. 2019 Sep;176:108575.

[281] Jiang L, Gonzalez-Diaz A, Ling-Chin J, Malik A, Roskilly AP, Smallbone AJ. PEF plastic synthesized from industrial carbon dioxide and biowaste. Nature Sustainability. 2020 Jun;3(9):761-7.

[282] Clarke RW, Rognerud EG, Puente-Urbina A, Barnes D, Murdy P, McGraw ML, et al. Manufacture and testing of biomass-derivable thermosets for wind blade recycling. Science. 2024 Aug;385(6711):854-60.

[283] Lavaux V, Lalevée J. Epoxy curing in mild and eco-friendly conditions: Towards bisphenol A-free systems. Progress in Polymer Science. 2024 Oct;157:101873.

[284] Türel T, Tomović Z. Chemically Recyclable and Upcyclable Epoxy Resins Derived from Vanillin. ACS Sustainable Chemistry & Engineering. 2023 Jun;11(22):8308-16.

[285] Mattar N, de Anda AR, Vahabi H, Renard E, Langlois V. Resorcinol-Based Epoxy Resins Hardened with Limonene and Eugenol Derivatives: From the Synthesis of Renewable Diamines to the Mechanical Properties of Biobased Thermosets. ACS Sustainable Chemistry & Engineering. 2020 Aug;8(34):13064-75.

[286] Łukaszczyk J, Janicki B, Kaczmarek M. Synthesis and properties of isosorbide based epoxy resin. European Polymer Journal. 2011 Aug;47(8):1601-6.

[287] La Rosa A, Blanco I, Banatao D, Pastine S, Björklund A, Cicala G. Innovative Chemical Process for Recycling Thermosets Cured with Recyclamines® by Converting Bio-Epoxy Composites in Reusable Thermoplastic—An LCA Study. Materials. 2018 Feb;11(3):353.

[288] La Rosa AD, Banatao DR, Pastine SJ, Latteri A, Cicala G. Recycling treatment of carbon fibre/epoxy composites: Materials recovery and characterization and environmental impacts through life cycle assessment. Composites Part B: Engineering. 2016 Nov;104:17-25.

[289] Kosinski S, Pastine SJ; Aditya Birla Chemicals USA Inc, assignee. Synthesis of and compositions containing diaminoacetals and diaminoketals. US11542224B2; 2023.

[290] Pastine SJ, Liang B, QIN B; CONNORA Tech Inc Connora Technologies Inc, assignee. Novel agents for reworkable epoxy resins. EP2646410B1; 2018.

[291] Li J, Xu PL, Zhu YK, Ding JP, Xue LX, Wang YZ. A promising strategy for chemical recycling of carbon fiber/thermoset composites: self-accelerating decomposition in a mild oxidative system. Green Chemistry. 2012 Nov;14(12):3260-3.

[292] Xu P, Li J, Ding J. Chemical recycling of carbon fibre/epoxy composites in a mixed solution of peroxide hydrogen and N,N-dimethylformamide. Composites Science and Technology. 2013 Jun;82:54-9.

[293] Das M, Chacko R, Varughese S. An Efficient Method of Recycling of CFRP Waste Using Peracetic Acid. ACS Sustainable Chemistry & Engineering. 2018 Feb;6(2):1564-71.

[294] Liu L, Liu X, Li X, Xu S, Wang Y. An Integrative Chemical Recycling Approach for Catalytic Oxidation of Epoxy Resin and in situ Separation of Degraded Products. Angewandte Chemie. 2024 Jun;136(26):e202405912.

[295] Ahrens A, Bonde A, Sun H, Wittig NK, Hammershøj HCD, Batista GMF, et al. Catalytic disconnection of C–O bonds in epoxy resins and composites. Nature. 2023 May;617(7962):730-7.

[296] Lefay C, Guillaneuf Y. Recyclable/degradable materials via the insertion of labile/cleavable bonds using a comonomer approach. Progress in Polymer Science. 2023 Dec;147:101764.

[297] Saitta L, Prasad V, Tosto C, Murphy N, Ivankovic A, Cicala G, et al. Characterization of biobased epoxy resins to manufacture eco-composites showing recycling properties. Polymer Composites. 2022 Dec;43(12):9179-92.

[298] Das A, Mahanwar P. A brief discussion on advances in polyurethane applications. Advanced Industrial and Engineering Polymer Research. 2020 Jul;3(3):93-101.

[299] Delavarde A, Savin G, Derkenne P, Boursier M, Morales-Cerrada R, Nottelet B, et al. Sustainable polyurethanes: toward new cutting-edge opportunities. Progress in Polymer Science. 2024 Apr;151:101805.

[300] Bello D, Herrick CA, Smith TJ, Woskie SR, Streicher RP, Cullen MR, et al. Skin Exposure to Isocyanates: Reasons for Concern. Environmental Health Perspectives. 2007 Mar;115(3):328-35. Publisher: Environmental Health Perspectives.

[301] Broughton E. The Bhopal disaster and its aftermath: a review. Environmental Health. 2005 May;4(1):6.

[302] Agency EC. Regulation (EC) No 1907/2006 of the European Parliament and of the Council of 18 December 2006 concerning the Registration, Evaluation, Authorisation and Restriction of Chemicals (REACH), consolidated version 2024; 2024.

[303] Mohamed M, Vuppalapati RR, Bheemreddy V, Chandrashekhara K, Schuman T. Characterization of polyurethane composites manufactured using vacuum assisted resin transfer molding. Advanced Composite Materials. 2015 Dec;24(sup1):13-31.

[304] Cuinat-Guerraz N, Dumont MJ, Hubert P. Environmental resistance of flax/bio-based epoxy and flax/polyurethane composites manufactured by resin transfer moulding. Composites Part A: Applied Science and Manufacturing. 2016 Sep;88:140-7.

[305] Guo Z, Ding X, Wang Y. How To Get Isocyanate? ACS Omega. 2024 Mar;9(10):11168-80.

[306] Niesiobędzka J, Datta J. Challenges and recent advances in bio-based isocyanate production. Green Chemistry. 2023;25(7):2482-504.

[307] Silva R, Barros-Timmons A, Quinteiro P. Life cycle assessment of fossil- and bio-based polyurethane foams:a review. Journal of Cleaner Production. 2023 Dec;430:139697.

[308] Wray HE, Luzzi S, D'Arrigo P, Griffini G. Life Cycle Environmental Impact Considerations in the Design of Novel Biobased Polyurethane Coatings. ACS Sustainable Chemistry & Engineering. 2023 May;11(21):8065-74.

[309] Polo Fonseca L, Duval A, Luna E, Ximenis M, De Meester S, Avérous L, et al. Reducing the carbon footprint of polyurethanes by chemical and biological depolymerization: Fact or fiction? Current Opinion in Green and Sustainable Chemistry. 2023 Jun;41:100802.

[310] Zhao L, Semetey V. Recycling Polyurethanes through Transcarbamoylation. ACS Omega. 2021 Feb;6(6):4175-83.

[311] Rossignolo G, Malucelli G, Lorenzetti A. Recycling of polyurethanes: where we are and where we are going. Green Chemistry. 2024.

[312] Del Amo J, Simón D, Ramos MJ, Rodríguez JF, De Lucas A, Borreguero AM. Scaled-up and economic assessment approach of the split-phase glycolysis process for the recycling of flexible polyurethane foam wastes. Journal of Material Cycles and Waste Management. 2022 May;24(3):1059-71.

[313] Heiran R, Ghaderian A, Reghunadhan A, Sedaghati F, Thomas S, Haghighi Ah. Glycolysis: an efficient route for recycling of end of life polyurethane foams. Journal of Polymer Research. 2021 Jan;28(1):22.

[314] Marson A, Masiero M, Modesti M, Scipioni A, Manzardo A. Life Cycle Assessment of Polyurethane Foams from Polyols Obtained through Chemical Recycling. ACS Omega. 2021 Jan;6(2):1718-24.

[315] Vanbergen T, Verlent I, De Geeter J, Haelterman B, Claes L, De Vos D. Recycling of Flexible Polyurethane Foam by Split-Phase Alcoholysis: Identification of Additives and Alcoholyzing Agents to Reach Higher Efficiencies. ChemSusChem. 2020;13(15):3835-43.

[316] Bech TB, Donslund BS, Kristensen SK, Skrydstrup T. Chemical separation of polyurethane *via* acidolysis – combining acidolysis with hydrolysis for valorisation of aromatic amines. Green Chemistry. 2024;26(14):8395-404.

[317] Raczyńska A, Góra A, André I. An overview on polyurethane-degrading enzymes. Biotechnology Advances. 2024 Dec;77:108439.

[318] Guicherd M, Ben Khaled M, Gueroult M, Nomme J, Dalibey M, Grimaud F, et al. An engineered enzyme embedded into PLA to make self-biodegradable plastic. Nature. 2024;631(8022):884-90.

[319] Denissen W, Winne JM, Du Prez FE. Vitrimers: permanent organic networks with glass-like fluidity. Chemical Science. 2016;7(1):30-8.

[320] Ruiz de Luzuriaga A, Martin R, Markaide N, Rekondo A, Cabañero G, Rodríguez J, et al. Epoxy resin with exchangeable disulfide crosslinks to obtain reprocessable, repairable and recyclable fiber-reinforced thermoset composites. Materials Horizons. 2016;3(3):241-7.

[321] Tobolsky AV. Stress Relaxation Studies of the Viscoelastic Properties of Polymers. Journal of Applied Physics. 1956 Jul;27(7):673-85.

[322] Russo PS. A Perspective on Reversible Gels and Related Systems. In: Reversible Polymeric Gels and Related Systems. vol. 350 of ACS Symposium Series. American Chemical Society; 1987. p. 1-21.

[323] Leibler L, Rubinstein M, Colby RH. Dynamics of reversible networks. Macromolecules. 1991 Aug;24(16):4701-7.

[324] Semenov AN, Rubinstein M. Thermoreversible Gelation in Solutions of Associative Polymers. 1. Statics. Macromolecules. 1998 Feb;31(4):1373-85.

[325] Rubinstein M, Semenov AN. Thermoreversible Gelation in Solutions of Associating Polymers. 2. Linear Dynamics. Macromolecules. 1998 Feb;31(4):1386-97.

[326] Chen X, Dam MA, Ono K, Mal A, Shen H, Nutt SR, et al. A Thermally Re-mendable Cross-Linked Polymeric Material. Science. 2002 Mar;295(5560):1698-702.

[327] Skene WG, Lehn JMP. Dynamers: Polyacylhydrazone reversible covalent polymers, component exchange, and constitutional diversity. Proceedings of the National Academy of Sciences. 2004 Jun;101(22):8270-5.

[328] Kloxin CJ, Scott TF, Adzima BJ, Bowman CN. Covalent Adaptable Networks (CANs): A Unique Paradigm in Cross-Linked Polymers. Macromolecules. 2010 Mar;43(6):2643-53.

[329] Bowman CN, Kloxin CJ. Covalent Adaptable Networks: Reversible Bond Structures Incorporated in Polymer Networks. Angewandte Chemie International Edition. 2012;51(18):4272-4.

[330] Montarnal D, Capelot M, Tournilhac F, Leibler L. Silica-Like Malleable Materials from Permanent Organic Networks. Science. 2011 Nov;334(6058):965-8.

[331] Winne JM, Leibler L, Du Prez FE. Dynamic covalent chemistry in polymer networks: a mechanistic perspective. Polymer Chemistry. 2019;10(45):6091-108.

[332] Meng F, Saed MO, Terentjev EM. Rheology of vitrimers. Nature Communications. 2022 Sep;13(1):5753.

[333] Zhang V, Kang B, Accardo JV, Kalow JA. Structure–Reactivity–Property Relationships in Covalent Adaptable Networks. Journal of the American Chemical Society. 2022 Dec;144(49):22358-77.

[334] Van Lijsebetten F, Debsharma T, Winne JM, Du Prez FE. A Highly Dynamic Covalent Polymer Network without Creep: Mission Impossible? Angewandte Chemie International Edition. 2022 Nov;61(48).

[335] Sala B, Gabrion X, Trivaudey F, Guicheret-Retel V, Placet V. Influence of the stress level and hygrothermal conditions on the creep/recovery behaviour of high-grade flax and hemp fibre reinforced GreenPoxy matrix composites. Composites Part A: Applied Science and Manufacturing. 2021 Feb;141:106204.

[336] McBride MK, Worrell BT, Brown T, Cox LM, Sowan N, Wang C, et al. Enabling Applications of Covalent Adaptable Networks. Annual Review of Chemical and Biomolecular Engineering. 2019 Jun;10(1):175-98.

[337] Elizalde F, H Aguirresarobe R, Gonzalez A, Sardon H. Dynamic polyurethane thermosets: tuning associative/dissociative behavior by catalyst selection. Polymer Chemistry. 2020;11(33):5386-96.

[338] Kloxin CJ, Bowman CN. Covalent adaptable networks: smart, reconfigurable and responsive network systems. Chemical Society Reviews. 2013 Aug;42(17):7161-73.

[339] Luo J, Demchuk Z, Zhao X, Saito T, Tian M, Sokolov AP, et al. Elastic vitrimers: Beyond thermoplastic and thermoset elastomers. Matter. 2022 May;5(5):1391-422.

[340] Krishnakumar B, Sanka RVSP, Binder WH, Parthasarthy V, Rana S, Karak N. Vitrimers: Associative dynamic covalent adaptive networks in thermoset polymers. Chemical Engineering Journal. 2020 Apr;385:123820.

[341] Vidil T, Llevot A. Fully Biobased Vitrimers: Future Direction toward Sustainable Cross-Linked Polymers. Macromolecular Chemistry and Physics. 2022 Feb:2100494.

[342] Vora N, Christensen PR, Demarteau J, Baral NR, Keasling JD, Helms BA, et al. Leveling the cost and carbon footprint of circular polymers that are chemically recycled to monomer. Science Advances. 2021 Apr;7(15):eabf0187.

[343] Taynton P, Ni H, Zhu C, Yu K, Loob S, Jin Y, et al. Repairable Woven Carbon Fiber Composites with Full Recyclability Enabled by Malleable Polyimine Networks. Advanced Materials. 2016 Apr;28(15):2904-9.

[344] Schoustra SK, Groeneveld T, Smulders MMJ. The effect of polarity on the molecular exchange dynamics in imine-based covalent adaptable networks. Polymer Chemistry. 2021;12(11):1635-42.

[345] Denissen W, Rivero G, Nicolaÿ R, Leibler L, Winne JM, Du Prez FE. Vinylogous Urethane Vitrimers. Advanced Functional Materials. 2015 Apr;25(16):2451-7.

[346] Yang R, Li W, Mo R, Zhang X. Recyclable and Degradable Vinylogous Urethane Epoxy Thermosets with Tunable Mechanical Properties from Isosorbide and Vanillic Acid. ACS Applied Polymer Materials. 2023 Apr;5(4):2553-61.

[347] Denissen W, Droesbeke M, Nicolaÿ R, Leibler L, Winne JM, Du Prez FE. Chemical control of the viscoelastic properties of vinylogous urethane vitrimers. Nature Communications. 2017 Mar;8(1):14857.

[348] Denissen W, De Baere I, Van Paepegem W, Leibler L, Winne J, Du Prez FE. Vinylogous Urea Vitrimers and Their Application in Fiber Reinforced Composites. Macromolecules. 2018 Mar;51(5):2054-64.

[349] Van Lijsebetten F, De Bruycker K, Winne JM, Du Prez FE. Masked Primary Amines for a Controlled Plastic Flow of Vitrimers. ACS Macro Letters. 2022 Jul;11(7):919-24.

[350] Engelen S, Dolinski ND, Chen C, Ghimire E, Lindberg CA, Crolais AE, et al. Vinylogous Urea—Urethane Vitrimers: Accelerating and Inhibiting Network Dynamics through Hydrogen Bonding. Angewandte Chemie. 2024;136(9):e202318412.

[351] Van Lijsebetten F, Maes S, Winne JM, Du Prez FE. Thermoswitchable catalysis to inhibit and promote plastic flow in vitrimers. Chemical Science. 2024;15(19):7061-71.

[352] Niu W, O'Sullivan C, Rambo BM, Smith MD, Lavigne JJ. Self-repairing polymers: poly(dioxaborolane)s containing trigonal planar boron. Chemical Communications. 2005;34(34):4342.

[353] Anderson L, Sanders EW, Unthank MG. Recyclable thermosets based on modified epoxy-amine network polymers. Materials Horizons. 2023;10(3):889-98.

[354] Liu Y, Tang Z, Wang D, Wu S, Guo B. Biomimetic design of elastomeric vitrimers with unparalleled mechanical properties, improved creep resistance and retained malleability by metal–ligand coordination. Journal of Materials Chemistry A. 2019 Dec;7(47):26867-76.

[355] Chen Y, Tang Z, Zhang X, Liu Y, Wu S, Guo B. Covalently Cross-Linked Elastomers with Self-Healing and Malleable Abilities Enabled by Boronic Ester Bonds. ACS Applied Materials & Interfaces. 2018 Jul;10(28):24224-31.

[356] Cromwell OR, Chung J, Guan Z. Malleable and Self-Healing Covalent Polymer Networks through Tunable Dynamic Boronic Ester Bonds. Journal of the American Chemical Society. 2015 May;137(20):6492-5.

[357] Rahman MA, Karunarathna MS, Bowland CC, Yang G, Gainaru C, Li B, et al. Tough and recyclable carbon-fiber composites with exceptional interfacial adhesion via a tailored vitrimer-fiber interface. Cell Reports Physical Science. 2023 Dec;4(12):101695.

[358] Hoyle CE, Lowe AB, Bowman CN. Thiol-click chemistry: a multifaceted toolbox for small molecule and polymer synthesis. Chemical Society Reviews. 2010;39(4):1355.

[359] Maiheu T, Laguzzi E, Slark AT, Du Prez FE. Debondable Epoxy-Acrylate Adhesives using B-Amino Ester Chemistry. ACS Applied Materials & Interfaces. 2024 Nov.

[360] Rizzo G, Saitta L, Dattilo S, Tosto C, Pergolizzi E, Ivankovic A, et al. Thermomechanical Characterization of an Unsaturated Polyester Vitrimer Synthesized Using a Titanium Transesterification Catalyst. ACS Applied Polymer Materials. 2023 Oct;5(10):8326-38.

[361] Rizzo G, Prasad V, Yasar M, Cicala G, Ivankovic A, Murphy N, et al. Investigation of mechanical properties and self-healing efficiency of carbon fibers composites infused with unsaturated polyester vitrimer. Polymer Composites. 2024;45(11):10404-17.

[362] Bakkali-Hassani C, Berne D, Ladmiral V, Caillol S. Transcarbamoylation in Polyurethanes: Underestimated Exchange Reactions? Macromolecules. 2022 Sep;55(18):7974-91.

[363] Huyan C, Liu D, Pan C, Wang D, Guo Z, Zhang X, et al. Thermally recyclable and reprocessable glass fiber reinforced high performance thermosetting polyurethane vitrimer composites. Chemical Engineering Journal. 2023 Sep;471:144478.

[364] Tao Y, Liang X, Zhang J, Lei IM, Liu J. Polyurethane vitrimers: Chemistry, properties and applications. Journal of Polymer Science. 2023;61(19):2233-53.

[365] Xu Y, Dai S, Bi L, Jiang J, Zhang H, Chen Y. Catalyst-free self-healing bio-based vitrimer for a recyclable, reprocessable, and self-adhered carbon fiber reinforced composite. Chemical Engineering Journal. 2022 Feb;429:132518.

[366] Schenk V, D'Elia R, Olivier P, Labastie K, Destarac M, Guerre M. Exploring the Limits of High-Tg Epoxy Vitrimers Produced through Resin-Transfer Molding. ACS Applied Materials & Interfaces. 2023 Oct;15(39):46357-67.

[367] Memon H, Wei Y, Zhang L, Jiang Q, Liu W. An imine-containing epoxy vitrimer with versatile recyclability and its application in fully recyclable carbon fiber reinforced composites. Composites Science and Technology. 2020 Oct;199:108314.

[368] Memon H, Liu H, Rashid MA, Chen L, Jiang Q, Zhang L, et al. Vanillin-Based Epoxy Vitrimer with High Performance and Closed-Loop Recyclability. Macromolecules. 2020 Jan;53(2):621-30.

[369] Yang W, Ding H, Zhou W, Liu T, Xu P, Puglia D, et al. Design of inherent fire retarding and degradable bio-based epoxy vitrimer with excellent self-healing and mechanical reprocessability. Composites Science and Technology. 2022 Nov;230:109776.

[370] Debsharma T, Amfilochiou V, Wróblewska AA, De Baere I, Van Paepegem W, Du Prez FE. Fast Dynamic Siloxane Exchange Mechanism for Reshapable Vitrimer Composites. Journal of the American Chemical Society. 2022 Jul;144(27):12280-9.

[371] Verdugo P, Santiago D, De La Flor S, Serra A. A Biobased Epoxy Vitrimer with Dual Relaxation Mechanism: A Promising Material for Renewable, Reusable, and Recyclable Adhesives and Composites. ACS Sustainable Chemistry & Engineering. 2024 Apr;12(15):5965-78.

[372] Maisonneuve L, Lamarzelle O, Rix E, Grau E, Cramail H. Isocyanate-Free Routes to Polyurethanes and Poly(hydroxy Urethane)s. Chemical Reviews. 2015 Nov;115(22):12407-39.

[373] Cornille A, Auvergne R, Figovsky O, Boutevin B, Caillol S. A perspective approach to sustainable routes for non-isocyanate polyurethanes. European Polymer Journal. 2017 Feb;87:535-52.

[374] Liang C, Jadidi Y, Chen Y, Gracida-Alvarez U, Torkelson JM, Hawkins TR, et al. Techno-economic Analysis and Life Cycle Assessment of Biomass-Derived Polyhydroxyurethane and Nonisocyanate Polythiourethane Production and Reprocessing. ACS Sustainable Chemistry & Engineering. 2024 Aug;12(32):12161-70.

[375] Poussard L, Mariage J, Grignard B, Detrembleur C, Jérôme C, Calberg C, et al. Non-Isocyanate Polyurethanes from Carbonated Soybean Oil Using Monomeric or Oligomeric Diamines To Achieve Thermosets or Thermoplastics. Macromolecules. 2016 Mar;49(6):2162-71.

[376] Mundo F, Caillol S, Ladmiral V, Meier MAR. On Sustainability Aspects of the Synthesis of Five-Membered Cyclic Carbonates. ACS Sustainable Chemistry & Engineering. 2024 Apr;12(17):6452-66.

[377] Blain M, Cornille A, Boutevin B, Auvergne R, Benazet D, Andrioletti B, et al. Hydrogen bonds prevent obtaining high molar mass PHUs. Journal of Applied Polymer Science. 2017 Dec;134(45):44958.

[378] Cornille A, Michaud G, Simon F, Fouquay S, Auvergne R, Boutevin B, et al. Promising mechanical and adhesive properties of isocyanate-free poly(hydroxyurethane). European Polymer Journal. 2016 Nov;84:404-20.

[379] Panchireddy S, Grignard B, Thomassin JM, Jerome C, Detrembleur C. Bio-based poly(hydroxyurethane) glues for metal substrates. Polymer Chemistry. 2018;9(19):2650-9.

[380] Blattmann H, Mulhaupt R. Multifunctional B-amino alcohols as bio-based amine curing agents for the isocyanate- and phosgene-free synthesis of 100% bio-based polyhydroxyurethane thermosets. Green Chemistry. 2016;18(8):2406-15.

[381] Fleischer M, Blattmann H, Mülhaupt R. Glycerol-, pentaerythritol- and trimethylolpropane-based polyurethanes and their cellulose carbonate composites prepared via the non-isocyanate route with catalytic carbon dioxide fixation. Green Chemistry. 2013;15(4):934.

[382] Blain M, Jean-Gérard L, Auvergne R, Benazet D, Caillol S, Andrioletti B. Rational investigations in the ring opening of cyclic carbonates by amines. Green Chem. 2014;16(9):4286-91.

[383] Ecochard Y, Caillol S. Hybrid polyhydroxyurethanes: How to overcome limitations and reach cutting edge properties? European Polymer Journal. 2020 Aug;137:109915.

[384] Monie F, Grignard B, Detrembleur C. Divergent Aminolysis Approach for Constructing Recyclable Self-Blown Nonisocyanate Polyurethane Foams. ACS Macro Letters. 2022 Feb;11(2):236-42.

[385] Bourguignon M, Grignard B, Detrembleur C. Water-Induced Self-Blown Non-Isocyanate Polyurethane Foams. Angewandte Chemie International Edition. 2022 Dec;61(51):1-10.

[386] Fortman DJ, Brutman JP, Hillmyer MA, Dichtel WR. Structural effects on the reprocessability and stress relaxation of crosslinked polyhydroxyurethanes. Journal of Applied Polymer Science. 2017 Dec;134(45):44984.

[387] Chen X, Li L, Jin K, Torkelson JM. Reprocessable Polyhydroxyurethane Network Exhibiting Full Property Recovery and Concurrent Associative and Dissociative Dynamic Chemistry via Transcarbamoylation and Reversible Cyclic Carbonate Aminolysis. Polymer Chemistry. 2017;8(6349):6349-55.

[388] Hu S, Chen X, Torkelson JM. Biobased Reprocessable Polyhydroxyurethane Networks: Full Recovery of Crosslink Density with Three Concurrent Dynamic Chemistries. ACS Sustainable Chemistry & Engineering. 2019 Jun;7(11):10025-34.

[389] Liu X, Yang X, Wang S, Wang S, Wang Z, Liu S, et al. Fully Bio-Based Polyhydroxyurethanes with a Dynamic Network from a Terpene Derivative and Cyclic Carbonate Functional Soybean Oil. ACS Sustainable Chemistry & Engineering. 2021 Mar;9(11):4175-84.

[390] Bakkali-Hassani C, Berne D, Bron P, Irusta L, Sardon H, Ladmiral V, et al. Polyhydroxyurethane covalent adaptable networks: looking for suitable catalysts. Polymer Chemistry. 2023;14(31):3610-20.

[391] Zheng J, Png ZM, Ng SH, Tham GX, Ye E, Goh SS, et al. Vitrimers: Current research trends and their emerging applications. Materials Today. 2021 Dec;51:586-625.

[392] Bourguignon M, Grignard B, Detrembleur C. Cascade Exotherms for Rapidly Producing Hybrid Nonisocyanate Polyurethane Foams from Room Temperature Formulations. Journal of the American Chemical Society. 2024 Jan;146(1):988-1000.

[393] Doley S, Dolui SK. Solvent and catalyst-free synthesis of sunflower oil based polyurethane through non-isocyanate route and its coatings properties. European Polymer Journal. 2018 May;102:161-8.

[394] Gomez-Lopez A, Panchireddy S, Grignard B, Calvo I, Jerome C, Detrembleur C, et al. Poly(hydroxyurethane) Adhesives and Coatings: State-of-the-Art and Future Directions. ACS Sustainable Chemistry & Engineering. 2021 Jul;9(29):9541-62.

[395] Gomez-Lopez A, Grignard B, Calvo I, Detrembleur C, Sardon H. Monocomponent Non-isocyanate Polyurethane Adhesives Based on a Sol–Gel Process. ACS Applied Polymer Materials. 2020 May;2(5):1839-47.

[396] Lambeth RH, Rizvi A. Mechanical and adhesive properties of hybrid epoxy-polyhydroxyurethane network polymers. Polymer. 2019 Nov;183:121881.

[397] Bähr M, Mülhaupt R. Linseed and soybean oil-based polyurethanes prepared via the non-isocyanate route and catalytic carbon dioxide conversion. Green Chemistry. 2012;14(2):483.

[398] Blattmann H, Fleischer M, Bähr M, Mülhaupt R. Isocyanate- and Phosgene-Free Routes to Polyfunctional Cyclic Carbonates and Green Polyurethanes by Fixation of Carbon Dioxide. Macromolecular Rapid Communications. 2014 Jul;35(14):1238-54.

[399] Schimpf V, Ritter BS, Weis P, Parison K, Mülhaupt R. High Purity Limonene Dicarbonate as Versatile Building Block for Sustainable Non-Isocyanate Polyhydroxyurethane Thermosets and Thermoplastics. Macromolecules. 2017 Feb;50(3):944-55.

[400] Schmidt S, Göppert NE, Bruchmann B, Mülhaupt R. Liquid sorbitol ether carbonate as intermediate for rigid and segmented non-isocyanate polyhydroxyurethane thermosets. European Polymer Journal. 2017 Sep;94:136-42.

[401] Karami Z, Kabiri K, Zohuriaan-Mehr MJ. Non-isocyanate polyurethane thermoset based on a bio-resourced star-shaped epoxy macromonomer in comparison with a cyclocarbonate fossil-based epoxy resin: A preliminary study on thermo-mechanical and antibacterial properties. Journal of CO2 Utilization. 2019 Dec;34:558-67.

[402] Wazeer A, Das A, Abeykoon C, Sinha A, Karmakar A. Composites for Electric Vehicles and Automotive Sector: A Review. Green Energy and Intelligent Transportation. 2022 Dec:100043.

[403] Loukopoulos A, Katsiropoulos CV, Pantelakis SG. Carbon footprint and financial evaluation of an aeronautic component production using different manufacturing processes. International Journal of Structural Integrity. 2019 Jun;10(3):425-35.

[404] Loukopoulos A, Katsiropoulos C, Pantelakis S. Life cycle assessment and cost analysis evaluation of a helicopter's canopy production using different manufacturing processes. MATEC Web of Conferences. 2018;188:01020.

[405] Silva D, Rocha R, Ribeiro F, Monteiro H. Environmental Impact of an Innovative Aeronautic Carbon Composite Manufactured via Heated Vacuum-Assisted Resin Transfer Molding. Sustainability. 2024 Jan;16(8):3253.

[406] Diez-Cañamero B, Mendoza JMF. Circular economy performance and carbon footprint of wind turbine blade waste management alternatives. Waste Management. 2023 Jun;164:94-105.

[407] Gennitsaris S, Sagani A, Sofianopoulou S, Dedoussis V. Integrated LCA and DEA approach for circular economy-driven performance evaluation of wind turbine end-of-life treatment options. Applied Energy. 2023 Jun;339:120951.

[408] Rajchel M, Kulpa M, Wiater A, Siwowski T. Repurposing a Decommissioned Wind Turbine Blade for Bridge Construction: An Experimental Investigation. Journal of Composites for Construction. 2025 Feb;29(1):04024084.

[409] Pietroluongo M, Padovano E, Frache A, Badini C. Mechanical recycling of an end-of-life automotive composite component. Sustainable Materials and Technologies. 2020 Apr;23:e00143.

[410] Vo Dong PA, Azzaro-Pantel C, Cadene AL. Economic and environmental assessment of recovery and disposal pathways for CFRP waste management. Resources, Conservation and Recycling. 2018 Jun;133:63-75.

[411] Meng F, McKechnie J, Pickering SJ. An assessment of financial viability of recycled carbon fibre in automotive applications. Composites Part A: Applied Science and Manufacturing. 2018 Jun;109:207-20.

[412] Gourier C, Bourmaud A, Le Duigou A, Baley C. Influence of PA11 and PP thermoplastic polymers on recycling stability of unidirectional flax fibre reinforced biocomposites. Polymer Degradation and Stability. 2017 Feb;136:1-9.

[413] Ibrahim H, Farag M, Megahed H, Mehanny S. Characteristics of starch-based biodegradable composites reinforced with date palm and flax fibers. Carbohydrate Polymers. 2014 Jan;101:11-9.

[414] Bourmaud A, Åkesson D, Beaugrand J, Le Duigou A, Skrifvars M, Baley C. Recycling of L-Poly-(lactide)-Poly-(butylene-succinate)-flax biocomposite. Polymer Degradation and Stability. 2016 Jun;128:77-88.

[415] Melelli A, Pantaloni D, Balnois E, Arnould O, Jamme F, Baley C, et al. Investigations by AFM of Ageing Mechanisms in PLA-Flax Fibre Composites during Garden Composting. Polymers. 2021 Jul;13(14):2225.

[416] Yousef S, Eimontas J, Striūgas N, Abdelnaby MA. Synthesis of value-added aromatic chemicals from catalytic pyrolysis of waste wind turbine blades and their kinetic analysis using artificial neural network. Journal of Analytical and Applied Pyrolysis. 2024 Jan;177:106330.

[417] Shen Y, Apraku SE, Zhu Y. Recycling and recovery of fiber-reinforced polymer composites for end-of-life wind turbine blade management. Green Chemistry. 2023;25(23):9644-58.

[418] Gu Y, Jérôme F. Bio-based solvents: an emerging generation of fluids for the design of eco-efficient processes in catalysis and organic chemistry. Chemical Society Reviews. 2013;42(24):9550.

[419] Calvo-Flores FG, Monteagudo-Arrebola MJ, Dobado JA, Isac-García J. Green and Bio-Based Solvents. Topics in Current Chemistry. 2018 Jun;376(3):18.

[420] Manarin E, Boumezgane O, Giannino A, De Fabritiis V, Griffini G, Turri S. Towards a zero-waste chemcycling of thermoset polymer composites: Catalyst assisted mild solvolysis for clean carbon fiber liberation and circular coating development. Sustainable Materials and Technologies. 2024 Sep;41:e01031.

[421] Jehanno C, Demarteau J, Mantione D, Arno MC, Ruipérez F, Hedrick JL, et al. Selective Chemical Upcycling of Mixed Plastics Guided by a Thermally Stable Organocatalyst. Angewandte Chemie International Edition. 2021 Mar;60(12):6710-7.

[422] Khopade KV, Chikkali SH, Barsu N. Metal-catalyzed plastic depolymerization. Cell Reports Physical Science. 2023 May;4(5):101341.

[423] Pillain B, Loubet P, Pestalozzi F, Woidasky J, Erriguible A, Aymonier C, et al. Positioning supercritical solvolysis among innovative recycling and current waste management scenarios for carbon fiber reinforced plastics thanks to comparative life cycle assessment. The Journal of Supercritical Fluids. 2019 Dec;154:104607.

[424] Kooduvalli K, Unser J, Ozcan S, Vaidya UK. Embodied Energy in Pyrolysis and Solvolysis Approaches to Recycling for Carbon Fiber-Epoxy Reinforced Composite Waste Streams. Recycling. 2022 Feb;7(1):6.

[425] Pimenta S, Pinho ST. Recycling carbon fibre reinforced polymers for structural applications: Technology review and market outlook. Waste Management. 2011 Feb;31(2):378-92.

[426] Butenegro JA, Bahrami M, Abenojar J, Martínez MA. Recent Progress in Carbon Fiber Reinforced Polymers Recycling: A Review of Recycling Methods and Reuse of Carbon Fibers. Materials. 2021 Jan;14(21):6401.

[427] Yu H, Potter KD, Wisnom MR. A novel manufacturing method for aligned discontinuous fibre composites (High Performance-Discontinuous Fibre method). Composites Part A: Applied Science and Manufacturing. 2014 Oct;65:175-85.

[428] Hecker MD, Longana ML, Eloi JC, Thomsen O, Hamerton I. Recycling end-of-life sails by carbon fibre reclamation and composite remanufacture using the HiPerDiF fibre alignment technology. Composites Part A: Applied Science and Manufacturing. 2023 Oct;173:107651.

[429] Fitzgerald AM, Wong N, Fitzgerald AVL, Jesson DA, Martin F, Murphy RJ, et al. Life Cycle Assessment of the High Performance Discontinuous Fibre (HiPerDiF) Technology and Its Operation in Various Countries. Sustainability. 2022 Feb;14(3):1922.

[430] Mantaux O, GILLET A, PEDROS M; Centre National De La Recherche Scientifique Cnrs Université De Bordeaux, assignee. Procédé de détissage et de réalignement de fibres de carbone. WO2016066975A1; 2016.

[431] Oliveux G, Bailleul JL, Gillet A, Mantaux O, Leeke GA. Recovery and reuse of discontinuous carbon fibres by solvolysis: Realignment and properties of remanufactured materials. Composites Science and Technology. 2017 Feb;139:99-108.

[432] Andrew JJ, Dhakal HN. Sustainable biobased composites for advanced applications: recent trends and future opportunities – A critical review. Composites Part C: Open Access. 2022 Mar;7:100220.

[433] Panchireddy S, Thomassin JM, Grignard B, Damblon C, Tatton A, Jerome C, et al. Reinforced poly(hydroxyurethane) thermosets as high performance adhesives for aluminum substrates. Polymer Chemistry. 2017;8(38):5897-909.

[434] Quienne B, Poli R, Pinaud J, Caillol S. Enhanced aminolysis of cyclic carbonates by beta-hydroxylamines for the production of fully biobased polyhydroxyurethanes. Green Chemistry. 2021;23(4):1678-90.

[435] Camara F, Benyahya S, Besse V, Boutevin G, Auvergne R, Boutevin B, et al. Reactivity of secondary amines for the synthesis of non-isocyanate polyurethanes. European Polymer Journal. 2014 Jun;55:17-26.

[436] Besse V, Camara F, Méchin F, Fleury E, Caillol S, Pascault JP, et al. How to explain low molar masses in PolyHydroxyUrethanes (PHUs). European Polymer Journal. 2015 Oct;71:1-11.

[437] Carré C, Ecochard Y, Caillol S, Averous L. From the synthesis of biobased cyclic carbonate to polyhydroxyurethanes: a promising route towards renewable NonIsocyanate Polyurethanes. ChemSusChem. 2019;12(15):3410-30.

[438] Ecochard Y, Leroux J, Boutevin B, Auvergne R, Caillol S. From multi-functional siloxane-based cyclic carbonates to hybrid polyhydroxyurethane thermosets. European Polymer Journal. 2019 Nov;120:109280.

[439] Cornille A, Blain M, Auvergne R, Andrioletti B, Boutevin B, Caillol S. A study of cyclic carbonate aminolysis at room temperature: effect of cyclic carbonate structures and solvents on polyhydroxyurethane synthesis. Polymer Chemistry. 2017;8(3):592-604.

[440] Capar O, Tabatabai M, Klee JE, Worm M, Hartmann L, Ritter H. Fast curing of polyhydroxyurethanes via ring opening polyaddition of low viscosity cyclic carbonates and amines. Polymer Chemistry. 2020;11(43):6964-70.

[441] Dicker MPM, Duckworth PF, Baker AB, Francois G, Hazzard MK, Weaver PM. Green composites: A review of material attributes and complementary applications. Composites Part A: Applied Science and Manufacturing. 2014 Jan;56:280-9.

[442] Tomita H, Sanda F, Endo T. Structural analysis of polyhydroxyurethane obtained by polyaddition of bifunctional five-membered cyclic carbonate and diamine based on the model reaction. Journal of Polymer Science Part A: Polymer Chemistry. 2001;39(6):851-9.

[443] Liu T, Zhou T, Yao Y, Zhang F, Liu L, Liu Y, et al. Stimulus methods of multi-functional shape memory polymer nanocomposites: A review. Composites Part A: Applied Science and Manufacturing. 2017 Sep;100:20-30.

[444] Ng F, Couture G, Philippe C, Boutevin B, Caillol S. Bio-Based Aromatic Epoxy Monomers for Thermoset Materials. Molecules. 2017 Jan;22(1):149.

[445] Saba N, Jawaid M, Alothman OY, Paridah MT. A review on dynamic mechanical properties of natural fibre reinforced polymer composites. Construction and Building Materials. 2016 Mar;106:149-59.

[446] Leitsch EK, Beniah G, Liu K, Lan T, Heath WH, Scheidt KA, et al. Nonisocyanate Thermoplastic Polyhydroxyurethane Elastomers via Cyclic Carbonate Aminolysis: Critical Role of Hydroxyl Groups in Controlling Nanophase Separation. ACS Macro Letters. 2016 Apr;5(4):424-9.

[447] Wan J, Zhao J, Zhang X, Fan H, Zhang J, Hu D, et al. Epoxy thermosets and materials derived from bio-based monomeric phenols: Transformations and performances. Progress in Polymer Science. 2020 Sep;108:101287.

[448] Chen X, Li L, Wei T, Venerus DC, Torkelson JM. Reprocessable Polyhydroxyurethane Network Composites: Effect of Filler Surface Functionality on Cross-link Density Recovery and Stress Relaxation. ACS Applied Materials & Interfaces. 2019 Jan;11(2):2398-407.

[449] Fortman DJ, Snyder RL, Sheppard DT, Dichtel WR. Rapidly Reprocessable Cross-Linked Polyhydroxyurethanes Based on Disulfide Exchange. ACS Macro Letters. 2018 Oct;7(10):1226-31.

[450] Brutman JP, Fortman DJ, De Hoe GX, Dichtel WR, Hillmyer MA. Mechanistic Study of Stress Relaxation in Urethane-Containing Polymer Networks. The Journal of Physical Chemistry B. 2019 Feb;123(6):1432-41.

[451] Zeng Y, Yang B, Luo Z, Pan X, Ning Z. Fully rosin-based epoxy vitrimers with high mechanical and thermostability properties, thermo-healing and closed-loop recycling. European Polymer Journal. 2022 Dec;181:111643.

[452] Zhao XL, Liu YY, Weng Y, Li YD, Zeng JB. Sustainable Epoxy Vitrimers from Epoxidized Soybean Oil and Vanillin. ACS Sustainable Chemistry & Engineering. 2020 Oct;8(39):15020-9.

[453] Di Mauro C, Malburet S, Graillot A, Mija A. Recyclable, Repairable, and Reshapable (3R) Thermoset Materials with Shape Memory Properties from Bio-Based Epoxidized Vegetable Oils. ACS Applied Bio Materials. 2020 Nov;3(11):8094-104.

[454] Delebecq E, Pascault JP, Boutevin B, Ganachaud F. On the Versatility of Urethane/Urea Bonds: Reversibility, Blocked Isocyanate, and Non-isocyanate Polyurethane. Chemical Reviews. 2013 Jan;113(1):80-118.

[455] Sarkar F, Akonda M, Shah DU. Mechanical Properties of Flax Tape-Reinforced Thermoset Composites. Materials. 2020 Dec;13(23):5485.

[456] Le Duigou A, Kervoelen A, Le Grand A, Nardin M, Baley C. Interfacial properties of flax fibre–epoxy resin systems: Existence of a complex interphase. Composites Science and Technology. 2014 Aug;100:152-7.

[457] Bobbink FD, van Muyden AP, Dyson PJ. *En route* to CO $_2$ -containing renewable materials: catalytic synthesis of polycarbonates and non-isocyanate polyhydroxyurethanes derived from cyclic carbonates. Chemical Communications. 2019;55(10):1360-73.

[458] Park SJ, Seo MK, Lee JR, Lee DR. Studies on epoxy resins cured by cationic latent thermal catalysts: The effect of the catalysts on the thermal, rheological, and mechanical properties. Journal of Polymer Science Part A: Polymer Chemistry. 2001;39(1):187-95.

[459] Beniah G, Liu K, Heath WH, Miller MD, Scheidt KA, Torkelson JM. Novel thermoplastic polyhydroxyurethane elastomers as effective damping materials over broad temperature ranges. European Polymer Journal. 2016 Nov;84:770-83.

[460] Pickering KL, Efendy MGA, Le TM. A review of recent developments in natural fibre composites and their mechanical performance. Composites Part A: Applied Science and Manufacturing. 2016 Apr;83:98-112.

[461] Panchireddy S. Transformation of CO2 into high performance polyhydroxyurethane adhesives and coatings [PhD Thesis]. ULiège - Université de Liège; 2018.

[462] Seychal G, Ocando C, Bonnaud L, De Winter J, Grignard B, Detrembleur C, et al. Emerging Polyhydroxyurethanes as Sustainable Thermosets: A Structure–Property Relationship. ACS Applied Polymer Materials. 2023 Jun;5(7):5567-81.

[463] Shokuhfar A, Arab B. The effect of cross linking density on the mechanical properties and structure of the epoxy polymers: molecular dynamics simulation. Journal of Molecular Modeling. 2013 Sep;19(9):3719-31.

[464] Li W, Ma J, Wu S, Zhang J, Cheng J. The effect of hydrogen bond on the thermal and mechanical properties of furan epoxy resins: Molecular dynamics simulation study. Polymer Testing. 2021 Sep;101:107275.

[465] Wang X, Gillham JK. Competitive primary amine/epoxy and secondary amine/epoxy reactions: Effect on the isothermal time-to-vitrify. Journal of Applied Polymer Science. 1991 Dec;43(12):2267-77.

[466] Khatoon H, Iqbal S, Irfan M, Darda A, Rawat NK. A review on the production, properties and applications of non-isocyanate polyurethane: A greener perspective. Progress in Organic Coatings. 2021 May;154:106124.

[467] Saha S, Mishra MK, Reddy CM, Desiraju GR. From Molecules to Interactions to Crystal Engineering: Mechanical Properties of Organic Solids. Accounts of Chemical Research. 2018 Nov;51(11):2957-67. Publisher: American Chemical Society.

[468] Meng M, Le HR, Rizvi MJ, Grove SM. 3D FEA modelling of laminated composites in bending and their failure mechanisms. Composite Structures. 2015 Jan;119:693-708.

[469] Seychal G, Ramasso E, Le Moal P, Bourbon G, Gabrion X, Placet V. Towards in-situ acoustic emission-based health monitoring in bio-based composites structures: Does embedment of sensors affect the mechanical behaviour of flax/epoxy laminates? Composites Part B: Engineering. 2022 Mar;236(3):109787.

[470] Seychal G, Van Renterghem L, Ocando C, Bonnaud L, Raquez JM. Towards sustainable reprocessable structural composites: Benzoxazines as biobased matrices for natural fibers. Composites Part B: Engineering. 2024 Mar;272:111201.

[471] Monti A, El Mahi A, Jendli Z, Guillaumat L. Mechanical behaviour and damage mechanisms analysis of a flax-fibre reinforced composite by acoustic emission. Composites Part A: Applied Science and Manufacturing. 2016 Nov;90:100-10.

[472] Madsen B, Thygesen A, Lilholt H. Plant fibre composites – porosity and stiffness. Composites Science and Technology. 2009 Jun;69(7-8):1057-69.

[473] Saba N, Jawaid M, Paridah MT, Al-othman OY. A review on flammability of epoxy polymer, cellulosic and non-cellulosic fiber reinforced epoxy composites: Flammability of Epoxy Polymer and Its Composites. Polymers for Advanced Technologies. 2015;27(5):577-90.

[474] An L, Li X, Jin C, Zhao W, Shi Q. An extrinsic welding method for thermosetting composites: Strong and repeatable. Composites Part B: Engineering. 2022 Oct;245:110224.

[475] Miranda Campos B, Fontaine G, Bourbigot S, Stoclet G, Bonnet F. Poly(l-lactide- co e-caprolactone) Matrix Composites Produced in One Step by In-Situ Polymerization in TP-RTM. ACS Applied Polymer Materials. 2022 Oct;4(10):6797-802.

[476] Mo XZ, Wei FX, Tan DF, Pang JY, Lan CB. The compatibilization of PLA-g-TPU graft copolymer on polylactide/thermoplastic polyurethane blends. Journal of Polymer Research. 2020 Jan;27(2):33.

[477] Eisoldt L, Smith A, Scheibel T. Decoding the secrets of spider silk. Materials Today. 2011 Mar;14(3):80-6.

[478] Coyne KJ, Qin XX, Waite JH. Extensible Collagen in Mussel Byssus: A Natural Block Copolymer. Science. 1997 Sep;277(5333):1830-2.

[479] Le Duigou A, Requile S, Beaugrand J, Scarpa F, Castro M. Natural fibres actuators for smart bio-inspired hygromorph biocomposites. Smart Materials and Structures. 2017 Dec;26(12):125009.

[480] Shi C, Li ZC, Caporaso L, Cavallo L, Falivene L, Chen EYX. Hybrid monomer design for unifying conflicting polymerizability, recyclability, and performance properties. Chem. 2021 Mar;7(3):670-85.

[481] Hernández A, Houck HA, Elizalde F, Guerre M, Sardon H, Du Prez FE. Internal catalysis on the opposite side of the fence in non-isocyanate polyurethane covalent adaptable networks. European Polymer Journal. 2022 Apr;168:111100.

[482] Yap K, Krantzman KD, Lavrich RJ. Inductive Effects on Intramolecular Hydrogen Bond Strength: An Investigation of the Effect of an Electron-Withdrawing CF_3 Group Adjacent to an Alcohol Hydrogen Bond Donor. The Journal of Physical Chemistry A. 2023 Sep;127(38):7892-7.

[483] Fortman DJ, Brutman JP, Cramer CJ, Hillmyer MA, Dichtel WR. Mechanically Activated, Catalyst-Free Polyhydroxyurethane Vitrimers. Journal of the American Chemical Society. 2015 Nov;137(44):14019-22.

[484] Schenk V, De Calbiac J, D'Elia R, Olivier P, Labastie K, Destarac M, et al. Epoxy Vitrimer Formulation for Resin Transfer Molding: Reactivity, Process, and Material Characterization. ACS Applied Polymer Materials. 2024 May;6(10):6087-95.

[485] Rekondo A, Martin R, Ruiz De Luzuriaga A, Cabañero G, Grande HJ, Odriozola I. Catalyst-free room-temperature self-healing elastomers based on aromatic disulfide metathesis. Mater Horiz. 2014;1(2):237-40.

[486] Altuna FI, Hoppe CE, Williams RJJ. Epoxy vitrimers with a covalently bonded tertiary amine as catalyst of the transesterification reaction. European Polymer Journal. 2019 Apr;113:297-304.

[487] Ghanbaralizadeh R, Bouhendi H, Kabiri K, Vafayan M. A novel method for toughening epoxy resin through CO2 fixation reaction. Journal of CO2 Utilization. 2016 Dec;16:225-35.

[488] Du R, Xu Z, Zhu C, Jiang Y, Yan H, Wu H, et al. A Highly Stretchable and Self-Healing Supramolecular Elastomer Based on Sliding Crosslinks and Hydrogen Bonds. Advanced Functional Materials. 2020 Feb;30(7):1907139.

[489] Seychal G, Nickmilder P, Lemaur V, Ocando C, Grignard B, Leclère P, et al. A novel approach to design structural natural fiber composites from sustainable CO 2 -derived polyhydroxyurethane thermosets with outstanding properties and circular features. Composites Part A: Applied Science and Manufacturing. 2024 Oct;185:108311.

[490] Perrin H, Vaudemont R, Del Frari D, Verge P, Puchot L, Bodaghi M. On the cyclic delamination-healing capacity of vitrimer-based composite laminates. Composites Part A: Applied Science and Manufacturing. 2024 Feb;177:107899.

[491] Hubbard AM, Ren Y, Picu CR, Sarvestani A, Konkolewicz D, Roy AK, et al. Creep Mechanics of Epoxy Vitrimer Materials. ACS Applied Polymer Materials. 2022 Jun;4(6):4254-63.

[492] Van Lijsebetten F, De Bruycker K, Spiesschaert Y, Winne JM, Du Prez FE. Suppressing Creep and Promoting Fast Reprocessing of Vitrimers with Reversibly Trapped Amines. Angewandte Chemie. 2022 Feb;134(9).

[493] Yu K, Taynton P, Zhang W, Dunn ML, Qi HJ. Reprocessing and recycling of thermosetting polymers based on bond exchange reactions. RSC Adv. 2014;4(20):10108-17.

[494] Bandegi A, Gray TG, Mitchell S, Jamei Oskouei A, Sing MK, Kennedy J, et al. Vitrimerization of crosslinked elastomers: a mechanochemical approach for recycling thermoset polymers. Materials Advances. 2023;4(12):2648-58.

[495] Liu T, Shao L, Zhao B, Chang Y, Zhang J. Progress in Chemical Recycling of Carbon Fiber Reinforced Epoxy Composites. Macromolecular Rapid Communications. 2022 Dec;43(23):2200538.

[496] Nakayama Y, Soeda F, Ishitani A. XPS study of the carbon fiber matrix interface. Carbon. 1990;28(1):21-6.

[497] Witik RA, Teuscher R, Michaud V, Ludwig C, Månson JAE. Carbon fibre reinforced composite waste: An environmental assessment of recycling, energy recovery and landfilling. Composites Part A: Applied Science and Manufacturing. 2013 Jun;49:89-99.

[498] Ma Y, Navarro CA, Williams TJ, Nutt SR. Recovery and reuse of acid digested amine/epoxy-based composite matrices. Polymer Degradation and Stability. 2020 May;175:109125.

[499] Kong C, Park H, Lee J. Study on structural design and analysis of flax natural fiber composite tank manufactured by vacuum assisted resin transfer molding. Materials Letters. 2014 Sep;130:21-5.

[500] Baroncini EA, Kumar Yadav S, Palmese GR, Stanzione JF. Recent advances in bio-based epoxy resins and bio-based epoxy curing agents. Journal of Applied Polymer Science. 2016 Dec;133(45):app.44103.

[501] Garipov RM, Sysoev VA, Mikheev VV, Zagidullin AI, Deberdeev RY, Irzhak VI, et al. Reactivity of Cyclocarbonate Groups in Modified Epoxy–Amine Compositions. Doklady Physical Chemistry. 2003 Nov;393(1-3):289-92.

[502] Monie F, Vidil T, Grau E, Grignard B, Detrembleur C, Cramail H. The Multifaceted Role of Water as an Accelerator for the Preparation of Isocyanate-Free Polyurethane Thermosets. Macromolecules. 2024 Sep.

[503] Alves M, Méreau R, Grignard B, Detrembleur C, Jérôme C, Tassaing T. DFT investigation of the reaction mechanism for the guanidine catalysed ring-opening of cyclic carbonates by aromatic and alkyl-amines. RSC Advances. 2017;7(31):18993-9001.

[504] Jaques NG, William De Lima Souza J, Popp M, Kolbe J, Lia Fook MV, Ramos Wellen RM. Kinetic investigation of eggshell powders as biobased epoxy catalyzer. Composites Part B: Engineering. 2020 Feb;183:107651.

[505] Rusnáková S, Kalová M, Jonšta Z. Overview of production of pre-preg, prototype and testing. IOP Conference Series: Materials Science and Engineering. 2018 Nov;448:012069.

[506] Seychal G, Ximenis M, Lemaur V, Grignard B, Lazzaroni R, Detrembleur C, et al. Synergetic Hybridization Strategy to Enhance the Dynamicity of Poorly Dynamic CO $_2$ -derived Vitrimers achieved by a Simple Copolymerization Approach. Advanced Functional Materials. 2024 Oct:2412268.

[507] Singh DK, Vaidya A, Thomas V, Theodore M, Kore S, Vaidya U. Finite Element Modeling of the Fiber-Matrix Interface in Polymer Composites. Journal of Composites Science. 2020 May;4(2):58.

[508] Dziendzikowski M, Kurnyta A, Dragan K, Klysz S, Leski A. In situ Barely Visible Impact Damage detection and localization for composite structures using surface mounted and embedded PZT transducers: A comparative study. Mechanical Systems and Signal Processing. 2016 Oct;78:91-106.

[509] Orduna L, Razquin I, Otaegi I, Aranburu N, Guerrica-Echevarría G. Ionic Liquid-Cured Epoxy/PCL Blends with Improved Toughness and Adhesive Properties. Polymers. 2022 Jun;14(13):2679.

[510] Corbin AC, Soulat D, Ferreira M, Labanieh AR, Gabrion X, Malécot P, et al. Towards hemp fabrics for high-performance composites: Influence of weave pattern and features. Composites Part B: Engineering. 2020 Jan;181:107582.

[511] Madsen B, Thygesen A, Lilholt H. Plant fibre composites – porosity and volumetric interaction. Composites Science and Technology. 2007 Jun;67(7):1584-600.

[512] Kersani M, Lomov SV, Van Vuure AW, Bouabdallah A, Verpoest I. Damage in flax/epoxy quasi-unidirectional woven laminates under quasi-static tension. Journal of Composite Materials. 2015 Feb;49(4):403-13.

[513] Ueki Y, Lilholt H, Madsen B. Experimental evaluation of stiffness predictions of multiaxial flax fibre composites by classical laminate theory. PLOS ONE. 2020;15(6):e0234701.

[514] Sturgeon MR, Kim S, Lawrence K, Paton RS, Chmely SC, Nimlos M, et al. A Mechanistic Investigation of Acid-Catalyzed Cleavage of Aryl-Ether Linkages: Implications for Lignin Depolymerization in Acidic Environments. ACS Sustainable Chemistry & Engineering. 2014 Mar;2(3):472-85.

[515] Xing M, Li Z, Zheng G, Du Y, Chen C, Wang Y. Recycling of carbon fiber-reinforced epoxy resin composite via a novel acetic acid swelling technology. Composites Part B: Engineering. 2021 Nov;224:109230.

[516] Yang X, Berthold F, Berglund LA. High-Density Molded Cellulose Fibers and Transparent Biocomposites Based on Oriented Holocellulose. ACS Applied Materials & Interfaces. 2019 Mar;11(10):10310-9.

[517] Pickering SJ. Recycling technologies for thermoset composite materials—current status. Composites Part A: Applied Science and Manufacturing. 2006 Aug;37(8):1206-15.

[518] Yan T, H Balzer A, M Herbert K, H Epps T, J Korley LT. Circularity in polymers: addressing performance and sustainability challenges using dynamic covalent chemistries. Chemical Science. 2023;14(20):5243-65.

[519] Mohanty AK, Vivekanandhan S, Pin JM, Misra M. Composites from renewable and sustainable resources: Challenges and innovations. Science. 2018 Nov;362(6414):536-42.

[520] Nouailhas H, Aouf C, Le Guerneve C, Caillol S, Boutevin B, Fulcrand H. Synthesis and properties of biobased epoxy resins. part 1. Glycidylation of flavonoids by epichlorohydrin. Journal of Polymer Science Part A: Polymer Chemistry. 2011 May;49(10):2261-70.

[521] Gennen S, Alves M, Méreau R, Tassaing T, Gilbert B, Detrembleur C, et al. Fluorinated Alcohols as Activators for the Solvent-Free Chemical Fixation of Carbon Dioxide into Epoxides. ChemSusChem. 2015 Jun;8(11):1845-9.

[522] Michaud V, Takahashi J, Verpoest I. LCA of Carbon Fibers: An Analysis of Available Data Sets PAN Based Carbon FibersAnalysis of Various Data Sets. In: Proceedings of the International Conference on Composite Materials,. Belfast; 2023. p. 1-20.

[523] European Commission Joint Research Centre . Clean Energy Technology Observatory, Advanced biofuels in the European Union: status report on technology development, trends, value chains & markets : 2023. LU: Publications Office; 2023.

[524] Tchana Toffe G. Life Cycle Evaluation of Manufacturing and Mechanical Properties for Novel Natural Fibre Composites [Doctor of Philosophy]. Hertfordshire,UK: University of Hertfordshire; 2020. Accepted: 2021-03-24T11:39:13Z.

[525] Wegmann S, Rytka C, Diaz-Rodenas M, Werlen V, Schneeberger C, Ermanni P, et al. A life cycle analysis of novel lightweight composite processes: Reducing the environmental footprint of automotive structures. Journal of Cleaner Production. 2022 Jan;330:129808.

[526] Jones C. Embodied Carbon Footprint Database; 2019.

[527] Venkatarama Reddy BV, Jagadish KS. Embodied energy of common and alternative building materials and technologies. Energy and Buildings. 2003 Feb;35(2):129-37.

[528] Bensadoun F, Vanderfeesten B, Verpoest I, Van Vuure AW, Van Acker K. Environmental impact assessment of end of life options for flax-MAPP composites. Industrial Crops and Products. 2016 Dec;94:327-41.

[529] Martín-Espejo JL, Gandara-Loe J, Odriozola JA, Reina TR, Pastor-Pérez L. Sustainable routes for acetic acid production: Traditional processes vs a low-carbon, biogas-based strategy. Science of The Total Environment. 2022 Sep;840:156663.

[530] Zhang C, Xue J, Yang X, Ke Y, Ou R, Wang Y, et al. From plant phenols to novel bio-based polymers. Progress in Polymer Science. 2022 Feb;125:101473.

[531] HABERT R, Viguie C. AVIS de l'Anses relatif à l'identification en tant que substance extrêmement préoccupante (SVHC) du résorcinol pour son caractère de perturbateur endocrinien. Maison Halfort, Paris: ANSES; 2020. 2018-SA-0110.

[532] Wu X, De bruyn M, Trimmel G, Zangger K, Barta K. High-Performance Thermoplastics from a Unique Bicyclic Lignin-Derived Diol. ACS Sustainable Chemistry & Engineering. 2023 Feb;11(7):2819-29.

[533] Winter JD, Deshayes G, Boon F, Coulembier O, Dubois P, Gerbaux P. MALDI-ToF analysis of polythiophene: use of trans-2-[3-(4-t-butyl-phenyl)-2-methyl-2-propenylidene]malononitrile-DCTB-as matrix. Journal of Mass Spectrometry. 2011 Mar;46(3):237-46.

[534] D20 Committee. Test Method for Tensile Properties of Plastics. ASTM International. 2022;22.

[535] Brutman JP, Delgado PA, Hillmyer MA. Polylactide Vitrimers. ACS Macro Letters. 2014 Jul;3(7):607-10.

[536] Sendeckyj G, Wang S, Steven Johnson W, Stinchcomb W, Chamis C. Mechanics of Composite Materials: Past, Present, and Future. Journal of Composites Technology and Research. 1989;11(1):3.

[537] Grimme S, Ehrlich S, Goerigk L. Effect of the damping function in dispersion corrected density functional theory. Journal of Computational Chemistry. 2011 May;32(7):1456-65.

[538] Besler BH, Merz Jr KM, Kollman PA. Atomic charges derived from semiempirical methods. Journal of Computational Chemistry. 1990;11(4):431-9.

[539] Puhurcuoğlu N, Arman Y. Parameter estimation of epoxy resin cure kinetics by dynamics DSC data. Polymers for Advanced Technologies. 2024 Jul;35(7):e6498.

[540] Liu Y, Tang Z, Chen Y, Zhang C, Guo B. Engineering of beta-Hydroxyl Esters into Elastomer–Nanoparticle Interface toward Malleable, Robust, and Reprocessable Vitrimer Composites. ACS Applied Materials & Interfaces. 2018 Jan;10(3):2992-3001.

[541] Ruiz De Luzuriaga A, Markaide N, Salaberria AM, Azcune I, Rekondo A, Grande HJ. Aero Grade Epoxy Vitrimer towards Commercialization. Polymers. 2022 Aug;14(15):3180.

[542] Si H, Zhou L, Wu Y, Song L, Kang M, Zhao X, et al. Rapidly reprocessable, degradable epoxy vitrimer and recyclable carbon fiber reinforced thermoset composites relied on high contents of exchangeable aromatic disulfide crosslinks. Composites Part B: Engineering. 2020 Oct;199:108278.

[543] Adjaoud A, Puchot L, Verge P. High-Tg and Degradable Isosorbide-Based Polybenzoxazine Vitrimer. ACS Sustainable Chemistry & Engineering. 2022 Jan;10(1):594-602.

[544] Pettazzoni L, Ximenis M, Leonelli F, Vozzolo G, Bodo E, Elizalde F, et al. Oxime metathesis: tuneable and versatile chemistry for dynamic networks. Chemical Science. 2024;15(7):2359-64.

[545] Wu J, Yu X, Zhang H, Guo J, Hu J, Li MH. Fully Biobased Vitrimers from Glycyrrhizic Acid and Soybean Oil for Self-Healing, Shape Memory, Weldable, and Recyclable Materials. ACS Sustainable Chemistry & Engineering. 2020 Apr;8(16):6479-87. Publisher: American Chemical Society.

[546] Fortman DJ, Sheppard DT, Dichtel WR. Reprocessing Cross-Linked Polyurethanes by Catalyzing Carbamate Exchange. Macromolecules. 2019 Aug;52(16):6330-5.

[547] Niu X, Wang F, Li X, Zhang R, Wu Q, Sun P. Using Zn2+ Ionomer To Catalyze Transesterification Reaction in Epoxy Vitrimer. Industrial & Engineering Chemistry Research. 2019 Apr;58(14):5698-706. Publisher: American Chemical Society.

[548] Tian PX, Li YD, Hu Z, Zeng JB. Flame-retardant epoxy vitrimers with high strength and high-Tg for recyclable carbon fiber-reinforced composites. Composites Communications. 2024 Apr;47:101870.